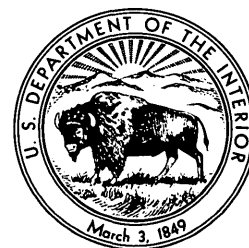


Short Papers in Geology Hydrology, and Topography Articles 120-179

G E O L O G I C A L S U R V E Y R E S E A R C H 1 9 6 2

G E O L O G I C A L S U R V E Y P R O F E S S I O N A L P A P E R 4 5 0 - D

*Scientific notes and summaries
of investigations prepared by
members of the Geologic, Water
Resources, and Topographic Divisions
in the fields of geology, hydrology,
topography, and related sciences*



UNITED STATES GOVERNMENT PRINTING OFFICE, WASHINGTON : 1962

UNITED STATES DEPARTMENT OF THE INTERIOR

STEWART L. UDALL, *Secretary*

GEOLOGICAL SURVEY

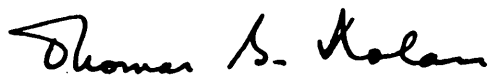
Thomas B. Nolan, *Director*

For sale by the Superintendent of Documents, U.S. Government Printing Office
Washington 25, D.C.

FOREWORD

This collection of 60 short papers on subjects in the fields of geology, hydrology, topography, and related sciences is the third of a series to be released during the year as chapters of Professional Paper 450. The papers in this chapter report on the scientific and economic results of current work by members of the Geologic, Water Resources, and Topographic Divisions of the United States Geological Survey. Some of the papers announce new discoveries or present observations on problems of limited scope; other papers draw conclusions from more extensive or continuing investigations that in large part will be discussed in greater detail in reports to be published in the future.

Chapter A of this series, to be published later in the year, will present a synopsis of results from a wide range of work done during the present fiscal year.



THOMAS B. NOLAN,
Director.

CONTENTS

	Page
Foreword.....	III
GEOLOGIC STUDIES	
Economic geology	
120. Age of some copper-bearing porphyries and other igneous rocks in southeastern Arizona, by S. C. Creasey and R. W. Kistler.....	D1
121. Thalenite from Teller County, Colorado, by J. W. Adams, F. A. Hildebrand, and R. G. Havens.....	6
122. Alteration as a guide to uranium ore, Shirley Basin, Wyoming, by E. N. Harshman.....	8
123. Alunite on Aspen Mountain, southwestern Wyoming, by J. D. Love and P. D. Blackmon.....	11
124. Clays in the Morrison Formation and their spatial relation to the uranium deposits at Ambrosia Lake, New Mexico, by H. C. Granger.....	15
Engineering geology	
125. Geology of Djatiluhur damsite and vicinity, West Java, Indonesia, by H. H. Waldron.....	21
Stratigraphy	
126. Precambrian(?) and Cambrian stratigraphy in Esmeralda County, Nevada, by J. P. Albers and J. H. Stewart.....	24
127. Cambrian Carrara Formation, Bonanza King Formation, and Dunderberg Shale east of Yucca Flat, Nye County, Nevada, by Harley Barnes, R. L. Christiansen, and F. M. Byers, Jr.....	27
128. Age and sequence of metasedimentary and metavolcanic formations northwest of New Haven, Connecticut, by C. E. Fritts.....	32
129. Age of the Leadville Limestone in the Glenwood Canyon, western Colorado, by W. E. Hallgarth and B. A. L. Skipp.....	37
130. Type sections for the Morrow Series, of Pennsylvanian age, and adjacent beds, Washington County, Arkansas, by L. G. Henbest.....	38
131. New members of the Bloyd Formation of Pennsylvanian age, Washington County, Arkansas, by L. G. Henbest....	42
132. The Eagle Valley Evaporite and its relation to the Minturn and Maroon Formations, northwest Colorado, by T. S. Lovering and W. W. Mallory.....	45
133. Jurassic stratigraphy in the McCarthy C-5 quadrangle, Alaska, by E. M. MacKevett, Jr., and R. W. Imlay.....	49
134. Some Late Cretaceous strand lines in southern Wyoming, by A. D. Zapp and W. A. Cobban.....	52
135. Tertiary volcanic and related rocks of the Republic area, Ferry County, Washington, by Siegfried Muessig.....	56
136. Geology of Tertiary rocks in Escambia and Santa Rosa Counties, western Florida, by O. T. Marsh.....	59
137. Stratigraphy and hydrology of the Juana Díaz Formation in the Yauco area, Puerto Rico, by I. G. Grossman.....	62
138. Pyroclastic deposits of Recent age at Mount Rainier, Washington, by D. R. Crandell, D. R. Mullineaux, R. D. Miller, and Meyer Rubin.....	64
Structural geology	
139. The Pine Mountain overthrust at the northeast end of the Powell Valley anticline, Virginia, by R. L. Miller.....	69
140. Gravity and magnetic anomalies in Gem Valley, Caribou County, Idaho, by D. R. Mabey and F. C. Armstrong....	73
141. Gravity, volcanism, and crustal deformation in the eastern Snake River Plain, Idaho, by T. R. LaFehr and L. C. Pakiser.....	76
142. Geohydrologic evidence of a buried fault in the Erda area, Tooele Valley, Utah, by J. S. Gates.....	78
143. Recurrent movement on the Canyon Creek fault, Navajo County, Arizona, by T. L. Finnell.....	80
144. Restudy of the Arrowhead fault, Muddy Mountains, Nevada, by C. R. Longwell.....	82
145. Correlation of granitic plutons across faulted Owens Valley, California, by D. C. Ross.....	86
146. Structural control of interior drainage, southern San Joaquin Valley, California, by G. H. Davis and J. H. Green..	89
147. Tertiary salt domes near San Pedro de Atacama, Chile, by R. J. Dingman.....	92
148. Zinc occurrence in the Serpent Mound structure of southern Ohio, by A. V. Heyl and M. R. Brock.....	95
Geophysics	
149. Thermoluminescence investigations at Meteor Crater, Arizona, by C. H. Roach, G. R. Johnson, J. G. McGrath, and T. S. Sterrett.....	98
150. Electrical and magnetic properties of a replacement-type magnetite deposit in San Bernardino County, California, by C. J. Zablocki.....	103
151. Determination of the magnetic polarity of rock samples in the field, by R. R. Doell and Allan Cox.....	105

Mineralogy, geochemistry, and petrology

152. Thermal expansion of ten minerals, by B. J. Skinner..... D109
153. Hydrothermal alteration in drill holes GS-5 and GS-7, Steamboat Springs, Nevada, by G. E. Sigvaldason and D. E. White..... 113
154. Precambrian gabbro in the central Front Range, Colorado, by R. B. Taylor and P. K. Sims..... 118

Geomorphology and glacial geology

155. Erosional features of snow avalanches, Middle Fork Kings River, California, by G. H. Davis..... 122
156. Configuration of the bedrock beneath the channel of the lower Merrimack River, Massachusetts, by E. A. Sammel... 125
157. Geology of Pleistocene deposits of Lake County, Indiana, by J. S. Rosenshein..... 127
158. Geology of the Vermilion end moraine, Nett Lake Indian Reservation, Minnesota, by R. F. Norvitch..... 130
159. Three pre-Bull Lake tills in the Wind River Mountains, Wyoming, by G. M. Richmond..... 132
160. Faulted Pleistocene strata near Jackson, northwestern Wyoming, by J. D. Love and D. W. Taylor..... 136

Paleontology and paleoecology

161. Late Cretaceous *Desmoscaphtes* Range Zone in the western interior region, by W. A. Cobban..... 140
162. The ostracode genus *Cytherelloidea*, a possible indicator of paleotemperature, by I. G. Sohn..... 144

Sedimentation

163. Wind directions in late Paleozoic to middle Mesozoic time on the Colorado Plateau, by F. G. Poole..... 147
164. Laboratory studies on deformation in unconsolidated sediment, by E. D. McKee, M. A. Reynolds, and C. H. Baker, Jr..... 151
165. Experiments on intraformational recumbent folds in crossbedded sand, by E. D. McKee, M. A. Reynolds, and C. H. Baker, Jr..... 155

Illustrative and mapping techniques

166. Edge isolation in photogrammetry and geologic photography, by A. B. Clarke..... 160
167. Shortcut method for the preparation of shaded-relief illustrations, by J. R. Stacy..... 165

HYDROLOGIC STUDIES**Ground water**

168. Winter ground-water temperatures along the Mullica River, Wharton Tract, New Jersey, by E. C. Rhodehamel and S. M. Lang..... 165
169. Relation of permeability and jointing in crystalline metamorphic rocks near Jonesboro, Georgia, by J. W. Stewart... 168
170. Aquifers in buried shore and glaciofluvial deposits along the Gladstone beach of glacial Lake Agassiz near Stephen, Minnesota, by R. W. Maclay and G. R. Schiner..... 170
171. Potential yield of deep water wells in the southern part of the Jicarilla Apache Indian Reservation and vicinity, San Juan Basin, New Mexico, by E. H. Baltz, S. W. West, and S. R. Ash..... 173
172. Compaction of the aquifer system and land subsidence in the Santa Clara Valley, California, by J. H. Green..... 175

Surface water

173. Use of short records of runoff to estimate a 25-year average runoff in the Potomac River basin, by W. S. Eisenlohr, Jr. 178
174. Use of regionalized flood-frequency curves in adjusting flow-duration curves, by G. A. Kirkpatrick and J. A. McCabe... 179
175. A control structure for measuring water discharge and sediment load, by E. V. Richardson and D. D. Harris..... 182
176. Use of a radioisotope to measure water discharge, by B. J. Frederick, C. W. Reck, and R. W. Carter..... 185

Quality of water

177. Solute degradation in the Potomac River basin, by H. R. Feltz and J. W. Wark..... 186
178. Foaming characteristics of synthetic-detergent solutions, by C. H. Wayman, J. B. Robertson, and H. G. Page..... 188
179. Surface tension of detergent solutions, by C. H. Wayman, J. B. Robertson, and H. G. Page..... 190

INDEXES

- Subject**..... 193
- Author**..... 195

GEOLOGICAL SURVEY RESEARCH 1962

SHORT PAPERS IN GEOLOGY, HYDROLOGY, AND TOPOGRAPHY, ARTICLES 120-179

GEOLOGIC STUDIES

ECONOMIC GEOLOGY

120. AGE OF SOME COPPER-BEARING PORPHYRIES AND OTHER IGNEOUS ROCKS IN SOUTHEASTERN ARIZONA

By S. C. CREASEY and R. W. KISTLER, Menlo Park, Calif.

Dating of the Mesozoic and early Cenozoic geologic events in southeastern Arizona is severely hampered by the scarcity of fossiliferous sedimentary rocks of these ages and by the isolation of individual mountain ranges. Isotopic age determinations, therefore, provide definite ages to replace permissive time intervals and aid in the correlation of geologic events from one range to another.

The K-Ar and Rb-Sr ages of biotites from some intrusive and extrusive rocks in southeastern Arizona are listed in table 120.1, and the location of the rocks sampled is shown on figure 120.1. Potassium was determined by flame photometer using lithium as an internal standard. Argon was extracted from the specimens using the technique described by Lipson (1958). Argon was analyzed with a Reynolds-type

TABLE 120.1.—Analytical data and isotopic ages of biotites from Arizona

K-Ar age determinations							
No. on fig. 120.1	Rock	Location	K (weight percent) ¹	K ⁴⁰ ×10 ⁻⁷ (moles per g)	*Ar ⁴⁰ ×10 ⁻¹¹ (moles per g)	Ar ⁴⁰ /K ⁴⁰	Age (m. y.)
1-----	Juniper Flat Granite ² -----	Northern Mule Mountains, Warren district.	5. 49	1. 71	171. 0	0. 01	163
2-----	Intrusive rhyolite-----	Tombstone district-----	7. 44	2. 32	87. 0	. 00375	63
3-----	Schieffelin Granodiorite-----	do-----	3. 33	1. 04	44. 6	. 00429	72
4-----	Equigranular granodiorite-----	Pima district-----	7. 28	2. 27	81. 0	. 00357	60
5-----	Quartz monzonite porphyry-----	do-----	5. 98	1. 87	61. 5	. 00329	56
6-----	Rhyolite tuff-----	do-----	7. 16	2. 23	74. 7	. 00335	57
7-----	Andesite dikes-----	do-----	3. 87	1. 21	16. 9	. 0014	24
8-----	Lost Gulch Quartz Monzonite-----	Globe-Miami district-----	7. 24	2. 26	83. 6	. 0037	62
9-----	Schultze Granite-----	do-----	7. 32	2. 28	77. 7	. 00341	58
10-----	Vitrophyre (dacite ash flow)-----	do-----	5. 67	1. 77	20. 4	. 00115	20
11-----	Granite Mountain Porphyry-----	Mineral Creek district-----	6. 86	2. 14	79. 6	. 00372	63
12-----	Quartz diorite porphyry-----	Banner district-----	6. 49	2. 02	73. 9	. 00366	62
13-----	Copper Creek granodiorite-----	Bunker Hill district-----	6. 27	1. 96	78. 8	. 00402	68
Rb-Sr age determinations							
No. on fig. 120.1	Rock	Location	Rb ⁸⁷ (ppm)	Normal Sr (ppm)	*Sr ⁸⁷ (ppm)	Sr ⁸⁷ /Rb ⁸⁷	Age (m. y.)
1-----	Juniper Flat Granite ² -----	Warren district-----	384	22. 2	0. 994	0. 00259	176
	do ² -----	do-----	388	21. 3	1. 017	. 00262	178

¹ Frank Walthall analyst.² Same sample used for Rb-Sr and K-Ar age determinations.

*Radiogenic.

Decay constants:

K⁴⁰: $\lambda_a = 0.584 \times 10^{-10} \text{ yr}^{-1}$, $\lambda_b = 4.72 \times 10^{-10} \text{ yr}^{-1}$; K⁴⁰ = $1.22 \times 10^{-4} \text{ g K}^{40} \text{ per g K}$.Rb⁸⁷: $\lambda = 1.47 \times 10^{-11} \text{ yr}^{-1}$; Rb⁸⁷ = $0.283 \text{ g Rb}^{87} \text{ per g Rb}$.

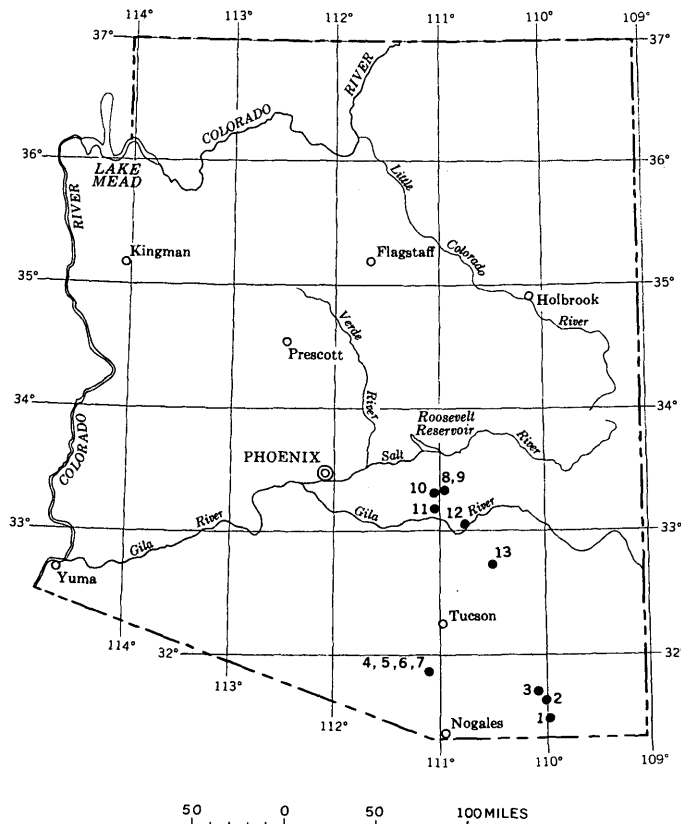


FIGURE 120.1.—Index map of Arizona showing location of igneous rocks sampled for the isotopic age determinations listed in table 120.1.

mass spectrometer by the geochronology group of the University of California, Berkeley. Rubidium and strontium were determined by isotope dilution techniques described by Goldich and others (1961, p. 8-35). The analytical determination of potassium and the mass spectrometric measurements of Ar, Rb, and Sr are accurate to about 2 percent. The probable error of an individual mineral age is about ± 4 percent.

Most of the intrusive rocks are related spatially either to ore deposits or to structures. These dates are a start toward establishing the age of mineralization of the porphyry copper and other deposits. In the following, the ages of the igneous rock will be discussed briefly in relation to the ore deposits of four general areas, each including one or more mining districts.

WARREN (BISBEE) AND TOMBSTONE DISTRICTS

Three intrusive rocks from the Warren and Tombstone districts were dated: The Juniper Flat Granite from the northern end of the Mule Mountains, intrusive rhyolite from south of Tombstone, and the Schieffelin Granodiorite from Tombstone. Gilluly (1956, p. 55) determined the age of the Juniper Flat Granite

to be post-Pennsylvanian (Horquilla Limestone) and pre-Lower Cretaceous (Bisbee Group). He also assigned a tentative Tertiary age to the intrusive rhyolite south of Tombstone on indirect geologic evidence (Gilluly, 1956, p. 106) and correlated it with the granite porphyry mapped by Ransome (1904) in the Warren district. The similarity in chemical composition of the intrusive rhyolite and the granite porphyry supports this correlation: both have an unusually high K_2O content. This correlation could not be tested by isotopic dating, however, for we were not able to obtain granite porphyry with fresh biotite.

Ransome (1904, p. 84) thought that the granite porphyry, the Juniper Flat Granite, and the Sacramento Porphyry (which is the host for disseminated copper ore at Bisbee) were comagmatic. Because the Juniper Flat Granite and the granite porphyry apparently had supplied pebbles to the basal conglomerate of the Bisbee Group of Early Cretaceous age, he assigned the entire rock suite and the ore deposits to the pre-Lower Cretaceous. Others, however, such as Tenney (1935, p. 225-227), believed that the Sacramento Porphyry and the spatially related ore deposits at Bisbee are Late Cretaceous or early Tertiary (Laramide).

The isotopic dating of the Juniper Flat Granite and the intrusive rhyolite do not establish the age of the Bisbee ore deposits. However, they do support Gilluly's conclusions that both Cenozoic and Mesozoic granitic rocks occur in the Bisbee area, that the apparent time interval between them is about 100 m.y. (million years), and that the deposits at Bisbee probably are related in time to only one of these.

Bain (1952), using the Pb^{207}/Pb^{206} ratio of uraninite from veins in the Bisbee district, suggested that the age of the Bisbee ore is 85 to 112 m.y. The radiogenic components of lead in the uraninites were small, however, and isotopic analyses of lead in the samples were not internally consistent. Under such conditions an unequivocal age determination is most difficult. Our data neither confirm nor contradict Bain's determinations.

The Schieffelin Granodiorite is the rock unit most closely related in time and space to the ore deposits at Tombstone (Gilluly, 1956, p. 160). The geologic age of the Schieffelin Granodiorite is post-Bronco Volcanics, which rests on the eroded surface of the Bisbee Group (Gilluly, 1956, p. 87). The isotopic age seems compatible with the position of the Schieffelin Granodiorite in the geologic sequence, and, as a working hypothesis, 72 m.y. can be used as the maximum age of the ore deposits at Tombstone.

The Schieffelin Granodiorite is younger than thrust faults in the Tombstone Hills. The age of the Schief-

felin therefore establishes a minimum age of 72 m.y. for the thrusts.

PIMA DISTRICT

K-Ar ages were determined for four igneous rocks from the Pima district: equigranular granodiorite, quartz monzonite porphyry, rhyolite tuff, and andesite dikes. These rocks and their general relations to each other, to the ore deposits, and to the structures in the area have been described by Cooper (1960, p. 72, 74, 76, and 89).

After a major orogeny that formed highly complex northwest-trending fault and fold structures in sedimentary and volcanic rocks of Cretaceous(?) age, the granodiorite and quartz monzonite porphyry were intruded. Although the geologic evidence is not unequivocal, Cooper (1960, p. 74) thought the granodiorite was older, but he gave no impression of a significant time break between the two intrusives. Cooper's views are supported by the K-Ar ages of the two rocks. According to Cooper (1960, p. 63) the quartz monzonite porphyry is spatially associated with ore deposits in the Pima district, and possibly is genetically related to them. This possible genetic relation, however, is indirect because the porphyry itself is the host for the disseminated copper ore. The K-Ar age of very slightly mineralized porphyry, 56 m.y., establishes a maximum age for the ore.

According to Cooper (1960), the Helmet Fanglomerate is younger than the ore deposits, and is cut by a large thrust (San Xavier thrust) which also is younger than the ore deposits. Both the San Xavier thrust and the Helmet Fanglomerate are transected by a narrow zone of andesite dikes. The K-Ar age of the andesite dikes establishes a minimum age for the thrusting and ore deposition.

The K-Ar dates give some information on the apparent ages of structural events in the Pima district. Here, thrusts and folds are older than 60 m.y., the age of the granodiorite, whereas in the Tombstone district, thrusts are older than 72 m.y., the age of the Schiefelin Granodiorite. A Late Cretaceous-early Tertiary period of deformation that includes thrusting long has been postulated for southeastern Arizona, and these apparent dates help to define it. In addition, Cooper (1960) recognized the San Xavier thrust in the Pima district as being a distinctly younger and independent structure. The age of the andesite dikes (24 m.y.) established a significant younger age limit for this thrust. Unfortunately a reliable older age limit was not obtained. The rhyolite tuff, which is older than the Helmet Fanglomerate, was dated with the hope that it, along with the andesite dikes, would

bracket the Helmet Fanglomerate and San Xavier fault within a small time span. The K-Ar age of the rhyolite tuff is virtually the same as that of the quartz monzonite porphyry, thus the time interval between the apparent maximum and minimum ages for the Helmet Fanglomerate and the San Xavier thrust is 32 m.y., a figure much larger than we anticipated. The similarity of the K-Ar ages of the quartz monzonite porphyry and rhyolite tuff, however, raises the problem of a possible genetic relation between the two.

The K-Ar ages of the four rocks in the Pima district suggest the following sequence of events:

1. Deformation intensely folded and faulted the volcanic and sedimentary rocks over 60 m.y. ago.
2. The quartz monzonite porphyry was mineralized no earlier than 56 m.y. ago.
3. The deposition of the Helmet Fanglomerate and the movement along the San Xavier thrust occurred less than 56 to 57 m.y. ago (the K-Ar ages of the quartz monzonite porphyry and the rhyolite tuff), and more than 24 m.y. ago (the K-Ar ages of the andesite dikes).

GLOBE-MIAMI DISTRICT

The Lost Gulch Quartz Monzonite and the Schultze Granite from the Globe-Miami district were dated by the K-Ar method. The Lost Gulch Quartz Monzonite is the host rock for the Castle Dome and Copper Cities disseminated copper deposits. Locally the Schultze Granite is also mineralized.

The Lost Gulch Quartz Monzonite is known to be post-Paleozoic, but there are no Mesozoic rocks in the area by which its age relative to that era can be determined. It is cut by granite porphyry that seems to be genetically related to the Schultze Granite, and on this basis the Schultze Granite was thought by Peterson (1954) to be younger. Peterson (1954) thought the extensive copper mineralization in the Globe-Miami district closely followed the intrusion of the Schultze Granite and granite porphyry and was the culminating event in the long period of igneous activity. The close spatial relation of the Lost Gulch Quartz Monzonite and Schultze Granite supports the close isotopic ages and, indirectly therefore, the general time of the igneous activity in the Globe-Miami district. Until further information on the age of the deposits is available, a tentative maximum age of 58 m.y. for the disseminated copper deposits seems reasonable.

In the Globe-Miami district, a large ash-flow deposit of post-mineralization dacite accumulated on a well-developed erosion surface. Here and there as much as several hundred feet of conglomerate (Whitetail Conglomerate) separates the dacite from the under-

lying rocks. The K-Ar age of the vitrophyre at the base of the dacite is 20 m.y. This age for the "cover rocks" is a minimum for the copper mineralization in the Globe-Miami district. Secondary enrichment in the Miami-Inspiration ore body is related to topography that antedates the Whitetail Conglomerate (Ransome, 1919, p. 173-174), which suggests that the ore is considerably older than the dacite.

MINERAL CREEK, BANNER, AND BUNKER HILL DISTRICTS

The Granite Mountain Porphyry from Ray (Mineral Creek district), the quartz diorite porphyry from Christmas (Banner district), and the granodiorite from Copper Creek (Bunker Hill district) were dated by the K-Ar method. These three districts are separated by about 40 airline miles, Christmas being roughly 15 airline miles southeast of Ray, and Copper Creek roughly 25 airline miles southeast of Christmas (fig. 120.1).

At Ray, the Granite Mountain Porphyry forms part of the disseminated copper deposit. At Christmas, pyrometamorphic copper deposits formed along the intrusive contacts of the quartz diorite porphyry and certain carbonate beds in the Paleozoic section, and at Copper Creek, the granodiorite is the host rock for perhaps 25 to 50 breccia pipes, many of which are mineralized.

The Granite Mountain Porphyry cuts only the Precambrian Pinal Schist, so that its age relative to younger rocks is indeterminate. Both the quartz diorite porphyry at Christmas and the granodiorite at Copper Creek intrude andesitic volcanic rocks. According to Frank Simons (written communication, 1962), the andesites intruded by the granodiorite appear to overlie unconformably a sequence of conglomerate and shale that he has correlated tentatively with the Pinkard Formation of Late Cretaceous age. Holmes (1960) dates the end of the Cretaceous at 70 ± 2 m.y. The isotopic ages of the quartz diorite porphyry at Christmas and the granodiorite at Copper Creek do not conflict with their ages as determined by their relation to other rocks, some of which have been dated by fossils, and until further information is available 62 and 68 m.y. are reasonable assumptions for the maximum age of the ore deposits at Christmas and Copper Creek respectively.

The K-Ar age of 63 m.y. for the Granite Mountain Porphyry is close to that of the quartz diorite porphyry at Christmas, the Schultze Granite, and the Lost Gulch Quartz Monzonite. Ransome's (1919, p. 67) geologic studies indicated a close genetic relation between the quartzose granitic rocks in the Globe-Miami, Ray, and Christmas areas. A close genetic

TABLE 120.2.—*Apparent maximum and minimum age of ore deposits in six mining districts in Arizona, based on K-Ar age of biotites in associated intrusive rocks*

Mining district	Rock	Maximum age (million years)	Minimum age (million years)
Tombstone-----	Schieffelin Granodiorite....	72	-----
Pima-----	Quartz monzonite porphyry.	56	24
Globe-Miami-----	Schultze Granite-----	58	20
Mineral Creek-----	Granite Mountain Porphyry.	63	-----
Bunker Hill-----	Granodiorite at Copper Creek.	68	-----
Banner-----	Quartz diorite porphyry at Christmas.	62	-----
Average-----			63
Mean-----			62-63
Range-----			16

relation implies a close time relation. On this basis, the K-Ar age of the Granite Mountain Porphyry is compatible with Ransome's geologic interpretations.

The apparent maximum and minimum age of ore deposits in the six mining districts based on the K-Ar age of biotites in the associated intrusive igneous rocks ("porphyries") are summarized in table 120.2. The significance that one attributes to the ages in the table depends on the extent to which one accepts a close time and genetic relation between the "porphyries" and the ore. In writing about the deposits at Ray and Miami 43 years ago, Ransome (1919, p. 166) lucidly stated the position of those of us who accept a close tie, but not a direct one:

Had no previous study been made of the copper deposits of the western United States and were observation restricted to one only of the two districts here described, the observer might well inquire whether the association of the ores with granitic or monzonitic porphyry is merely accidental or is an illustration of cause and effect. The present state of our information, however, leaves little room for this doubt. Not only at Ray and Miami but at Clifton, Bisbee, and Ajo in Arizona, at Ely in Nevada, at Santa Rita in New Mexico, and at Bingham in Utah, not to mention occurrences outside of this country, copper ores generally similar to those of Ray and Miami are closely associated with monzonite porphyry or with porphyry intermediate in character between monzonite porphyry and granite porphyry. In some of these districts the evidence for an essential genetic relationship between ore and porphyry is plain; in others it is more or less equivocal to anyone who permits himself to realize that some ores, even ores of copper, may occur in localities where there is nothing to suggest any connection between them and igneous activity. Taken collectively, however, the disseminated copper deposits of the southwestern United States present convincing evidence that the monzonitic porphyries, by which they are invariably accompanied, had something to do with their origin.

It is not to be supposed, however, that the now visible parts of these bodies of porphyry contributed in any active way to

ore deposition. They, like the neighboring schist, have themselves been altered by the ore-bearing solutions, and, where favorably situated, have been changed into protore just as the schist was changed under similar circumstances. Their significance lies in their testimony to the probable presence of much larger masses of similar igneous material below any depths likely to be reached in mining, and it is from these larger and deeper masses, which must have taken far longer to solidify and cool than the bodies now exposed by natural erosion and in the mines, that most of the energy and at least a part of the materials were derived to form the protore.

Following Ransome's beliefs, the data presented here suggest that the range in age of the ore deposits is essentially the range in K-Ar age of the "porphyries," that is, 56 to 72 m.y. On the Holmes (1960) time scale, the Cretaceous period ended 70 ± 2 m.y. ago and the Eocene 40 m.y. ago. Using these terminal dates, the ore deposits are early Tertiary, and the range in time of 16 m.y. seems small to us. We find considerable support in the data for the concept of a Laramide period of mineralization in southeastern Arizona.

REFERENCES

- Bain, G. W., 1952, The age of the "Lower Cretaceous" from Bisbee, Arizona, uraninite: *Econ. Geology*, v. 47, p. 305-315.
- Cooper, J. R., 1960, Some geologic features of the Pima mining district, Pima County, Arizona: *U.S. Geol. Survey Bull.* 1112-C, p. 63-103.
- Gilluly, James, 1956, General geology of central Cochise County, Arizona: *U.S. Geol. Survey Prof. Paper* 281, 169 p.
- Goldich, S. S., and others, 1961, The Precambrian geology and geochronology of Minnesota: *Minnesota Geol. Survey Bull.* 41, 193 p.
- Holmes, Arthur, 1960, A revised geological time-scale: *Edinburgh Geol. Soc. Trans.*, v. 17, pt. 3, p. 183-216.
- Lipson, Joseph, 1958, Potassium-argon dating of sedimentary rocks: *Geol. Soc. America Bull.*, v. 69, no. 2, p. 137-149.
- Peterson, N. P., 1954, Geology of the Globe quadrangle, Arizona: *U.S. Geol. Survey Geol. Quad. Map* GQ-41.
- Ransome, F. L., 1904, Geology and ore deposits of the Bisbee quadrangle, Arizona: *U.S. Geol. Survey Prof. Paper* 21, 168 p.
- 1919, The copper deposits of Ray and Miami, Arizona: *U.S. Geol. Survey Prof. Paper* 115, 192 p.
- Tenney, J. B., 1935, The copper deposits of Arizona, in *Copper resources of the world: Internat. Geol. Cong.*, 16th, Washington 1933, Rept., v. 1, p. 167-235.



121. THALENITE FROM TELLER COUNTY, COLORADO

By J. W. ADAMS, FRED A. HILDEBRAND, and R. G. HAVENS, Denver, Colo.

The yttrium silicate, thalenite, was first described by Carl Benedicks (1898) from the Österby pegmatite, Dalane, Sweden. Since its original discovery, thalenite has been found at one other locality in Sweden (Sjögren, 1906), in several pegmatites in Norway (Vogt, 1922; Schetelig, 1931; Bjørlykke, 1935), and two localities in North America.

The only published report of thalenite in North America was in a listing of mineral occurrences in Arizona by Galbraith and Brennan (1959, p. 90). They mention that the mineral was found at the Guy Hazen claims near Boulder Springs in Mohave County, but the source of their information was not given. Thalenite was tentatively identified by Alan G. King, U.S. Geological Survey, in material from this same group of claims in 1953, but this earlier work was not published. The tentative identification was confirmed in the course of the present study.

The second known occurrence of thalenite in North America is in pegmatite at the Snowflake feldspar mine, approximately 6½ miles northwest of Woodland Park in Teller County, Colo. Specimens of rock containing rare-earth minerals from this pegmatite were submitted to one of the authors by Mr. Roy Monett and Mr. Robert Beal of Woodland Park. These specimens were found to contain small amounts of thalenite.

The Snowflake feldspar mine was visited in September 1961 for the purpose of locating the position of the thalenite in the pegmatite, but the mineral could be found only in dump material. The pegmatite is in granite of the Pikes Peak batholith of Precambrian age.

The thalenite occurs in rare subhedral to anhedral crystals as much as 2 cm across. The mineral is found in a complex assemblage of perthitic microcline and yttrian fluorite, with minor allanite, fergusonite, zircon, xenotime, fluorite, albite-oligoclase, quartz, altered biotite, and molybdenite. Thalenite crystals are commonly partly enclosed in allanite, and both minerals appear to have been extensively replaced by fluorite.

Unaltered thalenite is clear and colorless, has a vitreous luster, and closely resembles quartz. Most of the thalenite from the Snowflake pegmatite, however, has a mottled appearance, being partly white or pale pink and partly pale yellow to orangish yellow. The pale-pink color probably is due to finely dispersed hematite. The yellow parts of the crystals effervesce weakly with cold hydrochloric acid and represent par-

tial alteration of the thalenite to an unidentified carbonate-bearing phase (strongest interplanar spacings are 6.42, 3.21, 3.38, 4.98, 7.31, 4.23, 3.53, 2.11 Å). In thin section the thalenite crystals are clear, transparent, and highly birefringent, and are veined by cloudy, apparently low-birefringent alteration products. Some crystals show marked zoning, accentuated by alteration.

The X-ray powder data for thalenite from the Snowflake pegmatite, Colorado, and from Österby, Sweden, are compared in table 121.1. The Österby thalenite was kindly supplied by Dr. Henrich Neumann, of the Mineralogisk-Geologisk Museum, Oslo, Norway. The powder data for the Colorado and Österby minerals agree reasonably well with the published X-ray diffraction diagram of the thalenite by Neumann and others (1957).

The optical properties and specific gravity of the Colorado thalenite determined from glassy colorless fragments are given below:

Refractive indices (Na):

$$\alpha = 1.719 \pm 0.002$$

$$\beta = 1.739 \pm 0.002$$

$$\gamma = 1.748 \pm 0.002$$

$$2V(-) = 67^{\circ}30''$$

$$\text{Specific gravity (pycnometer)} = 4.396$$

The value for $2V$ was determined with the universal stage by Edward J. Young, U.S. Geological Survey.

Thalenite is characterized by a distinct absorption spectrum. Under the microspectroscope the mineral shows a strong erbium absorption band in the green region of the spectrum, extending approximately from 520 to 526 m μ . This feature can be useful in distinguishing thalenite grains from other similar-appearing minerals.

A quantitative spectrophotographic analysis for the rare earths and semiquantitative analysis for other elements, together with determination of CO₂, H₂O+, and H₂O- are given in table 121.2.

The relative percentages of the lanthanide elements in the Colorado thalenite are plotted in figure 121.1 in the form suggested by Semenov and Barinskii (1958); their analysis of a Swedish thalenite (probably from Österby) is also shown in the figure for comparison. In the graph, separate curves connect the percentage values of elements of even and odd atomic number, so arranged that the pairs of lanthanides that are adjacent in the periodic table fall on the same ordinate line. This type of presentation shows the

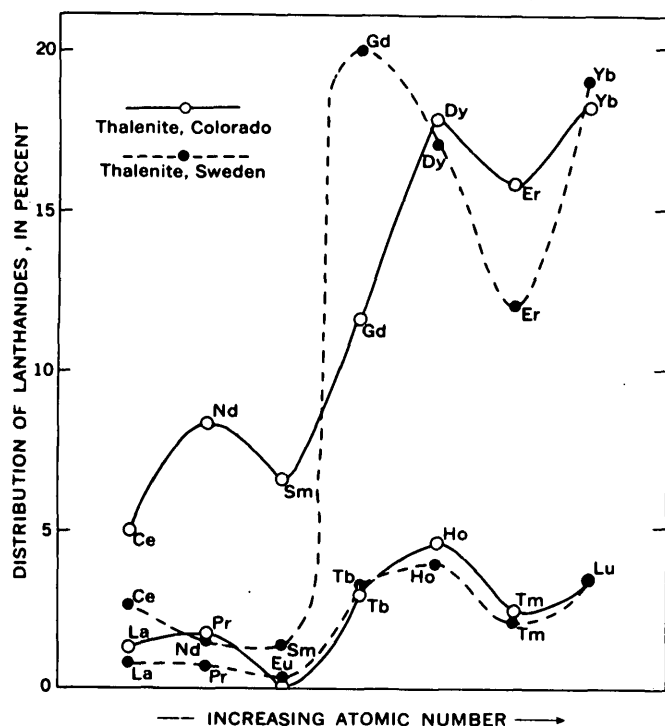


FIGURE 121.1.—Percentage distribution of lanthanide elements in thalenite from Colorado and Sweden. Upper pair of curves: elements of even atomic number. Lower pair: elements of odd atomic number.

general parallelism in distribution between odd-even pair members of the lanthanides as they occur in minerals.

The curves for the elements of odd atomic number in the two thalenite samples are strikingly similar, but marked differences appear between the plots of the elements of even atomic number. The Colorado thalenite is characterized by dysprosium and neodymium maximums in contrast to the gadolinium maximum found in the Swedish sample. Shifts in maximums, notably between the elements gadolinium, dysprosium, and ytterbium, may be noted by comparing the analyses of individual yttrium minerals from several localities (Semenov and Barinskii, 1958, table 1), but modern analyses of thalenite are so few that the extent of variability in this mineral is not known.

The absence or rarity of thalenite in most pegmatite areas appears to be due to the preferential deposition of yttrium as one or more of a large number of other yttrium minerals, notably xenotime, gadolinite, and the multiple oxides, or by its incorporation as a vicarious constituent in such species as fluorite, garnet, or allanite. From a study of the thalenite-bearing pegmatites of southern Norway, Schetelig (1931, p. 519) concluded that in these deposits the formation of thalenite was favored when there was (1) an ex-

TABLE 121.1.—X-ray diffraction powder data for thalenite from the Snowflake pegmatite, Teller County, Colo., and from Österby, Dalane, Sweden

Teller County, Colo.		Österby, Sweden		Teller County, Colo.		Österby, Sweden	
d (Å) ¹	I ²	d (Å) ¹	I ²	d (Å) ¹	I ²	d (Å) ¹	I ²
6.3	5	6.3	1	1.658	2	1.658	
6.07	4	6.07		1.645	2	1.645	
5.57	2	5.57		1.631	5	1.629	
5.50	20	5.50	25	1.616	4	1.613	
5.16	3	5.16		1.603	1	-----	
4.98	1	-----		1.583	.5	-----	
4.67	.5	-----		1.570	5	1.568	
4.44	5	4.44		1.558	2	1.558	
4.17	4	4.17		1.547	2	-----	
3.95	1	3.97		1.523	1	1.523	
3.79	25	3.79	30	1.510	2	1.490	
3.63	5	3.63		1.497	.7	-----	
3.49	4	3.51		1.478	2	1.480	
3.44	11	3.44	13	1.465	2	-----	
3.31	2	3.31		1.455	3	1.455	
3.27	18	3.27	18	1.445	1	-----	
3.16	18	3.16	18	1.429	.7	-----	
3.13	11	3.13	13	1.425	1	-----	
3.10	100	3.10	100	1.415	.7	1.414	
3.05	4	3.06		1.408	1	-----	
2.96	1	2.97		1.404	1	-----	
2.86	6	2.87		1.391	.7	1.391	
2.81	40	2.81	35	1.382	.7	-----	
2.75	30	2.76	18	1.370	2	1.370	
2.61	2	2.62		1.365	1	-----	
2.57	5	2.58	11	1.329	.5	-----	
2.51	4	2.51	7	1.315	2	1.316	
2.46	3	2.47		1.299	.7	-----	
2.42	1	2.44		1.282	1	-----	
2.40	3	2.41		1.254	2	1.255	
2.37	1	2.37		1.236	1	1.238	
2.34	3	2.34		1.218	1	1.221	
2.30	2	2.30		1.197	.7	1.202	
2.24	30	2.24	35	1.179	.7	1.185	
2.21	1	-----		1.169	2	1.170	
2.20	1	-----		1.160	2	1.163	
2.18	9	2.18	15	1.152	.7	1.153	
2.127	6	2.122	15	1.121	2	1.125	
2.103	.7	2.099		1.102	2	1.105	
2.076	.7	-----		1.083	2	1.086	
2.053	3	2.053		1.072	.7	-----	
2.027	2	2.027		1.058	2	1.061	
1.994	3	1.998		1.046	.7	1.051	
1.977	4	1.977		1.0277	1	1.0301	
1.953	2	1.953		1.0123	1	1.0145	
1.922	.7	-----		1.0049	.7	1.0019	
1.895	3	1.895		.9871	1	.9871	
1.873	7	1.873	11	.9685	.7	-----	
1.859	.7	-----		.9609	.7	.9615	
1.845	3	1.845		.9481	2	.9493	
1.817	4	1.821		.9422	.7	-----	
1.797	3	1.797		.9343	1	.9360	
1.781	2	1.781		.9288	1	.9310	
1.768	1	1.762		.9100	2	.9120	
1.746	.7	-----		.9032	2	.9070	
1.740	.7	-----		.8942	1	.8956	
1.728	1	1.725		.8884	.7	.8897	
1.716	4	1.716		.8827	.7	.8840	
1.704	2	1.707		.8743	.5	-----	
1.681	1	-----		.8629	1	.8633	
1.670	5	1.672					

¹ The diffraction patterns were taken with Debye-Scherrer powder cameras of 114.59-mm diameter using the Straumanis technique with Cu K α (Ni filter) radiation, $\lambda=1.5418$ Å. The cutoff point for these cameras is at a 2θ value of approximately 5°. Measurements were made with a Hilger-Watts film-measuring rule with a vernier precision of 0.05 mm. Shrinkage corrections were determined and applied to each film. There was no measurable α resolution of any lines.

² Intensities were measured with calibrated film strips prepared such that successive step exposures are related to each other by a factor of $\sqrt{2}$. Because the line intensities of Swedish thalenite were nearly identical with those of the Colorado thalenite, the intensities of only a few of the strongest lines of the Swedish sample were measured.

TABLE 121.2.—*Spectrographic analyses and CO₂ and H₂O determinations, in percent. Thalenite, Teller County, Colo.*[Analysts: R. G. Havens, U.S. Geological Survey (spectrographic); Blanche Ingram, U.S. Geological Survey (CO₂ and H₂O)]

QUANTITATIVE SPECTROGRAPHIC ANALYSES			
Y.....	32.6	Tb.....	0.72
La.....	.31	Dy.....	4.3
Ce.....	1.2	Ho.....	1.1
Pr.....	.42	Er.....	3.8
Nd.....	2.0	Tm.....	.59
Sm.....	1.6	Yb.....	4.4
Eu.....	<.01	Lu.....	.83
Gd.....	2.8		

SEMIQUANTITATIVE SPECTROGRAPHIC ANALYSES ^{1 2}			
Si.....	Major (>10 percent)	Ba.....	.015
Ca.....	2.0	Mg, Mn.....	.01
Fe.....	.15	B.....	.002
Al.....	.07	Be.....	.0007

H₂O— <0.1 H₂O + 0.95 CO₂ 1.9¹ Elements looked for but not detected: K, Ti, P, Ag, As, Au, Bi, Cd, Co, Cr, Cu, Ga, Ge, Hf, Hg, In, Mo, Nb, Ni, Pb, Pd, Pt, Re, Sb, Sc, Sn, Sr, Ta, Te, Th, Tl, U, V, W, Zn, Zr.² Due to interference by rare-earth lines, usual sensitivities did not apply for some elements.

cess of yttrium over available niobium, tantalum, and titanium for the formation of multiple-oxide minerals, and (2) insufficient beryllium to utilize all the remaining yttrium as gadolinite. These favorable conditions may prevail in the Snowflake and possibly

other pegmatites in the Pikes Peak batholith, but during the formation of most of these pegmatites there was a general availability of phosphorus and particularly fluorine so that yttrium was wholly utilized as xenotime or captured in the fluorite lattice.

REFERENCES

- Benedicks, Carl, 1898, Thalenit, ein neues Mineral aus Österby in Dalekarlien: Geol. Inst. Univ. Upsala Bull., v. 4, pt. 1, p. 1-15.
- Bjørlykke, arald, 1935, The mineral paragenesis and classification of the granite pegmatites of Iveland, Setesdal, southern Norway: Norsk geol. tidsskr., v. 14, p. 211-311.
- Galbraith, F. W., and Brennan, D. J., 1959, Minerals of Arizona, 3d ed.; Univ. Arizona Bull., v. 30, no. 2, 116 p.
- Neumann, Henrich, Sverdrup, Thor, and Saebø, P. Chr., 1957, X-ray powder patterns for mineral identification, III, Silicates: Norske Vidensk.-Acad. Oslo., I Mat-Nat Kl., no. 6, p. 16.
- Schetelig, Jabok, 1931, Remarks on thalenite from some new occurrences in southern Norway: Norsk geol. Tidsskr., v. 12, p. 507-519.
- Semenov, E. I., and Barinskii, 1958, The composition characteristics of the rare earths in minerals: Geochemistry, no. 4, p. 398-419. (A translation of Geokhimiya.)
- Sjögren, Hj., 1906, Thalenit från Åskagens kvartsbrott i Värmland: Geol. fören. förh., v. 28, p. 93-101.
- Vogt, Th., 1922, Über Thalenit von Hundholmen; Vid. selsk. Skr., I. Mat.-nat. Kl. v. 1, p. 19-45.



122. ALTERATION AS A GUIDE TO URANIUM ORE, SHIRLEY BASIN, WYOMING

By E. N. HARSHMAN, Denver, Colo.

Geologic investigations in the Shirley Basin, 35 miles south of Casper, Wyo., show that uranium ore is directly associated with altered sand. This association is a reliable exploration guide in this area and it may prove to be useful in exploring other areas with similar geologic histories.

The Shirley Basin contains one of the Nation's largest uranium-ore reserves. The ore bodies are in arkosic sands of the Wind River Formation of Eocene age. The Wind River sediments were derived from granitic rocks west and southwest of the area, were carried by streams flowing eastward, and were deposited in a basin eroded in rocks of Cretaceous and older age. The basin was elongate in a northwesterly direction and lay between the Laramie Mountains on

the northeast and the Shirley Mountains on the southwest.

The major ore deposits form a well-defined mineral belt along the western flank of a prominent ridge on the old basin surface. The belt strikes northwestward, has a known length of 7 miles, and is as much as 1½ miles wide. The position of the belt immediately west of the ridge has been related to favorable physical and chemical conditions produced in that area as the ridge was gradually buried by sand, silt, and clay of the Wind River Formation (Harshman, 1961).

Uraninite, the principal ore mineral, is believed to have been deposited from ground water circulating through the permeable members of the Wind River Formation. The age of the deposits is not known.

Exploration drilling and mining operations in the mineral belt have shown that the major Shirley Basin ore deposits are intimately related to large elongate bodies of greenish-yellow altered sand that are hereafter referred to as tongues. The altered sand has been recognized at various points along a 5-mile segment of the mineral belt and is believed to be present throughout the length of the belt. Alteration extends several thousand feet southward and eastward from the ore deposits, but due to paucity of data in non-ore-bearing areas the configurations and dimensions of the altered-sand tongues are not well known.

Near ore bodies the altered sand ranges from 10 to 40 feet in thickness and constitutes from 50 to 90 percent of the sandy beds in which it is found. The altered-sand tongues appear to thicken as the distance from their ends or sides increases.

The upper and lower surfaces of the altered-sand tongues are generally conformable with the regional dip of the Wind River Formation. Local sedimentary features such as crossbedding have almost no influence on the position of the altered-sand tongues and only

a minor influence on the character of the sharp contacts between altered and unaltered sand.

Figure 122.1 is a generalized section normal to the end of a tongue of altered sand. It illustrates the intimate relation of ore and calcite cement to altered sand, as well as the character of the contact between altered and unaltered sand. An altered-sand tongue may terminate in a simple cylindroidal surface or, as shown in this figure, the termination may be composed of several irregular lobes.

Ore is localized principally at the ends or sides of altered-sand tongues, although small ore bodies have been found along their top and bottom surfaces. Where the ends of altered-sand tongues are composed of several lobes, ore is concentrated on the convex side of each lobe.

Calcite and hematite also have been concentrated at the ends and sides of the altered-sand tongues. Calcite occurs at the contact of altered and unaltered sand, in ore on the convex side of the contact, and in gray sand beyond the outer limits of ore. Hematite, in bands and lenticular masses, is found in calcite associated

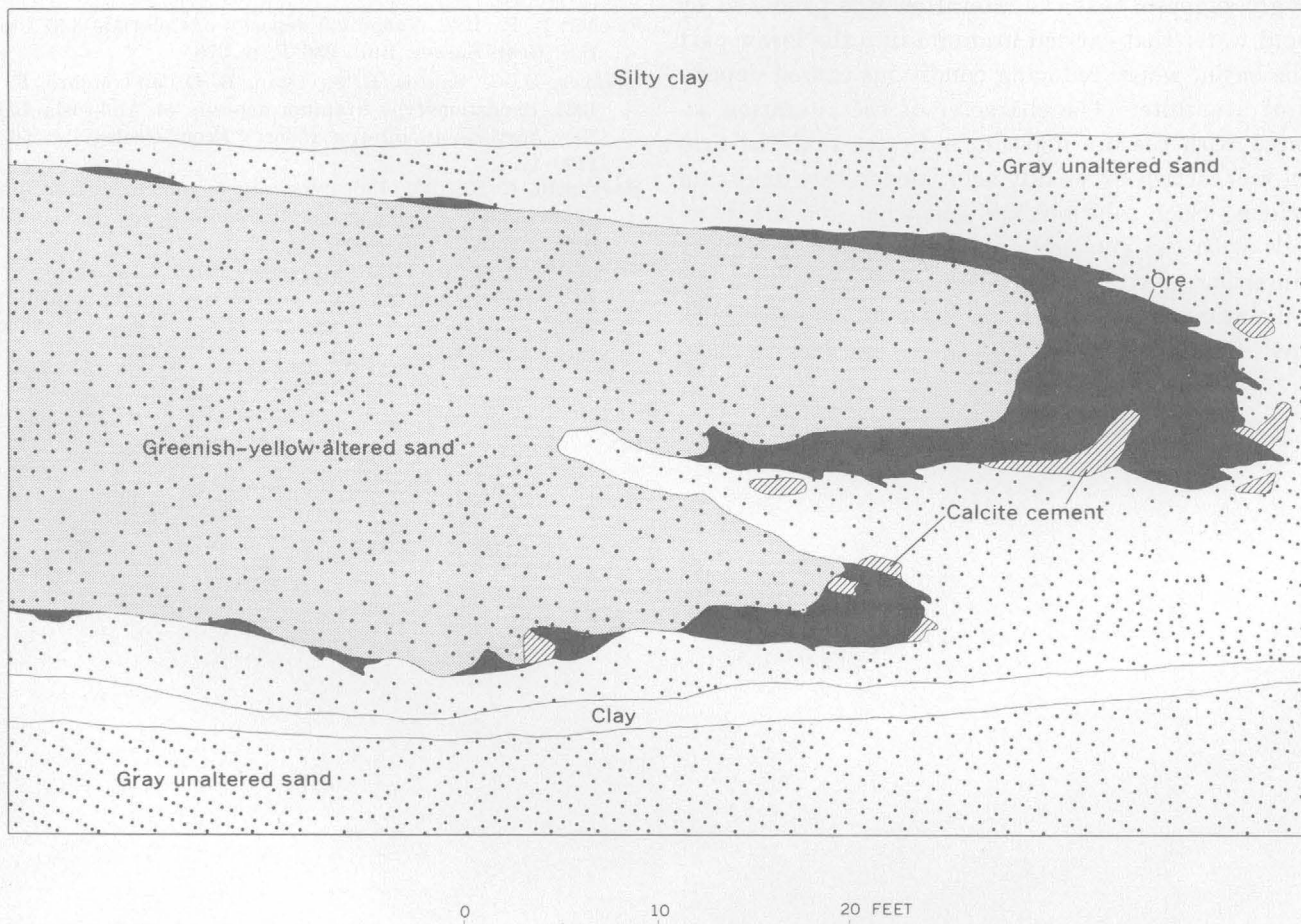


FIGURE 122.1.—Generalized section normal to end of altered-sand tongue showing relation of ore and calcite cement to altered sand.

with ore; it is less common in calcite beyond the outer margins of ore.

Studies to determine the differences between altered and unaltered sand are in progress. The results of these incomplete studies are shown in the table below.

	<u>Altered sand</u>	<u>Unaltered sand</u>
Color.....	Greenish-yellow.....	Gray.
Heavy minerals.	Pyrite, magnetite, and ilmenite, largely removed.	Pyrite, magnetite, and ilmenite present in significant amounts.
Clay minerals.	High-iron montmorillonite.	Low-iron montmorillonite.
Cement.....	Little or no calcite cement.	Considerable calcite cement.
Carbonaceous trash.	Incoherent and sooty.	Coherent, vitreous, coalified.

Other differences may be found as the studies are continued, and some of the differences noted above may prove to be characteristic only in limited areas of the mineral belt.

The intimate association of the Shirley Basin uranium deposits with large tongues of altered sand strongly suggests that the alteration was produced by ground water that carried uranium into the lower part of the basin, where reducing conditions caused deposition of uraninite. The character of the alteration associated with the ore deposits indicates that the uranium was carried by weakly acid, moderately oxidizing solutions. Such solutions are somewhat difficult to reconcile with the geologic environment of the Shirley Basin either now or in the past.

The intimate association of uranium deposits with altered zones of the kind described here may be char-

acteristic of other basins with geologic histories similar to that of the Shirley Basin. The practical application of this association in exploring for uranium deposits is apparent when the large size of an altered zone is contrasted with the relatively small size of an ore body.

Alteration of various kinds is recognized to be more or less closely related with ore deposits on the Colorado Plateau (Bowers and Shawe, 1961; Fischer, 1942; Granger and others, 1961; and others). Sharp and others (1955) describe ore deposits related to a contact between red and drab sandstone in the Powder River Basin, Wyo. These descriptions of alteration associated with deposits of different ages and of wide geographic distribution suggest that alteration of the host rocks may be a feature common to most primary uranium deposits in sandstone.

REFERENCES

- Bowers, H. E., and Shawe, D. R., 1961, Heavy minerals as guides to uranium-vanadium ore deposits in the Slick Rock district, Colorado: U.S. Geol. Survey Bull. 1107-B, p. 175-178.
- Fischer, R. P., 1942, Vanadium deposits of Colorado and Utah: U.S. Geol. Survey Bull. 936-P, p. 376.
- Granger, H. C., Santos, E. S., Dean, B. G., and Moore, F. B., 1961, Sandstone-type uranium deposits at Ambrosia Lake, New Mexico—an interim report: Econ. Geology, v. 56, p. 1193-1194.
- Harshman, E. N., 1961, Paleotopographic control of a uranium mineral belt, Shirley Basin, Wyoming: Art. 148 in U.S. Geol. Survey Prof. Paper 424-C, p. C4-C6.
- Sharp, W. N., McKeown, F. A., McKay, E. J., and White, A. M., 1955, Geology and uranium deposits of the Pumpkin Buttes area, Powder River Basin, Wyoming: U.S. Geol. Survey Prof. Paper 300, p. 373.



STRATIGRAPHY

The alunite-bearing claystone is in the upper part of a 100- to 330-foot-thick sequence of conglomerate, sandstone, limestone, and claystone on the south flank of Aspen Mountain. The basal unit is a conglomerate between 25 and 250 feet thick, composed chiefly of locally derived angular fragments of Cretaceous sandstone deposited unconformably across folded Cretaceous rocks of the Rock Springs uplift. This conglomerate has been illustrated, described, and called the Bishop Conglomerate by Rich (1910), Sears (1926, pl. 3; p. 21-22), and Bradley (1936, p. 173). However, the lack of similarity of this unit with the red quartzite cobble conglomerate typical of the Bishop in areas to the south suggests that they are not correlative; the conglomerate on Aspen Mountain is therefore called Bishop(?) in this article (see fig. 123.1).

Intertonguing with and overlying the basal conglomerate is a variable sequence of limestone, white alunite-bearing claystone, soft porous sandstone, and conglomerate. The upper part is exposed in the alunite trench and the rest was drilled nearby. In the southwest part of the Aspen Mountain area, lenses of light-gray dense limestone as much as 75 feet thick overlying the basal conglomerate are exposed in an area half a mile across (fig. 123.1; also Sears, 1926, p. 20-21). Some contain "bulbs" and laminated structures resembling algal reefs. This variable sequence, which has been warped into a gentle west-trending syncline, extends westward from the area shown in figure 123.1 for 2 miles to Antelope Butte, where a 250-foot section is exposed. It is chiefly very tuffaceous soft porous sandstone with some gray crystal vitric tuff composed of sodic plagioclase, biotite, amphibole, sanidine, sphene, curved colorless shards, obsidian, and pumice. The pyroclastic rocks at Antelope Butte may be in some way related to the alunite deposit.

Two sequences of highly altered strata are present along the crest of Aspen Mountain near the "zone of silicification" shown on figure 123.1. Both were mapped as Bishop Conglomerate by Schultz (1920, pl. 1) and Love and others (1955) but were called Blair Formation (Upper Cretaceous) by Sears (1926, pl. 2). Marine Cretaceous fossils were found in the lower of the two units, in a brown and gray silicified sandstone that contains secondary chert, at a locality a mile north-northeast of the alunite trench. The Cretaceous unit is overlain by several hundred feet of unfossiliferous chalky white tuffaceous siliceous sandstone, quartzite, and secondary chert that are believed to be of Tertiary age. The Tertiary sandstone contains abundant brightly twinned fresh-appearing plagi-

clase similar to that in the unaltered sandstone on Antelope Butte, but not recognized in sandstone of the type Blair Formation 10 miles north of Aspen Mountain. No basal conglomerate was observed in the Tertiary sequence, and the contact relationships are poorly exposed. The quartzite in both units resembles angular fragments of quartzite in the Bishop(?) Conglomerate in the alunite trench. The Tertiary unit and Bishop(?) Conglomerate are not differentiated on figure 123.1.

Limestone, claystone, sandstone, quartzite, and alunite were sampled for pollen and diatoms, but all proved barren. The age of the strata is therefore unknown, but at least the conglomeratic portion is younger than the post-middle Eocene arching of the Rock Springs uplift. The sequences may possibly be of Oligocene age (Love, 1960, p. 209), Miocene, or as young as Pliocene.

ALUNITE DEPOSIT

The alunite deposit is exposed in a bulldozer trench 40 feet long, 10 feet wide, and 30 feet deep in sec. 26, T. 17 N., R. 104 W., on the south flank of Aspen



FIGURE 123.2.—Alunite claystone in bulldozer pit, sec. 26, T. 17 N., R. 104 W., showing position of samples described in text and on figure 123.3.

Mountain. The alunite-bearing claystone appears to be stratified, as are the overlying beds, which dip about 2° S. The following section was measured with steel tape on the east face of the trench (fig. 123.2) :

Top of section.

Conglomerate, gray, with pink mottling, composed of unoriented angular fragments, several inches long, of light- and dark-gray and pink dense quartzite in a matrix of light-gray soft poorly cemented fine-grained sandstone that contains essentially no magnetic grains; sample 20-I was taken 3 feet above base -----

Sandstone, light-gray, fine-grained, soft, porous, poorly sorted; some large gray and purplish angular grains of quartzite(?); persistent bed with 2° S. dip; sample 20-H is representative -----

Conglomerate, gray, composed of angular unoriented quartzite fragments in a greenish sandy and clayey matrix; lenses of coarse- and fine-grained fragments -----

Sandstone, sandy siltstone, and claystone, light-gray to pale-green, soft, with angular to subrounded tabular quartzite fragments as much as 1 inch long; beds are lenticular; sandstone is porous, fine grained, and has few magnetic grains; more clayey and less sandy in lower part; base is breccia of gray angular quartzite fragments in a matrix of pink, white, and gray plastic claystone; sample 20-G is from upper 1 foot; sample 20-F is from 2 feet above base -----

Alunite-bearing claystone, snowy-white, with pink, lavender, and yellow secondary mottling; hard, blocky, plastic when wet; finely sandy in upper part and almost pure claystone in lower part; near base are small open vugs associated with inclusions of pale-greenish translucent soapy-feeling claystone; sample 20-E is of top 2 inches; 20-D is 2 feet below 20-E; 20-C is 2 feet below 20-D; 20-B is 1.5 feet below 20-C; 20-A is 2.5 feet below 20-B -----

Total thickness measured -----

The underlying 4 feet of strata is chiefly alunite but has not been analyzed.

The trench was located at the site of a core hole which completely penetrated the Tertiary section. No cuttings or electric logs are available, but it was reported that the base of the Bishop(?) Conglomerate is 301 feet below the alunite claystone and that within this interval are several additional white claystone beds of uncertain thickness (E. R. Keller, oral communication, 1962).

Nine samples, 20-A through 20-I, whose stratigraphic positions are indicated in the measured section, were analysed for grain-size distribution and mineral content with results as shown in figure 123.3. The mineral content was determined by X-ray diffractometer analysis.

Figure 123.3 shows that the lower part of the section is composed predominantly of fine-grained material grading upward to slightly coarser at the top of the alunite claystone (sample E). In samples E and F there are small angular chips of feldspar and quartz

in the matrix; an abrupt change to very coarse quartzitic material occurs in F. The percentage of sand-size quartz and feldspar particles continues to increase upward in the section.

The mineralogy of the section, shown in figure 123.3, is related directly to the grain-size distribution. Sample A, at the bottom of the section, contains approximately 90 percent fine-grained alunite with an intimate mixture of kaolinitic minerals and a trace of quartz. A chemical analysis by Wayne Mountjoy, of the U.S. Geological Survey, of the clay-size fraction from sample A indicates approximately 9 percent K₂O and 0.7 percent Na₂O. The theoretical K₂O content of pure alunite is 11.37 percent. As is indicated below, the K₂O content of two total samples is somewhat less than that in the clay-size fraction.

Analysis of total samples A and B is as follows (analyst: Harry Rose; Li₂O and Na₂O by Joseph Dinnin, using flame photometer) :

	Sample A	Sample B
SiO ₂ -----	8.0	16.0
Al ₂ O ₃ -----	32.0	29.5
Fe ₂ O ₃ -----	1.5	.4
MgO-----	.5	1.0
CaO-----	.1	.1
K ₂ O-----	6.8	5.8
TiO ₂ -----	.1	.1
SO ₃ -----	37.0	33.0
Li ₂ O-----	.01	.01
Na ₂ O-----	.58	.49
	<hr/> 86.59	<hr/> 86.4

There is probably at least 10 percent water. The alkali deficiency of 3 to 4 percent necessary to balance the Al₂O₃ as alunite may be accounted for by the presence of ammonia.

Figure 123.3 shows that above the richest alunite claystone (sample A), the abundance of kaolinitic minerals increases progressively as the alunite decreases, and more quartz appears in the sand fraction. Some montmorillonite-mica mixed-layer material and sparse feldspar appear in the upper part of the sequence.

The paucity of pyrite precludes oxidation of this mineral as the source of sulfur in the alunite. The alteration to alunite may have been accomplished by sulfate-bearing solutions of hydrothermal origin, but a source for such mineralizing waters has not been determined. On the other hand, this deposit may have originated in a manner somewhat different from that of most alunite deposits, because (a) the alunite-bearing claystone appears to be stratified, (b) it is half a mile from the area of intensely silicified rocks, (c) no igneous rocks are exposed within 20 miles, (d) a test

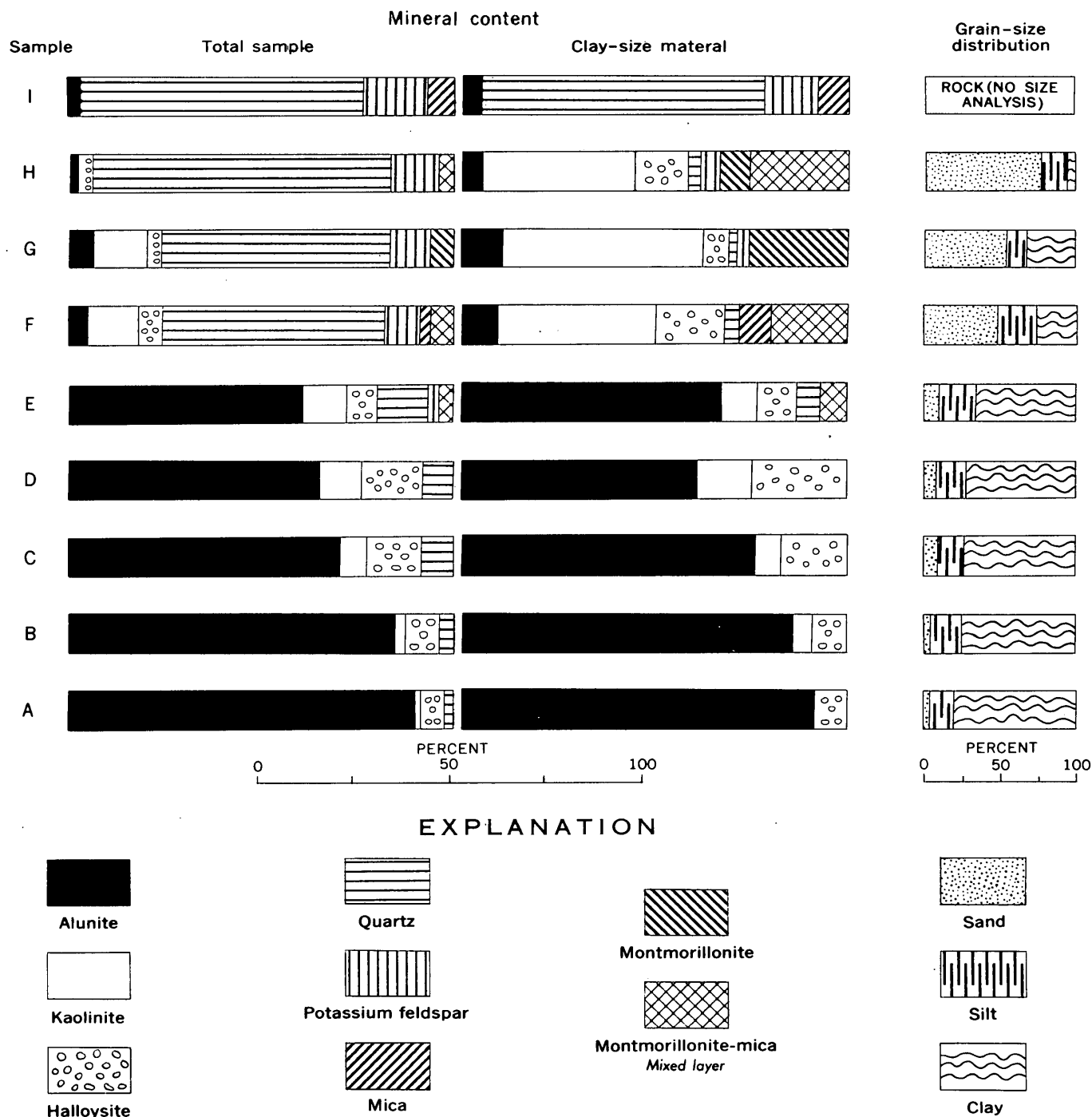


FIGURE 123.3.—Grain-size distribution and mineral content of total samples and mineral content of clay-size material in samples from section exposed in bulldozer trench, south flank of Aspen Mountain.

drilled for gas to a depth of 3,704 feet in the NE corner sec. 34, T. 17 N., R. 104 W. (fig. 123.1) penetrated no igneous rocks, although Cretaceous sandstone and shale were reported to be hard and silicified throughout the drilled section (E. R. Keller, oral communication, 1962), (e) a core hole drilled about 200 feet northwest of this well and a mile southwest of the

alunite trench penetrated 6 feet of white claystone at a depth of 145 feet, suggesting that the alunite may occur in beds of moderate extent, rather than in the more common hydrothermally precipitated "pods."

The age of the igneous activity in the Leucite Hills, 20 to 30 miles north of Aspen Mountain, is 1.25 million years or less, hence latest Pliocene (Bradley,

1961). If the alunite is related to this episode of igneous activity and was deposited as a bed more or less contemporaneously with strata here referred to the Bishop(?) Conglomerate, then this formation could be much younger than has been hitherto suspected.

The purity of the alunite deposit and the unusual features of its occurrence indicate the desirability of additional surface, subsurface, and laboratory studies directed toward determining its age, origin, and economic potential.

REFERENCES

Bradley, W. H., 1936, Geomorphology of the north flank of the Uinta Mountains: U.S. Geol. Survey Prof. Paper 185-I, p. 163-204.

- 1961, Geologic map of a part of southwestern Wyoming and adjacent states: U.S. Geol. Survey Misc. Geol. Inv. Map I-332.
- Love, J. D., 1960, Cenozoic sedimentation and crustal movement in Wyoming: *Am. Jour. Science*, v. 258-A, p. 204-214.
- Love, J. D., Weitz, J. L., and Hose, R. K., 1955, Geologic map of Wyoming: U.S. Geol. Survey.
- Rich, J. L., 1910, The physiography of the Bishop Conglomerate, southwestern Wyoming: *Jour. Geol.*, v. 18, p. 601-632.
- Schultz, A. R., 1920, Oil possibilities in and around Baxter Basin, in the Rock Springs uplift, Sweetwater County, Wyoming: U.S. Geol. Survey Bull. 702, 107 p.
- Sears, J. D., 1926, Geology of the Baxter Basin gas field, Sweetwater County, Wyoming: U.S. Geol. Survey Bull. 781, p. 13-27.



124. CLAYS IN THE MORRISON FORMATION AND THEIR SPATIAL RELATION TO THE URANIUM DEPOSITS AT AMBROSIA LAKE, NEW MEXICO

By HARRY C. GRANGER, Denver, Colo.

This investigation is a byproduct of studies being conducted on the uranium deposits at Ambrosia Lake, N. Mex. A prevailing hypothesis regarding the localization of layer and roll-type uranium deposits in sandstones proposes that the ore was deposited at an interface between two natural solutions of different characteristics (Shawe, Archbold, and Simmons, 1959). If this is so, differences in the type or degree of alteration on opposite sides of an ore layer might be reflected in the clay-mineral assemblage. While the writer was studying Ambrosia Lake ores, E. N. Harshman (Art. 122) found that both color and clay-composition differences exist on opposite sides of uranium-ore layers in Shirley Basin, Wyo., strengthening the conviction that a similar difference might be found at Ambrosia Lake.

All the samples were collected from the Morrison Formation, which contains many large uranium deposits in northwestern New Mexico. In this region the Morrison Formation consists of three members; from the bottom to top these are the Recapture Member, the Westwater Canyon Member, and the Brushy Basin Member. The Recapture is primarily a red to gray sandy mudstone containing many sandstone lenses. The Westwater Canyon is an arkosic to feldspathic sandstone that is red and hematitic throughout

much of the region except in areas near known uranium deposits, where it is commonly light gray and pyritic. The Brushy Basin is a gray to greenish-gray mudstone with scattered sandstone lenses.

In some places sandstones compositionally similar to the Westwater Canyon lie in channels cut in the upper part of the Brushy Basin. One of these, the Jackpile sandstone of local usage, at Laguna, contains two of the largest uranium deposits in the United States.

The Dakota Sandstone unconformably overlies the Morrison Formation, and although not formally divided, the lower part in this area commonly contains a preponderance of carbonaceous shales and impure coals. The upper part is massive coarse-grained cross-bedded sandstone.

The region under consideration is on the southern margin of the San Juan Basin (fig. 124.1) and, with local variations, the regional dip is northward. The southern margin of deposition of the Morrison corresponds rather closely to the margin of the San Juan Basin, and all the members of the Morrison thin and wedge out a few miles south of Ambrosia Lake. West of Ambrosia Lake near Gallup, however, and, by inference, southwest of Ambrosia Lake where these rocks have been removed by relatively recent erosion, the Morrison was gently truncated on the northern flank

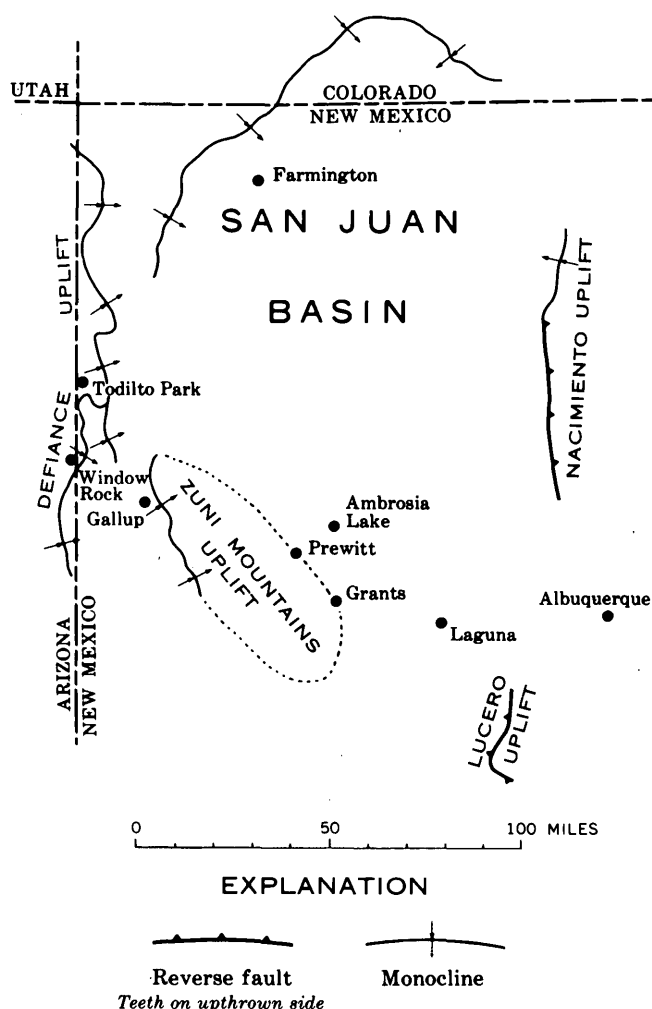


FIGURE 124.1.—Map showing generalized structural setting of Ambrosia Lake. (Adapted from Kelley and Clinton, 1958.)

of the ancestral Zuni Mountains by pre-Dakota erosion. The Dakota was, therefore, deposited on successively lower members of the Morrison westward and southwestward from Ambrosia Lake (fig. 124.2).

The primary uranium deposits in the Morrison Formation at Ambrosia Lake are largely in sandstones of the Westwater Canyon Member and were deposited in the undeformed rocks before faulting. They are layered ore bodies characterized by an accumulation of carbonaceous matter that coats sand grains and fills interstices (Granger, Santos, and others, 1961). The uranium occurs largely in the form of coffinite intimately associated with the carbonaceous material. The carbonaceous material is inferred to be a precipitate of humic acids derived from decaying plant matter either during Morrison or Dakota time.

Other, later, unoxidized uranium deposits are closely associated with the primary deposits at Ambrosia

Lake. These were created either by renewed introduction of uranium or by redistribution of the primary uranium without accompanying concentration of carbon and without apparent change in the clay content of the host rocks. They are later than and are partly controlled by faults, and are not further considered in this study.

Samples were collected by the writer and E. S. Santos. They were prepared for X-ray analysis by R. S. Roberts. Analysis of the data was the responsibility of the writer, who was greatly helped by consultations with J. C. Hathaway, P. D. Blackmon, and J. J. Hemley.

Widespread samples were taken to test the clay content of sandstones of the Morrison on a regional scale, and suites of closely spaced samples were taken to test the clay-mineral variation across primary ore layers. The sample suites across primary ore layers were selected so as to span the ore layer and extend far enough into the host rock on either side so that no further significant change in composition would be likely.

The samples (see table) were prepared and the clays were identified by X-ray diffraction methods according to the standard procedure followed in the laboratories of the U.S. Geological Survey. Thin sections of some of the samples were studied under a petrographic microscope.

MONTMORILLONITE

Montmorillonite is ordinarily the dominant clay mineral in the sandstones of the Westwater Canyon Member, where several tens of feet of mudstone of the Brushy Basin separates the Westwater Canyon from the Dakota Sandstone. Several samples were taken of sandstone of the Westwater Canyon Member well away from uranium deposits and where the Westwater Canyon was covered by mudstones of the Brushy Basin at the time of Dakota deposition. The sandstone was red and hematitic in most of these samples, although a sample from the upper part of the Westwater Canyon along the eastern margin of Todilto Park, approximately 75 miles northwest of Ambrosia Lake, consisted of buff, bleached-appearing sandstone. The clay fraction in each of these samples consisted largely of montmorillonite with various proportions of kaolinite. In some samples chlorite and hydrous mica (illite) were present, but in comparatively negligible amounts.

Microscopic studies of thin sections of sandstones from the Westwater Canyon suggest that the montmorillonite appears early in the genesis of the rocks, predominantly as a thin skin on sand grains. It is

Sample descriptions

Sample No.		Member	Description	Locality
Field	Laboratory			
23 G 61		Westwater Canyon	Sandstone ¹	Highway 68 southeast of Window Rock, Ariz.
24 G 61		do	do	East edge Todilto Park, N. Mex.
25 G 61		do	do ¹	Hogback 2 miles southeast of Gallup, N. Mex.
33 G 61a		do	Mudstone	First level, Mary #1 mine, Ambrosia Lake
56 G 61		do	Sandstone ¹	8 miles northeast of Gallup, N. Mex.
59 G 61		Brushy Basin	Mudstone	M-5 mine, 9 miles north of Prewitt, N. Mex.
60 G 61		do	do	Do.
74 G 61		do	Jackpile-type sandstone	Francis mine, 7 miles north of Prewitt, N. Mex.
75 G 61		Westwater Canyon	Sandstone	North of Prewitt, N. Mex.
76 G 61		do	do	12 miles north of Grants, N. Mex.
77 G 61b		do	Mudstone	Sec. 17 mine, Ambrosia Lake.
80 G 61b		do	do	Second level, Mary #1 mine, Ambrosia Lake.
91 G 61d		do	do	Poison Canyon mine, Ambrosia Lake.
100 G 61d		do	Mudstone gall	Sec. 30 mine, Ambrosia Lake.
19 G 59a-	271952-	do	Sample suite through ore layer in sandstone.	Sec. 15 mine, Ambrosia Lake.
19 G 59i	271960			
22 G 59a-	271961-	do	do	Sec. 25 mine, Ambrosia Lake.
22 G 59h	271968			
129 G 61a-	294479-	do	do	Do.
129 G 61k	294489			

¹ Westwater Canyon Member is directly overlain by Dakota Sandstone. The basal Dakota is not appreciably carbonaceous above samples 23 G 61, and 25 G 61, but is coal bearing above 56 G 61.

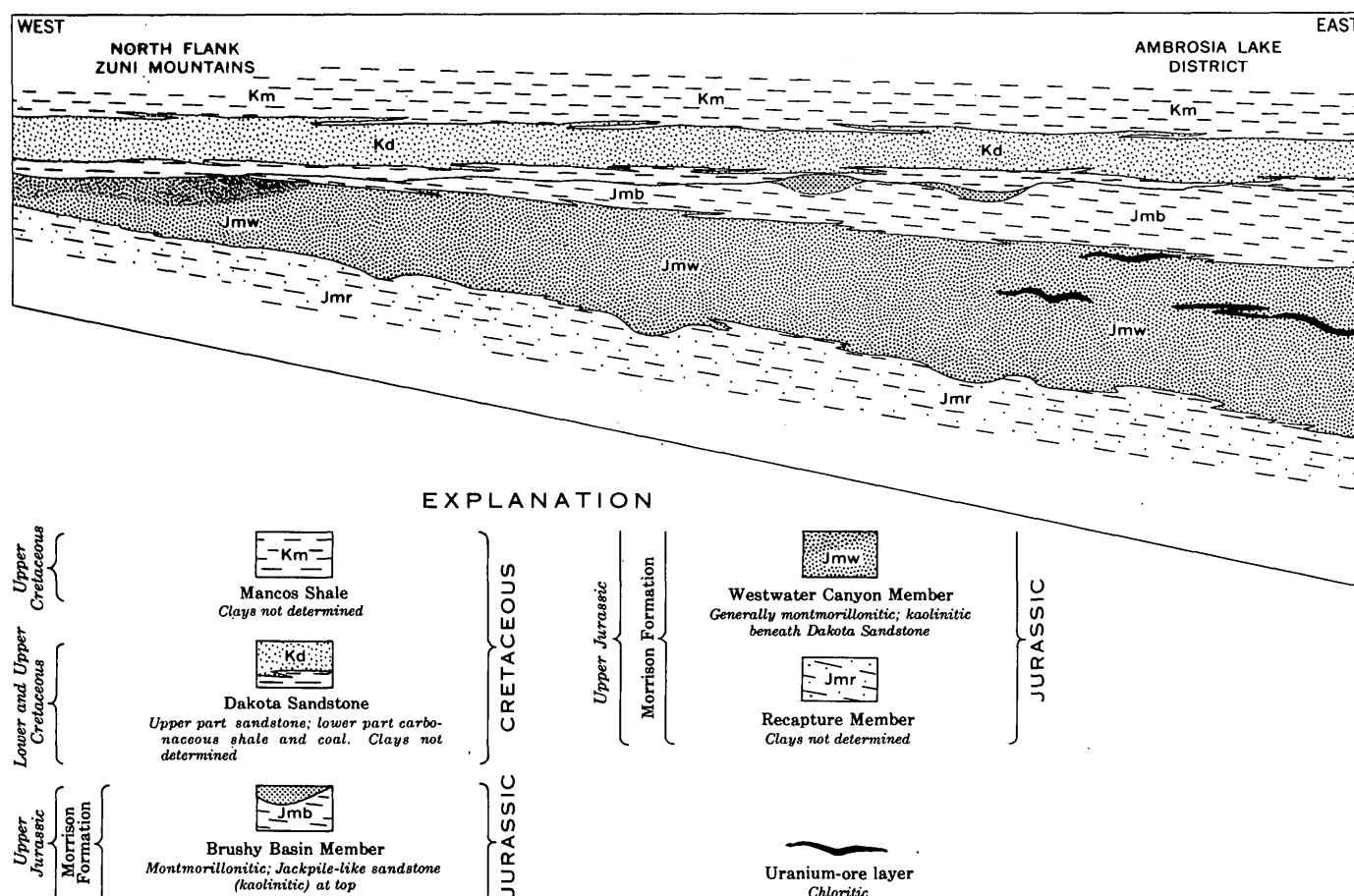


FIGURE 124.2.—Idealized reconstructed section extending westward from the Ambrosia Lake district.

inseparable from the extremely fine hematite stain that affects much of the rock.

The clay fraction from mudstone lenses and mudstone galls included in the Westwater Canyon is almost entirely montmorillonite; the clay that makes up the overlying thick mudstones in the Brushy Basin Member seems to have a similar composition. Presumably the montmorillonite in each of these mudstones and the montmorillonite in the sandstones are genetically related.

KAOLINITE

Kaolinite is present in most samples of sandstone from the Morrison Formation, but not in the mudstones. It seems to occur in two different forms of vastly different ages.

Almost pure kaolinite in a zone as much as 50 feet thick constitutes the clay fraction of sandstones of the Morrison in many places where they are directly overlain by the Dakota Sandstone, particularly where the basal Dakota contains abundant organic matter. The sandstone is almost pure white and consists largely of quartz and alkali feldspar grains in a nearly pure kaolinite matrix, although some mixed-layer mica-montmorillonite is present locally. Opaque iron minerals, mafic minerals, and plagioclase feldspars are missing.

J. S. Schlee and R. H. Moench (1961), L. B. Leopold (1943), and others have noted this kaolinitic zone in several places along the southern and southwestern margin of the San Juan Basin. They have observed that kaolinite-rich rocks directly underlie the erosion surface on which the Dakota rests, and have suggested that the kaolinite is a result of weathering and soil-forming processes in a humid climate before Dakota deposition. Their data do not permit a comparison between abundance of organic matter in the basal Dakota and occurrence of the kaolinite-rich zone.

Sandstones of the Westwater Canyon Member are red rather than being bleached nearly white, along Highway 68 southeast of Window Rock, Ariz., where the Dakota directly overlies the Westwater Canyon. A sample collected here contained montmorillonite and a greater proportion of kaolinite than is ordinarily present in the red sandstones of the Westwater Canyon. The basal Dakota at this locality, however, seems to be free of organic matter that may have caused bleaching and development of the abundant kaolinite found in the white sandstone.

Kaolinite is present in most samples of Morrison Sandstone even where several tens of feet of mudstones of the Brushy Basin separates the sandstone from the Dakota Formation. This kaolinite, however, forms scattered "nests" (J. A. Knox and J. W. Gruner,

1957) or aggregates as much as $\frac{1}{2}$ inch across that completely fill the interstices among the sand grains and cause the rock to be splotched with white spots. The larger nests occur in coarser grained sandstones. There seems to be no evidence that these kaolinite nests were derived locally by alteration of aluminous silicate minerals, nor is there yet any adequate evidence to link this kaolinite with the kaolinite produced in the sandstones directly below the Dakota. The available data suggest that this kaolinite is later than the faults that were formed long after deposition of the sedimentary sequence.

CHLORITE

Analyses of the clay-size fractions from suites of samples taken across primary ore layers disclosed that there is a rough correlation among the uranium, organic carbon, magnesium, and chlorite concentrations (fig. 124.3). There is evidence that as the uranium content rises the chlorite content also rises and the montmorillonite content diminishes. For purposes of comparison, therefore, the samples were heated to 400°C for $\frac{1}{2}$ hour and a ratio was derived from the heights of the resulting X-ray diffractometer patterns of the clays. The X-ray diffractometer peak height for chlorite ($2\theta \approx 6.2^\circ$) was related to the sum of the same chlorite peak height ($\approx 6.2^\circ$) plus the collapsed montmorillonite peak height at $2\theta \approx 8.6^\circ$. This ratio was then expressed as a percentage and plotted as shown on figure 124.3. The graphs strongly suggest that montmorillonite may have been converted to chlorite within the primary ore layers.

Chlorite also occurs sparingly in some of the samples of sandstone collected away from ore, but its content is generally insignificant.

CONCLUSIONS

Evidence obtained from X-ray analyses, field observations, and examination of thin sections suggests that montmorillonite is the earliest clay mineral in the Morrison Formation. Where sandstones in the Morrison are overlain by a pre-Dakota erosion surface, the montmorillonite and certain other minerals are commonly displaced or replaced by kaolinite. Within primary ore layers, chlorite has developed, evidently at the expense of the montmorillonite. The paragenetic relationship between chlorite and the kaolinite noted above is not known.

The kaolinite that forms white nests in the Morrison sandstones in so many places seems to be much later than any of the above minerals. It occupies interstices in the ore layers and elsewhere. Wherever it is seen, it overlies the montmorillonite and chlorite that form

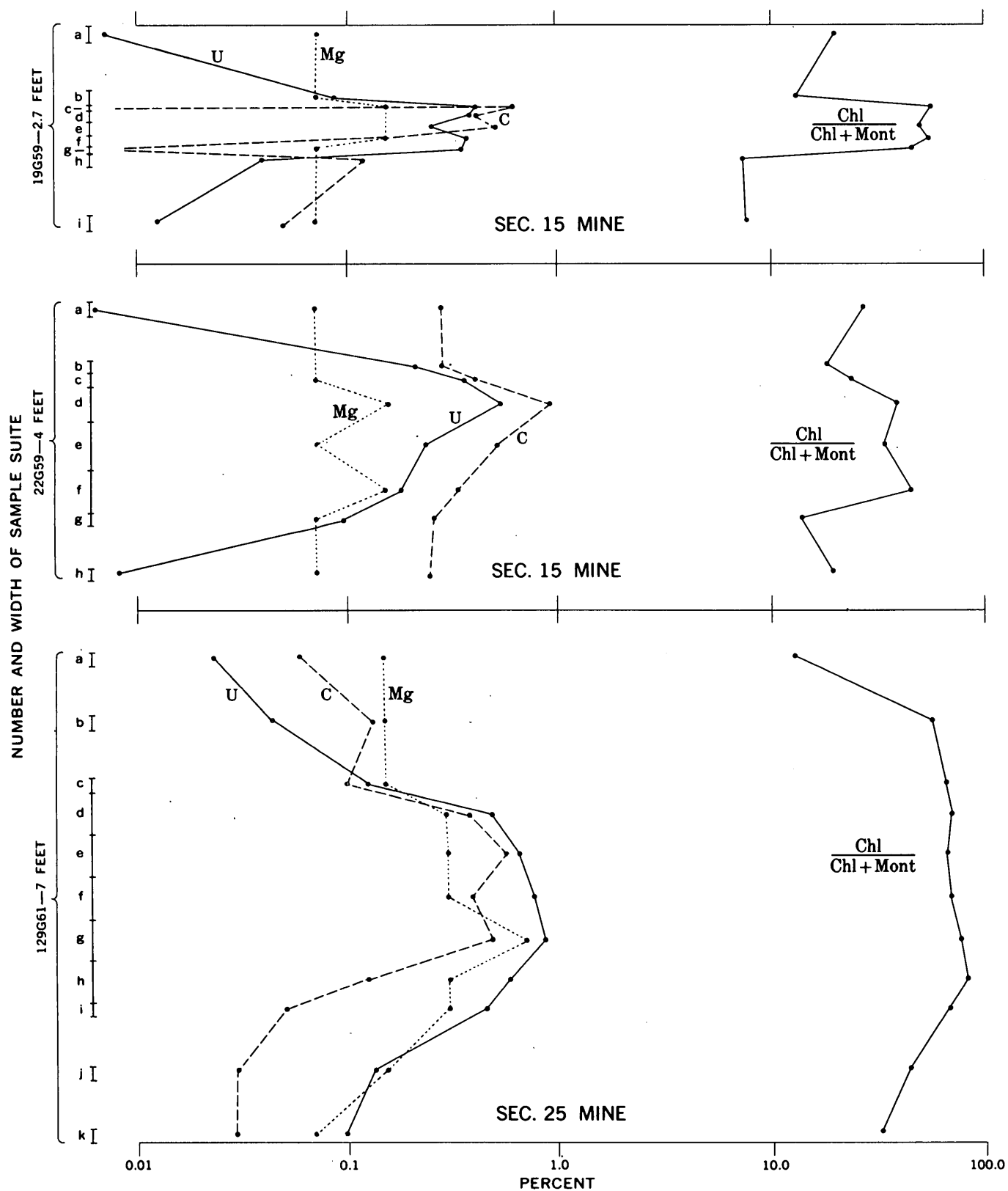


FIGURE 124.3—Correlation between concentrations of chlorite, magnesium (Mg), uranium (U), and carbon (C) across ore layers. Chl, chlorite; Mont, montmorillonite

thin coatings on the sand grains. It is not known if the kaolinite nests are related to the kaolinite that underlies the pre-Dakota erosion surface, but certainly the nests seem to be much later.

Montmorillonite is believed to be the normal clay component in all parts of the Morrison Formation along the southern margin of the San Juan Basin in New Mexico. It seems very likely that the montmorillonite, both in the sandstones and the mudstones of the Morrison, was derived from alteration of volcanic ash that was incorporated in the sediments (Waters and Granger, 1953). In some places, before Dakota deposition, sandstones in the Morrison were exposed at an erosion surface on which the Dakota was later deposited. It may be that this surface represents a moist soil-building cycle, and that kaolinite was formed near the erosion surface by weathering of feldspars. Possibly, the formation of kaolinite beneath this surface is related to soil building as a result of humic-acid solutions draining from the boggy, organic-rich terrain on which the basal coals and carbonaceous shale beds of the Dakota were deposited. Whatever the cause, the fact that this intensive alteration and leaching might, in some way, be related to the genesis of the uranium deposits should not be overlooked.

Within the primary uranium-ore layers, which also contain concentrations of organic carbon, magnesium, and various metallic elements, the normal montmorillonite seems to give way to chlorite. Very likely the anomalous magnesium is contained in the chlorite.

It is not known whether the chlorite was formed during the period of uranium mineralization or

whether it represents a slow progressive alteration of the montmorillonite under chemical conditions imposed, in part, by the organic material during the ages subsequent to mineralization.

REFERENCES

- Granger, H. C., Santos, E. S., and others, 1961, Sandstone-type uranium deposits at Ambrosia Lake, New Mexico—an interim report: *Econ. Geology*, v. 56, p. 1179-1210.
- Kelley, V. C., and Clinton, N. J., 1958, Fracture systems and tectonic elements of the Colorado Plateau: U.S. Atomic Energy Comm. RME-108, issued by the U.S. Atomic Energy Comm., Office of Tech. Inf. Extension, Oak Ridge, Tenn.
- Knox, J. A., and Gruner, J. W., 1957, Mineralogy of the Ambrosia Lake uranium deposits in McKinley County, New Mexico, in Annual report for Apr. 1, 1956 to Mar. 31, 1957: U.S. Atomic Energy Comm. RME-3148, issued by the U.S. Atomic Energy Comm., Office of Tech. Inf. Extension, Oak Ridge, Tenn.
- Leopold, L. B., 1943, Climatic character of the interval between the Jurassic and Cretaceous in New Mexico and Arizona: *Jour. Geology*, v. 51, no. 1, p. 56-62.
- Schlee, J. S., and Moench, R. H., 1961, Properties and genesis of "Jackpile" sandstone, Laguna, New Mexico, in Peterson, J. A., and Osmond, J. C., eds., *Geometry of sandstone bodies, a symposium*: Am. Assoc. Petroleum Geologists, 240 p.
- Shawe, D. R., Archbold, N. L., and Simmons, G. C., 1959, Geology and uranium-vanadium deposits of the Slick Rock district, San Miguel and Dolores Counties, Colorado: *Econ. Geology*, v. 54, p. 395-415.
- Waters, A. C., and Granger, H. C., 1953, Volcanic debris in uraniferous sandstones, and its possible bearing on the origin and precipitation of uranium: U.S. Geol. Survey Circ. 224.



ENGINEERING GEOLOGY

125. GEOLOGY OF DJATILUHUR DAMSITE AND VICINITY, WEST JAVA, INDONESIA

By HOWARD H. WALDRON, Bandung, Indonesia

Work done in cooperation with the Geological Survey of Indonesia

Djatiluhur is the site of the first major multipurpose dam to be constructed in Indonesia. Completion of the dam, now under construction, will provide water for increased irrigation and for additional electrical power, both vitally needed for this densely populated part of Indonesia. This investigation was undertaken as part of a cooperative program between the U.S. Geological Survey and the Geological Survey of Indonesia, under the auspices of the International Cooperation Administration.

The dam is to be a zoned, rockfill structure with a sloping impervious core. When completed the dam will have a height of about 100 meters, a crest length of about 1,125 meters, and a maximum width at the base of about 575 meters. Total volume of the structure, including cofferdams, will be in excess of 10 million cubic meters. A giant hollow reinforced concrete tower, 90 meters in diameter and 110 meters in height, will be embedded in the upstream face of the dam to serve as a glory-hole type spillway, provide for turbine and irrigation intakes, and house all of the power-generating equipment.

Djatiluhur lies in the "Bogor Zone" (Bemmelen, 1949, p. 645), a complex belt of hills and mountains that form the southern border of the coastal or lowland plain of West Java (fig. 125.1). This zone consists principally of folded and faulted young Tertiary marine sedimentary rocks intruded by many igneous masses (Ludwig, 1933). The damsite is located in a gorge of the Tjitarum River where it cuts through a ridge of folded sedimentary strata. Relief ranges from 25 meters to about 200 meters near the damsite;

elevations are higher south of the damsite, principally on the hills and ridges that are underlain by igneous rocks.

The rocks of the Djatiluhur area range in age from late Tertiary through Quaternary; rocks older than Miocene do not crop out in this part of West Java. Most of the area is underlain by Tertiary sedimentary rocks, chiefly marine shale and siltstone but with some fine-grained sandstone and a few strata of limestone interbedded with the shale. Several thousand meters of marine sedimentary rocks accumulated, after which deposition ceased and the rocks were folded, faulted, and intruded by a variety of intermediate and basic igneous rocks during latest Tertiary time. Subsequently the rocks were deeply eroded and partly buried by Quaternary alluvial sedimentary deposits. General geology of the damsite is shown in figure 125.2.

Fine-grained facies of sedimentary rocks prevail in the area. Silty shale and siltstone predominate, but some clay shale and claystone also occur. For the most part the rocks are dark gray or bluish to greenish gray where fresh, but commonly they are various shades of brown where oxidized or weathered. Most are calcareous and fossiliferous; microfossils are very numerous, and invertebrate macrofossils also are found in some of the strata. The sandstone beds are predominantly fine grained and range in composition from light-colored quartzose sandstone to dark-colored graywacke sandstone. Many are calcareous, and most are fossiliferous. The rocks range in grain size and composition from quartzose through limy sandstone to sandy limestone, or in some places to nearly pure limestone; and from quartzose sandstone through siltstone to silty shale. A few of the rocks are tuffaceous, and some are glauconitic. The lenses and beds of limestone are mostly a fossiliferous-fragmental limestone that consists of fossil fragments cemented in a matrix of crystalline limestone and grains of sand, silt, and clay. Most strata are well sorted; stratification ranges from well bedded to obscurely bedded or massive. Argillaceous rocks are commonly fissile or shaly but may range from laminated to massive claystone.

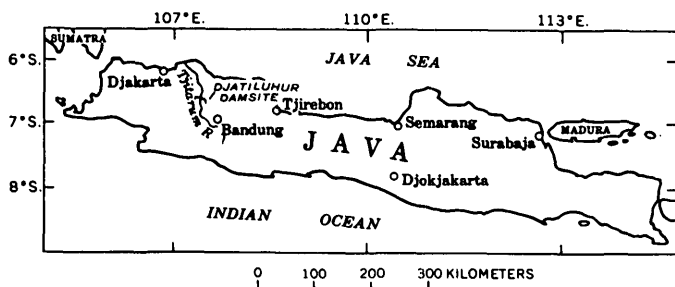
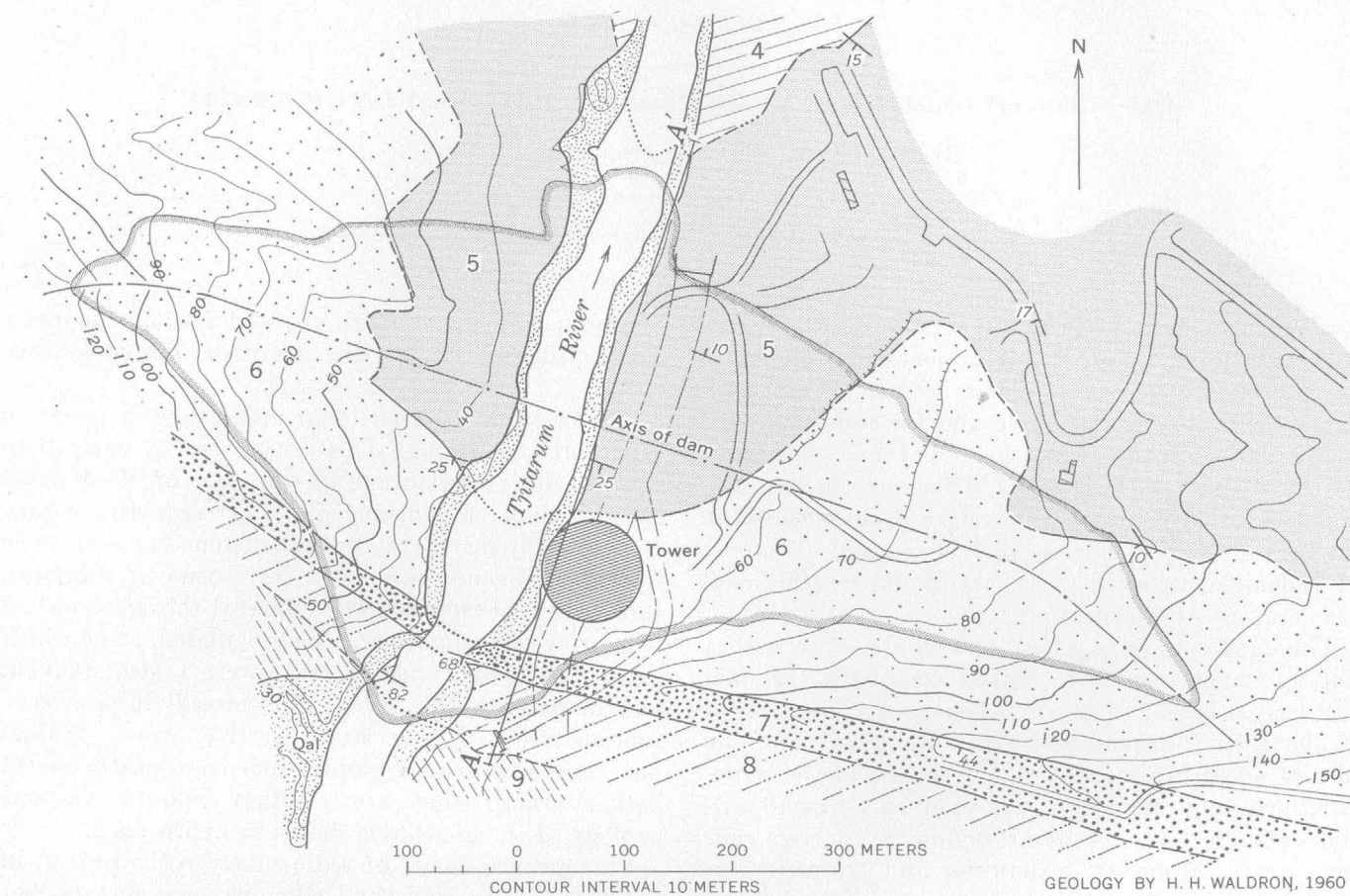


FIGURE 125.1.—Index map showing location of Djatiluhur dam site in West Java.



EXPLANATION

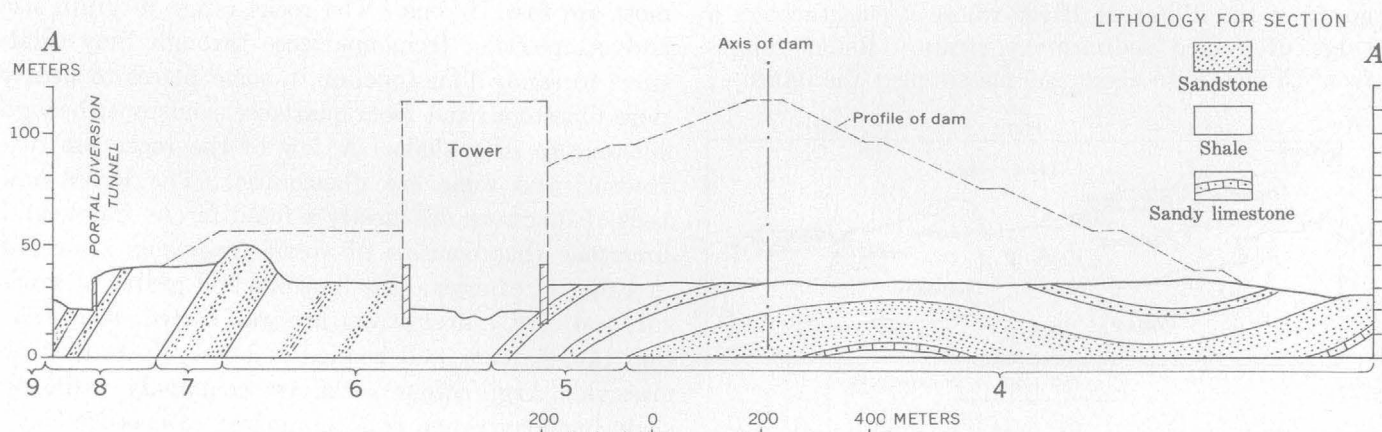
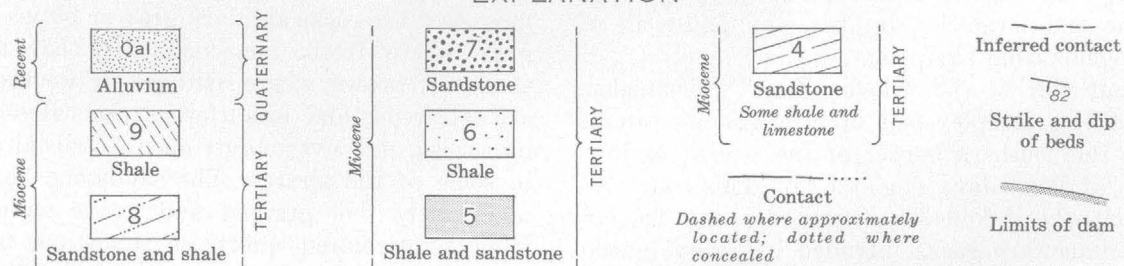


FIGURE 125.2.—Generalized geologic map and section of Djatiluhur damsite, West Java.

A variety of igneous rocks have intruded the Tertiary sedimentary rocks. Most of these are intermediate, or intermediate to basic in composition—hornblende andesite, augite andesite, alkalic basalt, hornblende diorite porphyry, and so forth. Most of the rocks are light gray and contain prominent phenocrysts of feldspars and mafic minerals in a fine-grained matrix. Solid rock is rarely exposed; most of the hills are nearly completely mantled with large blocks and boulders of igneous rock in a clayey matrix of altered ash. Where exposed, the igneous rocks range in structure from columnar to massive; many are platy. Locally, near the intrusive masses, the shale and siltstone have been altered by heat and pressure into low-grade metamorphic rocks such as argillite and hornfels.

All the Tertiary sedimentary rocks were folded and faulted, probably during Pliocene time. Structural details are difficult to interpret due to limited exposures and the lack of marker beds, but the major structure of the area consists of the south limb of a large anticline or anticlinorium, the north limb of which is absent due to faulting. The strata dip southward, almost homoclinally, but some minor gentle folds occur on the flank of the major anticline (fig. 125.2). In general, dips are low, 15° – 20° , but locally they may be as high as 80° . A major fault displaces the older strata both north and east of the damsite. Ludwig (1933) mapped this feature as a large thrust fault on the basis of evidence farther east, although evidence within the mapped area indicates that it is a normal high-angle fault at least locally, the relative movement of which has been downward to the north and east. Other smaller normal faults are present, but none were observed to underlie the foundation of the dam. Minor adjustment to deformation, however, is represented throughout the area by numerous joints and by small displacements of less than 1 to 2 meters. Grouting of the jointed sandstone and limestone will be necessary in places to assure adequate control of seepage.

Unconformably overlying the Tertiary strata are alluvial and lahar deposits of very late Pliocene or early Pleistocene age. These deposits normally consist of coarse volcanic sand and pebble-cobble alluvial

gravel at the base, overlain disconformably by a lahar deposit of varying thickness. The lahar deposit is an unsorted, compact mixture of volcanic sand and gravel, including large boulders, in a matrix of silt and clay. In upland areas, the lahar is deeply weathered to a red lateritic soil; at depth, however, it is relatively fresh and gray. Maximum thickness of the lahar is more than 75 meters. Younger Quaternary deposits include late Pleistocene terrace deposits in the Tjitarum valley, and modern alluvium underlying the valley bottoms and flood plains of the Tjitarum River and its tributaries. The terrace deposits consist of moderately weathered alluvial sand and gravel, some overbank deposits of lacustrine silt and clay, and the remnants of at least one thin lahar deposit. Maximum thickness of these deposits is about 35 to 40 meters.

The engineering characteristics and physical properties of the various rocks and soils in the Djatiluhur area are not well known, but preliminary observations and tests by the author and others, and soil tests being made by the engineering consulting firm of Coyne and Bellier, of Paris, France, indicate that the rocks at the proposed site are favorable for the support of heavy structures, and that the rocks and soils comprising the walls of the reservoir are favorable for containment of impounded waters. Numerous geologic factors were of prime importance in determining the final design of the dam. Some of these are (1) the difficulties inherent in the construction of a concrete dam on a predominantly shale foundation, (2) potential seismicity of the area, (3) lack of nearby adequate sources of materials of construction for either a concrete or an earth-fill structure, and (4) adequate nearby source of sound igneous rock suitable for construction of a rock-fill structure.

REFERENCES

- Bemmelen, R. W. van, 1949, *The geology of Indonesia*, v. 1A, General geology of Indonesia and adjacent archipelagoes: The Hague, Government Printing Office, Indonesia Bur. of Mines Spec. Ed., 732 p.
- Ludwig, O., 1933, *Toelichting bij Blad. 30 (Poewakarta): Geological map of Indonesia, 1:100,000*, Dienst Minjb. Ned. Ind., 45 p.



STRATIGRAPHY

126. PRECAMBRIAN(?) AND CAMBRIAN STRATIGRAPHY IN ESMERALDA COUNTY, NEVADA

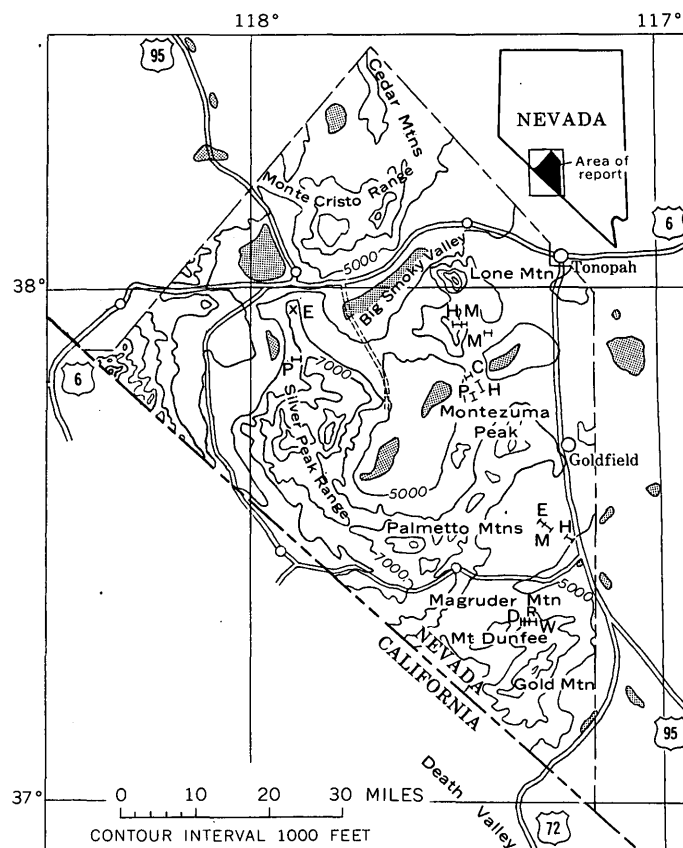
By J. P. ALBERS and J. H. STEWART, Menlo Park, Calif.

Work done in cooperation with the Nevada Bureau of Mines

In 1960 the U.S. Geological Survey began a study of Esmeralda County, Nev., as a part of a program of county mapping done in cooperation with the Nevada Bureau of Mines. By the end of the 1961 field season most of the exposed Precambrian(?) and Cambrian rocks had been mapped and the stratigraphic section largely worked out. The purpose of this paper is to record the pertinent stratigraphic information.

In gross aspect, the section closely resembles that recently described by Nelson (1962, p. 139-144) in the White and Inyo Mountains, Calif., and the names used by Nelson for Lower Cambrian and underlying rocks are applied in Esmeralda County. We are indebted to Nelson for showing us part of the section in the field during 1960, and also to E. H. McKee, who had worked out the geology of the Magruder Mountain area, Esmeralda County (fig. 126.1) prior to 1960 and applied Nelson's terminology to the Precambrian(?) and Cambrian rocks exposed there. McKee kindly showed us this section in detail and also worked part time with us during 1961.

Included in the section are 3 units, the Wyman, Reed, and Deep Spring Formations, that have yielded no fossils and are therefore regarded as probably of Precambrian age; 4 units, the Campito, Poleta, Harkless, and Mule Spring Formations, that contain abundant olenellid trilobites and other fossils of Early Cambrian age; and 1 unit, the Emigrant Formation, of Middle and Late Cambrian age. The total thickness of this section is at least 13,000 feet, of which about 3,600 feet is Precambrian(?), 7,500 feet is Lower Cambrian, and 1,900 feet is Middle and Upper Cambrian (fig. 126.2). The Lower Cambrian rocks in the Silver Peak region were named the Silver Peak Formation by Turner (1902, p. 264-265). Later, the term Silver Peak was used by Walcott (1908, p. 185) in a group sense for part of this series of rocks. Because of the vague original usage of the term Silver Peak, and also because it includes too many rock types to be usable as a modern map unit, Nelson (1962, p. 144) has abandoned the term. Accordingly,



EXPLANATION

E	D
Emigrant Formation	Deep Spring Formation
M	R
Mule Spring Limestone	Reed Dolomite
H	W
Harkless Formation	Wyman Formation
P	—
Poleta Formation	Location of measured section
C	x
Montenegro Member of Campito Formation	Type locality of Emigrant Formation

FIGURE 126.1.—Index map of Esmeralda County, showing location of measured sections of Precambrian(?) and Cambrian rocks. Letters show formations measured at each section. Shaded areas are basins.

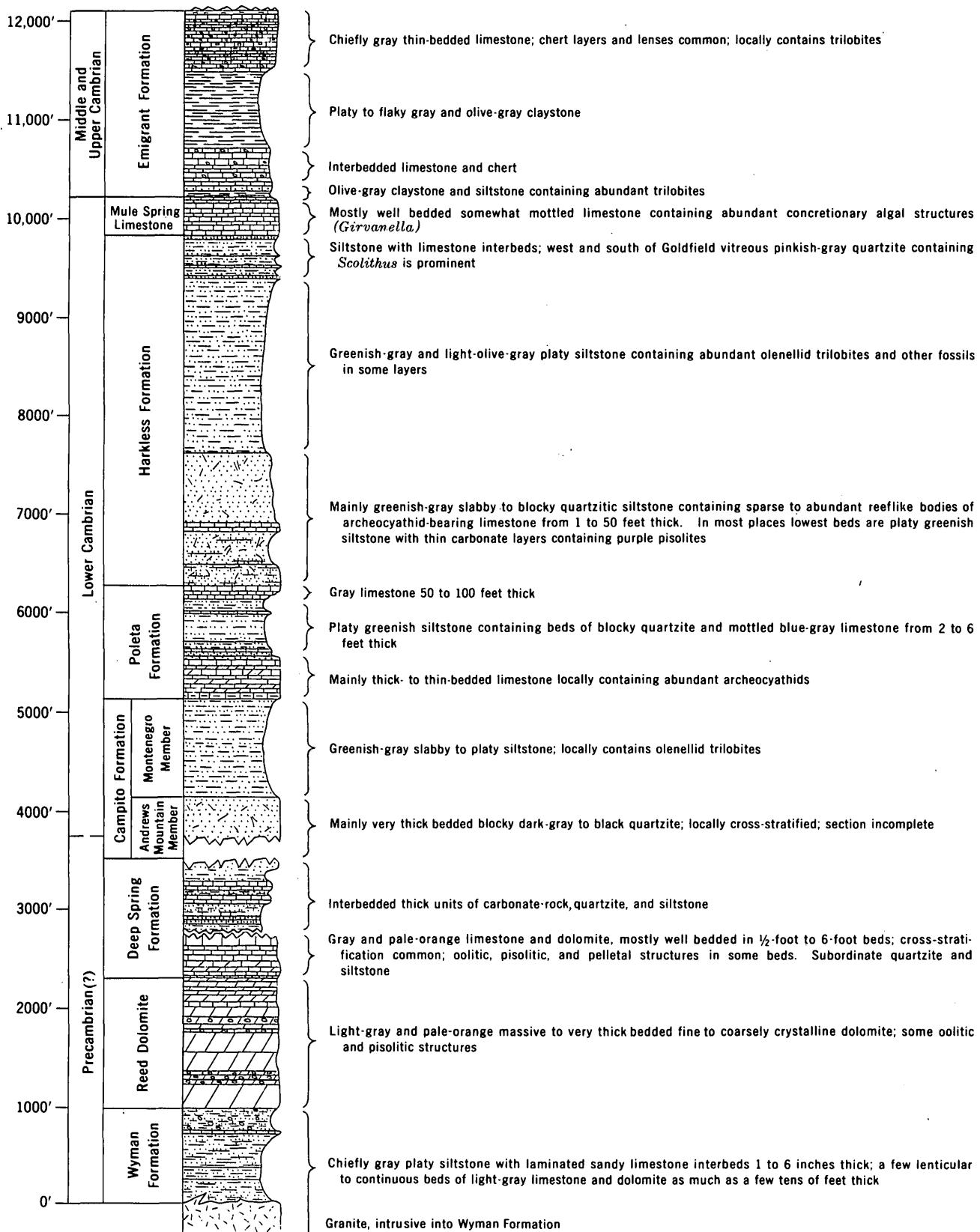


FIGURE 126.2.—Generalized composite section of Precambrian(?) and Cambrian rocks, Esmeralda County.

Nelson's terminology, slightly amended, is applied to the rocks in Esmeralda County, which includes the type area of the Silver Peak of former usage.

The Wyman Formation, consisting chiefly of platy siltstone, interlayered thin sandy limestone beds, and local fairly thick lenses of gray limestone and dolomite, is the oldest map unit in the county and, as shown diagrammatically on figure 126.2, its lower boundary is an intrusive contact, where observed in the area mapped. The maximum exposed thickness of the Wyman is not much more than 1,000 feet, but the amount of section cut out is not known. In most places the Wyman is metamorphosed to spotted hornfels or schist, but on the west flank of Mount Dunfee (fig. 126.1) it is only slightly metamorphosed and clearly lies conformably beneath the Reed Dolomite, which consists mainly of massive very thick bedded light-gray commonly coarsely crystalline dolomite. Similar conformable relations between the Wyman and the Reed were seen east of Lone Mountain. Elsewhere in the county the Reed rests in some places in thrust relation on the Wyman, and in other places the structural relation of the two units is obscure. Accordingly, Nelson's (1962, p. 140-141) observation that an unconformity separates the Wyman and Reed Formations is not supported by our findings in Esmeralda County. The wide lithologic variation in the Wyman at its contact with the Reed may be due to a combination of original lenticularity of beds within the Wyman and a thrust relation in some places between the Wyman and Reed, rather than to an unconformity.

The name Reed Dolomite is herein retained, in preference to Nelson's (1962, p. 141) Reed Formation, because the unit is composed almost entirely of thick-bedded very-light-gray to yellowish-gray dolomite. It is a distinctive unit that forms prominent outcrops.

The Deep Spring Formation, which overlies the Reed, is composed mainly of distinctly bedded limestone and dolomite, much of which shows cross-stratification, and subordinate quartzite and siltstone. Biscuit-shaped algal growths, pisolites, and pelletal structures are common. The contact between the Reed and the Deep Spring is well exposed in the section on Mount Dunfee and is clearly conformable.

The uppermost part of the Deep Spring Formation and the lower part of the overlying Campito Formation are not exposed on Mount Dunfee where the contact between these two units is a fault. However, E. H. McKee¹ has found these two formations to be

conformable in the east end of Magruder Mountain a few miles to the west (fig. 126.1). The Andrews Mountain and Montenegro Members of the Campito Formation, as subdivided by Nelson (1962, p. 141), are distinctive lithologic units in Esmeralda County and are highly useful in working out the complex structural pattern. The Andrews Mountain Member is mainly dark-gray blocky quartzite, and the Montenegro Member is largely greenish-gray siltstone. The Montenegro Member contains abundant olenellid trilobites; we have not found any fossils lower in the section. Thus the boundary between the Cambrian and Precambrian is not certainly fixed. Nelson (1962, p. 140) indicates that olenellid trilobites occur in the upper part of the Andrews Mountain Member. It therefore seems likely that at least the upper part of this member in Esmeralda County is Lower Cambrian.

The limestone that forms the lower part of the Poleta Formation contains abundant archeocyathids and forms a very useful marker. This carbonate unit seems to differ greatly in thickness from place to place, but we have not been able to ascertain how much of the variation is due to original lenticularity and how much to structural slicing. The rest of the Poleta Formation is a sequence of platy siltstones containing locally abundant trilobites interlayered with blocky quartzite beds and bluish-gray mottled limestone beds, and capped by a limestone unit 50 to 100 feet thick that contains sparse archeocyathids. The upper part of the Poleta is also a highly distinctive map unit.

The blocky quartzitic siltstone that makes up the lower part of the Harkless Formation (fig. 126.2) is recognized mainly by the small reeflike masses of archeocyathid limestone that it contains and by its greenish-gray color. The unit is absent in many parts of Esmeralda County, and we attribute this mainly to structural complications. The greenish-gray platy siltstone that forms the upper part of the Harkless is very difficult to distinguish from the Montenegro Member of the Campito Formation except by the fauna that it contains.

The upper part of the Harkless Formation in the Montezuma Peak area west of Goldfield includes beds of limestone and sandy limestone interbedded with platy siltstone and quartzite that, according to Nelson (oral communication, 1960), resemble the younger Saline Valley Formation of the northern Inyo and White Mountains (Nelson, 1962, p. 142). Similar beds also have been recognized about a mile northeast of Mount Dunfee. This unit is not present everywhere, however, and where present it has been included in the Harkless Formation. In the hills northwest of the junction between U.S. 95 and State Highway 3

¹ McKee, E. H., 1962, The stratigraphy and structure of a portion of the Magruder Mountain-Soldier Pass quadrangles, California-Nevada: California Univ. Ph.D. thesis, 108 p.

and in the hills 6 miles south of Goldfield and west of U.S. 95, the uppermost Harkless includes beds of coarse vitreous pinkish-gray quartzite, some of which contain *Scolithus*. This quartzite was also recognized as a bed about 2 to 4 feet thick, west of Montezuma Peak where it seems to pinch out. It has not been found elsewhere. These quartzite beds lithologically resemble and may correlate with the unit named the Zabriskie Quartzite Member of the Wood Canyon Formation by Hazzard (1937, p. 309) in the Nopah Range, Inyo County, Calif.

The name Mule Spring Limestone is herein used in preference to the Mule Spring Formation of Nelson (1962, p. 142) because the unit consists everywhere of distinctly bedded commonly mottled limestone and is a conspicuous marker unit that crops out prominently. Except where it is extremely metamorphosed, the Mule Spring is readily identified by the abundant concretionary algal structures (*Girvanella*) that it contains.

In several localities a few miles southwest of Goldfield the Mule Spring Limestone of Early Cambrian age is overlain conformably by siltstones containing trilobites identified by A. R. Palmer (written communication, 1960) as of Middle Cambrian age. These

siltstones in turn are overlain by a sequence of limestone with interlayered chert, by claystone, and finally by thin-bedded limestone with cherty interbeds. This last unit has yielded fossils of Late Cambrian age. The entire sequence above the Mule Spring Formation is considered to be the Emigrant Formation and its age is revised to include Middle as well as Late Cambrian rocks. However, details of the stratigraphy of the Emigrant, particularly the uppermost part, have not yet been satisfactorily worked out.

From the relations seen, it is our interpretation that the entire sequence of Precambrian(?), Lower Cambrian, and Middle and Upper Cambrian rocks in Esmeralda County is conformable.

REFERENCES

- Hazzard, J. C., 1937, Paleozoic section in the Nopah and Resting Springs Mountains, Inyo County, California: California Div. Mines Rept. 33, p. 289-339.
 Nelson, C. A., 1962, Lower Cambrian-Precambrian succession, White-Inyo Mountains, California: Geol. Soc. America Bull., v. 73, p. 139-144.
 Turner, H. W., 1902, A sketch of the historical geology of Esmeralda County, Nevada: Am. Geologist, v. 29, p. 261-272.
 Walcott, C. D., 1908, Cambrian sections of the Cordilleran area: Smithsonian Misc. Colln., v. 53, no. 5, p. 167-230.



127. CAMBRIAN CARRARA FORMATION, BONANZA KING FORMATION, AND DUNDERBERG SHALE EAST OF YUCCA FLAT, NYE COUNTY, NEVADA

By HARLEY BARNES, ROBERT L. CHRISTIANSEN, and F. M. BYERS, JR., Denver, Colo.

Work done in cooperation with U.S. Atomic Energy Commission

The Cambrian rocks underlying the Upper Cambrian Windfall Formation (Barnes and Byers, 1961) in the northeast corner of the Nevada Test Site (fig. 127.1) are described in this article. The section includes the Lower and Middle Cambrian Carrara Formation, the Middle and Upper Cambrian Bonanza King Formation, and the Upper Cambrian Dunderberg Shale. It now seems advisable to apply the name Carrara Formation (Cornwall and Kleinhampl, 1961), rather than the names Latham Shale, Chambless Limestone, and Cadiz Formation (Barnes and Palmer, 1961), to the entire transitional sequence between the quartzites of the Lower Cambrian Wood Canyon Formation and

the carbonates of the Bonanza King Formation (fig. 127.2). This change in usage was suggested by A. R. Palmer (written and oral communications, October and November, 1961) following field examination of many sections below the Bonanza King Formation in southern Nevada and adjacent parts of California, because the Chambless Limestone cannot be correlated across the region with certainty. Palmer has also provided all fossil identifications used in this article.

CARRARA FORMATION

The Carrara Formation east of Yucca Flat is about 1,960 feet thick and is divided into 7 subunits. Sub-

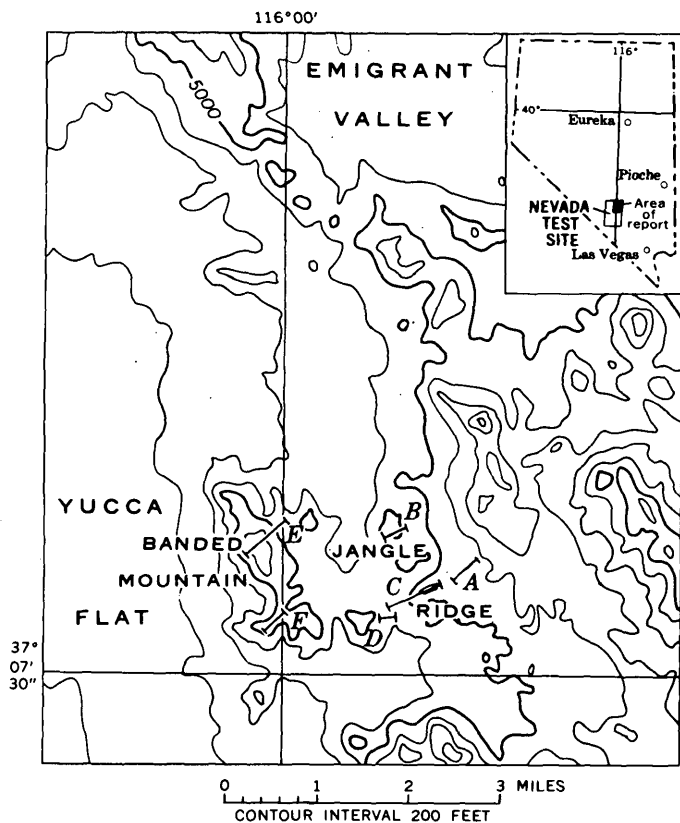


FIGURE 127.1.—Map of part of Nevada Test Site east of Yucca Flat, Nye County, Nev., showing location of measured sections. A, subunits 1-5 of Carrara Formation; B, Jangle Limestone Member and subunit 7 of Carrara Formation; C and D, Papoose Lake Member of Bonanza King Formation; E and F, Banded Mountain Member of Bonanza King Formation; G, Dunderberg Shale.

units 1, 2, and 3 were correlated by Johnson and Hibbard (1957, p. 338) with the Pioche Shale of the Groom district, subunit 4 (p. 338) with the Lyndon Limestone of the Groom district, and subunit 5 (p. 339) with the Chisholm Shale of the Groom district. The Jangle Limestone of Johnson and Hibbard (1957, p. 339) is here recognized as a member of the Carrara Formation. Subunit 7, the highest of the subunits, is equivalent to the lower part of Johnson and Hibbard's Yucca Flat Formation (1957, p. 340).

The lower half of the Carrara Formation consists of interbedded shale, siltstone, and limestone and is divided into three subunits. The lowest subunit is 85 feet thick and consists of dark-yellowish-orange to pale-olive fissile clay shale and siltstone, grayish-red to yellowish-brown thin-bedded very fine grained micaceous sandstone and quartzite, and a little yellowish-brown to grayish-red thin-bedded sandy limestone. The subunit is gradational with the underlying Zabriskie Quartzite Member of the Wood Canyon Formation of Hazzard (1937, p. 309), and the basal

contact is placed at the lowest occurrence of fissile shale. The second subunit of the Carrara is about 285 feet thick and consists of laminated to thin-bedded medium-dark-gray to grayish-red limestone and silty limestone with interbedded fissile clay shale. The limestone and silty limestone have fairly regular to platy bedding and split into plates and shaly chips. Trilobite fragments are common. This subunit forms two low ridges underlain by limestone, with an intervening saddle eroded in shale. The third subunit is about 540 feet thick and consists of pale-brown to grayish-red fissile clay shale and laminated to thin-bedded micaceous siltstone and sandstone with minor amounts of interbedded limestone and silty limestone. It forms a conspicuous brownish outcrop band.

Subunits 4 and 5 and the Jangle Limestone Member of the Carrara Formation form two persistent zones of ridge-forming limestone with a less resistant shale between. Subunit 4 contains about 310 feet of light-to medium-dark-gray limestone with interbedded pale-red to dark-yellowish-orange shale, siltstone, and silty limestone. The rocks are thin bedded to laminated, with some discontinuous cusped laminae. Locally the limestone is conspicuously oolitic and contains abundant *Girvanella* and trilobite fragments. Subunit 5 contains about 170 feet of pale-reddish-brown to dark-yellowish-orange fissile clay shale with interbedded laminated to thin-bedded silty limestone. About 100 feet above the base of the subunit is a persistent ledge-forming 3-foot bed of medium-dark-gray limestone mottled with discontinuous cusped laminae of pale-red siltstone, similar to the Jangle Limestone Member. The Jangle Limestone Member of the Carrara Formation is about 280 feet thick and consists of thin-bedded to laminated medium-gray limestone and silty limestone, much of which is mottled. The characteristic mottling results from the interlayering of dark-yellowish-orange to pale-reddish-brown discontinuous cusped laminae with medium-gray laminae. The lower and upper parts of the member form ledges, and about 135 feet in the middle forms slopes and contains abundant irregular laminae of silty limestone. *Girvanella* is locally abundant.

The uppermost subunit of the Carrara Formation is about 290 feet thick and comprises rocks transitional between the underlying shales and silty limestones and the overlying limestones and dolomites of the Bonanza King Formation. All but the lower 50 feet of this transitional unit was included by Barnes and Palmer (1961, p. C102) in the Bonanza King Formation, but recent detailed work has shown that the lithology of subunit 7 is more like the Carrara Formation with its shales and silty limestone than the Bonanza King

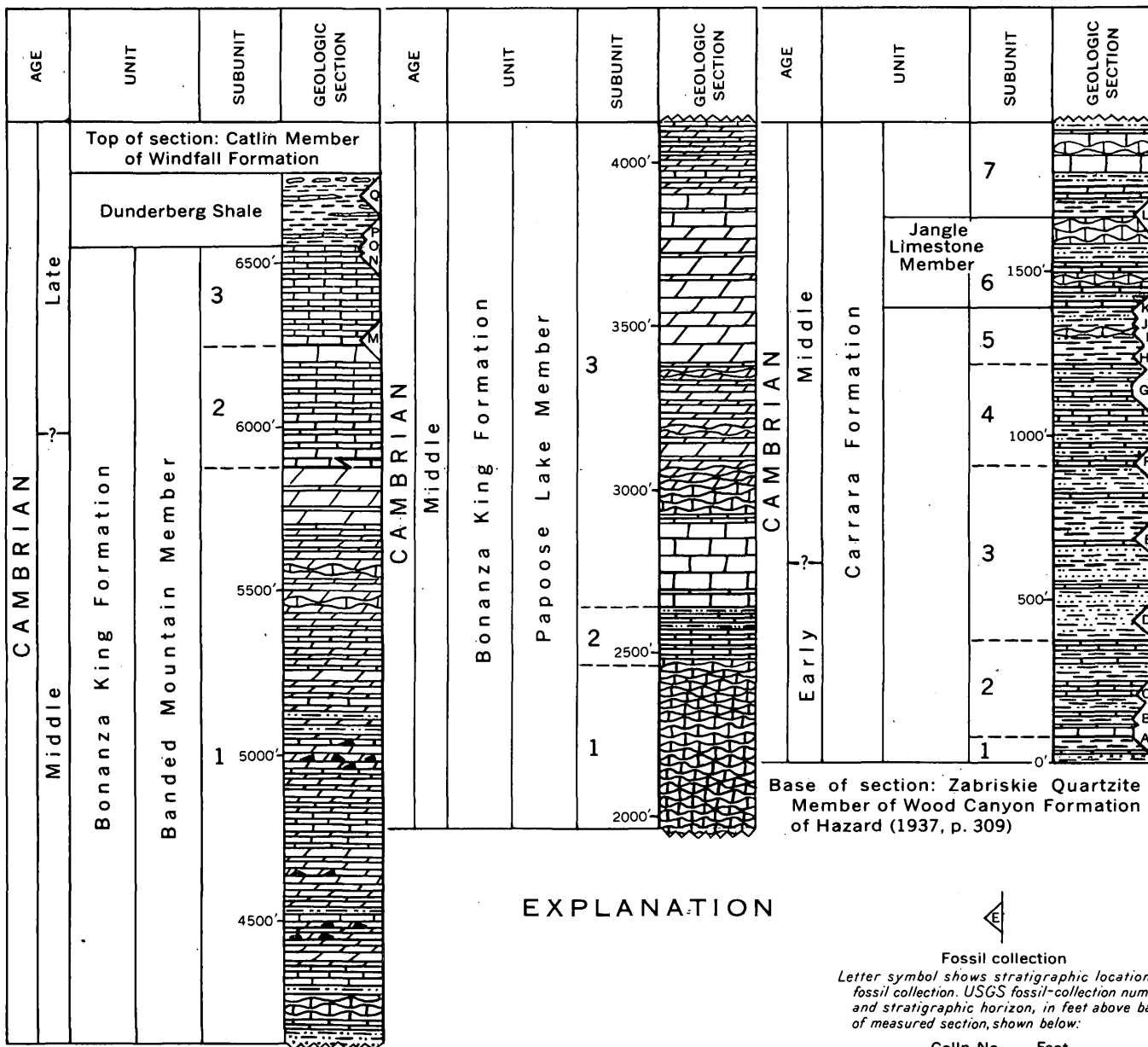


FIGURE 127.2.—Section of Carrara Formation, Bonanza King Formation, and Dunderberg Shale measured east of Yucca Flat, Nevada Test Site (fig. 127.1).

Formation with its carbonate rocks relatively free of detrital materials. The characteristic lithology of the subunit is medium- to dark-gray thin-bedded limestone with irregularly distributed brownish- to reddish-weathering laminae of siltstone and dolomite. All gradations occur from well-bedded interlaminated limestone and siltstone to rocks with the mottled appearance of the underlying Jangle Member. In addition to these silty limestones, subunit 7 includes abundant light-gray poorly bedded limestones that typically contain small white irregularly shaped blebs of coarsely crystalline calcite. Near the top of the subunit, zones a few feet thick of mottled gray limestone characteristic of the lower part of the Bonanza King Formation are rather common. The top of the subunit is placed at the top of the highest silty bed in the transitional sequence. The discontinuity of individual silty beds that define the top of the unit results in thickness variations of as much as several tens of feet.

The age of the Carrara Formation is Early and Middle Cambrian. Early Cambrian fossils of the *Olenellus* zone occur in subunits 2 and 3, from 85 to 440 feet stratigraphically above the base of the formation (fig. 127.2, A-D). A single small collection from near the middle of subunit 3 contains the earliest Middle Cambrian *Wenchemnia-Stephenaspis* zone (fig. 127.2, E). Fossils probably equivalent to the early Middle Cambrian *Kochaspis-Plagiura* zone are found near the base of subunit 4 (fig. 127.2, F). Middle Cambrian fossils from the *Albertella* zone occur in subunits 4, 5, and 6 (fig. 127.2, H-K) and from the *Glossopleura* zone near the base of subunit 7 (fig. 127.2, L).

BONANZA KING FORMATION

The Bonanza King Formation on the east side of Yucca Flat is subdivided into two members: the Papoose Lake Member, about 2,160 feet thick, and the Banded Mountain Member, about 2,440 feet thick (Barnes and Palmer, 1961, p. C103). The formation is equivalent to the upper part of Johnson and Hibbard's Yucca Flat Formation (1957, p. 340).

The Papoose Lake Member comprises three subunits. Approximately the lower fifth of the member is made up of a distinctive dark-gray limestone thinly interbedded and interlaminated with slightly coarser grained medium-gray limestone. The laminae have somewhat irregular cusped forms, giving the rock a mottled appearance in two shades of gray. The subunit weathers to dark massive subrounded exposures. The basal subunit is equivalent to unit A of the upper

part of Johnson and Hibbard's Yucca Flat Formation (1957, p. 341). The overlying subunit of the Papoose Lake Member is well-bedded laminated to thin-bedded light- to medium-gray limestone with minor dolomite and several thin zones containing brownish-weathering siltstone laminae. The subunit contains virtually the only clastic material in the member and is a good local stratigraphic marker. The upper two-thirds of the Papoose Lake Member is more heterogeneous than either of the other subunits. It consists of three lithologic types in varied order. Much of it is well-bedded light- to medium-gray thick-bedded dolomite and limestone. Light- to medium-gray laminated dolomite and limestone are dominant near the top of the member. The third lithologic type in this subunit is dark-gray dolomite with very irregular and cusped thin beds and massive-weathering forms. Within these dark beds are abundant small white arcuate calcite stringers suggestive of shell profiles. This third type generally occurs in lenticular bodies a few feet thick, but the lowest of these is about 170 feet thick and persists throughout the area.

The Papoose Lake Member in many places has been altered to a rather coarsely crystalline light-gray to faintly yellowish-gray dolomite with wispy remnants of the original rock types. Locally this dolomitization is stratigraphically controlled, but in different places it has affected virtually every part of the member. In the northwestern corner of the Jangle Ridge quadrangle it has obliterated the original lithologic character of almost the entire unit. The member has a measured thickness of 2,160 feet, but the measured section had to be offset in an altered zone and was correlated on some of the wispy remnants within it. The resulting measurement may be slightly in error.

The overlying Banded Mountain Member of the Bonanza King Formation has three local subunits. The lowest of these is about 1,765 feet thick and is a strikingly banded sequence of laminated to thin tabular beds of light-gray dolomite and dark-gray limestone. The conspicuous color bands range in width from several inches to 15 feet. Dolomite predominates over limestone except for the basal 230 feet and a sequence extending from 600 to 735 feet above the base. Scattered nodules and lenticular beds of dark-brown-weathering chert and silty limestone are found at intervals throughout the subunit. The basal 230 feet is a good stratigraphic marker. It is largely thin-bedded but massive-weathering resistant dark-gray limestone mottled in various shades of gray, yellowish brown, and grayish orange; it also contains less resistant laminated to thin-bedded yellowish-brown

to very-pale-orange silty limestone. The mottling of the dark-gray limestone comes largely from the irregular cusped form of the thin beds and in appearance is reminiscent of mottled beds near the base of the Bonanza King Formation. The lowest 40 feet of the 230-foot sequence is yellowish-brown silty limestone, the "brown-weathering siliceous carbonate" referred to by Barnes and Palmer (1961, p. C102-C103).

The middle and upper subunits of the Banded Mountain Member form two broadly contrasting light and dark outcrop bands. The contrast is increased by the deeply pitted weathering of the darker rocks in the upper subunit as opposed to the smoothly rounded weathering of the lighter rocks in the middle subunit. The light-colored middle subunit contains about 375 feet of thick to very thin tabular beds of light- to yellowish-gray limestone, and has probably formed by alteration of darker beds. Its upper contact is conformable but sharp, its lower contact gradational. The upper subunit contains 300 feet of dark- to light-gray limestone in tabular to somewhat irregular thin beds. The upper 10 feet of the subunit is composed of dark-yellowish-brown and medium-gray thin to laminated irregular beds of limestone that contain much bituminous material and weather brownish gray. The middle and upper subunits of the Banded Mountain Member are equivalent to units C and D of the upper part of Johnson and Hibbard's Yucca Flat Formation (1957, p. 341).

The age of the Bonanza King Formation is Middle and Late Cambrian. Late Cambrian fossils of the *Crepicephalis* zone are found at the base of subunit 3 of the Banded Mountain Member and 40 feet below the top of that subunit (fig. 127.2 M-N). Three feet higher (fig. 127.2 N) are fossils of the *Aphelaspis* zone. Other Late Cambrian fossils representing an unnamed zone occur 10 feet below the top of the subunit (fig. 127.2, O).

DUNDERBERG SHALE

The Dunderberg Shale, 225 feet thick, is composed of pale-reddish brown fissile clay shale with thin interbeds of limestone. The shale is easily eroded and poorly exposed, but the thin-bedded limestone forms ledges, closely spaced in the upper fourth of the formation. Thin platy to wavy medium-gray beds of limestone in the lower part of the Dunderberg weather brownish gray and are similar to the limestone in the top 10 feet of the Bonanza King Formation. Limestone in the upper part of the Dunderberg Shale is light olive gray and occurs in flattened concretions and thin nodular and wavy beds; it is similar to the ledge-forming nodular limestone at the base of the overlying Catlin Member of the Windfall Formation.

The age of the Dunderberg Shale is Late Cambrian. *Dunderbergia*-zone fossils of early Late Cambrian Dresbach age are found at several levels (fig. 127.2, P-Q) in the formation. The basal beds of the overlying Windfall Formation contain trilobites of the *Elvinia* zone of middle Late Cambrian Franconia age.

REFERENCES

- Barnes, Harley, and Byers, F. M., Jr., 1961, Windfall Formation (Upper Cambrian) of Nevada Test Site and vicinity, Nevada: Art. 188 in U.S. Geol. Survey Prof. Paper 424-C, p. C103-C106.
- Barnes, Harley, and Palmer, A. R., 1961, Revision of stratigraphic nomenclature of Cambrian rocks, Nevada Test Site and vicinity, Nevada: Art. 187 in U.S. Geol. Survey Prof. Paper 424-C, p. C100-C103.
- Cornwall, H. R., and Kleinhampl, F. J., 1961, Geological map of Bare Mountain quadrangle, Nye County, Nevada: U.S. Geol. Survey Geol. Quadrangle Map GQ-157.
- Hazzard, J. C., 1937, Paleozoic section in the Nopah and Resting Springs Mountains, Inyo County, California: California Jour. Mines and Geology Rept. 33, State Mineralogist, p. 273-339.
- Johnson, M. S., and Hibbard, D. E., 1957, Geology of the Atomic Energy Commission Nevada Proving Grounds area, Nevada: U.S. Geol. Survey Bull. 1021-K, p. 333-384.



128. AGE AND SEQUENCE OF METASEDIMENTARY AND METAVOLCANIC FORMATIONS NORTHWEST OF NEW HAVEN, CONNECTICUT

By CRAWFORD E. FRITTS, Denver, Colo.

Work done in cooperation with the Connecticut State Geological and Natural History Survey

Metasedimentary and metavolcanic formations northwest of New Haven, Conn. (fig. 128.1), are near the eastern edge of a broad belt of rocks of Precambrian to Paleozoic age that extends from Long Island Sound through western New England to Canada. These rocks underwent the progressive regional metamorphism described, in part, by Barth (1936). Age determinations on micas from southeastern New York and southwestern Connecticut suggest that the metamorphism occurred about 365 million years ago (Long and Kulp, 1958, p. 604). According to a recent revision of the geologic time scale (Kulp, 1961, p. 1111) the metamorphism occurred in Middle to Late Devonian time. The age of the metamorphosed rocks, therefore, must be Devonian or older.

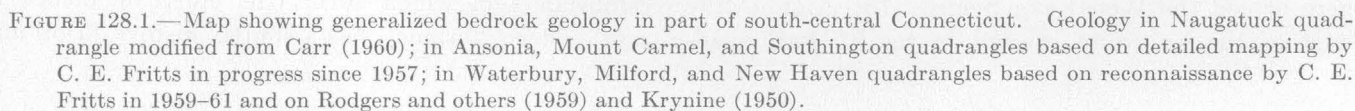
Geologic ages ranging from Precambrian to Silurian and Devonian are assigned here to the Connecticut rocks on the basis of correlation with an established stratigraphic succession in southeastern Vermont. Direct correlation is impossible now, because mapping in the intervening area is incomplete, no fossils have been found in the Connecticut rocks, and some formations are covered by strata of Late Triassic age in central Connecticut and Massachusetts. The rocks in Vermont and Connecticut, however, are similar and occupy comparable structural and stratigraphic positions in and

near a series of partly preserved domes east of the Green Mountain anticlinorium (Thompson, 1952, p. 20, pl. 4; Emerson, 1917, pl. 10; Rodgers and others, 1959, fig. 2). Possible equivalence of formations was postulated on the basis of reconnaissance mapping by Rodgers (Rodgers and others, 1959, p. 6, 14, 15), and the stratigraphic section was modified in the course of recent detailed mapping by the author in the Ansonia, Mount Carmel, and Southington quadrangles. The sequence from Waterbury Gneiss to Wepawaug Schist in Connecticut appears to be approximately equivalent to the sequence from Mount Holly Complex to Waits River Formation in Vermont, as shown in the table below.

The metasedimentary and metavolcanic formations in Connecticut discussed in this article are cut by several intrusives mentioned here for convenience, although some of them are not directly related to the subject under consideration. The Woodtick Gneiss, named here for Woodtick, Conn., in the Southington quadrangle, intruded the Waterbury Gneiss but is not known to have intruded rocks stratigraphically above this formation. The Prospect Gneiss (formerly part of the Prospect Porphyritic Gneiss) and the Ansonia Gneiss (formerly the Ansonia Granite of Carr, 1960) intruded the Straits Schist and the Southington Moun-

Approximate equivalence of metasedimentary and metavolcanic formations in south-central Connecticut and southeastern Vermont

Connecticut		Vermont		Geologic age
Interpretation of nomenclature of Rodgers and others (1959, p. 14, 15)	Nomenclature of Fritts	Nomenclature of Doll and others (1961)		
“Main body” of Orange Phyllite	Wepawaug Schist	Waits River Formation Northfield Formation		Devonian and Silurian
Milford Chlorite Schist	Metavolcanic and metasedimentary rocks, undivided	Missisquoi Formation	Barnard Volcanic Member	Ordovician
West-central part of Orange Phyllite	Derby Hill Schist		Moretown Member	
West edge of Orange Phyllite and upper part of The Straits Schist Member of the Hartland Formation	Southington Mountain Schist	Stowe Formation Ottawquechee Formation Pinney Hollow Formation		Ordovician and Cambrian
Lower part of The Straits Schist Member of the Hartland Formation	Straits Schist	Hoosac Formation		Cambrian
Waterbury Gneiss	Waterbury Gneiss	Mount Holly Complex		Precambrian



tain Schist but are not known to have intruded overlying formations. The Woodbridge Granite, named here for Woodbridge, Conn., in the Mount Carmel quadrangle, intruded the Wepawaug Schist before the climax of progressive regional metamorphism in Devonian time (Fritts, 1962). The ages of these four intrusives are discussed briefly below. Formations intruded by these rocks are overlain unconformably by the New Haven Arkose, which is part of the Newark Group of Late Triassic age. The West Rock Diabase, named here for West Rock in the New Haven quadrangle, intruded the New Haven Arkose at about the time that the Talcott Basalt of the Newark Group was extruded above the arkose. The age of this diabase, therefore, is Late Triassic. The Buttress Diabase, named here for a topographic feature known locally as The Buttress in the New Haven quadrangle, intruded West Rock Diabase at The Buttress, and is Triassic or younger in age.

The stratigraphic section recognized by Rodgers (Rodgers and others, 1959, p. 14) was deduced, in part, from the distribution of formations near the Waterbury dome (fig. 128.1). Formations were eroded from the western side of the dome after faulting and eastward tilting of the region during and (or) after Late Triassic time. East and south of the dome, however, the stratigraphic sequence is more complete, and most formations trend north-northeast. The easternmost formation (Milford Chlorite Schist of former usage) was assumed to be the youngest.

The present interpretation of stratigraphy and structure in the map area differs from that of Rodgers in several ways: (1) The Prospect Gneiss, which was interpreted as a granitized metasediment (Rodgers and others, 1959, p. 37), is believed to be a metamorphosed igneous rock, as suggested by Gregory (Rice and Gregory, 1906, p. 103). The Prospect forms stocks in the staurolite and kyanite zones, where the intensity of progressive regional metamorphism was too low to have formed the gneiss by granitization. (2) Metasedimentary rocks formerly included in the Prospect Gneiss, in the upper part of The Straits Schist Member of the Hartland Formation of Rodgers (Rodgers and other, 1959), and in the western part of the Orange Phyllite, were remapped and are here named the Southington Mountain Schist. (3) The names Orange Phyllite and Milford Chlorite Schist are here abandoned. (4) Rocks formerly assigned to the west-central part of the Orange Phyllite are here named the Derby Hill Schist, and rocks formerly assigned to the "main body" of the Orange Phyllite are here named the Wepawaug Schist. (5) Amphibolite west of the staurolite isograd in the Milford quad-

range, formerly mapped as a lens of hornblende gneiss in the Orange Phyllite, is physically continuous with lower grade metavolcanic rocks mapped as Milford Chlorite Schist by Rodgers and others (1959) farther east. (6) The rocks formerly mapped as Milford Chlorite Schist underlie rather than overlie the Wepawaug Schist (formerly the "main body" of Orange Phyllite). In the southeastern corner of the Ansonia quadrangle, bedding in both formations strikes northeast and dips 30° – 70° NW. Beds are right side up. Along the western side of the area of exposure of the Wepawaug, however, beds are nearly vertical and tops face east. The Wepawaug overlies the Derby Hill Schist on the west, and metavolcanic and meta-sedimentary rocks, undivided, on the east. The map pattern (fig. 128.1) suggests an unconformity beneath the Wepawaug. The center of the Wepawaug is characterized by numerous small north-plunging folds, because the formation occupies the trough of a tight north-plunging syncline.

The Waterbury Gneiss is part of a basement complex, which forms the core of the Waterbury dome (fig. 128.1). The name Waterbury Gneiss is restricted here to metasedimentary rocks that underlie Straits Schist. The predominant rock is a fine-grained well-banded paragneiss composed of quartz, biotite, muscovite, oligoclase, kyanite, garnet, microcline, and magnetite. This rock contains more alumina and iron oxide in the form of kyanite and magnetite, respectively, than other paragneisses in the map area. The Waterbury also contains subordinate medium- to coarse-grained schists composed of quartz, muscovite, oligoclase, biotite, garnet, and ilmenite or magnetite. Waterbury Gneiss is highly contorted in many places and is characterized by more complex textures than overlying formations (Fritts, 1962). The Waterbury is believed to have undergone progressive regional metamorphism more than once. The formation also contains numerous irregular bodies of felsic to intermediate meta-igneous rocks not known to have intruded overlying formations. There is no apparent relationship between emplacement of the meta-igneous rocks and formation of the Waterbury dome. For example, the largest body of Woodtick Gneiss, a quartz dioritic intrusive rock, is not in the center of the dome. Furthermore, the textures of these intrusives resemble the textures of Waterbury Gneiss rather than those of younger rocks. It is believed that emplacement of the meta-igneous rocks and a first metamorphism of Waterbury Gneiss occurred in pre-Straits time. The Mount Holly Complex of Precambrian age, which forms the cores of domes in southeastern Vermont, has a similar history (Doll and

others, 1961). A Precambrian (?) age, therefore, is assigned to the Waterbury and Woodtick Gneisses.

The Straits Schist is a relatively clean pelitic formation which overlies the Waterbury Gneiss unconformably, underlies the Southington Mountain Schist, and wraps around the core of the Waterbury dome. Straits Schist is the lower part of a unit named The Straits Schist Member of the Hartland Formation by Rodgers (Rodgers and others, 1959, p. 40). The predominant rock is a medium- to coarse-grained unbanding schist composed of quartz, muscovite, biotite, oligoclase, staurolite, kyanite (in the kyanite zone only), and ilmenite. In the Southington quadrangle, the formation also contains subordinate amphibolite and minor plagioclase-rich paragneiss, which are believed to represent metamorphosed graywacke or tuff. Straits Schist commonly is uncrumpled, although it is crumpled in some places along the southern side of the Waterbury dome. In contrast to Waterbury Gneiss, Straits Schist is characterized by simple textures and uniform grain size. The schist probably underwent progressive regional metamorphism only once. The Straits is similar to the Hoosac Schist of Early Cambrian age, which unconformably overlies rocks of Precambrian age in Massachusetts and Vermont (Herz, 1961; Doll and others, 1961). Thus, a Cambrian (?) age is assigned to the Straits Schist.

The Southington Mountain Schist includes all meta-sedimentary and metavolcanic rocks above the Straits Schist and below the Derby Hill Schist. The type locality of the Southington Mountain Schist is near New Britain Reservoir on Southington Mountain in the Southington quadrangle. Interlayered medium-grained paragneiss and fine- to medium-grained graphitic muscovite schist predominate. The formation is characterized by ribbon-like banding. The thickness of bands ranges from less than 1 inch to several tens of feet, but commonly is only a few inches. In the kyanite zone, schist bands contain quartz, muscovite, biotite, oligoclase, garnet, staurolite, kyanite, and chlorite; paragneiss contains quartz, sodic plagioclase, biotite, muscovite, garnet, staurolite, and minor kyanite (near the base of the formation). Amphibolite bands believed to represent metamorphosed graywacke or tuff are thinner but more numerous in this formation than in the Straits Schist. The formation also contains minor calc-silicate rocks and impure marble. The Southington Mountain Schist occupies a position comparable to that of rocks mapped above the Hoosac Schist as Pinney Hollow, Ottauquechee, and Stowe Formations, undifferentiated, near domes in southeastern Vermont (Doll and others, 1961). The age of the Pinney Hollow is Early Cambrian, the age

of the Ottauquechee is Middle Cambrian, and the age of the Stowe is Late Cambrian and Early Ordovician (Cady, Albee, and Murphy, 1962). The age of the Southington Mountain Schist, therefore, is Cambrian (?) and Ordovician (?).

The Derby Hill Schist, which overlies the Southington Mountain Schist, contains fine-grained thinly laminated argillaceous metatuff and impure quartzite. The Derby Hill Schist is named here for Derby Hill in the Ansonia quadrangle, Connecticut. The type locality is on the west side of the hill. The metatuff predominates and is characterized by layers a few millimeters thick composed almost entirely of muscovite, which are separated by layers of similar thickness composed of quartz and layers of intergrown albite and chlorite. Numerous veins and lenses of younger quartz have been injected between these layers. In northern exposures the schist is characterized by conspicuous shear cleavage, but to the south the rock is crumpled rather than sheared. A quartzitic member west of the Housatonic River in the Ansonia quadrangle probably is continuous with impure quartzite exposed east of the river in the Milford quadrangle. This member strongly resembles parts of the Savoy Schist (Ordovician) of Massachusetts and the Moretown Formation of Vermont. The age of the Moretown, which overlies the Stowe, is believed to be Middle Ordovician (Cady, 1960, p. 554). Thus, an Ordovician (?) age is assigned to Derby Hill Schist.

The metavolcanic and metasedimentary rocks, undivided, south and east of the Wepawaug Schist include intrusive and extrusive metadiabase and metabasalt, chlorite schist, amphibolite, meta-agglomerate, minor serpentinized limestone, and phyllite. The intrusives and extrusives apparently represent the climax of local volcanic activity in Ordovician time. These rocks, which overlie Derby Hill Schist, occupy a position comparable to that of the Barnard Volcanic Member of the Missisquoi Formation of Doll and others (1961). The Cram Hill Formation, which occupies a similar position in northern Vermont, is believed to be Middle Ordovician in age (Currier and Jahns, 1941, p. 1496).

The Wepawaug Schist is named for the Wepawaug River in the Ansonia quadrangle, Connecticut. The type locality is along this river south of Wepawaug Reservoir. Wepawaug Schist consists mainly of interlayered fine- to medium-grained argillaceous, siliceous, and minor calcareous rocks of chlorite to kyanite grade. In the chlorite zone (east of the garnet isograd) the predominant rock is carbonaceous phyllite composed mainly of quartz, muscovite, chlorite, and minor albite. Some layers a few inches thick are

quartz rich and others are muscovite rich. West of the garnet isograd, the rocks are fine to medium grained and consist of interbanded quartz-rich paragneiss and carbonaceous or graphitic muscovite schist. Garnet, biotite, staurolite, and kyanite are present in rocks of appropriate composition and metamorphic grade. Garnets are found on the low-grade side of the biotite isograd in this area, because the ratio MgO/FeO in Wepawaug Schist is low. In the staurolite and kyanite zones, the formation also contains subordinate thin bands of amphibolite. Bodies of subordinate impure crystalline limestone as much as 75 feet thick and 450 feet long are widespread, but are more numerous in the upper part of the formation. The limestone, which is approximately 50 percent calcite, is medium dark gray to medium bluish gray where fresh, but weathered surfaces have brown rinds as much as 1 inch thick, which are composed of quartz, muscovite, chlorite, and other silicate minerals. Similar limestones are characteristic of the Waits River Formation and a few are found in the underlying Northfield Slate of Vermont. The Northfield is Middle Silurian and the Waits River is Silurian and Devonian in age (Cady, 1960, p. 556). A Silurian and Devonian age, therefore, is assigned to the Wepawaug Schist.

The metasedimentary and metavolcanic formations in the map area were deposited during three main cycles of sedimentation. The predominant paragneiss of the Waterbury Gneiss, which contains moderate amounts of alumina and iron oxide, probably was derived from an area that underwent deep weathering and perhaps laterization. Deposition of the Waterbury was followed by progressive regional metamorphism and emplacement of the Woodtick Gneiss and other meta-igneous rocks in Precambrian time. The Straits, Southington Mountain, and Derby Hill Schists, and the overlying metavolcanic and metasedimentary rocks, undivided, reflect transition from relatively clean pelitic sediments to impure geosynclinal sediments in which volcanic debris was abundant. These rocks were deposited in Cambrian and Ordovician time before the Taconic orogeny. During a period of renewed subsidence after the Taconic orogeny, the Wepawaug Schist was deposited unconformably on older rocks. All of the metasedimentary and metavolcanic formations were folded or refolded and underwent progressive regional metamorphism

in Middle to Late Devonian time during the Acadian orogeny. The Prospect and Ansonia Gneisses, which intruded rocks unconformably beneath the Wepawaug Schist, probably were emplaced during either the Taconic or the Acadian orogeny, and are Ordovician or Devonian in age. The Woodbridge Granite, which intruded the Wepawaug Schist, probably was emplaced during the Acadian orogeny, and is Devonian in age.

REFERENCES

- Barth, T. F. W., 1936, Structural and petrologic studies in Dutchess County, New York, pt. 2, Petrology and metamorphism of the Paleozoic rocks: *Geol. Soc. America Bull.*, v. 47, no. 6, p. 775-850.
- Cady, W. M., 1960, Stratigraphy and geotectonic relationships in northern Vermont and southern Quebec: *Geol. Soc. America Bull.*, v. 71, no. 5, p. 531-576.
- Cady, W. M., Albee, A. L., and Murphy, J. F., 1962, Bedrock geology of the Lincoln Mountain quadrangle, Vermont: U.S. Geol. Survey Geol. Quad. Map GQ-164 (in press).
- Carr, M. H., 1960, The bedrock geology of the Naugatuck quadrangle: Connecticut Geol. and Nat. History Survey Quad. Rept. 9, 25 p.
- Currier, L. W., and Jahns, R. H., 1941, Ordovician stratigraphy of central Vermont: *Geol. Soc. America Bull.*, v. 52, no. 9, p. 1487-1512.
- Doll, C. G., and others, 1961, Centennial geologic map of Vermont: Vermont Geol. Survey.
- Emerson, B. K., 1917, Geology of Massachusetts and Rhode Island: U.S. Geol. Survey Bull. 597, 289 p.
- Fritts, C. E., 1962, Bedrock geology of the Mount Carmel and Southington quadrangles, Connecticut: U.S. Geol. Survey open-file rept.
- Herz, Norman, 1961, Bedrock geology of the North Adams quadrangle, Massachusetts-Vermont: U.S. Geol. Survey Geol. Quad. Map GQ-139.
- Krynine, P. D., 1950, Petrology, stratigraphy, and origin of the Triassic sedimentary rocks of Connecticut: Connecticut Geol. and Nat. History Survey Bull. 73, 247 p.
- Kulp, J. L., 1961, Geologic time scale: *Science*, v. 133, no. 3459, p. 1105-1114.
- Long, L. E., and Kulp, J. L., 1958, Age of the metamorphism of the rocks of the Manhattan prong: *Geol. Soc. America Bull.*, v. 69, no. 5, p. 603-606.
- Rice, W. N., and Gregory, H. E., 1906, Manual of the geology of Connecticut: Connecticut Geol. and Nat. History Survey Bull. 6, 273 p.
- Rodgers, John, Gates, R. M., and Rosenfeld, J. L., 1959, Explanatory text for preliminary geological map of Connecticut, 1956: Connecticut Geol. and Nat. History Survey Bull. 84, 64 p.
- Thompson, J. B., Jr., 1952, Southern Vermont, in *Guidebook for field trips in New England*: Geol. Soc. America, 65th Ann. Mtg., Nov. 10-12, 1952.



129. AGE OF THE LEADVILLE LIMESTONE IN THE GLENWOOD CANYON, WESTERN COLORADO

By W. E. HALLGARTH and BETTY A. L. SKIPP, Denver, Colo.

The Leadville Limestone in the Glenwood Canyon near Glenwood Springs in western Colorado contains endothyrid faunas which may be useful in determining the age of the formation. The Early Mississippian age currently recognized by the U.S. Geological Survey was determined from macrofossils studied by Girty (1903). Near the Colorado and Utah State line, however, rocks of Meramec (Late Mississippian) age have been recognized (Rothrock, 1960), and on the basis of more recent work the Leadville in the White River Plateau area may range from Kinderhook to Meramec in age as inferred from the occurrence of *Eumetria verneuilliana* (Hall) (N. W. Bass and S. A. Northrop, written communication, 1962). The endothyrid faunas likewise suggest that a part of the Leadville may be as young as Meramec.

The Leadville Limestone is well exposed near the east end of the canyon at the Garfield and Eagle County line where it consists of two recognizable parts (fig. 129.1). The lower part, about 85 feet thick, is a sequence of interbedded sandy and cherty limestone and dolomite beds which includes the Gilman Sandstone as a basal member. The age of the lower

part is probably Kinderhook and Osage. The upper part, about 80 feet thick, is formed by massive oolitic cliff-forming limestone which contains endothyrids only in the lower half.

Three genera of Foraminifera were identified in the Leadville—*Plectogyra tumula* Zeller, *Endothyra* aff. *E. scitula* Toomey (*E. symmetrica* Zeller), and *Septaglomospiranella* sp. Lipina.

In the Cordilleran trough area *Plectogyra tumula* is in rocks no younger than Osage, and *Endothyra scitula* is restricted to Meramec (Zeller, 1957, p. 694; Skipp, 1961). In the Glenwood Canyon area *Plectogyra tumula* and *Endothyra* aff. *E. scitula* occur in similar distinct zones. *Plectogyra tumula* occurs most abundantly in a zone about 20 feet thick in the lower part of the oolitic limestone and only sparingly in the overlying 15 feet of limestone. A few *Endothyra* aff. *E. scitula* and one *Septaglomospiranella* were found in a 10-foot zone about 40 feet above the base of the unit. None was found in the upper 35 feet of the Leadville, and its age remains uncertain. However, because rocks of Chester age have not been found in western Colorado, the upper part may be of Meramec age also. *Septaglomospiranella* has been found only in the Tournaisian (Lower Mississippian equivalent) of the Soviet Union (Lipina, 1955), but in the Redwall Limestone Skipp has found it rarely in the lower Meramec.

Zonation and correlation of the endothyrid faunas in the Cordilleran geosyncline area by Zeller (1957), and more recently in the Idaho and northern Arizona areas by Skipp, suggest that the Leadville in the Glenwood Canyon area may be as young as Meramec. Therefore, the boundary between rocks of Osage and Meramec age, as inferred from the endothyrid faunas, seems to be in the massive oolitic cliff-forming limestone where stratigraphic breaks are not apparent and deposition may have been continuous. However, there appears to be a rather sharp faunal break at the base of the *Endothyra* aff. *E. scitula* zone which may be the boundary between the Osage and Meramec.

REFERENCES

- Girty, G. H., 1903, The Carboniferous formations and faunas of Colorado: U.S. Geol. Survey Prof. Paper 16, 546 p.
Lipina, O. A., 1955, Foraminifera of the Tournaisian Stage and upper part of Devonian of the Volga-Ural region and

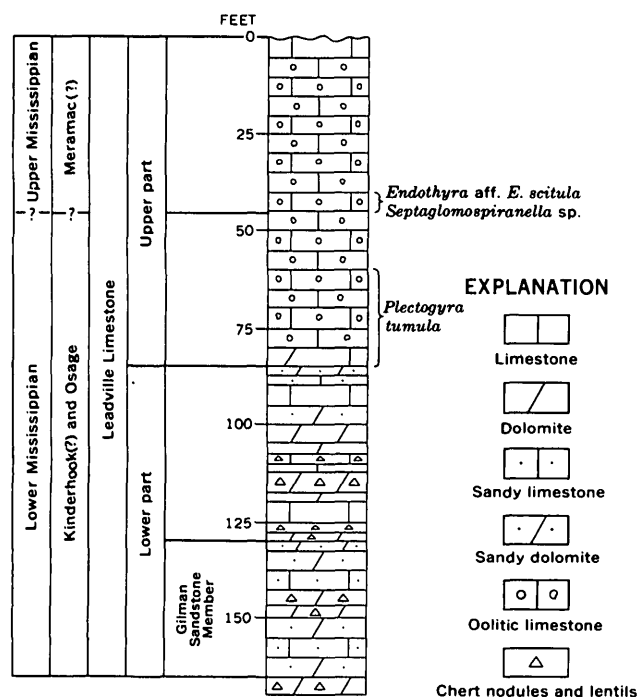


FIGURE 129.1.—Section of Leadville Limestone in Glenwood Canyon showing fossil zones.

western slopes of the Central Urals [Foraminifery turneiskogo iarusu i verkhnei chasti devona Volgo-Ural'skoi oblasti i zapadnogo sklona Srednego Urala]: Trudy IGN, AN-SSSR, No. 163 (geol. seriia no. 70), p. 46.

Rothrock, D. P., 1960, Devonian and Mississippian Systems in Colorado, in Guide to geology of Colorado: Geol. Soc. America, p. 17-23.

Skipp, Betty A. L., 1961, Stratigraphic distribution of endothyroid Foraminifera in Carboniferous rocks of the

Mackay quadrangle, Idaho: Art. 236 in U.S. Geol. Survey Prof. Paper 424-C, p. C239-C244.

Toomey, D. F., 1961, *Endothyra scitula*, new name for *E. symmetrica* Zeller, preoccupied: Cushman Lab. Foram. Research Contr., v. 12, pt. 1, p. 26.

Zeller, E. J., 1957, Mississippian endothyroid Foraminifera from the Cordilleran geosyncline: Jour. Paleontology, v. 31, p. 679-704.



130. TYPE SECTIONS FOR THE MORROW SERIES OF PENNSYLVANIAN AGE, AND ADJACENT BEDS, WASHINGTON COUNTY, ARKANSAS

By LLOYD G. HENBEST, Washington, D.C.

The Morrow Series in Washington County, Ark., is the standard of reference and the type section for the Lower Pennsylvanian rocks of the midcontinent region. The Washington County section contains the most varied and comprehensive record of Early Pennsylvanian life so far reported in a single succession. This article designates a type section, lists characteristic exposures, and outlines the history of the name of each named unit of the Morrow and adjacent beds

in Washington County (fig. 130.1), with the exception of the newly named Dye Shale and Trace Creek Shale Members of the Bloyd Formation, which are described in the accompanying Article 131. The stratigraphic units herein treated are described in figure 131.1 of that article.

PITKIN LIMESTONE, MISSISSIPPIAN

The Pitkin Limestone of Mississippian (Chester) age was named by Ulrich (1904, p. 109), who substituted the name Pitkin Limestone for the term "*Archimedes* Limestone" of Owen (1858, p. 34, 115), Simonds (1891, p. 55), and other authors in northwest Arkansas. It was named from exposures in the vicinity of the Pitkin Post Office, Washington County. The nearest, the most extensively and conspicuously exposed, and the most informative section of the Pitkin Limestone in the vicinity of Pitkin is in the 30- to 50-foot cliff along the West Fork of White River at the west base of Bloyd Mountain. This cliff, half a mile long, near the center of the west side of sec. 4, T. 14 N., R. 30 W., is hereby designated as the type section. The Pitkin Limestone as represented in this cliff has generally been consistently identified, defined, and mapped by Simonds, Purdue, and later authors in northwest Arkansas and adjacent Oklahoma. Purdue (1907, map), however, misidentified a small area of Prairie Grove Limestone at the Pitkin Post Office as the Pitkin Limestone. This understandable error does not affect the designation of a type locality because Purdue was not the author of the term Pitkin and did not express an intent to revise the name, and the type section designated above repre-

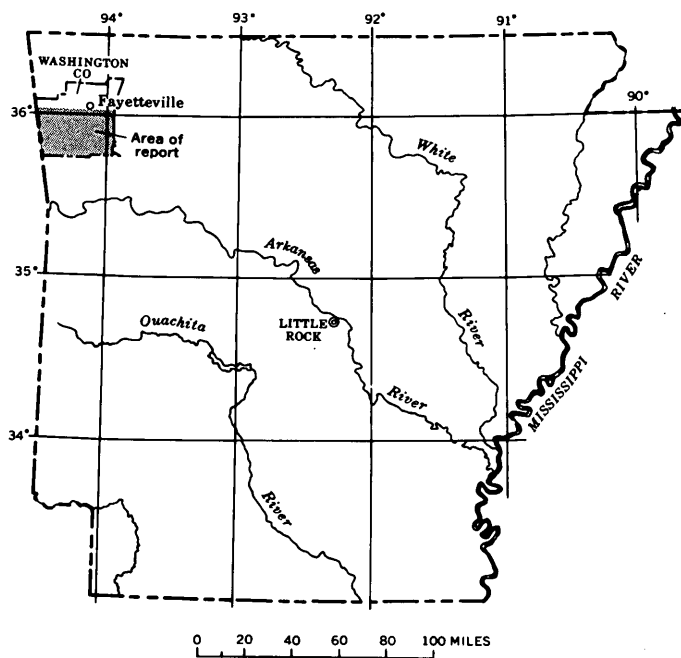


FIGURE 130.1.—Index map of northwestern Arkansas, showing area that contains type sections for Morrow Series in southern part of Washington County.

sents the Pitkin as identified and as mapped by everyone, including Purdue himself.

MORROW SERIES, PENNSYLVANIAN

The rock sequence in northwest Arkansas now known as the Morrow Series was first recognized by the paleobotanist Lesquereux (1860). Lesquereux was also the first to recognize that the rocks of the Morrow Series belong in the Pennsylvanian (Upper Carboniferous) rather than in the Mississippian (Lower Carboniferous) System. Until 1895, however, other paleontologists and geologists classed the Morrow as Mississippian because it contains *Pentremites* and certain other marine, metazoan fossils that characterize the Mississippian.

The "Pentremital Limestone" and the "coal bearing shale" of early authors were included in the "Boston Group" of the Branner Survey (*in* Simonds, 1891, p. XIII), but the flora was restudied by White (1895, p. 316-318; 1900, p. 817) and the fauna was reviewed by Ulrich (1904, p. 109-113) and Girty (1905, p. 8), all of whom confirmed the age determined by Lesquereux. The term Boston was both a homonym and a synonym of previous stratigraphic names. Ulrich (1904, p. 109) substituted the term Morrow for Boston without designating a type area. A year later Adams and Ulrich (1905, p. 4) stated that "The name is derived from the post office of Morrow, in Washington County, Ark., just south of which a high hill affords a nearly complete section of the formation." This statement constitutes a first revision. The "high hill" can be no other than Hale Mountain.

HALE FORMATION

The Hale Formation was described and named by Simonds (1891, p. 75-82) as the "Washington Shale and Sandstone." Simonds' term proved to be a junior homonym. Taff (1905, p. 4) renamed the unit as the "Hale Sandstone Lentil" (now classed as a formation) from its characteristic development in Hale Mountain. He presented significant information on the character and distribution of the formation and included the unit in his geologic map. In another publication the same year, Adams and Ulrich (1905, p. 4) briefly mentioned the name in the text, but did not include it elsewhere in the text or in the columnar section and geologic map, which indicates that recognition of the division was an afterthought following Taff's work. Other confirmation of Taff's authorship appears in reports by Purdue (1907, p. 3) and Purdue and Miser (1916, p. 14), which deal with closely connected areas. Those authors were intimately associated with the geology, geologists, and surveys involved. It is not known whether the Adams and Ulrich or the Taff

folio was published the first in 1905, but it is now known that Taff was the true author of the name. It therefore seems that Taff's priority should be accepted regardless of uncertainty on the exact date of publication, and it thus seems that Wilmarth (1938, p. 896) and Henbest (1953, p. 1936) were mistaken in crediting Adams and Ulrich as the authors.

The most complete and informative exposure of the Hale Formation in Hale Mountain is in a very small area in and around a box canyon beginning at a high waterfall over the Prairie Grove Member of the Hale. This locality is near the center of the north side of Hale Mountain in a ravine that heads at the Hale Mountain School near the center of the west side, sec. 7, T. 13 N., R. 32 W. (Henbest, 1953, p. 1948, no. 3). This section comprises a typical development of the unit and is hereby designated as the type locality of the Hale Formation. The exposure described by Giles and Brewster (1930, p. 131) is not nearly so complete.

The Cane Hill Member of the Hale Formation was first recognized as a stratigraphic entity by Simonds (1891, p. 75), who described it as the lower division of his "Washington Shale and Sandstone." Though the name Washington was found by Taff (1905, p. 4) to be unavailable, a restudy (Henbest, 1953, p. 1938) confirmed Simonds' stratigraphic observations and determined that the lower shale division of the Hale is a mappable unit. The name Cane Hill Member was applied because of typical development of the unit " * * * in the southern part of Washington County, in the vicinity of Cane Hill * * *" (1953, p. 1938). The exposures in the hillside and cuts on the west side of State Highway 59 about 3 miles along the road east of south from Evansville in the SW $\frac{1}{4}$ SE $\frac{1}{4}$ sec. 35, T. 13 N., R. 33 W., at the common boundary of Washington and Crawford Counties (part of loc. 1, p. 1949) were cited as the most complete and typical section of the Cane Hill. This section is hereby designated as the type for the member. Here, the Cane Hill consists of (a) a basal limestone conglomerate lying unconformably on the top of the Pitkin Limestone, (b) finely lamellar dark, shaly siltstone and claystone, and (c) alternating shaly sandstone and siltstone changing upward into increasingly flaggy, ripple-marked sandstone bearing *Conostichus* Lesquereux and abundant arthropycid burrows. The common boundary of the Cane Hill and Prairie Grove is here defined as lying at the base of the lowest massive, bench-forming calcareous sandstone unit of the Prairie Grove Member about 65 feet above the top of the Pitkin Limestone. In this type section the Cane Hill seems to intergrade with the Prairie Grove Member. In the

ravine about a third of a mile north from this type section, the Prairie Grove lies directly on the Pitkin. From the possible explanations that were cited by Henbest (1953, p. 1949) for the absence of the Cane Hill at this locality, an intraformational unconformity or channeloid contact was adopted with some doubt. Restudy suggests that truncation by creep deserves more consideration than originally thought.

The Prairie Grove Member of the Hale Formation was described and named by Henbest (1953, p. 1940) from characteristic sections in the mountains around the Prairie Grove community, Washington County. The Prairie Grove Member probably includes most or all of the sandstone part of the "Washington Shale and Sandstone" of Simonds (1891, p. 75). It also includes a part, locally, of the rocks identified by Simonds and later authors as the "Pentremital" or Brentwood Limestone, but does not include any part of the Brentwood Limestone Member of the Bloyd Formation as restricted by Henbest (1953).

The type section of the Prairie Grove Member is hereby designated as the section in the hillside and canyon along State Highway 59 in the E $\frac{1}{2}$ sec. 35, T. 13 N., R. 33 W. The type section of the Prairie Grove is contiguous with that of the Cane Hill Member and the area of exposure extends northward to the head of the canyon near the mountain pass. This locality is in and near the southwest corner of Washington County, 2 to 3 miles east of south along Highway 59 from Evansville and 3 to 4 miles west of south from Hale Mountain. The type sections of the Cane Hill and Prairie Grove Members are the same as localities 1 and 2 of Henbest (1953, p. 1949). The top of the Prairie Grove at this locality is drawn at the base of the first shale bed, 2 feet or more thick, above the uppermost massive, honeycombed (arthrophycid) calcareous sandstone of the Prairie Grove Member.

BLOYD FORMATION

The Bloyd Formation was described and was named after Bloyd Mountain by Purdue (1907, p. 3). A type area was not specified. The section in the southwest part of Bloyd Mountain extending from the center of the E $\frac{1}{2}$ sec. 3 to the center, north side of sec. 4, T. 14 N., R. 30 W., is hereby designated as the type section of the Bloyd Formation.

The name Brentwood Limestone, now classed as a member of the Bloyd Formation, was substituted by Ulrich (1904, p. 109) for the name "Pentremital Limestone" of Owen (Owen, Peter, and others, 1860, p. 115), Simonds (1891, p. 83), and others. This member was named from Brentwood Station (now des-

erted), but a type area was not delimited, as was the custom of the time in that type areas were loosely construed. The top of the Brentwood is exposed in the riverbed at Brentwood Station and in cuts along the railroad to the north, but the exposures are so incomplete or are so deeply involved with creep that they comprise poor standards of reference. Fortunately, the most complete, fossiliferous, and characteristic section of the Brentwood Limestone Member is exposed near Brentwood in the cut on the east side of U.S. Highway 71 and the West Fork of White River, from a tenth to a half mile south of the mouth of Mill Creek. This section is in the center of the N $\frac{1}{2}$ sec. 16, T. 14 N., R. 30 W. As previously restricted and defined by Henbest (1953, p. 1943), the Brentwood at this locality is 40 to 45 feet thick, contains an 18-foot dark shale at the base, and terminates above in a marine limestone unit. The top of the Brentwood is truncated by an unconformity beneath the basal conglomerates and plant-bearing shaly sandstone of the Woolsey Member. The Brentwood Limestone and limestone facies of the Prairie Grove have been confused at many localities. The type locality herein specified was chosen as the primary standard of reference for definition of the Brentwood and for locating the common boundary of the Hale and Bloyd Formations.

The Woolsey Member of the Bloyd Formation was named by Henbest (1953, p. 1943) after characteristic exposures near Woolsey Station. The section on the south and west side of Bloyd Mountain from the center, E $\frac{1}{2}$ sec. 3 to the center, north side, sec. 4, T. 14 N., R. 30 W., is hereby selected as the type section. The Woolsey Member is composed of terrestrial rocks. The sequence consists, beginning at the base, of (a) a local conglomerate containing detritus derived from the preceding Brentwood, rarely with quartz gravel or with shaly sandstone and siltstone bearing impressions of aerial parts of plants, (b) fossil soil below the Baldwin coal (c) Baldwin coal, and (d) terrestrial shale (0-13 feet thick) with coal stringers and aerial parts of plants. The Woolsey sequence terminates at the angular unconformity beneath the marine conglomeratic caprock of the Baldwin coal. The coal bed in the Woolsey was named the Baldwin coal by Croneis (1930, p. 87) after Baldwin Station, near the area formerly mined in Robinson Mountain, Washington County.

The Kessler Limestone Member was described and named by Simonds (1891, p. 26, 103-105) from its " * * * occurrence in Kessler Mountain * * * high up on the slope * * * in 16 N. 30 W." Kessler Mountain is in R. 31 W., not R. 30 W. Two limestones

(including the highly variable caprock of the Baldwin coal) occur "high up on the slope" of Kessler Mountain. The upper and most consistently calcareous bed was designated by Henbest (1953, p. 1944-1945) as the true Kessler. Simonds' description of the Kessler indicates that in a few other localities the caprock of the Baldwin coal was misidentified as the Kessler. Those horizons may have been confused in the type area that he designated, but at most localities in Washington County it is evident that Simonds identified the Kessler as the relatively pure, commonly oolitic, locally exfoliating limestone, 60 to 90 feet above the Baldwin coal. The "conglomeratic" appearance, which he noted as an identifying mark of the Kessler, is produced by algal-foraminiferal concretions, namely *Osagia* and *Ottomisia* both of Twenhofel, 1919. In a few places, subsequent authors have likewise confused the Kessler and the caprock of the Baldwin coal, but in general all have agreed on its identification.

To clarify and stabilize an accepted usage, the section of the Kessler on the west side of a shallow saddle near the north end of the highest part of the Kessler Mountain ridge, where erosion has removed the caprock (Greenland Sandstone Member of the Atoka Formation), is hereby designated as the type locality of the Kessler Limestone Member of the Bloyd Formation. This locality is near the center, SE $\frac{1}{4}$ sec. 25, T. 16 N., R. 31 W. The Kessler Limestone Member here is 5 to 15 feet thick. It forms a low bench, locally shows exfoliation, has an abundance of *Ottomisia* Twenhofel, 1919, and *Osagia* Twenhofel, 1919, in the upper part. The Kessler lies 22 feet below the base of the Greenland Sandstone Member, which caps Kessler Mountain, and lies 70 feet above the dark-brown calcareous sandstone caprock of the Baldwin coal.

ATOKA SERIES, PENNSYLVANIAN

The Greenland Sandstone Member of the Atoka Formation was named by Henbest (1953, p. 1946-1947) from characteristic exposures in the mountains near Greenland, Washington County. From the characteristic sections originally cited, the section in the southwest face of Bloyd Mountain in the NW $\frac{1}{4}$ sec. 3 and N $\frac{1}{2}$ sec. 4, T. 14 N., R. 30 W., is hereby designated as the type section of the Greenland Sandstone Member of the Atoka Formation.

REFERENCES

Adams, G. I., and Ulrich, E. O., 1905, Description of the Fayetteville quadrangle, Arkansas-Missouri: U.S. Geol. Survey Geologic Atlas, Folio 119, 6 p., 2 figs., topog. map, geol. map, table.

- Cronis, C. G., 1930, Geology of the Arkansas Paleozoic area, with especial reference to oil and gas possibilities: Arkansas Geol. Survey Bull. 3, 457 p., 30 figs., 45 pls., maps, tables.
- Giles, A. W., and Brewster, E. B., 1930, Hale Mountain section in northwest Arkansas: American Assoc. Petroleum Geologists Bull., v. 14, p. 121-138, 2 figs.
- Girty, G. H., 1905, The relations of some Carboniferous faunas: Washington Acad. Sci. Proc., v. 7, p. 1-26.
- Henbest, L. G., 1953, Morrow Group and lower Atoka Formation of Arkansas: American Assoc. Petroleum Geologists Bull., v. 37, p. 1935-1953, 2 figs.
- Lesquereux, L., 1860, Botanical and paleontological report of the Geological Survey of Arkansas, p. 295-319, 6 pls., in Owen, D. D., Peter, R., and others, Second report of a geological reconnaissance of the middle and southern counties of Arkansas . . . 1859 and 1860: Philadelphia, C. Sherman & Son, 433 p., 19 pls., woodcuts, 2 maps, tables.
- Mather, K. F., 1915, The fauna of the Morrow Group of Arkansas and Oklahoma: Denison Univ. Sci. Lab. Bull. v. 18, p. 59-284, 16 pl.
- Owen, D. D., Elderhorst, W., and Cox, E. T., 1858, First report of a geological reconnaissance of the northern counties of Arkansas made during the years 1857 and 1858: Little Rock, Ark., Johnson & Yerkes, 256 p., 10 pls. (listed), woodcuts, columnar sections, tables.
- Owen, D. D., Peter, R., Lesquereux, L., and Cox, E. T., 1860, Second report of a geological reconnaissance of the middle and southern counties of Arkansas . . . 1859 and 1860: Philadelphia, C. Sherman & Son, 433 p., 19 pls., woodcuts, 2 maps, tables.
- Purdue, A. H., 1907, Description of the Winslow quadrangle, Arkansas-Indian Territory: U.S. Geol. Survey Geol. Atlas, Folio 154, 6 p., topog. map, geol. map, columnar section, 4 figs.
- Purdue, A. H., and Miser, H. D., 1916, Description of the Eureka Springs and Harrison quadrangles, Arkansas-Missouri: U.S. Geol. Survey Geol. Atlas, Folio 202, 21 p., 2 topog. maps, 2 geol. maps, 9 pls., 13 figs., columnar section, 8 structure sections, 2 tables.
- Simonds, F. W., 1891, The geology of Washington County: Geol. Survey Arkansas Ann. Rept. 1888, v. 4, pt. 1, 154 p., 2 pls., unnumbered pls. and figs., geol. map.
- Taff, J. A., 1905, Description of the Tahlequah quadrangle, Indian Territory—Arkansas: U.S. Geol. Survey Geol. Atlas, Folio 122, 7 p., 2 figs., topog. map, geol. map, columnar section, structure section, tables.
- Ulrich, E. O., 1904, Determination and correlation of formations, in Adams, G. I., Ulrich, E. O., and others, Zinc and lead deposits of northern Arkansas: U.S. Geol. Survey Prof. Paper 24, p. 90-113.
- White, C. David, 1895, The Pottsville Series along New River, West Virginia: Geol. Soc. America Bull., v. 6, p. 305-320, 2 figs., 2 tables.
- 1900, The stratigraphic succession of the fossil floras of the Pottsville Formation in the southern anthracite coal field, Pennsylvania: U.S. Geol. Survey 20th Ann. Rept. pt. 2, p. 749-930, pls. 180-193.
- Wilmarth, M. G., 1938, Lexicon of geologic names of the United States: U.S. Geol. Survey Bull. 896, 2396 p.

131. NEW MEMBERS OF THE BLOYD FORMATION OF PENNSYLVANIAN AGE, WASHINGTON COUNTY, ARKANSAS

By LLOYD G. HENBEST, Washington, D.C.

The Bloyd Formation is the upper of two formations of the Morrow Series at its type locality in Washington County, Ark. The Brentwood Limestone Member (Ulrich, 1904), Kessler Limestone Member (Simonds, 1891), and the Woolsey Member (Henbest, 1953) were named during previous studies of the Morrow Series. Two marine shale members, which constitute two-thirds of the Bloyd sequence, remained unnamed.

In a field conference in 1961 with H. D. Miser and M. Gordon, of the U.S. Geological Survey, and with J. H. Quinn, University of Arkansas, it was agreed that the two shale members are mappable and useful in describing the geology of Washington County and that this writer would both name those two unnamed members and designate type sections for the previously named units of the Morrow.

The lithic composition, stratigraphic relations, and sedimentary structures of the Morrow Series are indicated in figure 131.1.

DYE SHALE MEMBER

The rocks of the Bloyd Formation that lie between the top of the terrestrial Woolsey Member and the base of the Kessler Limestone Member are here named the Dye Shale Member from a characteristic development in Bloyd Mountain, whose sides are partly drained by Dye Creek. The type locality of the Dye Member is here designated to coincide with the type locality of the Bloyd Formation as designated in Article 130; that is, from the E $\frac{1}{2}$ sec. 3 to the center of the north side of sec. 4, T. 14 N., R. 30 W.

The Dye Shale Member is widely distributed and mappable in Washington County. The Dye and the Trace Creek Shale Members are similar in composition. They are poorly exposed and are identified chiefly by their position relative to the Woolsey and the Kessler Members which have marked, lithic features. The extension of the Dye Shale Member westward into Oklahoma has not been determined because the bracketing units change into indistinct units.

Rapid lateral changes eastward, in the area where the Morrow has been removed by the White River, have introduced complications in tracing the Dye Shale Member as well as other Morrow units eastward from Washington County. With the exception of

fossils and of the coal bed, no lithic property or bedding structure in the Morrow Series or in the adjacent parts of the Atoka Series of Washington County is known to be exclusively characteristic of the unit in which it is found.

Especially good exposures of the Dye Shale Member, besides the type locality, are those in the hillside and railway cuts at the south edge of Brentwood, in the northeast part of Fayetteville in the SW $\frac{1}{4}$ NE $\frac{1}{4}$ SW $\frac{1}{4}$ sec. 10, T. 16 N., R. 30 W., and in slopes around Mount Sequoyah (formerly East Mountain), on the east side of Fayetteville.

The Dye Shale Member is 60 to 110 feet thick. By far the greater part of the member consists of dark-gray to black shaly siltstone and claystone. Thin lenticular limestone beds and calcareous zones are present here and there. Most of these are definitely recognizable as of marine origin. The remainder of the unit appears to be marine. The organic-matter and sulfide content of the Dye is rather low at most places. Deposition in shallow, rather poorly circulated, muddy sea water is evident.

The basal unit of the Dye Shale Member is informally called the "caprock of the Baldwin coal" by the writer. The caprock is widely distributed in Washington County. The caprock and the Baldwin coal in the underlying Woolsey Member are the most consistent and easily recognized markers in the Morrow Series of Washington County. The caprock ranges from 0 to 25 feet in thickness. It is conglomeratic; commonly consists mainly of calcareous sandstone; locally contains quartz gravel up to 14 mm across; commonly crossbedded; contains marine fossils; and commonly lies with erosional discordance on the underlying terrestrial beds of the Woolsey Member. It was the basal sediment of an advancing sea. The chocolate color of the caprock is a result of chemical weathering by acid from oxidation of sulfides in the underlying Baldwin coal and should not be interpreted as a deposit of subaerially weathered, reworked limestone. The caprock of the Baldwin coal has been confused at many localities with the Kessler Limestone Member by earlier workers.

With the exception of the caprock of the Baldwin coal, the Dye Shale Member generally forms a subdued topographic surface. Though the mineral composition of the Dye is favorable for soil formation, its impervi-

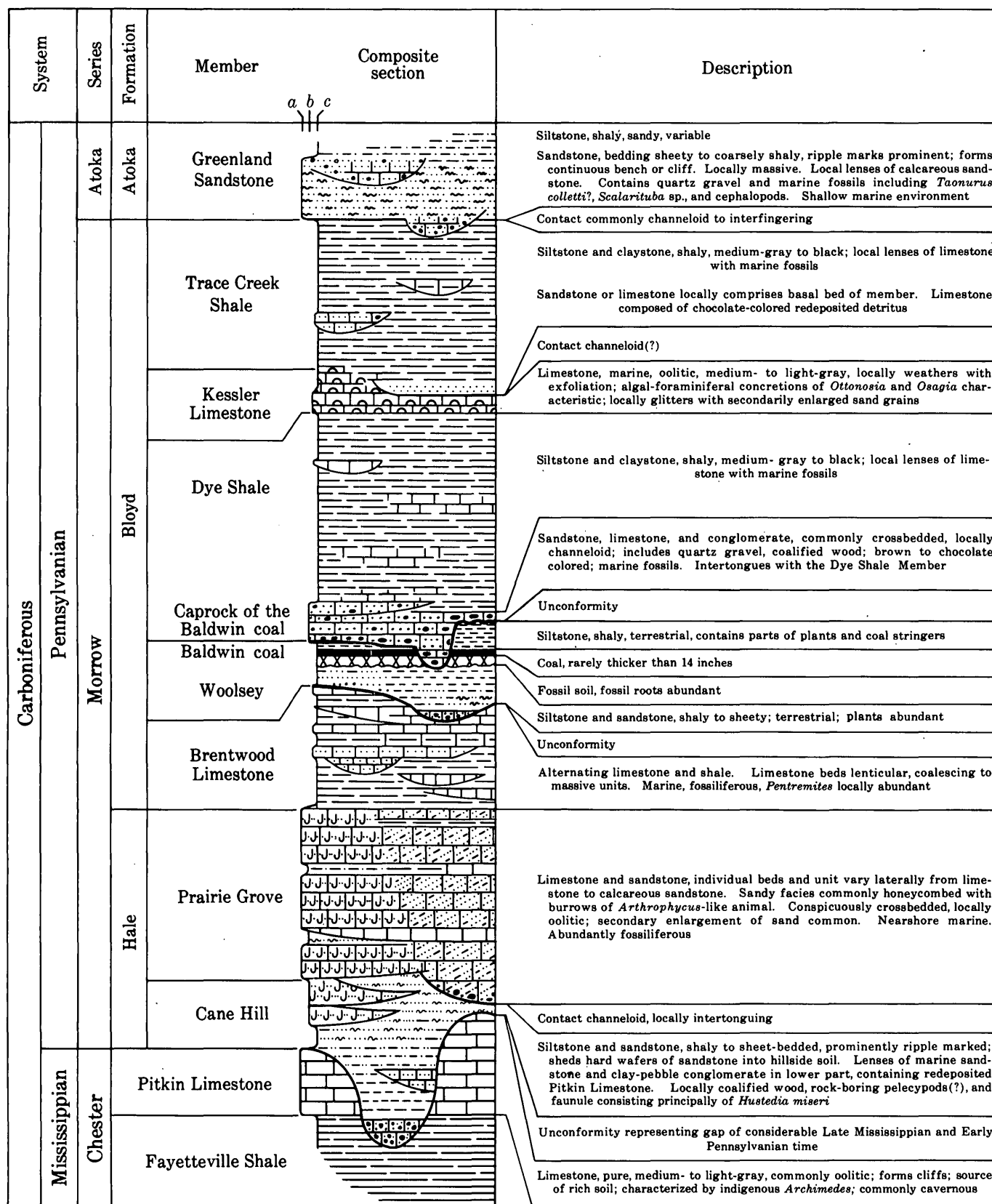


FIGURE 131.1.—Composite section of Morrow Series and adjacent rocks in Washington County, Ark. Topographic expression of rock units is shown on left side of column: *a*, forms prominent cliffs or rock-controlled surfaces; *b*, forms local cliffs or benches; and *c*, forms subdued surfaces. Vertical scale, 1 inch equals approximately 60 feet.

ousness to water and consequent low storage and circulation capacity promotes excessive drying during droughts. This generally results in poor vegetation cover or scrubby forest with glades, rapid erosion, and poor soil.

Fossils are scarce in the Dye Member. It is dated as of late Morrow age chiefly by its stratigraphic position. It directly overlies the well-known floral zone of the Baldwin coal of late middle or early late Pottsville age (White, 1895, 1900) and overlies the faunal zone of the Brentwood Limestone Member fauna, both of which are middle Early Pennsylvanian age. It underlies the Kessler Limestone Member, whose fauna is related to the Morrow assemblages (Ulrich, 1904, p. 110; Girty, 1905, p. 8; Mather, 1915, p. 67).

TRACE CREEK SHALE MEMBER

The rocks that lie between the top of the Kessler Limestone Member of the Bloyd Formation and the base of the Greenland Sandstone Member of the Atoka Formation are here named the Trace Creek Shale Member of the Bloyd Formation. The member is named from its development in Bloyd Mountain, whose slopes are partly drained by Trace Creek. Its type locality is here designated as congruent with that of the Bloyd Formation; that is, the southwest part of Bloyd Mountain from the center of the E $\frac{1}{2}$ sec. 3 to the center of the north side of sec. 4, T. 14 N., R. 30 W.

The Trace Creek Shale Member is widely distributed and mappable in Washington County. Though the Trace Creek Member probably extends both westward into the edge of Oklahoma and eastward from Washington County, its extensions outside Washington County are obscured by lateral changes in the Morrow Series. Besides the type locality, two especially characteristic exposures of the Trace Creek are found at the type locality of the Kessler Limestone Member near the center of the SE $\frac{1}{4}$ sec. 25, T. 16 N., R. 31 W., on the west side of a saddle formed by an erosional gap in the Greenland Sandstone Member of the Atoka Formation, which caps Kessler Mountain. This saddle is on the crest and near the north end of Kessler Mountain. The other locality is a half mile southeast of Brentwood Station. The localities cited above as characteristic for the Dye Shale Member are equally informative for the Trace Creek Shale Member.

The Trace Creek Shale Member is composed of marine dark-gray to black shaly siltstone and claystone with minor local, thin, calcareous zones, and limestone or calcareous sandstone lenses. Its thickness is generally 60 to 70 feet, but at the Kessler Mountain exposure cited above it is only 20 feet thick beneath the quartz gravelstone conglomerate of the Greenland Sandstone Member of the Atoka Formation. The maximum thickness of about 125 feet so far recognized is near the southwest corner of Washington County. The Trace Creek generally forms a subdued surface. It is impervious and commonly forms a poor soil with limited vegetation cover and scrubby forest with glades.

The Trace Creek Shale Member locally intergrades with the underlying Kessler Limestone Member. At some localities, however, the basal beds consist of medium-textured sandstone or chocolate-colored redeposited limestone derived from the Kessler. The stratigraphic relations with the Atoka vary from angular erosional contact with the Greenland Sandstone Member to possibly an interfingering with Atoka sediments. The Trace Creek has yielded few fossils and its age is determined principally by its position beneath the Atoka Series of Middle Pennsylvanian age and above the faunal zone of the Kessler Limestone Member of late Morrow age.

REFERENCES

- Girty, G. H., 1905, The relations of some Carboniferous faunas: Washington Acad. Sci. Proc., v. 7, p. 1-26.
- Henbest, L. G., 1953, Morrow Group and lower Atoka Formation of Arkansas: Am. Assoc. Petroleum Geology Bull., v. 37, p. 1935-1953, 2 figs.
- Mather, K. F., 1915, The fauna of the Morrow Group of Arkansas and Oklahoma: Denison Univ. Sci. Lab. Bull., v. 18, p. 59-284, 16 pl.
- Simonds, F. W., 1891, The geology of Washington County: Geol. Survey Arkansas Ann. Rept. 1888, v. 4, pt. 1, 154 p., 2 pls., unnumbered pls. and figs., geol. map.
- Ulrich, E. O., 1904, Determination and correlation of formations, in Adams, G. I., Ulrich, E. O., Purdue, A. H., and Burchard, E. H. Zinc and lead deposits of northern Arkansas: U.S. Geol. Survey Prof. Paper 24, p. 90-113.
- White, D. David, 1895, The Pottsville Series along New River, West Virginia: Geol. Soc. America Bull., v. 6, p. 305-320, 2 figs., 2 tables.
- 1900, The stratigraphic succession of the fossil floras of the Pottsville Formation in the southern anthracite coal field, Pennsylvania: U.S. Geol. Survey 20th Ann. Rept. pt. 2, p. 749-930, pls. 180-193.



132. THE EAGLE VALLEY EVAPORITE AND ITS RELATION TO THE MINTURN AND MAROON FORMATIONS, NORTHWEST COLORADO

By T. S. LOVERING and W. W. MALLORY, Denver, Colo.

Regional paleogeographic maps (Mallory, 1960, fig. 5) show that in Pennsylvanian and Early Permian time two elements of the ancestral Rocky Mountains, the Uncompahgre and the Front Range highlands, dominated the geography of Colorado. Between them was a basin of deposition, now called the Eagle or Maroon basin by local geologists, which is separate from the analogous Paradox basin of equivalent age on the southwest side of the Uncompahgre highland. The Minturn quadrangle, in which this study was made, is on the northeast flank of the Eagle (or Maroon) basin (fig. 132.1).

Most of the sedimentary rocks exposed in the Minturn quadrangle are of Pennsylvanian and Permian age. Coarse clastic rocks dominate the sequence, but siltstone and carbonate marker beds are common, and an evaporite section is present in the northwestern part of the quadrangle. The relation of the clastic sequence to the evaporite facies has posed a problem.

Two formations, the Minturn and the Maroon, comprise the coarse clastic facies. The Minturn Formation, about 6,000 feet thick (Tweto, 1949, p. 204), is primarily gray, tan, and dull maroon shale, sandstone, grit, and coarse conglomerate; shale is more abundant in the upper part. A few dolomite beds occur in the lower part of the formation, many limestones in the middle, and a few limestones in the upper part. Many of the carbonate beds abruptly change lithology along strike from nearly pure carbonate to grit or other clastic rocks containing little or no carbonate. Many of the limestones in the middle of the formation a few miles southeast of the town of Minturn contain porous dolomite reefs many times thicker than the bedded limestone a short distance away. At least the lower five-sixths of the Minturn Formation is of Des Moines age (Tweto, 1949, p. 205-206) as determined by the presence of abundant fossils in the thin limestone beds.

The overlying Maroon Formation, about 2,000 feet thick, is similar to the Minturn in lithology but contains much more siltstone. Its bright brick-red color contrasts with the dull purplish-red and grayish-tan colors of the Minturn. Except for some long-ranging plants, no fossils have been found in the Maroon Formation in the Minturn quadrangle, but its age is inferentially Pennsylvanian and Permian because it lies conformably upon the Minturn Formation of Des Moines and younger age and is overlain by the

Chinle Formation of Late Triassic age (Lovering and Tweto, 1944, p. 50).

Of critical significance in distinguishing the Minturn from the Maroon is the Jacque Mountain Limestone Member, designated by Tweto (1949, p. 204) as the uppermost member of the Minturn Formation. At its type locality on Jacque Mountain, 23 miles south-southeast of section J1 of this article (fig. 132.1D), the unit is 21 feet thick; at section J1 it is 27 feet thick. According to Tweto (written communication, Jan. 31, 1962) the lithology is strikingly similar in both localities and is divisible into three parts. The top 5 or 6 feet of the member at both localities is gray medium-grained oolitic limestone, locally sandy. Beneath this upper unit is a thin zone containing detrital material: a 2-foot calcareous red siltstone at Jacque Mountain, and a 2-foot cross-bedded biotite-rich pinkish limestone at section J1. The lower 20 feet of the member is gray limestone. The upper part of this lower unit is mottled pink and green, and is locally oolitic and fossiliferous; the lower part is dense to lithographic.

The lithologic homogeneity of the Jacque Mountain from its type locality to section J1 as mapped by Lovering and Tweto (1944) in the Minturn quadrangle is in sharp contrast to the facies changes observed when the bed is followed westward a short distance, as from section J1 to section J10 (fig. 132.1C). Maps and sections made by the writers in 1961 show that the 27-foot thickness of the Jacque Mountain Limestone Member at section J1 thickens to about 140 feet of strata of equivalent age but dissimilar lithology at J8 (the entire measured interval at J8). From section J1 to section J10, the Jacque Mountain Limestone Member splits into discrete tongues, and terminates a short distance west of J10. Many of the tongues thicken locally into small reefs or banks near their terminus in the evaporite facies (fig. 132.1C).

Because the Maroon and Minturn Formations have similar lithology, it is essential in mapping them that the Jacque Mountain Limestone Member or its recognizable equivalent be present. Fortunately, the member is easily traced in the Minturn quadrangle except in the northwestern part where the Jacque Mountain terminates in the evaporite sequence. Murray (1958, p. 52, and fig. 2) has indicated that the evaporite sequence exposed in the valley of the Eagle River between Minturn and Wolcott is equivalent in

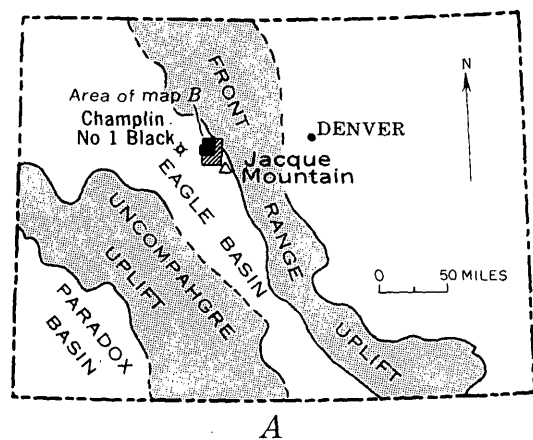
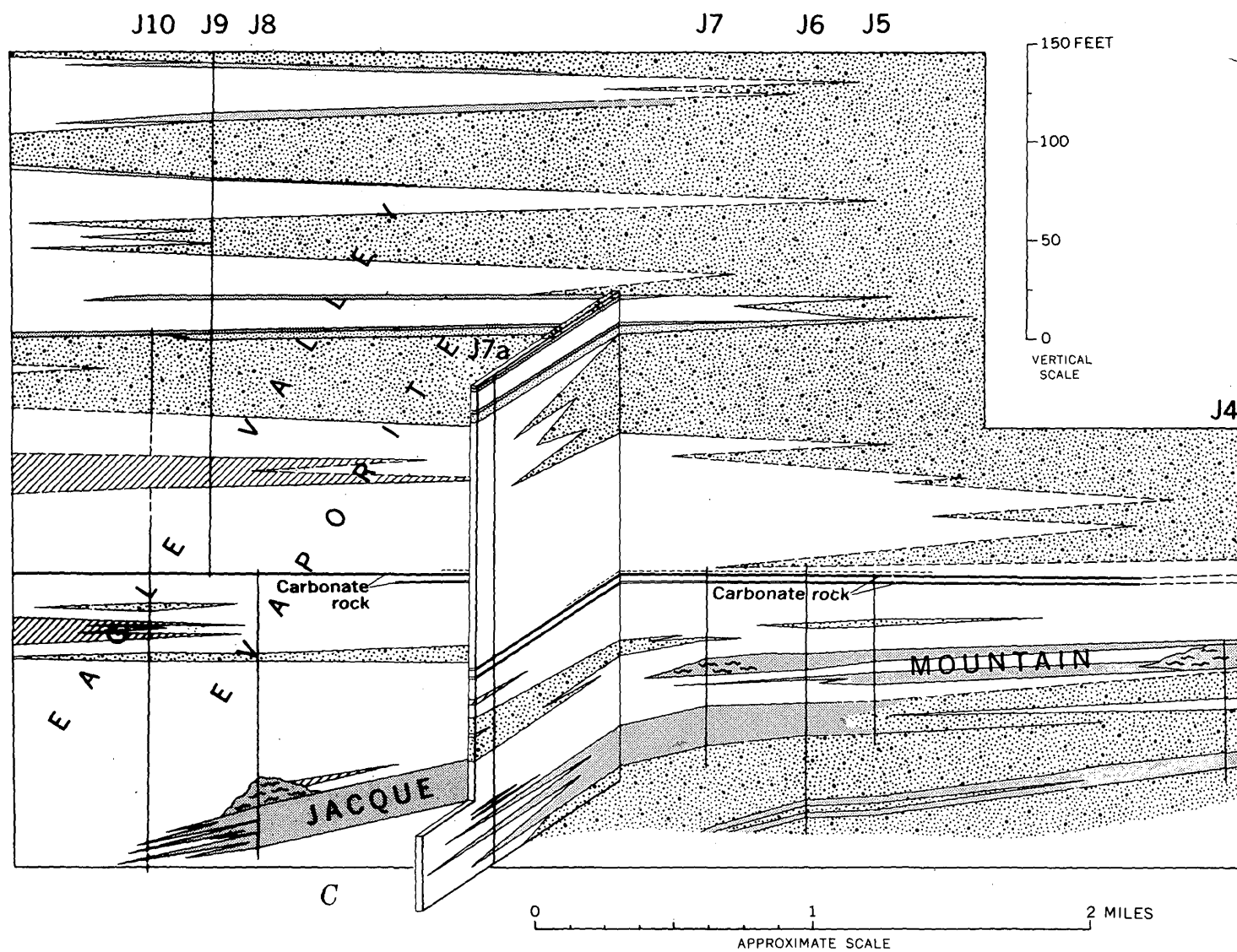
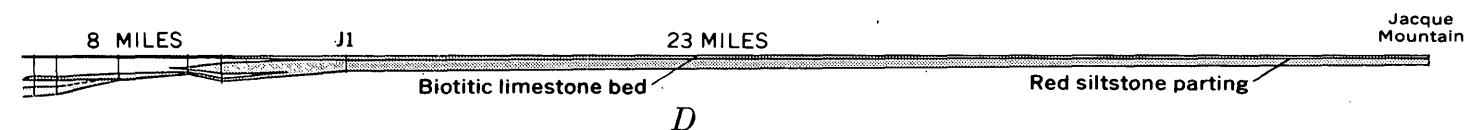
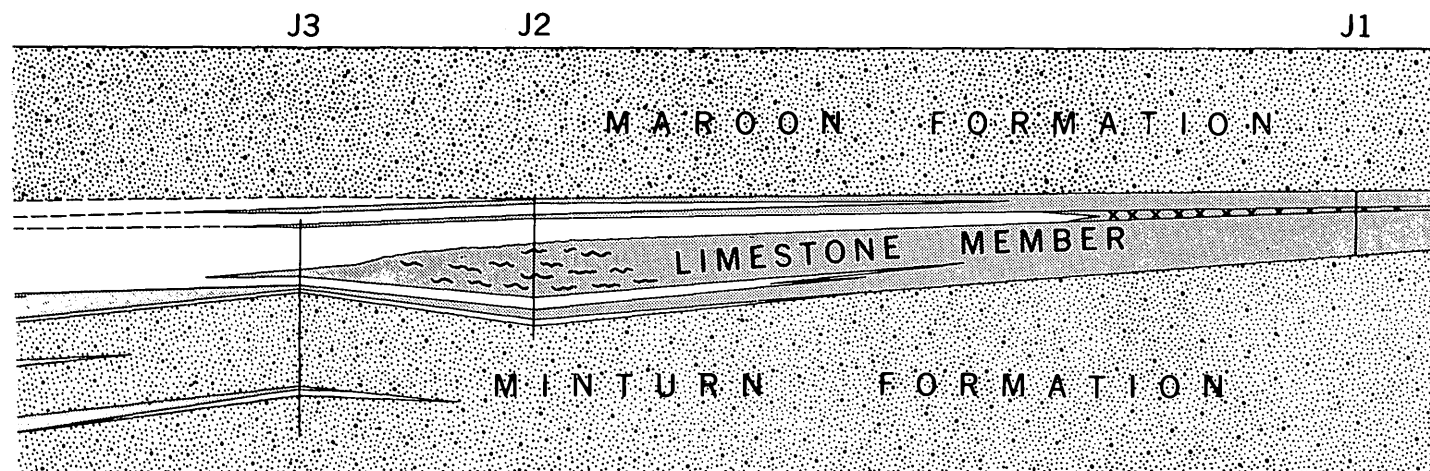
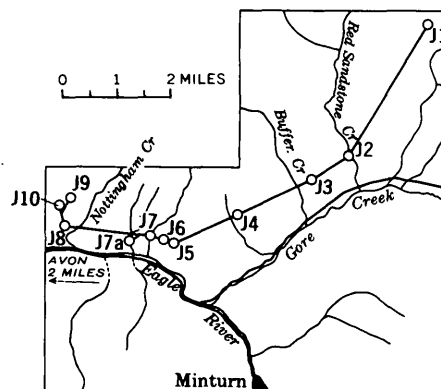
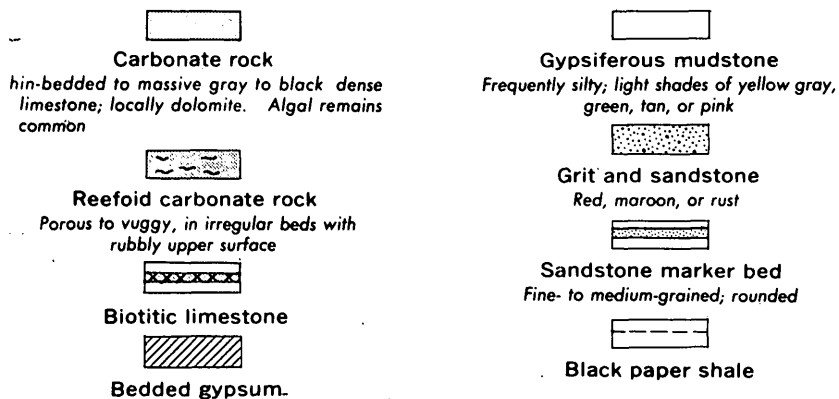


FIGURE 132.1.—A, Map of Colorado showing major paleogeographic features for Pennsylvanian time and location of the Minturn quadrangle, the Champlin No. 1 Black well, and Jacques Mountain. B, Part of the Minturn quadrangle, showing location of the measured sections. C, Stratigraphic section illustrating interrelation of the Eagle Valley, Maroon, and Minturn Formations, and Jacques Mountain Limestone Member of the Minturn Formation in the vicinity of Minturn, Colo. Actual measured intervals are shown by vertical lines; horizontal extensions of the section between and beyond measured intervals are reasonable interpolations consistent with general stratigraphy observed in the field. D, A small section with little vertical exaggeration showing regional variation in thickness of the Jacques Mountain Limestone Member.

EXPLANATION



age only to beds contained within the Minturn Formation, but field study shows that bedded gypsum and gypsiferous mudstones of the evaporite sequence inter-tongue with parts of both the Maroon and Minturn Formations. Because the Minturn and the Maroon Formations are not distinguishable as cartographic units in the evaporite sequence, the name Eagle Valley Evaporite is here proposed for the gypsiferous sequence exposed in Eagle Valley of the Eagle River in the vicinity of Avon, Colo. The sequence extends from Tracer Creek about a mile northwest of the mouth of Gore Creek, to Red Canyon about 9 miles west-northwest.

The type section is established as measured sections J8 and J9 on the interfluvial west of Nottingham Creek, north side of Eagle River, in secs. 6 and 7, T. 5 S., R. 81 W., Eagle County, Colo. The Eagle Valley Evaporite in this area is predominantly gypsiferous mudstone and siltstone, usually light colored, which contains bedded gypsum and a few cherty dark gray limestone beds about 1 foot thick. Also included are beds of reddish shale and siltstone. The formation forms smoothly rounded slopes partly covered by a veneer of slump detritus owing to the soft, easily weathered character of the rock. The topographic expression and color of the Eagle Valley Evaporite

contrasts strongly with the brighter colors and massive ledges of the Minturn and Maroon Formations into which it tongues. At the type locality the lower part of the formation is covered by alluvium of the Eagle River, and the upper part is in brush or aspen-covered slopes where its contact with an overlying tongue of Maroon Formation is obscure. Farther west the gypsiferous sequences are thicker, contain more bedded gypsum, and may have a definite top and base, but the type area is chosen near Avon because here the age and the relation of the Eagle Valley Evaporite to the Maroon and Minturn Formations and the Jacque Mountain Limestone Member can be demonstrated.

In Red Canyon, red gypsiferous siltstone beds of the Eagle Valley Evaporite are conformably overlain by the Chinle Formation of Triassic age; the siltstones merge with the uppermost Maroon Formation to the northeast and lie upon dull-colored or gray gypsiferous mudstones and bedded gypsum.

The Eagle Valley Evaporite dips west at Red Canyon and extends an indefinite distance west and northwest into the central part of the Eagle basin. Near Eagle, Colo., about 16 miles west of Avon, 4,700 feet of evaporite-bearing rocks occur in a well, the Champlin No. 1 Black (sec. 4, T. 5 S., R. 84 W.). These rocks are anhydritic gypsiferous mudstone and siltstone with abundant halite casts and some bedded halite. At the surface the rocks are red gypsiferous clastics that have been identified as the Maroon For-

mation. Evaporite-bearing strata are present from the surface down to the top of the Belden Shale, which regionally underlies the Minturn Formation. Evidence in the Black well and at Red Canyon therefore suggests that west of the type area the Eagle Valley Evaporite is the time equivalent of all of the Minturn Formation and much of the Maroon Formation.

The regional evidence indicates that while coarse clastics of the Minturn and Maroon Formations were being deposited near the shores of the trough by waters ranging in salinity from fresh or brackish to normal marine, salts of the Eagle Valley Evaporite were precipitating from supersaline brines a few miles offshore in more rapidly subsiding parts of the trough.

REFERENCES

- Lovering, T. S., and Tweto, O. L., 1944, Preliminary report with map on geology and ore deposits of the Minturn quadrangle, Colorado: U.S. Geol. Survey open-file report, 115 p.
- Mallory, W. W., 1960, Outline of Pennsylvanian stratigraphy of Colorado, in *Guide to the geology of Colorado*: Geol. Soc. America, jointly with Rocky Mtn. Assoc. Geologists and Colorado Sci. Soc., p. 23-33.
- Murray, H. F., 1958, Pennsylvanian stratigraphy of the Maroon Trough, in *Symposium on Pennsylvanian rocks of Colorado*: Rocky Mtn. Assoc. Geologists, p. 47-57.
- Tweto, O. L., 1949, Stratigraphy of the Pando area, Eagle County, Colorado: *Colorado Sci. Soc. Proc.*, v. 15, no. 4, p. 149-235.



133. JURASSIC STRATIGRAPHY IN THE MCCARTHY C-5 QUADRANGLE, ALASKA

By E. M. MacKEVETT, JR., and R. W. IMLAY, Menlo Park, Calif., and Washington, D.C.

Previously undescribed fossiliferous Jurassic marine sedimentary rocks having a cumulative thickness of more than 9,000 feet are well exposed in the McCarthy C-5 quadrangle, Alaska, where they were mapped by MacKevett and M. C. Blake, Jr., during 1961. Provisional field identifications of fossils by D. L. Jones, of the U.S. Geological Survey, facilitated the mapping, and paleontologic studies by Imlay determined the geologic ages of the Jurassic rocks.

The 15- by 22½-minute McCarthy C-5 quadrangle is in rugged terrain having a relief in excess of 11,000 feet on the southern flank of the Wrangell Mountains, about 200 miles east of Anchorage (fig. 133.1).

Moffit (1938), during his extensive reconnaissance mapping in the general region, recognized only two small patches of Jurassic rocks within the McCarthy C-5 quadrangle, and he grouped most of the Jurassic rocks with Cretaceous rocks or with the McCarthy Shale of Late Triassic age.

The nearest exposed Jurassic sequence that has been mapped in detail is in the Talkeetna Mountains A-1, A-2, and B-1 quadrangles in the Nelchina area, about 150 miles northwest of McCarthy (fig. 133.1). Grantz (1960a, b) described this fossiliferous Jurassic section as being over 15,000 feet thick and consisting of Lower Jurassic submarine volcanic and sedimentary rocks, Middle Jurassic nearshore sandstone, and Upper Jurassic siltstone, sandstone, and conglomerate.

The Jurassic rocks in the McCarthy C-5 quadrangle consist of fossiliferous shelf strata of Early, Middle(?), and Late Jurassic age. These rocks occupy a belt as much as 10 miles wide that extends northward across the quadrangle (fig. 133.2). Most of the rocks dip northward at low angles, but locally they form open folds. Faults that cut the Jurassic strata commonly strike northward, are nearly vertical, and have apparent right-lateral displacement.

The Jurassic rocks consist of a conformable sequence that appears to overlie the McCarthy Shale of Late Triassic age conformably, and is unconformably overlain by Cretaceous marine sedimentary rocks or by Tertiary continental and lacustrine sedimentary rocks that are intercalated with the basal part of the Wrangell Lava. A hiatus separates the rocks of Early Jurassic age from younger Jurassic rocks, and other gaps probably occur within the Jurassic sequence despite the apparent conformity of the stratigraphic succession.

The Lower and Middle(?) Jurassic strata, which constitute about a third of the Jurassic section, consist chiefly of limestone and shale. The overlying thick Upper Jurassic sequence consists dominantly of shale but locally contains sandstone and conglomerate in its higher part.

Five Jurassic units are delineated on the map (fig. 133.2), and a summary of the lithology, the indicated geologic age, and the stratigraphic range of the important fauna of the Jurassic rocks is shown in figure 133.3. The lowermost of these, J1, is composed of light- to medium-brown-weathering silty limestone and shale, contains mollusks of Sinemurian age, and overlies the evenly bedded McCarthy Shale, which weathers dark brown. This unit is overlain by a distinctive sandy and silty limestone unit, J1s, that contains abundant fossils of the Early Jurassic pectenid *Weyla*. Prof. S. W. Muller, of Stanford University, has examined several of the *Weylas* and believes that they are indicative of a Pliensbachian (Early Jurassic) age (oral communication, 1961). The unit forms bold outcrops and is an excellent marker that is traceable across the quadrangle.

These Lower Jurassic rocks are locally overlain by reddish-brown shale and limestone, Js, that contain diagnostic ammonites indicative of a Middle(?) or possibly an early Late Jurassic age.

A widespread unit composed mainly of shale, Jsh,

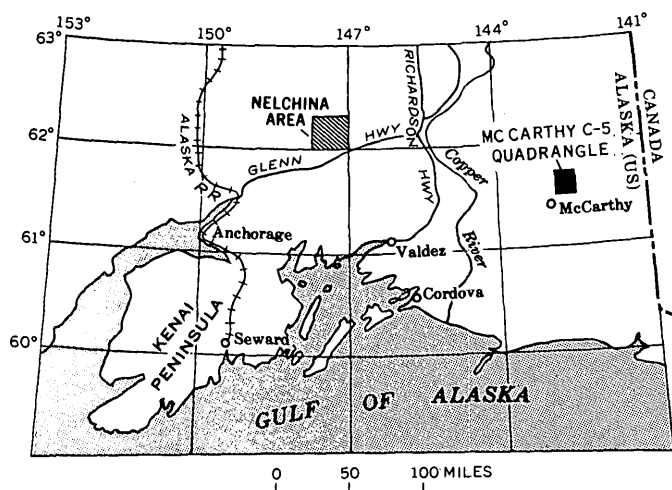
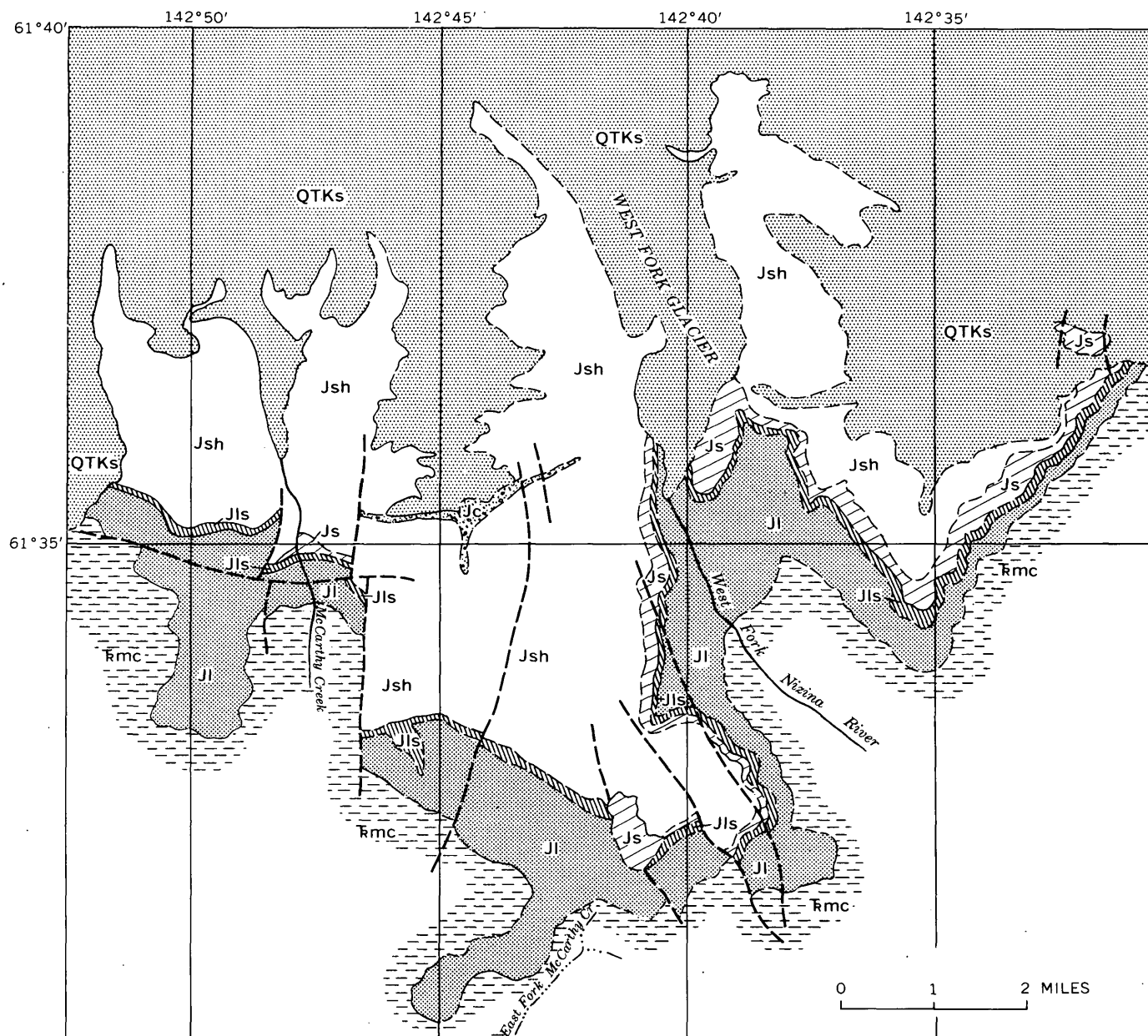


FIGURE 133.1.—Index map of part of Alaska showing the location of the McCarthy C-5 quadrangle.



EXPLANATION

Contact
Dashed where approximately located

Fault
Dashed where approximately located

FIGURE 133.2.—Generalized geologic map showing the distribution of Jurassic rocks in the McCarthy C-5 quadrangle. QTKs, Sedimentary and volcanic rocks, Cretaceous or Tertiary, and surficial deposits, Quaternary; Jsh, shale, and Js, conglomerate, Upper Jurassic; Js, shale and limestone, Middle(?) and Upper Jurassic; Jls, limestone, and Jl, limestone and shale, Lower Jurassic; rmc, McCarthy Shale, Upper Triassic.

LITHOLOGY	Cretaceous or Tertiary rocks	THICKNESS (FEET)	APPROXIMATE RANGE OF CHARACTERISTIC FOSSILS	STAGE	SERIES
Mainly dark-gray shale	Jsh		<i>Belemnites</i>		
Conglomerate	Jc	0-650	<i>Buchia rugosa</i> (Fisher)		
Interbedded conglomerate sand stone and shale					
Mainly dark-gray shale that weathers brown, subordinate limestone, siltstone, and lime- stone concretions	Jsh	5000	<i>Buchia concentrica</i> (Sowerby) <i>Buchia mosquensis</i> (Von Buch) <i>Partschiceras</i> sp. <i>Amoeboceras</i> (<i>Priondoceras</i>) sp.	Kimmeridgian and Oxfordian	Upper Jurassic
Red-brown shale and silty limestone	Jls	0-1000	<i>Reineckeia</i> ?, <i>Kheraiceris</i> ? sp. <i>Procerites</i> ? sp., <i>Inoceramus</i> cf. <i>I. ambiguus</i> Eichwald	Early Callovian and Bathonian(?)	Middle(?) and Upper Jurassic
Mainly silty limestone, minor coquina	Jls	150-300	<i>Weyla</i> sp., <i>Gryphaea</i> sp., <i>Chlamys</i> sp. <i>Crucillobiceras</i> sp.	Pliensbachian	
Gray silty limestone and limestone intercalated with dark-gray shale	Jls	1500-2300	<i>Entolium</i> (?) <i>semiplicatum</i> (Hyatt) <i>Psiloceratacid ammonites</i> <i>Arnioceras</i> sp.	Sinemurian and Hettangian(?)	Lower Jurassic

McCarthy Shale
(Triassic)

FIGURE 133.3.—Generalized columnar section and descriptions of Jurassic rocks in the McCarthy C-5 quadrangle. Letter symbols in the lithologic section are explained in the caption for figure 133.2.

directly overlies either the shale and limestone unit (Js) or the subjacent limestone unit (Jls) with apparent conformity. It contains abundant *Buchias* and a few diagnostic ammonites. Brown-weathering sandstone that occurs high in the upper shale unit is locally transitional into a pebble or cobble conglomerate, Jc (figs. 133.2, 133.3). An angular unconformity marks the contact between the Jurassic and the Cretaceous or Tertiary rocks.

REFERENCES

- Grantz, Arthur, 1960a, Geologic map of Talkeetna Mountains (A-2) quadrangle, Alaska, and the contiguous area to the north and northwest: U.S. geol. Survey Misc. Geol. Inv. Map I-313.
- 1960b, Geologic map of Talkeetna Mountains (A-1) quadrangle and the south third of Talkeetna Mountains (B-1) quadrangle, Alaska: U.S. Geol. Survey Misc. Geol. Inv. Map I-314.
- Moffit, F. H., 1938, Geology of the Chitina Valley and adjacent area, Alaska: U.S. Geol. Survey Bull. 894, 137 p.



134. SOME LATE CRETACEOUS STRAND LINES IN SOUTHERN WYOMING

By A. D. ZAPP and W. A. COBBAN, Denver, Colo.

Eastward withdrawal of the sea across most of southern Wyoming during the Campanian Stage was interrupted by several partial readvances of the sea, as recorded by superposition of tongues of marine strata on tongues of nonmarine strata. The larger regressive-transgressive cycles so recorded are described in this article, and the strand-line positions indicated by the seaward and landward limits of the tongues are shown on figure 134.1.

This is a brief progress report on a field investigation begun in August 1961; the work thus far has not included subsurface studies. A similar report on a comparable investigation in the adjoining area to the south was published earlier by the authors (Zapp and Cobban, 1960).

Gratitude is expressed to H. J. Hyden for the use of certain unpublished data in the area near the town of Rock River.

For purposes of this study, the rocks were classified broadly into marine and nonmarine facies, with two subfacies distinguished in each category. The general lithology and the geographic and stratigraphic distribution of these facies, and their relation to named stratigraphic units, are summarized on figure 134.2. The fossil zones are numbered to correspond to those used in the area to the south (Zapp and Cobban, 1960, fig. 112.2); zone F9 of this report includes zones F9 and F10 of the earlier report.

The strata exhibit considerable variation in thickness of time-equivalent units. For example, the zones of *Baculites perplexus* and *Baculites eliasi* are separated by about 1,000 feet of strata in the northeastern part of the area; in the Rawlins area the stratigraphic separation is twice as great. We attribute such variation in thickness to differential subsidence during sedimentation.

Extreme depositional thinning and some local truncation of beds beneath Cretaceous unconformities obscure the normal transgressive-regressive relations in the area northwest of the town of Lamont (fig. 134.2, sections 6-8). Time-equivalent strata that are normally separated by more than 4,000 feet of strata, as at locality 8 (figs. 134.1, 134.2), are virtually in contact at locality 6. The strata comprising the Mesaverde Formation at locality 7 similarly wedge out almost completely in a westward direction—by depositional thinning and perhaps partly by truncation—about $4\frac{1}{2}$ miles west of locality 7. About 4 miles

west of locality 7, in the south half of sec. 36, T. 27 N., R. 90 W., a pronounced unconformity is evident in the rocks lower in the stratigraphic section. Approximately the upper two-thirds of a sequence of about 1,000 feet of massive sandstone and siltstone pinches out eastward as a result of truncation before deposition of an overlying shale unit. The rocks above and below the unconformity are of marine origin, indicating submarine planation. The extreme local tectonic differentiation apparent in the Lamont area is, to the knowledge of the authors, unique in the predominantly marine facies of the Cretaceous rocks of western interior United States. Pronounced local thinning of the Mesaverde Formation in this area was first pointed out by Fath and Moulton (1924, p. 27).

The oldest regressive-transgressive cycle here enumerated is that reflected in the Rock Springs Formation and correlative strata (figs. 134.1 and 134.2, R_1 and T_1). Actually it consists of more than one cycle, as the sea margin oscillated within a rather narrow belt during the accumulation of more than 1,000 feet of strata. An extraordinary thickness of massive marine sandstones was formed in the seaward portion of this belt of oscillation, and a short distance seaward from the seaward margin.

Present evidence suggests that the Rock Springs regressive-transgressive cycle is represented along the Book Cliffs in east-central Utah by the regressive Kenilworth coal zone of the Blackhawk Formation and the overlying marine-transgressive middle shale member of the Blackhawk Formation (Fisher, 1936, pl. 7, col. 1). This indicates that the strand line trended approximately S. 25° W. from the southern margin of figure 134.1 across the Uinta Basin in Utah. Also, the Rock Springs regressive deposits are at least approximately equivalent to the most seaward nonmarine rocks of the Menefee Formation of the type Mesaverde Group in the San Juan Basin of southwestern Colorado and northwestern New Mexico. The nonmarine rocks of the Menefee Formation wedge out along a line that trends about N. 60° W. across the northeastern part of the San Juan Basin (Zapp, 1949).

Following the upper Rock Springs transgression (T_1), the sea retreated—perhaps with minor readvances—about 80 miles eastward (R_2), then readvanced about 20 to 30 miles (T_2). The regressive and transgressive phases of this cycle are direct correlatives of the Castlegate-Rim Rock regression and the

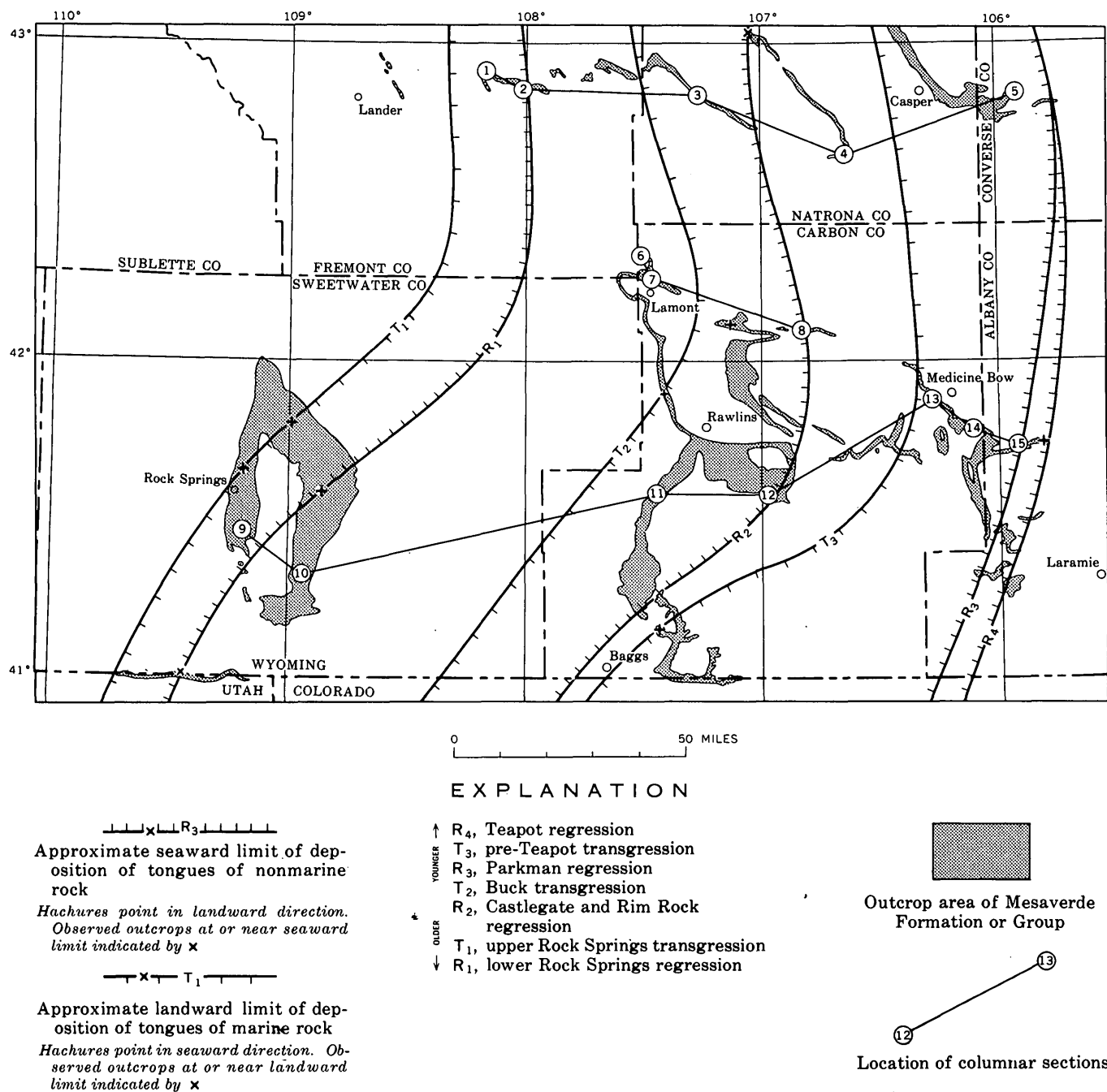


FIGURE 134.1.—Map of part of southern Wyoming, showing location of columnar sections (fig. 134.2), and general location and trend of certain regressive and transgressive strand lines during part of Late Cretaceous time, as inferred from outcrop studies.

Buck transgression, respectively, of the area to the south (Zapp and Cobban, 1960), so the previous nomenclature is retained in this article. The strata of the transgressive phase in both areas have yielded species of *Baculites* referable to the zone of *Baculites perpleurus* Cobban.

The sea margin then retreated to a point approximately midway between points 12 and 13 on figure

134.1. There, exposures in the northwestern part of Halleck Ridge show eastward lateral replacement by marine rocks of the lower 300 feet of the nonmarine part of the Mesaverde Formation. The sea margin oscillated within a belt a few miles wide during the deposition of these rocks. This feature is similar in stratigraphic position and relations to the lower Iles regressive-transgressive cycle in Colorado (Zapp and

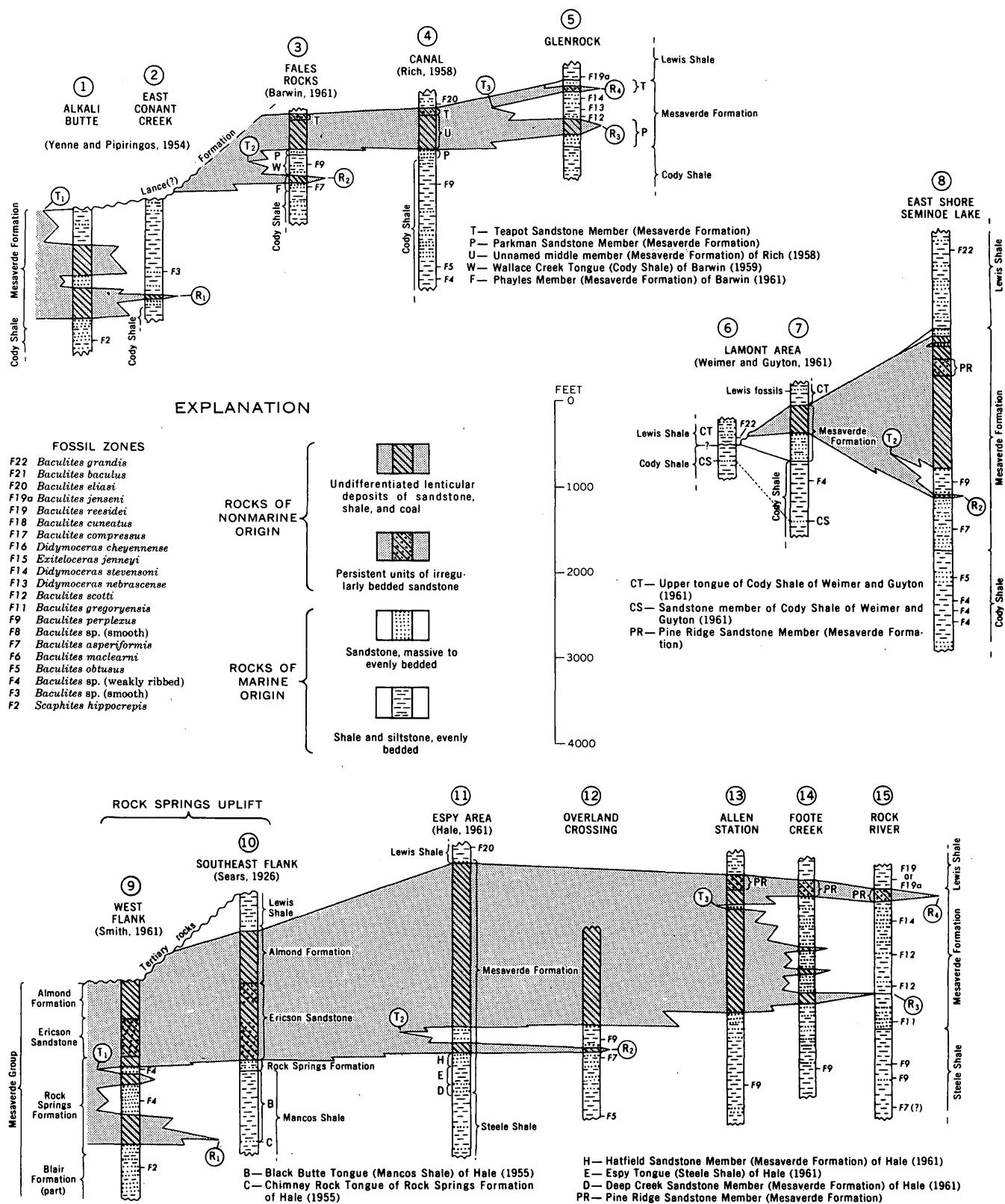


FIGURE 134.2.—Generalized columnar sections of the Mesaverde Formation and adjacent rocks in part of southern Wyoming, showing distribution of facies and correlation of named stratigraphic units. For location of sections and explanation of T's and R's, see figure 134.1. Sections are modified after the authors cited.

Cobban, 1960). The strand line at this time is not shown on figure 134.1.

This was followed by retreat of the strand line to the position of the Parkman regression (R_3) as shown on figure 134.1. The Parkman regression is comparable in stratigraphic position to the middle Iles-Palisade regression of the area to the south (Zapp and Cobban, 1960) but may be slightly older.

The sea margin then readvanced, with several subordinate oscillations, to the position shown as the pre-Teapot transgression (T_3) on figure 134.1. This is the approximate or exact equivalent of the upper Iles-lower Mount Garfield transgression of the area to the south (Zapp and Cobban, 1960). A marine tongue exposed about 14 miles northeast of Baggs (fig. 134.1) is now believed to be a product of this transgression; previously (Zapp and Cobban, 1960, loc. Y), it was thought to represent a later transgression.

The sea margin then retreated to a position near the east edge of the area, and this is termed the Teapot regression (R_4). It is correlated with the lower Williams Fork-lower Bowie regression of Colorado (Zapp and Cobban, 1960). The Teapot regression is marked in the Medicine Bow area by the Pine Ridge Sandstone Member and associated coaly rocks. The Pine Ridge Sandstone Member is extensively exposed in the area between Rawlins and Lamont, and in that area it resembles the Ericson Sandstone of the Rock Springs area. The Pine Ridge Sandstone may represent a tongue of the upper part of the Ericson Sandstone.

The Teapot regression was followed by extensive readvance of the sea and by deposition of the thick marine Lewis Shale. In the southern part of the area this advance of the sea margin exceeded 150 miles, to the vicinity of Rock Springs. In the northern part of the area, the transgression was less than half as extensive, and was interrupted by a major regressive movement (Rich, 1958, p. 2442).

The marine Lewis Shale, at least east of the longitude of Baggs, includes the time equivalent of the upper Williams Fork regressive tongue of Colorado (Zapp and Cobban, 1960). That tongue has not been recognized in Wyoming.

REFERENCES

- Barwin, J. R., 1959, Facies of the Mesaverde Formation: Am. Assoc. Petroleum Geologists, Rocky Mtn. Sec., 1959 Geological Record: p. 139-142.
- , 1961, Stratigraphy of the Mesaverde Formation in the southern part of the Wind River Basin, Wyoming, in Wyoming Geol. Assoc. Guidebook 16th Ann. Field Conf., Green River, Washakie, Wind River, and Powder River Basins, 1961: p. 173.
- Fath, A. E., and Moulton, G. F., 1924, Oil and gas fields of the Lost Soldier-Ferris district, Wyoming: U.S. Geol. Survey Bull. 756, p. 27.
- Fisher, D. J., 1936, The Book Cliffs coal field in Emery and Grand Counties, Utah: U.S. Geol. Survey Bull. 852, p. 13, pl. 7.
- Hale, L. A., 1955, Stratigraphy and facies relationships of the Montanan Group in south-central Wyoming, northeastern Utah, and northwestern Colorado, in Wyoming Geol. Assoc. Guidebook 10th Ann. Field Conf., Green River Basin, 1955: p. 90-92.
- , 1961, Late Cretaceous (Montanan) stratigraphy, eastern Washakie Basin, Carbon County, Wyoming, in Wyoming Geol. Assoc. Guidebook 16th Ann. Field Conf., Green River, Washakie, Wind River, and Powder River Basins, 1961: p. 130, 131, 133.
- Rich, E. I., 1958, Stratigraphic relation of latest Cretaceous rocks in parts of Powder River, Wind River, and Big Horn Basins, Wyoming: Am. Assoc. Petroleum Geologists Bull., v. 42, no. 10, p. 2442.
- Sears, J. D., 1926, Geology of the Baxter Basin gas field, Sweetwater County, Wyoming: U.S. Geol. Survey Bull. 781-B, pl. V.
- Smith, J. H., 1961, A summary of stratigraphy and paleontology, Upper Colorado and Montanan Groups, south-central Wyoming, northeastern Utah, and northwestern Colorado, in Wyoming Geol. Assoc. Guidebook 16th Ann. Field Conf., Green River, Washakie, Wind River, and Powder River Basins, 1961: pl. I.
- Weimer, R. J., and Guyton, J. W., 1961, Geology of the-Muddy Gap-Lamont area, Wyoming, in Wyoming Geol. Assoc. Guidebook 16th Ann. Field Conf., Green River, Washakie, Wind River, and Powder River Basins, 1961: p. 143.
- Yenne, K. A., and Pipiringos, G. N., 1954, Stratigraphic sections of Cody shale and younger Cretaceous and Paleocene rocks in the Wind River Basin: U.S. Geol. Survey Oil and Gas Inv. Chart OC-49.
- Zapp, A. D., 1949, Geology and coal resources of the Durango area, La Plata and Montezuma Counties, Colorado: U.S. Geol. Survey Oil and Gas Inv. Prelim. Map 109.
- Zapp, A. D., and Cobban, W. A., 1960, Some Late Cretaceous strand lines in northwestern Colorado and northeastern Utah: Art. 112 in U.S. Geol. Survey Prof. Paper 400-B, p. B246-B249.

135. TERTIARY VOLCANIC AND RELATED ROCKS OF THE REPUBLIC AREA, FERRY COUNTY, WASHINGTON

By SIEGFRIED MUESSIG, Los Angeles, Calif.

A thick sequence of Tertiary volcanic rocks and related sedimentary and intrusive rocks were found during recent mapping (Muessig and Quinlan, 1959) to underlie large parts of the Republic and the eastern half of the Aeneas quadrangles (fig. 135.1). These rocks include flows, tuffs, breccias, intrusive bodies, and lake beds; their composition ranges from rhyodacite to basalt. With the exception of the intrusives, these rocks are confined to the large northeast-trending Republic graben (fig. 135.1) that occupies the greater part of the Republic quadrangle and part of the Aeneas quadrangle.

This sequence is here divided into four new formations. From oldest to youngest these are the O'Brien Creek Formation, Sanpoil Volcanics, Scatter Creek

Rhyodacite, and Klondike Mountain Formation. All have been traced northward into the adjacent Curlew quadrangle, and all except the Klondike Mountain have been traced southward into adjacent quadrangles.

O'BRIEN CREEK FORMATION

The basal Tertiary formation in the Republic area is the O'Brien Creek Formation, which consists largely of water-laid tuff and some conglomerate; it is here named for typical exposures along the North Fork of O'Brien Creek, the type section (fig. 135.1). The O'Brien Creek Formation underlies most of the Republic graben but crops out principally along the sides of the graben, although some outcrops are near its center in the northern part of the Republic quad-

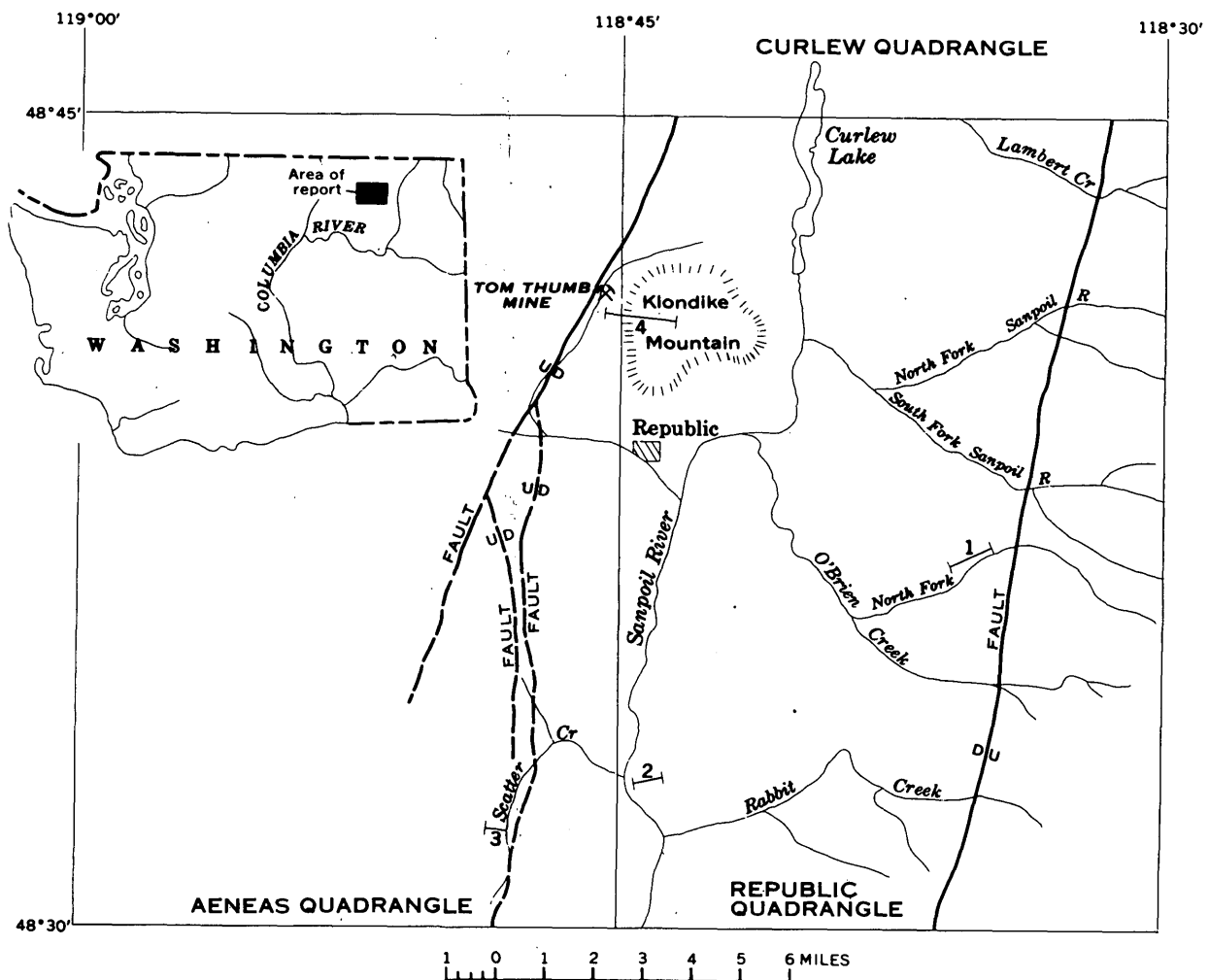


FIGURE 135.1.—Index map of the Republic area showing type localities of the four new formations: (1) O'Brien Creek Formation, (2) Sanpoil Volcanics, (3) Scatter Creek Rhyodacite, and (4) Klondike Mountain Formation.

range. Here the O'Brien Creek unconformably overlies metamorphosed sedimentary rocks of Paleozoic age.

A complete section of the O'Brien Creek Formation is nowhere exposed; hence, the total thickness of this formation cannot be determined accurately. Both the lithology and thickness of the formation differ from place to place. Along the east side of the graben north of the North Fork of the Sanpoil River the formation is at least 4,200 feet thick, and 7 miles south of here at the south edge of the Republic graben it is 2,300 feet thick. On the west side of the graben along Scatter Creek, 1,350 feet of the formation is exposed.

The greater part of the O'Brien Creek Formation consists of a white to greenish-white water-laid crystal tuff. Crystal fragments, 1 to 4 mm in diameter, make up as much as 70 percent of this rock. Plagioclase, quartz, and orthoclase crystals are the major constituents, but biotite, sericite, sphene, apatite, calcite, magnetite, and pyrite are present in minor amounts. This crystal tuff commonly contains a few rock fragments that range from a fraction of an inch to several inches in diameter. Locally the fragments constitute as much as 30 percent of the rock. These fragments are characteristically chips of phyllite or argillite, with minor more equidimensional clasts of greenstone, quartzite, and granitic rocks. The matrix is ash.

Two other types of rock occur locally in this formation. One is dark fine-grained water-laid tuff that resembles shale. In some places this tuff contains carbonized plant debris and in one place to the east of Curlew Lake it contains several thin beds of lignite. The other rock type is boulder conglomerate, beds of which have been found both in the upper and lower parts of the formation. In some places the boulders are mainly argillite, phyllite, and schist, and in other places they are mainly quartz monzonite and granodiorite.

Plant fossils from the dark tuff east of Curlew Lake were reported by R. W. Brown to be Eocene(?) in age. The O'Brien Creek Formation is thus assigned an Eocene(?) age. The formation is roughly correlative with the Kettle River Formation of Daly (1912), which is found to the north in British Columbia; it is the dacite flow conglomerate of Umpleby (1910) and the breccia-conglomerate of Lindgren and Bancroft (1914).

SANPOIL VOLCANICS

The Sanpoil Volcanics is a thick sequence of rhyodacite and quartz latite flows and minor tuff and flow breccia that conformably overlies the O'Brien Creek Formation and unconformably underlies the Klondike

dike Mountain Formation. This formation is here named after the Sanpoil River valley, whose walls are carved in this unit for many miles south of Republic. The type locality is 7 miles south of Republic. The Sanpoil has the most extensive exposures of any rock unit in the graben, and south of Republic the outcrops are nearly continuous from one side of the graben to the other. The base of the Sanpoil is placed at the base of the first flows that overlie the water-laid tuffs of the O'Brien Creek Formation.

The Sanpoil Volcanics, like the O'Brien Creek Formation, varies in thickness from place to place. The formation is approximately 4,000 feet thick on the east side of Klondike Mountain.

The greater part of the Sanpoil Volcanics is made up of light-gray to black, brown-weathering rhyodacite or quartz latite flows. These flows commonly form prominent outcrops that in places show prominent flow banding. The rhyodacite or quartz latite is a porphyritic rock with the phenocrysts generally making up less than 50 percent of the rock. The mafic minerals, hornblende and biotite, make up about 60 percent of the phenocrysts. Plagioclase (An_{35-65}) constitutes most of the remaining 40 percent. Augite and hypersthene are present in some flows. Accessory minerals include apatite, magnetite, sphene, leucoxene, zircon, and calcite. The groundmass consists of partly devitrified brown glass.

Locally, fine-grained light-yellowish-brown tuffs are found interbedded with the flows. Rock fragments in the tuffs are few and are generally glass.

Flow breccias crop out along the Sanpoil River in the southern part of the area. They consist of numerous brown angular pieces of rhyodacite as much as 8 inches across in a matrix of similar material.

Fossils were not found in the Sanpoil Volcanics, but it is herein assigned an Eocene(?) age; it underlies the Klondike Mountain Formation, which contains Oligocene fossils, and overlies the O'Brien Creek, which contains probable Eocene fossils.

SCATTER CREEK RHYODACITE

The name Scatter Creek Rhyodacite is here given to the widespread porphyritic intrusive rocks that are younger than the O'Brien Creek Formation but older than the Klondike Mountain Formation. The name comes from Scatter Creek in the southeastern part of the Wauconda quadrangle, where excellent exposures of this rock occur at the type locality along the road leading up this creek (fig. 1). The greater part of the Scatter Creek is found in the graben along its east and west margins, although some Scatter Creek intrusives occur outside the graben. The Scatter Creek cuts metamorphosed sedimentary rocks of Permian

age, quartz monzonite of Cretaceous age, the O'Brien Creek Formation, and in a few places the Sanpoil Volcanics. It forms dikes, sills, or irregular intrusive bodies. The Scatter Creek in part closely resembles some of the flows of the Sanpoil Volcanics. Although in a few places the intrusive relations between these two rocks are clear cut, in other places the two appear to grade into one another.

The Scatter Creek Rhyodacite is a light-gray to dark-greenish-gray, brown-weathering porphyritic rock. Phenocrysts have an average length of about 1 mm and consist principally of plagioclase (An_{30-45}), and of hornblende and biotite, which are in a few places altered to chlorite, sphene, calcite, and epidote. Augite, sanidine, and quartz are also present in some places. Accessory minerals include magnetite, apatite, and zircon. The groundmass is generally partly devitrified glass. Although the greater part of the Scatter Creek is rhyodacite, quartz latite is common and several other rock types also occur.

This formation is probably of about the same age as the Sanpoil Volcanics, although part of it at least is younger than the older part of the Sanpoil. It is herein assigned an Eocene or Oligocene age.

KLONDIKE MOUNTAIN FORMATION

The name Klondike Mountain Formation is here given to the volcanic rocks that unconformably overlie the Sanpoil Volcanics and the Scatter Creek Rhyodacite; the volcanic rocks are the youngest in the Republic area. The name comes from Klondike Mountain, north of Republic, whose top and western slope, herein designated the type locality, are underlain by pyroclastic rocks and flows of this formation. The Klondike Mountain is divided into three members: (1) a lower member of mostly fine-grained water-laid tuff, (2) a middle member of coarse pyroclastic rocks, and (3) an upper member of basalt flows. The lower member is well known for excellent plant fossils that have been found in it, and because of this importance is here named the Tom Thumb Tuff Member after the Tom Thumb mine, $3\frac{1}{2}$ miles north of Republic (fig. 135.1).

The Klondike Mountain Formation crops out in a fairly narrow band along the west side of the graben from about 3 miles south of Republic northward into the adjoining Curlew quadrangle. The outcrop area of the Tom Thumb Tuff Member is much more limited in extent and is not found more than 5 miles north of Republic. An angular unconformity separates the formation from the underlying Sanpoil Volcanics. The base of the formation is placed at the base of a thin volcanic breccia at the bottom of the Tom Thumb,

or where this member is not present, at the base of the thick volcanic breccia that elsewhere is the middle member of the formation. An angular unconformity also separates the Tom Thumb from the middle member; the upper two members are apparently conformable.

The thickness of the members varies from place to place. The Tom Thumb has a maximum thickness of about 1,900 feet 2 miles northwest of Republic; it thins abruptly, and is absent a little more than a mile to the east of this point. The middle member is about 800 feet thick, and the upper member is 200 feet thick on Klondike Mountain. In the adjoining Curlew quadrangle both members are much thicker.

The Tom Thumb Member consists of two units. The basal unit is volcanic breccia, conglomerate, and tuff. This unit has both rounded and angular volcanic fragments as much as several feet across in a fine- to coarse-grained tuffaceous matrix. Overlying this and making up the greater part of the member is a fine-grained well-sorted water-laid light-tan to orange tuff that contains abundant plant debris.

The middle member consists of buff coarse volcanic breccias made up of angular fragments of porphyritic latite, as much as several feet in diameter, in a tuffaceous matrix. This member also contains a few olive-gray to buff basalt flows.

The upper member is a brownish-black porphyritic basalt. The phenocrysts are principally labradorite with some phenocrysts of augite, hypersthene, and olivine. These are set in a groundmass containing abundant microlites of andesine, augite, and magnetite.

Numerous fossil plants have been found in the Tom Thumb Member. These have been dated as Oligocene by R. W. Brown (1959, p. 127). The formation is accordingly assigned an Oligocene age. However, the middle and upper members of the Klondike Mountain may be younger than Oligocene.

REFERENCES

- Brown, R. W., 1959, A bat and some plants from the upper Oligocene of Oregon: *Jour. Paleontology*, v. 33, p. 125-129.
- Daly, R. A., 1912, Geology of the North American Cordilleran at the forty-ninth parallel: *Canada Geol. Survey Mem.* 38, p. 2, 857 p.
- Lindgren, Waldemar, and Bancroft, Howland, 1914, The Republic mining district, in Bancroft, Howland, The ore deposits of northeastern Washington: *U.S. Geol. Survey Bull.* 550, p. 133-166.
- Muessig, S. J., and Quinlan, J. J., 1959, Geologic map of the Republic and part of the Wauconda quadrangles, Washington: *U.S. Geol. Survey open-file report*.
- Umpleby, J. B., 1910, Geology and ore deposits of the Republic mining district: *Washington Geol. Survey Bull.* 1, 65 p.

136. GEOLOGY OF TERTIARY ROCKS IN ESCAMBIA AND SANTA ROSA COUNTIES, WESTERN FLORIDA

By OWEN T. MARSH, Waynesville, N.C.

Work done in cooperation with the Florida Geological Survey, Escambia County, Santa Rosa County, and the city of Pensacola

This summary of the geology of Escambia and Santa Rosa Counties, Fla. (fig. 136.1), is based primarily on samples from and electric logs of 60 oil test holes and 13 deep water wells. The fossils were identified by S. M. Herrick, Ruth Todd, Druid Wilson, and Estella Leopold, of the U.S. Geological Survey; G. A. Cooper, of the U.S. National Museum; and H. S. Puri, of the Florida Geological Survey. The stratigraphic units are described below in ascending order.

STRATIGRAPHY

The Hatchetigbee Formation, the youngest formation of the Wilcox Group (lower Eocene) in westernmost Florida, consists chiefly of gray silty micaceous clay and averages 315 feet in thickness (fig. 136.2). It also contains some glauconitic shale, siltstone, and shaly limestone. Fossils include foraminifers, corals, echinoids, and abundant mollusks.

The Tallahatta Formation (Claiborne Group, mid-

dle Eocene) is of variable lithology, consisting mostly of hard light-gray calcareous shale and siltstone with numerous beds of gray limestone and poorly sorted sand. It averages 255 feet in thickness. Foraminifers and a few gastropods are present.

In the Florida panhandle (Puri and Vernon, 1959, p. 42) and southern Escambia County, Ala. (Winter, 1954, p. 127), a thick section, predominantly of limestone, has been correlated with the Lisbon Formation of middle Eocene age. In the western part of the panhandle this sequence is chiefly a grayish shaly glauconitic limestone with some shale and averages about 500 feet in thickness. This section is so different from the Lisbon at its type locality in Alabama that, pending further study, it is referred to here as the Lisbon Formation equivalent. The basal part of the Lisbon equivalent is locally rich in glauconite and phosphate. About 40 species of foraminifers, as well as a few ostracodes, echinoids, worm tubes, and other fossils of middle Eocene age were identified from the formation.

The Ocala Limestone (Jackson Group, upper Eocene) underlies the western panhandle at depths ranging from 290 to 1,940 feet below sea level. The Ocala averages 165 feet in thickness within the area and thickens eastward across the panhandle. The formation is a light-gray to chalky-white limestone composed mainly of foraminifers, mollusks, corals, echinoids, and other fossils. More than 60 species of foraminifers were identified.

Unconformably overlying the Ocala Limestone is the Bucatunna Clay Member of the Byram Formation (Vicksburg Group, middle Oligocene). The Bucatunna averages 125 feet in thickness in Escambia and Santa Rosa Counties but thins eastward and pinches out about 32 miles east of the area (Marsh, 1962, p. 246). The Bucatunna is a dark-gray soft silty to sandy clay. Although it contains few fossils, 26 species of foraminifers were identified.

The Chickasawhay Limestone (upper Oligocene) and Tampa Limestone (lower Miocene) cannot be distinguished lithologically in the western panhandle except in a few places and are therefore shown in figure 136.2 as undifferentiated. The Chickasawhay consists of gray vesicular limestone and dolomitic limestone with some light-brown dolomite. Fragments of these rocks have a characteristic knobby texture. The Tampa Limestone is hard, light gray to

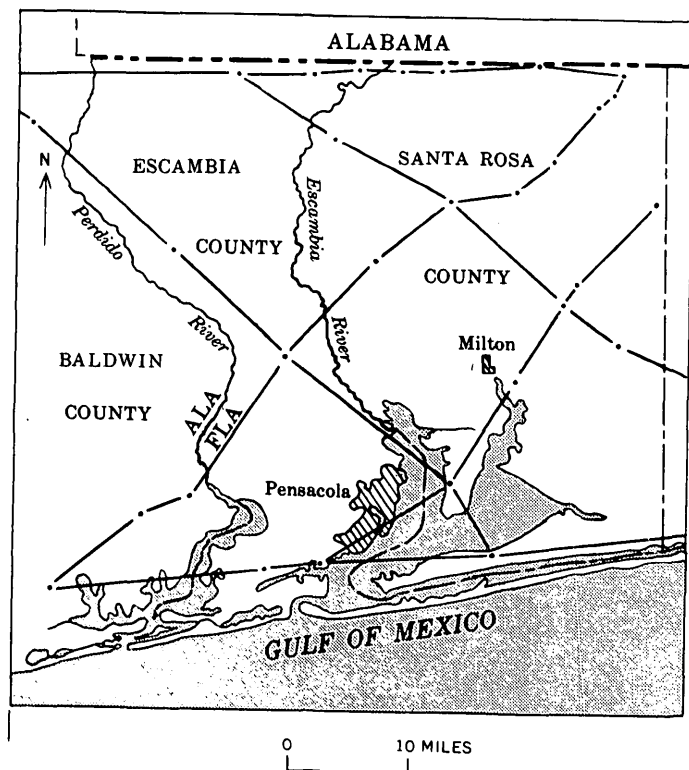


FIGURE 136.1.—Map of Escambia and Santa Rosa Counties, Fla., showing location of fence diagram in figure 136.2. Dots show location of wells.

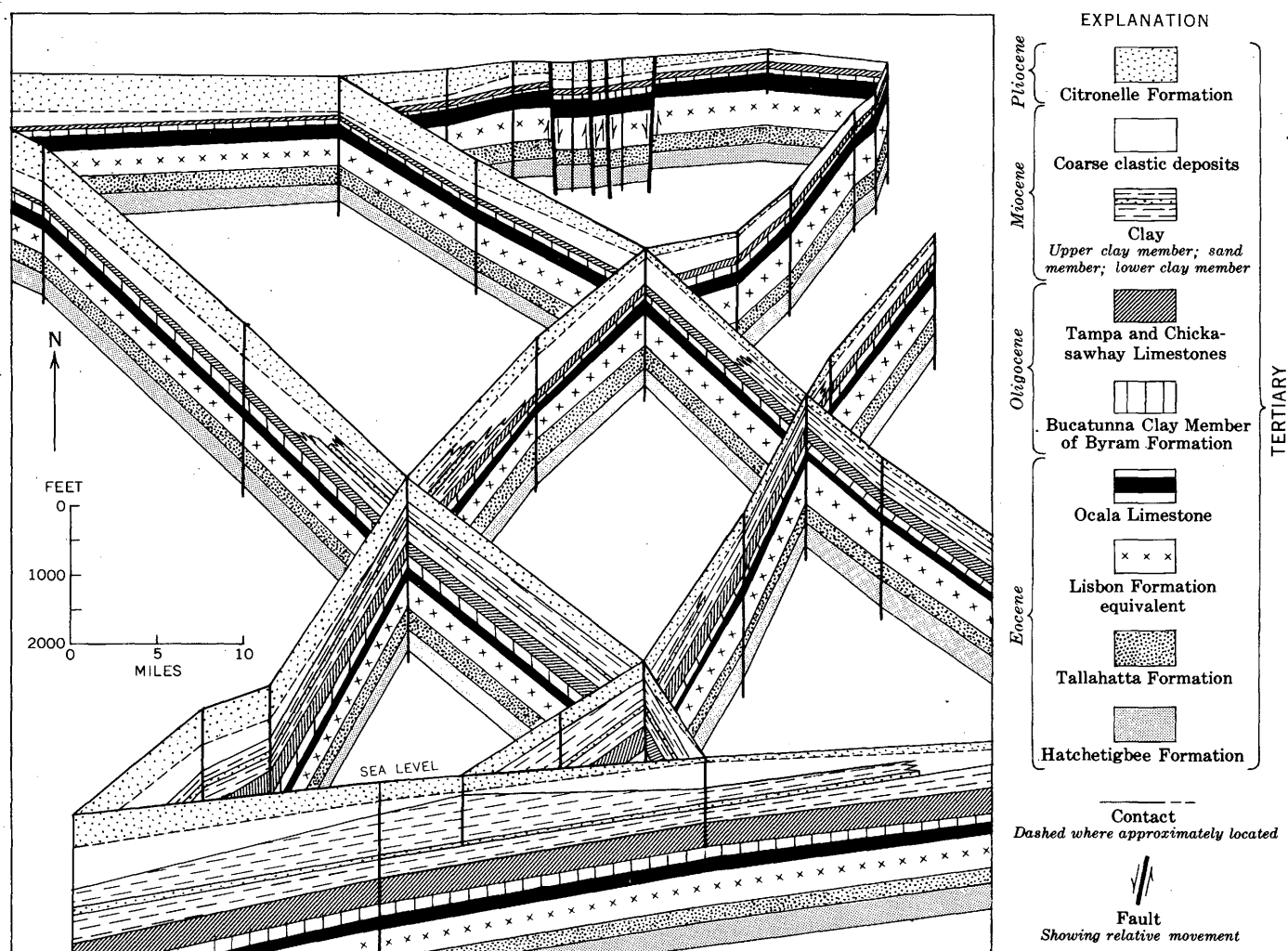


FIGURE 136.2.—Fence diagram of geologic formations in Escambia and Santa Rosa Counties, Fla., and Baldwin County, Ala. Datum is mean sea level. Contacts are generalized and beds above sea level are omitted. Short vertical lines are water wells; long vertical lines are oil test holes.

grayish white, and is generally not dolomitic. It is less vesicular and contains more clay than the Chickasawhay. The Chickasawhay Limestone underlies the entire area and thickens from about 30 to 130 feet toward the Gulf of Mexico. The Tampa, however, is present only in the southern half of the area, where it has a maximum thickness of 270 feet. Both formations contain diagnostic foraminifers; in addition, 10 species of mollusks were identified from the Tampa.

A new stratigraphic unit of middle Miocene age overlies the Tampa and Chickasawhay Limestones. The unit comprises a lower member and an upper member, each composed of tough gray sandy clay, separated by a thin bed of sand (fig. 136.2). In Escambia and Santa Rosa Counties the Miocene clay unit ranges from about 380 to 980 feet in thickness. A few miles north of Pensacola the clay interfingers

with unnamed coarse clastic deposits of the same age, discussed in the next paragraph. The lower member terminates 28 miles east of the area, where it is unconformably overlain by the Citronelle Formation; the upper member terminates in southeastern Santa Rosa County by interfingering with the unnamed coarse clastic deposits. Thus, the Miocene clay is wholly confined to the subsurface. The clay is micaceous and contains carbonized plant remains. In places, thick beds of mollusk shells occur near the top of the upper member. Sixty-four species of foraminifers were identified from the formation.

A thick sequence of brown to gray very fine to very coarse pebbly sand and gravel rests upon the Miocene clay in the southern part of the area and upon the Chickasawhay Limestone in the northern part. Pending further study, these beds are referred to by the

Florida Geological Survey as "unnamed coarse clastics." The unit contains lenses of carbonaceous clay and siltstone as much as 180 feet thick. Beds of minute mollusk shells are found throughout the coarse clastic deposits and serve to distinguish these beds from the Citronelle Formation. Diagnostic mollusks and foraminifers date the coarse clastics as chiefly middle Miocene, although at four localities late Miocene fossils were found.

The Citronelle Formation of Pliocene age is lithologically similar to the unnamed coarse clastics except for the virtual absence of shells in the Citronelle. The exact thickness of the Citronelle in westernmost Florida is uncertain because it is capped by lithologically similar marine terrace deposits of Pleistocene age. However, the formation probably ranges from about 40 to about 800 feet in thickness. Layers of sand cemented by iron oxides are common in the Citronelle, and in the upper part, thin zones of charcoal are found. Samples of logs penetrated by wells at depths of 50 to 200 feet have a fresh appearance that suggests they are thousands rather than millions of years old. Quaternary pollen, identified by Estella Leopold in samples of the Citronelle collected by the writer, suggests a possible Pleistocene age for the formation. Other fossils include mollusk shells in well samples from depths of 20 to 300 feet, and locally abundant kaolinite tubes that were probably the burrows of aquatic animals.

STRUCTURE

A northwestward-trending graben (fig. 136.2) enters the area from Alabama on the north. In Florida it is bounded on the west by the Jay fault (not previously recognized) and on the east by the Foshee fault. The Pollard and South Pollard faults within the graben have lesser offsets. At the Pollard oil field, 2 miles north of the area, oil is produced from structural traps along some of these faults (Winter, 1954, p. 126). Recurrent movement on all these faults, contemporaneous with deposition of the beds, took place over many millions of years. This caused the beds on the downthrown side of each fault to be thicker than the corresponding beds on the upthrown side, thus the throw increases with depth. The ultimate cause of the graben faulting may have been withdrawal of support by lateral flowage of salt at great depths beneath the area. The Mississippi salt dome basin, a southeastward-trending concentration of salt dome, lies only 32 miles to the northwest and trends directly toward the western Florida panhandle.

REFERENCES

- Marsh, O. T., 1962, Relation of Bucatunna Clay Member (Byram Formation, Oligocene) to geology and ground water of westernmost Florida: *Geol. Soc. America Bull.*, v. 73, p. 243-252.
- Puri, H. S., and Vernon, R. O., 1959, Summary of the geology of Florida and a guidebook to the classic exposures: *Florida Geol. Survey Spec. Pub.* 5, 255 p.
- Winter, C. V., Jr., 1954, Pollard field, Escambia County, Ala.: *Gulf Coast Assoc. Geol. Soc. Trans.*, v. 4, p. 121-142.



137. STRATIGRAPHY AND HYDROLOGY OF THE JUANA DÍAZ FORMATION IN THE YAUCO AREA, PUERTO RICO

By I. G. GROSSMAN, San Juan, Puerto Rico

Work done in cooperation with the Commonwealth of Puerto Rico

Reconnaissance geologic mapping for a water-resources investigation in southwestern Puerto Rico included an area of about 50 square miles extending east from Yauco to Guayanilla and south to the Caribbean Sea. The northwestern part, covering about 15 square miles near Yauco (fig. 137.1), produced new stratigraphic information of hydrologic significance.

The northern part of the mapped area is underlain by a complex of Cretaceous igneous, sedimentary, and metamorphic rocks. South of the complex, clastic sedimentary rocks of the Juana Díaz Formation of middle Oligocene age are exposed in an east-trending belt. Still farther south is an east-trending belt of the Ponce Limestone of Oligocene and Miocene age (Zapp and others, 1948).

The name Juana Díaz was first used as a local term by Berkey (1915), who estimated the beds to be about 3,000 feet thick. Mitchell (1922), who made the first geologic map of southwestern Puerto Rico, used the name for a formation estimated to be only 750 feet thick. Zapp and others (1948) subdivided the formation into three members: an upper shale member about 460 feet thick, a middle member of sandy limestone and limy shale about 1,230 feet thick, and a lower member of sandy conglomerate about 460 feet thick. They suggested that the main basin of deposition was in the eastern part of the belt of exposure near Santa Isabel, about 30 miles east of Yauco, because the oldest clastic rocks were believed to be confined to that area. Slodowski (1956, p. 107) recognized two comparatively large areas of clastic rocks at Yauco separated by a thin belt of Quaternary surficial deposits, which he mapped as the Juana Díaz and Ponce Formations, undifferentiated.

The present study indicates that a sizeable basin filled with clastic rocks of the Juana Díaz extends from south of Palomas northward about 2.8 miles. The basin may also extend southward from Palomas, but it is covered by the overlying Ponce Limestone. Faulted Juana Díaz crops out as far as 2.5 miles southeast of Palomas (not shown on map). Northwest of Palomas the Juana Díaz ends abruptly just outside the west boundary of the area of figure 137.1, where the formation is in contact with the Cretaceous rocks. To the east the bedrock is covered by alluvial

sediments of the Rio Yauco, but beds of the Juana Díaz crop out on the east side of the river, in a belt about a mile wide, near the east boundary of the area.

Northwest of Yauco a striking basal conglomerate of the Juana Díaz is made up of abundant ellipsoidal

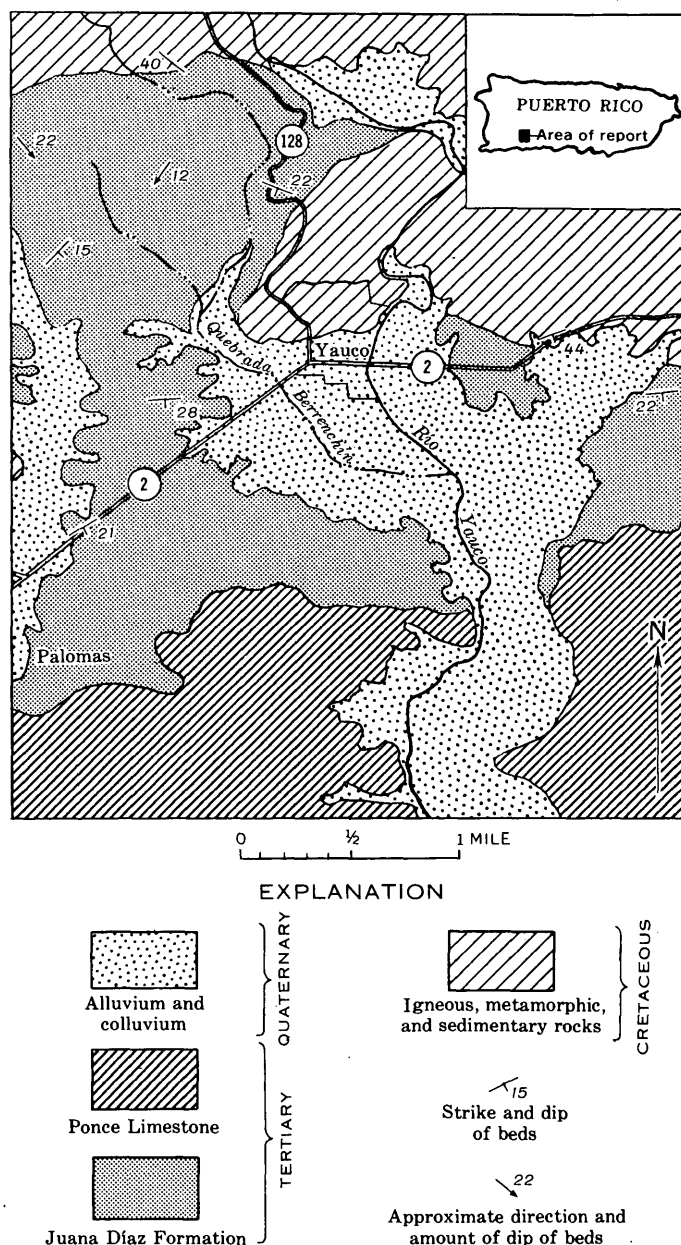


FIGURE 137.1.—Geologic map of the Yauco area.

boulders and large cobbles of hard Cretaceous rocks. This is overlain west of Yauco by cobble and pebble conglomerate, which in turn is overlain southwest of Yauco by sandstone and pebble conglomerate. In general the coarsest materials are to the north and the finest to the south, although there is considerable interbedding. Slodowski (1956) assigned this sequence to the lower and middle members of the Juana Díaz Formation. The present study indicates that lithologically most of it belongs to the lower member.

The Juana Díaz Formation strikes generally east-west and dips gently about 10° – 28° S. The regional dip of the Cretaceous rocks is also south, but the dips are commonly steeper. The beds in the northeastern part of the basin dip southwestward, and those in the northwestern part dip southeastward. Although the observations are few, they indicate that the long axis of the basin is approximately north-south.

The Juana Díaz was computed to be at least 4,000 feet thick along a line extending northward from near Palomas, by conservatively assuming an average dip of 15° . Possibly this great thickness is only apparent, resulting from unrecognized duplication of the section or reversal of dip, owing to faulting or folding. Indeed, the present investigation has disclosed faulting of the Juana Díaz and adjacent units with appreciable displacement in the central San Francisco area, about 2.5 miles southeast of Palomas (not shown on map). However, the relatively uniform dip and gradation in grain size suggest that the beds near Yauco are relatively undisturbed.

If detailed investigation confirms the estimated thickness of the conglomerate at Yauco and its assignment to the lower member of the Juana Díaz Formation, the composite maximum thickness, when the middle and upper members are added, may be 5,500 feet. The three members do not attain their maximum thickness at any one place however. In fact, the lower member may be a fresh-water or brackish-water deposit, as suggested by the embayed shape and orientation of the axis of the basin near Yauco, which is perpendicular to the east-trending Cretaceous source area to the north. The formation does not thicken eastward along the south coastal

plain of Puerto Rico as formerly believed (Zapp and others, 1948). Rather, the maximum thickness is probably near Yauco, where the occurrence of coarser clastic rocks requires revision of the older notion that these are confined to the eastern type area near Juana Díaz.

The intergranular spaces of the conglomerate are filled with sand and finer material, and the poor sorting results in low porosity and permeability. A well drilled for water in a lowland about halfway between Palomas and Yauco penetrated about 75 feet of clastic rocks of the Juana Díaz but yields only about 5 gallons per minute. The water is so highly mineralized that it is unsuitable for human consumption and is used for stock only. The poor chemical quality suggests slow circulation of ground water. The few wells tapping the Juana Díaz Formation elsewhere in Puerto Rico are generally on hillsides, hence it has been difficult to determine whether their low yields result from the impermeable character of the formation or from their unfavorable topographic location. If this example is typical, lithology is a more important influence on yield than topography. By contrast, a well tapping alluvium just south of Yauco yields several hundred gallons per minute of potable water which is used for irrigation. The higher yield and lower mineralization are due to better sorting of the alluvial sand and gravel, looser packing, and lack of cementing material. The resulting higher permeability affords better opportunity for recharge from surface water in Quebrada Berrenchín. The Juana Díaz Formation is thus a relatively unproductive aquifer even at Yauco, where it seems to attain its maximum known thickness.

REFERENCES

- Berkey, C. P., 1915, Geological reconnaissance of Porto Rico: New York Acad. Sci. Annals, v. 26, p. 13.
- Mitchell, G. J., 1922, The geology of the Ponce District, Porto Rico: New York Acad. Sci., Sci. Survey of Porto Rico and the Virgin Islands, v. 1, pt. 3, p. 229–300.
- Slodowski, T. R., 1956, Geology of the Yauco area, Puerto Rico: Princeton Univ. and Industrial Lab., Puerto Rico Admin. de Fomento, 130 p.
- Zapp, A. D., Bergquist, H. R., and Thomas, C. R., 1948, Tertiary geology of the coastal plains of Puerto Rico: U.S. Geol. Survey Oil and Gas Inv. Prelim. Map 85, sheet 2.



138. PYROCLASTIC DEPOSITS OF RECENT AGE AT MOUNT RAINIER, WASHINGTON

By DWIGHT R. CRANDELL, DONAL R. MULLINEAUX, ROBERT D. MILLER; and MEYER RUBIN:
Denver, Colo.; Washington, D.C.

A study of surficial deposits in Mount Rainier National Park has led to the recognition of six distinctive layers of relatively light-colored pyroclastic debris on the flanks of Mount Rainier volcano, and on neighboring slopes of the Cascade Range. On slopes and ridgetops the layers locally are included in deposits totaling less than 6 feet in thickness. In terrace deposits in the valleys, however, the layers may be separated by tens of feet of debris flows and alluvium.

Only two of these ash layers are known to have originated at Mount Rainier. Two other pyroclastic layers become progressively coarser and thicker toward Mount St. Helens, 50 miles to the south-southwest. These layers merge with the two sheets of pumice northeast of Mount St. Helens described by Carithers (1946, p. 16), who recognized that they were erupted by Mount St. Helens and were carried as far as Mount Rainier.

The six layers are light colored and are prominent and individually distinctive. Because they were initially deposited over wide areas and are still locally preserved, they are useful for subdividing, correlating, and dating Recent surficial deposits.

Study of the Recent pyroclastic deposits near Mount Rainier began during investigation of the Osceola Mudflow, and most of these six light-colored layers were described briefly in a section measured on the northeast side of the volcano (Crandell and Waldron, 1956). In the present study, the stratigraphy and distribution of the ash layers on and near Mount Rainier were studied by Crandell and Miller, and the stratigraphy of the pumice at Mount St. Helens and the petrography of the pyroclastic layers were examined by Mullineaux. Radiocarbon ages of interbedded organic matter were determined by Rubin.

DESCRIPTION

The 6 pyroclastic deposits include 3 composed chiefly of pumice of lapilli size or larger, and 3 of vitric and crystal ash. Most of the layers can be recognized in the field by color, size range, and stratigraphic position; laboratory study of constituent minerals and glass confirms field identifications and distinguishes those that appear outwardly similar. In many places these distinctive layers are separated by beds of dark sand, some of which probably are lithic

ash from Mount Rainier. Arbitrary letter symbols are here assigned to the distinctive ash layers to permit future additions to the sequence without changes of nomenclature. The mineralogy, source, and age of the pyroclastic deposits are summarized in the following tables, and the deposits are compared with Recent events in the valleys of the Nisqually and White Rivers.

LAPILLI AND ASH LAYER R

Layer R consists of brownish-yellow (10YR 6/6) ash and lapilli as much as 30 mm in diameter and occurs in the north and east parts of the park. The lapilli are dark to light-brown andesitic pumice, cinders, and dense rock fragments which lie in an oxidized matrix of similar rock fragments and crystals. The glass in most lapilli is dark brown and turbid, and much of it is crowded with crystallites. The refractive index of glass in different fragments ranges from about 1.52 to about 1.57.

Northeast of Mount Rainier layer R decreases from a thickness of about 6 inches 7 miles from the summit of the volcano to 2½ inches 10 miles away. It was not seen on the southwest flank of Mount Rainier during detailed mapping there. Its coarse texture and apparent thinning away from the volcano in a north-

TABLE 138.1—Mineralogy of the pyroclastic layers

Pyroclastic layer	Source of pyroclastic material	Fe-Mg minerals		Refractive index of glass
		Mineral ¹	Abundance ²	
G-----	Unknown-----	hy hb ag oxh	D S A S	1.52-1.53 and 1.49-1.50
W-----	Mount St. Helens.	hy hb	D A	1.49-1.50
C-----	Mount Rainier--	hy hb ag	D S A	1.50-1.53 ³
Y-----	Mount St. Helens.	hy hb	R D	1.50-1.51
O-----	Mount Mazama--	hy hb ag	D A A	1.50-1.51
R-----	Mount Rainier--	hy hb ag oxh	V V V V	1.52-1.57 ³

¹ hy, hypersthene; hb, hornblende; ag, augite; oxh, oxyhornblende.

² D, >50 percent; A, 5-50 percent; S, <5 but ubiquitous; R, rare; absent in some samples; V, varied.

³ In various pumice fragments.

TABLE 138.2—Age of pyroclastic deposits

Pyroclastic layer	Source of pyroclastic material	Radiocarbon age and sample nos. ¹ of organic matter (years)	Inferred age of pyroclastic layers (years)	Correlative unit in measured section of Crandell and Waldron (1956)	Principal events in valleys of Nisqually and White Rivers	
G-----	Unknown-----	-----	>65-<215	8	Recession of glaciers	Deposition of debris flows and alluvium on valley floors
W-----	Mount St. Helens-----	290 ± 200 (W-1120) 320 ± 200 (W-1119)	300			
C-----	Mount Rainier-----	1,640 ± 250 (W-922) 2,550 ± 200 (W-930) 2,980 ± 250 (W-1118)	1,000-3,000	7	Advance of glaciers	
Y-----	Mount St. Helens-----	3,500 ± 250 (W-1115) 4,000 ± 250 (W-1116)	3,200	6		
O-----	Mount Mazama-----	4,800 ± 300 (L-223A)	6,500	5	Osceola Mudflow	
R-----	Mount Rainier-----	8,750 ± 280 (W-950)	>8,750	3		

¹ W, U.S. Geological Survey; L, Lamont Geological Observatory.

easterly direction indicate that it originated in an eruption of Mount Rainier. The layer is well exposed in a road cut 1.1 miles east of Sunrise Lodge at Yakima Park on the northeast side of Mount Rainier.

Layer R underlies carbonized wood dated as about 8,750 years old, but it postdates the glaciation of late Wisconsin age at Mount Rainier.

ASH LAYER O

Ash layer O consists chiefly of light-yellowish-brown (10YR 6/4) to yellow (10YR 7/6) silt to sand-size pumiceous glass and crystals, and at some places aggregates of iron oxide and clay. Particles in this ash have an iron-oxide-rich film, beneath which crystals and glass are clear and seem to be unaltered.

The thickness of ash layer O near Mount Rainier ranges from 2 to 5 inches. The ash occurs all around the volcano, but we have not attempted to trace it beyond the park boundaries. It overlies layer R in road cuts at Yakima Park, where it is about 2 inches thick.

Radiocarbon analysis of carbonized wood underlying layer O gave an age of about 8,750 years. In the White River valley, the ash underlies the 4,800-year-old Osceola Mudflow (Crandell and Waldron, 1956). According to Ray E. Wilcox, U.S. Geological Survey (oral communication, 1962), the mineralogic and petrographic characteristics of ash layer O correspond closely to those of the pumice and ash from the eruption of Mount Mazama that formed the Crater Lake caldera in southern Oregon. This eruption is considered to have occurred about 6,500 years ago (Williams, 1953, p. 46).

LAPILLI AND ASH LAYER Y

Layer Y in the park is a relatively thick deposit of dacitic pumice lapilli and vitric and crystal ash, and is generally very pale brown (10YR 7/4) to light yellowish brown (10YR 6/4). It is the most widespread, thickest, and most conspicuous of the Recent pyroclastic deposits at Mount Rainier. In addition, it is the only ash layer in these deposits in which pyroxene is rare. It is well exposed in a road cut adjacent to State Highway 5, 1.8 miles east of Ashford, Wash., where it is 22 inches thick.

A progressive decrease in grain size from south to north is apparent: 5 miles south of the summit the layer contains lapilli as large as 12 mm, and more than 30 percent of the deposit is larger than 1 mm, but 7 miles northeast of the summit the largest fragments are about 3 mm, and only about 5 percent of the layer is larger than 1 mm. Layer Y extends at least to Keechelus Lake (fig. 138.1) 25 miles northeast of Mount Rainier, where fragments as large as 1 mm have been found.

Layer Y is about 2 feet thick in the Nisqually River valley just west of the park, only 8 inches thick 4 miles east of Elbe, and is absent at Elbe. In addition, it is about 1 foot thick in all but the southeastern part of the park, where it is thin or absent. Southwest from Mount Rainier it increases markedly in grain size and thickness toward Mount St. Helens; near Randle it is as much as 4 feet thick and contains fragments as large as 3 inches.

Its stratigraphic position, distribution, and southwesterly increase in size and thickness clearly indicate

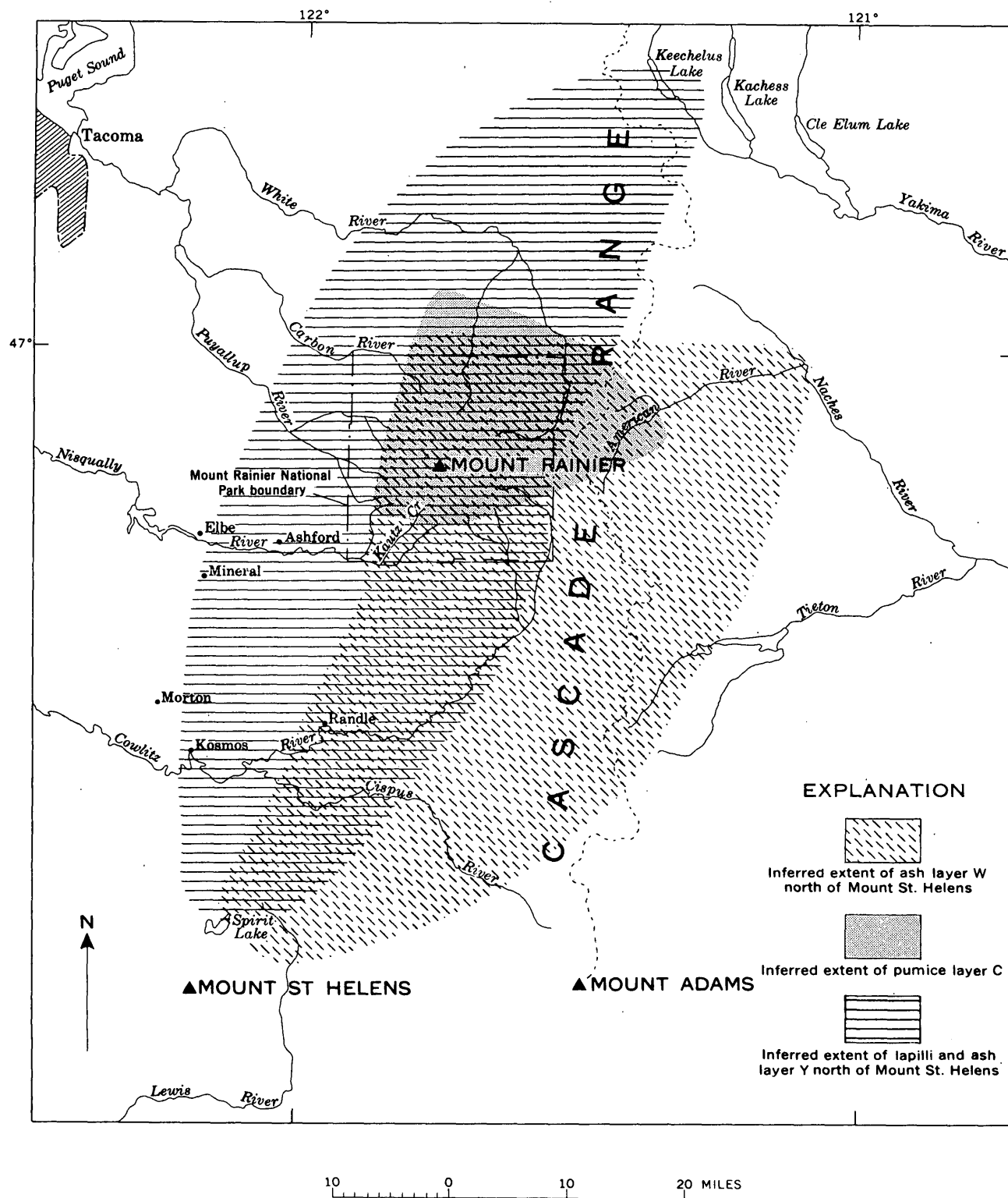


FIGURE 138.1.—Inferred extent of ash and lapilli layers W, Y, and C.

that layer Y is the same as the "older pumice" of the Cowlitz River valley described by Carithers (1946, p. 16). Layer Y is not exposed on the flanks of Mount St. Helens, for the present cone postdates it.

Ash layer Y is estimated to be about 3,200 years old: radiocarbon ages of about 2,500 and 3,000 years were obtained from organic matter above it, and ages of 3,500 and 4,000 years from below it (see table).

PUMICE LAYER C

By far the coarsest pyroclastic material in the recent sequence is the pale-yellow (5Y 8/3) to olive-gray (5Y 5/2) and black pumice layer C, which contains fragments as large as a foot in maximum dimension. This layer also contains dense lithic ash and lapilli. Glass in the most common pumice is andesitic (refractive index about 1.52–1.53), although fragments of dacitic glass have been found whose refractive index is between 1.50 and 1.51. The layer is thickest and the pumice coarsest on the north and east sides of Mount Rainier, where it was first described by Smith (1898, p. 418). The pumice is abundant at ground surface at Yakima Park, where fragments are as large as 2½ inches in diameter. It commonly is 8 to 12 inches thick as far as 12 miles from the summit of the volcano, but only 4 inches thick 15 miles from the summit. Scattered fragments as large as half an inch are present in the American River valley at a point 18 miles east of Mount Rainier. On the south and west sides of Mount Rainier the pumice decreases more abruptly in grain size and thickness, and generally it is absent more than 4 miles from the summit. At one locality on the south flank of Mount Rainier, material similar to layer C occurs in agglutinated masses as large as 3 feet in diameter.

Samples of pumice resembling layer C from the southwest flank of the volcano lack hornblende, although samples from the northeast side all contain at least small amounts of hornblende. Though not clearly established, the pumice lacking hornblende may represent a separate eruption.

The hornblende-bearing pumice layer on the northeast side of the volcano has not been dated directly, but as it occurs between layers W and Y, its age is bracketed by dates of about 300 and 3,200 years. No pumice was seen on a terrace in the White River valley about half a mile downstream from the position of the terminus of the Emmons Glacier in 1910. This terrace is inferred to have been forested for at least 1,000 years (Sigafos and Hendricks, 1961); thus, layer C presumably is older than 1,000 years.

ASH LAYER W

Ash layer W at Mount Rainier is a thin layer of coarse to very coarse sand-size dacitic pumice and smaller crystals, pumice, and glass shards; it ranges in color from white (2.5Y 8/2) to light gray (2.5Y 7/2) or pale yellow (2.5Y 8/4). It is generally recognizable by its size range, color, and thickness; a distinctive mineralogic feature is the high refractive index of its hypersthene (n_x about 1.71) as compared to that of the hypersthene in the other layers younger than layer R (n_x about 1.69).

This ash layer occurs in the eastern two-thirds of Mount Rainier National Park, and extends beyond the park boundaries in all directions except west and northwest (fig. 138.1). Layer W is almost continu-

Section measured in the east bank of Kautz Creek about 3,000 feet upstream from Wonderland Trail Bridge across creek

	ft.	in.
21. Debris flow; boulders and cobbles in medium- to fine-sand matrix. Deposited in October 1947-----	2-8	
20. Duff, silty, dark-grayish-brown; contains roots and wood fragments-----		6
19. Boulders, 1 to 4 feet in diameter, in stratified coarse sand and granule matrix-----	3	
18. Sand, fine to medium, gray, horizontally stratified and interbedded with layers of yellowish-gray silt-----	2	
17. Duff; contains fragments of carbonized wood-----		2
16. Silt and fine sand, yellowish-gray, horizontally bedded; contains pebbles and granules near top-----	1	
15. Duff and roots (radiocarbon sample W-1120, 290 ± 200 years)-----		¼-½
14. Sand, fine, gray-----		¼-½
13. Ash layer W-----		½-2
12. Sand, fine, gray-----		½
11. Duff, wood and carbonized wood fragments (radiocarbon sample W-1119, 320 ± 200 years)-----		½-1½
10. Sand, fine to medium, gray; contains scattered cobbles-----		6
9. Debris flow; pebbles and cobbles in compact sand and granule matrix; gray-----	2	
8. Sand, medium, mostly horizontally stratified but has some faint crossbedding; contains reworked ash of layer Y, and wood fragments-----	5	
7. Debris flow; boulders and cobbles in fine- to medium-sand and granule matrix-----	2	6
6. Duff mixed with gray fine sand; contains fragments of charcoal-----		½-2
5. Sand, fine, gray; contains reworked pumice of layer Y, and wood fragments-----	½-2	
4. Debris flow; boulders as large as 4 feet in diameter in gray sand and granule matrix-----	15	
3. Sand, fine to medium, stratified, lenticular-----	1-3	
2. Lapilli and ash layer Y-----		8
1. Pebble to boulder gravel and sand-----	1.0+	

ously exposed adjacent to the highway between Longmire and Van Trump Creek in the park, where it is 2 inches thick. The ash increases in thickness from about $\frac{1}{2}$ to 2 inches from the northern to the southern boundary of the park, while the ratio of coarse sand to finer sand increases from about 15:85 to 40:60. Southwest of the park, layer W continues to increase in thickness and grain size; near Randle, for example, it is several inches thick and contains pumice lapilli as large as 8 mm. On the north flank of Mount St. Helens, it is as much as 20 feet thick and contains pumice fragments 2 feet in diameter. Between Mount St. Helens and Mount Rainier, this layer is the younger, light-gray pumice deposit of Carithers (1946, p. 16).

Radiocarbon analyses of carbon from duff layers just above and below ash layer W in the valley wall of Kautz Creek on the south side of Mount Rainier (see measured section) suggest an age of about 300 years.

ASH LAYER G

Ash layer G is the youngest pyroclastic layer recognized at Mount Rainier and is a discontinuous layer $\frac{1}{4}$ to $\frac{1}{2}$ inch thick in the modern forest duff. It consists principally of reddish-gray (10YR 5/2) silt to very fine sand-size crystals, but also contains both brown turbid glass (refractive index about 1.52–1.53) and clear glass (about 1.49–1.50) that probably are andesitic and dacitic, respectively. It is distinguished from other ash layers by its color, fine size, stratigraphic position, and by containing a wider variety of dark minerals than other layers younger than lapilli and ash layer R (see table). The variety of minerals and glass suggests the possibility that this layer contains ash from two volcanoes, perhaps Mount Rainier and Mount St. Helens, but this has not been verified by other evidence. The ash overlies layer W along the highway between Longmire and Van Trump Creek in the park, where it is $\frac{1}{2}$ inch thick. The lateral extent of the ash is not known, although it seems to be absent west of the park.

The ash is on a moraine formed about the middle

of the 18th century, but is absent on a moraine formed about A.D. 1900.

OLDER ASH LAYER OR LAYERS

At least one partly oxidized crystal ash layer lies below layer R, and also postdates the last glaciation of Wisconsin age. This has been seen at only a few places, and its distribution, source, and stratigraphic relations are not well known, so that it cannot be said to be the deposit of a single ash fall. It is similar in color, thickness, and texture to ash layer O, but differs in that it contains a markedly wider variety of minerals and larger proportion of crystals. Despite its age of probably more than 10,000 years, the older ash contains much clear glass. The fine texture of the layer suggests that it did not originate at Mount Rainier.

CONCLUSIONS

Preliminary work on Recent pyroclastic deposits on the flanks of Mount Rainier volcano indicates that at least 2 and probably 3 of the most distinctive, thickest, and most widespread layers were erupted by other volcanoes. The two pyroclastic layers originating from Mount Rainier are characterized by abundant andesitic glass and lithic fragments, and those derived from other volcanoes by dacitic glass.

REFERENCES

- Carithers, Ward, 1946, Pumice and pumicite occurrences of Washington: Washington Div. Mines and Geology Rept. Inv. 15, 78 p.
- Crandell, D. R., and Waldron, H. H., 1956, A Recent volcanic mudflow of exceptional dimensions from Mount Rainier, Washington: *Am. Jour. Sci.*, v. 254, p. 349–362.
- Mullineaux, D. R., and Crandell, D. R., 1960, Late Recent age of Mount St. Helens volcano, Washington: Art. 143 in U.S. Geol. Survey Prof. Paper 400-B, p. B307–B308.
- Sigafoos, R. S., and Hendricks, E. L., 1961, Botanical evidence of the modern history of Nisqually Glacier, Washington: U.S. Geol. Survey Prof. Paper 387-A.
- Smith, G. O., 1898, The rocks of Mount Rainier: U.S. Geol. Survey 18th Ann. Rept., pt. 2, p. 416–423.
- Williams, Howel, 1953, The ancient volcanoes of Oregon, 2d ed.: Oregon State System of Higher Education: Condon Lecture Publications, 68 p.



STRUCTURAL GEOLOGY

139. THE PINE MOUNTAIN OVERTHRUST AT THE NORTHEAST END OF THE POWELL VALLEY ANTICLINE, VIRGINIA

By RALPH L. MILLER, Washington, D.C.

The Pine Mountain overthrust underlies the entire Cumberland overthrust block in the tristate area of Virginia, Kentucky, and Tennessee. The block is rectangular in shape, 125 miles long from northeast to southwest, and 25 miles wide from southeast to northwest (fig. 139.1). On the northwest side of the block, coal measures of Pennsylvanian age are preserved at the surface in the Middlesboro syncline. On the southeast side, rocks as old as Middle Cambrian are exposed along the axis of the Powell Valley anticline. The stratigraphic position of the Pine Mountain overthrust, along which the block moved to the northwest, is now known at a number of different localities as a result of recent detailed geologic mapping and from deep wells that cross the fault. Most of the deep drilling has been in the Middlesboro syncline in Kentucky and in the coal-bearing parts of adjacent Vir-

ginia where the fault is a bedding-plane fault near the base of the Chattanooga shale of early usage.

Along the Powell Valley anticline the fault is exposed in central Lee County, Va. in fensters in the Rose Hill region (Miller and Fuller, 1954) and the Jonesville region (Miller and Brosgé, 1954). Northeast of central Lee County, the fault is not known to be exposed nor have any wells been drilled that are known to have reached the fault. However, recent detailed mapping of the Big Stone Gap 7½-minute quadrangle that includes parts of Lee, Wise, and Scott Counties suggests that the fault zone comes to the surface in the valley bottom of Powell River southwest of the town of Big Stone Gap. Here a strongly deformed zone in the lower part of the Chattanooga shale of early usage is exposed just above the valley floor, and the deformed zone may be seen in a dozen

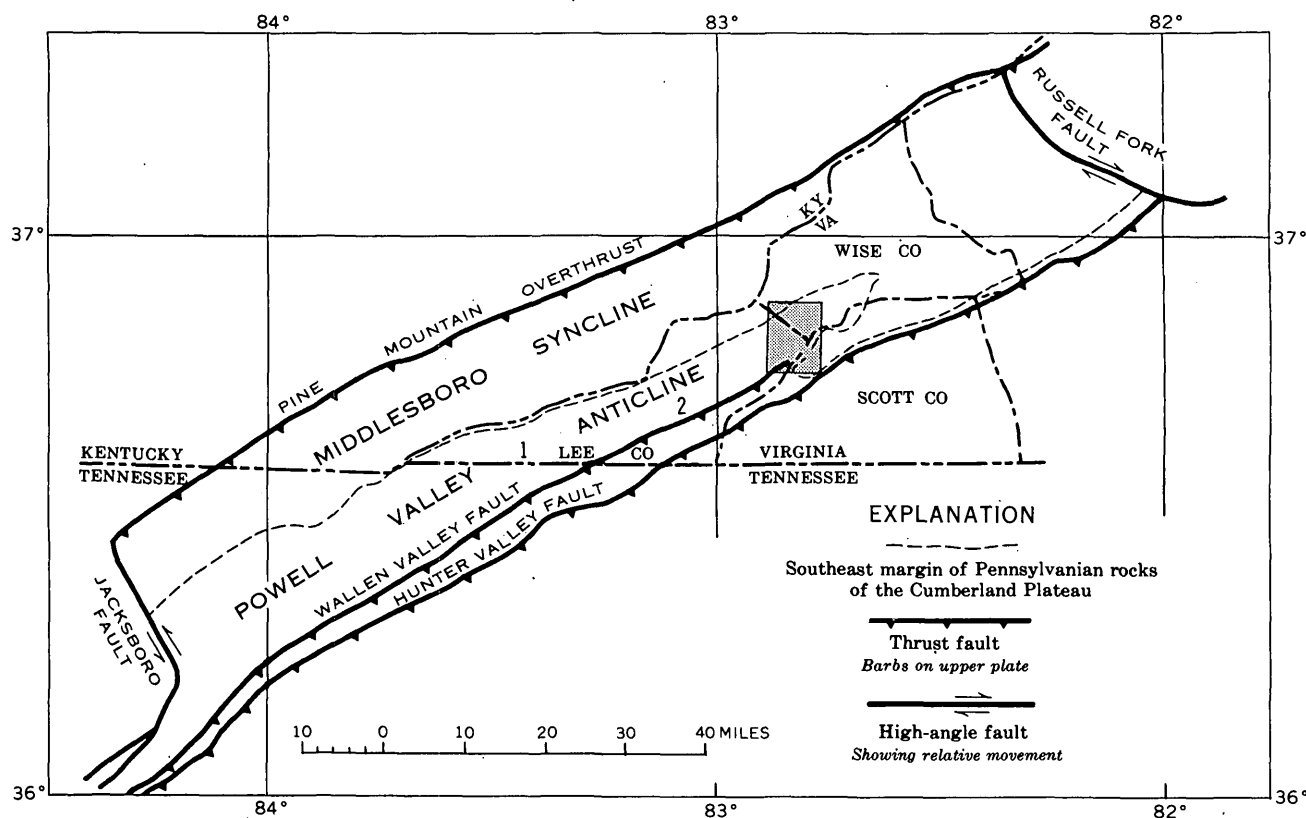


FIGURE 139.1.—Index map of the Cumberland overthrust block showing major structures, location of the Big Stone Gap quadrangle (shaded), location of the Rose Hill district (1), and location of the Jonesville district (2).

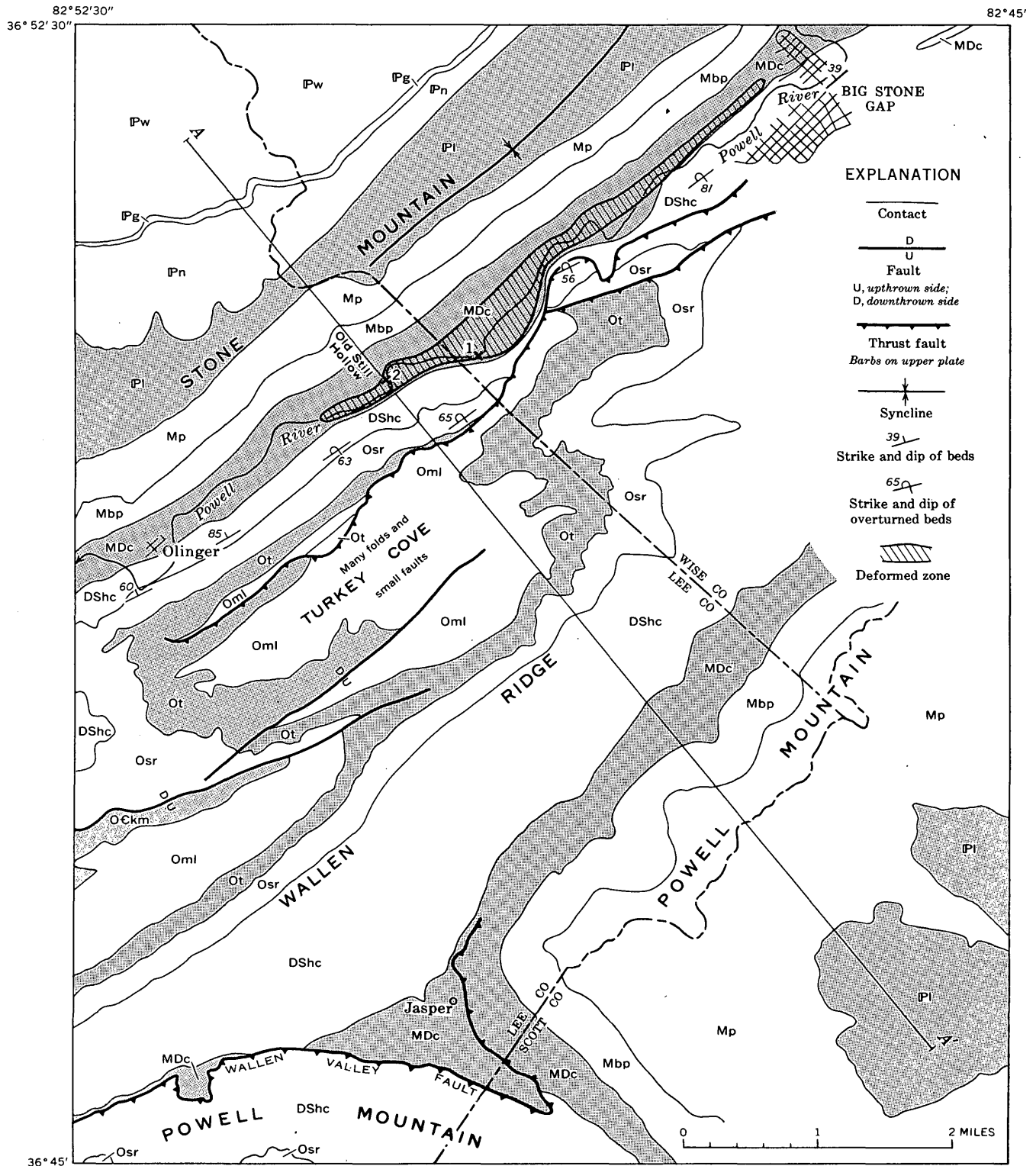


FIGURE 139.2.—Generalized geologic map of the Big Stone Gap quadrangle, showing the location of the deformed zone in the Chattanooga shale of early usage, and of structure section A-A' (fig. 139.3). Formations, shown by symbols, are as follows: Pw, Wise Formation; Pg, Gladeville Sandstone; Pn, Norton Formation; Pl, Lee Formation; Mp, Pennington Group; Mbp, Bluefield Formation, Greenbrier Limestone, and Price Sandstone; MDc, Chattanooga shale of early usage; DShc, sandstone (Helderberg as used by Stose, 1923), Hancock Limestone, Clinton Formation, and Clinch Sandstone; Osr, Sequatchie Formation and Reedsville Shale; Ot, Trenton Limestone; Oml, lower Middle Ordovician limestone formations; Ockm, Knox Group and Maynardville Limestone. Localities 1 and 2 are exposures of black shale referred to in text.

outcrops. A line drawn on the map to enclose all these outcrops forms an elongate narrow area along the valley bottom stretching from a point along the Powell River opposite downtown Big Stone Gap southwest for $4\frac{1}{4}$ miles to a point about $1\frac{1}{2}$ miles northeast of the town of Olinger (fig. 139.2). The greatest width of this area is about 0.4 mile, but it averages about 0.15 mile. Within the area thus delineated, every outcrop that could be found was of intricately deformed black shale assigned here to the lower part of the Chattanooga shale. No outcrops of any other formation were seen, nor was any of the black shale within this area undeformed as it is in many other places in the Big Stone Gap quadrangle.

One of the two largest exposures of the deformed black shale is at the base of a nearly vertical bluff just above water level on the south bank of the Powell River about 500 feet east of the Lee County-Wise County line (fig. 139.2, loc. 1). Here the beds are nearly completely upside down, with deformed black shale at water level overlain by similar but undeformed black shale of the lowest part of the Chattanooga, by sandstone (Helderberg as used by Stose, 1923), and by Hancock Limestone (Upper Silurian) at the top of the bluff. The other very good exposure, also in a nearly vertical bluff, is on the north bank of the Powell River below the Louisville and Nashville Railroad tracks, 3,200 feet due west of where the county line crosses the Powell River (fig. 139.2, loc. 2). Here the beds are right side up. Strongly deformed black shale at river level is overlain by much less deformed black shale of the lower part of the Chattanooga, which is overlain by undeformed, though steeply dipping, siltstone and shale of the middle and upper parts of the formation.

In both of these good exposures, and in the other 10 much smaller ones, the shale is hackly instead of breaking along smooth surfaces. Slickensided carbonaceous surfaces are abundant, and changes of dip are extreme within a matter of a few feet or a few tens of feet. If the outcrop is big enough, small faults or well-developed chevron folds are visible.

The "top" of the deformed zone along the valley rises only a few tens of feet above river level, so that it may be described as nearly flat in spite of the fact that older beds on the south side of the river and younger beds on the north side of the river are steeply dipping, whether right side up or overturned.

The Chattanooga shale has been mapped in many other places in the Big Stone Gap quadrangle. Only in the vicinity of the town of Jasper does it show the type of deformation described above, and here it is clearly demonstrable that the Wallen Valley fault, a large Appalachian-type low-angle fault, is a bedding-

plane fault within the lower part of the formation (fig. 139.2).

The evidence above has led the writer to postulate that another large low-angle fault lying entirely within the lower part of the Chattanooga shale comes to the surface south of the Powell River and dips downward beneath the surface again on the north side of the river. The outcrops that we see along the $4\frac{1}{4}$ -mile belt are parts of the deformed zone of this fault. The most logical fault to be present here is the Pine Mountain overthrust, which is known from broad regional evidence and from drilling to lie within the Chattanooga shale beneath the Middlesboro syncline.

A structure section incorporating the above interpretation of the subsurface structure is presented here, reduced and generalized, as figure 139.3. The position of the section is shown in figure 139.2. In the section the Pine Mountain fault zone comes to the surface in the valley of the Powell River and lies at shallow depths beneath Turkey Cove at the southeast, where numerous folds and faults in lower Middle Ordovician limestone formations suggest a major fault not too far below. These folds and faults are too small to show at the scale of figures 139.2 and 139.3. The amount of displacement inferred on the Pine Mountain fault is about 2 miles as indicated by the offset of the Knox Group in figure 139.3. As yet, no way has been found to measure or calculate the displacement in this region. The amount shown may be too small, but it is probably not too large.

The Pine Mountain fault zone is shown on figure 139.3 as a line, because of space limitations at the small scale of the section. Actually the line where it breaks the surface should be interpreted as representing the top of the deformed zone of the fault, rather than the plane or planes along which greatest movement occurred. No major fault plane was seen along the Powell River valley. The fault plane may be concealed beneath the river alluvium and colluvium of the lowest slopes of the mountains on both sides, or more likely it lies at shallow depth beneath the bedrock surface of the valley floor.

According to the above interpretation of the deformed zone and the overthrust fault, a large anticline would underlie the overthrust. Formations older than the Chattanooga would be present in normal order downward to basement. In a direction normal to the section, the anticline in pre-Chattanooga rocks as well as the deformed zone would plunge gently beneath the surface both to the northeast and the southwest, thus forming a large closed structure. This anticline may extend far beyond the $4\frac{1}{4}$ -mile distance along which the deformed zone is exposed.

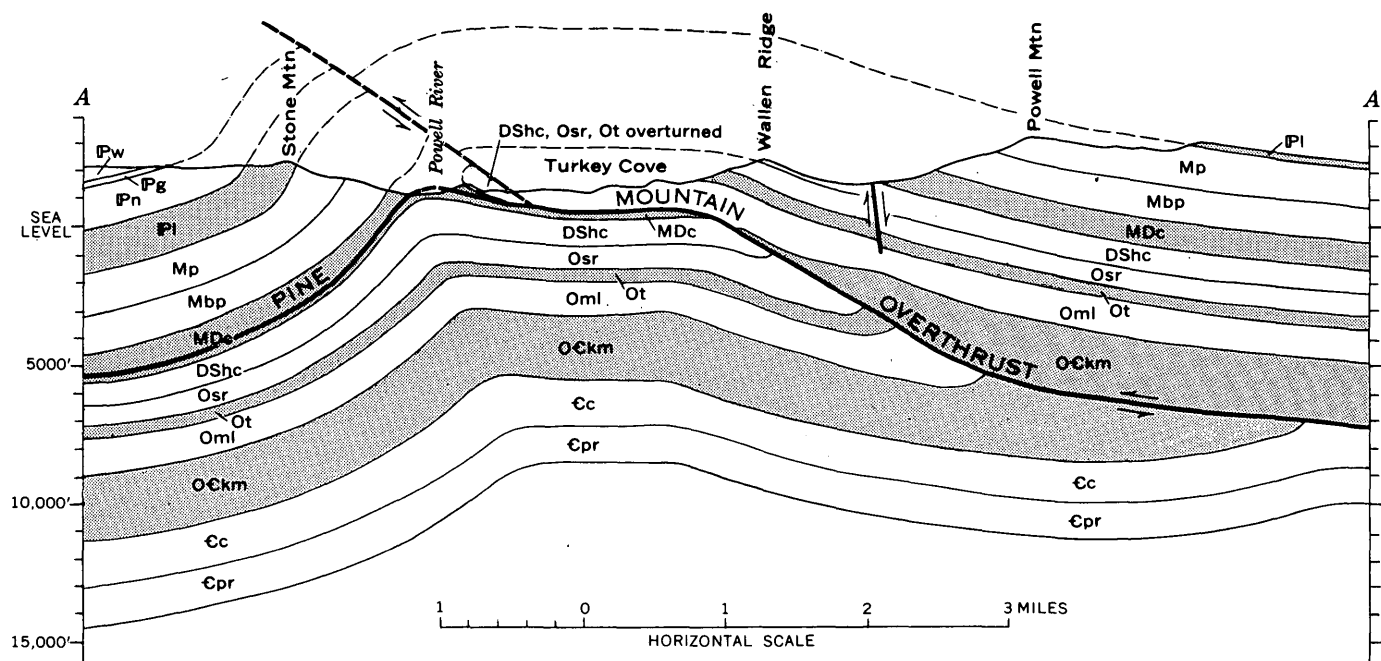


FIGURE 139.3.—Structure section along line A-A', figure 139.2. Formation symbols are the same as on figure 139.2 with the addition of the following subsurface formations: Cc, Conasauga Shale; Cpr, Pumpkin Valley Shale and Rome Formation.

Two alternative interpretations of the subsurface structure have been considered. The first of these postulates that the fault deforming the Chattanooga shale in the Powell River valley is a much smaller branch of the Pine Mountain overthrust, which either rejoins the Pine Mountain fault somewhere beneath Stone Mountain or dies out northwest in the subsurface. The other interpretation, suggested by Leonard Harris (oral communication, 1962), is that the deformation of the Chattanooga shale in the Powell River valley is the result of very great compression of the shale in the core of a strongly overturned syncline, the analog of the faulted overturned anticline just south of the Powell River and on the north side of Turkey Cove (figs. 139.2 and 139.3). In either alternative interpretation, the main Pine Mountain fault would be nearly flat at a depth of about 3,500 to 4,000 feet beneath Turkey Cove and would crosscut stratigraphically but not topographically upward from the base of the Maynardville Limestone to the Chattanooga shale beneath the Powell River valley and Stone Mountain. Neither of the two alternative interpretations seems to explain the features of the surface geology as satisfactorily as the interpretation diagrammed in figure 139.3, but lacking any subsurface data, the alternative interpretations cannot be eliminated.

In the structure section shown here, the Trenton

Limestone, which produces oil in central Lee County, is estimated to lie at a depth of 2,500 to 3,000 feet beneath Turkey Cove. In either of the alternative interpretations, the Trenton Limestone in the stationary block at the same location might lie about 6,000 feet beneath the surface.

Possibly additional mapping in the Powell Valley southwest and northeast of the Big Stone Gap quadrangle will shed more light on the location of the Pine Mountain overthrust within the quadrangle. Probably, however, the first and favored interpretation presented here can be verified only by drilling. If figure 139.3 is approximately correct in its major subsurface outlines, a well drilled along or a short distance south of the south edge of the Powell River valley would be an interesting test of oil and gas possibilities in the pre-Devonian formations.

REFERENCES

- Miller, R. L., and Brosgé, W. P., 1954, Geology and oil resources of the Jonesville district, Lee County, Virginia: U.S. Geol. Survey Bull. 990, 240 p.
- Miller, R. L., and Fuller, J. O., 1954, Geology and oil resources of the Rose Hill district—the Fenster area of the Cumberland overthrust block—Lee County, Virginia: Virginia Geol. Survey Bull. 71, 383 p.
- Stose, G. W., 1923, Pre-Pennsylvanian rocks, in Geology and mineral resources of Wise County and coal-bearing portions of Scott County, Virginia: Virginia Geol. Survey Bull. 24, p. 22-62.



140. GRAVITY AND MAGNETIC ANOMALIES IN GEM VALLEY, CARIBOU COUNTY, IDAHO

By DON R. MABEY and FRANK C. ARMSTRONG, Menlo Park, Calif., and Spokane, Wash.

In southeastern Idaho about 30 miles east of Pocatello, a northward-trending valley lies between the Portneuf and Fish Creek Ranges on the west and the Chesterfield Range, Soda Springs Hills, and Bear River Range on the east. The central part of this valley is called Gem Valley, and the northern and southern parts are known as Portneuf and Gentile Valleys, respectively (fig. 140.1). Gem Valley as used in this report includes Portneuf Valley and the north end of Gentile Valley.

Gem Valley is about 35 miles long and 7 miles wide. Elevations range from about 5,000 to 5,800 feet above sea level in the valley and to as high as 9,200 feet in the ranges. The divide between the Great Salt Lake drainage basin to the southeast and the Columbia River drainage basin to the northwest crosses the

valley near its center. Bear River enters the valley from the east, bends sharply southward, and flows out the south end of the valley through a narrow gorge into Cache Valley and on into Great Salt Lake. The Portneuf River, which is a tributary of the Snake River, enters the valley at the north end and flows out southwestward through a canyon on the northwest side of the valley.

The central part of the valley is underlain by Pleistocene basalt lava flows. Prior to the extrusion of these flows Bear River is thought to have flowed northward in Gem Valley and to have left the valley by way of the Portneuf River canyon to join the Snake River. When the flows were extruded they apparently dammed Gem Valley and diverted the prelava Bear River, causing it to flow southward and eventually to spill over into the Lake Bonneville drainage basin (Bright,¹ p. 206-246). Data presented here were obtained to determine if gravity and magnetic surveys could produce new data about the thickness of the basalt flows and underlying sediments in the valley that would bear on the valley's origin.

GRAVITY SURVEY

Gravity observations were made at about 150 stations in the valley and at a few stations in the nearby mountains. The data reduced to the simple Bouguer anomaly using an elevation correction of 0.06 mgals (milligals) per foot and contoured at a 5-mgal interval are shown in figure 140.1. The largest gravity feature is a low of about 35 mgals with the lowest values on the east side of the valley southeast of Chesterfield. A second area of low-gravity closure extends southward beyond the limits of the map and is separated from the northern low by a gravity high in the area of the topographic divide between Bancroft and Grace.

The dominant local gravity anomalies in the Basin and Range physiographic province are produced by the density contrast that usually exists between the Cenozoic rocks and the generally more dense older rocks. Smaller anomalies are produced by density differences within the pre-Cenozoic rocks and within the Cenozoic rocks. The rocks in the ranges adjoining Gem Valley are mostly sedimentary rocks of Paleozoic age overlain locally by Tertiary sedimentary

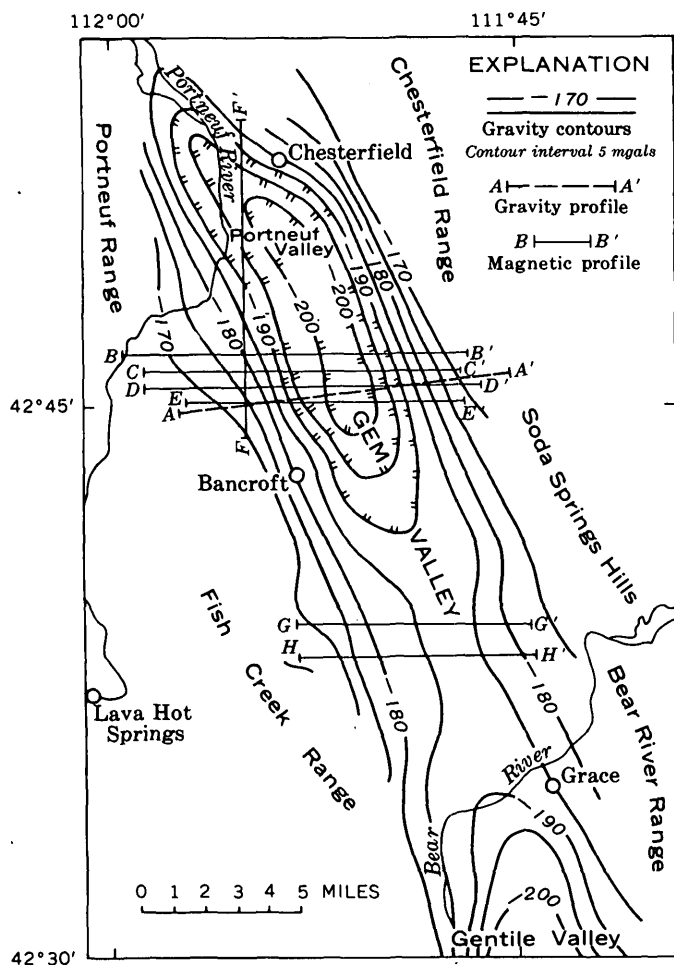


FIGURE 140.1.—Bouguer-anomaly map of Gem Valley, and lines of profiles shown on figures 140.2 and 140.3.

¹ Bright, R. C., 1960, Geology of the Cleveland area, southeastern Idaho: Utah Univ. Master's thesis, 262 p.

rocks. The rocks underlying the cover of Quaternary alluvium and lava in the valley probably are Tertiary sedimentary rocks underlain by Paleozoic sedimentary rocks similar to those exposed in the ranges. As Mesozoic rocks had been largely stripped from the ancestral Bear River Range by Early Cretaceous time, it seems unlikely that significant areas of Mesozoic rocks are preserved under the Quaternary alluvium and lavas of the central part of the valley, but some may be present in the northern part.

Densities of the sedimentary rocks were not determined. A density contrast, however, of 0.4 or 0.5 g per cm^3 between Cenozoic and pre-Cenozoic sedimentary rock has proved applicable in other areas of the Basin and Range province. The average density of 7 samples of basalt collected along Bear River is 2.64 g per cm^3 . This density is near the estimated density of the pre-Cenozoic rocks. As no large density contrast exists between the basalt and the pre-Cenozoic rocks, a thickness of a few hundred feet of basalt will not have an appreciable effect upon the large gravity lows in Gem Valley.

The gravity anomaly on profile *A-A'* (fig. 140.2) across the northern low could be produced by a depression filled with material having a density 0.5 g per cm^3 lower than the enclosing rock and a maximum thickness of about 9,000 feet. The gravity low probably is produced mostly by Cenozoic sedimentary rocks; in the northern part of the valley Mesozoic sedimentary rocks may also contribute to the gravity low. The density of the Mesozoic rocks is probably greater than the Cenozoic rocks but less than the Paleozoic rocks. The lowest part of the northern low is coincident with a small topographic low on the basalt surface, which may indicate that subsidence of the valley has continued since the extrusion of the basalt—

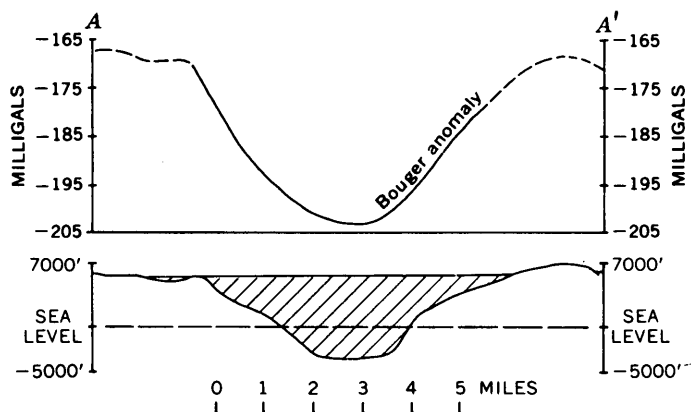


FIGURE 140.2.—The gravity anomaly along profile *A-A'*, in northern Gem Valley, and an interpretation of the gravity low. Density of material (shaded) beneath gravity low is 0.5 g per cm^3 lower than enclosing rock.

a conclusion supported elsewhere by the presence of fault scarps in the basalt along the east side of Gem Valley near the gravity divide in the valley. The steep gradients on both sides of the gravity low shown on profile *A-A'* (fig. 140.2) suggest that the deepest depression is bounded by normal faults on the east and west sides—a conclusion in agreement with Mansfield's (1929, p. 60) suggestion that the Chesterfield Range may be a horst, and with recent work in the Bear River Range east of Grace which also supports the theory of a horst-graben relationship for Gem Valley and the adjacent ranges.

A gravity high which approximately coincides with the topographic divide separates the northern depression from a depression of similar size but undetermined configuration near the center of the southern part of the valley. As it does not seem likely that the basalt flows can thicken enough over the topographic divide to account completely for the gravity high (a thickening of about 4,000 feet would be required), the gravity high is interpreted as a topographic high on the surface of Paleozoic rocks underlying the valley.

Because the density of the lava is very near that of the Paleozoic rocks in the ranges, gravity observations proved ineffective in determining the thickness of the lava where the Portneuf River leaves the valley. Only very detailed gravity surveys could possibly detect small gravity highs which might be associated with thickening of the lava in channels within the valley.

MAGNETIC SURVEY

The lava in Gem Valley is highly magnetic, in contrast to the almost nonmagnetic sedimentary rocks in the valley and adjacent ranges. Quantitative interpretation of the anomalies is difficult, however, because most magnetic anomalies associated with volcanic flows are produced in large part by remanent magnetism that usually has an erratic distribution.

Seven total-intensity magnetic profiles were flown 750 feet above the land surface in the valley (fig. 140.3). Over the flows the magnetic field is irregular but has no large changes in the general level of the field. The irregular character of the field is a good criterion for inferring the presence of basalt near the surface. The northern limit of the basalt is indicated on profile *F-F'* by the abrupt change in the character of the magnetic anomalies about 3 miles south of *F'*. In this area the basalt thins northward, and as it is probably only a few feet thick at its northern edge, the magnetic anomaly at the edge is not large.

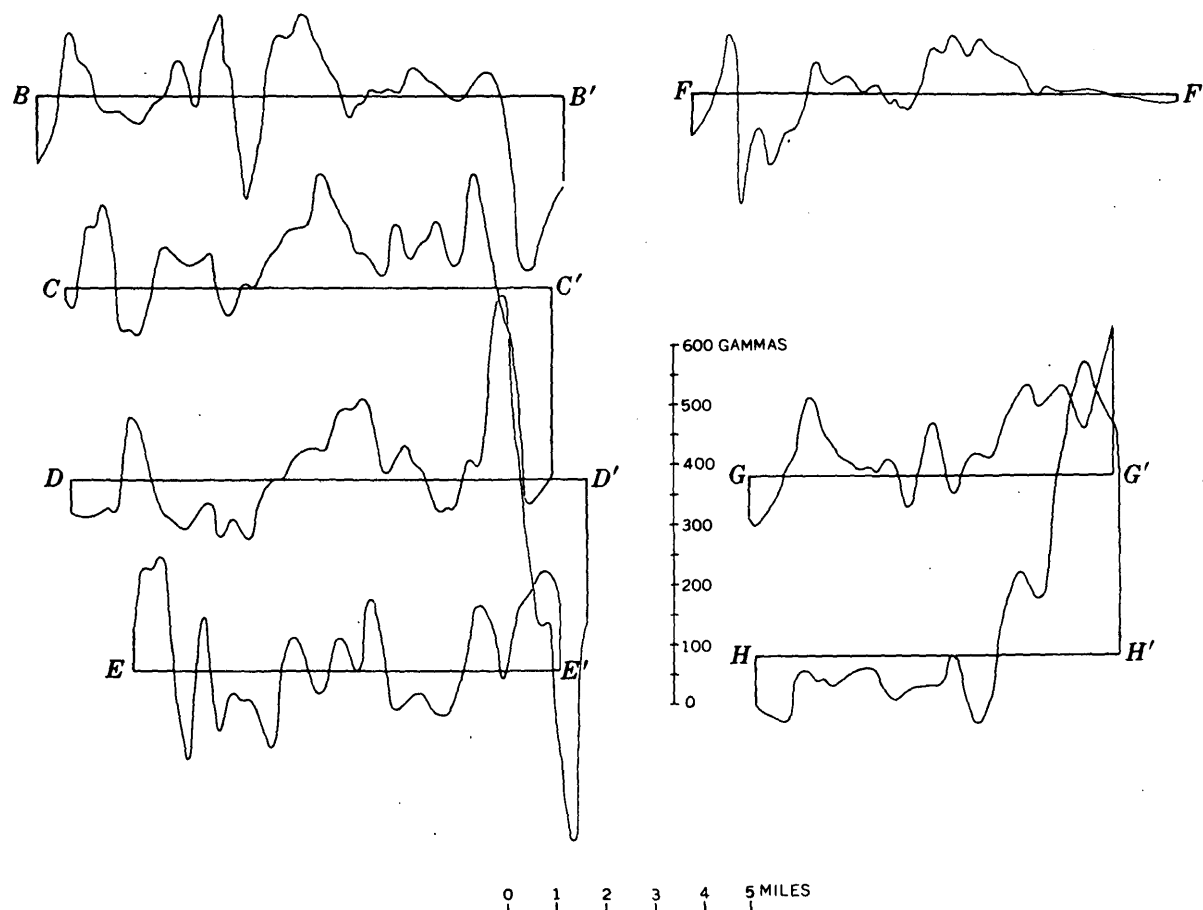


FIGURE 140.3.—Aeromagnetic profiles of Gem Valley. Flight elevation was 750 feet above land surface.

The magnetic fluctuation of several hundred gammas near the east end of profiles *B-B'*, *C-C'*, and *D-D'* approximately coincides with the east margin of the basalt exposed in the valley. These large fluctuations indicate an abrupt termination of a thick basalt pile. The shape of the east end of profile *E-E'* and the location of *E'* suggest that *E'* is close to, but not east of, the east edge of the thick pile of basalt, as are points *B'*, *C'*, and *D'*. Although profiles *B-B'* through *E-E'* are only half a mile apart only the larger magnetic fluctuations can be correlated between adjoining profiles. The high near the center of *B-B'*, *C-C'*, and *D-D'* may indicate an area of thicker basalt that filled a prebasalt topographic low over the deepest bedrock depression indicated by the gravity low.

The magnetic high near the east end of profile *H-H'* and the start of a high at the east end of *G-G'* (fig. 140.3) occur approximately over a group of basalt scoria cones and prominent collapse features in the

basalt. The cones and collapse features are alined so that they trend a little west of north and approximately parallel the west front of the Bear River Range and the Soda Springs Hills at this locality. The trend of the cones and collapse features also approximately parallels a set of faults that cuts the basalts in the valley and the Paleozoic rocks in the ranges to the east. At the crest of the north end of the Bear River Range, basalt flows have been extruded from three centers located on similarly trending faults. The magnetic highs at the east ends of profiles *G-G'* and *H-H'* are thus interpreted as indicating the position and trend of a fault zone along which basalt rose to the surface and furnished lava for some of the flows in the valley.

REFERENCE

- Mansfield, G. R., 1929, Geography, geology, and mineral resources of the Portneuf quadrangle, Idaho: U.S. Geol. Survey Bull. 803, 110 p.



141. GRAVITY, VOLCANISM, AND CRUSTAL DEFORMATION IN THE EASTERN SNAKE RIVER PLAIN, IDAHO

By T. R. LaFEHR and L. C. PAKISER, Denver, Colo.

Work done in cooperation with the Advanced Research Projects Agency, Department of Defense, as part of project VELA UNIFORM

A regional gravity survey in the eastern part of the Snake River Plain, Idaho, was made in 1961 as a continuation of the gravity network established by Hill and others (1961) in the western part of the Snake River Plain. Seven hundred and seven gravity stations were established, and the measurements were reduced to the simple-Bouguer anomaly assuming a density of 2.67 g per cm³ for the rocks above sea level. The resulting data were plotted on a map and contoured at an interval of 10 milligals (fig. 141.1).

The Snake River traverses more than 400 miles from the Teton Mountains, Wyo., across southern Idaho to the Oregon-Idaho border. Over most of this course it follows the crescent-shaped, broad structural depression known as the Snake River Plain, most of whose 19,000 square miles is north of the river. The plain

can be divided into two parts, western and eastern, approximately along long 114°30' W. The western plain trends west and northwest; the eastern plain trends east and northeast.

The low gravity relief of the eastern plain strongly contrasts with the high-amplitude anomalies of the western plain (Hill and others, 1961). There are four major gravity features in the eastern plain: (1) a broad high, which is an extension of the series of large gravity highs of the western plain; (2) a set of elongated, alternating lows and highs which trend normal to the axis of the eastern plain; (3) a series of small local highs on the southern and southeastern boundaries of the plain; and (4) a prominent low, centered over Mud Lake, in the northern part of the surveyed area (fig. 141.1).

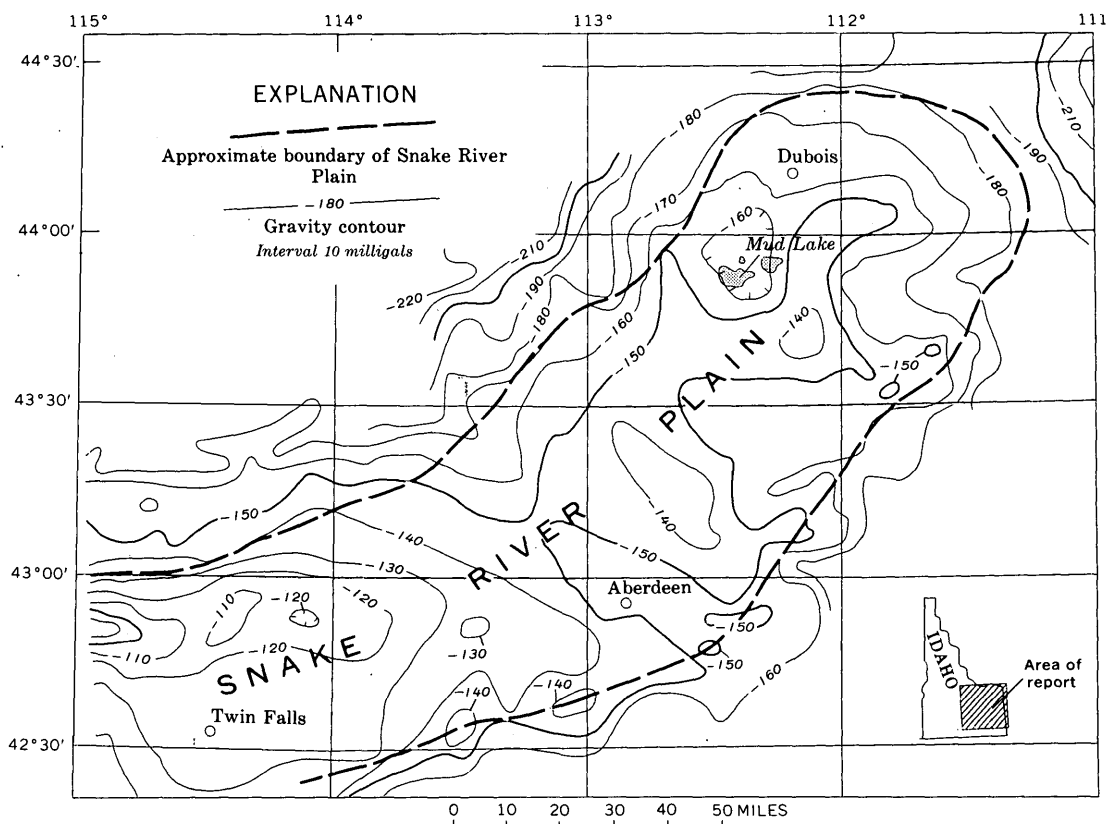


FIGURE 141.1—Simple Bouguer-anomaly map of the eastern Snake River Plain, Idaho.

Snake River Basalt of Quaternary age is exposed at the surface over almost all of the eastern plain. Because the steepest gravity gradients occur over the mountains to the north and south of the eastern plain (in some places a considerable distance away from the edge of the basalt) it is presumed that these gradients, for the most part, result from large-scale geologic features. The generalized regional gravity anomaly could be caused by a local upward displacement of the base of the earth's crust of about 6 km, from a normal crustal thickness of about 40 km. This estimate is based on depth estimation formulas (Bott and Smith, 1958; LaFehr, 1962) and two-dimensional graticule analysis.

RELATIONS OF GRAVITY AND GEOLOGY

The alternating lows and highs imply relatively near-surface geologic relief, although that relief may not be directly related to the mountains whose axes are cut nearly at right angles by the Snake River Plain. Of particular structural importance is a widespread series of silicic volcanic rocks (largely rhyolite) of Miocene or Pliocene age that underlie the basalts of the Snake River Group. These silicic volcanic rocks occur in the mountains on both sides of the plain. Because they tend to dip toward the plain, Kirkham (1931, p. 471-481) concluded that the plain had been downwarped. Geologic and drilling information indicate that the rhyolite floor under the later basalt flows has considerable relief, which implies a variation in near-surface densities that could cause the gravity anomalies. With an assumed density contrast of about 0.3 g per cm³ between the basement complex and the denser basalt, residual anomalies reveal thickness variations of the basalts of Quaternary age ranging from a few hundred to as much as 5 thousand feet.

The gravity low at Mud Lake (fig. 141.1) is attributed to an accumulation of less than 2,000 feet of lacustrine deposits that crop out over a wide area in this part of the plain. This estimate is based on an assumed density contrast of -0.5 g per cm³.

COMPARISON OF THE EASTERN AND WESTERN PLAINS

The remarkable difference between the gravity fields of the eastern and western parts of the Snake River Plain demands a searching inquiry for other differences—geologic, topographic, or tectonic—which are, as yet, not established in the literature. The change in the gravity pattern occurs approximately where the axis of the plain is most strongly bent. The down-

warp hypothesis (Kirkham, 1931), which has been ruled out for the western plain (Malde, 1959; Hill and others, 1961), remains a possible explanation for the eastern plain. The eastern plain is transverse to the major topographic trends of the region. Fingerlike extensions of the mountain ranges face each other on opposite sides of the plain. The western plain also is bordered by mountains, but their trends do not seem to be so distinctly broken by the plain.

A study of earthquake epicenters in the United States (Woollard, 1958) outlines areas of recent tectonic activity. On the basis of these patterns, Malde (1959, p. 272) states: "The crustal break implied by the gravity measurements is possibly expressed by a line of earthquake epicenters that extends diagonally from Puget Sound, across the Columbia River Plateau, along the northern boundary of the western Snake River Plain, and thence across the plain to northern Utah." This suggests a basic difference between the western and eastern plains: The western plain may be structurally controlled by a major break in the earth's crust; the eastern plain cannot be structurally controlled by this proposed break.

The lava in the western plain probably escaped along or near this crustal break and along adjoining long fissures, giving the gravity field its en echelon character. The main channels of escape for the basalts of the eastern plain, in contrast, may be vents or short fissures, causing the circular and oblong gravity highs along the boundary. It may be significant that they are aligned on the south and southeast boundary. It is perhaps along or near a fault, delineating this edge of the plain, that the magma found its escape.

The extensive fissure flows that predominated in the early formation of the western plain probably filled a large graben. The formation of the eastern depression has almost certainly been accompanied by faulting, but the regional structural control of the western plain is seemingly not a factor in the depression of the eastern plain, as manifested in their different gravity fields, recent tectonic history, and topographic settings. The accumulations of basalt has been less in the east and has filled troughs or valleys in an undulating subsurface floor rather than a large regional graben.

REFERENCES

- Bott, M. P. H., and Smith, R. A., 1958, The estimation of the limiting depth of gravitating bodies: *Geophys. Prosp.*, v. 6, no. 1, p. 1-10.
- Hill, D. P., Baldwin, H. L., and Pakiser, L. C., 1961, Gravity, volcanism, and crustal deformation in the Snake River

- Plain, Idaho: Art. 105 in U.S. Geol. Survey Prof. Paper 424-B, p. B248-B250.
- Kirkham, V. R. D., 1931, Snake River downwarp: Jour. Geology, v. 39, no. 5, p. 456-482.
- LaFehr, T. R., 1962, The estimation of depth using gravity data [abs.]: Geophysics Yearbook, p. 267.

- Malde, H. E., 1959, Fault zone along northern boundary of western Snake River Plain, Idaho: Science, v. 130, no. 3370, p. 272.
- Woollard, G. P., 1958, Tectonic activity and earthquake epicenters: Am. Geophys. Union Trans., v. 39, no. 6, p. 1135-1150.



142. GEOHYDROLOGIC EVIDENCE OF A BURIED FAULT IN THE ERDA AREA, TOOEELE VALLEY, UTAH

By JOSEPH S. GATES, Salt Lake City, Utah

Work done in cooperation with the Utah State Engineer

Differences in water-level fluctuations, chemical quality of ground water, altitude of the piezometric surface, and gravity on either side of a discontinuous ridge that crosses the Erda area, in Tooele Valley, Utah, suggest that a fault causes a ground-water barrier at the ridge; the ridge probably is a surface expression of the fault. The fault may be a branch or extension of the Occidental fault (fig. 142.1) into

Tooele Valley, and it is termed the Occidental(?) fault in this article. Its position is inferred chiefly from the piezometric surface and from the surface ridge, and is shown in figure 142.2. The fault zone may cover a wider area than that shown, and the line of faulting may consist of 2 faults, 1 trending north and 1 trending northwest, instead of 1 curving fault.

Gravity studies in Tooele Valley by W. W. Johnson¹ indicate a normal fault near the ridge, down-thrown to the southwest, which is shown in figure 142.2A for comparison. D. R. Mabey of the U.S. Geological Survey, who collected gravity data in the northern Oquirrh Mountains area, concludes (written communication, Dec. 27, 1961) that a fault trends a little west of north from the northwest corner of sec. 28, T. 2 S., R. 4 W., although he doubts that this fault could be extended to the southeast on the basis of gravity data.

The discontinuous ridge that crosses the Erda area from southeast to northwest (fig. 142.2A) contains gravel and boulders as large as 5 feet in diameter as far as 3½ miles from the front of the Oquirrh Mountains, in contrast to finer material that forms the surface on either side of the ridge. The gravel and boulders may have been deposited as a mudflow along the base of a fault scarp that since has been eroded. The deposit crops out prominently because the gravely material is more resistant to erosion than the adjacent finer material.

Ground-water conditions on opposite sides of the ridge differ considerably, as has long been known by local residents. Differences in the decline in water

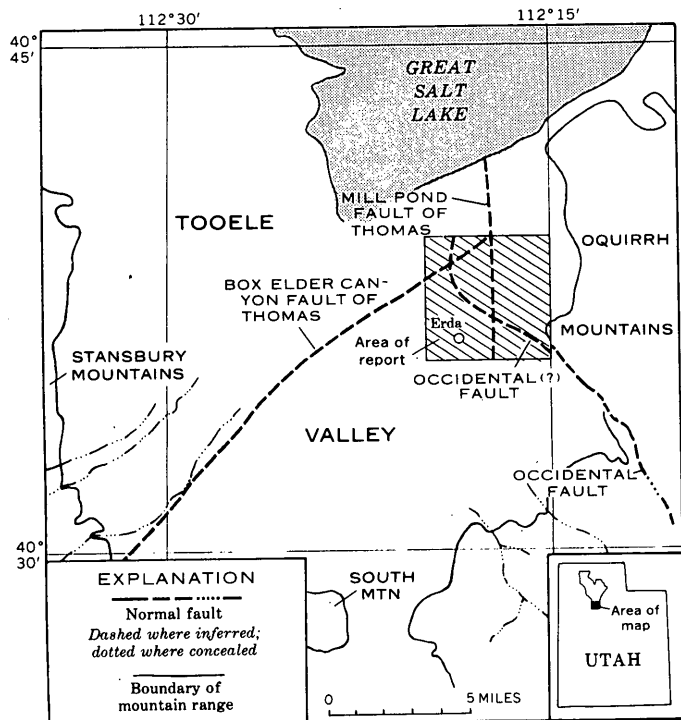
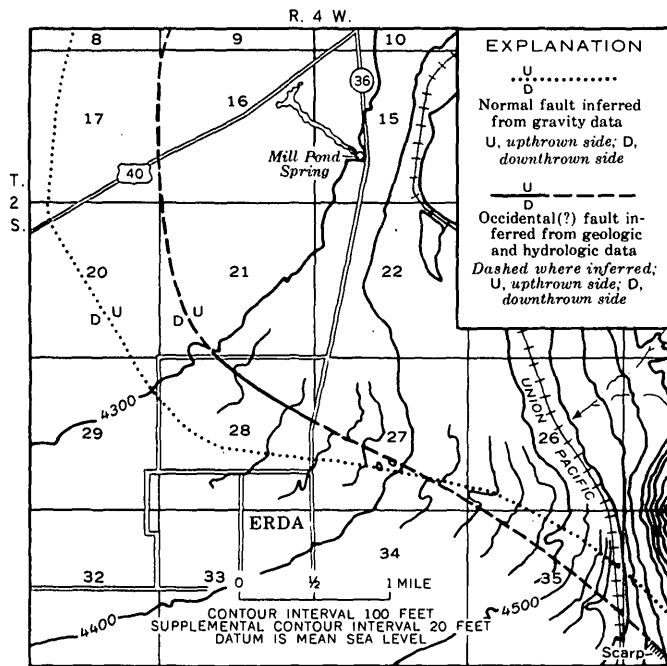
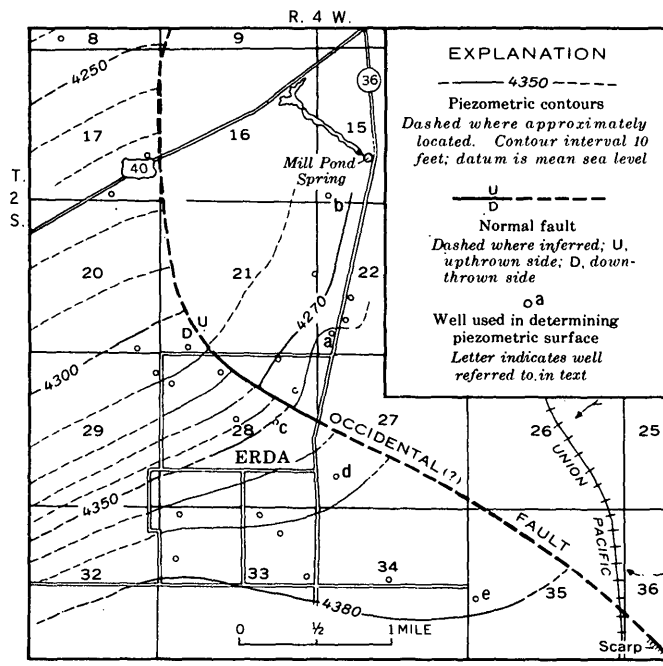


FIGURE 142.1.—Map showing the area described in this report, the Occidental and the Occidental(?) faults, and the Mill Pond and Box Elder Canyon faults as described by Thomas (1946).

¹ Johnson, W. W., 1958, Regional gravity survey of part of Tooele County, Utah: Utah Univ. M.S. thesis, 38 p.

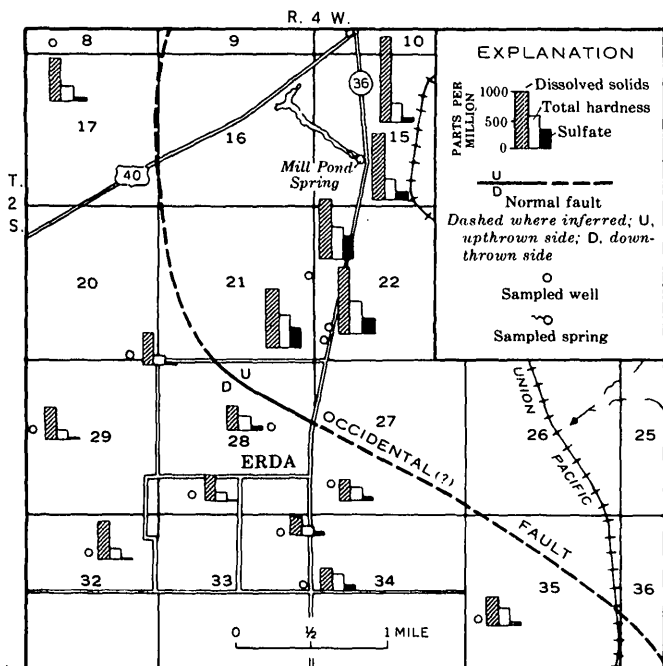


A



C

FIGURE 142.2.—Map of the Erda area showing position of the Occidental(?) fault relative to the following geologic and hydrologic evidence used by the author to infer the fault position: A, discontinuous ridge shown by contours and the position of a fault inferred by Johnson from gravity data, B, chemical character of representative samples of ground water, C, piezometric surface as of June 1959.



B

levels on the two sides of the ridge during the 1959 irrigation season indicated a ground-water barrier in the vicinity of the ridge. From spring to fall of 1959, the water level northeast of the ridge declined 1.2 feet in well a and 1.1 feet in well b (fig. 142.2C). In contrast, southwest of the ridge the water level declined 9.3 feet in well c, 5.0 feet in well d, and 3.3 feet in well e.

Chemical analyses of representative samples of ground water show a difference in quality of water on either side of the ridge (fig. 142.2B). Ground water northeast of the ridge contains more dissolved mineral matter and it has an especially high hardness and sulfate content, compared to that southwest of the ridge. This difference in quality can be demonstrated only for water from aquifers at shallow depths because northeast of the ridge the analyses are of samples from a spring and from wells less than 140 feet deep.

A map of the piezometric surface (fig. 142.2C) indicates a ground-water barrier at or very near the ridge. In wells northeast of the ridge, the altitude of the piezometric surface is 50 to 70 feet lower than that in wells southwest of the ridge. Some of the difference may be a result of measuring water levels of deeper wells southwest of the ridge and shallower wells to the northeast, because in Tooele Valley the deeper artesian aquifers have higher water levels than the shallower artesian aquifers. However, water levels in some wells of about the same depth on either side of the ridge differ by 50 to 70 feet, so a lack of hydraulic connection, and not a variation of well depths, is the cause of the large differences in water levels.

The discontinuous surface ridge intersects the Oquirrh Mountains near a range-front fault scarp

which is assumed to be the eastern limit of the trace of the fault through the Erda area (fig. 142.2A). Thomas (1946, p. 148) concluded that this scarp was an expression of the Occidental fault, which had been defined in the Bingham mining district about 8 miles south-east of Erda. The trace of the Occidental fault (Cook, 1961, pl. 1) and the trace of the Occidental(?) fault through the Erda area are nearly parallel and almost join at the mountain front (fig. 142.1). Thomas (1946, p. 149-150) considered the faults along the west front of the Oquirrh Mountains, which probably include the fault that passes through Erda, to be basin-and-range type faults of Tertiary and Quaternary age. James, Smith, and Welsh (1961, p. 56), however, state that the Occidental fault in the Bingham district is older than the basin-and-range type faults. The offset in the valley fill that causes the ground-water barrier may represent a basin-and-range type of fault movement along the older Occidental fault.

Thomas (1946, p. 147-152) described several faults in Tooele Valley, including the Box Elder Canyon and Mill Pond faults crossing the Erda area as shown on figure 142.1. Water-level and water-quality data collected in the present investigation, and Johnson's gravity data, suggest that the Box Elder Canyon fault does not cross Tooele Valley along the projection of its surface trace in Box Elder Canyon as interpreted

by Thomas. Also, the Mill Pond fault, instead of trending south from Mill Pond Spring as interpreted by Thomas, probably trends southeast from the spring roughly parallel to the Union Pacific Railroad tracks. Because the existence of the one and the location of the other are questionable they are not shown on figure 142.2.

The Utah State Engineer does not encourage the drilling of new wells in the Erda area because ground water in the area may be fully appropriated. Recognition of the Occidental(?) fault, however, may lead to additional ground-water development in the Erda area, because an increase in withdrawal of water from the relatively undeveloped area northeast of the fault should not lower water levels in the more highly developed area southwest of the fault.

REFERENCES

- Cook, D. R., ed., 1961, *Geology of the Bingham mining district and northern Oquirrh Mountains*: Utah Geol. Soc. Guidebook 16, 145 p.
- James, A. H., Smith, W. H., and Welsh, J. E., 1961, *General geology and structure of the Bingham district, Utah*, in Cook, D. R., ed., *Geology of the Bingham mining district and northern Oquirrh Mountains*: Utah Geol. Soc. Guidebook 16, p. 49-69.
- Thomas, H. E., 1946, *Ground water in Tooele Valley, Tooele County, Utah*: Utah State Engineer Tech. Pub. 4, in Utah State Engineer 25th Bienn. Rept., p. 91-238.



143. RECURRENT MOVEMENT ON THE CANYON CREEK FAULT, NAVAJO COUNTY, ARIZONA

By TOMMY L. FINNELL, Denver, Colo.

The southwestern part of Navajo County, Ariz., lies within the Basin and Range physiographic province, but it is characterized, in general, by flat-lying sedimentary rocks which are continuous with the structurally simple rocks of the Colorado Plateaus province to the north.

A major fault, here named the Canyon Creek fault, has been traced along strike for about 11 miles in southwestern Navajo County, (fig. 143.1) and it also extends southward for about 30 more miles in Gila County (A. F. Shride, oral communication, 1962). The fault strikes generally N. 10° W. and is nearly vertical. For about 9 miles the fault is near the base of a rugged scarp facing westward on a broad valley oc-

cupied by Canyon Creek and Oak Creek. Near the south end of Chediski Farms, the scarp disappears and the fault follows the bed of Canyon Creek for about a mile. North of Chediski Farms the fault extends about a mile before it passes into a monocline.

Evidence for two distinct periods of movement with opposite sense is observed along the Canyon Creek fault—the early movement raised beds of Pennsylvanian age on the west; the later movement raised a gravel deposit and a basic flow of late Tertiary or Quaternary age on the east.

The maximum stratigraphic throw on the Canyon Creek fault at Chediski Farms is about 840 feet upward on the west. At the north end of Chediski

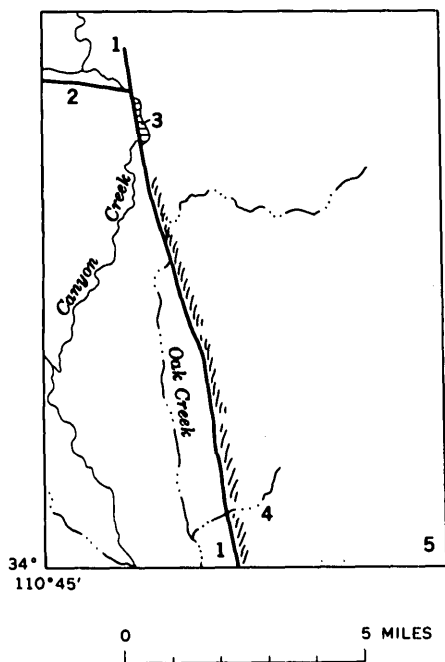


FIGURE 143.1.—Sketch map of the southwestern corner of Navajo County, Ariz. 1, Canyon Creek fault; 2, Lost Tank Canyon fault; 3, Chediski Farms; 4, Cliff House Canyon; 5, Spotted Mountain.

Farms, the westward trending Lost Tank Canyon fault joins the Canyon Creek fault and absorbs about 600 feet of the stratigraphic throw by downward displacement of the north block. About a mile north of the junction with the Lost Tank Canyon fault, the Canyon Creek fault passes into the anticlinal bend of an eastward-dipping monocline, which has about 600 feet of structural relief on the base of the Naco Formation (Pennsylvanian). The Canyon Creek fault near Chediski Farms is clearly post-Pennsylvanian in age and it may be Laramide or younger.

Southward from Chediski Farms the relative displacement on the fault remains upward on the west but the amount of throw diminishes gradually to about 500 feet at Cliff House Canyon, where the Dripping Spring Quartzite (Precambrian) on the west is in fault contact with the Troy Quartzite (Precambrian) on the east.

West of the fault on the south rim of Cliff House Canyon the Dripping Spring Quartzite is overlain by a gravel deposit of late Tertiary or Quaternary age, and this in turn is overlain by a basic flow about 60 feet thick. The gravel beds are dragged to dips of 80° W. along the fault, and the flow also seems to be dragged, indicating that the block west of the fault has been downthrown.

The basic flow west of the fault is very similar to a flow that rests on gravel on Spotted Mountain about 4 miles to the east, and, assuming that they are faulted portions of a single flow that covered a surface of low relief, the postflow displacement is about 1,300 feet upward on the east. The original upthrow on the west side of the Canyon Creek fault at this point, thus, may have been as much as 1,800 feet.

Where the Canyon Creek fault has been traced in Gila County, by A. F. Shride, gravel deposits of late Tertiary or Quaternary age are faulted upward on the east, and the deformation is considered to be the result of basin-range block faulting.

The early movement on the Canyon Creek fault apparently displaced beds upward as much as 1,800 feet on the west. Later movement apparently displaced gravel deposits of late Tertiary or Quaternary age upward as much as 1,300 feet on the east. The late movement probably represents basin-range deformation which followed the previously established line of weakness northward into an area of Colorado Plateaus structure.



144. RESTUDY OF THE ARROWHEAD FAULT, MUDDY MOUNTAINS, NEVADA

By C. R. LONGWELL, Menlo Park, Calif.

The Muddy Mountains, in Clark County, Nev., have rugged relief developed on Paleozoic carbonate rocks in an extensive flat thrust plate. A steep scarp at the north side of the range marks the location of the Arrowhead fault, a structural east-west boundary between the high mountain mass and the lower ridges of the North Muddy Mountains (fig. 144.1). These ridges, extending northward to the valley of the Muddy River, are developed on a structural pattern radically different from that south of the Arrowhead fault

(Longwell, 1949, pls. 1, 5). A belt of large folds, in part recumbent, extends from the Arrowhead fault northward through the western part of the North Muddy Mountains.

An early study of the area led to conviction that movement on the Arrowhead fault had an important left-lateral component (Longwell, 1928, p. 110-111, pl. 1, fig. 6). That interpretation regarded the steep fault as genetically related to the thrust and associated folds, serving to accommodate differences in

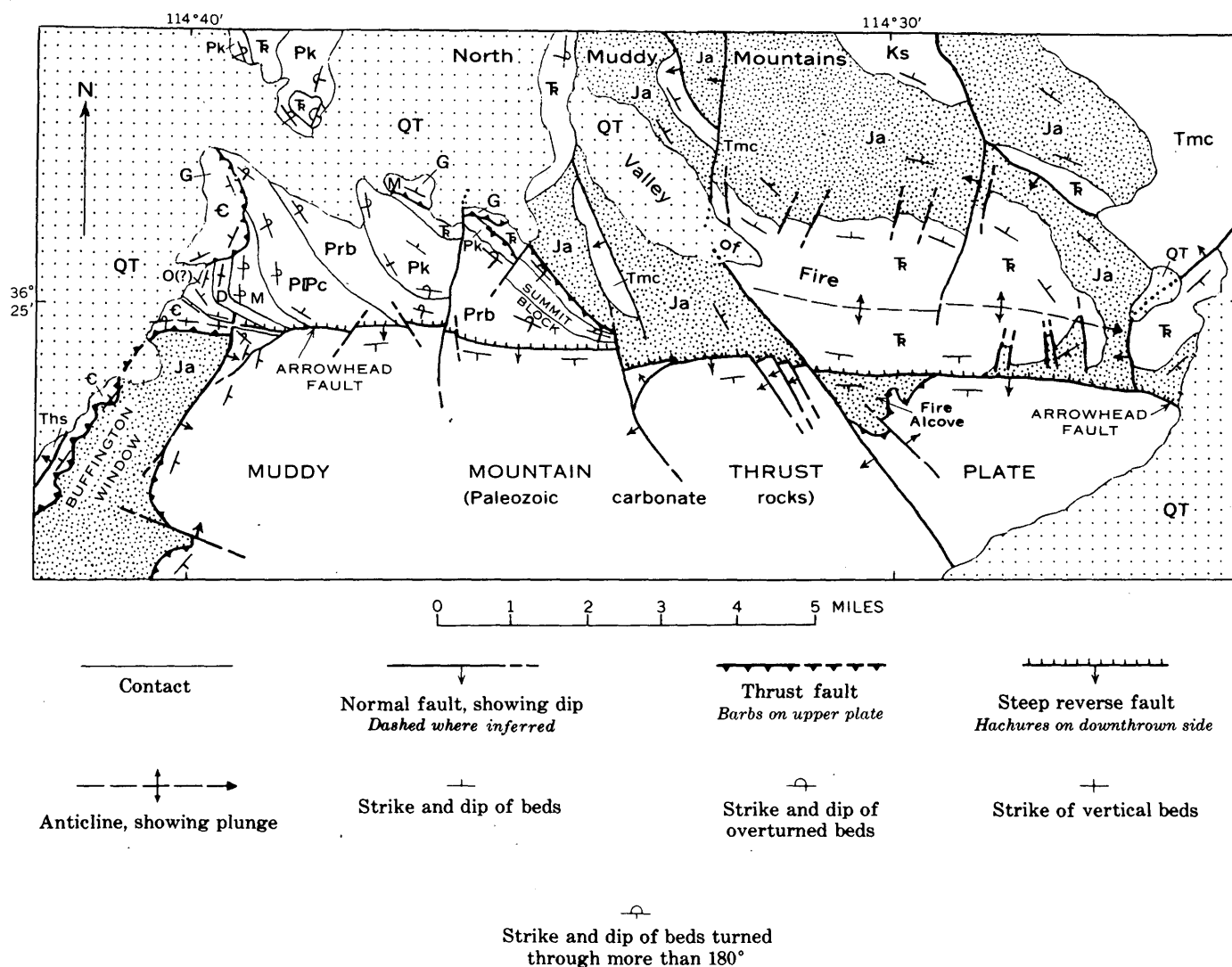


FIGURE 144.1.—Major structural features in the Muddy Mountain area. C and O, rocks of Cambrian and Ordovician(?) age; D, Devonian carbonate rocks; M, Mississippian carbonate rocks; PPc, Callville Limestone (Permian and Pennsylvanian); Prb, Permian red beds; Pk, Kaibab Limestone (Permian); T, Triassic rocks; Ja, Aztec Sandstone (Jurassic?); Ks, Cretaceous sedimentary rocks; Ths, Horse Spring Formation (Tertiary); Tmc, Muddy Creek Formation (Tertiary); QT, Quaternary and Tertiary deposits; G, remnant of Glendale thrust plate.

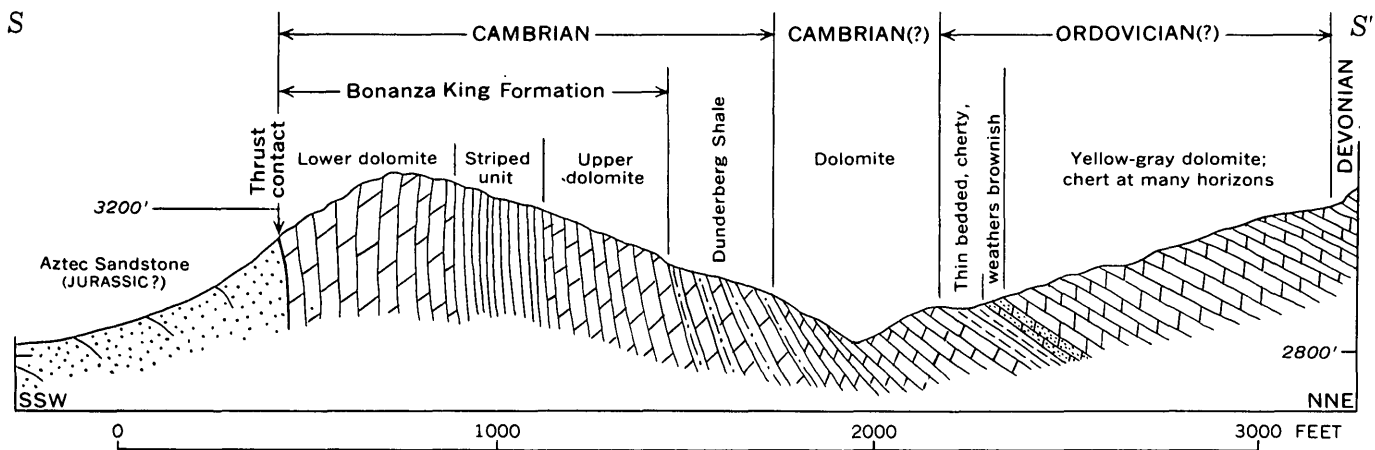


FIGURE 144.2.—Structure section across the monocline at west end of Arrowhead fault (on line $S-S'$, fig. 144.3).

deformation in adjacent major blocks. Parts of the structural pattern seem to indicate strong strike-slip movement. In the North Muddy Mountains, structural elements that trend generally north bend toward the southeast as they are traced toward the Arrowhead fault. This suggestion of drag effect from left-lateral movement is particularly impressive in the Summit thrust block, at the southwest border of the Valley of Fire.

A detailed study of the North Muddy Mountains revealed that near the west border of the range the Arrowhead fault passes into a steep monoclinical fold (Longwell, 1949). North of this fold, formations that make up the Muddy Mountain thrust plate are overturned beneath a thrust at a higher structural level, the Glendale thrust. Scattered remnants of the Glendale thrust plate overlie much-deformed younger strata in a belt extending more than 20 miles to the north.

The dying out of the Arrowhead fault in the monocline has important implications to be considered in analysis of the overall structural pattern. As the major blocks north and south of the fault are united in the monocline, the suggestion of large-scale strike-slip movement on the fault must be illusory. Such a component of movement would be possible only to the extent that deformation by folding or thrusting may have shortened the block on one side of the fault relative to the adjacent block. Thrusting and folding in the western part of the North Muddy Mountain belt perhaps caused enough local shortening to account for a limited strike-slip component on the fault.

Another important deduction from the union of blocks in the monocline concerns the northward extent of the Muddy Mountain thrust. Directly south of the Arrowhead scarp the plate was displaced, relatively eastward, through the full width of its present ex-

posure. The down-dropped part of the plate north of the fault must have moved eastward with the block to which it is attached in the monocline. Therefore the Muddy Mountain thrust must extend an unknown distance northward beneath a concealing cover of sedimentary formations (Longwell, 1949, p. 938, 940).

In the fall of 1961, with Leonard Palmer as field assistant, I began remapping the Muddy Mountain area on the topographic sheets now available. We gave particular attention to the Arrowhead fault and monocline. The valley of a stream that winds through the area of the monocline provides almost perfect exposures of the stratigraphic units (fig. 144.2). Sections measured in detail across the monocline agree closely with sections measured in the thrust plate east of the Buffington window; this agreement is in the succession of distinctive stratigraphic units, and in total thickness. The earlier map (Longwell, 1949, pl. 1) errs in extending the Arrowhead fault considerably too far west; the section exposed in the monocline is intact through a distance of at least a mile inside the border of the range. Farther east there is increasing displacement on the Arrowhead reverse fault, with cutting out of successive formations north of it (fig. 144.3).

Displacement on steep faults northeast of the Buffington window has played a part in adjustment from large upthrow on the Arrowhead fault to strong bending in the monocline. A northeast-trending fault against which the folding ends probably was itself deformed under pressure, as suggested by abrupt changes in its strike and dip. West of this fault a part of the monocline hooks strongly southward, with much local bending and fracturing. Displacement on the fault dies out rapidly southwestward toward the east margin of the window, where it intersects a normal fault along which rocks of the thrust plate have

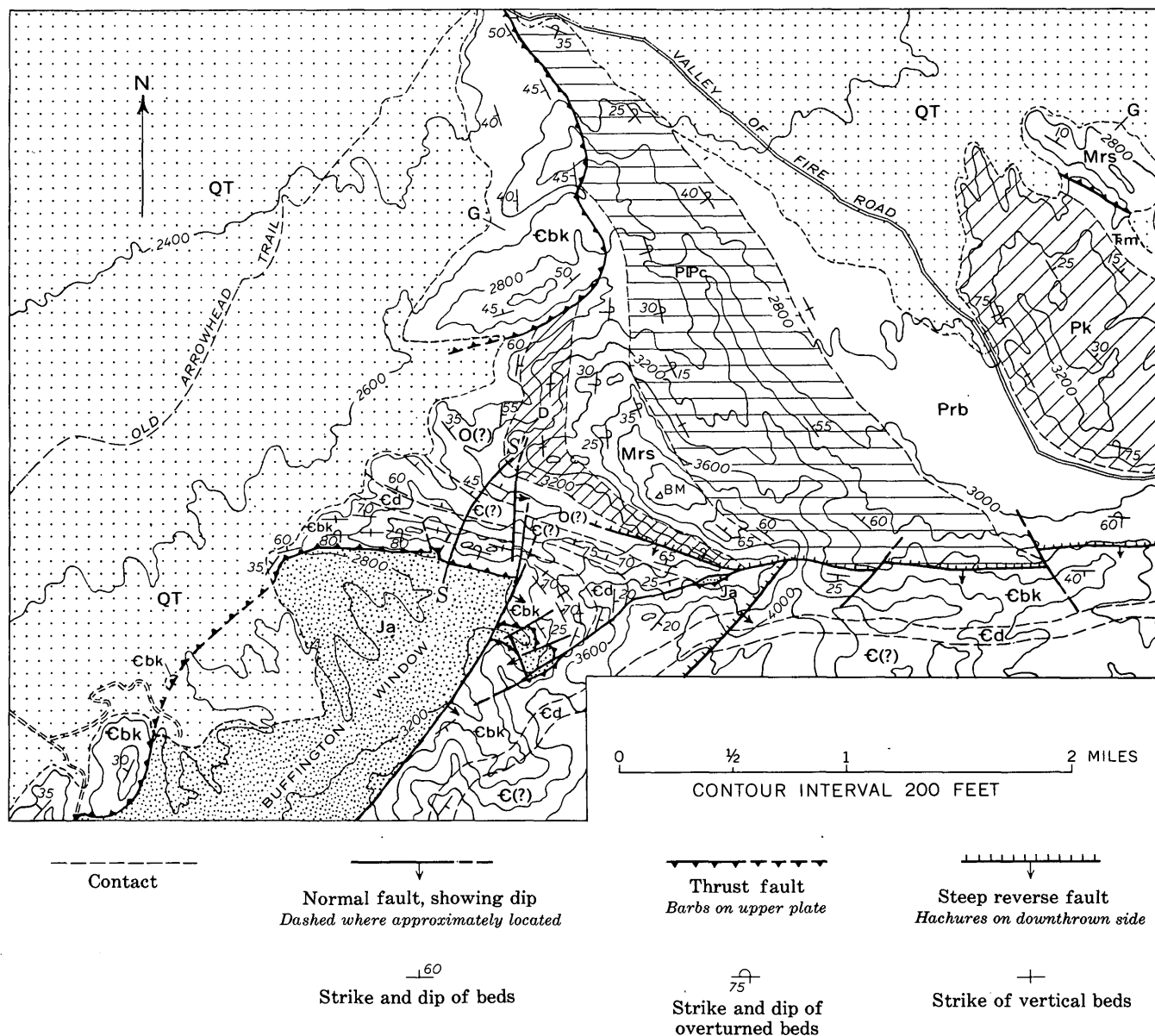


FIGURE 144.3.—Map showing details of structure near west end of Arrowhead fault. Cbk, Bonanza King Formation; Cd, Dunderberg Shale; Cu and Ou, unnamed units of Cambrian(?) and Ordovician(?) age; D, Devonian carbonate rocks; Mrs, Rogers Spring Limestone (Mississippian); Fm, Moenkopi Formation (Triassic). Other symbols for formations, and also structure symbols, as in figure 144.1. S-S', approximate line of structure section, figure 144.2.

been dropped against Aztec Sandstone. East of this normal fault the base of the plate and the underlying sandstone are exposed locally in two valleys.

North of the Buffington window, where successive formations in the Muddy Mountain plate dip steeply northward, units of Devonian and later age are overturned eastward beneath the Glendale thrust (fig. 144.3). A conspicuous bend in strike of the older formations from west to northwest and north indicates that these units also were transected and upturned in the Glendale thrusting. As these overridden forma-

tions constitute the Muddy Mountain plate, clearly the Glendale thrust is at a higher structural level. A westward divergence in strike along the monoclinical axis results from intersection by the monocline of two structural units very different in character. In the Muddy Mountain plate, bedding is essentially parallel to the surface of thrusting. Where this planar unit, dipping westward, is bent strongly down along an east-west axis, the resulting pattern is a sharp curve in strike southward from the monocline. But northward tilting of formations that were turned up be-

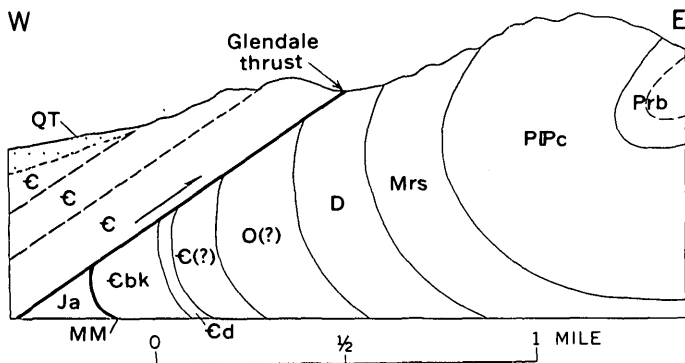


FIGURE 144.4.—General relation, in section, between the Muddy Mountain thrust and the Glendale thrust, northwest of the Buffington Window. MM, base of Muddy Mountain thrust plate. Other symbols as in figures 144.1 and 144.3.

neath the Glendale thrust, followed by erosion, has produced the pattern with curvature northward from the axis.

The Glendale belt of thrusting and folding must have extended farther south, above the area of the Buffington window. After the two major thrusts were displaced by the Arrowhead fault and monocline, erosion removed the higher structure from the area of uplift. If the Glendale thrust is extrapolated from the southernmost exposure of the plate, it should extend southwestward beneath the cover of alluvial deposits west of the range, where presumably it transects the Muddy Mountain thrust (fig. 144.4).

Study of a large and complex structural unit should consider all reasonable possibilities of origin and history. An obvious hypothesis may assume the Arrowhead fault to be a normal fault with downthrow on the south. Under this concept the North Muddy Mountains would represent a footwall block from which the Muddy Mountain thrust plate was eroded following uplift. The concept fails under several tests, one of them involving the monocline north of the Buffington window. Passing of a south-dipping normal fault into a flexure should result in a monocline dipping southward, not northward. Moreover in ex-

cellent exposures along the fault east of the monocline, beds on the north are bent sharply upward, testifying in convincing fashion to reverse movement against strong frictional resistance. Evidence of this kind is cumulative in a detailed study of the fault zone.

The pattern that suggests important left-lateral movement on the Arrowhead fault merits analysis. Flexures that trend northwest in the high Muddy Mountain mass south of the fault imply that such trends may have been common, before the fault was in operation, in a wide belt that included the Summit block and neighboring ridges. Probably the pronounced curvature at the southeast end of the Summit ridge and similar structural details in neighboring ridges reflect northward pressure, while the fault was active, against blocks in which northwest trends were the result of earlier deformation.

Exposures in the embayment known as Fire Alcove, 9 to 10 miles east of the Buffington window, have particular interest. There the thrust plate, on Aztec Sandstone, has the same succession of stratigraphic units of Cambrian age found in the lower part of the plate at the west side of the range. Bedding in the plate is essentially parallel to the thrust contact. The plate and the underlying Aztec Sandstone of Jurassic(?) age dip steeply southward from the Arrowhead fault. Along the fault the sandstone is in contact with formations of Triassic age. It is clear, therefore, that displacement on the Arrowhead fault is not restricted to the thrust plate, as was assumed in the concept that movement on the fault was largely strike-slip and genetically related to the thrusting. The throw on the steep reverse fault north of Fire Alcove, as reckoned from thicknesses of the transected formations, exceeds 10,000 feet (Longwell, 1949, fig. 7, p. 940).

REFERENCES

- Longwell, C. R., 1928, Geology of the Muddy Mountains, Nevada: U.S. Geol. Survey Bull. 798, 152 p.
 ——— 1949, Structure of the northern Muddy Mountain area, Nevada: Géol. Soc. America Bull., v. 60, p. 923-968.



145. CORRELATION OF GRANITIC PLUTONS ACROSS FAULTED OWENS VALLEY, CALIFORNIA

By DONALD C. ROSS, Menlo Park, Calif.

Work done in cooperation with the California Division of Mines and Geology

This article presents evidence for the correlation of the Santa Rita Flat pluton in the Inyo Mountains with the Tinemaha Granodiorite, of Cretaceous age, in the Sierra Nevada (Bateman, 1961). Such a correlation places a limit on the amount of lateral movement along the faults that bound or lie beneath Owens Valley.

Geologic mapping in the east-central Sierra Nevada during the past several years has focused attention on correlating areally separate granitic masses within the composite Sierra Nevada batholith. The most recent product of this work is a report by Bateman (1961) in which he established several formal granitic formations in the Bishop area.

Bedrock in the Inyo Mountains, across Owens Valley from the Sierra, consists predominantly of Paleozoic sedimentary rocks into which are intruded granitic plutons, some of batholithic proportions. In the Independence quadrangle, D. C. Ross, F. K. Miller, and R. J. Pickering have delineated several large plutons, one of which, the Santa Rita Flat pluton, bears a close resemblance to the Tinemaha Granodiorite of the Sierra Nevada (fig. 145.1). Examination of these two masses in the field and comparison of modal and chemical data suggest that they are correlative. This is the first time that a single lithologic unit has been correlated across Owens Valley, although broad correlations based on the regional pattern have been proposed (Bateman and others, 1962). Folded Paleozoic sedimentary and Mesozoic volcanic strata of the Inyo Mountains strike obliquely across Owens Valley toward the Sierra Nevada and may be correlative with metamorphosed remnants of grossly similar lithologies in the Sierra Nevada. Moore and Hopson (1961) have also suggested that a swarm of mafic dikes in the eastern Sierra is correlative across Owens Valley with similar dikes on strike in the southern Inyo Mountains.

The criteria for correlating areally separated granitic plutons are: (1) similarity of appearance—in particular similarity of textures and structures; (2) similarity of composition; and (3) compatible intrusive relations, and hence similar age.

The textural and mineralogical similarity of the Santa Rita Flat pluton and the Tinemaha Granodiorite is striking. Both masses have about the same

percentage of dark minerals and a range in grain size of 2 to 5mm. Both contain widespread tabular to equant phenocrysts of K-feldspar as long as 2 cm, which have irregular borders and are commonly studded with dark minerals. Scattered relatively well formed hornblende crystals that are generally 1 to 2 cm long are characteristic of the Santa Rita Flat pluton, and were also observed in outcrops of the Tinemaha Granodiorite. Lenticular mafic inclusions in the Tinemaha Granodiorite, described by Bateman (1961) as numerous and defining a foliation, are widespread in the Santa Rita Flat pluton, but they are rarely abundant and only locally define a foliation.

The compositional similarity and the similar average specific gravity of these two masses also suggest

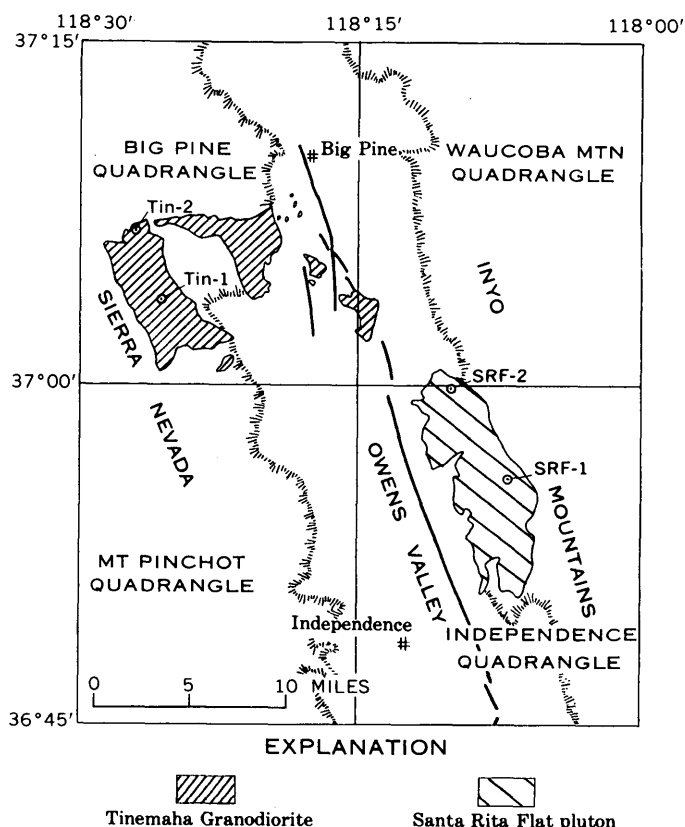


FIGURE 145.1.—Map showing outcrop area of Santa Rita Flat pluton and Tinemaha Granodiorite. Faults along which there was movement in the 1872 earthquake in Owens Valley are shown as heavy black lines. Location of chemically analyzed samples is shown by small circled dots.

TABLE 145.1.—*Modal data of Santa Rita Flat pluton and Tinemaha Granodiorite*

	Average modes ¹	
	Santa Rita Flat pluton	Tinemaha Granodiorite ²
Plagioclase.....	36	42.3
K-feldspar.....	31	24.5
Quartz.....	20	19.2
Biotite.....	4	4.6
Hornblende.....	6	6.0
Other.....	3	3.4
Average specific gravity.....	2.70	2.72
Hornblende: biotite.....	1.5:1	1.3:1
Dark-mineral content (color index).....	13	14

¹ In volume percent.² Data on average mode from Bateman (1961).

correlation. Abundant modal data show that the two bodies have similar percentages of quartz, biotite, and hornblende, but somewhat different percentages of plagioclase and K-feldspar (table 145.1). Hornblende in excess of biotite, which is characteristic of both bodies but quite unusual in rocks of the central Sierra Nevada, is a key factor in the suggested correlation.

The triangular plots of individual modes on figure 145.2 (points show quartz, plagioclase, and K-feldspar recomputed to 100 percent) show that although the Santa Rita Flat pluton has a more restricted compositional range and relatively more K-feldspar than the Tinemaha Granodiorite, the modal field of the Santa Rita Flat pluton encloses nearly two-thirds of the modal plots of the Tinemaha Granodiorite specimens.

Chemical data (table 145.2 and fig. 145.3) are limited to only two analyses from each mass, and these analyses are not of average specimens in the sense of having modes near the centers of their respective modal fields. Caution must be observed therefore in using the limited chemical data to draw conclusions about these granitic masses whose modal, and hence compositional, range is great. It seems reasonable to conclude, however, that though the chemical data neither confirm nor deny correlation, they are compatible with the correlation of these masses.

The intrusive relations, and hence the age relations of these masses, cannot be compared because the Santa Rita Flat pluton is not in contact with other granitic plutons. Both masses, however, are cut by abundant dark-colored dikes of the type described by Moore and Hopson (1961).

In summary, each of the two masses discussed here has persistent mappable characteristics. Further, the similarity of the masses suggests that both are part of an originally continuous granitic intrusive, though the

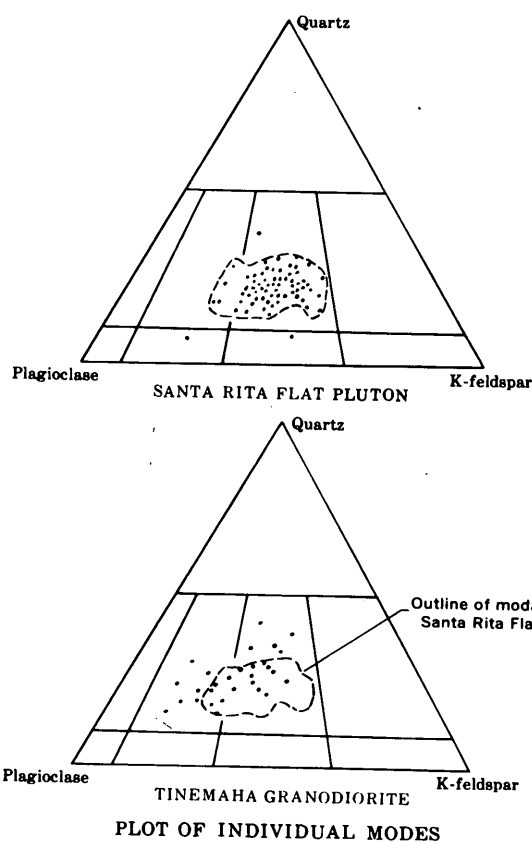
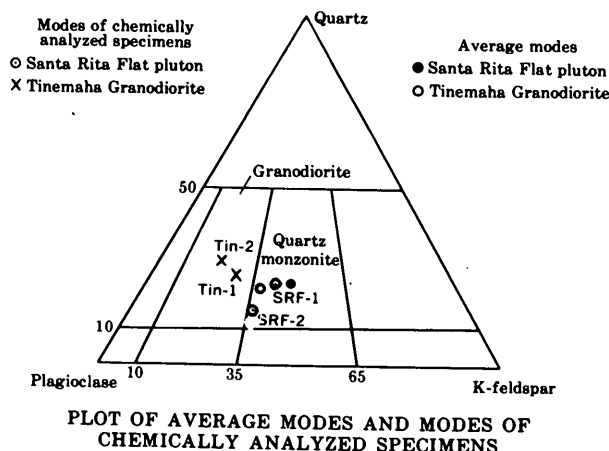


FIGURE 145.2.—Plots of modal data of the Santa Rita pluton and Tinemaha Granodiorite. Data on individual modes are from Bateman (written communication, 1962).

connection may be at some depth. The overall northwest trend of the two plutons (fig. 145.1), parallel to the regional trend of many granitic masses in the central Sierra, suggests a present-day connection beneath the Cenozoic deposits of Owens Valley. However, the several-mile gap between the easternmost outcrops of Tinemaha Granodiorite and the Santa Rita Flat pluton precludes more than speculation on

TABLE 145.2.—Chemical analyses and norms of Santa Rita Flat pluton and Tinemaha Granodiorite

	SRF-1 ¹	SRF-2 ¹	Tin-1 ²	Tin-2 ³
CHEMICAL ANALYSES				
SiO ₂ -----	66.4	61.3	62.82	65.77
Al ₂ O ₃ -----	14.9	15.9	15.44	14.34
Fe ₂ O ₃ -----	2.6	3.1	2.59	2.10
FeO-----	2.0	3.0	3.17	2.62
MgO-----	1.6	2.2	2.35	2.02
CaO-----	3.9	5.3	5.04	4.24
Na ₂ O-----	3.0	3.3	3.15	3.18
K ₂ O-----	4.1	3.4	3.72	3.76
H ₂ O-----	.73	.85	.65	.56
TiO ₂ -----	.48	.64	.64	.60
P ₂ O ₅ -----	.26	.36	.30	.24
MnO-----	.08	.10	.11	.10
CO ₂ -----	.05	.05	.01	.08
NORMS				
Q-----	23.5	15.7	16.69	21.42
or-----	24.5	20.0	22.20	22.24
ab-----	25.2	27.8	26.71	27.25
an-----	15.0	18.6	16.68	13.34
di-----	2.0	4.0	5.16	5.66
hy-----	3.9	5.6	6.18	4.32
mt-----	3.7	4.4	3.74	3.02
il-----	.9	1.2	1.22	1.22
ap-----	.7	1.0	.69	.34
Total-----	99.4	98.5	99.27	98.81
Normative plagioclase---	An ₃₇	An ₄₀	An ₃₈	An ₃₃

¹ Rapid rock analysis. Analysts: P. L. D. Elmore, I. H. Barlow, S. D. Botts, G. Chioe.

² Standard rock analysis (Bateman 1961, p. 1525-1526.)

³ Standard rock analysis (Bateman, written communication 1962).

this point. Also, at least minor disruption of the postulated originally continuous body must have occurred along the trend of the 1872 earthquake faults.

The correlation of these plutons across Owens Valley affects interpretations of the structural history of the region. Hill (1954, p. 10) suggests that Owens Valley may be the course of a major strike-slip fault. More recently Pakiser (1960) invokes strike-slip movement to help account for the origin and distribution of Cenozoic volcanic rocks in Owens Valley. Strike-slip faulting undoubtedly took place along some of the faults shown on figure 145.1 during the Owens Valley earthquake of 1872; however, Bateman (1961, p. 493) suggests that strike-slip movement was sub-

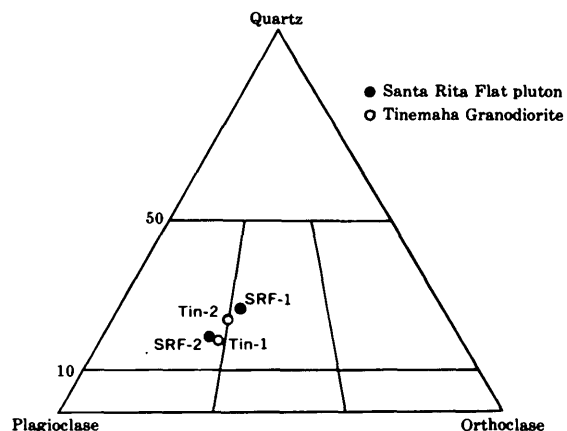


FIGURE 145.3.—Plot of normative quartz, orthoclase, and feldspar.

ordinate to dip-slip movement in the Cenozoic structural development of the region. Moore and Hopson (1961, p. 258) suggest a limitation on strike-slip movement in Owens Valley of a few miles at most since Cretaceous time, based on the strike continuation of a swarm of mafic dikes across the valley. The correlation of the Santa Rita Flat pluton with the Tinemaha Granodiorite supports the view that strike-slip movement along the present course of Owens Valley is limited to a few miles at most since the emplacement of the Sierra Nevada batholith.

REFERENCES

- Bateman, P. C., 1961, Willard D. Johnson and the strike-slip component of fault movement in the Owens Valley, California, earthquake of 1872: *Seismol. Soc. America Bull.*, v. 51, no. 4, p. 483-493.
- Bateman, P. C., Clark, L. D., and others, 1962, The Sierra Nevada batholith—a synthesis of recent work across the central part: U.S. Geol. Survey Prof. Paper 414-D. (In press)
- Hill, M. L., 1954, Tectonics of faulting in southern California, in Jahns, R. H., ed., *Geology of southern California*: California Div. Mines Bull. 170, chap. 4, pt. 1, p. 5-13.
- Moore, J. G., and Hopson, C. A., 1961, The Independence dike swarm in eastern California: *Am. Jour. Sci.*, v. 259, p. 241-259.
- Pakiser, L. C., 1960, Transcurrent faulting and volcanism in Owens Valley, California: *Geol. Soc. America Bull.*, v. 71, p. 153-160.

146. STRUCTURAL CONTROL OF INTERIOR DRAINAGE, SOUTHERN SAN JOAQUIN VALLEY, CALIFORNIA

By GEORGE H. DAVIS and J. H. GREEN, Washington, D.C., and Sacramento, Calif.

The southern part of the San Joaquin Valley, under the present water regime, is a basin of interior drainage. The streams tributary to the southern part of the valley drain to natural sumps in the center of the San Joaquin Valley, the largest of which is called Tulare Lake Bed. The low point of Tulare Lake Bed is 178 feet above sea level; the divide to the north is 210 feet above sea level (fig. 146.1). Before the first diversions for irrigation about 90 years ago, the area was not permanently a basin of interior drainage. During periods of high runoff, Tulare Lake would fill to an elevation of 210 feet and would discharge north to the San Joaquin River and thence to the Pacific Ocean. Playas or salt flats did not form because through-flowing water periodically flushed out accumulated salt.

The principal tributary to Tulare Lake Bed, the Kings River, is peculiar because under both natural and regulated conditions it splits—part of the water flows south to Tulare Lake and part north to the San Joaquin River. During low and normal stages, most of the water flows to Tulare Lake Bed; during high stage much spills north to the San Joaquin.

Two principal explanations have been advanced to account for the interior drainage of the southern San Joaquin Valley. One advocated by Mendenhall and others (1916, p. 21), W. M. Davis (1933, p. 224), Hinds (1952, p. 150), and many others explains the interior drainage as due to damming of the valley by the growth of the alluvial fans of the Kings River from the east and Los Gatos Creek from the west. The other explanation suggests that Tulare Lake Bed is the site of a structural downwarp and that active tectonic subsidence is the cause of the topographic depression (G. H. Davis and others, 1939, p. 29).

The theory of damming by alluvial-fan growth implies that the formation of Tulare Lake occurred during the present cycle of deposition and presumes that through drainage was the rule before the supposed damming. If this theory is valid, the sedimentary record should reflect these events. Maintenance of an alluvial dam across the axis of the valley would require continuing deposition of the fans. For example, the soils on the divide north of Tulare Lake Bed should be typical Recent alluvial-fan materials, the lacustrine soils of Tulare Lake Bed should be merely

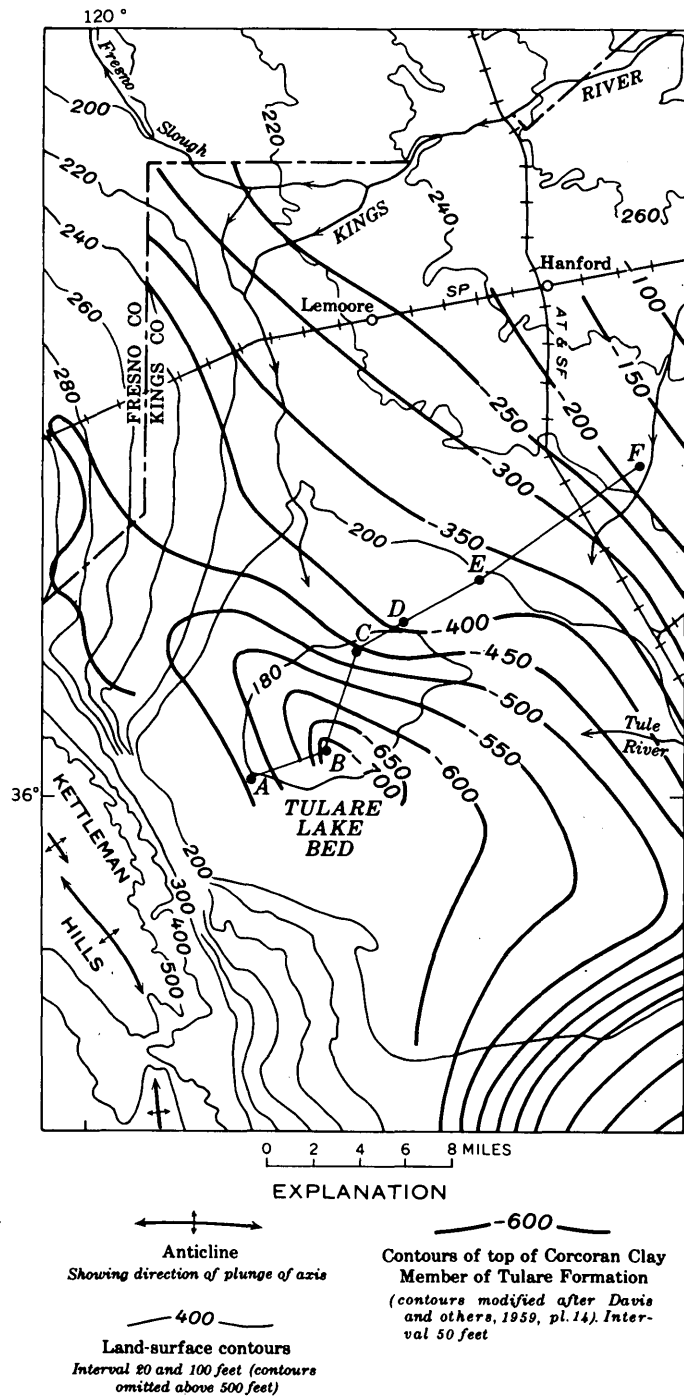


FIGURE 146.1.—Topography and structure of the Tulare Lake Bed area, San Joaquin Valley, Calif.

a veneer, and the subsurface deposits of the lake bed should be alluvial deposits typical of the axis of the valley.

The alternate theory is that Tulare Lake Bed is the surface expression of a structural depression flanking the Kettleman Hills anticlinal structure. Subsurface evidence collected in recent years offers strong support for this theory, as discussed below.

The surface soils in the area of the divide north of Tulare Lake are not typical alluvial-fan soils. Instead, a belt of clay "soils of the valley basins," indicative of deposition under conditions of poor surface drainage, extends northward from Tulare Lake Bed toward Fresno Slough (Retzer and others, 1946, fig. 3) and separates the Kings River alluvial fan from that of Los Gatos Creek. Furthermore, the soils of the toe of the Los Gatos fan are classified by Retzer and others as "soils of the old alluvial fans and valley plains," and not as Recent alluvial-fan deposits. These old fan soils belong to the Lethent series, which are characteristically heavy textured, calcareous, and show considerable profile development. Taken together these features indicate that the Lethent soils are not accumulating under the present regime but are a relic of a previous cycle of deposition. Under present conditions of drainage, Los Gatos Creek deposits nearly all its load on the upper slope of the fan several miles west of the valley axis.

The lacustrine soils of Tulare Lake Bed are not a veneer over typical alluvial deposits of the valley axis as might be expected under the alluvial-dam theory. Instead, fine-grained deposits that are almost entirely silt and clay, indicating deposition in still water, extend to great depth. For example, well A (fig. 146.2) penetrated clayey deposits to a depth of 2,750 feet below sea level before encountering substantial amounts of sand, and well B penetrated clayey material to 1,865 feet below sea level where it entered a sand 249 feet thick. Wells in the Tulare Lake Bed area remote from the Kings River fan penetrate little or no sand in the upper several hundred feet; the lack of sand beds indicates that for a long period there was no through-flowing trunk stream along the valley axis. Moreover, the typical gray, blue, or black color of the deposits indicates deposition in a reducing environment, which would be expected in an area of poor drainage such as a lake or swampy area.

The lithology and structure of the subsurface deposits as shown on figure 146.2 also support the structural theory. To the northeast, on the Kings River fan, the subsurface deposits consist of thin-bedded silty and sandy materials to a depth of more than 1,200 feet, as shown by the electric log of well F. This

sequence is interrupted by about 75 feet of diatomaceous lacustrine clay—the Corcoran Clay Member of the Tulare Formation—which has been traced in the subsurface throughout more than 5,000 square miles of the axial part of the San Joaquin Valley (Frink and Kues, 1954, fig. 3; Davis and others, 1959, pl. 14.)

The structural contours of figure 146.1, showing the configuration of the Corcoran Clay Member, outline a structural depression whose axis passes through Tulare Lake Bed; the depression is elongated parallel to the trend of the Kettleman Hills. The closure on the Corcoran is on the order of 300 feet, compared to a topographic closure of about 30 feet (fig. 146.1). Frink and Kues (1954, fig. 2) show that the Corcoran attains its maximum thickness of more than 120 feet in the Tulare Lake area, suggesting that a topographic and structural low prevailed there before and during the widespread Corcoran lacustrine episode. This suggests that some of the relief on the Corcoran was due to deposition on the sloping bed of a lake; however, the lithology of the deposits above and below the Corcoran in most of the San Joaquin Valley suggests that the gradient of the valley floor was little different than at present. Thus, the authors believe that the closure on the Corcoran is due chiefly to post-depositional structural warping.

Sandy alluvial deposits of the Kings River fan, which are generally conformable with the Corcoran in the northeastern part of the section on figure 146.2, pinch out to the west or grade into thick-bedded, well-sorted sands as shown by the electric logs of wells C and D. The predominance of sand and the thick bedding suggest deposition as deltaic deposits along a lake shore, rather than as stream-channel deposits. The thick sand sequence penetrated by well C either pinches out or dips steeply toward well B. Most likely, the clayey deposits above -1,865 feet (sea-level datum) at well B are the fine-grained equivalents of the thick sands of well C. The absence of coarse alluvial deposits to depths of more than 2,000 feet beneath Tulare Lake Bed in the central part of the San Joaquin Valley indicates that through flow has not drained the valley during the interval represented by the upper 2,000 feet of deposits. The presence of dark silt and clay along the axis of the valley trough and thick probable beach sands to the east suggests that a lacustrine environment has been maintained for a long interval at the site of the present Tulare Lake Bed. Maintenance of such an environment requires continued relative subsidence of the area, otherwise the depression would have filled with sediments and through drainage would have been established. The present topography and drainage, therefore, are interpreted as resulting chiefly from the continued tectonic

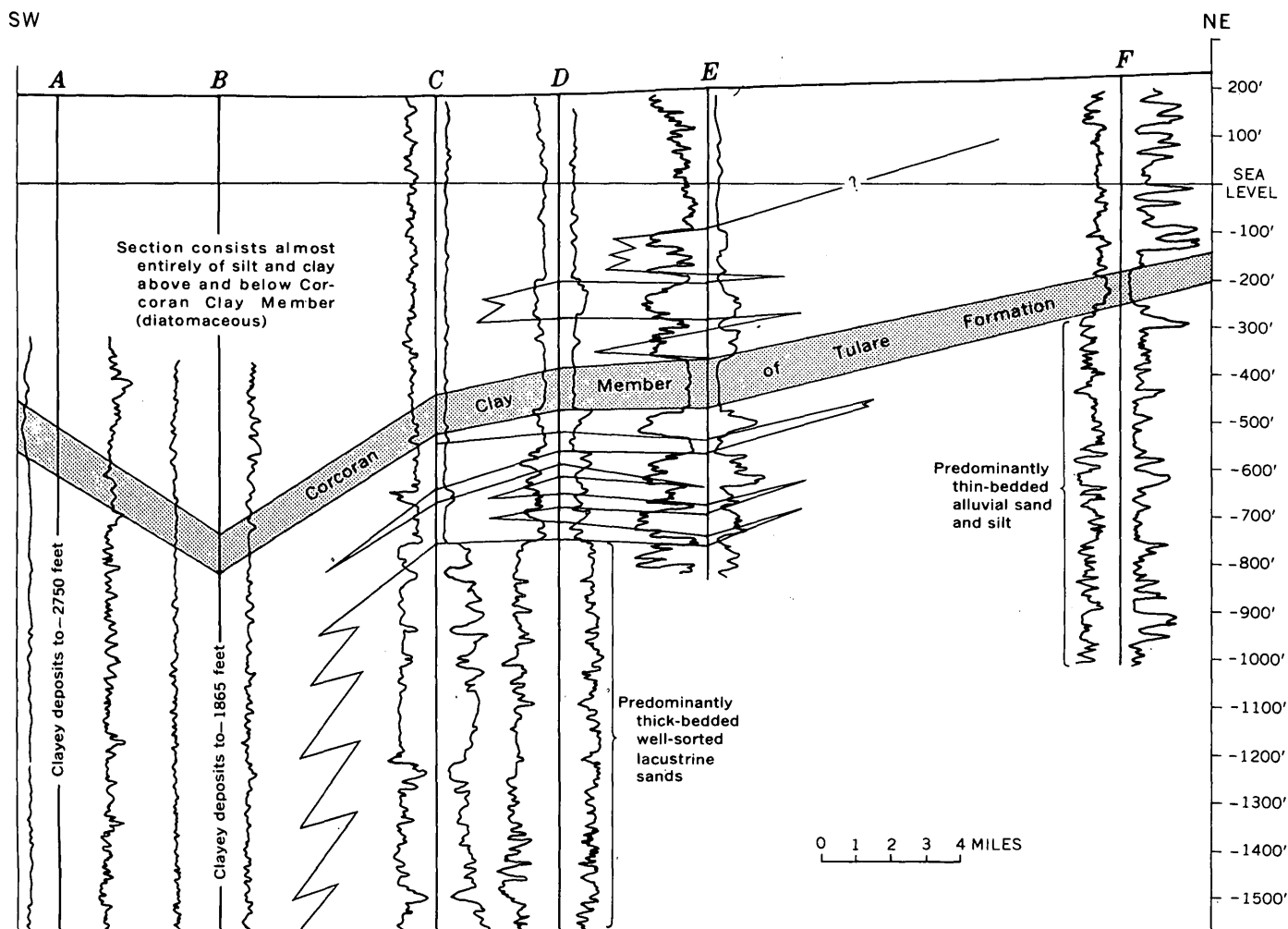


FIGURE 146.2.—Diagrammatic geologic section across Tulare Lake Bed based on electric logs of water wells and oil-test wells. Spontaneous-potential curve on left, resistivity curve on right at each well; scales not uniform. Alinement of section shown on figure 146.1.

subsidence of a synclinal structure paralleling the Kettleman Hills anticlinal structure, rather than from damming of the drainage of the valley by alluvial-fan growth.

REFERENCES

- Davis, G. H., Green, J. H., Olmsted, F. H., and Brown, D. W., 1959, Ground-water conditions and storage capacity in the San Joaquin Valley, Calif.: U.S. Geol. Survey Water-Supply Paper 1469.
- Davis, W. M., 1933, The lakes of California: California Jour. Mines and Geology, v. 29, nos. 1 and 2.
- Frink, J. W., and Kues, H. A., 1954, Corcoran Clay—A Pleistocene lacustrine deposit in San Joaquin Valley, Calif.: Am. Assoc. Petroleum Geologists Bull., v. 38, no. 11, p. 2357-2371.
- Hinds, N. E. A., 1952, Evaluation of the California landscape: California Div. Mines Bull. 158.
- Mendenhall, W. C., Dole, R. B., and Stabler, Herman, 1916, Ground water in San Joaquin Valley, Calif.: U.S. Geol. Survey Water-Supply Paper 398.
- Retzer, J. L., Gardner, R. A., Koehler, L. F., and Cole, R. C., 1946, Soil survey of Kings County, Calif.: U.S. Dept. Agriculture Ser. 1938, no. 9, 102 p.

147. TERTIARY SALT DOMES NEAR SAN PEDRO DE ATACAMA, CHILE

By ROBERT J. DINGMAN, Santiago, Chile

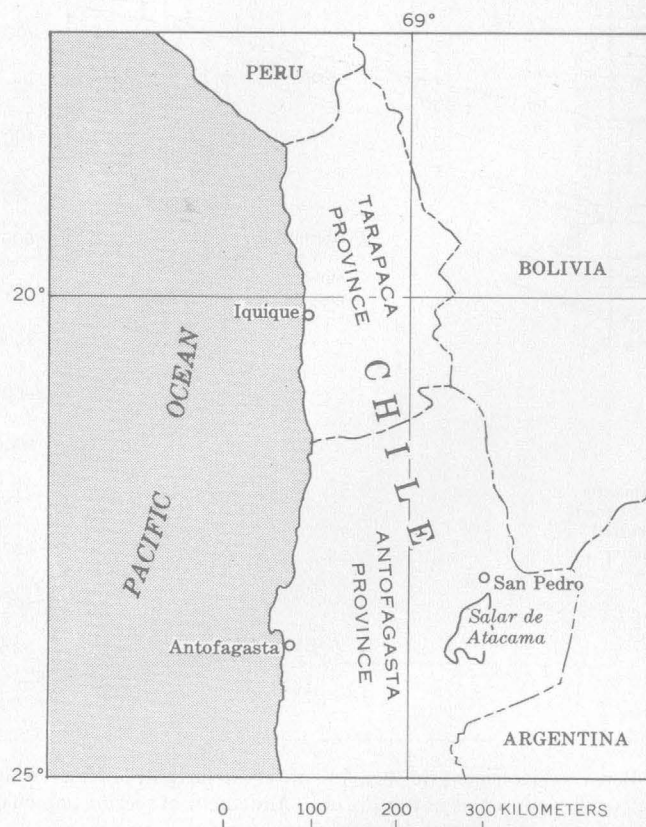
Work done in cooperation with the Instituto de Investigaciones Geológicas, Santiago, Chile

FIGURE 147.1.—Index map of Chile showing location of Salar de Atacama.

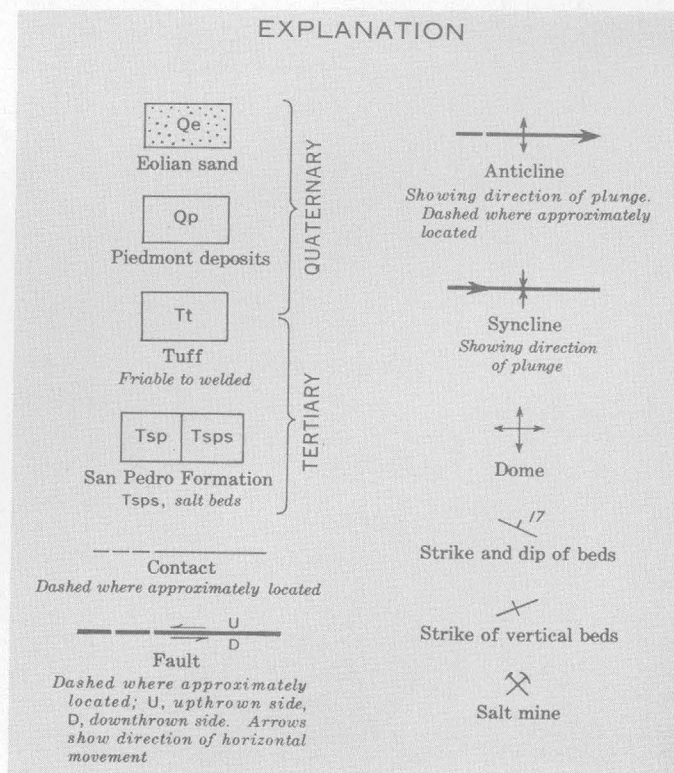
The Cerros de la Sal, in the west-central part of Antofagasta Province, Chile, form a narrow ridge approximately 45 miles long trending N. 20° E. along the western border of the Salar de Atacama (fig. 147.1). The area is extremely arid and the village of San Pedro has an average annual rainfall of less than 2 inches, although it is at an elevation of over 8,000 feet.

The area was mapped in August 1961 as a part of a ground-water investigation in the Salar de Atacama. The author was assisted part of the time by Ernesto Pérez, geologist of the Instituto de Investigaciones Geológicas. Prof. S. E. Hollingworth and Roy Rutland, of the University of London, spent several days in the area and made many helpful suggestions concerning the structure of the area. No detailed geologic mapping had previously been done in this

area. Various authors had mentioned the structure of the Cerros de la Sal, however, and had called them either salt domes or salt anticlines; Brüggén (1950) called them both.

The oldest rocks exposed in the northern part of the basin containing the Salar de Atacama are continental deposits of the Salinas de Purilactis Formation of Jurassic(?) age (Brüggén, 1950). The formation is composed of approximately 1,800 feet of fine-grained well-stratified basin-type deposits with a few intercalated beds of evaporites including salt, gypsum, and anhydrite.

The Salinas de Purilactis Formation is overlain by approximately 15,000 feet of continental sediments of the Purilactis Formation of Cretaceous age (Brüggén, 1950). The Purilactis Formation is subdivided into three members, as yet unnamed, that are herein referred to as the lower, middle, and upper members. The upper and lower members of the Purilactis Formation are relatively coarse-grained clastic sediments.



Explanation for figure 147.2.



FIGURE 147.2.—Aerial photograph showing the geology of the Cerros de la Sal.

The middle member is composed of fine-grained red-bed sediments and evaporite deposits typical of deposition in continental basins under arid conditions.

The San Pedro Formation of early Tertiary age (Brüggen, 1950) is of continental origin and is composed of more than 6,900 feet of sediments and evaporite deposits. In the Cerros de la Sal it was possible to distinguish two types of deposit in the formation consisting predominantly of fine-grained clastic sediments and of salt beds (fig. 147.2). The few conglomerate beds in the sedimentary sequence contain well-rounded phenoclasts, many of which were derived from the conglomerates of the upper member of the Purilactis Formation. The salt beds of the San Pedro Formation are apparently the result of redeposition and further concentration of the evaporite salts from the Jurassic(?) and Cretaceous formations.

The San Pedro Formation is overlain by rhyolitic tuffs of late Tertiary age, which are in turn overlain by Quaternary piedmont deposits.

The Cerros de la Sal are formed by a series of domes and doubly plunging synclines and anticlines. They are bounded on the east by a well-exposed border fault of unknown displacement, and there is evidence of a fault along the western border. The attitude of beds of well-stratified clastic sediments ranges from very steeply dipping to slightly overturned on the flanks of the major structures. In many localities the tops of the clastic beds can be determined by primary sedimentary features. In places the salt beds appear to be structureless on the surface, due to the masking effect of a mantle of salt up to 1 meter thick, which has resulted from leaching and subsequent redeposition on the surface following the infrequent rains. Primary structure in the salt beds may be observed in fresh exposures. The stratification of the salt beds is easily seen on aerial photographs (fig. 147.2).

Faulting within the domes consists of minor vertical to high-angle normal faults. The boundary faults are nearly vertical with the downthrown blocks on the side away from the Cerros de la Sal. North of the area covered by figure 147.2 the upper Tertiary strata on the flanks of the Cerros are displaced by low-angle (14°) thrust faults trending north to N. 30° E.

Folding and doming of the San Pedro Formation began before the deposition of the upper Tertiary tuffs, and continued to the present. The tuffs were deposited as a blanket over the pre-existing topography. In some localities they are flatlying and rest with sharp unconformity on the San Pedro Formation. In other localities they are conformable with the San Pedro

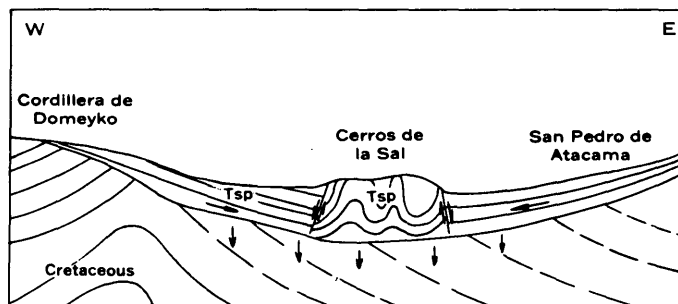


FIGURE 147.3.—Schematic section through the Cerros de la Sal showing how gravitational gliding could have produced local folding of the Cerros de la Sal (arrows indicate direction of movement). Tsp, San Pedro Formation.

clastic sediments and have been tilted up to 90° , thus indicating continued development of the structures after the deposition of the tuffs.

The author considers that (1) the preservation of bedding within the salt, (2) the parallelism of bedding between the clastic beds and the salt, and (3) the complete lack of inclusions or fragments of older rock within the salt beds are strong arguments against deep-seated diapiric folding being an important force in the formation of these structures. On the other hand, complex structures in Tertiary beds cannot be the product of regional tectonics in an area where the underlying Cretaceous strata are gently folded. Probably the Atacama basin subsided under the lower Tertiary sedimentary load, resulting in a slight tilting of the unconsolidated Tertiary sediments toward the center of the basin (fig. 147.3). Gravitational gliding toward the center of the basin, along beds of salt or gypsum in the San Pedro Formation, produced horizontal compression resulting in the upfolding of the Cerros de la Sal. This process of subsidence, gliding, and folding probably continued throughout the rest of the Tertiary and Quaternary and may still be active.

There is no evidence in either the salt domes or in the regional geology to indicate marine deposition of the sediments related to these structures. The Cerros de la Sal may be unique in that they demonstrate well-exposed salt domes and anticlines in Tertiary continental sediments.

SELECTED BIBLIOGRAPHY

- Brüggen, Juan, 1950, *Fundamentos de la geología de Chile*: Santiago, Chile, Instituto Geográfico Militar.
- Felsch, J., 1933, *Informe preliminar sobre los reconocimientos geológicos de los yacimientos petroleros en la cordillera de la provincia de Antofagasta*: Minas Petróleo Bull., v. 2, no. 18, p. 411-422.
- Harrington, H. J., 1961, *Geology of parts of Antofagasta and Atacama Provinces, northern Chile*: Am. Assoc. Petroleum Geologists Bull., v. 45, no. 2.

148. ZINC OCCURRENCE IN THE SERPENT MOUND STRUCTURE OF SOUTHERN OHIO

By ALLEN V. HEYL and MAURICE R. BROCK, Beltsville, Md.

Zinc minerals occur in dolomite shatter breccia¹ exposed in the west-central part of the Serpent Mound "cryptovolcanic structure" (Bucher, 1936, p. 1060-1064). The occurrence is particularly interesting because it is located in the central part of one of the most unusual and controversial structures in the central United States, and because zinc minerals have not been reported previously in southern Ohio (Ralph J. Bernhazen, State Geologist of Ohio, oral communication to Heyl, 1961). The structure is 32 miles southwest of Chillicothe, Ohio, and is centered about 2 miles east-northeast of Loudon, a small town on Ohio Route 73 (fig. 148.1).

The zinc minerals are present in several places in a low hill that lies east of a township road extending northward through the structure from Ohio Route 73. The hill forms a low westward-trending prong 2 to 3 acres in area that extends out from a large plateau of higher elevation that contains the core of the Serpent Mound structure. The parts of the hill where the zinc minerals were found are almost without soil and are covered with weathered fragments of gray dolomite shatter breccia. The dolomite lies within a unit mapped by Bucher (1936) as the Peebles and Greenfield Formations of Middle and Late Silurian age. The shatter breccia is exposed in a small quarry at the east edge of the township road. Most of the angular breccia fragments are less than an inch across and have been rotated slightly or transported during brecciation at most only a few feet. Shallow gullies expose less weathered but equally shattered rock.

The shatter breccia undoubtedly was formed by the explosion which shaped the Serpent Mound structure. Bucher (1936, p. 1074-1081) suggested that this structure formed by an explosion at depth due to the sudden liberation of pent-up gases from an incipient volcano (cryptovolcano). More recently other geologists, including Boon and Albritton (1936), Dietz (1961a, 1961b), and Cohen and others (1961), proposed that the Serpent Mound structure was produced by meteor impact followed by explosion of the meteor at depth. The main evidence cited by them for meteoric impact is the absence of igneous material or related mineralization, and the presence of two pressure phenomena—shatter cones and the silica mineral coesite. Coesite

crystallizes only at high pressures (Chao and others, 1960).

After the shatter breccia was formed, recrystallization of dolomite grains at the interfaces of the fragments resulted in cementation of the breccia. The cemented rock was then broken a second time as shown by small shear zones and open fractures which locally cut the breccia. These shear zones and fractures contain most of the zinc.

The zinc minerals consist of coarse- to medium-grained sphalerite which is partly weathered to smithsonite and hydrozincite. Loose fragments of rock estimated to contain 5 to 20 percent zinc and weighing as much as a few pounds are common at several places on the hill. Commonly the sphalerite crystals have red or reddish-brown cores surrounded by an orange zone and a pale-yellow rim. Most sphalerite is in the form of slightly fractured coarse grains with irregular boundaries against the buff to gray dolomite breccia which it has replaced (fig. 148.2). Sphalerite also fills, or partly fills, small vugs and open fractures. Gentle fracturing followed the deposition of sphalerite, and late-stage dolomite was introduced into the shear zones as an intimate mixture that forms the main gangue. Still later, hydrocarbon and more dolomite were deposited as veinlets that crosscut the sphalerite and gangue.

The probable sequence of tectonic events and ore deposition is as follows:

A. Initial structural events.

1. Development of shatter-breccia during the main stages of formation of the Serpent Mound structure, probably under high pressures, with subsequent cementation.
2. Localized shearing and fracturing of cemented shatter-breccia.

B. Hypogene stages and associated tectonic events.

1. Deposition of sphalerite as coarse replacement crystals in dolomite and as open-space fillings.
2. Gentle fracturing of sphalerite and breccia.
3. Limited replacement of sphalerite and breccia by dolomite, in part along fractures.
4. Renewed shattering locally.
5. Introduction of fine-grained hydrocarbon and associated dolomite in veinlets crosscutting the sphalerite and gangue.

C. Supergene stages.

1. Alteration of the sphalerite to smithsonite.
2. Local further oxidation and minor deposition of hydrozincite.

¹ Shatter breccia as used in this article refers to a breccia of one lithology, more or less completely crushed, in which many small dislocations between fragments can be recognized.

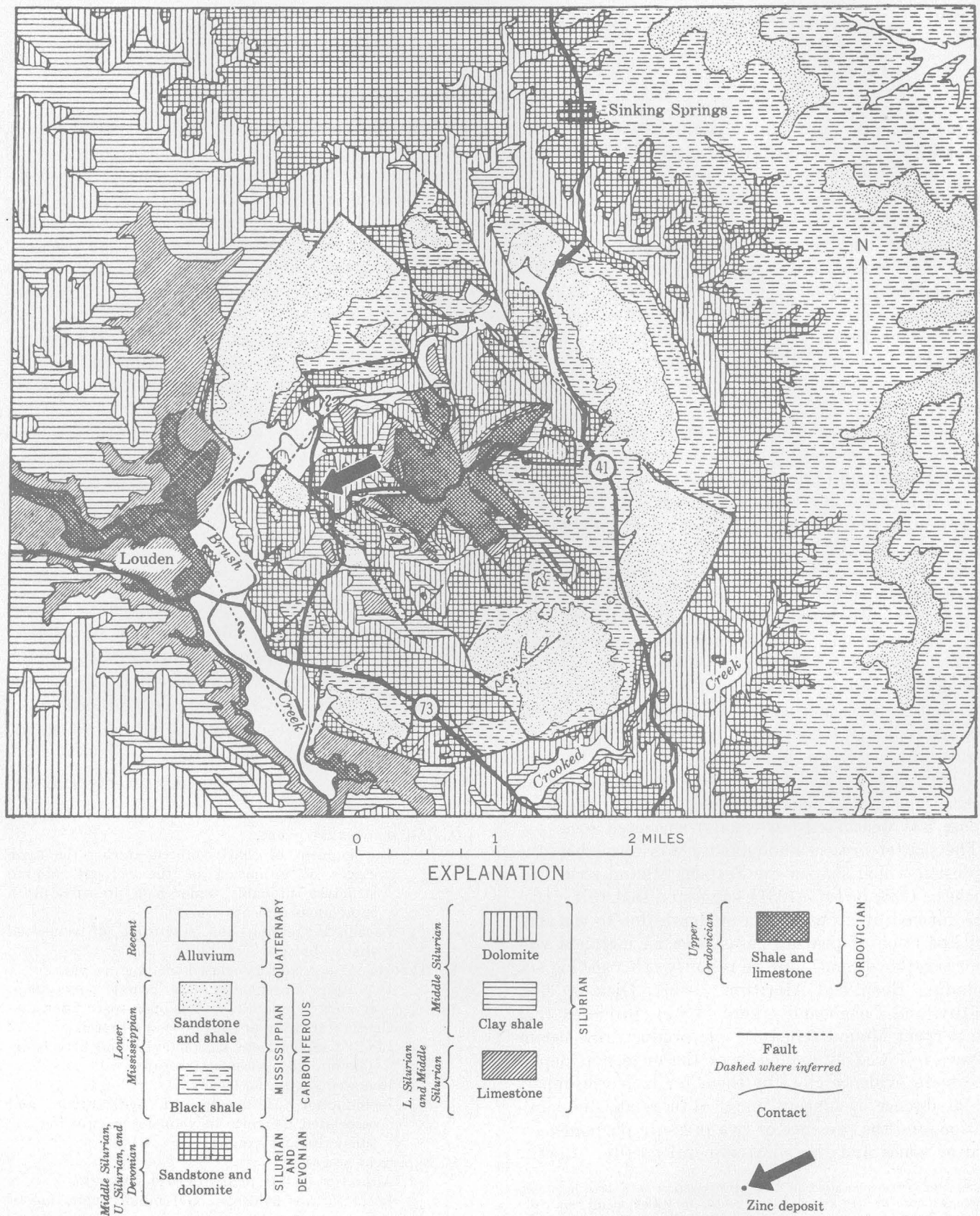


FIGURE 148.1.—Geologic map of the Serpent Mound area showing location of the zinc occurrence. Geology after Bucher (1936, fig. 4).

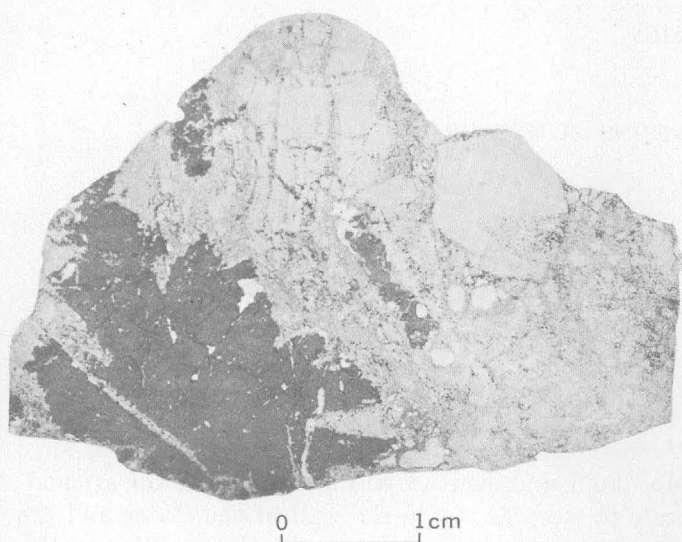


FIGURE 148.2.—Photograph of a thin section showing slightly deformed sphalerite (darkest gray areas) in coarse replacement crystals in dolomite breccia. The very-light-gray fragments are host-rock dolomite. The mottled-gray areas are microbrecciated host rock cemented by post-sphalerite dolomite, which also locally replaced sphalerite (gray veinlets). The sphalerite is veined by a still later stage of hydrocarbon and dolomite (black and white veinlets).

Much of the sphalerite is coated by smithsonite and hydrozincite. These supergene zinc minerals are fine grained, massive, and brown, buff, gray, and white. Most of the smithsonite, a direct-replacement product of sphalerite, is porous and spongy, but some is dense and chertlike in appearance. Brown cellular boxworks of the typical "drybone" variety are fairly common. The boxworks are formed by smithsonite directly replacing sphalerite along cleavages and fractures, but some of the sphalerite between cleavages is dissolved and removed in ground water without redeposition, leaving a smithsonite boxwork. Further oxidation of the boxwork replaced a little of the smithsonite with white hydrozincite. The abundance of sphalerite at the surface implies that supergene alteration of sphalerite is limited to shallow depths.

The brief reconnaissance study indicates that the zinc occurrences are small, but they are distributed over much of the 2 or 3 acres of exposed outcrop. The

zinc may not be abundant enough to form a commercial-grade deposit, but it should be a useful starting point to search for better deposits in this unprospected part of the Midwest.

Geologically important are the facts that: (1) the zinc is in all respects epigenetic to the wallrocks and host fractures; the coarse crystal habit and gentle shattering of the sphalerite indicate it was deposited after the Serpent Mound structure had ceased major movement and after the breccia was cemented; (2) the ore solutions used previously formed fractures as channelways; (3) the sphalerite is younger than the youngest strata involved in the structure and thus is post-Mississippian in age; and (4) sphalerite deposition was followed by two later periods of minor shattering and dolomite deposition.

The several stages of fracturing and mineralization of the sphalerite suggest that the enclosing Serpent Mound structure also developed in several related stages over a considerable period of geologic time. Such a complex history is incompatible with the hypothesis that the structure was formed by meteoric impact and explosion of an imbedded meteor. The multistage structural history and the occurrence of zinc is compatible with the hypothesis that later stages of recurring deep-seated volcanic explosions (Bucher, 1936) were accompanied and followed by mineralization.

REFERENCES

- Boon, J. D., and Albritton, C. C., 1936, Meteoric impact craters and their possible relationship to "cryptovolcanic structures": *Field and Lab.*, v. 5, p. 1-9.
- Bucher, W. H., 1936, Cryptovolcanic structures in the United States: *Internat. Geol. Cong.*, 16th, Washington, 1933, Rept., v. 2, p. 1055-1084.
- Chao, E. C. T., Shoemaker, E. M., and Madsen, B. M., 1960, First natural occurrence of coesite: *Science*, v. 132, no. 3421, p. 220-222.
- Cohen, A. J., Bunch, T. E., and Reid, A. M., 1961, Coesite discoveries establish cryptovolcanoes as fossil meteorite craters: *Science*, v. 134, no. 3490, p. 1624-1625.
- Dietz, R. S., 1961a, Astroblemes: *Sci. Am.*, v. 205, no. 2, p. 50-58.
- , 1961b, Vredefort ring structure: meteoric impact scar?: *Jour. Geology*, v. 69, no. 5, p. 494-516.



GEOPHYSICS

149. THERMOLUMINESCENCE INVESTIGATIONS AT METEOR CRATER, ARIZONA

By C. H. ROACH, G. R. JOHNSON, J. G. McGRATH, and T. S. STERRETT, Denver, Colo.

Work done in cooperation with the National Aeronautics and Space Administration

Preliminary study of rocks from the vicinity of Meteor Crater that have been shocked by hypervelocity impact in the laboratory indicates that the thermoluminescence of some of these rocks is affected by shock. Field studies at Meteor Crater, Ariz., have been undertaken to determine whether the thermoluminescence of the rocks was affected by the shock propagated by impact of the meteorite.

Two characteristics of thermoluminescence of rocks shocked under laboratory conditions vary with the strength of the shock: (a) the total amount of thermoluminescence (area under the glow curve) decreases systematically with distance from the shock origin and, therefore, with decreasing peak shock pressure; and (b) in some rock types strong shock causes the low-temperature peak to have a greater amplitude than the high-temperature peak (Roach and others, 1961). These two characteristics of thermoluminescence are being used to help reconstruct the history of shock propagation at Meteor Crater.

GEOLOGY OF METEOR CRATER

The geology of Meteor Crater has been described by E. M. Shoemaker (1960) as follows: The crater lies in the southern part of the Colorado Plateau in north-central Arizona. Near the crater, the surface of the Plateau has a very low relief and is underlain by well-exposed, nearly flat lying beds of Permian and Triassic age. The crater lies near the crest or upper axis of a gentle monoclinial fold, a type of structure characteristic of this region. The strata are broken by widely spaced northwest-trending normal faults, generally many miles in length but with only a few tens of feet to about a hundred feet displacement. Two sets of regional vertical joints are present near the crater; one set is subparallel to the normal faults and the other set is at right angles to the first set.

Meteor Crater is a bowl-shaped depression 600 feet deep and about three-fourths of a mile in diameter encompassed by a ridge or rim that rises 100 to 200 feet above the surrounding plain. Rocks exposed in the crater, in ascending stratigraphic order, are: the upper part of the Coconino Sandstone (Permian), about

9 feet of Toroweap Formation (Permian), 270 feet of Kaibab Limestone (Permian), and about 40 feet of reddish-brown sandstone and siltstone of the Wupatki Member of the Moenkopi Formation (Triassic). Moenkopi and Kaibab strata are turned up at moderate to steep angles in the wall of the crater and are locally overturned in the rim. The bedrock in the rim is overlain by a complex sequence of Pleistocene debris. Original bedrock stratigraphy is preserved, inverted, in the debris units. Pleistocene and Recent alluvium rests uncomfortably on all of the debris units as well as on bedrock.

The structural and geologic characteristics of Meteor Crater are fully explained by impact of a large meteorite in late Pleistocene time. The meteorite, with a density of about 7.85 g per cc, has been estimated by Shoemaker (1960) to have had an impact velocity of about 15 km per sec, a diameter of about 80 feet, and a total kinetic energy of 1.4 to 1.7 megatons TNT equivalent.

THERMOLUMINESCENCE OF BEDS

The thermoluminescence of all stratigraphic units exposed in Meteor Crater and of all units in the Quaternary debris is being studied; to date, however, emphasis has been focused on three easily identified individual beds or narrow stratigraphic intervals exposed in the rim of the crater. In order of depth below the original pre-impact surface these are: (a) a reddish-brown calcareous siltstone bed of the Moenkopi Formation about 25 feet below the pre-impact land surface; (b) the "lower massive sandstone" (McKee, 1954) of the Moenkopi Formation, about 35 feet below the pre-impact surface; and (c) a marker bed, the "geode bed," of the alpha member (Cadigan, 1957) of the Kaibab Limestone, about 50 feet below the pre-impact surface. Samples from each of these beds were taken at several places around the rim of the crater (figs. 149.1, 149.2, 149.3).

Both the total thermoluminescence and the relative height of the low-temperature peak suggest that all samples of the siltstone bed of the Moenkopi Formation have been subjected to shock (fig. 149.1). Varia-

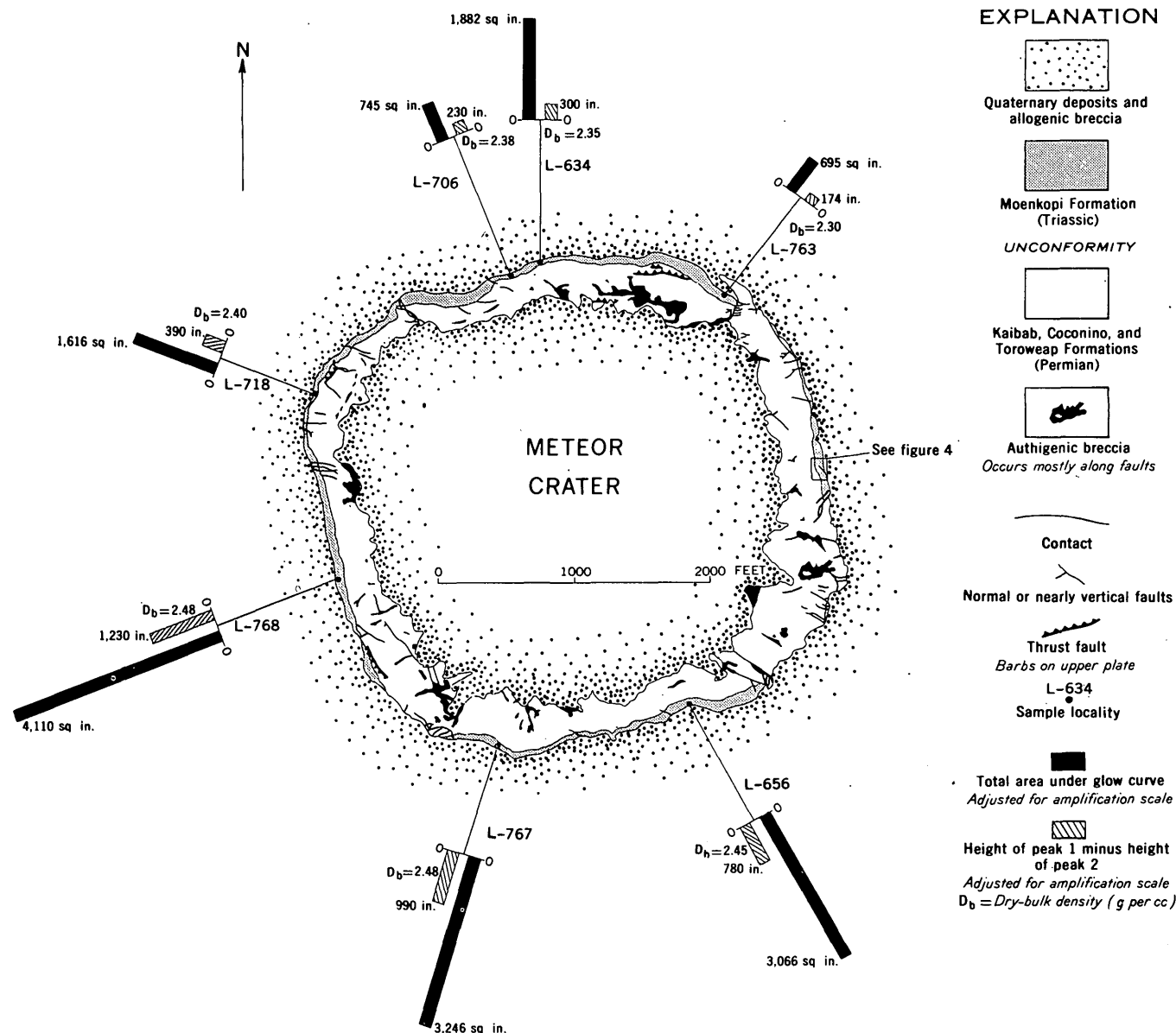


FIGURE 149.1.—Thermoluminescence characteristics of siltstone of the Moenkopi Formation in the rim of Meteor Crater.

tion of both of these characteristics suggests that the strength of the shock was greatest in samples from the south half of the crater rim. Three closely spaced samples were taken where the siltstone bed is exposed in an overturned fold on the east rim of the crater (fig. 149.4). The glow curves suggest that the overturned and axial regions of the fold were subjected to stronger shock than the normal limb. Variation of the dry-bulk density of the siltstone correlates with variation in the thermoluminescence characteristics (figs. 149.1, 149.4). A permanent increase of bulk density was probably produced by shock.

Thermoluminescence characteristics of samples of the lower massive sandstone of the Moenkopi Forma-

tion are less distinctively of the shocked type than are those of the overlying siltstone bed (149.2). All samples except L-722 from the northeast corner of the crater, however, exhibit glow curves of the type produced by shock (positive value of peak 1 minus peak 2). Sample L-722 is from near a prominent tear fault associated with an overturned flap of the east wall of the crater, and it is possible that the local stress distribution during the formation of this tear fault is the cause of the anomaly in thermoluminescence. The strength of the shock in the lower massive sandstone appears to have been greatest in the southeast quadrant of the crater. As in the siltstone there is a general tendency for samples having the greatest amount

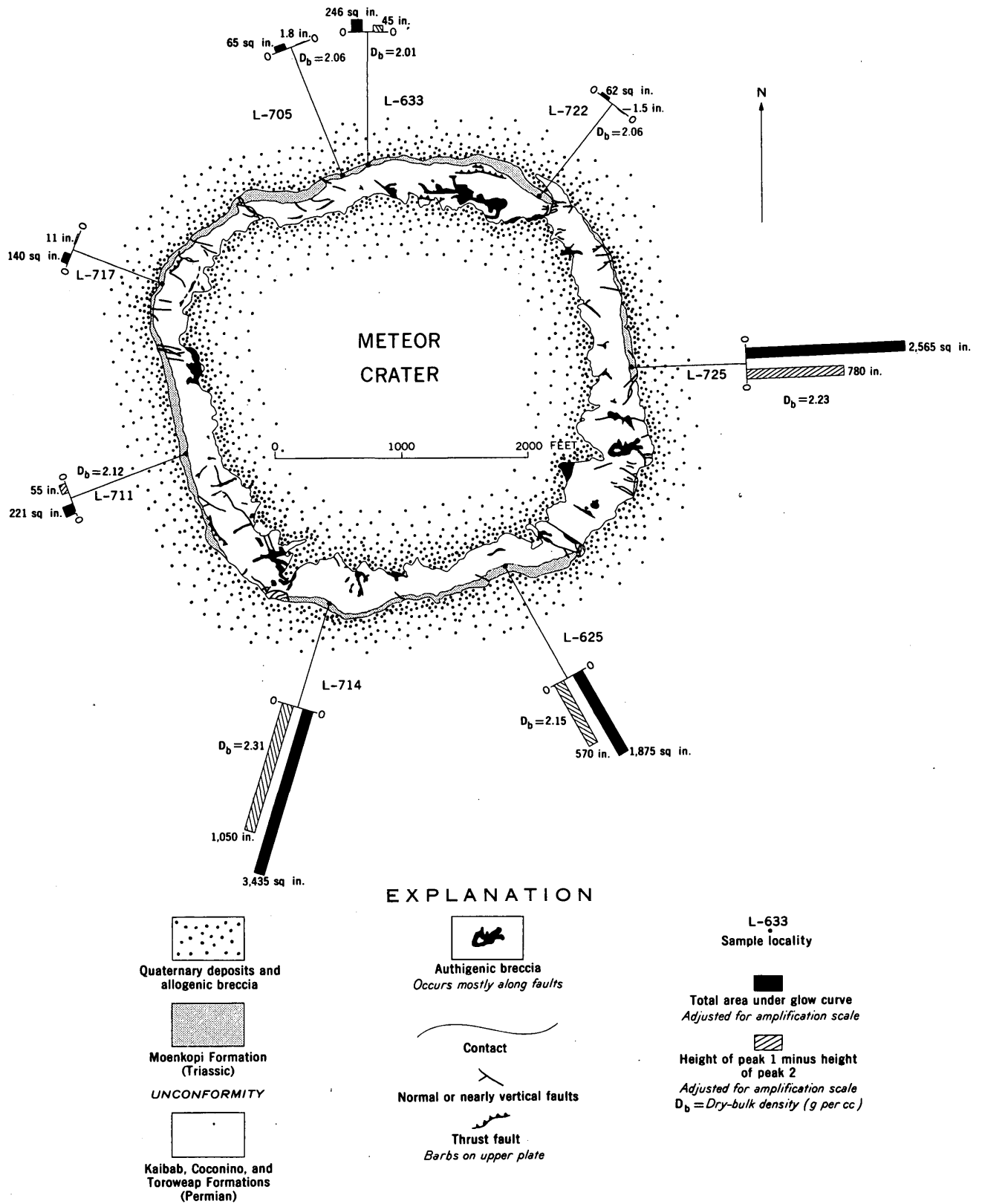


FIGURE 149.2.—Thermoluminescence characteristics of the lower massive sandstone of the Moenkopi Formation in the rim of Meteor Crater.

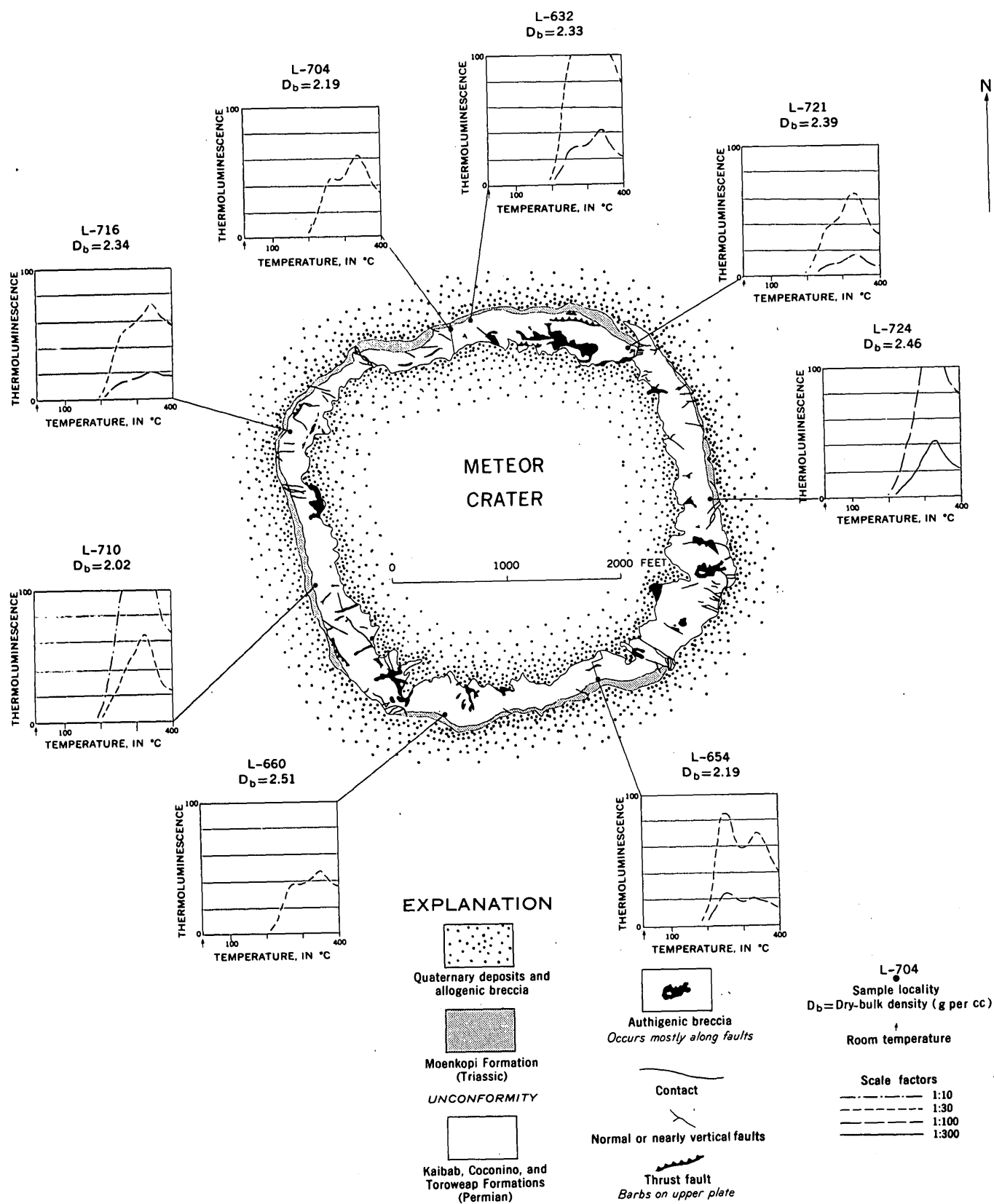


FIGURE 149.3.—Thermoluminescence characteristics of the geode bed of the alpha member of the Kaibab Limestone in the rim of Meteor Crater.

of thermoluminescence to have the highest dry-bulk density, indicating that the lower massive sandstone bed was exposed to greater permanent compression in the southeast quadrant of the crater rim than elsewhere.

Glow curves of samples from the geode bed of the Kaibab Limestone exhibit a complex pattern of variation with respect to position along the crater rim (fig. 149.3). Only sample L-654, from the southeast corner of the crater rim, yielded a glow curve indicative of strong shock (positive value of peak 1 minus peak 2). No correlation is apparent between the thermoluminescence and dry-bulk density of samples of the geode bed as exists for the siltstones and sandstone beds in the overlying Moenkopi Formation. The geode bed contains numerous vugs, however; this feature makes it difficult to obtain a representative bulk-density measurement from the small core specimens that are normally used for bulk-density measurements. A larger number of bulk-density measurements will be required to determine a representative value for a significant volume of rock at any sampling locality.

Comparison of the thermoluminescence of samples of the three marker beds taken from a measured section on the north rim of the crater with those from a corresponding section on the southeast rim (figs. 149.3, 149.5) shows that rocks exposed in the southeast quadrant of the crater appear to have received the strongest

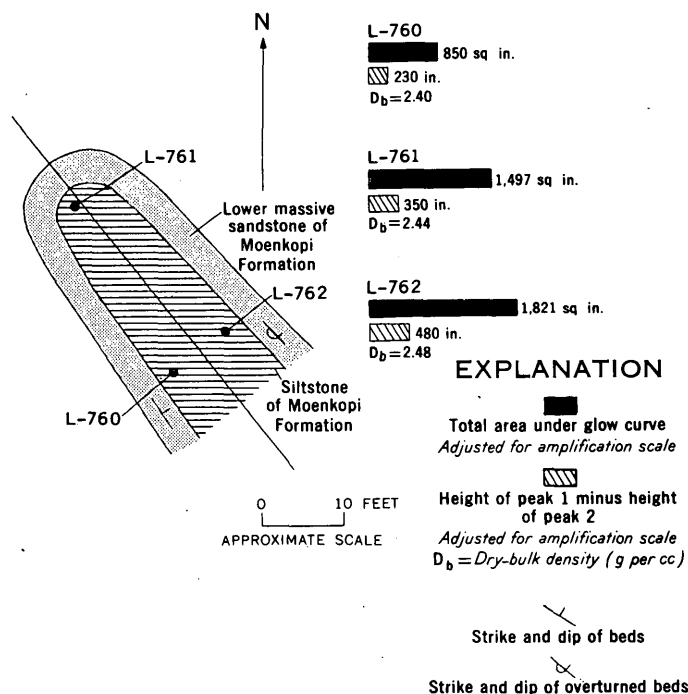


FIGURE 149.4.—Diagrammatic sketch of an overturned fold on the east rim of Meteor Crater.

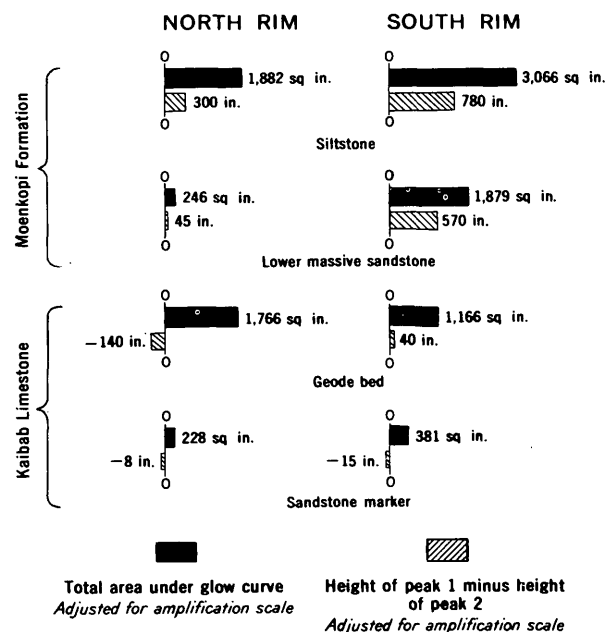


FIGURE 149.5.—Thermoluminescence of marker beds in the rim of Meteor Crater.

shock, and rocks along the northern part of the crater appear to have been shocked least. At greater depths rocks also seem to have been more strongly shocked in the southeast part of the crater than elsewhere.

Glow curves obtained from samples L-710 and L-724 from the geode marker bed differ from all other glow curves obtained from Meteor Crater to date in that they have only one peak—the high-temperature peak. The absence of a low-temperature peak in glow curves of these samples cannot be completely explained at this time. Carbonate samples that normally have two-peak glow curves will yield a glow curve having only a high-temperature peak if they are subjected to high temperature (200°C to 250°C), or are recrystallized. Further study is planned to determine the conditions which might account for the somewhat unique glow curves of these two samples.

CONCLUSIONS

Preliminary study suggests that thermoluminescence may be used as a guide to the stress history of rocks exposed in the rim of Meteor Crater, Ariz. The areal and stratigraphic variations of shock strength are probably recorded by the changes in the thermoluminescence in rocks exposed in the rim of the crater. Variations in bulk density are correlated with the variations in thermoluminescence in the siltstone and "lower massive sandstone", of the Moenkopi Formation.

The present study suggests that the point of impact and upper part of the path of penetration of the meteorite may have lain southeast of the center of the crater. As the crater rim is probably roughly centered about the center of gravity of the total energy delivered during penetration of the meteorite (Shoemaker, 1960, p. 431), the results of this study suggest that the meteorite was moving from southeast to northwest. Additional study is needed, however, before definite conclusions can be drawn.

The present study also suggests that thermoluminescence techniques might be useful in the study of cryptovolcanic structures (Bucher, 1936), which are structures thought by some to have originated by impact mechanism rather than by volcanic processes (Shoemaker and Eggleton, 1961). Thermoluminescence investigations of some of these "possible impact" structures are now underway.



REFERENCES

- Bucher, W. H., 1936, Cryptovolcanic structures in the United States: *Internat. Geol. Cong.*, 16th, Washington, D.C., 1933, Rept., v. 2, p. 1055-1084.
- Cadigan, R. A., 1957, Lithologic studies: U.S. Atomic Energy Comm. TEI Rept. 700.
- McKee, E. D., 1954, Stratigraphy and history of the Moenkopi Formation of Triassic age: *Geol. Soc. America Mem.* 61, 133 p.
- Roach, C. H., Johnson, G. R., McGrath, J. G., and Spence, F. H., 1961, Effects of impact on thermoluminescence of Yule marble: Art. 272 in *U.S. Geol. Survey Prof. Paper* 424-C, p. C342-C346; also in *U.S. Geol. Survey Astrogeologic Studies Semiann. Prog. Rept. to NASA*, Aug. 25, 1960 to Feb. 25, 1961, p. 82-90.
- Shoemaker, E. M., 1960, Penetration mechanics of high velocity meteorites, illustrated by Meteor Crater, Arizona: *Internat. Geol. Cong.*, 21st, Copenhagen, 1960, Rept., pt. 18, p. 418-434.
- Shoemaker, E. M., and Eggleton, R. E., 1961, Terrestrial features of impact origin: *Geophysical Laboratory—Lawrence Radiation Laboratory Cratering Symposium Proc.*, UCRL-6438, pt. I, p. A1-A27.

150. ELECTRICAL AND MAGNETIC PROPERTIES OF A REPLACEMENT-TYPE MAGNETITE DEPOSIT IN SAN BERNARDINO COUNTY, CALIFORNIA

By CHARLES J. ZABLOCKI, Denver, Colo.

An electrical-properties survey was made of the rocks penetrated by 5 exploration drill holes about 20 miles south of Daggett, San Bernardino County, Calif. The work was done as part of a program of the U.S. Geological Survey to determine the electrical properties of rocks in selected mineralized areas. The holes were drilled by the Columbia Iron Mining Co.¹ to evaluate a replacement-type magnetite deposit associated with siliceous metasedimentary and metavolcanic rocks, limestone, marble, and monzonite. Resistivity, induced-polarization, and magnetic-susceptibility measurements were made in 5 drill holes which ranged from 250 feet to 2,800 feet in depth.

Siliceous metasedimentary and metavolcanic rocks that overlie the magnetite-bearing zones are brecciated and fractured in many places. Resistivities measured in these sections are relatively low, ranging from 100 to 500 ohm-meters. Resistivities of more than 2,000 ohm-meters were measured in fine-grained nonporous limestone, skarn, and slightly fractured marble and limestone. In some of these rocks, disseminated pyrite

is abundant, but only where pyrite was reported as being massive is the resistivity substantially reduced. In the magnetite-bearing rocks, the resistivities are less than 1 ohm-meter where the magnetite exceeds about 20 percent by volume. This very low resistivity is due to solid conduction through connected grains of magnetite. The resistivity of a part of the footwall monzonite, which underlies a major zone of mineralized rock, is about 1,500 ohm-meters.

The only significant induced polarization response (3 percent) was measured in metasedimentary rocks containing about 4 percent disseminated pyrite. Measurements in the ore zones could not be made because of the high conductivity of the ore.

Magnetic-susceptibility logs indicate an average susceptibility of 0.18 cgs unit for the magnetite deposit. Magnetic-susceptibility logs in monzonite indicate a value of about 0.01 cgs unit, which corresponds to about 5 percent magnetite by volume.

Parts of resistivity and magnetic-susceptibility logs in magnetite-bearing siliceous metasedimentary rocks are shown in figure 150.1. A short-normal resistivity array with a 4-inch electrode spacing was used in order

¹ The cooperation of the Columbia Iron Mining Co., particularly of Dr. Rodger H. Chapman, is gratefully acknowledged.

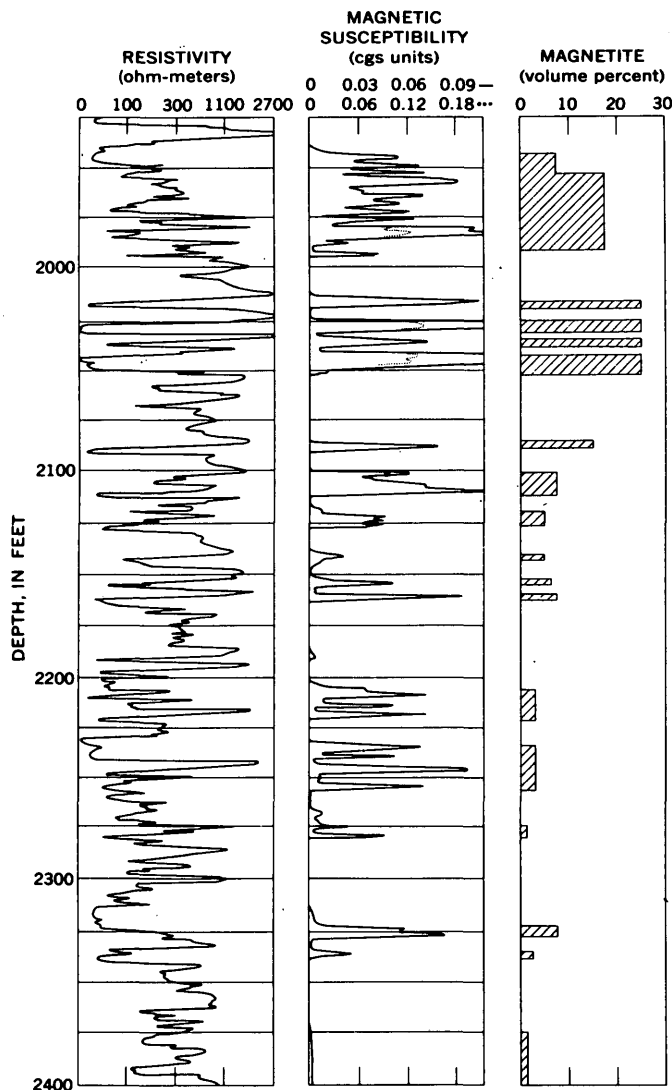


FIGURE 150.1.—Parts of geophysical logs from a diamond-drill hole in magnetite-bearing siliceous metasedimentary rocks, San Bernardino County, Calif. Resistivity is departure corrected; magnetite content estimated visually.

to resolve the resistivities of thin layers or zones. The maximum resistivity that could be measured was limited by this relatively small electrode spacing as well as by the borehole diameter and resistivity of the borehole fluid. For these particular boreholes, the maximum resistivity that could be measured was about 3,000 ohm-meters. Therefore, where an apparent resistivity of about 3,000 ohm-meters was measured, the rocks probably have a true resistivity considerably greater. Laboratory measurements made on 8 representative samples ranged from 3,500 ohm-meters to 15,000 ohm-meters. This is in accordance with their very low intergranular porosity (less than 1 percent).

The resistivity log in figure 150.1 indicates extremely low resistivities for 2 zones at 2,030 and 2,045 feet. The low resistivities are due to solid conduction through connected grains of magnetite. Highly fractured zones are indicated on the log by intervals of low resistivity at 2,230 and 2,315 feet.

The magnetic-susceptibility log shows good correlation with the assay log, in which the magnetite was estimated visually. Better correlation would be expected if a chemical assay over closer intervals had been available. The example demonstrates that this type of logging tool may be used to detect thin seams of magnetite as well as small variations in the ore-grade zones. Also, with a magnetic susceptibility log, assay samples could be chosen so that relatively uniform intervals would be included in each sample length instead of choosing them arbitrarily.

The table below shows the average values of resistivity and magnetic susceptibility for the rock types penetrated.

Summary of average values of resistivity and magnetic susceptibility for the rock types penetrated, San Bernardino County, Calif.

Rock type	Average resistivity, in ohm-meters	Magnetic susceptibility in cgs units
Siliceous metasedimentary and volcanic (highly fractured).....	100-500	Nil
Fine-grained limestone and skarn (unfractured).....	>2,500	Nil
Marble-limestone (unfractured).....	>2,500	Nil
Monzonite (fractured).....	1,500	0.01
Mineralized zones (<20 percent Fe_3O_4).....	500-1,500	.002-.04
Mineralized zones (>20 percent Fe_3O_4).....	<1	.04-.30

It is interesting to note that, in general, 20 percent magnetite by volume is required to render the rock conductive. In contrast, measurements made on some magnetite-bearing rocks in the western part of the Gogebic iron range, Wisconsin (Zablocki and Keller, 1957) showed that solid conduction occurred where the magnetite content was as little as 6 percent by volume. The difference is due to the mode of occurrence of the magnetite. In the replacement deposit, the magnetite occurs as medium to coarse grains and crystals disseminated throughout the host rock. In the Gogebic range, the magnetite occurs in thin beds and anastomosing bands which render the rock conductive over a large volume because of the continuity through the grains.

REFERENCE

- Zablocki, C. J., and Keller, G. V., 1957, Borehole geophysical logging methods in the Lake Superior district, in *Drilling symposium, 7th annual, exploration drilling*: Minneapolis, Minnesota Univ. Center for Continuation Study, p. 15-24.

151. DETERMINATION OF THE MAGNETIC POLARITY OF ROCK SAMPLES IN THE FIELD

By RICHARD R. DOELL and ALLAN COX, Menlo Park, Calif.

The directions of remanent magnetization of most rocks of post-Eocene age may be divided into two groups: a normal group, in which the remanent-magnetization vectors have roughly the same direction as the present geomagnetic field at the sampling locality; and a reversed group, in which the remanent-magnetization vectors are directed nearly opposite to the present geomagnetic field. At all localities over the earth, the present geomagnetic field is close to that which would be produced by a magnetic dipole (that is, a short bar magnet) at the center of the earth with its *north magnetic pole* directed toward the *south geographic pole*. The resulting magnetic field at the earth's surface is directed toward the north geographic pole and is inclined to the horizontal at different angles appropriate to the geographic latitude of the sampling area. The appropriate angle of the inclination, I , is given by:

$$I = \arctan (2 \tan \theta)$$

where θ is the geographic latitude, assigned a positive value in the northern hemisphere and a negative value south of the equator. Correspondingly, the inclination is positive in the northern hemisphere, indicating inclinations below the horizontal, and negative in the southern hemisphere, specifying inclinations above the horizontal. Figure 151.1A shows this relationship graphically and also, therefore, indicates the average orientation at different latitudes for rocks of the normal group. Figure 151.1B shows the relation for rocks of the reversed group.

The occurrence and distribution of reversely magnetized rocks have been interpreted as evidence that the polarity of the earth's magnetic field has reversed 20 or more times since the Eocene. The best stratigraphic evidence now available indicates that the two most recent reversals occurred in the Pleistocene (Matuyama, 1929; Hospers, 1954; Rutten, 1960; Doell and Cox, 1961a). Transitions from one polarity to the other are observed to occur within very narrow stratigraphic intervals, and since all geomagnetic-field theories require that the transitions be contemporaneous over the entire earth, these horizons may prove very useful for stratigraphic correlation.

However, it cannot be assumed that all reversely magnetized rocks were formed when the geomagnetic field was reversed, because at least one of the ferromagnetic minerals found in rocks is known to be self

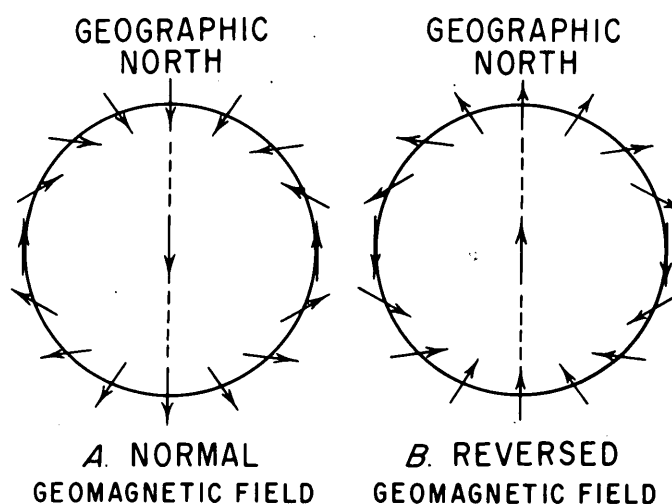


FIGURE 151.1.—Directions of the geomagnetic field at various latitudes expected for (A) a normal geomagnetic field (present configuration) and (B) a reversed geomagnetic field.

reversing (Uyeda, 1958). This mineral, a solid solution of ilmenite and hematite, acquires a magnetization exactly opposing the applied geomagnetic field when it is cooled from above its Curie temperature in the laboratory. Moreover, the possibility of self reversals that cannot be reproduced in the laboratory has been suggested (Néel, 1951; Verhoogen, 1956, 1962). Detailed laboratory analysis for the presence of reproducible self-reversing properties is always desirable, but field study of the stratigraphic distribution of normally and reversely magnetized rocks throughout geologic units may provide even more critical evidence concerning the presence or absence of self reversals. For example, rare occurrences of both normal and reversed magnetizations within the same lava flow or small intrusion (Asami, 1956; Strangway, 1961) clearly indicate self reversal whether or not this property can be reproduced in the laboratory. However, most of the field evidence now available indicates that natural self reversals are rare, since it is much more common to find the same magnetic polarity in rocks with vastly different mineralogies which were magnetized at the same time. For example, many lava flows and the sediments baked by them have the same polarity, whereas none have been found with opposing polarities (Brunhes, 1906; Roche, 1953; Einarsson and Sigurgeirsson, 1955; Wilson, 1961). Similarly, normal and reversed zones usually follow time horizons in thick stratigraphic sequences but

transgress petrologic horizons, indicating that self reversals are probably absent. Preliminary measurements in the field are therefore valuable as a guide for more detailed sampling and laboratory study, and where consistency of polarity can be established among samples of different mineralogy from the same time horizon, such field measurements should suffice for purposes of mapping and correlation.

This article describes a technique for using a declination gradiometer and a small portable magnetometer to measure the magnetic polarity of oriented hand samples. Although the sensitivity of the magnetometer described is not great enough to measure most sediments, it is quite sufficient to measure almost all igneous rocks and some of the more strongly magnetized sediments.

In making such determinations in the field, it is important to recognize and avoid rocks that have been struck by lightning. The strong magnetic field of one lightning bolt may realine the remanent magnetization of rocks in an area 5 to 25 meters in diameter, completely masking the original magnetic polarity (Cox, 1961; Graham, 1961). A simple way to determine where lightning has struck is to measure the local magnetic anomalies adjacent to the outcrop in question, since the strong magnetic fields associated with lightning bolts induce intense remanent magnetizations which in turn cause large anomalies within a few tens of centimeters from the outcrop. Although such gradients may be readily determined with a geologist's compass using a distant point as a reference, we have found a simple declination gradiometer much easier to use.

The gradiometer consists of two small oil-damped moving-card-type magnetic compasses mounted in simple gimbals at opposite ends of a rigid rod about half a meter in length (fig. 151.2). The compasses are arranged with their index marks parallel so that a difference in their readings, divided by their separation, yields the declination gradient in degrees per meter. With at least one of the compasses held immediately adjacent to the outcrop, local declination

anomalies are quickly located. Gradients of 20° to 60° per meter are quite common along ridges in areas of high lightning incidence. For most lava flows, the absence of gradients greater than 5° per meter over an outcrop area greater than 2 meters in length indicates that samples near the center of the outcrop will be free from the effects of lightning. The exact value of the gradient to be used as a criterion for the absence of lightning effects depends upon the amount and type of ferromagnetic minerals present in the rock.

For measuring the magnetic polarity of igneous rocks by the techniques described here, any magnetometer having a directionally sensitive detector that can be alined perpendicular to the earth's magnetic field may be used. The magnetometer should be capable of measuring fields as small as 25 gammas (25×10^{-5} oersteds) for typical basaltic extrusive rocks, 5 gammas for rhyolites, and about 1 gamma for acidic intrusive rocks. Our instrument is of the saturable-core or fluxgate type and is a modification of a design by Serson and Hannaford (1956). The detector head of this magnetometer is 1.5 cm in diameter by 10 cm in length and is mounted on a small aluminum tripod with a universal head. It is connected by an electrical cable (fig. 151.3) to a battery-powered electronics unit measuring 16 cm \times 16 cm \times 15 cm and weighing about 2 kilograms. The detector is sensitive to the magnetic-field component exactly parallel to its axis but does not respond to magnetic-field components perpendicular to the axis.

Before determining the polarity of an oriented rock specimen, the sensitivity of the instrument must be properly adjusted and the detector axis alined exactly perpendicular to the local geomagnetic field. This may be done by placing the detector in a horizontal and roughly east-west orientation and, with the sensitivity control initially set to a low value, rotating the detector about a vertical axis until the indicating meter reads near the center zero. The sensitivity is then increased, generally causing the meter to deflect away from the center position, and the detector is carefully reoriented to again bring the meter to a zero center reading. A test signal, equivalent to a 15-gamma change in the magnetic field along the detector axis, is applied after each increase in sensitivity, and the above steps are repeated until the meter reads near the zero center and the test signal indicates a sensitivity sufficient to measure the rocks being studied.

When adjusted in this manner with the detector axis exactly perpendicular to the local geomagnetic field, small magnetic fields directed parallel to the detector axis can be measured; moreover, the detector

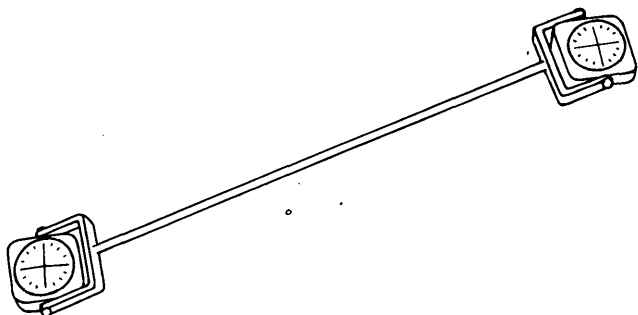


FIGURE 151.2.—The declination gradiometer.

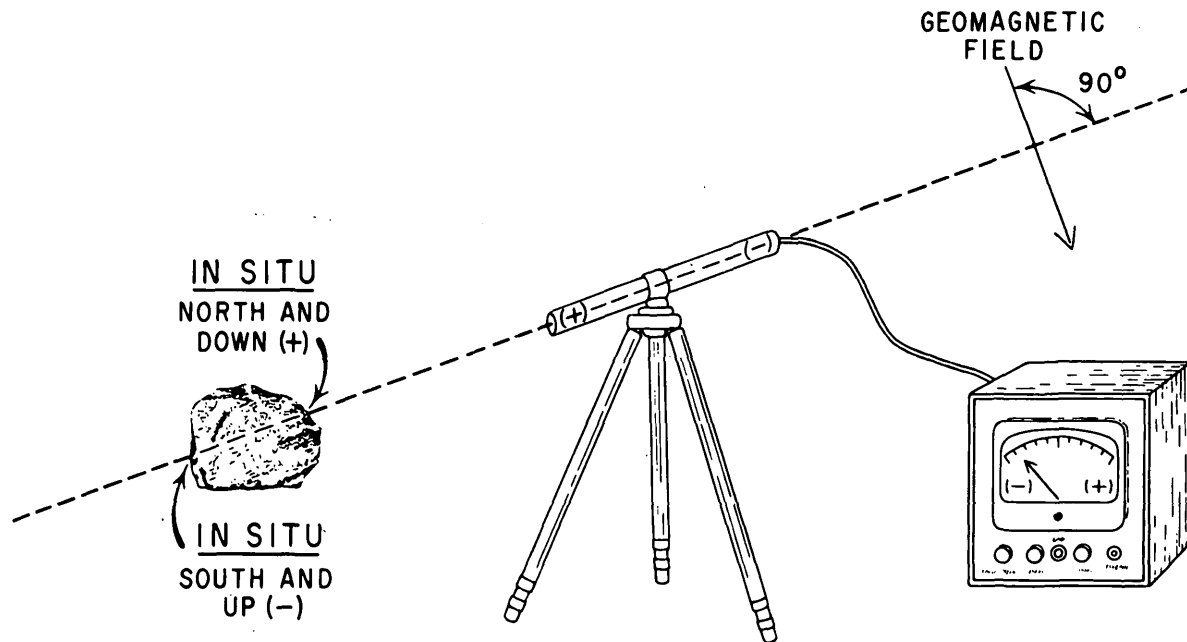


FIGURE 151.3.—Portable magnetometer depicted measuring the magnetic polarity of a reversely magnetized sample from the northern hemisphere.

is polarity sensitive—a magnetic field directed from magnetic west to east will cause a meter deflection to the right, say, whereas a field in the opposite direction will cause a deflection to the left. To determine the “sense” of the meter deflection, the following procedure may be used to calibrate a new instrument:

- (1) One end of the detector head is arbitrarily marked (+).
- (2) The needle of a compass is clamped and the compass is placed 1 or 2 meters from the (+) end of the detector head so that the needle is parallel to and in line with the detector axis and has its positive or north-seeking end directed toward the detector head.
- (3) The compass is moved toward the detector head, keeping the needle in line with the detector axis, and the direction of the meter deflection as the compass needle approaches the detector is marked (+). This is the deflection to be expected if the positive or north-seeking end of a remnant-magnetization vector approaches the (+) of the detector; conversely, a deflection in the opposite direction indicates that the magnetically negative or south-seeking end of the vector is approaching the detector.

As mentioned earlier, rocks of post-Eocene age that are unaffected by lightning may be expected to have a direction of remanent magnetization, after correction for any postemplacement tilting, directed to the north and inclined to the horizontal at an angle appropriate to the sampling latitude (see fig. 151.14). If the rock is *normally* magnetized, the positive end of the magnetization vector is in this direction, and if *reversely* magnetized, the negative end. It is thus

necessary to orient or mark the sample by some means before it is removed from the outcrop so that this expected direction of magnetization within the sample may be determined.

The magnetic polarity may be measured as follows:

- (1) Holding the sample in its in situ position, a (+) sign is marked at the north end of a vector originating at the center of the sample and parallel to the “normal” field direction as described above, that is, trending north and, between lat. 30° and 50° N., plunging 49° to 67°; a (—) sign is marked at the opposite end of this vector.
- (2) The sample is held 1 meter from the detector with the (+) and (—) signs both aligned with the detector axis and with the (+) signs of the detector and samples closest together.
- (3) The sample is moved toward the detector; if the meter deflection is in the (+) direction, the sample is magnetically normal, and conversely, if the meter deflection is in the (—) direction, the sample is reversed.

To avoid erroneous determinations due to shape effects or magnetization directions at large angles to the expected direction, the determination should be repeated by moving the (—) end of the sample toward the (+) end of the detector. The polarity measurement is reliable only if the meter deflects in the opposite direction. It is also reassuring to repeat

the determination on at least two additional oriented samples from the same unit, separated from each other as much as possible—preferably at least 10 to 20 meters—and if possible representing different mineralogies and different rates of cooling.

With some care, the direction of magnetization of equidimensional samples that are neither clearly normal nor reversed may be estimated by keeping the sample at a fixed distance from the detector head and finding the orientation that gives a maximum deflection.

An important characteristic of this method of measuring magnetic polarity of hand samples in the field is that only the remanent magnetization is measured. The induced magnetization of the sample, which is parallel to the geomagnetic field and proportional to its strength, gives rise to lines of magnetic flux at right angles to the detector axis and is thus not measured.

In the course of sampling lava flows from the islands of Hawaii (Doell and Cox, 1961b) and Kauai, from Owens Valley, from near Lake Tahoe, Calif., and from near Reno, Nev., we have used the techniques described above to determine the magnetic polarity of lava flows from which oriented cores were also drilled and studied in detail in the laboratory. The following is a summary of all field polarity measurements that have also been accompanied by more detailed laboratory measurements.

Normal flows correctly identified	96
Normal flows incorrectly identified as reversed	1
Reversed flows correctly identified	23
Reversed flows incorrectly identified as normal	1
Flows with intermediate directions or inconsistent magnetizations incorrectly identified as either normal or reversed	4
Flows with intermediate directions or inconsistent magnetizations so identified	5-10
	(no record)

We would like to note further that most of the incorrect determinations were made before we gained experience in using the method.

Although a geologist's compass may also be used to determine strongly magnetized parts of some lava flows (Einarsson, 1957; Rutten, 1960, Muehlberger and Baldwin, 1958) the portable magnetometer greatly extends the range of magnetic intensities and rock types that may be measured by the geologist in the field.

REFERENCES

- Asami, E., 1956, A palaeomagnetic consideration on the remanent magnetization of the basalt layers at Kawajiri-misaki, Japan: *Jour. Geomagnetism and Geoelectricity*, v. 8, p. 147-155.
- Brunhes, B., 1906, Recherches sur la direction d'aimantation des roches volcaniques (¹): *Jour. de Physique*, 4th series, v. 5, p. 705-724.
- Cox, Allan, 1961, Anomalous remanent magnetization of basalt: *U.S. Geol. Survey Bull.* 1083-E, p. 131-160.
- Doell, R. R., and Cox, Allan, 1961a, Paleomagnetism: *Advances in Geophysics*, v. 8, p. 221-313.
- 1961b, Palaeomagnetism of Hawaiian lava flows: *Nature*, v. 192, p. 645-646.
- Einarsson, T., 1957, Magneto-geological mapping in Iceland with the use of a compass: *Philos. Mag.*, v. 6, p. 232-239.
- Einarsson, T., and Sigurgeirsson, Th., 1955, Rock magnetism in Iceland: *Nature*, v. 175, p. 892.
- Graham, K. W. T., 1961, The re-magnetization of a surface outcrop by lightning currents: *Royal Astron. Soc. Geophys. Jour.*, v. 6, p. 85-102.
- Hospers, J., 1954, Reversals of the main geomagnetic field, III: *Koninkl. Nederlandse Akad. Wetensch. Proc.*, v. 57, p. 112-121.
- Matuyama, Motonori, 1929, On the direction of magnetization of basalt in Japan, Työsen, and Manchuria: *Japan Acad. Proc.*, v. 5, p. 203-205.
- Muehlberger, W. R., and Baldwin, B., 1958, Field method for determining direction of magnetization as applied to late Cenozoic basalts of northeastern New Mexico: *Jour. Geophys. Research*, v. 63, p. 353-360.
- Néel, M. L., 1951, L'inversion de l'aimantation permanente des roches: *Annales Géophysique*, v. 7, p. 90-102.
- Roche, A., 1953, Sur l'origine des inversions d'aimantation constatées dans les roches d'Auvergne: *Acad. Sci. [Paris] Comptes Rendus*, v. 236, p. 107-109.
- Rutten, M. G., 1960, Paleomagnetic dating of younger volcanic series: *Sonderdruck Geol. Rundschau*, v. 49, p. 161-167.
- Serson, P. H., and Hannaford, W. L. W., 1956, A portable electrical magnetometer: *Canadian Jour. Technology*, v. 1, p. 232-243.
- Strangway, D. W., 1961, Magnetic properties of diabase dikes: *Jour. Geophys. Research*, v. 66, p. 3021-3032.
- Uyeda, S., 1958, Thermo-remanent magnetism as a medium of palaeomagnetism, with special reference to reverse thermo-remanent magnetism: *Japanese Jour. Geophysics*, v. 2, p. 1-123.
- Verhoogen, J., 1956, Ionic ordering and self-reversal of magnetization in impure magnetites: *Jour. Geophys. Research*, v. 61, p. 201-209.
- 1962, Oxidation of iron-titanium oxides in igneous rocks: *Jour. Geology*, v. 70, p. 168-181.
- Wilson, R. L., 1961, Palaeomagnetism in Northern Ireland: *Royal Astron. Soc. Geophys. Jour.*, v. 5, p. 45-69.

MINERALOGY, GEOCHEMISTRY, AND PETROLOGY

152. THERMAL EXPANSION OF TEN MINERALS

By BRIAN J. SKINNER, Washington, D.C.

A new heating stage for the X-ray diffractometer described by Skinner, Stewart, and Morgenstern (1962) has been used to measure the thermal expansion of 5 sulfides, 2 selenides, 2 silicates, and 1 carbonate. Measurement and alignment procedures were the same as those described by Skinner, Clark, and Appleman (1961). For each substance several diffraction lines were measured at each temperature by oscillating over each line at $\frac{1}{4}^\circ 2\theta$ per minute. Copper $K\alpha$ radiation ($\alpha_1 = 1.54050\text{\AA}$) was used in all cases. Measurements were made at irregular temperature intervals and in random order to permit evaluation of any irreversible changes occurring in the sample and to ensure that the measurements were the same for both rising and falling temperatures.

Diffraction peaks were measured at the intersection of the weighted centerline with an average background level. The precision or reproducibility of measurement is 0.01 percent, and comparison of our silver expansion measurements with those of Hume-Rothery and Reynolds (1938) suggest that the accuracy is at least 0.03 percent.

Because of their use in thermodynamic calculations, molar volumes (cc per mol) have been calculated from the unit-cell edge measurements at each temperature. Molar volumes were calculated using $6.02472 \times 10^{23} \text{ mol}^{-1}$ for Avogadro's number (DuMond and Cohen, 1953). The molar volumes are, therefore, gram-formula volumes on the physical scale of atomic weights. The change in molar volume with temperature can be conveniently expressed by the general function

$$V = A/T + B + CT + DT^2,$$

where V is the molar volume in cc per mol and T is the absolute temperature. The constants A , B , C , and D were found with a digital computer by the method of least squares. The thermal expansion coefficient can be found by differentiating the function analytically. The determined cell edges and calculated molar volumes are listed in table 152.1. The constants of the derived functions are listed in table 152.2.

THERMAL EXPANSION OF GALENA, CLAUSTHALITE, AND CADMIAN GALENA

Galena, clausthalite, and cadmian galena are isostructural, with space group $Fm\bar{3}m$, $Z = 4$. The syn-

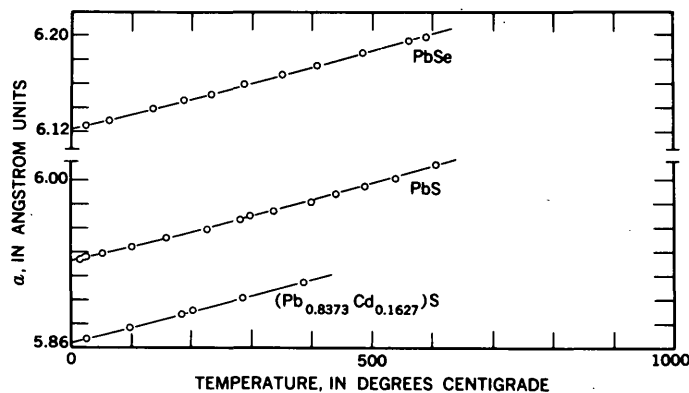


FIGURE 152.1.—Change in cell edge (a) of galena (PbS), clausthalite (PbSe), and a cadmian galena with change in temperature.

thetic PbS, PbSe, and a cadmian galena, with the reported composition $(\text{Pb}_{0.8373}\text{Cd}_{0.1627})\text{S}$, that were used for the present study were prepared and described by Bethke and Barton (1961). The thermal expansion, measured in a vacuum, was computed from the measured positions of the (420), (422), and (511) reflections. Plots of unit-cell edge versus temperature (fig. 152.1) are nearly parallel for the three compounds. The cell edges of PbS and PbSe at 25°C , and of the cadmian galena at 26.2°C in table 152.1 are those reported by Bethke and Barton (1961). The parameters of the functions describing the molar volume expansions are given in table 152.2.

The only previous expansion measurements of PbS are those by Pfaff (1859) and Sharma (1951). Pfaff observed a 0.15-percent linear expansion between 20°C and 100°C . In the present study a 0.162-percent increase was observed in the same interval. Sharma (1951) measured the linear expansion of a galena crystal by the interferometer method. The data are in good agreement below 300°C , but from 300° to his highest temperature of measurement, 375°C , Sharma observed a significantly greater expansion than that found in the present study. The reason for the disagreement above 300°C is not known.

THERMAL EXPANSION OF SPHALERITE, STILLEITE, AND A CADMIAN SPHALERITE

Sphalerite (ZnS), stilleite (ZnSe), and a cadmian sphalerite with the reported composition ($\text{Zn}_{0.9382}\text{Cd}_{0.0618}\text{S}$) are cubic and isostructural, space group $F\bar{4}3m$, $Z = 4$. The synthetic ZnSe used for the present study is that reported by Bethke and Barton (1961). The cadmian sphalerite was prepared for the study by P. M. Bethke. Expansions were computed from measurements of the (331) and (422) reflections at various temperatures.

The cell edge versus temperature plots for the three compounds are essentially parallel (fig. 152.2), analogous to the behavior of the three galena-type compounds. The cell edge of sphalerite at 25°C in table 152.1 is that reported by Skinner, Barton, and Kullerud (1959) and of ZnSe at 25°C by Bethke and Barton (1961).

Parameters of the functions describing the molar volume expansions are given in table 152.2. It is significant that in both the sphalerite-type and the galena-type compounds described, compositional differences do not markedly change the slope of the expansion curves (figs. 152.1 and 152.2).

THERMAL EXPANSION OF WURTZITE

Wurtzite (ZnS) is hexagonal, space group $P6_3mc$, $Z = 2$. Synthetic wurtzite with the 2-layer ($2H$) stacking sequence was synthesized at 1100°C . The expansions of a and c were computed from the measured positions of the (210), (300), (203), and (114) reflections at various temperatures. The expansion is anisotropic but continuous over the temperature range of measurement. Parameters of the function describing the molar volume expansion are given in table 152.2.

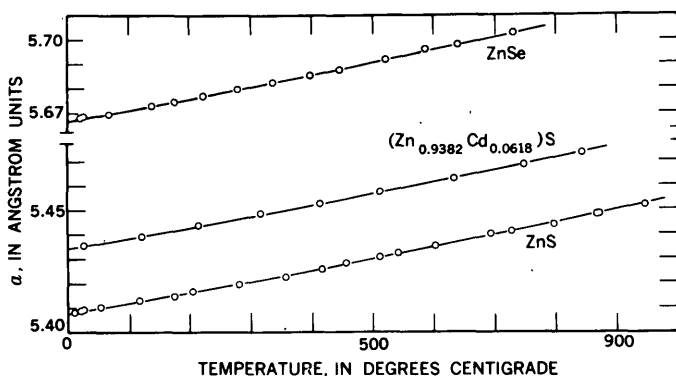


FIGURE 152.2.—Change in cell edge (a) of sphalerite (ZnS), stilleite (ZnSe), and a cadmian sphalerite with change in temperature.

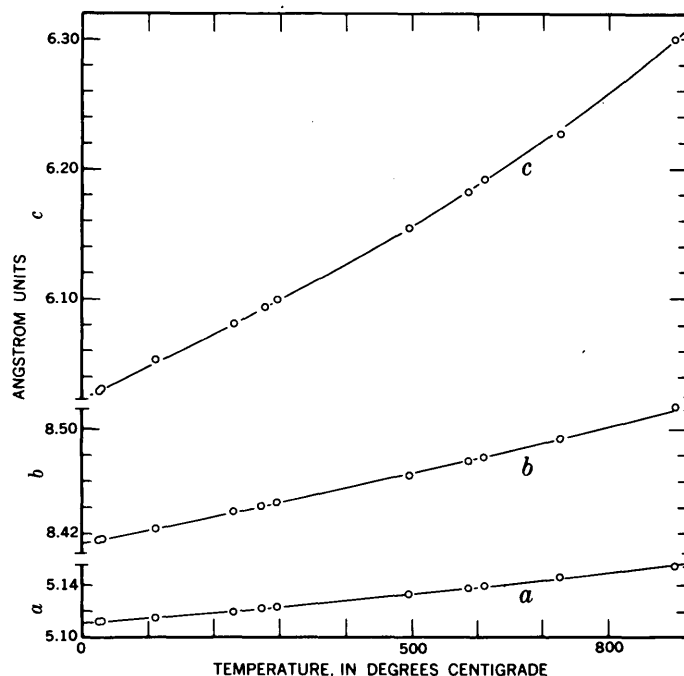


FIGURE 152.3.—Change in cell edges (a , b , c) of strontianite (SrCO_3) with change in temperature, demonstrating the large anisotropism of expansion.

THERMAL EXPANSION OF STRONTIANITE

Strontianite (SrCO_3) is orthorhombic, space group $Pnam$, $Z = 4$. The thermal expansion of analytical reagent-grade SrCO_3 was measured under 1 atmosphere of CO_2 pressure up to 900°C , from the measured displacement of the (200), (041), and (002) reflections.

The expansion is strongly anisotropic (fig. 152.3), the relative expansion of the c -axis being several times greater than that of the a -axis. Parameters of the function describing the molar volume expansion are given in table 152.2.

THERMAL EXPANSION OF COESITE

Coesite (SiO_2) is monoclinic, but dimensionally hexagonal, with $a = c$ and $\beta = 120^\circ$. Zoltai and Buerger (1959) chose to orient coesite in the monoclinic first setting to emphasize its dimensional hexagonal symmetry so that $a = b$ and $\gamma = 120^\circ$, and in this setting the space group is $B2/b^1$, $Z = 16$.

A synthetic coesite synthesized at 1100°C and 40 kilobars pressure by F. R. Boyd was used for the expansion measurements and the expansion calculated from the movement of the ($\bar{4}21$) and (170) reflections. Coesite remains dimensionally hexagonal, within the resolution of the present measurements, up to 1045°C .

¹ In the standard or monoclinic second setting, the space group is $C2/c$.

If significant deviations from hexagonal dimensions occurred (that is, $a \neq b$ or $\gamma \neq 120^\circ$), the X-ray reflections would become broad and eventually split. Because this did not happen, at least up to 1045°C , only 2 independent measurements were necessary for determining the thermal expansion, instead of the 4 reflections normally required to characterize a monoclinic crystal uniquely. The parameters of the molar volume expansion function are given in table 152.2.

THERMAL EXPANSION OF FORSTERITE

Forsterite (Mg_2SiO_4) is orthorhombic, space group $Pbnm$, $Z = 4$. The sample studied was a synthetic forsterite prepared by H. S. Yoder, Jr. The measured cell edges at 25°C are in reasonable agreement with those reported by Yoder and Sahama (1957) and by Swanson and Tatge (1953) for pure forsterite.

TABLE 152.1—Unit-cell edges and molar volumes at different temperatures of ten minerals

Temperature ($^\circ\text{C}$)	a (Å)	b (Å)	c (Å)	V (cc per mol)
Galena (PbS)				
15.0	5.9339			31.470
22.0	5.9352			31.491
25.0	5.9358			31.500
53.5	5.9389			31.550
101.0	5.9440			31.631
159.0	5.9517			31.754
217.0	5.9582			31.858
281.0	5.9665			31.992
298.2	5.9700			32.048
336.0	5.9738			32.109
399.2	5.9812			32.229
441.2	5.9879			32.337
489.2	5.9943			32.441
540.0	6.0010			32.550
607.0	6.0122			32.732
Clausthalite (PbSe)				
25.0	6.1254			34.616
26.5	6.1257			34.621
63.0	6.1294			34.684
136.0	6.1393			34.852
187.2	6.1460			34.967
233.0	6.1509			35.050
287.0	6.1595			35.198
350.1	6.1673			35.332
408.3	6.1746			35.457
485.5	6.1850			35.637
562.0	6.1948			35.806
591.0	6.1987			35.874
Cadmian galena [(Pb_{0.8373}Cd_{0.1627})S]				
25.0	5.8674			30.424
26.2	5.8676			30.427
98.2	5.8768			30.570
184.2	5.8880			30.745
202.0	5.8907			30.788
285.3	5.9014			30.956
388.0	5.9144			31.161

TABLE 152.1—Unit-cell edges and molar volumes at different temperatures of ten minerals—Continued

Temperature ($^\circ\text{C}$)	a (Å)	b (Å)	c (Å)	V (cc per mol)
Sphalerite (ZnS)				
11.0	5.4084			23.828
20.1	5.4090			23.836
23.2	5.4092			23.838
25.0	5.4093			23.840
54.4	5.4104			23.854
118.3	5.4130			23.889
175.7	5.4148			23.912
205.5	5.4165			23.935
280.0	5.4195			23.975
357.2	5.4226			24.016
416.1	5.4257			24.057
456.0	5.4280			24.087
512.6	5.4307			24.124
542.1	5.4324			24.146
602.3	5.4352			24.184
693.5	5.4400			24.248
727.0	5.4411			24.263
797.7	5.4444			24.307
867.0	5.4481			24.356
870.5	5.4485			24.362
946.0	5.4520			24.409
Sillite (ZnSe)				
20.0	5.6680			27.426
25.0	5.6685			27.434
67.1	5.6694			27.447
138.4	5.6728			27.496
175.2	5.6743			27.518
222.5	5.6764			27.548
279.1	5.6793			27.591
337.0	5.6821			27.631
398.0	5.6851			27.675
446.2	5.6873			27.707
521.5	5.6914			27.767
586.0	5.6958			27.832
639.2	5.6978			27.861
731.1	5.7029			27.936
Cadmian sphalerite [(Zn_{0.9382}Cd_{0.0618})S]				
25.0	5.4354			24.188
100.0	5.4389			24.233
214.5	5.4438			24.299
316.5	5.4485			24.362
414.0	5.4524			24.414
511.2	5.4574			24.481
633.3	5.4629			24.555
747.0	5.4686			24.632
843.1	5.4734			24.697
Wurtzite (ZnS)				
25.0	3.8232		6.2565	23.858
131.5	3.8260		6.2610	23.910
244.8	3.8293		6.2668	23.973
359.5	3.8343		6.2717	24.054
477.5	3.8379		6.2781	24.124
556.7	3.8411		6.2839	24.187
607.0	3.8434		6.2849	24.220
678.5	3.8464		6.2884	24.271
689.8	3.8468		6.2896	24.281
781.9	3.8510		6.2938	24.350
829.0	3.8533		6.2973	24.393
909.0	3.8570		6.3018	24.457

TABLE 152.1.—Unit-cell edges and molar volumes at different temperatures of ten minerals—Continued

Temperature (°C)	a (Å)	b (Å)	c (Å)	V (cc per mol)
Coesite (SiO₂)				
24.3	7.1517	-----	12.3791	20.647
128.0	7.1534	-----	12.3828	20.663
238.5	7.1560	-----	12.3864	20.685
350.5	7.1586	-----	12.3907	20.706
464.2	7.1617	-----	12.3957	20.732
603.0	7.1655	-----	12.4030	20.767
672.3	7.1677	-----	12.4066	20.786
780.0	7.1712	-----	12.4125	20.815
872.0	7.1746	-----	12.4181	20.845
991.3	7.1785	-----	12.4254	20.880
1045.3	7.1807	-----	12.4290	20.899
Forsterite (Mg₂SiO₄)				
25	4.758	10.214	5.984	43.802
81.1	4.760	10.220	5.987	43.87
113.7	4.761	10.223	5.989	43.90
161.9	4.763	10.229	5.992	43.97
206.3	4.766	10.234	5.995	44.04
291.6	4.769	10.245	6.000	44.15
358.2	4.772	10.253	6.007	44.27
425.5	4.776	10.264	6.014	44.41
530.6	4.779	10.282	6.020	44.55
572.3	4.783	10.289	6.026	44.67
661.6	4.788	10.305	6.031	44.82
742.7	4.793	10.316	6.036	44.95
904.2	4.802	10.344	6.055	45.30
1041.8	4.810	10.368	6.069	45.59
1127.1	4.816	10.382	6.077	45.77
Strontianite (SrCO₃)				
25.0	5.1120	8.4145	6.0286	39.058
30.0	5.1125	8.4155	6.0306	39.080
112.2	5.1150	8.4235	6.0530	39.281
230.1	5.1199	8.4370	6.0810	39.564
272.5	5.1226	8.4410	6.0935	39.685
296.0	5.1235	8.4440	6.0994	39.745
495.0	5.1330	8.4650	6.1548	40.280
585.5	5.1380	8.4755	6.1820	40.548
610.2	5.1400	8.4785	6.1922	40.645
725.5	5.1465	8.4926	6.2270	40.993
900.0	5.1558	8.5175	6.3000	41.670

The linear expansions parallel to the three crystallographic axes, computed from the measured positions of the (112), (140) and (211) reflections, can be compared qualitatively with the expansions observed by Kozu and others (1934) for a natural olivine with the composition forsterite 89.9 percent, fayalite 10.1. In both cases the relative expansions parallel to the *b* and *c* axes are approximately equal, but the expansion parallel to the *a* axis is considerably less. The only previous measurement reported for a pure forsterite is that of Rigby and Green (1941), who measured the bulk expansion of a random aggregate of forsterite grains. The percentage volume expansion from 20°C

TABLE 152.2.—Coefficients in the equation $V = \frac{A}{T} + B + CT + DT^2$

[The function is calculated by the method of least squares, giving the value at 298.2° Absolute (25° C) three times the weight of other values. The agreement of fit is shown by the standard deviation between the observed and calculated values]

Substance	A	B	C	D	Standard deviation
Galena (PbS).....	-47.689	31.304	0.9244×10^{-3}	8.5232×10^{-7}	0.008
Clausthalite (PbSe).....	58.105	33.621	2.7618×10^{-3}	-2.7220×10^{-7}	.006
(Pb _{0.8375} Cd _{0.1625})S.....	125.58	28.922	4.0642×10^{-3}	-14.623×10^{-7}	.003
Sphalerite (ZnS).....	24.427	23.552	$.6865 \times 10^{-3}$	$.0084 \times 10^{-7}$.003
Stilleite (ZnSe).....	30.002	27.100	$.7649 \times 10^{-3}$	$.3994 \times 10^{-7}$.004
(Zn _{0.9382} Cd _{0.0618})S.....	-5.014	24.056	$.4719 \times 10^{-3}$	$.9725 \times 10^{-7}$.003
Wurtzite (ZnS).....	11.407	23.659	$.4946 \times 10^{-3}$	1.4501×10^{-7}	.003
Strontianite (SrCO ₃).....	-129.21	39.214	$.5082 \times 10^{-3}$	14.259×10^{-7}	.009
Coesite (SiO ₂).....	2.451	20.596	$.1212 \times 10^{-3}$	$.8147 \times 10^{-7}$.001
Forsterite (Mg ₂ SiO ₄).....	45.31	43.21	1.368×10^{-3}	$.3.113 \times 10^{-7}$.011

to 1000°C observed by Rigby and Green (1941) is 3.42 percent, in comparison to the 3.86 percent observed in the present study. This should be considered only fair agreement, and indicates a need for further independent measurements.

REFERENCES

- Bethke, P. M., and Barton, P. B., Jr., 1961, Unit-cell dimension versus composition in the systems PbS-CdS, PbS-PbSe, ZnS-ZnSe, and CuFeS_{1.90}-CuFeSe_{1.90}: Art. 114 in U.S. Geol. Survey Prof. Paper 424-B, p. B266-B270.
- DuMond, J. W. M., and Cohen, E. R., 1953, Least squares adjustment of the atomic constants, 1952: Rev. Modern Physics, v. 25, p. 691-708.
- Hume-Rothery, W., and Reynolds, P. W., 1938, A high-temperature Debye-Scherrer camera: Royal Soc. London Proc., v. A167, p. 25-34.
- Kozu, S., Ueda, J., and Tsurumi, S., 1934, Thermal expansion of olivine: Imp. Acad. Japan Proc., v. 10, p. 83-86.
- Pfaff, F., 1859, Untersuchungen über die Ausdehnung der Krystalle durch die Wärme: Poggendorff, Ann. der Physik und Chemie, B107, p. 148-154.
- Rigby, G. R., and Green, A. T., 1941, Thermal expansion characteristics of some calcareous and magnesium minerals: British Ceram. Soc. Trans., v. 41, p. 123-143.
- Sharma, S. S., 1951, Thermal expansions of crystals VIII—Galena and pyrite: Indian Acad. Sci. Proc., v. 34, p. 72-75.
- Skinner, B. J., Barton, P. B., Jr., and Kullerud, G., 1959, Effect of FeS on the unit cell edge of sphalerite—A revision: Econ. Geol., v. 54, p. 1040-1046.
- Skinner, B. J., Clark, S. P., Jr., and Appleman, D. E., 1961, Molar volumes and thermal expansions of andalusite, kyanite and sillimanite: Am. Jour. Sci., v. 259, p. 651-668.
- Skinner, B. J., Stewart, D. B., and Morgenstern, J. C., 1962, A new heating stage for the X-ray diffractometer: Am. Mineral., v. 47, p. 962-967.
- Swanson, H. E., and Tatge, E., 1953, Standard X-ray diffraction patterns: Natl. Bur. Standards Circ. 539, v. 1, 95 p.
- Yoder, H. S., Jr., and Sahama, Th. G., 1957, Olivine X-ray determinative curve: Am. Mineral., v. 42, p. 475-491.
- Zoltai, T., and Buerger, M. J., 1959, The crystal structure of coesite the dense, high-pressure form of silica: Zeitschr. Kristallographie, v. 111, p. 129-141.

153. HYDROTHERMAL ALTERATION IN DRILL HOLES GS-5 AND GS-7, STEAMBOAT SPRINGS, NEVADA

By GUDMUNDUR E. SIGVALDASON¹ and DONALD E. WHITE, Menlo Park, Calif.

Sigvaldason and White (1961) described briefly the hydrothermal mineral assemblages in two drill holes (GS-1 and GS-2) in the Low and High Terraces, respectively, at Steamboat Springs and included bibliographic references to previous work.

DRILL HOLE GS-5

Drill hole GS-5 is on the Main Terrace near the principal flowing springs and is between the drill holes previously described on the low and high terraces respectively. Semiquantitative abundance of the principal minerals and other pertinent data are shown in figure 153.1; analyses of the altered rocks are shown in table 153.1. The most abundant clay mineral is mixed-layer illite-montmorillonite. The expandable montmorillonite component constitutes about 20 to 25 percent of the mixed layers in much of the granodiorite, but 10 percent or less in the dikes and in the most completely altered granodiorite. Below 350 feet, a relatively well-crystallized hydrothermal mica occurs with $n_\alpha > 1.55$ and with high birefringence, and is here called "sericite." This mineral probably grades into the more abundant illite-montmorillonite, characterized optically by finer grain size, $n_\alpha < 1.55$ and typically near 1.53, and lower birefringence. All of the hydrothermal mica is of the 1 Md dioctahedral type, now recognized also in cores from GS-2, and with less certainty in cores from GS-1 and GS-7, where it is greatly dominated by montmorillonite. Chlorite with a relatively high iron content is present in small amount throughout the core and is generally more abundant in the altered dikes than in granodiorite. The intensity ratios of the (001) and (002) X-ray peaks suggest that chlorite has a higher Mg content in the upper part of the andesite dike than elsewhere.

Hydrothermal K-feldspar is relatively abundant from about 100 to 300 feet in depth, generally replacing plagioclase irregularly, and is commonly marginal to patches of completely argillized plagioclase. The sodic rims of zoned plagioclase crystals are very resistant to alteration. The andesine cores of crystals are commonly replaced completely in the upper part of the hole by illite-montmorillonite and K-feldspar.

Below 300 feet K-feldspar is increasingly scarce, and the original zoned plagioclase is commonly "homogenized" to albite or sodic oligoclase with abundant patches and flecks of clay minerals or calcite; excess calcium is removed. Original hornblende and biotite are completely altered throughout the hole, but original quartz and orthoclase are stable or metastable. Chalcedony-quartz-calcite veins occur below 84 feet, with calcite as an abundant component below 175 feet; vein thicknesses range up to about 8 feet. Stibnite is relatively common near the surface, decreasing in abundance downward to 94 feet; it has not been observed from greater depths.

The mineral assemblages in drill hole GS-5 are similar to those of GS-2 of the High Terrace in the downward decrease in hydrothermal K-feldspar and plagioclase, and in the general increase downward in clay minerals (see Sigvaldason and White, 1961, for possible explanations). Addition of potassium is nowhere as notable in GS-5 as in the upper 300 feet of GS-2. At least in part this is related to proportions of reactive calcic plagioclase and perhaps even to structural states of plagioclase in plutonic rocks and in volcanic rocks. The present composition of the thermal waters of the two terraces is similar (Sigvaldason and White, 1961, p. D121).

DRILL HOLE GS-7

Drill hole GS-7 is situated in the Silica Pit area on higher ground a mile west of the flowing springs (White, 1955, p. 110-111). Although thermal potassium-bearing waters probably discharged from this area several hundred thousand years ago, activity at present and in the recent past consists of the rise of steam, CO₂, and H₂S into a perched body of water dominantly of meteoric origin, with a well-defined water table near a depth of 112 feet. In contrast to the discharging water of the active spring terraces, the perched water body contains bicarbonates and sulfates almost to the exclusion of chloride, boron, and cations of external origin. Possible origins of this type of water have been reviewed briefly by White (1957, p. 1649-1651, 1655). H₂S rises above the water table and oxidizes near the surface to form sulfuric acid.

¹ Present address, University Research Institute, Reykjavik, Iceland.

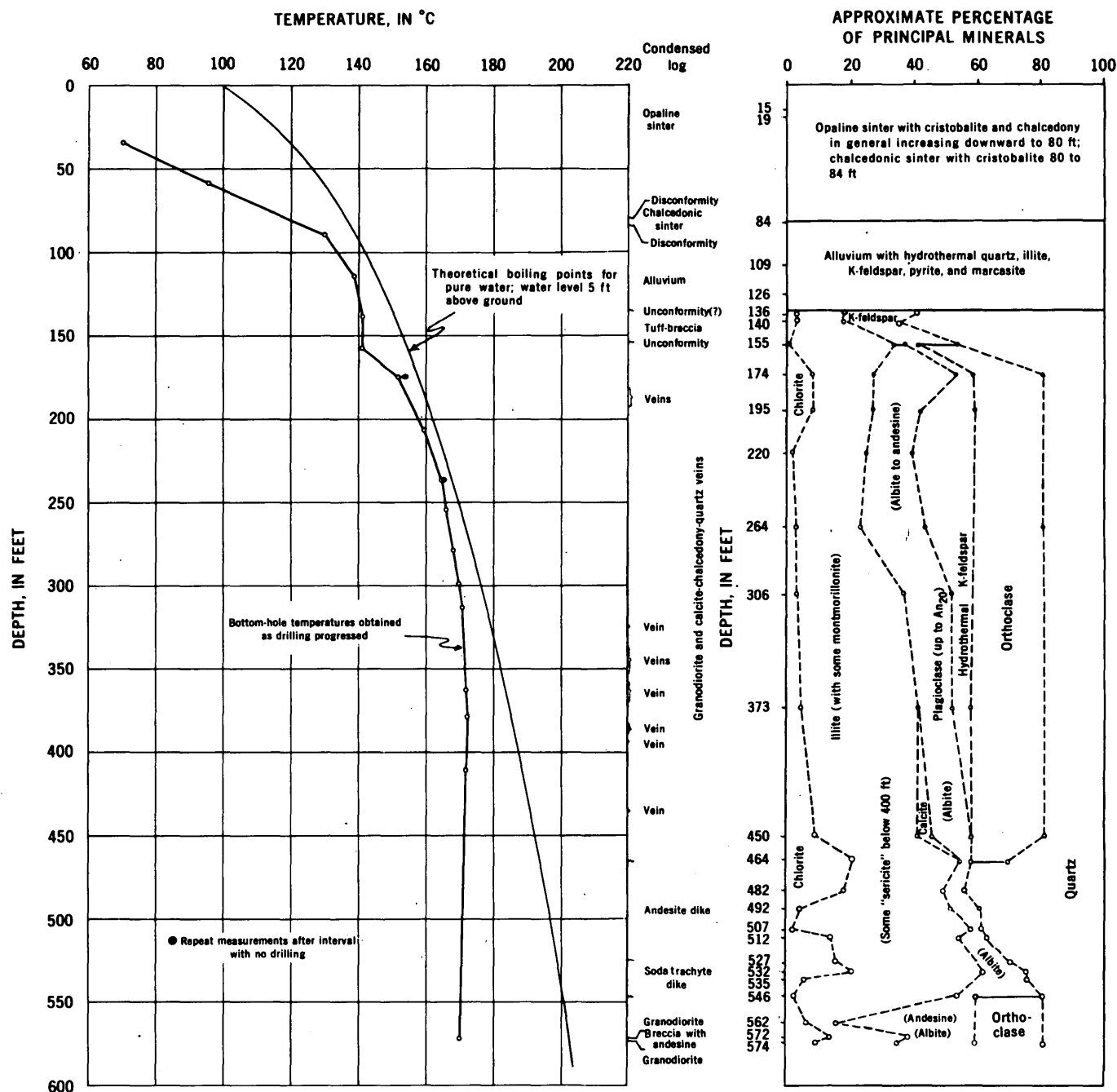


FIGURE 153.1.—Data from drill hole GS-5, main terrace, Steamboat Springs. Altitude of ground level is 4,661 feet.

The striking differences in the mineral assemblages (fig. 153.2 and table 153.2) from the surface to depths of more than 150 feet are related to downward per-

colation of very acid water (pH probably initially 1 to 2) through porous siliceous residues of previously leached granodiorite. Opal has the X-ray pattern of

TABLE 153.1.—Analyses of hydrothermally altered rocks of drill hole GS-5

[Analyzed by rapid methods by L. Shapiro, H. F. Phillips, K. E. White, S. M. Berthold, and E. A. Nygaard]

	Rock type, and depth, in feet						
	Opaline sinter	Black opal sinter	Chalcedony-opal sinter	Arkosic sediments	Chalcedony vein (?)	Granodiorite	Granodiorite
	15	19	84	109	126	155	306
SiO ₂	95.2	91.9	96.3	97.2	89.2	81.0	69.9
Al ₂ O ₃25	.11	.72	10.3	4.8	9.6	14.6
FeO.....	.0	.0	.05	.5	.8	.3	.0
Fe ₂ O ₃ ¹0	.0	.05	.4	.0	.3	.0
MgO.....	.04	.00	.02	.25	.30	.31	.44
CaO.....	.18	.70	.26	.92	.30	.45	.93
Na ₂ O.....	.22	.26	.24	1.1	.22	.66	2.4
K ₂ O.....	.10	.18	.16	5.6	1.3	4.3	5.8
TiO ₂00	.06	.16	.34	.16	.16	.30
P ₂ O ₅00	.01	.00	.02	.00	.00	.07
MnO.....	.00	.01	.00	.01	.00	.00	.01
CO ₂	<.05	<.05	<.05	<.05	<.05	<.05	<.05
H ₂ O.....	3.7	6.6	1.6	1.6	1.3	1.3	1.2
FeS ₂13	.11	.52	1.4	1.6	1.5	3.6
Total as reported.....	99.8	99.9	100.0	101.6	100.0	99.9	99.3
Specific gravity (powder).....	2.16	2.06	2.40	2.58	2.66	2.64	2.68
Specific gravity (lump).....	2.04	1.92	2.07	2.41	2.55	2.56	2.52
Prominent hydrothermal minerals. ²	Opal, (chalcedony, stibnite, calcite).	Cristobalite, (quartz, stibnite).	Chalcedony, cristobalite, (pyrite, calcite).	Quartz, K-feldspar, illite-montmorillonite, (pyrite).	Chalcedony, illite-montmorillonite, (K-feldspar, pyrite, marcasite).	Quartz, illite-montmorillonite, (K-feldspar, calcite, pyrite, hematite).	Illite ($n\gamma \sim 1.545$) chlorite, K-feldspar, (albite, pyrite).

	Granodiorite	Andesite dike	Andesite dike	Trachytic andesite dike	Granodiorite	Granodiorite
	450	482	512	532	562	574
SiO ₂	65.4	65.4	66.6	64.0	68.0	67.1
Al ₂ O ₃	13.6	16.4	16.1	16.5	16.0	14.5
FeO.....	.3	.8	.3	.7	2.1	1.9
Fe ₂ O ₃ ¹1	.4	.0	.7	.8	.4
MgO.....	1.0	.70	1.4	1.1	.61	.68
CaO.....	4.2	.65	.31	.94	2.5	1.4
Na ₂ O.....	2.0	.66	.84	2.8	3.2	3.2
K ₂ O.....	4.4	4.2	4.2	4.0	3.5	4.6
TiO ₂30	.52	.47	.49	.47	.49
P ₂ O ₅08	.20	.23	.09	.12	.08
MnO.....	.10	.06	.00	.03	.10	.11
CO ₂	2.6	<.05	<.05	.08	.68	.67
H ₂ O.....	2.0	5.2	3.4	4.2	1.3	2.8
FeS ₂	3.2	5.2	5.8	4.3	.80	.77
Total as reported.....	99.3	98.4	99.4	99.9	100.2	98.7
Specific gravity (powder).....	2.66	2.68	2.76	2.68	2.66	2.62
Specific gravity (lump).....	2.29	2.21	2.33	2.38	2.49	2.35
Prominent hydrothermal minerals. ²	Illite-montmorillonite, "sericite", albite, chlorite (calcite, pyrite).	Illite-montmorillonite, quartz, chlorite, albite, (pyrite).	Illite-montmorillonite, quartz, chlorite, albite, (pyrite).	Illite-montmorillonite, quartz, albite, chlorite, (pyrite, calcite).	Illite-montmorillonite, chlorite, (calcite, "sericite", pyrite).	Illite-montmorillonite, chlorite, albite, (calcite, hematite).

¹ Or total Fe as Fe₂O₃.² Approximate order of abundance; minor minerals in parentheses.

cristobalite to a depth of 32 feet but is amorphous at greater depths. The perched body of ground water is strongly acid immediately below the water table to 132 feet, where kaolinite is most abundant. At 133 feet montmorillonite abruptly becomes dominant and is abundant at all greater depths. Kaolinite was not found below 238 feet, marking the lower limit of in-

fluence of sulfuric acid of surficial origin. The basal (001) X-ray reflection of the montmorillonite is uniformly near 15 Å, indicating a Ca-Mg type similar to the dominant type in GS-1 (Sigvaldason and White, 1961), and this is supported by double low-temperature differential thermal analysis peaks characteristic of many Ca-montmorillonites. Chlorite is

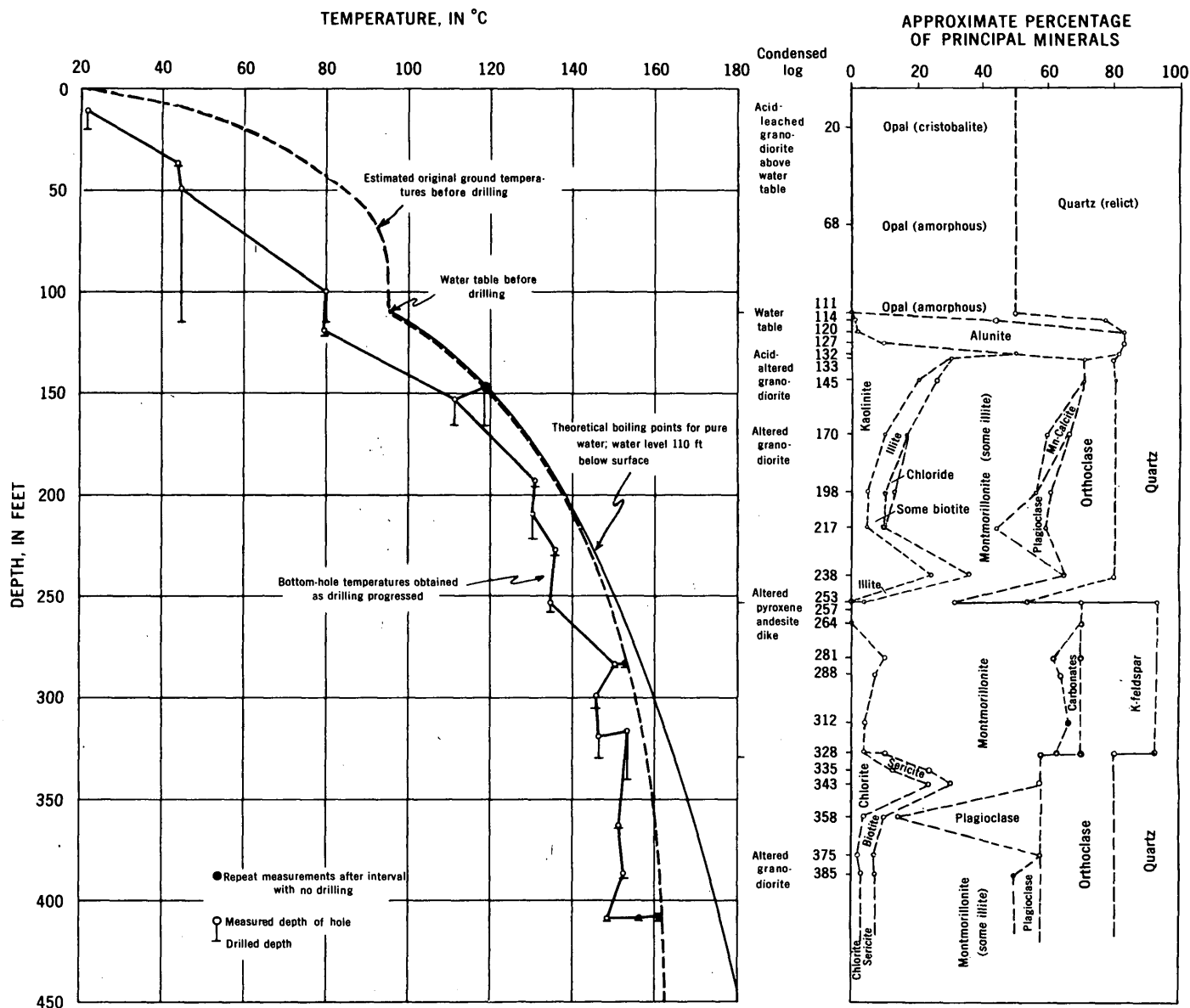


FIGURE 153.2.—Data from drill hole GS-7, Silica Pit area, Steamboat Springs. Altitude of ground level is about 5,025 ft.

present below 270 feet and also occurs in small amounts at 198 feet. Below 330 feet "sericite," optically similar to that of GS-5, is found. Relict biotite occurs only in relatively fresh rocks containing some unreplaced andesine.

The active agent for the deep alteration in drill

hole GS-7 is CO_2 . Potassium is not being supplied from depth at the present time but probably was in the past. Excess potassium and aluminum in the rocks immediately below the water table (table 153.2) were supplied by acid leaching of rocks near the surface.

TABLE 153.2.—Analyses of hydrothermally altered rocks of drill-hole GS-7

[Analyzed by rapid methods by L. Shapiro, H. F. Phillips, K. E. White, S. M. Berthold, and E. A. Nygaard; Sb by F. N. Ward]

	Rock type, and depth, in feet							
	Granodiorite	Granodiorite	Granodiorite	Granodiorite	Granodiorite	Granodiorite	Granodiorite	Granodiorite
	20	68	111	114	120	127	133	145
SiO ₂	95.4	92.0	90.5	56.9	21.8	26.8	69.4	69.6
Al ₂ O ₃68	.76	.58	15.1	29.0	27.9	15.6	12.0
FeO.....	.06	.0	.0	.0	.0	.0	.0	.1
Fe ₂ O ₃ ¹01	.01	.00	.03	.00	.00	2.1	2.6
MgO.....	.14	.04	.12	.04	.12	.08	.53	.62
CaO.....	.13	.18	.18	.20	.31	.32	.22	.28
Na ₂ O.....	.08	.14	.16	4.1	7.9	7.4	3.0	2.2
K ₂ O.....	.38	.44	.56	.28	.26	.30	.32	.22
TiO ₂00	.01	.02	.16	.42	.30	.06	.04
P ₂ O ₅00	.01	.00	.00	.01	.00	.09	.12
MnO.....	<.05	.07	.06	.23	.18	.08	.12	<.05
CO ₂	3.8	2.2	1.9	6.9	11.4	10.5	7.3	8.7
H ₂ O.....	.04	3.0	5.8	3.0	1.6	1.4	2.2	3.4
FeS ₂	0	0	0	13.7	27.7	25.7	0	0
SO ₃								
Total as reported.....	100.8	98.9	99.9	100.6	100.7	100.8	100.9	99.9
Sb (in ppm).....	.9	2.2	2.0	1.6	.8	.8	-----	1.0
Specific gravity (powder).....	2.17	2.32	2.36	2.52	2.79	2.76	2.50	2.46
Specific gravity (lump).....	1.52	1.30	1.57	2.26	2.36	2.41	-----	2.21
Prominent hydrothermal minerals. ²	Cristobalite, (anatase, barite).	Opal, (pyrite, anatase).	Opal, pyrite, (marcasite, anatase, barite).	Alunite, opal, (pyrite, marcasite, anatase?).	Alunite, (opal, pyrite, marcasite, kaolinite?).	Alunite, kaolinite, (marcasite, pyrite).	Montmorillonite, kaolinite, (alunite, pyrite).	Montmorillonite, kaolinite, (illite, marcasite, pyrite).

	Granodiorite	Granodiorite	Andesite dike	Andesite dike	Granodiorite	Granodiorite	Granodiorite
	170	217	264	281	335	358	385
SiO ₂	61.3	66.9	58.0	54.2	68.6	68.8	69.7
Al ₂ O ₃	12.5	14.6	17.8	17.1	15.4	14.8	15.2
FeO.....	.5	.0	.16	1.2	1.2	1.6	.8
Fe ₂ O ₃ ¹0	.0	.5	.4	.4	.4	.1
MgO.....	1.6	2.0	1.9	2.9	1.8	1.2	1.0
CaO.....	4.5	1.4	2.2	5.0	.71	2.2	1.6
Na ₂ O.....	.40	1.2	.64	1.8	.35	3.6	2.3
K ₂ O.....	3.6	4.1	3.2	3.0	5.3	3.9	4.1
TiO ₂26	.30	.46	.50	.37	.30	.31
P ₂ O ₅06	.07	.20	.36	.07	.06	.07
MnO.....	.25	.13	.06	.73	.04	.04	.02
CO ₂	2.9	.07	.18	3.0	<.05	.08	<.05
H ₂ O.....	8.1	7.5	13.8	8.5	5.3	1.4	4.4
FeS ₂	3.7	1.7	.77	1.5	.56	.28	.41
SO ₃	0	0	0	0	0	-----	-----
Total as reported.....	99.7	100.0	99.9	100.2	100.1	98.7	100.0
Sb (in ppm).....	1.0	.7	.5	-----	2.3	1.0	1.3
Specific gravity (powder).....	2.44	2.52	2.28	2.46	2.60	2.62	2.53
Specific gravity (lump).....	2.30	2.35	1.98	2.42	2.16	2.57	2.41
Prominent hydrothermal minerals. ²	Montmorillonite, kaolinite, illite, Mn-calcite, (pyrite).	Montmorillonite, kaolinite, illite, (pyrite).	Montmorillonite, K-feldspar (pyrite, calcite)	Montmorillonite, K-feldspar (?) ankerite (?) chlorite, (pyrite).	Illite-montmorillonite, chlorite, sericite, (pyrite).	Illite-montmorillonite, chlorite, (pyrite, calcite).	Illite-montmorillonite, (chlorite, sericite, pyrite).

¹ Or total Fe as Fe₂O₃.² In order of abundance; minor minerals in parentheses.

REFERENCES

- Sigvaldason, G. E., and White, D. E., 1961, Hydrothermal alteration of rocks in two drill holes at Steamboat Springs, Washoe County, Nevada: Art. 331 in U.S. Geol. Survey Prof. Paper 424-D, p. D116-D122.
- White, D. E., 1955, Thermal springs and epithermal or deposits, in Bateman, A. M., ed., Economic geology, pt. 1: Urbana, Ill., Economic Geology Publishing Co., p. 99-154.
- 1957, Thermal waters of volcanic origin: Geol. Soc. America Bull., v. 68, p. 1637-1658.



154. PRECAMBRIAN GABBRO IN THE CENTRAL FRONT RANGE, COLORADO

By R. B. TAYLOR and P. K. SIMS, Denver, Colo., and Minneapolis, Minn.

Precambrian gabbro, a rock type not previously reported from the Front Range of Colorado, has been found southwest of Fraser in the Vasequez Mountains and west of Apex on the east slope of the Front Range (fig. 154.1). Though the two areas are 25 miles apart, the rocks are linked by lithologic similarities and by their age relative to known Precambrian events. The gabbros are characterized by calcic plagioclase, orthopyroxene, and clinopyroxene, and generally contain some younger amphibole and mica. The gabbro plutons were emplaced late in a period of deformation and metamorphism in which the older rocks of the region attained the sillimanite-almandine facies. Contact aureoles have been incompletely meta-

morphosed to the pyroxene hornfels facies. Continuing regional metamorphism and later local deformation partly retrograded the rocks within the plutons.

Two lenticular plutons of gabbro have been outlined in the Keyser Creek area southwest of Fraser (fig. 154.1). The larger one, the Upson Creek pluton, is about 4 miles in length and 1½ miles in maximum width. The smaller mass, the Cook Creek pluton, is 1½ miles long and almost a mile wide. The bodies trend northeastward and have subconcordant, steeply dipping contacts that follow the regional trend of the gneissic structure in the country rock. Near-vertical internal flow structures trending northeast are evident in most outcrops.

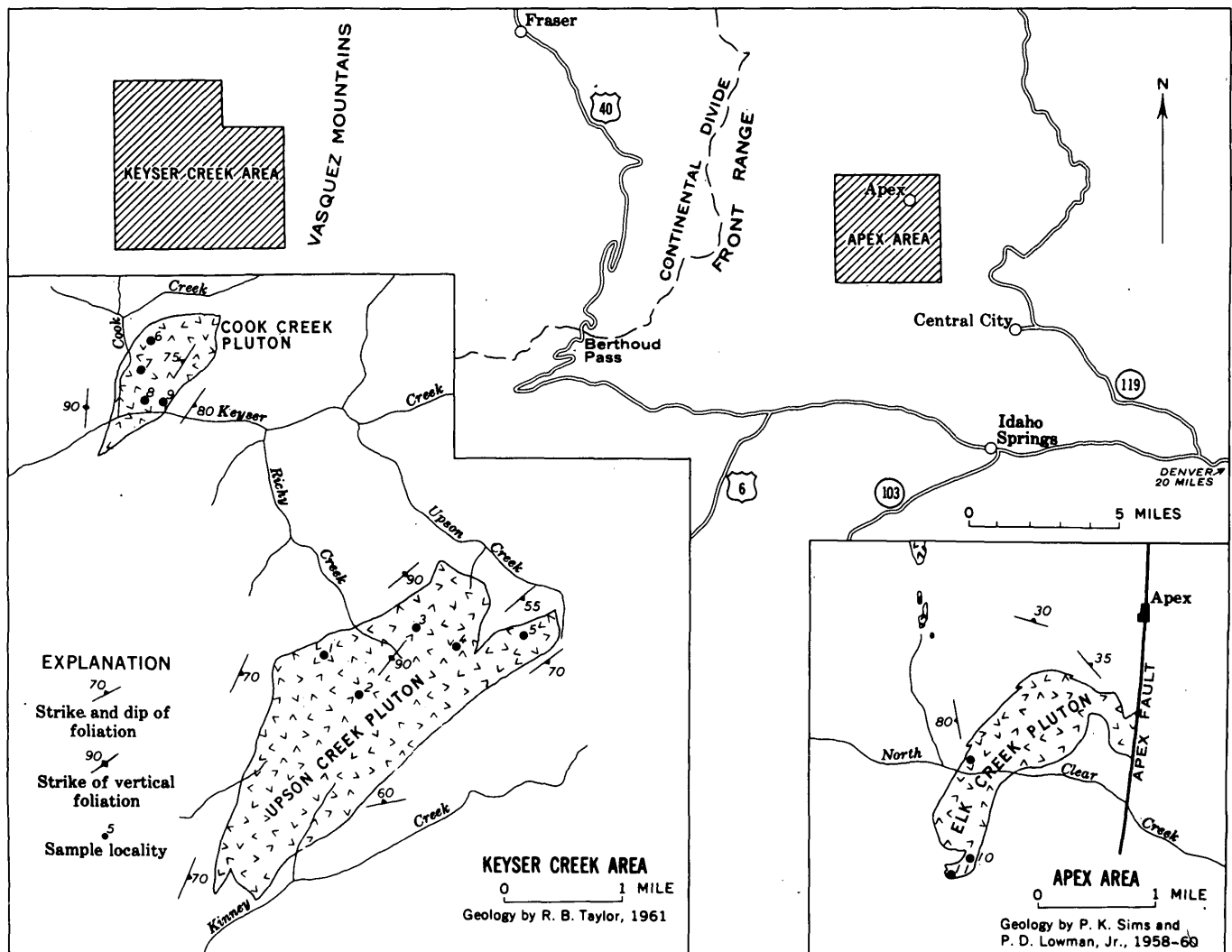


FIGURE 154.1.—Index map and geologic sketch map of gabbro plutons (patterned areas) in the central Front Range.

The largest body in the Apex area, the Elk Creek pluton, is a hook-shaped mass about 2 miles in total length and $\frac{3}{4}$ of a mile in maximum width that lies on the crest of a complex anticline. Several bodies less than 1,000 feet in maximum dimension occur near this mass. Unlike the bodies southwest of Fraser, these have a massive internal structure. The only foliated parts, so far as is known, are lenticular zones confined to the eastern side of the Elk Creek pluton and are interpreted as protoclastic in origin.

The gabbroic rocks in both areas are dark gray, medium to coarse grained, and generally equigranular. Rare inequigranular feldspathic varieties have plagioclase crystals as much as 2 inches in size, and melanocratic varieties may have a luster mottling produced by randomly oriented large poikiloblastic hornblende crystals. The composition ranges from melagabbro to quartz diorite (see table), but most samples are either gabbro or pyroxene diorite. The Upson Creek and Cook Creek plutons, because of their characteristic bytownite and bronzite, have affinities with ultrabasic rocks (Leake, 1958, p. 159). The rocks of the Apex area are less basic, are characterized by intermediate plagioclase, and locally contain substantial amounts of quartz. The gabbros tend to weather spheroidally to subrounded boulders, to coarse grus or, under forest cover, to a distinctive sticky dark-brown soil laden with fragments of metamorphic xenoliths and granitic material from crosscutting dikes.

The gabbro has a typical hypidiomorphic or xenomorphic granular texture. The marginal phases in the Keyser Creek area have a diabasic texture, with pyroxene intersertal to plagioclase laths (fig. 154.2A). Hornblende surrounds most pyroxene crystals and has scalloped contacts against adjoining plagioclase grains. Coarser gabbro from the interior of the plutons has a strong planar structure defined by flow-oriented plagioclase and pyroxene crystals in a mosaic intergrowth (fig. 154.2B). The gabbro of the Apex area is massive and has interlocking plagioclase and pyroxene crystals; more rarely, the mafic minerals occur in aggregates with synneusis texture. In both areas gabbro varieties much modified by metamorphic retrograding are characterized by large ragged grains of replacement amphibole that virtually obliterate the primary igneous texture (fig. 154.2C).

Plagioclase is the dominant mineral in most of the gabbro (see table). In the Apex area it is slightly zoned calcic andesine or, rarely, labradorite. In the Keyser Creek area, it is strongly zoned and ranges from about An_{50} to An_{85} . Simple zoning with calcic cores and sodic rims and with growth patterns following crystal faces is characteristic. An irregular pattern is superimposed on many crystals in hornblende-rich gabbro; sodic zones follow grain margins and are especially wide adjacent to hornblende, and calcic plagioclase is confined to remnants of cores or to parts adjacent to orthopyroxene crystals. The regular sim-

Modes (volume percent) and mineralogic data for representative samples of gabbroic rocks

[Localities shown on fig. 154.1, except for 13, 14, and 15; modes from Apex area by D. J. Gable, U.S. Geological Survey]

	Keyser Creek area									Apex area					
	Upson Creek pluton					Cook Creek pluton				Elk Creek pluton			Scattered bodies		
	1	2	3	4	5	6	7	8	9	10	11	12	13	14	15
Plagioclase.....	70	56	68	50	58	52	35	36	48	71	65	46	9	2	34
Orthopyroxene.....	8	13	8	20	8	-----	-----	-----	6	7	1	4	51	43	2
Clinopyroxene.....	<1	-----	-----	6	1	-----	-----	-----	1	1	6	11	<1	19	-----
Amphibole.....	14	19	16	20	27	41	61	58	42	7	11	2	35	28	38
Biotite.....	5	<1	4	-----	3	6	1	3	2	6	6	10	5	6	17
Magnetite-ilmenite..	<1	11	3	1	1	<1	1	<1	<1	4	4	10	<1	1	4
Apatite.....	<1	<1	<1	<1	<1	<1	<1	<1	<1	<1	<1	<1	-----	-----	<1
Quartz.....	1	<1	1	2	2	1	2	2	<1	4	4	13	-----	-----	5
Chlorite.....	-----	<1	<1	-----	-----	<1	<1	<1	-----	<1	<1	2	-----	-----	-----
Calcite.....	-----	-----	<1	<1	<1	-----	-----	-----	-----	<1	-----	<1	<1	-----	-----
Pyrrhotite.....	-----	-----	-----	<1	-----	-----	-----	-----	-----	-----	-----	-----	-----	-----	-----
Sericite.....	<1	<1	<1	-----	-----	<1	<1	<1	<1	<1	-----	-----	-----	-----	-----
Zircon.....	-----	-----	-----	-----	-----	-----	-----	-----	-----	<1	-----	<1	-----	-----	-----
Epidote.....	-----	-----	-----	-----	-----	-----	-----	-----	-----	-----	2	1	-----	1	<1
Potassium feldspar..	-----	-----	-----	-----	-----	-----	-----	-----	-----	-----	-----	1	-----	-----	-----
Allanite.....	-----	-----	-----	-----	-----	-----	-----	-----	-----	-----	-----	<1	-----	-----	-----
Sphene.....	-----	-----	-----	-----	-----	-----	-----	-----	-----	-----	-----	<1	-----	-----	-----
Plagioclase, An content.....	66-82	65-85	60-70	72-78	57-68	55-75	50-62	50-57	55-70	46	46	41	56	54	48
Orthopyroxene, n_y	1. 685	1. 695	1. 696	1. 696	1. 702	1. 654	1. 651	1. 656	1. 697	-----	-----	-----	1. 684	1. 694	-----
Amphibole, n_y	1. 662	1. 663	1. 663	1. 662	1. 665	-----	-----	-----	1. 663	-----	-----	-----	-----	-----	-----



FIGURE 154.2.—Photomicrographs of gabbroic rocks. *A*, Diabasic gabbro, locality 9, Cook Creek pluton. *B*, Feldspathic gabbro, locality 2, Upson Creek pluton. *C*, Hornblende gabbro, locality 7, Cook Creek pluton. All photomicrographs are $\times 20$, with crossed nicols.

ple zoning is interpreted as an igneous feature developed during free growth in a melt. The irregular zoning is interpreted as a metamorphic feature developed during amphibolization.

Both orthopyroxene and clinopyroxene are present in most samples. The orthopyroxene is dominantly bronzite (N_v ranges from 1.684 to 1.702) in subhedral crystals that have conspicuous schiller structure resulting from thin plates of an unidentified brown translucent mineral aligned parallel to the optic plane. Other discontinuous lamellae may be clinopyroxene or hornblende. As augite lamellae at a small angle to the (101) plane in the orthopyroxene were not seen, it is inferred that the original form of crystallization was orthopyroxene rather than pigeonite. The clinopyroxene is a nearly colorless variety of augite, occurring in subhedral crystals having small oriented inclusions of opaque minerals. With few exceptions the clinopyroxene is partially replaced by hornblende that follows grain margins or forms a cuneiform intergrowth inside the grain controlled by cleavage. In contrast, the orthopyroxene is characteristically rimmed by hornblende and retains most of its crystal outline.

The amphibole in most gabbro samples is a pleochroic dark-green hornblende (N_v ranges from 1.662 to 1.665). Its contacts with other minerals are sharp, regular, and usually scalloped. It closely resembles the hornblende in the regionally metamorphosed hornblende-plagioclase gneiss. In some samples the plagioclase and clinopyroxene have been partially replaced by green hornblende, and the orthopyroxene by a colorless amphibole, perhaps tremolite. In the most metamorphosed gabbro a light-blue-green hornblende (N_v ranges from 1.651 to 1.656) with ragged outlines replaces plagioclase and both pyroxenes. It is associated with sodic labradorite, perhaps also a recrystallization mineral, and with minerals of the epidote group.

Black opaque grains, chiefly titaniferous magnetite, are locally abundant. In the well-foliated rocks they may be flow oriented in part, but in the more massive rocks they appear to be interstitial to plagioclase and pyroxene. Red-brown biotite is variable in amount, is closely associated with the other ferromagnesian minerals, and generally occurs along the cleavage of pyroxene or hornblende. Quartz is common in the gabbroic rocks of the Apex area as anhedral interstitial grains, blebs in other minerals, and in myrmekitic intergrowths with plagioclase and biotite. Other minerals present in small amount are potassium

feldspar, allanite, sphene, and apatite (see table). Epidote, sericite, calcite, and chlorite occur in some of the more intensely altered rocks.

Striking contact-metamorphic aureoles have formed in the biotite gneisses around the larger intrusions. The most intense metamorphism is around the Upson Creek pluton, probably because it is larger and more basic than the other plutons. Locally, wallrock within about 40 feet of the contact has been transformed to a breccia of blocky, fist-sized fragments of quartz-rich gneiss in a matrix of coarsely crystalline sillimanite, cordierite, biotite, plagioclase, garnet, and quartz. These minerals apparently grew in the matrix after it became sufficiently mobile to flow around pieces of more refractory layers. Outside the breccia zone, the gneiss has been recrystallized to a coarser grained rock with a granoblastic texture; more than 300 feet from the contact, half-inch garnets formed in some of the layers and inch-long sillimanite prisms in others. The characteristic mineral assemblage of the regionally metamorphosed biotite gneisses—quartz-fibrolitic sillimanite-biotite-microcline-plagioclase—has been modified to a disequilibrium assemblage: quartz-biotite-prismatic sillimanite-plagioclase-cordierite-garnet-spinel-magnetite. The matted hairlike crystals of fibrolitic sillimanite were converted to prismatic sillimanite crystals commonly 1–2 mm long, but as much as 2½ cm long. The prisms in some places follow old mineral-lineation directions, but in other places have no preferred orientation. The greenish-tan to brown biotite of the normal gneiss has been partly converted to strongly pleochroic orange- to red-brown biotite, and partly to cordierite, magnetite, sillimanite, and spinel. The cordierite forms small anhedral twinned grains with abundant inclusions of magnetite, and is commonly rimmed by aggregates of tiny sillimanite crystals. The garnet is poikiloblastic, and typically contains biotite and magnetite. Tiny rounded blebs of spinel occur within cordierite or garnet. Hypersthene appears with clinopyroxene in some of the contact rocks. These mineralogic changes in the contact aureole represent the incomplete adjustment of these rocks to the pyroxene hornfels facies of contact metamorphism.

The country rocks adjacent to the Elk Creek pluton have been recrystallized and sheared. In the contact zone the biotite gneisses are coarser grained than similar rocks away from the intrusion. Sillimanitic gneisses are changed locally to inequigranular rocks containing discoidal aggregates of sillimanite, phlog-

opitic mica, and green spinel. Biotite-quartz-plagioclase gneiss is locally reconstituted to an orthopyroxene-biotite-quartz-plagioclase rocks with a felted texture. At one locality along the east contact, microcline-bearing gneiss is sheared to a flaser gneiss and bleached for a distance of nearly 50 feet from the contact; quartz forms lens-shaped aggregates with strong lineation, and biotite is changed to chlorite.

The gabbro was emplaced during the waning stages of the older, major Precambrian deformation recognized in the central part of the Front Range (Moench, Harrison, and Sims, 1962). The subconcordant contacts of all the masses and the phacolithic form of the Elk Creek pluton (fig. 154.1) relate the gabbro to the older deformation. The general lack of metamorphic structures within the gabbro suggests that it was emplaced too late to have been much deformed by the older folding. These interpretations are supported by relations observed in the Upson Creek pluton. This pluton is cut by dikes of biotite-muscovite granite which are similar to rocks known to predate the second deformation recognized a short distance to the north. It cuts small bodies of granodiorite similar in structure and composition to the syntectonic Boulder Creek Granodiorite of the central Front Range.

The gabbros of the Keyser Creek area were emplaced after the thermal maximum, equivalent to the sillimanite-almandine-orthoclase facies, of the older Precambrian deformation and metamorphism. A temperature difference between the gabbro magma and the country rocks, which may be estimated as possibly more than 500°C, was sufficient to produce extensive metamorphism and local melting of the country rock and chilling of the margins of the pluton. After crystallization, green hornblende formed at the expense of pyroxene and plagioclase. Wager (1932) and Leake (1958) point out that hornblende in this quantity in basic and ultrabasic rocks is probably the result of metamorphism and not of crystallization from a melt. Later, during the younger Precambrian deformation, light-blue-green amphibole, epidote, and other minerals locally replaced the older minerals. This change is most evident in the Cook Creek pluton, which is in an area affected by the younger deformation. The Upson Creek pluton is less modified and is in an area less affected by the younger folding. The changes associated with the younger deformation are attributed to retrograde metamorphism; they parallel those described by James (1955) for the transition from the staurolite to the biotite zone.

The gabbro in the Apex area seems to have had a more complex history, and formed from a far less basic magma. The hornblende, quartz, and potassium feldspar may have formed from the interstitial liquid late in the crystallization of the magma, or they may be metamorphic minerals. The cooling of the magma in the environment of regional metamorphism, and the succeeding metamorphic history make it nearly impossible to distinguish between igneous, deuteric, and metamorphic stages of crystallization.

REFERENCES

- Leake, B. E., 1958, The Cashel-Lough Wheelaun intrusion, Co. Galway: *Proc. Roy. Irish Acad.*, v. 59, B, p. 155-203.
- James, H. L., 1955, Zones of regional metamorphism in the Precambrian of northern Michigan: *Geol. Soc. America Bull.*, v. 66, p. 1455-1488.
- Moench, R. H., Harrison, J. E., and Sims, P. K., 1962, Precambrian folding in the Idaho Springs-Central City Area, Front Range, Colorado: *Geol. Soc. America Bull.*, v. 73, p. 35-58.
- Wager, L. R., 1932, Geology of the Roundstone district, Co. Galway: *Proc. Roy. Irish Acad.*, v. 41, B, p. 46-72.



GEOMORPHOLOGY AND GLACIAL GEOLOGY

155. EROSIONAL FEATURES OF SNOW AVALANCHES, MIDDLE FORK KINGS RIVER, CALIFORNIA

By GEORGE H. DAVIS, Washington, D.C.

Work done in cooperation with the National Park Service

Snow avalanches are one of the principal means by which high mountains are eroded and sculptured. They and their effects have been studied extensively in Europe, especially in the Alps, where avalanches pose a constant threat to life and property. In the United States, however, they have received little attention because our high mountains are sparsely inhabited; the damage by snow avalanches is mainly to highways and railroads.

Avalanche sculpture is especially well developed along the canyon of the Middle Fork of the Kings River in the Sierra Nevada, Calif. In parts of the canyon not scoured by glaciers, snow avalanches have been the dominant erosional process throughout Quaternary time.

The Middle Fork of the Kings River rises near Mount Goddard on the crest of the Sierra Nevada and flows generally southwestward to its junction with the South Fork. The junction is about 10 miles downstream from "Kings Canyon," the popular name for the accessible and well-known part of the canyon of the South Fork. Most of the drainage basin of the Middle Fork is above an altitude of 10,000 feet. The Middle Fork flows in a steep-walled canyon, which in much of its course has the U-shaped cross section characteristic of glaciated valleys. The canyon is one of the deepest and steepest in the Sierra Nevada; in its

most spectacular reach (fig. 155.1), extending from Tehipite Valley upstream 8 miles to Simpson Meadow, the walls rise 4,000 to 5,000 feet within a mile horizontal distance (fig. 155.2) where they merge with a rolling upland surface (fig. 155.3). The physiography closely resembles and its geomorphic development parallels that of Yosemite Valley, 75 miles northwest, which has been so ably described by Matthes (1930) in his classic paper on the geologic history of Yosemite Valley.

Precipitation in the high parts of the Sierra Nevada occurs mainly as snow, between November and May, and the water is stored in that form until the late spring and early summer melting. Indeed, three quarters of the total discharge of the Kings River runs off to the San Joaquin Valley between March 1 and June 30. At Blackcap Basin, altitude 10,300 feet, 10 miles north of the Middle Fork, the average depth of snow on April 1st is about 8 feet and its water content is 35 inches.

Massive granitic rocks of the Sierra Nevada batholith form the floor of most of the drainage basin of the Middle Fork although, locally, roof pendants of metamorphosed sandstone and siltstone with lesser amounts of marble and volcanic rocks have been preserved. Along the walls of the U-shaped canyon upstream from Tehipite Valley, only granitic rocks are

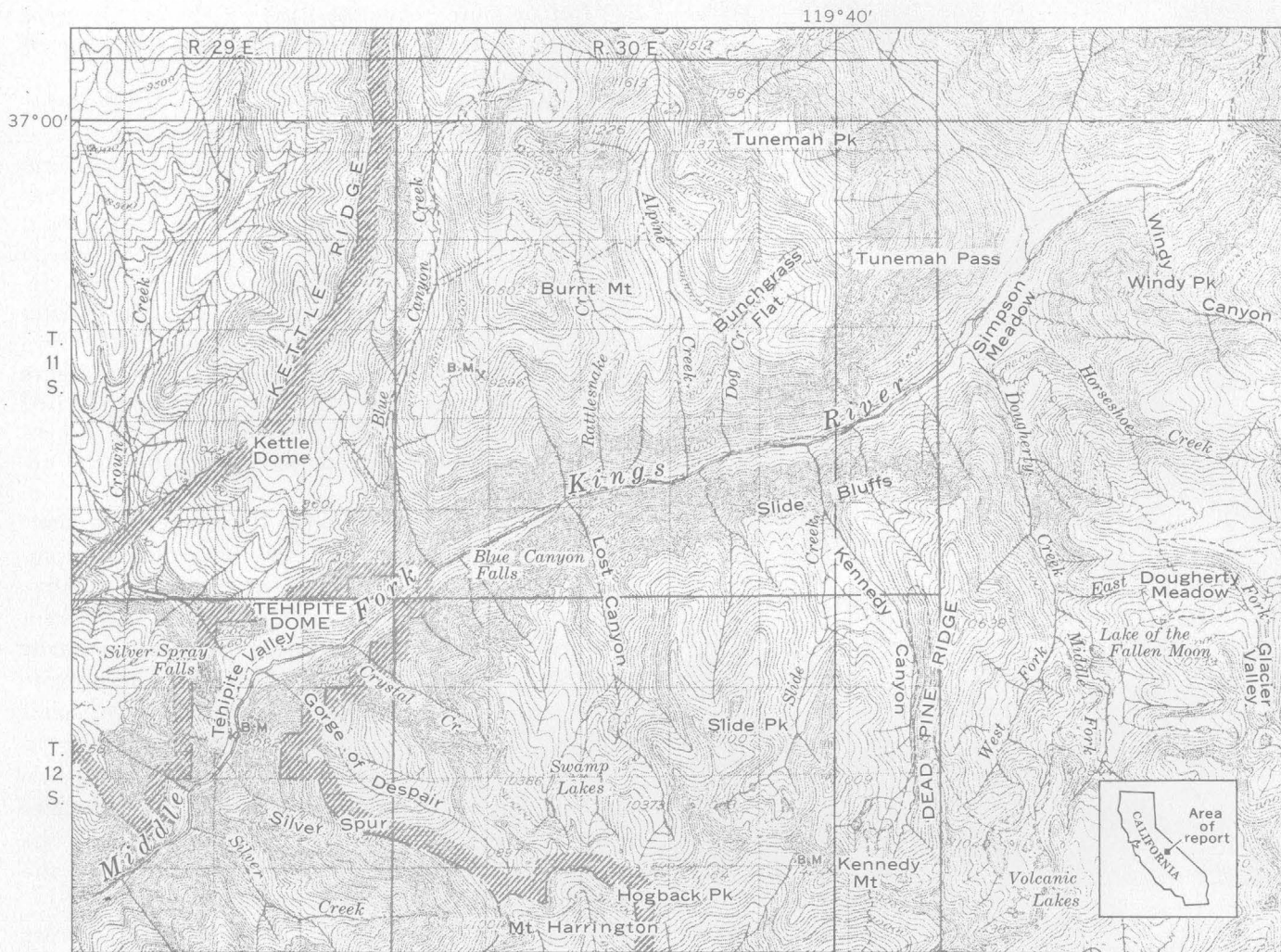


FIGURE 155.1.—Topographic map of canyon of the Middle Fork of the Kings River, Calif. Scale: 125,000; contour interval, 100 feet. Base from U.S. Geol. Survey Topographic Map, Sequoia and Kings Canyon National Parks, Calif.



FIGURE 155.2.—View northeastward up canyon of the Middle Fork of the Kings River, from north wall overlooking Tehipite Valley (center foreground). Tehipite Dome, upper left.



FIGURE 155.3.—Snow chutes and attenuated rock ribs carved by avalanches, south wall of canyon of the Middle Fork of the Kings River. Lost Canyon, left foreground.



FIGURE 155.4.—View eastward up face of Windy Peak from Simpson Meadow, showing two generations of avalanche chutes. Shallow grooves on lower slope represent post-glacial avalanche erosion; deep chutes above in unglaciated part of canyon are probably Pleistocene.

exposed. Northeastward-trending vertical master joints have determined the profile and orientation of the sheer cliffs in the steep-walled canyon section. Glacial excavation broadened the bottom of the canyon, but triangular facets above the active glacial scouring are the site of some of the most impressive avalanche sculpture.

Avalanche sculpture is especially well developed along the southeast wall of the canyon of the Middle Fork of the Kings River between Tshipite Valley and Lost Canyon. Here many of the cliffs have a fluted surface, on which straight smooth gullies alternate with rock ribs (fig. 155.3). Matthes (1938) applied the name "snow chutes" to similar features in the Mount Whitney area. The chutes have a hyperbolic cross section and, where closely spaced as on figure 155.3, the dividing ridges are attenuated ribs that rise

200 feet or more above the flanking chutes. In some places the ribs have been broken to form rows of separate spires.

The snow chutes commonly are wider at the upper end than at the lower end. In many places several chutes on the upper walls of the canyon join to form a single chute downslope. Matthes (1938) noted that most chutes terminate at the upper limit of glacial scouring, and this is generally true also in the canyon of the Middle Fork. He concluded from this that virtually all the chute sculpturing took place in Pleistocene time. However, at Windy Peak (fig. 155.1) two generations of chutes can be seen, as shown in figure 155.4: an upper set of deep chutes above the glaciated zone, and numerous shallow chutes on the lower slopes that evidently have formed since the last glacial retreat.

Matthes ascribed the chutes to abrasion by snow and entrained rock debris. Windblown snow accumulates at the top of the cliff in the form of a massive cornice; sudden breaking of the cornice initiates a snow avalanche. Rock fragments and granules made available by exfoliation of the granitic rocks provide the abrasive action. In the Kings River area, small amounts of talus were poised ready for sliding in some chutes, but most chutes contained little debris and only small bodies of talus debris abutted the toes of the cliffs. These observations suggest that the movement of rock debris is a minor factor in the formation of avalanche chutes.

Erosional features of avalanche origin of a different sort are avalanche scour pits, a good example of which can be seen on the floor of Grouse Meadow on Blue



FIGURE 155.5.—View westward across Grouse Meadow and Blue Canyon Creek, showing avalanche scour pit, upper center. Pond (shown by arrow) is about 60 by 25 feet.

Canyon Creek (fig. 155.5). Grouse Meadow is a nearly level alluviated valley at an altitude of 8,500 feet, about 3 miles upstream from the confluence of Blue Canyon Creek and the Middle Fork of the Kings River. Just to the west, Kettle Ridge rises to 10,500 feet in 0.7 mile. At the foot of Kettle Ridge, on a gentle rise on the floor of Grouse Meadow, is a natural pond about 60 feet long by 25 feet wide and 8 to 10 feet deep, looking very much like a swimming pool. The depression is enclosed at its down valley end by an embankment of rock and soil which appears almost to have been pushed up by a bulldozer. The location of the pond at the foot of Kettle Ridge and the large boulders scattered around the rim suggest avalanche

origin, and the pit containing the pond is interpreted as an avalanche scar. Presumably, a snow avalanche tumbled down the mountain and shoved the soil outward and forward to form a rim; then the snow melted and left behind a depression filled with water. Spring flow from the slope above keeps the pond almost brimfull, and discharge is mainly by seepage through the banks.

REFERENCES

- Matthes, F. E., 1930, Geologic history of the Yosemite Valley: U.S. Geol. Survey Prof. Paper 160.
 ——— 1938, Avalanche sculpture in the Sierra Nevada of California: Internat. Assoc. Hydrology Bull. 23, p. 631-637.



156. CONFIGURATION OF THE BEDROCK BENEATH THE CHANNEL OF THE LOWER MERRIMACK RIVER, MASSACHUSETTS

By EDWARD A. SAMMEL, Boston, Mass.

Work done in cooperation with the Massachusetts Department of Public Works

Geologic mapping and previous seismic investigations in northeastern Massachusetts have disclosed the existence of buried bedrock valleys which presumably represent the traces of a preglacial drainage pattern and are the site of highly productive water-bearing deposits (Baker, Healy, and Hackett, 1961). This article reports further data on the configuration of bedrock in the lower Merrimack River valley obtained recently during an investigation of groundwater resources in the valley. The current investigation indicates that the bedrock surface below the river channel is shallow in much of the reach downstream from Haverhill, although depths of more than 100 feet were noted at places.

A seismic profile was made during September 1961 in portions of the Merrimack River channel along a 20-mile reach between Haverhill and the mouth of the river, near Plum Island, Mass. (fig. 156.1). The area is included in the Haverhill, Newburyport West, and Newburyport East 7½-minute topographic quadrangles of the Geological Survey. The methods used in making the profile were standard reflection tech-

niques, employing a broad-band penetrating echo sounder installed in a 40-foot launch. The fieldwork was done under contract by Alpine Geophysical Associates, Inc., of Norwood, N.J., and the seismic records were interpreted by Hartley Hoskins of the Woods Hole Oceanographic Institution.

The seismic signal was produced by a repeating underwater spark source towed about 50 feet behind the boat at a speed of about 3 knots. Reflected signals were received in a transducer, also towed 50 feet behind the boat and about 3 feet beneath the surface of the water. The amplified signal from the transducer was continuously recorded on electrosensitized paper by a standard recording instrument. Hoskins and Knott (1961) give a detailed description of the general method and types of instruments used.

Bedrock reflections were generally well defined in the eastern half of the traverse except in outcrop areas where the bedrock surface was at shallow depths that approximated the median wavelength of the seismic signal. East of Newburyport, bedrock deeps overlain by horizontally bedded sediments were clearly

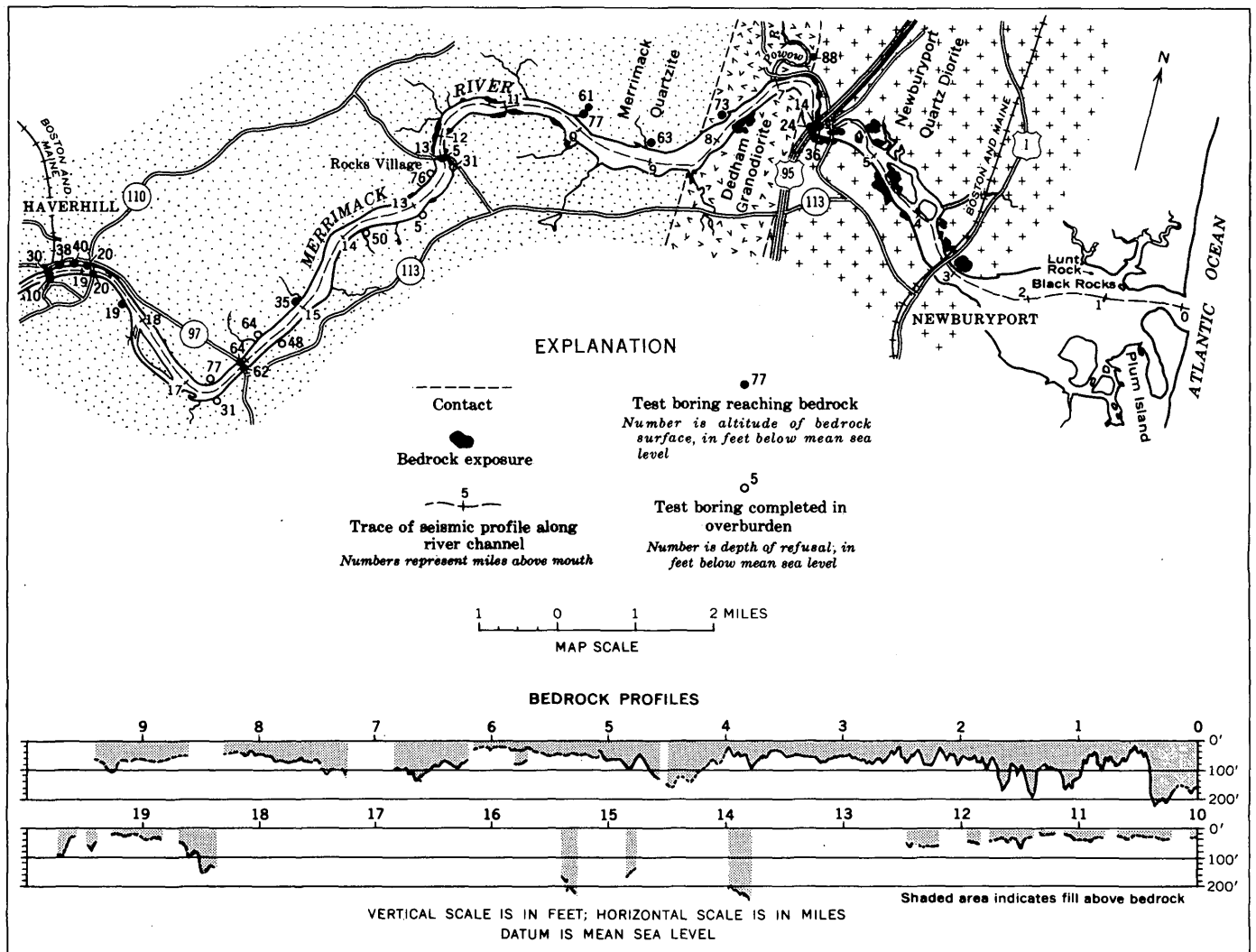


FIGURE 156.1.—Bedrock profile beneath the channel of the lower Merrimack River, Mass., made with a continuous seismic reflection profiler. Plan view shows geology (Clapp, 1921) and bedrock altitudes from test borings.

shown; depths greater than 100 feet were found between miles 1 and 2, 4 and 5, and 6 and 7 (fig. 156.1).

The seismic record was generally unsatisfactory in the reach between Rocks Village and Haverhill. In most of this reach continuous reflections were not received from bedrock, although at a few points near miles 14 and 15 reflections were recorded that indicated bedrock depths on the order of 200 feet. The instrument used was not suitable for recording signals from depths greater than 200 feet, therefore it is possible that bedrock was more than 200 feet deep in most of the 6-mile reach upstream from Rocks Village. A more reasonable explanation for the lack of bedrock signals, however, is that the bedrock is at a

depth of less than 200 feet, but that the seismic reflections were attenuated due to the lithologic character of the fill or the nature of the bedrock contact.

Test borings made along the bank of the Merrimack River upstream from Rocks Village during the spring of 1962 indicate that the fill consists chiefly of gravelly material, in contrast to clay, silt, and fine sand in the downstream reach. The borings, which were carried to bedrock or to refusal, suggest that the bedrock surface is less than 200 feet below sea level in the questionable reach. Bedrock was found near 40 feet below sea level above mile 19, at about 60 feet near mile 16, and at 35 feet at mile 15. The deepest points confirmed by borings were below 76 feet below sea

level just upstream from Rocks Village and below 77 feet between miles 16 and 17.

The geologic implications of the seismic records remain to be clarified by further mapping, seismic exploration, and test drilling. In particular, further work will be needed to relate the configuration of the bedrock surface to the history of glacial deposition in the region.



REFERENCES

- Baker, J. A., Healy, H. G., and Hackett, O. M., 1961, Ground-water conditions in the Wilmington-Reading Area, Massachusetts: U.S. Geol. Survey open-file report, 162 p.
- Clapp, C. H., 1921, Geology of the igneous rocks of Essex County, Massachusetts: U.S. Geol. Survey Bull. 704, 132 p.
- Hoskins, Hartley, and Knott, S. T., 1961, Geophysical investigation of Cape Cod Bay, Massachusetts, using the continuous seismic profiler: Jour. Geology, v. 69, no. 3, p. 330-340.

157. GEOLOGY OF PLEISTOCENE DEPOSITS OF LAKE COUNTY, INDIANA

By J. S. ROSENSHEIN, Indianapolis, Ind.

Work done in cooperation with the Division of Water Resources, Indiana Department of Conservation

Evaluation of subsurface geologic data, collected as part of a ground-water investigation in northwestern Indiana, has led to a tentative differentiation of the glacial drift underlying Lake County, Ind. (fig. 157.1) into four distinctive lithologic units. These units are economically significant to the county as they serve as important sources of water supply. The lithologic units range in age from early Pleistocene to Recent and locally form a stratigraphic sequence more than 250 feet thick. They extend eastward and westward into adjacent counties in Indiana and Illinois. The subsurface geology of the units provides additional facts that may lead to a more comprehensive interpretation of the glacial history of the county. This history to date is based chiefly on interpretation of surface expression of deposits as described by Leverett and Taylor (1915), Wayne (1956, 1958), Zumberge (1960), and R. J. Vig (written communication, 1959).

The distribution and relationship of each unit are shown in the generalized sections on figure 157.2. The location of these sections is shown in figure 157.1. The oldest lithologic unit, tentatively designated unit 4, underlies about 500 square miles of the county and consists chiefly of till that is a gray to bluish-gray pebbly, sandy, silty clay, locally hard and compact. It ranges in thickness from 0 to more than 150 feet and in age from early Pleistocene to Illinoian. The till represents drift deposited during at least the Kansan and Illinoian Glaciations. The unit contains sev-

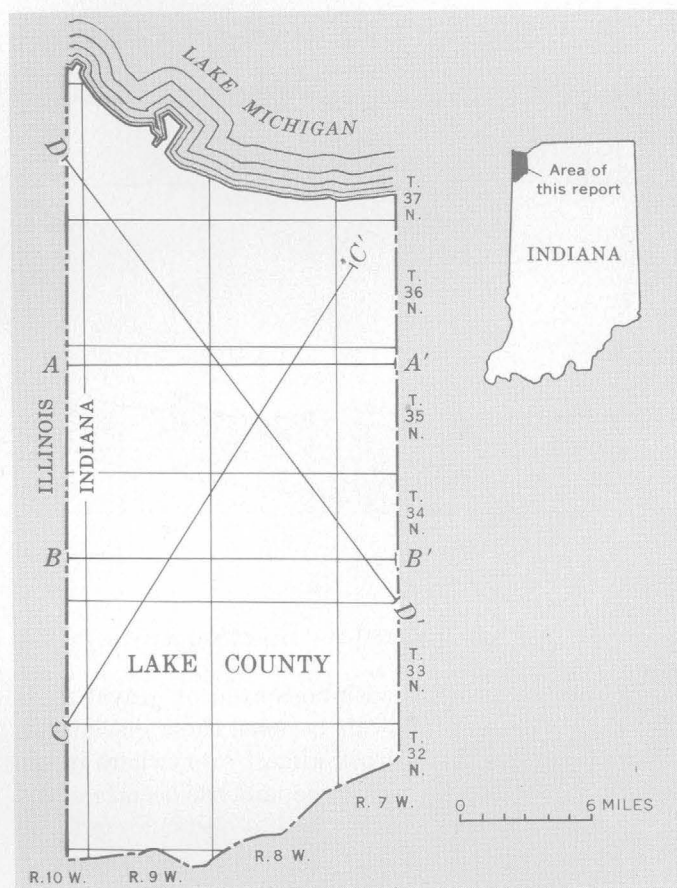


FIGURE 157.1.—Index map showing lines of sections (fig. 157.2), Lake County.

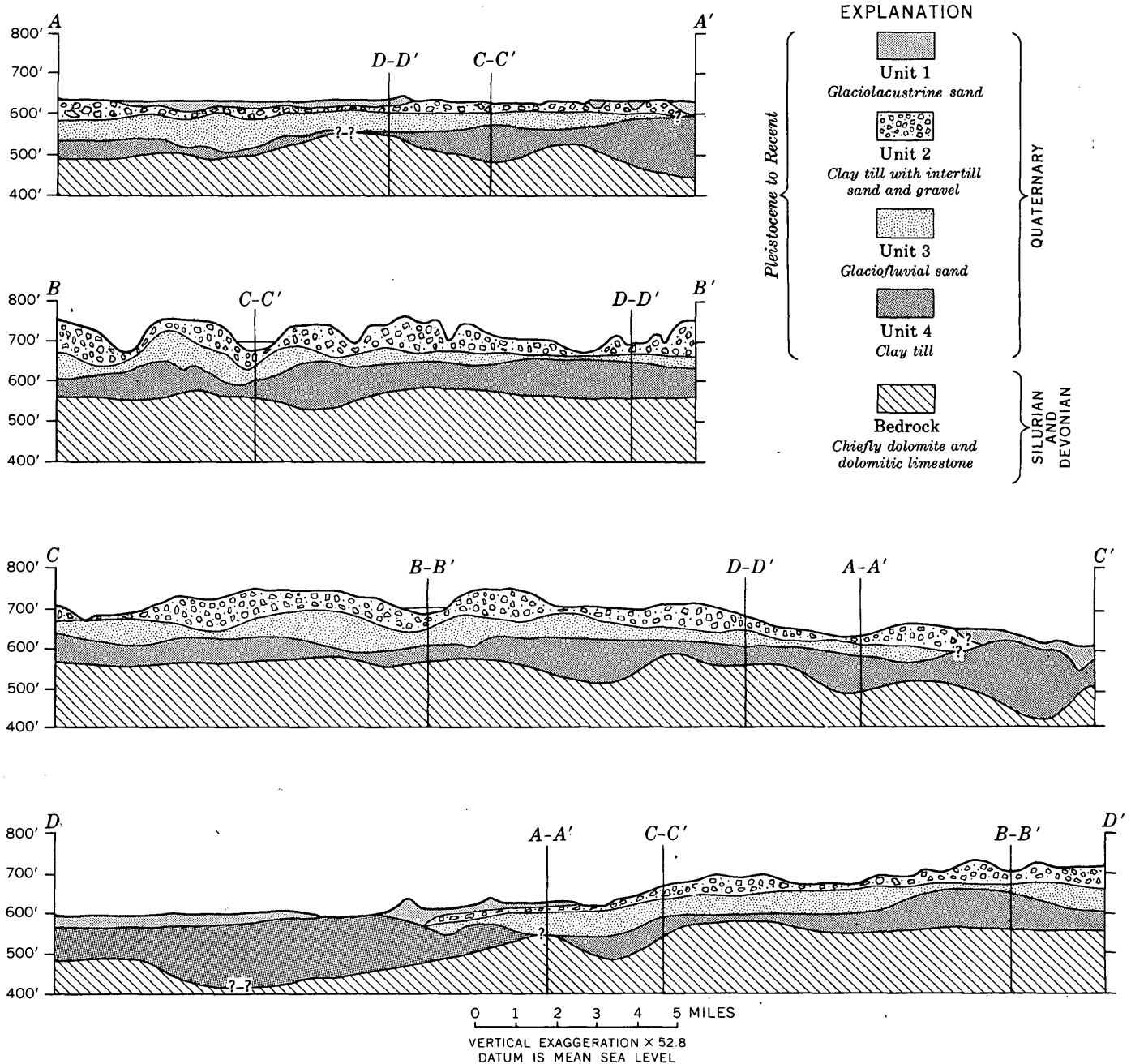


FIGURE 157.2.—Generalized sections showing lithologic units in glacial drift of Lake County.

eral relatively thin discontinuous sand or gravel zones that may represent intervals between these glaciations. The till mantles the bedrock almost everywhere in the county, except locally where the unit has been removed by postdepositional erosion, and it rests disconformably upon rocks of Silurian, Devonian, and Mississippian(?) ages. Locally in the northern part of the county the basal part of the unit consists of relatively thin sand or gravel. This sand or gravel partly fills the deeper parts of several preglacial valleys whose

streams flowed northeastward toward the area underlying Lake Michigan.

Unit 4 is overlain disconformably in the southern two-thirds of the county by an extensive glaciofluvial deposit, tentatively designated unit 3, that is primarily of Illinoian age. Unit 3 consists chiefly of sand with some interbeds of sand and gravel, and very locally of thick clay. The unit ranges in thickness from 0 to 100 feet and underlies about 370 square miles of the county. It is thickest along its northern edge (fig.

157.2, sections *A-A'* and *D-D'*) and in the western part of the county (fig. 157.2, sections *A-A'* through *D-D'*) where locally it thickens toward Illinois (fig. 157.2, section *B-B'*). Postdepositional erosion has removed part of the unit in the western half of the county. The erosion accounts for the marked thickening and thinning of the unit here in relatively short lateral distances. This erosion took place during Sangamon time when several interglacial streams, which flowed northward and westward into Illinois, cut deeply into the unit.

The former stream system has somewhat influenced the topography of the present land surface. Several lakes occupy elongate depressions that coincide with these Sangamon interglacial valleys.

In the broad sandy plain in the southern quarter of the county, unit 3 grades upward into glaciofluvial and associated windblown sand that ranges in age from late Wisconsin to Recent. This younger sand, generally less than 10 feet thick, forms the upper part of unit 3. It is somewhat silty and clayey and is locally interbedded with layers of organically rich silt and clay of relatively small areal extent.

Unit 3 is overlain by a mantle of till that extends to the surface and forms the terminal and ground moraines of the Valparaiso morainic system. This surface expression is somewhat influenced by the topography of the underlying deposits of pre-Wisconsin age. The till, tentatively designated as unit 2, ranges in thickness from 0 to about 100 feet and in age from early to late Wisconsin. The unit underlies about 300 square miles in the central three-quarters of the county. It consists of a lower till member of early(?) Wisconsin age, a relatively thin intertill sand and gravel member, and an upper till member of late Wisconsin age. This sequence in part has been recognized by R. J. Vig (written communication, 1959). The lower till member is gray to bluish-gray pebbly, sandy clay that is locally hard. It ranges in thickness from 0 to about 80 feet, and contains discontinuous lenses of sand and gravel of small areal extent. The lower till

member is overlain by a relatively thin sand and gravel member that is not present throughout the county but where present separates the upper till member from the lower till member. The upper till member is buff, yellow, or brown somewhat sandy, silty clay that ranges in thickness from 0 to about 60 feet and is late Wisconsin in age. This till is exposed at the surface in many parts of the county and comprises the surface material of the Valparaiso morainic system.

Unit 2 is overlain along its northern edge by glacio-lacustrine sand, silt, and clay, that is herein tentatively designated unit 1. Unit 1 consists chiefly of fine to medium sand that is interbedded with zones of beach gravel, silt, and clay, all of which are locally organically rich. Along the eastern edge of the county the unit consists of alternating layers of thinly laminated silt and clay as much as 30 feet thick. Unit 1 was deposited on units 2 and 4 upon a surface that sloped gently, about 10 feet per mile, toward Lake Michigan.

Unit 1 ranges in thickness from 0 to about 70 feet. It underlies about 140 square miles of the county. The deposit is of late Wisconsin to Recent age and marks the transition period in the glacial history of Lake County between the formation of glacial Lake Chicago and the formation of Lake Michigan.

REFERENCES

- Leverett, Frank, and Taylor, F. B., 1915, *The Pleistocene of Indiana and Michigan and the history of the Great Lakes*: U.S. Geol. Survey Mon. 53, 529 p.
- Rosenshein, J. S., 1961, *Ground-water resources of northwestern Indiana, preliminary report—Lake County*: Indiana Dept. Conserv., Div. Water Resources Bull. 10, 229 p.
- Wayne, W. J., 1956, *Thickness of drift and bedrock physiography of Indiana north of the Wisconsin glacial boundary*: Indiana Dept. Conserv., Geol. Survey Prog. Rept. 7, 70 p.
- , 1958, *Glacial geology of Indiana*: Indiana Dept. Conserv., Geol. Survey Atlas Mineral Resources Map 10.
- Zumberge, J. H., 1960, *Correlation of Wisconsin drifts in Illinois, Indiana, Michigan, and Ohio*: Geol. Soc. America Bull., v. 71, no. 8, p. 1,177–1,188.

158. GEOLOGY OF THE VERMILION END MORAINE, NETT LAKE INDIAN RESERVATION, MINNESOTA

By RALPH F. NORVITCH, St. Paul, Minn.

Work done in cooperation with the U.S. Department of Health, Education, and Welfare

Recent geologic mapping of glacial deposits on the Nett Lake Indian Reservation, 35 miles south of Rainy Lake in northernmost Minnesota, indicates that the St. Louis sublobe of the Keewatin ice sheet did not completely override the Vermilion end moraine as previously supposed, and that wave erosion by glacial Lake Agassiz locally washed out and reworked parts of the Vermilion moraine.

The segment of the Vermilion end moraine that traverses the Nett Lake Indian Reservation forms a prominent ridge where it crosses the eastern boundary of the reservation at an altitude of more than 1,500 feet; it reaches a peak altitude greater than 1,550 feet in secs. 1 and 2, T. 64 N., R. 22 W. From this peak it diminishes in altitude westward and merges with the surrounding lake plain at an altitude of about 1,350 feet in the west-central part of the reservation.

End-moraine deposits are missing in a gap about $3\frac{1}{2}$ miles wide in the southeastern part of T. 65 N., R. 23 W. Evidently, the moraine was eroded away by wave action of glacial Lake Agassiz at the 1,360-foot stage. The moraine can be traced northwestward from sec. 16, T. 65 N., R. 23 W., where it forms a subdued ridge trending northwestward to the boundary of the reservation (see fig. 158.1).

The Vermilion end moraine was probably formed during a readvance of the Rainy ice lobe in late Cary time (Wright, 1956, p. 19). Immediately south of the shallow body of water forming Nett Lake, the highest part of the moraine consists largely of sand and some gravel but contains many huge boulders derived from local bedrock. Except for their erratic positions many of the boulders might be interpreted as bedrock outcrops. Although drill-hole evidence is

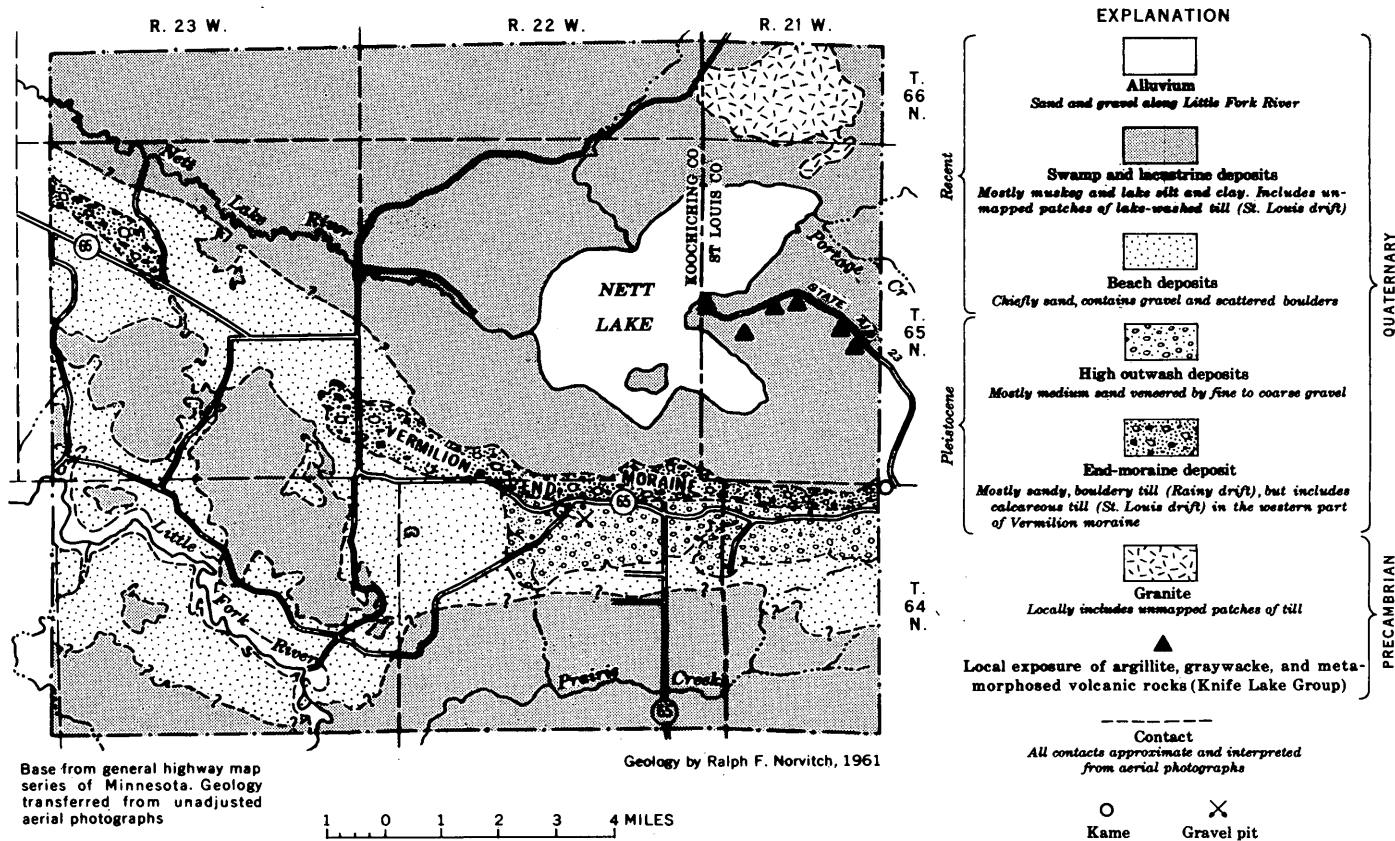


FIGURE 158.1.—Surficial geology of the Nett Lake Indian Reservation.

Surficial deposits of the Nett Lake Indian Reservation, Minn.

Era	Period	Epoch	Glaciation	Stade	Unit	Description	Topographic situation
Cenozoic	Quaternary	Recent			Swamp and lacustrine deposits and alluvium.	Swamp deposits consist of silty clay and peat, range in thickness from 0 to 7 feet, cap laustrine clay and St. Louis till. Alluvial deposits consist of sand and silt.	Covers most of low-lying area. Alluvial deposits are along Little Fork River.
					Beach deposits	Mainly well-sorted sand but contain some boulders. Formed along shore of glacial Lake Agassiz at 1,360-foot stage.	Sandy slopes near Vermilion moraine.
		Pleistocene	Wisconsin	Mankato	St. Louis drift	Mostly gray to buff pebbly calcareous clay till that contains abundant shale and limestone pebbles. Till has been washed by a glacial lake in low areas.	Thinly mantles western part of Vermilion moraine up to 1,400 feet and occurs as isolated patches of ground moraine in low areas.
				Cary	High outwash	Mostly medium-grained sand veneered by gravel, presumably deposited in front of Vermilion moraine.	Flanks southern margin of Vermilion moraine in southeastern part of reservation above 1,400 feet altitude.
					Rainy drift	Sandy, bouldery till; includes fragments of metamorphic, igneous, and sedimentary rocks.	Forms Vermilion moraine. Altitude ranges from 1,350 to 1,550 feet.
					Knife Lake Group.	Dark dense argillite, slate, and granite.	Forms isolated knobs near Vermilion moraine and low ridges in north-eastern part of reservation.
Precambrian							

not available, the prominence of the morainal ridge in this vicinity is interpreted as the result of accumulation on a bedrock high.

According to Leverett (1932, p. 56), the Vermilion end moraine in this area was thinly coated by drift deposited by the St. Louis sublobe of the Keewatin ice sheet in Mankato time. However, the author was not able to find St. Louis drift above an altitude of 1,400 feet on the Vermilion moraine. The drift of the St. Louis sublobe contains abundant limestone and shale pebbles, whereas drift of the Rainy lobe, which forms the bulk of the Vermilion end moraine, contains some limestone pebbles but no shale. The Rainy drift is predominantly a sandy, bouldery till derived from coarsely crystalline igneous rocks, whereas the St. Louis drift consists largely of gray (buff where oxidized) pebbly calcareous lake-washed clay till. A high kame in the NW $\frac{1}{4}$ sec. 3, T. 64 N., R. 22 W., consisting mostly of Rainy lobe material and containing limestone but no shale, occurs at an altitude of nearly 1,450 feet. In contrast, a lower kame at about 1,400 feet, in the SW $\frac{1}{4}$ sec. 34, T. 65 N., R. 21 W., about a quarter of a mile east of the reservation boundary, contains a high percentage of limestone and shale pebbles definitely deposited by the St. Louis sublobe. The absence of shale fragments above 1,400 feet suggests that St. Louis sublobe drift was not de-

posited above this altitude. Although overriding of the western part of the Vermilion moraine in the Nett Lake area by ice of the St. Louis sublobe probably contributed, in part, to subsequent erosion of that part of the moraine by lake washing, the St. Louis sublobe probably did not override the Vermilion moraine in the central and eastern parts of the area.

The number and size of the boulders in the Vermilion end moraine decrease eastward and westward from the highest part of the moraine. Many boulders lie on the surface as if deposited from ice rafts; however, they are aligned parallel to the trend of the end moraine and lie at different altitudes. Boulders probably were concentrated in the gap, where the Vermilion moraine is missing, by removal of the finer materials of the moraine deposits by wave action of glacial Lake Agassiz. The lake covered a large part of the Nett Lake Reservation up to altitudes of nearly 1,360 feet (Leverett, p. 133 and pl. 1). Leverett refers to a higher beach encircling the prominent ridge south of Nett Lake, but the author was unable to find evidence of a higher beach. A high-level deposit of outwash, which might be interpreted as beach material, occurs above a 1,400-foot altitude immediately south of the Vermilion end moraine in the eastern half of the area. Although the central part of this body of outwash consists largely of medium sand, it probably

was not deposited by Lake Agassiz because it is at an altitude of 1,400 feet, well above any known Lake Agassiz shoreline. The age of this high-level outwash deposit is probably late Cary, the same as that of the Vermilion moraine.

Further evidence that the moraine has been lake washed is an extensive body of lake or beach sand in the west-central part of the area presumably derived from reworking of morainal deposits in the area now occupied by the gap. A less extensive body of lacustrine sand flanks the outwash deposit south of

the eastern part of the Vermilion moraine. Apparently the lake surface was not high enough to erode the sand from the outwash.

REFERENCES

- Leverett, Frank, 1932, Quaternary geology of Minnesota and parts of adjacent States: U.S. Geol. Survey Prof. Paper 161, 149 p., 5 pl.
 Wright, H. E., Jr., 1956, Sequence of glaciation in eastern Minnesota, field trip no. 3, in Geol. Soc. America Guidebook Series: Minneapolis meeting, p. 1-24.



159. THREE PRE-BULL LAKE TILLS IN THE WIND RIVER MOUNTAINS, WYOMING

By GERALD M. RICHMOND, Denver, Colo.

The sequence of Pleistocene glaciations in the Wind River Mountains of Wyoming as defined by Blackwelder (1915) consisted of three "glacial stages," from oldest to youngest, the Buffalo, Bull Lake, and Pinedale. Because of the clarity of Blackwelder's original descriptions, these units, here called glaciations in conformity with the code of the American Commission on Stratigraphic Nomenclature (1961), have long served as a standard sequence for correlation in Wyoming (Fryxell, 1930, Bradley, 1936; Horberg, 1940) and the terms Bull Lake and Pinedale are receiving increasing recognition as such throughout the Rocky Mountain region (Horberg, 1954; Richmond, 1954, 1960a). Some subdivision of the units has resulted from later studies and it is the purpose of this article to show that, at least locally, three glaciations are represented by deposits called the Buffalo Till.

Deposits of the younger glaciations may be briefly summarized. Those of the Pinedale Glaciations include three sets of moraines and related outwash terraces (Richmond, 1948; Holmes, 1951; Holmes and Moss, 1955) on the basis of which an early, a middle, and a late stade of the Pinedale Glaciation have been inferred (Richmond, 1960a, 1960b, 1961). In some areas, a humic or weakly oxidized soil stratigraphically separates deposits of the early and middle stades.

Deposits of the Bull Lake Glaciation include two sets of moraines and associated outwash terraces on the basis of which an early and a late stade of the Bull Lake Glaciation have been inferred, (Fryxell,

1930; Richmond, 1948, 1960a; Holmes, 1951; Blackwelder, 1950; Holmes and Moss, 1955). The fact that in the La Sal Mountains, Utah, and in Glacier National Park, Mont., a maturely developed zonal soil stratigraphically separates deposits of the early stade from those of the late (Richmond, 1960a), and that near desiccation of Lake Bonneville occurred during the soil-forming interval (Morrison, 1961; Richmond, 1961) suggests that the two stades represent two distinct glaciations.

Deposits called Buffalo Till in the Wind River Mountains tend to lie above or beyond the outer limits of younger tills. Some are extensive, but others are small patches or merely a zone of erratic boulders. Most are sheetlike deposits capping interstream divides, 200 to more than 1,000 feet above trunk streams, which has led many writers to conclude that they are older than the canyons. However, the fact that some deposits of the Buffalo Till occur at or near stream level and are separated from the deposits on the divides by erosion of the canyons (Holmes and Moss, 1955; Richmond, 1957) suggests, as Blackwelder (1915) thought possible, that the Buffalo Till may represent more than one glaciation.

In general, the deposits lack morainal form, but some, especially those in the valleys, display large, smooth, mature moraines. Along the mountain front, the till is related to 2 and in places 3 outwash gravel terraces, a further suggestion of multiple glaciation.

The till is commonly compact and consists of unsorted and unsized angular to subangular pebbles to boulders in a sandy to silty arkosic matrix. It contains more silt and clay than do younger tills. The contained rock fragments are mostly crystalline, both fresh and decomposed. The granite weathering ratio, according to Blackwelder (1931), is 0-30-70. However, the writer believes that most of the rotted material, including the arkosic grus in the matrix, is derived secondarily either from deeply rotted crystalline rocks underlying the high Tertiary erosion surfaces of the range, or from the abundant deeply decomposed crystalline boulders in conglomerate of Tertiary age that flanks the range.

Surface exposures of the till are commonly weathered to a thick very strongly developed soil. In its pedalfers facies, the upper part of the B horizon of the soil is a reddish (2.5YR-7.5YR) residual leached clay in which most crystalline rocks tend to be deeply decomposed. The lower part of the B horizon is similar but yellowish brown (7.5YR-10YR) and contains less altered rock. In the pedocal facies of the soil, the B horizon rests on a thick Cca horizon intensively enriched in calcium carbonate. These soils, however, are commonly so stripped by erosion that only the lower part of the B horizon or merely remnants of the Cca horizon are preserved.

Superimposed tills, included in deposits called the Buffalo Till (Blackwelder, 1915), were found by the writer on the northeast flank of the Wind River Mountains at Bull Lake and at Dinwoody Lake (fig. 159.1). On the north side of Bull Lake, the escarpment of Cedar Ridge exposes three lithologically distinct tills, separated by disconformities and, locally, by the eroded remnants of soils. The deposits are

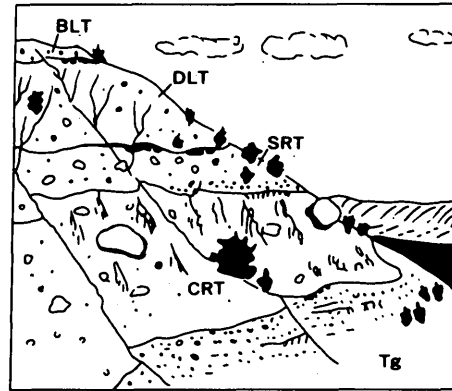


FIGURE 159.2.—Part of the south side of Cedar Ridge at Bull Lake. BLT, Bull Lake Till (30-40 ft thick); DLT, Dinwoody Lake Till (60-70 ft thick); SRT, Sacagawea Ridge Till (20 ft thick); CRT, Cedar Ridge Till (40-50 ft thick); Tg, conglomerate of Tertiary age.

overlain disconformably by the Bull Lake Till, here in its type area, and rest on an erosion surface cut across gently tilted conglomerate of Tertiary age (fig. 159.2). On the north side of Upper Dinwoody Lake, in the escarpment of Sacagawea Ridge, the middle and upper of the three tills are also exposed beneath the Bull Lake Till and above the conglomerate of Tertiary age. The conspicuous lithologic characteristics of the tills assure correlation between the two localities. Detailed stratigraphic sections of these exposures are given below.

The oldest of the three tills is here named the Cedar Ridge Till from Cedar Ridge on the north side of Bull Lake. The middle till is named the Sacagawea Till from Sacagawea Ridge on the north side of Upper Dinwoody Lake, and the youngest till is named the Dinwoody Lake Till.

No specific correlation of any one of the three tills could be established with the Buffalo Till in its type area on the North Fork of the Snake River (Blackwelder, 1915) where, unfortunately, the overlying Bull Lake Till is so extensive that typical deposits of the Buffalo Till are rarely exposed.

Section in the escarpment of Cedar Ridge on the north side of Bull Lake, center sec. 31, T. 3 N., R. 3 W.

[Locality 1, fig. 159.1]

Pinedale Till:

Stripped surface soil, light-brown (7.5YR 4/4); loose stony, silty fine sand; thin calcareous coatings on stones.....

Thick-
ness
(feet)

1-2

Till, light-gray (10YR 7/2); loose, stony, silty sand. Stones subangular to angular, range from pebbles to boulders, a few soled, faceted, or striated; most of fresh crystalline rock, but some of sedimentary rock. mostly limestone.....

15-20

Disconformity.

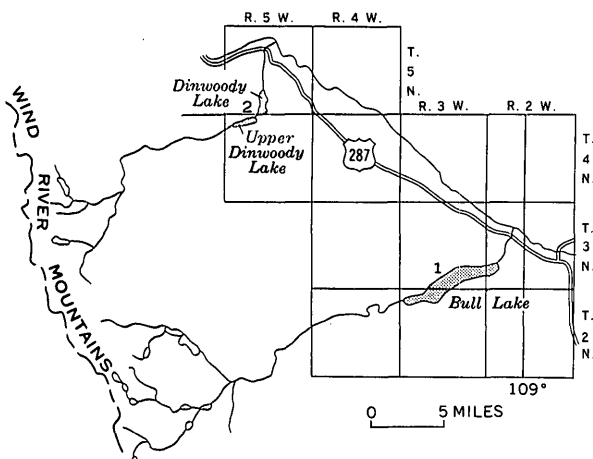


FIGURE 159.1.—Sketch map showing location of Bull Lake and Dinwoody Lake, on the northeast side of the Wind River Mountains, and location of stratigraphic sections described in text.

Section in the escarpment of Cedar Ridge on the north side of Bull Lake, center sec. 31, T. 3 N., R. 3 W.—Continued

[Locality 1, fig. 159.1]

Bull Lake Till:

Till, brown (7.5YR 4/4–6/4) to light-olive-brown (2.5Y 5/4); compact, stony, silty sand. Resembles Pine-dale Till except in color, hardness, and weathering, and has more large boulders..... 30–40

Disconformity.

Dinwoody Lake Till:

Till, light-brown (7.5YR 6/4) to light-yellowish-brown (10YR 6/4); compact, massive, stony silty sand, very bouldery. Matrix has distinctive pinkish hue owing to silt derived from Mesozoic red beds. A few stones soled, faceted, or striated. About half of rock material crystalline, about half sedimentary. Layers of pinkish bedded silt and local lenses of angular gravel and sand at base..... 60–70

Disconformity.

Sacagawea Ridge Till:

Stripped B horizon of soil, reddish-brown (5YR 5/4); compact, stony, sandy, clayey silt; structureless. Till, pale-brown (10YR 6/3) to light-yellowish-brown (10YR 6/4); compact, massive, stony sandy silt. Stones angular to rounded, range from pebbles to boulders; a few soled, faceted, or striated; most of crystalline rock, in part fresh, in part stained brown and decomposed. Latter are rounded and appear to be derived from underlying conglomerate of Tertiary age. A few stones of hard or crumbly limestone and sandstone and a very few of dark porphyritic volcanic rock. Thin layers of pinkish silt in lower part derived from Mesozoic redbeds..... 20

Sand and gravel; beds of medium-grained gray, pepper and salt sand and clean fine sand, 2 to 3 feet thick, overlying angular pebble and cobble gravel of crystalline rock in an arkosic sandy matrix..... 10

Disconformity.

Cedar Ridge Till:

Stripped soil, B horizon, yellowish-brown (10YR 5/4); compact, stony, sandy, clayey till; structureless, weakly calcareous; locally developed on lenses of sandy angular gravel at top of till..... 0–1.3

Cca horizon, very-pale-brown (10YR 7/4); compact, stony, sandy silt; strongly impregnated with calcium carbonate, strong platy structure. Like B horizon, locally developed on lenses of sandy angular gravel at top of till..... 0–3

Till, light-brownish-gray (10YR 6/2); massive, unsorted, compact, stony, silty sand; contains a few huge boulders; local lenses of angular gravel as thick as 15 ft at top. Stones like those in overlying tills but most fresh crystalline rock..... 40–50

Disconformity.

Soil, B horizon, light-brown (7.5YR 6/4); massive, clayey silt; partly leached; probably loess or colluvium (only locally preserved). Carbonate extends down fractures and around cobbles in underlying conglomerate to depth of 5–6 ft..... 0–2

Angular unconformity.

Conglomerate of Tertiary age:

Cobbles and boulders of crystalline rock in a matrix of arkosic sand; compact, crudely bedded. Material stained brown and many stones decomposed..... 150–200

Section in escarpment of Sacagawea Ridge on the north side of Upper Dinwoody Lake; center, sec. 31, T. 5 N., R. 5 W.

[Locality 2, fig. 159.1]

Stripped surface soil, B horizon, brown (7.5YR 4/4); loose, silty fine sand, eolian..... 1/2–1

Bull Lake Till:

Soil, Cca horizon, light-brown (7.5YR 6/4); stony, silty sand. Calcareous coatings on cobbles and boulders..... 1–2

Till, yellowish-brown (10.5YR 5/4); locally light olive brown (2.5YR 5/4); compact, friable, silty sand and unsorted, unsized subangular to angular pebbles to boulders. Numerous large boulders. Most stones fresh crystalline rock, but some decomposed and some sedimentary rock, mostly limestone. A few soled, faceted, or striated..... 15–40

Disconformity.

Dinwoody Lake Till:

Soil, B horizon, dark-brown (7.5YR 4/4); stony, clayey silt, structureless..... 2–3

Till, light-brown (7.5YR 6/4) to light-yellowish-brown (10YR 6/4); compact, stony, silty sand. Has distinct pinkish cast owing to fine silt derived from Mesozoic red beds. Fewer boulders than Bull Lake Till. Stones are angular to subangular; a few striated; most of fresh crystalline rock, but some of sedimentary rock, mostly limestone. A few rounded boulders of brown decomposed crystalline rock derived from nearby conglomerate of Tertiary age..... 30–40

Silt and fine gravel, bedded, probably outwash..... 15–20

Disconformity.

Sacagawea Ridge Till:

Stripped soil, Cca horizon, yellowish-brown (10YR 5/6); stony, sandy silt. Calcareous coatings along fractures and around stones. Rocks in till immediately beneath zone of fractures are crumbly..... 5–6

Till, pale-brown to light-yellowish-brown (10YR 6/3–6/4); compact, stony, silty sand. Stones mostly crystalline rock; high proportion rounded boulders of brown decomposed granitic rock derived from nearby conglomerate of Tertiary age. A few are sedimentary rock and a very few pebbles are dark dense porphyritic volcanic rock..... 50–60

Quartz sand and arkosic sand; clean, bedded, probably outwash..... 10–15

Angular unconformity.

Conglomerate of Tertiary age:

Cobbles and boulders rounded to subrounded, of crystalline rock in arkosic sandy matrix. Material stained brown and most cobbles and boulders deeply decomposed. Deposit crudely bedded..... ±200

The tills in the above sections vary somewhat in thickness along the escarpments. On Cedar Ridge, the Dinwoody Lake Till is in places more than 100 feet thick. The soils are not continuous horizons, but are preserved locally along intertill contacts and are so stripped by erosion that only their lower parts remain. Thus the colors are not as red nor is the material as clayey as that of the upper part of more fully preserved pre-Bull Lake soils in the area.

On the southeast side of Bull Lake, the Dinwoody Lake Till forms a broad, smooth moraine which extends eastward into outwash gravel on a terrace above and beyond the moraines of the Bull Lake Glaciation and about 360 feet above the Wind River. In the same area, the Saçagawea Ridge Till and the Cedar Ridge Till come to the surface and extend into outwash gravel on still higher terraces, 520 and 660 feet respectively, above the Wind River (fig. 159.2).

A hypothesis for the erosional history in the Wind River Mountains in pre-Bull Lake time is suggested by the distinctive lithologic differences of the three tills and their relation to terraces. Prior to glaciation, the conglomerate of Tertiary age completely covered the Mesozoic red beds and was itself cut by a pedimentlike erosion surface on which a soil had at least locally developed.

The Cedar Ridge Till, consisting predominantly of fresh crystalline rocks, was obviously derived from the interior of the range rather than from the conglomerate on which it was deposited. The erosion surface on the conglomerate, over which the ice advanced, is about 1,000 feet above the present canyon floor at the mountain front, and the associated outwash-gravel terrace lies about 660 feet above the Wind River.

The composition of the Saçagawea Ridge Till, a mixture of fresh crystalline detritus, abundant rounded brownish-stained decomposed crystalline boulders from the conglomerate of Tertiary age, and small amounts of Paleozoic and Mesozoic sedimentary rock, suggests that the ice was advancing in a valley cut in the conglomerate of Tertiary age beneath which Mesozoic sedimentary rocks were locally exposed. The top of the Mesozoic rocks is about 200 feet below the older pediment on the conglomerate and about 800 feet above the canyon floor; the outwash terrace associated with the Saçagawea Ridge Till is about 150 feet below that associated with the Cedar Ridge Till and 510 feet above the Wind River. The valley down which the ice advanced in Saçagawea Ridge time was therefore about 200 feet deep at the mountain front and 150 feet deep in the basin.

The composition of the Dinwoody Lake Till, predominantly a pink silty sand containing abundant fresh crystalline and sedimentary rock, but little material from the conglomerate of Tertiary age, suggests that the ice advanced down a canyon cut well into the Mesozoic red beds from which its pinkish color is derived. At its maximum, the ice filled the canyon, overflowing the conglomerate of Tertiary age and

overlying tills to form a lateral moraine on the canyon rim. The fact that along the Wind River the outwash terrace associated with the Dinwoody Lake Till is 360 feet above the river, whereas that associated with the Bull Lake Till is only 150 to 200 feet above, suggests that the floor of the canyon down which the ice advanced in Dinwoody Lake time may have been about 500 feet below the pediment and 400 to 500 feet above the present canyon floor at the mountain front.

The Cedar Ridge Till, the Saçagawea Ridge Till, and the Dinwoody Lake Till are believed to be equivalent to three pre-Bull Lake, "pre-Wisconsin" tills having similar topographic and stratigraphic settings in the La Sal Mountains, Utah, and in Glacier National Park, Mont. (Richmond, 1957). They may also be equivalent to the Rocky Flats Alluvium (oldest), Verdos Alluvium, and Slocum Alluvium of the Denver Basin, which in turn are correlated with the Nebraskan, Kansan, and Illinoian Glaciations of the midcontinent region (Scott, 1960). However, for purposes of correlation in the Rocky Mountain region, the terms Cedar Ridge Glaciation, Saçagawea Ridge Glaciation, and Dinwoody Lake Glaciation are proposed from the type localities of their respective tills.

REFERENCES

- American Commission on Stratigraphic Nomenclature, 1961, Code of stratigraphic nomenclature: Am. Assoc. Petroleum Geologists Bull., v. 45, p. 645-665.
- Blackwelder, Elliot, 1915, Post-Cretaceous history of the mountains of central western Wyoming: Jour. Geology, v. 23, p. 97-117, 193-217, 307-340.
- 1931, Pleistocene glaciation in the Sierra Nevada and Basin Range: Geol. Soc. America Bull., v. 42, p. 865-922.
- 1950, Pleistocene geology of the Green River Basin, Wyoming: Wyoming Geol. Assoc. 5th Ann. Field Conf., Southwestern Wyoming: Casper, Wyo., 196 p.
- Bradley, W. H., 1936, Geomorphology of the north flank of the Uinta Mountains: U.S. Geol. Survey Prof. Paper 185-I, 204 p.
- Fryxell, F. M., 1930, Glacial features of Jackson Hole, Wyoming: Augustana Library Pub. 13, 128 p.
- Holmes, G. W., 1951, The regional significance of the Pleistocene deposits in the Eden Valley, Wyoming, p. 93-100, in Moss, J. H., Early man in the Eden Valley: Univ. Pennsylvania Mus. Mon., 124 p.
- Holmes, G. W., and Moss, J. H., 1955, Pleistocene geology of the southwestern Wind River Mountains, Wyoming: Geol. Soc. America Bull., v. 66, p. 629-654.
- Horberg, Leland, 1940, Geomorphic problems and glacial geology of the Yellowstone Valley, Park County, Montana: Jour. Geology, v. 48, p. 275-303.
- 1954, Rocky Mountain and continental Pleistocene deposits in the Waterton region, Alberta, Canada: Geol. Soc. America Bull., v. 65, p. 1093-1150.

- Morrison, R. B., 1961, New evidence on the history of Lake Bonneville from an area south of Salt Lake City, Utah: Art. 333 in U.S. Geol. Survey Prof. Paper 424-D, p. D125-D127.
- Richmond, G. M., 1948, Modification of Blackwelder's sequence of Pleistocene glaciation in the Wind River Mountains, Wyoming [abs.]: Geol. Soc. America Bull., v. 59, p. 1400-1401.
- 1954, Modification of the glacial chronology of the San Juan Mountains, Colorado: Science, v. 119, p. 614-615.
- 1957, Three pre-Wisconsin glacial stages in the Rocky Mountain region: Geol. Soc. America Bull., v. 68, p. 239-262.
- 1960a, Glaciation of the east slope of Rocky Mountain National Park, Colorado: Geol. Soc. America Bull., v. 71, p. 1371-1382.
- 1960b, Correlation of Alpine and continental glacial deposits of Glacier National Park and adjacent High Plains, Montana: Art. 98 in U.S. Geol. Survey Prof. Paper 400-B, p. B223-B224.
- 1961, New evidence of the age of Lake Bonneville from moraines in Little Cottonwood Canyon, Utah: Art. 334 in U.S. Geol. Survey Prof. Paper 424-D, p. D127-D128.
- Scott, G. R., 1960, Subdivision of the Quaternary alluvium east of the Front Range near Denver, Colorado: Geol. Soc. America Bull., v. 71, p. 1541-1544.



160. FAULTED PLEISTOCENE STRATA NEAR JACKSON, NORTHWESTERN WYOMING

By J. D. LOVE and D. W. TAYLOR, Laramie, Wyo., and Washington, D.C.

Unique and structurally complex unnamed Quaternary units, 8 igneous and 13 sedimentary, are present near the town of Jackson. Two of the sedimentary units—one lacustrine and the other eolian—that contain mollusks in some abundance are discussed in this article. Both units are significant because (a) they indicate widely divergent environments of deposition; (b) they are cut by normal faults and, inasmuch as the younger unit contains shell material within the age range of carbon-14, they furnish data on timing, magnitude, and characteristics of localized Pleistocene and Recent faulting; (c) the mollusks provide correlation with similar assemblages elsewhere in the Western States; (d) the record of local and regional crustal instability is pertinent to major construction projects in the Jackson area.

LACUSTRINE SEQUENCE

Excavations between 1958 and 1961 at 3 localities north of Jackson (fig. 160.1, locs. 1, 2, 3) exposed 25-50 feet or more of olive-drab to gray claystone, siltstone, thin white concretionary marl beds, light-gray very soft fine- to coarse-grained sandstone, and brown andesitic grit and conglomerate. The andesitic debris consists of red and black deeply weathered angular fragments derived from directly adjacent flows of porphyritic andesite that comprise the youngest and locally the thickest (more than 1,100 feet) of the Quaternary igneous units in the area. Fossil mollusks characteristic of a lacustrine environment (Tay-

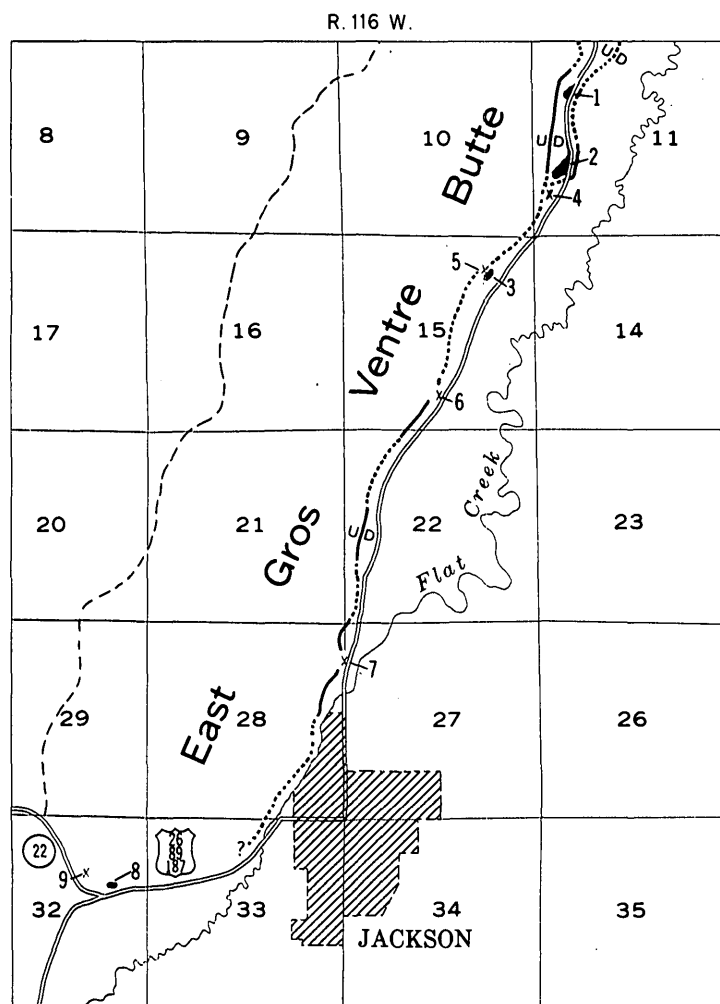
lor, 1960) are found in all but the coarsest lithologies (see table).

Occurrence, by localities, of fossil shells in the lacustrine sequence and in loess

[All localities (fig. 160.1) are in Teton County, Wyo. Geographic data are from U.S. Geol. Survey Grand Teton National Park map (1951), 1:62,500. Numbers in parentheses are U.S. Geol. Survey Cenozoic locality number, and collector's field number]

Species	Lacustrine sequence			Loess				
	1	2	3	4	5	6	7	9
Fresh-water clams:								
<i>Anodonta?</i> -----	×							
<i>Pisidium compressum</i> Prime--	?	×						
Fresh-water snails:								
<i>Valvata humeralis</i> Say-----		×						
<i>Valvata utahensis</i> Call-----	×	×						
<i>Carinifex newberryi</i> (Lea)-----	×	×	×					
Land snails:								
<i>Pupilla muscorum</i> (Linnaeus)---					×	×	×	×
<i>Vallonia cyclophorella</i> Sterki---					×	×	×	×
cf. <i>Succinea</i> -----					×	×	×	×
<i>Discus shimeki cockerelli</i> Pilsbry.					×		×	
<i>Oreohelix</i> -----				×				

- (22605; T61-38; L61-60A, unit 6); 1,000 feet east of west line and 1,400 feet south of north line of sec. 11, T. 41 N., R. 116 W.; road cut on west side of U.S. Highways 26, 89, 187.
- (22606; T61-51; L61-61); 900 feet east of west line and 2,000 feet north of south line of sec. 11, T. 41 N., R. 116 W.; road cut on west side of U.S. Highways 26, 89, 187.
- (22607; T61-48); 1,100 feet south of north line and 1,250 feet west of east line of sec. 15, T. 41 N., R. 116 W.; cut 100 feet west of the Old Wyoming Chuck Wagon Restaurant.
- (22608; T61-50; L61-63); 1,150 feet north of south line and 500 feet east of west line of sec. 11, T. 41 N., R. 116 W.; road cut on west side of U.S. Highways 26, 89, 187 at first turnout on west side of highway, south of bend.
- (22609; T61-49); same as locality 3, but shells are from loess overlying lacustrine sequence.
- (22610; L61-69); 800 feet north of south line and 2,650 feet west of east line of sec. 15, T. 41 N., R. 116 W.; road cut on west side of U.S. Highways 26, 89, 187.
- (22611; L61-226); 1,200 feet south along section line from NW cor. sec. 27, T. 41 N., R. 116 W.; road cut on west side of U.S. Highways 26, 89, 187.
- (22642 and 22643; L61-95A and B); 1,700 feet south of north line and 1,700 feet west of east line of sec. 32, T. 41 N., R. 116 W.; north wall of excavation for cement-mix plant.



EXPLANATION

- Contact
Dashed where approximately located
- High-angle fault
Dashed where approximately located; dotted where concealed
U, upthrown side; D, downthrown side
- Fossiliferous loess locality
- Outcrop of lacustrine sequence
- West margin of East Gros Ventre Butte

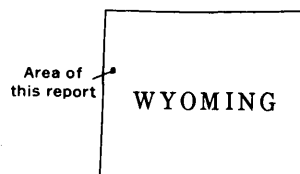
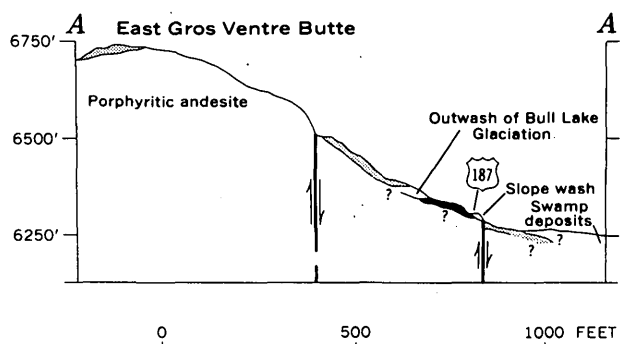
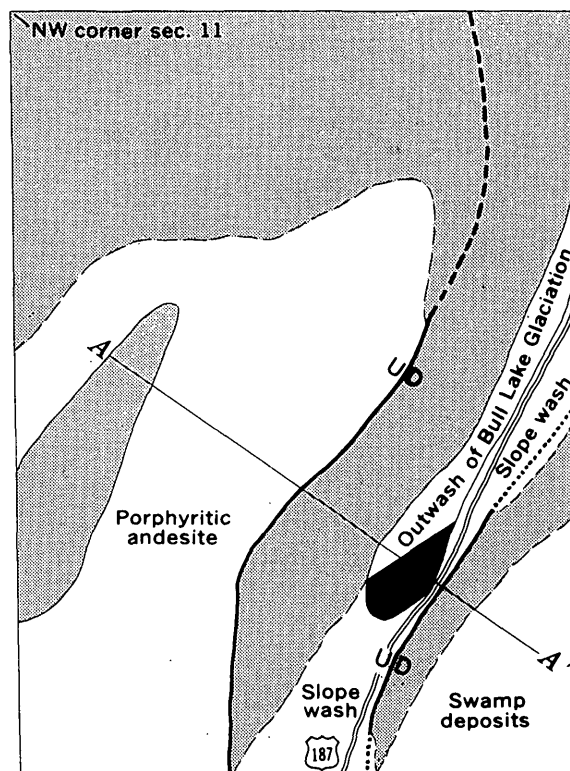


FIGURE 160.1.—Index map showing localities and features described in text, and geologic sketch map and section of Quaternary deposits and volcanic rocks at locality 1. Deposits of Recent age: slope wash and swamp deposits. Deposits of Pleistocene age: loess (stipple); outwash of Bull Lake Glaciation; lacustrine sequence (solid black); and porphyritic andesite.

In another excavation west of Jackson (fig. 160.1, loc. 8), the lacustrine sequence is composed of 17 feet of unfossiliferous dark-gray to brown soft plastic blocky claystone, light-tan soft fine-grained sandstone, and conglomerate. The conglomerate here contains fragments of gray basalt derived from an adjacent Quaternary igneous unit, 500 feet thick, and older than the andesite at localities 1, 2, and 3.

Regional relations indicate that the lacustrine sequence was deposited unconformably across the truncated edges of rocks ranging in age from Paleozoic to Quaternary. The sequence was faulted before the last pre-Bull Lake glaciation (possibly the Buffalo Glaciation, which is generally considered to be of pre-Wisconsin age).

The correlation of this lacustrine sequence with similar strata in other parts of Jackson Hole (Love, 1960, p. 212-213) has not been established. Therefore, the size and duration of the lake in which the strata accumulated are not known. Two species found in the lacustrine sequence (*Carinifex newberryi* and *Valvata humeralis*) live in Lake Tahoe, California-Nevada, at depths between 120 and 300 feet (Hanna and Smith, 1938). Lake Tahoe has an area of about 300 square miles, a maximum depth of 1,628 feet, and a mean depth of about 800 feet according to Hutchinson (1957). The former lake in Jackson Hole might have been of the same order of magnitude.

INTERPRETATION OF MOLLUSKS OF LACUSTRINE SEQUENCE

The lacustrine sequence is the only Pleistocene unit in Jackson Hole known to contain locally extinct species. The occurrence of *Valvata utahensis*, unknown elsewhere in Wyoming, is evidence of relative antiquity.

Association of *Carinifex newberryi* and *Valvata utahensis* has been recorded in a number of localities in Idaho and Utah (Taylor, 1960). The oldest occurrence known is in the American Falls area, southeastern Idaho (Trimble and Carr, 1961). There, *V. utahensis* is found in the fine-grained dominantly lacustrine Raft Formation. The overlying basal gravel of the American Falls Lake Beds containing *V. utahensis* and *Carinifex* records an episode of greatly increased flow in the Snake River. At this time, pebbles were transported long distances down a broad, low-gradient valley. The simplest interpretation (but not the only possible one) is that the lacustrine sequence near Jackson is correlative with part of the Raft Formation, and the pre-Bull Lake glaciation with the basal gravel of the American Falls Lake Beds. If this correlation is correct an Illinoian, or

Yarmouth and Illinoian, age for these events and deposits in Jackson Hole is most likely.

Of the five species of mollusks found in the lacustrine sequence (see table), *Valvata utahensis* and *Carinifex newberryi* live in either lakes or large slow-moving streams, whereas the other three may also live in small creeks only a few feet wide. Living and fossil occurrences of *V. utahensis* and *Carinifex* are discontinuous (Taylor, 1960); their presence in Jackson Hole implies the persistence of a suitable lacustrine habitat, perhaps continuing from Pliocene time. The subsequent local extinction of *V. utahensis* suggests that the pre-Bull Lake (possibly Buffalo) glaciation was the first, and perhaps the only time that Jackson Hole was largely filled with ice.

POST-BULL LAKE LOESS

Loess deposited during the interval between the Bull Lake and Pinedale Glaciations (medial and youngest of Pleistocene age in this region) covers large areas near Jackson (Fryxell, 1930). Average thickness is 10 to 20 feet, with maximum of about 50 feet. The loess consists of white to light-tan homogeneous massive soft porous silt, in places containing one or more secondary white calcareous layers. It overlies outwash of the Bull Lake Glaciation (figs. 160.2 and 160.3) with angular unconformity in some places and with apparent conformity in others. Elsewhere, the loess was deposited on a surface of considerable relief cut in older rocks. Figures 160.2 and 160.3 show the relations of the loess, outwash, and lacustrine sequences. One carbon-14 age determination

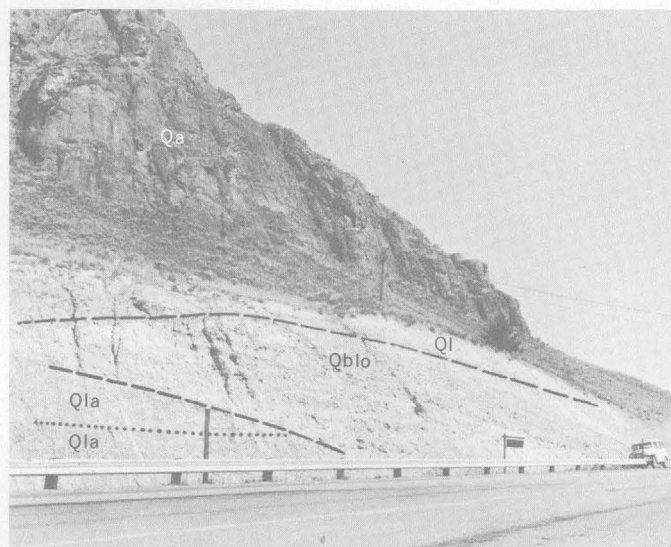


FIGURE 160.2.—Quaternary sequences at locality 1; fault scarp of porphyritic andesite (Qa); post-Bull Lake loess (Ql); tilted outwash of Bull Lake Glaciation (Qblo); lacustrine sequence (Qla), with dotted line marking main fossil zone.

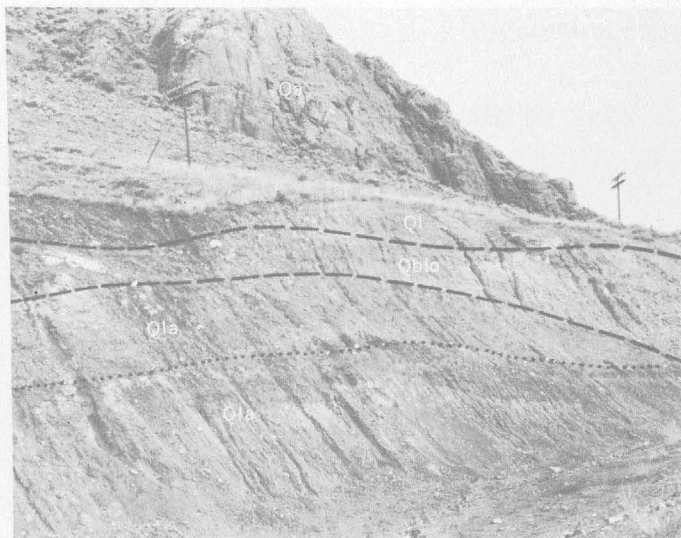


FIGURE 160.3—Lacustrine sequence (Qla) at locality 1, folded into gentle anticline delineated by main fossil zone (dotted line); photograph overlaps left margin of figure 160.2 and shows same units marked by same symbols.

suggests that the Bull Lake outwash may be about 27,000 years old (Love, 1956, p. 149). The loess contains land snails in most outcrops. Carbon-14 ages of $13,980 \pm 700$ (W-1078; loc. 6) and $15,300 \pm 500$ (W-1071; loc. 7) years have been determined from shell material (Meyer Rubin, written communication, 1962; measurement done in laboratory of U.S. Geol. Survey). The maximum development of the Pine-dale Glaciation in the central part of Jackson Hole may have been between 8,000 and 9,000 years ago (Love, 1956, p. 150).

STRUCTURE INVOLVING THE LACUSTRINE SEQUENCE AND LOESS

The lacustrine sequence was downdropped 300 feet or more along a normal fault (fig. 160.1) at the base of the porphyritic andesite cliff shown in figures 160.2 and 160.3. Most of this displacement was prior to Buffalo Glaciation. The downfaulted remnants of the lacustrine sequence were protected by the andesite and basalt cliffs at the time the Buffalo ice overrode and scoured East Gros Ventre Butte.

A second episode of normal faulting along a divergent and more extensive line of weakness occurred, in part at least, within the last 13,000–15,000 years, after the post-Bull Lake loess was deposited. During this episode, the valley of Flat Creek was down-dropped 200 feet or more along a high-angle fault on the east side of East Gros Ventre Butte (fig. 160.1). The freshness of some parts of the scarp suggests that, at least locally, movement continued into Recent time. Renewed movement likewise occurred during this episode along the fault that had previously downdropped the lacustrine sequence at locality 1.

Mild earthquakes are common in this area, but no severe ones have been recorded in the 75 years of continuous settlement. A comparison of similar Quaternary movements in the northern part of Jackson Hole with those associated with the Hebgen earthquake of 1959, 90 miles north of Jackson, has been presented elsewhere (Love, 1961). The Quaternary geologic history of this region suggests that additional crustal movements can be expected, and this probability is, therefore, pertinent to the planning, design, and location of major construction projects in the Jackson area.

REFERENCES

- Fryxell, F. M., 1930, Glacial features of Jackson Hole, Wyoming: Augustana Library Pubs. No. 13, 129 p.
- Hanna, G. D., and Smith, A. G., 1938, The mollusks of Lake Tahoe: Nautilus, v. 52, p. 34–36.
- Hutchinson, G. E., 1957, A treatise on limnology; v. 1, Geography, physics, and chemistry: New York, John Wiley and Sons, 1015 p.
- Love, J. D., 1956, Summary of geologic history of Teton County, Wyoming, during Late Cretaceous, Tertiary, and Quaternary times: Wyoming Geol. Assoc., Guidebook, 11th Ann. Field Conf., p. 140–150.
- 1960, Cenozoic sedimentation and crustal movement in Wyoming: Am. Jour. Science, v. 258–A, p. 204–214.
- 1961, Reconnaissance study of Quaternary faults in and south of Yellowstone National Park, Wyoming: Geol. Soc. America Bull., v. 72, p. 1749–1764.
- Taylor, D. W., 1960, Distribution of the freshwater clam *Pisidium ultramontanum*; a zoogeographic inquiry: Am. Jour. Science, v. 258–A, p. 325–334.
- Trimble, D. E., and Carr, W. J., 1961, Late Quaternary history of the Snake River in the American Falls region, Idaho: Geol. Soc. America Bull., v. 72, p. 1739–1748, 1 pl.



PALEONTOLOGY AND PALEOECOLOGY

161. LATE CRETACEOUS *DESMOSCAPHITES* RANGE ZONE IN THE WESTERN INTERIOR REGION

By W. A. COBBAN, Denver, Colo.

Ammonites belonging to the genus *Desmoscaphites* are widely distributed in the western interior of the conterminous United States. This widespread occurrence combined with its narrow stratigraphic range makes this genus an important and useful guide fossil. Reeside (1927a, distribution table) listed the known localities of the genus up through 1926. At that time only one species (*D. bassleri* Reeside) was known. Since then another species (*D. erdmanni* Cobban) has been described and several new localities for both species have been discovered. The purpose of the present paper is to point out the characteristic features of the genus and its species, draw attention to the more important associated fossils, verify the age determination, and bring up to date all that is known of the distribution of *Desmoscaphites*.

SCOPE OF THE GENUS

Reeside (1927a, p. 16) established the genus *Desmoscaphites* to include moderate-sized scaphitoid ammonites that have stout well-rounded whorls, small umbilicus, constrictions on the early juvenile whorls, numerous primary and secondary ribs on the adult body chamber, and suture with trifold first lateral lobe. To this definition the present writer adds that the primary ribs on the adult body chamber terminate in small ventrolateral nodes, the numerous secondary ribs on the body chamber are evenly spaced or almost evenly spaced where they cross the venter, and all the lobes of the suture are trifold or tend to be trifold.

Of the two described species of *Desmoscaphites*, the genotype, *D. bassleri* Reeside (1927a, p. 16, pl. 21, figs. 17-21; pl. 22, figs. 8-12) is characterized by numerous secondary ribs on the adult body chamber and these tend to cross the venter with even spacing. There are 6 to 9 secondaries to each primary rib on the body chamber. The slightly older species, *D. erdmanni* Cobban (1951a, p. 38, pl. 21, figs. 10-23), has 4 to 6 secondaries for each primary rib and, in addition, the secondary ribs are a little more widely spaced along the venter in the middle part of the adult body chamber than near the aperture.

IMPORTANT ASSOCIATED FOSSILS

In the western interior region the distinctive pelecypod *Inoceramus patootensis* de Loriol first appears in the *Desmoscaphites erdmanni* Range Zone and per-

sists up through the *D. bassleri* Range Zone and into the middle part of the *Scaphites hippocrepis* Range Zone. Likewise, *Scaphites leei* Reeside first appears with *D. erdmanni*, ranges up through the *D. bassleri* Range Zone, and persists into at least the lower part of the *S. hippocrepis* Range Zone. On the other hand *Clioscaphites novimexicanus* (Reeside) is a common associate of *D. erdmanni* but is unknown with *D. bassleri*, and the ammonite described by Reeside (1927a, p. 15, pl. 12, figs. 1-8) as *Puzosia* (*Latidorsella*) *mancosensis* is found with *D. bassleri* but not with the older *D. erdmanni*. *Baculites thomi* Reeside is the most common baculite associated with both *D. erdmanni* and *D. bassleri* but ranges up into slightly younger rocks. In the western interior, all the known occurrences of the free-swimming crinoids *Uintacrinus* and *Marsupites* seem to lie in the *Desmoscaphites* Range Zone and most may be with *D. bassleri*.

AGE

In terms of the standard stages of the Upper Cretaceous, Reeside (1927b, p. 28) originally assigned *Desmoscaphites bassleri* to the Santonian and later (1944) to the upper part of that zone. *Desmoscaphites erdmanni* also has been placed high in the Santonian (Cobban, 1951b, p. 2197; Cobban and Reeside, 1952, correlation chart). This late Santonian Age for both species of *Desmoscaphites* is suggested by the following factors: (1) *Uintacrinus* and *Marsupites*, which seem to be confined to the *Desmoscaphites* Range Zone, occur in Europe in the upper part of the Santonian (for example, Heinz, 1928, pl. 3), (2) *Scaphites hippocrepis* (DeKay), which occurs immediately above the *Desmoscaphites* Range Zone, is a well known guide fossil to the lower part of the Campanian Stage in Europe, and (3) *Inoceramus cordiformis* Sowerby, which is associated with *Clioscaphites vermiciformis* (Meek and Hayden) in rocks a little below those containing *Desmoscaphites erdmanni*, is considered of middle Santonian Age (for example, Seitz, 1956, p. 4, 5).

Scaphites hippocrepis was recorded with *D. bassleri* in the Telegraph Creek Member of the Cody Shale in south-central Montana (Reeside, 1927a, loc. 11208 in distribution table; also see Thom, and others, 1935, p. 56). The writer has not been able to locate the specimen or specimens on which this record was made.

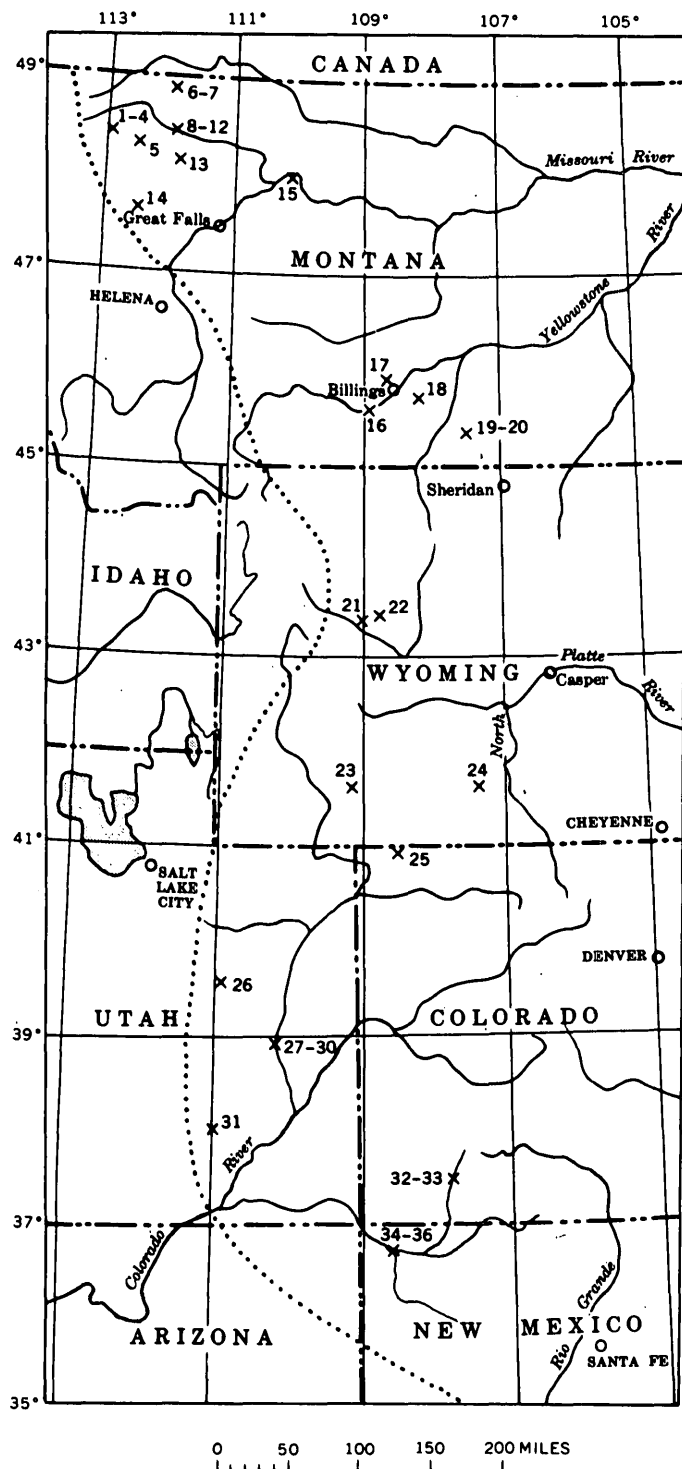


FIGURE 161.1.—Localities of Geological Survey collections of *Desmoscaphites*. Numbers refer to the description of localities in the table. Dotted line represents the approximate position of the shoreline during the age span of *Desmoscaphites* (the position of this line in Arizona and New Mexico is after Pike, 1947, fig. 7, line 7).

Inasmuch as *Scaphites leei*, which closely resembles small forms of *S. hippocrepis*, is the only scaphite associated with *D. bassleri* in the collections at hand, it probably is the scaphite from locality 11208.

DISTRIBUTION

Desmoscaphites is known from 36 Geological Survey Mesozoic localities in the western interior region (fig. 161.1). In addition the genus has been recorded from a few localities in southwestern Colorado and northwestern New Mexico by Pike (1947, p. 23, 26, 27, 43). Katich (1956, p. 118; 1959, p. 27) reports the genus in eastern Utah and western Colorado but does not give specific localities.

The Geological Survey localities and species of *Desmoscaphites* are given in the following list.

Localities at which *Desmoscaphites* was collected

No. on figure 161.1	Geological Survey Mesozoic locality	Fossil	Description, collector, and date
1----	7143	<i>Desmoscaphites bassleri</i> .	Top of ridge south of Lake Creek, about 2 miles east of Basin Mountain and 12 miles west of Browning (approximately in SW¼ sec. 8, T. 32 N., R. 13 W.), Glacier County, Mont. Virgelle Sandstone. T. W. Stanton and M. R. Campbell, 1911.
2----	21413	<i>Desmoscaphites</i> sp.	About 7 miles northwest of East Glacier, in NW¼NE¼ sec. 15, T. 32 N., R. 13 E., Glacier County, Mont. Virgelle Sandstone. C. E. Erdmann, 1955.
3----	24739	-----do-----	South Fork of Cut Bank Creek in NW¼SE¼ sec. 4, T. 32 N., R. 12 W., Glacier County, Mont. Virgelle Sandstone. F. E. Turner, 1953.
4----	D937	-----do-----	Southeast side of U.S. Highway 2 about 7 miles northeast of East Glacier, in SE¼SW¼NE¼ sec. 25, T. 32 N., R. 12 W., Glacier County, Mont. Virgelle Sandstone. B. R. Alto, 1956.
5----	7138	<i>Desmoscaphites bassleri</i> .	About 10 miles east of East Glacier, in NW¼ sec. 26, T. 31 N., R. 11 W., Glacier County, Mont. Virgelle Sandstone. T. W. Stanton and M. R. Campbell, 1911.

Localities at which *Desmoscaphites* was collected—Continued

No. on figure 161.1	Geological Survey Mesozoic locality	Fossil	Description, collector, and date
6----	20299	<i>Desmoscaphites erdmanni</i> .	5 miles northwest of Kevin, in NE¼NW¼ sec. 24, T. 35 N., R. 4 W., Toole County, Mont. Marias River Shale, 101 ft below top. C. E. Erdmann and others, 1956.
7----	21667	----do-----	5 miles northwest of Kevin, in NE¼NE¼NW¼ sec. 24, T. 35 N., R. 4 W., Toole County, Mont. Marias River Shale, 23 ft below top. C. E. Erdmann, R. W. Imlay, and J. B. Reeside, Jr., 1944.
8----	21419	----do-----	8 miles west of Shelby at head of ravine 3 miles north of Marias River, in NE¼ sec. 31, T. 32 N., R. 3 W., Toole County, Mont. Marias River Shale, from limestone concretions 10 ft below top. W. A. Cobban, 1948.
9----	21420	<i>Desmoscaphites bassleri</i> .	8 miles west of Shelby, in NE¼ sec. 31, T. 32 N., R. 3 W., Toole County, Mont. Telegraph Creek Formation, from thin-bedded sandstone 24-35 ft above base. W. A. Cobban, 1948.
10---	D688	<i>Desmoscaphites erdmanni</i> .	9 miles west-southwest of Shelby, in E½NW¼NE¼ sec. 31, T. 32 N., R. 3 W., Toole County, Mont. Marias River Shale, from 5 ft below top. C. E. Erdmann, 1955.
11---	D692	----do-----	9 miles west-northwest of Shelby, in S½SW¼NW¼ sec. 31, T. 32 N., R. 3 W., Toole County, Mont. Marias River Shale, from 29.5 ft below top. W. L. Rohrer, 1955.
12---	D694	----do-----	Same locality as D692. Marias River Shale, from 9.5 ft below top. W. L. Rohrer, 1955.
13---	D666	<i>Desmoscaphites</i> sp.	About 10 miles northwest of Conrad, in SE¼NE¼ sec. 28, T. 29 N., R. 4 W., Pondera County, Mont. Telegraph Creek Formation, from 105 ft above base. B. R. Alto, 1955.

Localities at which *Desmoscaphites* was collected—Continued

No. on figure 161.1	Geological Survey Mesozoic locality	Fossil	Description, collector, and date
14---	D1128	<i>Desmoscaphites bassleri</i> ?	SE¼SW¼ sec. 28, T. 22 N., R. 8 W., Teton County, Mont. Telegraph Creek Formation. M. R. Mudge, J. J. Halbert, and M. B. Slaughter, 1956.
15---	1404	<i>Desmoscaphites erdmanni</i> .	Missouri River 4 or 5 miles below mouth of Marias River, Mont. Upper part of Marias River Shale. T. W. Stanton and W. H. Weed, 1894.
16---	D3302	----do-----	About 2 miles south of Park City, in SW¼NW¼ sec.-6, T. 3 S., R. 23 E., Carbon County, Mont. Colorado Shale, 50 ft below top of Niobrara Member. J. R. Gill, 1961.
17---	11208	<i>Desmoscaphites bassleri</i> .	SW¼ sec. 26, T. 1 S., R. 27 E., Yellowstone County, Mont. Telegraph Creek Formation. W. T. Thom, Jr., 1922.
18---	10902	----do-----	About 20 miles west of Hardin, in sec. 27, T. 1 S., R. 30 E., Big Horn County, Mont. Telegraph Creek Formation. W. T. Thom, Jr., 1921.
19---	10750	----do-----	Between Shoulderblade Butte and St. Xavier Mesa, near south quarter-corner sec. 27, T. 4 S., R. 33 E., Big Horn County, Mont. From soft sandstone below Virgelle Sandstone Member of Eagle Sandstone. T. W. Stanton and W. T. Thom, Jr., 1921.
20---	10752	----do-----	Between Shoulderblade Butte and St. Xavier Mesa, near south quarter-corner sec. 27, T. 4 S., R. 33 E., Big Horn County, Mont. Near base of Telegraph Creek Formation. T. W. Stanton and W. T. Thom, Jr., 1921.
21---	21752	----do-----	South of Dry Muddy Creek, in SE¼SW¼ sec. 22, T. 6 N., R. 1 W., Fremont County, Wyo. Cody Shale, from 1,300 ft below top. J. B. Reeside, Jr., and others, 1949.

Localities at which *Desmoscaphites* was collected—Continued

No. on figure 161.1	Geological Survey Mesozoic locality	Fossil	Description, collector, and date
22---	23110	<i>Desmoscaphites bassleri</i> .	East Sheep Creek in NW¼ SE¼NE¼ sec. 23, T. 6 N., R. 2 E., Freemont County, Wyo. Cody Shale, from about 1,275 ft below top. J. B. Reeside, Jr., and others, 1950.
23---	22102	----do-----	Six miles northeast of Rock Springs, in sec. 14, T. 19 N., R. 104 W., Sweetwater County, Wyo. Baxter Shale, from 785 ft below top. L. A. Hale, 1950.
24---	D3051	----do-----	About 12 miles south of Rawlins, in SE¼SW¼ sec. 23, T. 19 N., R. 88 W., Carbon County, Wyo. Steele Shale, from a limestone concretion 180 ft above base. J. H. Smith, 1961.
25---	11706	----do-----	Near Vermilion Creek, in SW¼NW¼ sec. 12, T. 10 N., R. 101 W., Moffat County, Colo. Mancos Shale, from 2,275 ft above base. J. D. Sears, W. H. Bradley, and J. B. Reeside, Jr., 1923.
26---	D2509	----do-----	5 miles north-northwest of Price, in SE¼NE¼ sec. 30, T. 13 S., R. 10 E., Carbon County, Utah. Mancos Shale, from lowest of 3 sandstone units making up Emery Sandstone Member. A. D. Zapp and W. A. Cobban, 1960.
27---	13247	----do-----	1 mile east of Desert, in SE¼ T. 20 S., R. 14 E., Emery County, Utah. Mancos Shale, from concretion 1,710 ft above base. E. M. Spieker and J. B. Reeside, Jr., 1925.
28---	13248	----do-----	Same locality as 13247. Mancos Shale, from 1,750 ft above base. E. M. Spieker and J. B. Reeside, Jr., 1925.
29---	13249	----do-----	Same locality as 13247. Mancos Shale, from 1,900 ft above base. E. M. Spieker and J. B. Reeside, Jr., 1925.
30---	13250	----do-----	Same locality as 13247. Mancos Shale, from 1,920 ft above base. E. M. Spieker and J. B. Reeside, Jr., 1925.

Localities at which *Desmoscaphites* was collected—Continued

No. on figure 161.1	Geological Survey Mesozoic locality	Fossil	Description, collector, and date
31---	13280	<i>Desmoscaphites bassleri</i> .	4 miles east of old Box Bar ranch, in sec. 27, T. 31 S., R. 8 E., Garfield County, Utah. Mancos Shale, 545 ft below Emery Sandstone Member. James Gilluly and J. B. Reeside, Jr., 1925.
32---	10434	----do-----	Just west of Durango, in center of sec. 13, T. 35 N., R. 10 W., La Plata County, Colo. Mancos Shale, 1,000 ft below top. T. C. Hopkins, 1920.
33---	10484	----do-----	Just west of Durango, in NW¼SE¼ sec. 13, T. 35 N., R. 10 W., La Plata County, Colo. Mancos Shale, 1,000 ft below top. J. B. Reeside, Jr., 1920.
34---	10141	----do-----	West foot of Hogback Mountain, in sec. 32, T. 30 N., R. 16 W., San Juan County, N. Mex. Mancos Shale, 280 ft below top. Harvey Bassler, 1917.
35---	12005	----do-----	About 8 miles east of Shiprock, in SW¼NE¼ sec. 20, T. 30 N., R. 16 W., San Juan County, N. Mex. Mancos Shale, 190 ft below top. J. B. Reeside, Jr., 1923.
36---	12013	----do-----	East of Shiprock, in NE¼ NE¼ sec. 30, T. 30 N., R. 16 W., San Juan County, N. Mex. Mancos Shale, 435 ft below top. J. B. Reeside, Jr., 1923.

REFERENCES

- Cobban, W. A., 1951a, Scaphitoid cephalopods of the Colorado Group: U.S. Geol. Survey Prof. Paper 239, 42 p. [1952].
- 1951b, Colorado Shale of central and northwestern Montana and equivalent rocks of Black Hills: Am. Assoc. Petroleum Geologists Bull., v. 35, no. 10, p. 2170-2198.
- Cobban, W. A., and Reeside, J. B., Jr., 1952, Correlation of the Cretaceous formations of the western interior of the United States: Geol. Soc. America Bull., v. 63, no. 10, p. 1011-1044.
- Heinz, Rudolf, 1928, Das Inoceramen-Profil der oberen Kreide Lüneburgs: Niedersächsische geol. Ver. [Hannover] Jahrb., no. 21, p. 65-81.
- Katich, P. J., 1956, Some notes on the Cretaceous faunas of eastern Utah and western Colorado, in Intermountain Assoc. Petroleum Geologists, Guidebook 7th Ann. Field Conf., East-central Utah, 1956: p. 116-119.

- Katich, P. J., 1959, Late Cretaceous faunal zones, western Colorado, in Rocky Mtn. Assoc. Geologists, Guidebook 11th Ann. Field Conf., Washakie, Sand Wash, and Piceance Basins, 1959: p. 26-29.
- Pike, W. S., Jr., 1947, Intertonguing marine and nonmarine Upper Cretaceous deposits of New Mexico, Arizona, and southwestern Colorado: Geol. Soc. America Mem. 24, p. 1-103.
- Reeside, J. B., Jr., 1927a, The cephalopods of the Eagle Sandstone and related formations in the western interior of the United States: U.S. Geol. Survey Prof. Paper 151, 87 p.
- 1927b, The scaphites, an Upper Cretaceous ammonite group: U.S. Geol. Survey Prof. Paper 150-B, p. 21-40.
- 1944, Maps showing thickness and general character of the Cretaceous deposits in the western interior of the United States: U.S. Geol. Survey Oil and Gas Prelim. Map 10.
- Seitz, O., 1956, Über Ontogenie, Variabilität und Biostratigraphie einiger Inoceramen: Palaeont. Zeitschr., v. 30, p. 3-6.
- Thom, W. T., Jr., Hall, G. M., Wegemann, C. H., and Moulton, G. F., 1935, Geology of Big Horn County and the Crow Indian Reservation, Montana: U.S. Geol. Survey Bull. 856, 200 p.



162. THE OSTRACODE GENUS *CYTHERELLOIDEA*, A POSSIBLE INDICATOR OF PALEOTEMPERATURE

By I. G. SOHN, Washington, D.C.

Invertebrate fossils have been used as a means of interpreting paleotemperatures since Neumayr's work on climatic zones of the Jurassic and Lower Cretaceous. Neumayr (1883, p. 283), in turn, refers to earlier workers such as Römer (1852, p. 20-26) who mentioned the climatic influence on the distribution of rudistids. Accumulated paleoclimatological data recently have been summarized by Nairn (1961) and by Schwarzbach (1961).

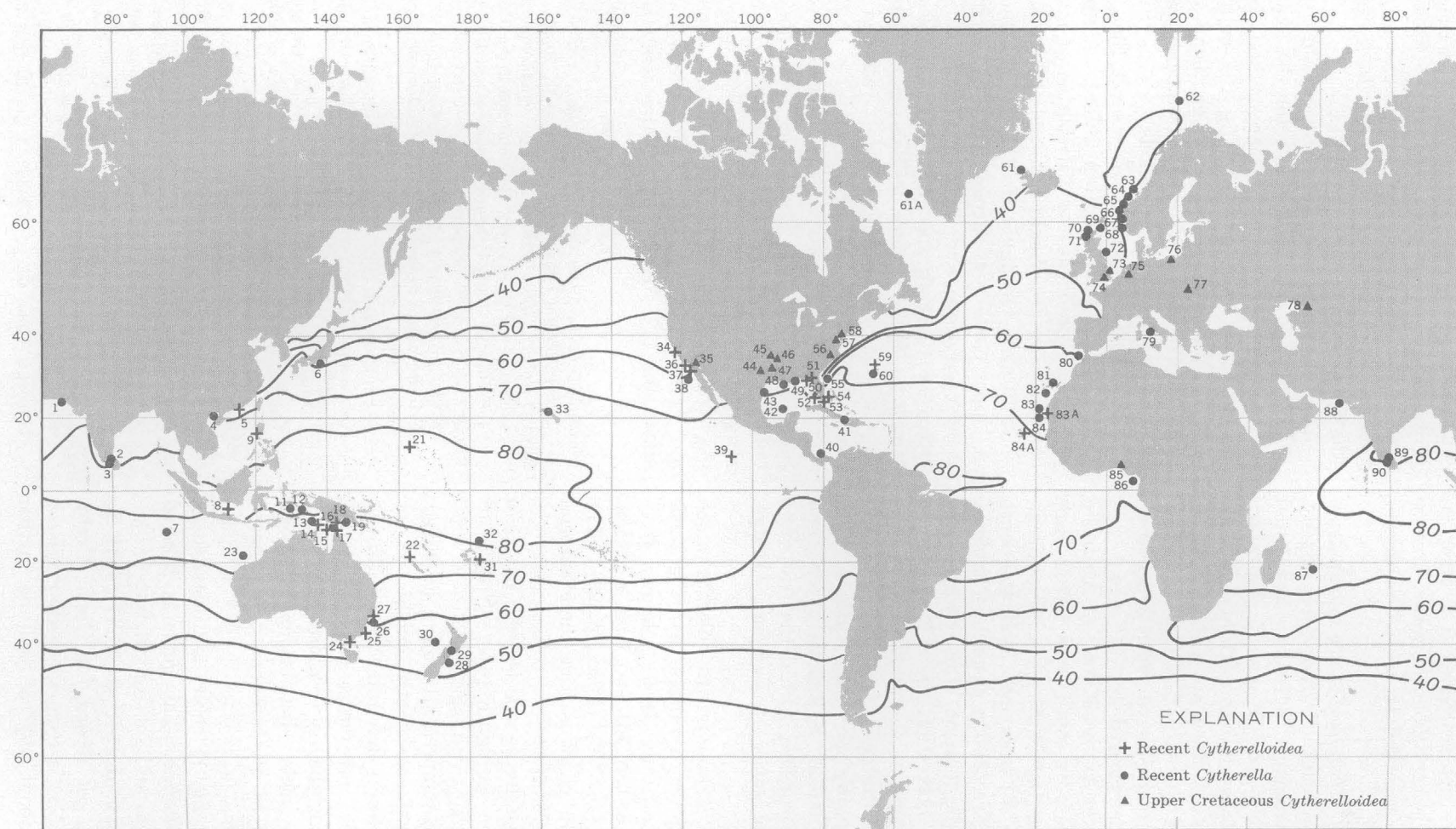
Data are here recorded for an ostracode genus known from the Jurassic to Recent. Because paleotemperature interpretations from other sources are available for the Upper Cretaceous, data for Upper Cretaceous and Recent species of this genus are presented.

As with other organisms the distribution of marine ostracodes is controlled in part by temperature. Living representatives of this subclass are recorded from a minimum temperature of 0.0°C (32°F) at 1,900 fathoms (Brady, 1880, p. 29) to 31°C (87.8°F) at depths of less than a fathom (Kornicker, 1961, p. 59). Except for Elofson's (1941, p. 442-455) and Neale's (1959, 1961) works on Pleistocene and Recent boreal forms, precise data on temperature ranges of individual taxa are not published. A statement by Kornicker (1962), that representatives of the family Cytherellidae from the Bahama Banks would probably not survive at or below 13°C (55.4°F) for extended periods, suggested the research upon which this preliminary report is based.

I am grateful to Dr. L. S. Kornicker, Texas Agricultural and Mechanical College, for sending me a copy of the typescript of his forthcoming report; to Prof. Edwin C. Allison, San Diego State College, Calif., for unpublished information on ostracodes near Clipperton Island (fig. 162.1, loc. 39), and to one of his students, John C. Holden, for information on an Upper Cretaceous species of *Cytherelloidea* in California.

The genus *Cytherelloidea* was erected by Alexander (1929, p. 55) to segregate species with ornamented shells from the marine benthonic species that were previously assigned to *Cytherella* Jones (1849, p. 28). Published descriptions and illustrations of all the living species of *Cytherella* were examined in order to determine which species actually belong to *Cytherelloidea*. The localities from which living species of *Cytherelloidea* have been recorded, and a few unpublished occurrences, are shown on figure 162.1.

Superposition of calendar-month isocrymes of surface-water temperature (Hutchins and Scharff, 1947, pl. 2) on this map limits the distribution of living species of *Cytherelloidea* to areas having a minimum temperature of approximately 10°C (50°F). Calendar-month isocrymes as defined by Hutchins and Scharff (1947, p. 266) are isotherms that connect points which cool down to the same extremes as measured in monthly mean temperatures. Although *Cytherelloidea* is a benthonic genus, a correction due to the decrease of temperature with depth is not made



Base from US Navy Hydrographic Office chart 1262b, July 1941

FIGURE 162.1.—Map showing the distribution of living species of *Cytherelloidea* and *Cytherella* and Upper Cretaceous species of *Cytherelloidea*, and calendar-month isocrymes (degrees Fahrenheit) from Hutchins and Scharff (1947).

because precise data are not available. The error introduced by this fact is negligible, however, because most of the species are recorded from shallow depths to 46 fathoms.

Only two species of *Cytherelloidea* are known from depths lower than 46 fathoms. *C. irregularis* (Brady, 1880) and *C. auris* Chapman, 1941, occur at 435 and 470 fathoms respectively. *C. irregularis* is known from "one or two detached valves" (Brady, 1880, p. 178) from the vicinity of Bermuda (fig. 162.1, loc. 59) where the isocryme is close to 21.1°C (70°F), and any decrease of temperature due to depth will be well above the minimum determined for the genus. *C. auris* is recorded from the southeast coast of Australia (loc. 25) at 33 miles east by south from Green Cape (lat 37°21'20" S., long 150°24'25" E.), at approximately the 12.8°C (55°F) isocryme. Both the depth and the location of this record are suspect (Chapman, 1941, p. 152) because the location is in the area of a steep slope. A slight correction to the west would place this species in bottom temperatures above the minimum postulated for this genus.

The distribution of living species of *Cytherelloidea* is bounded roughly by lat 40° S. and lat 37° N., and by the 10°C (50°F) isocryme, within the temperate and tropical biogenetic zones of Vaughan (Hedgepeth, 1957, p. 364).

The genus *Cytherella* appears to tolerate much wider temperature and depth ranges than *Cytherelloidea*. *Cytherella lata* Brady, 1880, is known from 675 fathoms (Brady, 1880, p. 15) and from a bottom temperature of 4.9°C (40.8°F) (idem., p. 23). The geographic range of this genus is from the equatorial region to the Arctic lat 73° N..

Localities from which living species of *Cytherella* are recorded are shown on figure 162.1. Species of *Cytherella* are associated with species of *Cytherelloidea* only within the temperature limits discussed, but *Cytherella* is found consistently outside of the minimum temperature limits determined for *Cytherelloidea*, suggesting that temperature is probably the major factor that controls the distribution of *Cytherelloidea*. Additionally, this distribution supports Alexander's separation of *Cytherelloidea* as a genus distinct from *Cytherella*.

Douglass (1960, text fig. 1) shows the distribution of the foraminifer *Orbitolina*. This genus is inferred to have lived in tropical and subtropical waters having a temperature range of 15°C to 35°C (59°F to 95°F). The northernmost record for Upper Cretaceous species of *Orbitolina* is from southern England, about lat 51° N. or about 3½° of latitude farther

south than species of *Cytherelloidea* of the same age. It therefore seems consistent that the probable minimum temperature during Late Cretaceous time at the northern limit from which *Cytherelloidea* is recorded was not less than 10°C (50°F).

A temperature range for Western Europe of about 15°C to 21°C (59°F to 70°F) for the Maestrichtian was inferred by oxygen isotope methods by Lowenstam and Epstein (1954 p. 226, fig. 10), and by Bowen (1961). This range inferred by geochemical methods is compatible with the minimum temperatures inferred above by paleontologic methods.

If the basic assumption is correct that the genus did not adapt with time to a different minimum temperature requirement, the distribution of fossil species of *Cytherelloidea* should give some clues as to paleotemperature. On figure 162.1 are shown the locations of Upper Cretaceous species of this genus from North America, Europe, and Africa. Each point represents from one to seven species, and from one to several samples. *Cytherelloidea williamsoniana* (Jones) and *C. chapmani* (Jones and Hinde), recorded by Chapman (1917, p. 51, 52) from the Upper Cretaceous of southwestern Australia, are not used because they are probably from Lower Cretaceous sediments. The distribution of the genus during Late Cretaceous time ranged from Nigeria (fig. 162.1, loc. 85), about lat 6½° N., to North Germany (loc. 76), about lat 54° N., and from about long 55° E. in Russia (loc. 73) to about long 117° W. in the United States (loc. 35).

REFERENCES

- Alexander, C. I., 1929, Ostracoda of the Cretaceous of north Texas: Texas Univ. Bull. 2907, 134 p., 10 pls.
- Bowen, Robert, 1961, Oxygen isotope paleotemperature measurements on Cretaceous Belemnoida from Europe, India and Japan: Jour. Paleontology, v. 35, p. 1077-1084, 3 figs.
- Brady, G. S., 1880, Report on the Ostracoda dredged by H. M. S. *Challenger* during the years 1873-1876: Report Sci. Results Voyage H. M. S. *Challenger*, Zoology, v. 1, pt. 3, 184 p., 44 pls.
- Chapman, Frederick, 1917, Monograph of the Foraminifera and Ostracoda of the Gingga Chalk: Australia Geol. Survey Bull. 72, 81 p., 14 pls.
- , 1941, Report on foraminiferal soundings and dredgings of the F. I. S. "Endeavor" along the continental shelf of the south-east coast of Australia: Royal Soc. South Australia Trans., v. 65, no. 2, p. 145-211, pls. 7-9.
- Douglass, R. C., 1960, Revision of the family Orbitolinidae: Micropaleontology, v. 6, p. 249-270, 6 pls., 3 text figs.
- Elofson, Olof, 1941, Zur Kenntnis der marinen Ostracoden Schwedens mit besonder Berücksichtigung des Skageraks: Geologiska Bidrag från Uppsala, v. 19, p. 215-534, 52 text figs.
- Hedgepeth, J. W., 1957, Marine biogeography, in Treatise on marine ecology and paleoecology, v. 1, Ecology: Geol. Soc. America Mem. 67, p. 359-382, 1 pl., 16 text figs.

- Hutchins, L. W., and Scharff, Margaret, 1947, Maximum and minimum monthly mean sea surface temperature charted from the "World Atlas of sea surface temperatures": Jour. Marine Research, v. 6, p. 264-268, 2 pls., text fig. 69.
- Jones, T. R., 1849, A monograph of the Entomostraca of the Cretaceous of England: Palaeontographical Soc. London, 40 p., 7 pls.
- Kornicker, L. S., 1961, Ecology and taxonomy of Recent Bairdiinae (Ostracoda): Micropaleontology, v. 7, p. 55-70, 1 pl.
- 1962, Ecology and description of Bahamian Cytherellidea (Ostracoda): Micropaleontology. (In press)
- Lowenstam, H. A., and Epstein, S., 1954, Paleotemperatures of the post-Aptian Cretaceous as determined by the oxygen isotope method: Jour. Geol., v. 62, p. 207-248, 22 text figs.
- Nairn, A. E. N., 1961, Descriptive paleoclimatology: New York, Interscience Publishers, 380 p., illus.
- Neale, J. W., 1959, *Normanicythere* gen. nov. (Pleistocene to Recent) and the division of the ostracod family Trachyleberididae: Paleontology, v. 2, p. 72-93, pls. 13, 14, text figs. 1-5.
- 1961, *Normanicythere leioderma* (Norman) in North America: Paleontology, v. 4, p. 424.
- Neumayr, M., 1883, Über klimatische Zonen während der Jura- und Kreidezeit: Kais. Akad. Wissenschaften. Math.-Naturwiss. Classe, Denkschr., v. 47, p. 277-310, 1 map.
- Römer, Ferdinand, 1852, Die Kreidebildungen von Texas und ihre organischen Einschlüsse: Bonn, A. Marcus, 100 p., 11 pls.
- Schwarzbach, Martin, 1961, Das Klima der Vorzeit: Stuttgart, Ferdinand Enke Verlag, 2d ed., 275 p., 134 text figs.



SEDIMENTATION

163. WIND DIRECTIONS IN LATE PALEOZOIC TO MIDDLE MESOZOIC TIME ON THE COLORADO PLATEAU

By F. G. POOLE, Denver, Colo.

Work done in cooperation with the U.S. Atomic Energy Commission

The cross-stratified eolian sandstones of late Paleozoic to middle Mesozoic age on the Colorado Plateau are here divided into four major age groups: (a) the Weber Sandstone, of Pennsylvanian and Permian age, the White Rim, Cedar Mesa, and De Chelly Sandstone Members of the Cutler Formation, and the De Chelly and Coconino Sandstones, of Permian age; (b) the Wingate Sandstone and tongues of Wingate Sandstone in the upper part of the Chinle Formation, of Late Triassic age, and the Dinosaur Canyon Sandstone Member of the Moenave Formation, of Late Triassic(?) age; (c) the Nugget Sandstone, of Early Jurassic age, Navajo Sandstone, of Jurassic and Triassic(?) age, and Aztec Sandstone, of Jurassic(?) age, and tongues of Navajo Sandstone in the Kayenta Formation, of Late Triassic(?) age; and (d) the Carmel Formation, of Middle and Late Jurassic age, and the Entrada, Bluff, Junction Creek, and Cow Springs Sandstones, of Late Jurassic age. No correlation or stratigraphic position of these subunits is implied within the four major groups.

The portions of the sandstone units described in this paper are interpreted as dominantly eolian, although they contain some fluvial or marine strata, be-

cause their lithology and sedimentary structures are physically similar to modern dune deposits. Only a small proportion of the Weber, Dinosaur Canyon, and Carmel is considered eolian. The sandstones are, in general, light colored and are composed chiefly of quartz grains with subordinate amounts of feldspar, chert, and clay minerals. The bonding medium for the grains consists both of silica cement, in the form of quartz overgrowths and microcrystalline quartz, and of carbonate cement. Grains range in size from very fine to coarse sand, with fine sand usually predominating. Most of the sandstones are moderately to well sorted. Sand grains range from subangular to well rounded; the larger grains are generally the better rounded. Pitting and frosting of the grains are common.

Sedimentary structures consist of wedge-planar and subordinate tabular-planar, lenticular-trough, and lenticular-simple sets of cross strata. The lower boundary of a planar set is a plane surface of erosion; the lower boundary of a trough set is a curved surface of erosion; and the lower boundary of a simple set is a nonerosional surface (McKee and Weir, 1953). The deposits are composed almost exclusively of steeply

dipping cross strata, averaging between 20° and 30°, that formed on the lee sides of dunes. Sets of cross strata are separated by gently inclined erosional or depositional surfaces. The thickness of the sets ranges from about 2 feet to over 100 feet, and the length of the cross strata ranges from 5 feet to over 100 feet. Parallel asymmetrical ripple marks of long wavelength and low amplitude are numerous. The ripple index ranges from 20 to 50.

Many features that are characteristic of modern dune deposits (McKee, 1957; Bagnold, 1954) are also characteristic of the sandstones studied. Both have (a) a high quartz content, indicative of a mature sediment, probably the result of several cycles of sedimentation; (b) a comparatively limited range of rock particle sizes (c) a high degree of rounding and sorting; and (d) pitting and frosting of the grains, probably resulting from abrasion by saltation. Modern dune deposits are composed almost exclusively of steeply dipping cross strata that form on the lee slopes; the gently dipping cross strata of windward sides, which slope in the opposite direction, rarely are preserved. Initial dips on the lee side of modern dunes usually range from 29° to 34°, which is the angle of repose for dry very fine to medium-grained sand; measured lee-side dips of the ancient cross strata studied, however, average 5° to 10° less because the more steeply dipping cross strata at the top of each set were eroded prior to deposition of the overlying set. Dune deposits are made up of large- and medium-scale cross strata, and large-scale eolian cross-strata sets are dominantly wedge shaped. Eolian ripples are restricted to the parallel asymmetrical type with a high index, and they are subparallel to the dip direction of the cross strata on the lee slope and flanks of dunes.

The direction of transport of the sand is determined by measuring the direction of the steepest dips near the top of each cross-strata set. At each locality, measurements were taken within a particular stratigraphic unit and were averaged to obtain a resultant wind direction. Due to the consistency in dip directions of the cross strata, 50 readings were usually sufficient to obtain a significant trend. Each arrow shown in figure 163.1 represents the resultant dip direction of cross strata in a particular sandstone unit in the four major age groups at one or more localities.

PENNSYLVANIAN AND PERMIAN TIME

The orientation of cross strata indicates that prevailing winds during Pennsylvanian and Permian time were from the north and northeast during deposition of the upper part of the Weber Sandstone; from

the northwest, north, and northeast for the White Rim and the Coconino Sandstone; from the northwest for the Cedar Mesa Sandstone Member; and from the north and northeast for the De Chelly (fig. 163.1A).

Regional stratigraphic relations of the Pennsylvanian and Permian units indicate that these sandstones tongue into marine strata westward and into continental strata eastward. These sandstone bodies are present along a north-south trending belt that is believed to represent a coastal-plain dune area in the western part and an inland-desert environment in the eastern part. This belt extends south-southwestward from southwestern Wyoming through eastern Utah into central Arizona. A southerly wind direction during deposition of these sandstones is shown in figure 163.1A.

TRIASSIC TIME

The orientation of cross strata indicates prevailing winds from the northwest, with subordinate west winds, in Triassic time during deposition of the Wingate Sandstone; northwest and northeast winds for the tongues of Wingate Sandstone in the upper part of the Chinle Formation; and west winds for the Dinosaur Canyon Sandstone Member of the Moenave Formation (fig. 163.1B). Cross-strata orientations in local eolian sandstone units in the "lower massive sandstone" of McKee (1954) in the Moenkopi Formation indicate winds from the northwest during Early and Middle(?) Triassic time. The cross-strata measurements of the "lower massive sandstone" were made in two localities in northeastern Arizona.

The local windblown sand bodies in the Moenkopi Formation of Early and Middle(?) Triassic age are believed to be dune accumulations marginal to a marine environment. The Wingate Sandstone and related sand bodies in the upper part of the Chinle Formation, all of Late Triassic age, are associated only with continental sediments and probably accumulated in an interior-desert environment. Prevailing winds blew toward the southeast during Triassic time (fig. 163.1B).

LATE TRIASSIC(?) AND EARLY JURASSIC TIME

Cross-strata orientations indicate dominant north and northeast winds in Late Triassic(?) and Early Jurassic time during deposition of the Nugget and Aztec Sandstones. Northwest winds prevailed during

FOOTNOTES TO FIGURE 163.1

¹ Wilson, R. F., 1959, The stratigraphy and sedimentology of the Kayenta and Moenave formations, Vermilion Cliffs region, Utah and Arizona: Stanford Univ. Ph. D. thesis, 337 p.

² Cadigan, R. A., 1952, The correlation of the Jurassic, Bluff, and Junction Creek Sandstones in southeastern Utah and southwestern Colorado: Pennsylvania State College Master's thesis, 163 p.

³ Harshbarger, J. W., 1949, Petrology and stratigraphy of Upper Jurassic rocks of central Navajo Reservation, Arizona: Arizona Univ. Ph.D. thesis.

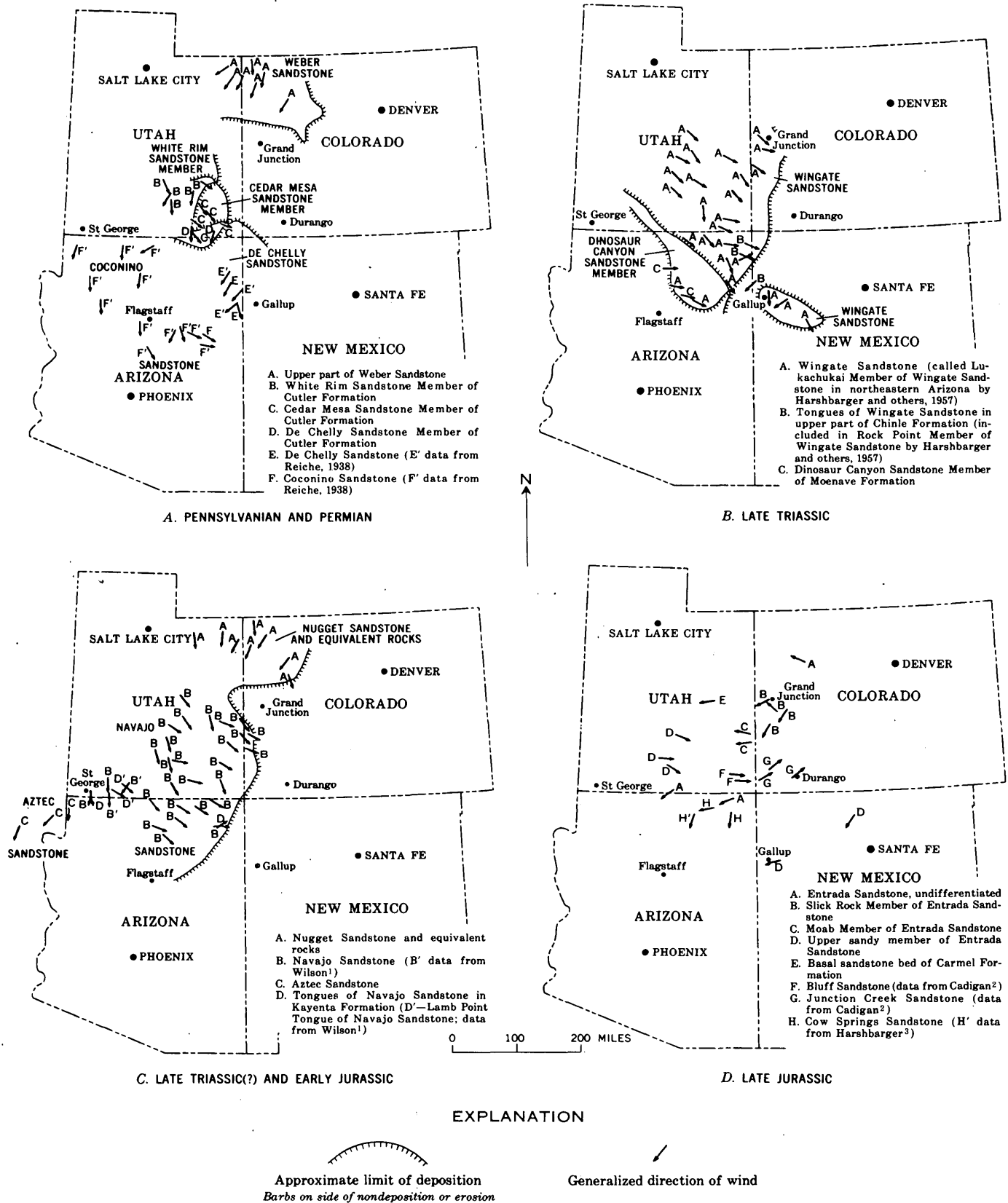


FIGURE 163.1.—Wind directions during late Paleozoic to middle Mesozoic time, Colorado Plateau.

deposition of the Navajo Sandstone except in southwest Utah and northwest Arizona, where north winds dominated. Winds from the northwest were dominant during deposition of the tongues of Navajo Sandstone in the underlying Kayenta Formation (fig. 163.1C).

The writer believes that the Aztec Sandstone is equivalent to the Navajo Sandstone. Part of the Nugget Sandstone in northeast Utah and northwest Colorado is believed to be correlative with the Navajo of central Utah.

The sandstones of Late Triassic(?) and Early Jurassic age were deposited by prevailing winds blowing toward the south (fig. 163.1C). These sand bodies, like the Wingate Sandstone, are associated only with continental deposits and probably accumulated in a vast interior-desert basin extending southwestward from central Wyoming through Utah, northern Arizona, southeastern Nevada, and into southern California.

LATE JURASSIC TIME

Cross-strata orientations indicate dominant northeast and east winds during Late Jurassic time when the Entrada Sandstone was deposited, except during deposition of the upper sandy member in south-central Utah, when a northwest and west wind prevailed (fig. 163.1D). Winds from the north and northeast prevailed during deposition of the Cow Springs Sandstone; from the west and southwest for the Bluff and Junction Creek Sandstones; and an east wind prevailed when the sandstone at the base of the Carmel Formation of Middle and Late Jurassic age was deposited (fig. 163.1D). The Bluff and Junction Creek are equivalent sandstone units.

The sandstones of Late Jurassic age show a dominant southwest to west direction of transport of sand, except for the upper part of the Entrada Sandstone in south-central Utah and the Bluff-Junction Creek Sandstones, which show an east to northeast direction of transport (fig. 163.1D). Most of the eolian sandstones of Late Jurassic age are associated with marine strata in the western part of the study area, and they probably represent coastal-plain dune accumulations formed by reworking of beach deposits and regressive marine sands. Most of the Cow Springs Sandstone and the sandstones in the eastern part of the area probably accumulated in an inland-desert environment.

INTERPRETATIONS

The sandstone units discussed in this paper are typical wind deposits comparable to modern dunes. The sandstones associated with marine strata are believed to be dominantly coastal-plain dune deposits derived from unconsolidated beach and regressive

marine sands. Eolian sandstones associated with continental strata may have been derived from unconsolidated marine and marginal marine sands that were transported landward, where they became associated with terrestrial sediments. On the other hand, these eolian sandstones may have been derived largely from older rocks exposed upwind. The sandstone bodies tend to thicken downwind, and many of them are thickest near their downwind limit.

Dip directions of cross strata indicate that late Paleozoic and early Mesozoic winds on the Colorado Plateau and adjacent areas were relatively constant and blew in a southerly direction throughout much of that time (Poole, 1957). Local variations in wind direction were probably controlled by such factors as seasonal fluctuation in winds, relative position of land and sea, and the configuration and relief of landmasses. The consistency in dip directions of cross strata in these eolian deposits indicate northerly winds with great regularity and strength similar to our present-day northeast trade winds, which blow southwesterly (Poole, 1957). The consistency of cross-strata dip bearings in a southerly direction suggests that in late Paleozoic and early Mesozoic time a broad belt of strong and persistent northerly winds was present in the Colorado Plateau area between lat. 35° N. and 43° N. This belt of "northerlies" may represent an ancient tradewind belt that extended from the equatorial zone to lat. 43° N. and beyond, or perhaps an expanded equatorial belt pushed the trade-wind belt northward. Persistent northerly winds in the Colorado Plateau area may have been due to a relatively stable high-pressure cell that was situated over the late Paleozoic-middle Mesozoic sea to the west. The clockwise movement of air around this high-pressure center would result in perennial "northerlies" in the eastern part of the high-pressure system. Another possible explanation is the hypothesis of polar wandering (Creer, Irving, and Runcorn, 1954). Measurements of remanent magnetism in rocks of the Colorado Plateau indicate that during late Paleozoic time the earth's magnetic pole in the northern hemisphere was in an area west of Japan and that during early Mesozoic time it was north of Mongolia, whereas during middle Mesozoic time it was near the present geographic pole, as indicated by magnetism in Upper Jurassic rocks (Cox and Doell, 1960; Collinson and Runcorn, 1960). If the earth's rotational axis were coincident with the axis of the mean geomagnetic dipole during the geologic past, the Colorado Plateau area would be within the northern hemisphere trade-wind belt during late Paleozoic and early Mesozoic time, providing that the ancient planetary wind belts were similar to the present-day wind system.

Divergent winds during deposition of some sandstones of Late Jurassic age, for example the upper part of the Entrada Sandstone (that is, upper sandy member and Moab Member) (fig. 163.1*D*), are believed to be the result of seasonal changes in wind direction due to local physiography as the shoreline fluctuated east-west. These divergent wind patterns may be due to monsoon winds or modified trade winds, or may represent the initial shift in the Colorado Plateau wind system from northerly to westerly winds. The easterly and northeasterly directions of transport indicated by the Bluff and Junction Creek Sandstones suggest deposition by westerly winds. The eolian Chuska Sandstone, of Miocene(?) age, in north-eastern Arizona and northwestern New Mexico was deposited by winds from the south-southwest (Wright, 1956), indicating the existence of the westerly wind belt on the Colorado Plateau in Tertiary time.

SELECTED BIBLIOGRAPHY

- Bagnold, R. A., 1954, The physics of blown sand and desert dunes: Reprint, London, Methuen and Co., Ltd., 265 p.
- Collinson, D. W., and Runcorn, S. K., 1960, Polar wandering and continental drift: evidence from paleomagnetic observations in the United States: *Geol. Soc. America Bull.*, v. 71, no. 7, p. 915-958.
- Cox, A., and Doell, R. R., 1960, Review of paleomagnetism: *Geol. Soc. America Bull.*, v. 71, no. 6, p. 645-768.
- Creer, K. M., Irving, E., and Runcorn, S. K., 1954, The direction of the geomagnetic field in remote epochs in Great Britain: *Jour. Geomagnetism and Geoelectricity*, v. 6, no. 4, p. 163-168.
- Harshbarger, J. W., Repenning, C. A., and Irwin, J. H., 1957, Stratigraphy of the uppermost Triassic and the Jurassic rocks of the Navajo Country: U.S. Geol. Survey Prof. Paper 291, 74 p.
- McKee, E. D., 1954, Stratigraphy and history of the Moenkopi Formation of Triassic age: *Geol. Soc. America Mem.* 61, 133 p.
- 1957, Primary structures in some recent sediments: *Am. Assoc. Petroleum Geologists Bull.*, v. 41, no. 8, p. 1707-1747.
- McKee, E. D., and Weir, G. W., 1953, Terminology for stratification and cross-stratification in sedimentary rocks: *Geol. Soc. America Bull.*, v. 64, no. 4, p. 381-389.
- Poole, F. G., 1957, Paleowind directions in late Paleozoic and early Mesozoic time on the Colorado Plateau as determined by cross strata [abs.]: *Geol. Soc. America Bull.*, v. 68, no. 12, p. 1870.
- Reiche, P., 1938, An analysis of cross laminations in the Cocolino sandstone: *Jour. Geology*, v. 46, no. 7, p. 905-932.
- Wright, H. E., Jr., 1956, Origin of the Chuska sandstone, Arizona and New Mexico: A structural and petrographic study of a Tertiary eolian sediment: *Geol. Soc. America Bull.*, v. 67, no. 4, p. 413-434.
- Wright, J. C., Shawe, D. R., and Lohman, S. W., 1963, Definition of members of the Entrada Sandstone in east-central Utah and west-central Colorado: *Am. Assoc. Petroleum Geologists Bull.* (In press)



164. LABORATORY STUDIES ON DEFORMATION IN UNCONSOLIDATED SEDIMENT¹

By EDWIN D. MCKEE, MAX A. REYNOLDS,² and CLAUD H. BAKER, JR., Denver, Colo., Canberra, Australia, and Denver, Colo.

Many structural forms produced through deformation of unconsolidated strata have been described and a voluminous literature has developed on this subject. Such structures occur in nearly all types of sedimentary rock and in all parts of the geologic column. They have been classified and interpreted in many different ways.

A series of experiments on deformation in stratified and cross-stratified sediments is being conducted in the sedimentation laboratory of the U.S. Geological

Survey in Denver, Colo. Each of the deformational processes described below has been applied to sand, clay, and alternations of each, and to saturated (that is, subaqueous), wet, and dry (subaerial) sediments. Because many minor variables such as depth of water, degree of pressure, and others affect the final structure pattern, each experiment has been repeated many times in order to ascertain the principal factors involved.

Definitions.—The purely descriptive term *contorted stratification*, recently defined (Dott and Howard, 1962, p. 120) as "all disturbed stratification, regardless of inducing agent or agents * * *" is applied in this paper in the same sense. Probable synonyms are soft-

¹ The experimental work described in this article was done by M. A. Reynolds and Claud Baker, Jr. under the direction of Edwin D. McKee. Mr. Y. Nir of the Geological Survey of Israel assisted during the early stages.

² Geologist, Australian Bureau of Mineral Resources.

rock deformation (Rettger, 1935, p. 272), gnarly bedding (McKee, 1938, p. 106), and disturbed structure as used by others. All of these terms imply deformation at any time after deposition, but before lithification, and by any process. Mostly the structures are restricted to single sets of strata or cross strata with rock units above and below entirely unaffected. They are intraformational features.

Terms that have definite genetic implications, such as slump folds (Rigby, 1958, p. 310), flow structure (Cooper, 1943, p. 190), and glacial contortion (Fairbridge, 1947, p. 105), are considered undesirable where interpretation is involved. Likewise those that have time connotations, as contemporaneous deformation (Lahee, 1914, p. 790) and penecontemporaneous deformation, are avoided in this investigation.

Some terms applied to deformation of unconsolidated sediment are restricted to particular kinds of structures and may be considered subtypes of contorted stratification. They include convolute bedding, crenulated bedding, prolapsed bedding, overturned folds, and others.

Basic types of deformed strata.—Contorted stratification, based on physical form, may be grouped into four principal classes. These include among many others (1) highly irregular structures in which strata appear crumpled and twisted, rather than folded, (2) regularly folded strata in which the axes are either horizontal or dip with low angle, (3) strata folded with axes essentially vertical, and (4) strata broken into a series of separate, nearly parallel, miniature thrusts or related tight folds.

Terminology for basic types.—Terms applied to the principal types or classes of contorted stratification have been used differently by different authors and in a very loose sense by many. For this reason a descriptive, nongenetic terminology is applied in this investigation as indicated below.

Highly irregular, crumpled and twisted strata are referred to as *irregularly contorted beds*. This usage is similar to that of Kuenen (1949, p. 368), who described Carboniferous rock of Pembrokeshire as "twisted, drawn out, or compressed in such a manner as to suggest kneading more than simple folding."

Regularly folded strata with structures systematically bent to give the appearance of U's or V's on their sides are termed *intraformational recumbent folds*. "Overturned" as applied to cross strata by Potter and Glass (1958, p. 20) and by Stewart (1961, p. B129) is probably synonymous, but "recumbent" is preferred as it more precisely describes the normal attitude of the folds in terms of structural geology. The terms "prolapsed bedding" (Wood and Smith, 1957, p. 172)

and "deformed ripple-drift bedding" (Prentice, 1960, p. 217) also seem to refer to this type of structure.

Strata forming series of folds with nearly vertical axes are termed *convolute bedding*. This term was proposed by Kuenen (1953b, p. 1056) to describe laminae within a single set showing distortion that "gradually increases upward to intensive but rather regular folds and then dies out gradually." The term "crinkled bedding" used by Migliorini is a synonym according to Kuenen (1953a, p. 15), and various other terms such as "crenulated bedding," "curled bedding," and "corrugation" probably also refer to this structure. No genetic connotation is implied in the term as used here, although some geologists relate it to specific environments or processes.

Repeated miniature thrust faults and related overturned fold structures within a stratification unit are designated as *intraformational thrust structures*. These commonly are distributed along a single stratification set with axes tending to dip in one direction. They have been referred to as decollement structures (Hansen and others, 1961, p. 1415).

Relation of type of sediment to deformation.—The type of structure developed in any particular situation depends, in part, on the kind of unconsolidated sediment that is subjected to deformation. Rigid discrete particles of sand react to forces of compression and tension very differently from clayey material, which tends to slide and slip under stress of lateral pressure. Thus, in experimental work typical intraformational recumbent folds of the type defined above have been developed only in sand, whereas intraformational thrust structures were formed best where clay layers occur between units of sand, as was convolute bedding under stress of vertical loading.

Differences in structure also depend to some extent on whether the sediment involved is saturated; that is, under water, wet but with water drained off, or completely dry. The experiments of Rettger (1935, p. 286-288) have indicated the importance of this factor, and in the current investigations comparative tests have been made to ascertain its influence with respect to the forming of each structural type.

Relation of physical process to deformation.—Four principal processes have been invoked by geologists to explain contorted stratification. These are (1) gravity slumping, (2) drag, as from an overriding force, (3) overloading, from above or from one side, and (4) modification by boring organisms, root growth, or gas bubbles. The first three of these have been tested in laboratory experiments involved in the present study.

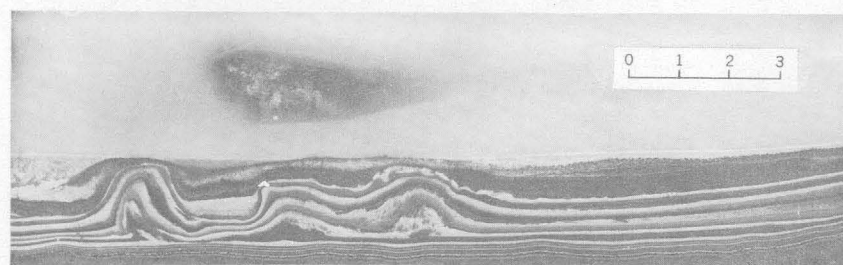
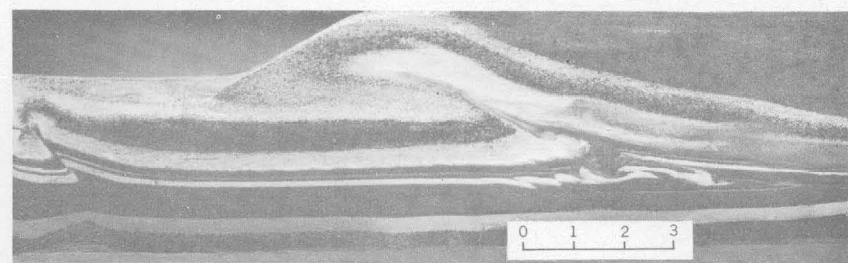
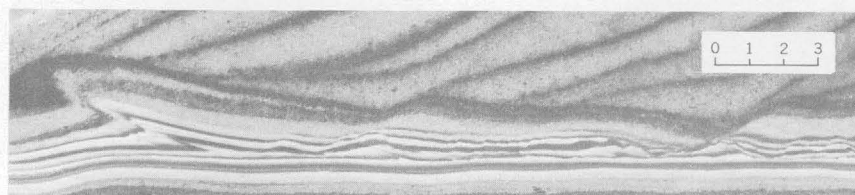
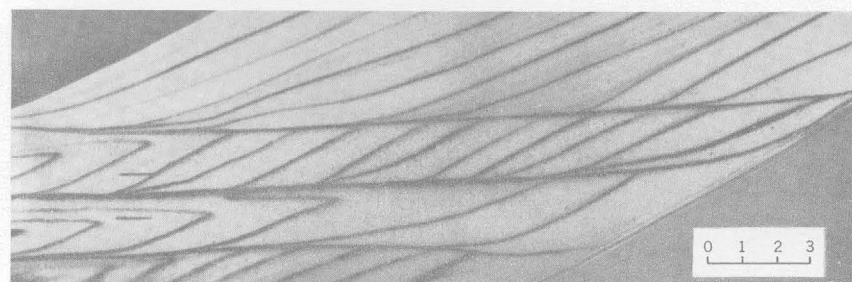
*A**B**C**D**E*

FIGURE 164.1.—*A*, Convolute bedding developed in laminated mud layers between sand layers by vertical loading. Sandbag, responsible for contortions, partly visible in milky water above strata. *B*, *C*, Intraformational thrust structures in laminated mud layers formed by progressive loading of sand from right to left. *D*, *E*, Intraformational recumbent folds developed in saturated sand by water currents forcing a mass of sand from right to left across top of foresets. Scale is in inches.

Gravity slumping in unconsolidated sediments may result from weight increase at top of depositional slope, increase in water saturation, oversteepening, or undercutting of a depositional slope. It may be triggered by external impulses such as water movement or earthquakes (Rigby, 1958, p. 310; Hallam, 1960, p. 57). Regardless of cause, the results probably are similar. Slumping may occur on subaerial, as well as subaqueous slopes, but with somewhat different results.

Surface drag by an overriding force is commonly developed where masses of sediment are moved across a recently deposited surface by torrential or other strong currents. Similar forms result from glacial push (Fairbridge, 1947), and from subglacial drag, as suggested by numerous authors (Slater, 1927a, 1927b; Jacobson and Scott, 1937; Öpik, 1958, p. 58; Hansen and others, 1961, p. 1415). A distinction between gravity slumping and drag structures has been emphasized by Rettger (1935, p. 282), and he lists some criteria for distinguishing between the types of deformation.

Deformation resulting from overloading is of two principal types (Prentice, 1960, p. 220). One type may be referred to as vertical loading and is caused by local differences in a load settling from above. Such local settling has been attributed to turbidity currents (Kuenen and Menard, 1952, p. 90), but it may result from sediment raised by storm waves, from windblown sand or from volcanic pyroclastics dropping out of the atmosphere, and probably from other causes. The second type is horizontal load flowage which results from the weight of sediment accumulating on the margin of a current-fed deposit, as when a delta cone advances across a surface.

Alteration of stratification and cross-stratification by the boring of animals, the growth of plants, or the migration of gas or liquid (Stewart, 1956) is not discussed here as it has not been included in the laboratory program. The usual changes brought about by these processes, however, are of a highly irregular or nonsymmetrical type.

Conclusions.—Experiments to date have demonstrated that in saturated mud layers alternating with sand layers, convolute bedding can be formed by vertical loading (fig. 164.1A); intraformational thrust structures can be developed by horizontal flowage from progressive loading in a given direction (fig. 164.1B and C). Intraformational recumbent folds can be formed in saturated sand by the overriding force of a sand mass pushed forward by strong currents (fig. 164.1D and E). The experiments on re-

cumbent folds are described in detail in Article 165; subsequent reports will discuss other types of contorted bedding as the work on each is completed.

REFERENCES

- Cooper, J. R., 1943, Flow structures in the Berea Sandstone and Bedford Shale of central Ohio: *Jour. Geology*, v. 51, no. 3, p. 190-203.
- Dott, R. H., Jr., and Howard, J. K., 1962, Convolute laminations in non-graded sequences: *Jour. Geology*, v. 70, no. 1, p. 114-120.
- Fairbridge, R. W., 1947, Possible causes of intraformational disturbances in the Carboniferous varve rocks of Australia: *Royal Soc. New South Wales Jour. and Proc.*, v. 81, pt. 2, p. 99-121.
- Hallam, A., 1960, The White Lias of the Devon coast: *Geol. Assoc. Proc.*, v. 71, pt. 1, p. 47-60.
- Hansen, E., Porter, S. C., Hall, B. A., and Hills, A., 1961, Decollement structures in glacial-lake sediments: *Geol. Soc. America Bull.*, v. 72, p. 1415-1418.
- Jacobson, R., and Scott, T. R., 1937, The geology of the Korpuperril Creek area, Bacchus Marsh: *Royal Soc. Victoria Proc.*, v. 50 (n.s.), p. 110-156.
- Kuenen, Ph. H., 1949, Slumping in the Carboniferous rocks of Pembroke: *Geol. Soc. London Quart. Jour.*, v. 104, p. 365-385.
- , 1953a, Graded bedding, with observations on the Lower Paleozoic rocks of Britain: *Verhandl. Kon. Ned. Akad. Wet.*, Eerste reeks, pt. 20, no. 3, 47 p.
- , 1953b, Significant features of graded bedding: *Am. Assoc. Petroleum Geologists Bull.*, v. 37, no. 5, p. 1044-1066.
- Kuenen, Ph. H., and Menard, H. W., 1952, Turbidity currents, graded and non-graded deposits: *Jour. Sed. Petrology*, v. 22, no. 2, p. 83-96.
- Lahee, F. H., 1914, Contemporaneous deformation: A criterion for aqueoglacial sedimentation: *Jour. Geology*, v. 22, no. 8, p. 786-790.
- McKee, E. D., 1938, Environment and history of the Toroweap and Kaibab Formations of northern Arizona and southern Utah: Washington, D.C., Carnegie Inst. Washington, pub. 492, 268 p., 48 pl.
- Öpik, A. A., 1958, The geology of the Canberra City District: *Bur. Mineral Resources Australia Bull.* 32.
- Potter, P. E. and Glass, H. D., 1958, Pennsylvanian petrology and sedimentation in southern Illinois: A vertical profile: *Illinois Geol. Survey Rept. Inv.* 204, 60 p.
- Prentice, J. E., 1960, Flow structures in sedimentary rocks: *Jour. Geology*, v. 68, no. 2, p. 217-224.
- Rettger, R. E., 1935, Experiments on soft-rock deformation: *Am. Assoc. Petroleum Geologists, Bull.*, v. 19, no. 2, p. 271-292.
- Rigby, J. K., 1958, Mass movements in Permian rocks of Trans-Pecos, Texas: *Jour. Sed. Petrology*, v. 28, no. 3, p. 298-315.
- Slater, G., 1927a, The structure of the disturbed deposits of Møns Klint, Denmark: *Royal Soc. Edinburgh Trans.*, v. 55, pt. 2, no. 12, p. 289-302.
- , 1927b, The disturbed glacial deposits in the neighborhood of Lønstrup near Hjørring, North Denmark: *Royal Soc. Edinburgh Trans.*, v. 55, pt. 2, no. 13, p. 303-315.

- Stewart, H. B., 1956, Contorted sediments in modern coastal lagoon explained by laboratory experiments: *Am. Assoc. Petroleum Geologists Bull.*, v. 40, no. 1, p. 153-179.
- Stewart, J. H., 1961, Origin of cross-strata in fluvial sandstone layers in the Chinle Formation (Upper Triassic) on the

- Colorado Plateau: *Art 54 in U.S. Geol. Survey Prof. Paper 424-B*, p. B127-B129.
- Wood, Alan, and Smith, J. A., 1957, The sedimentation and sedimentary history of the Aberystwyth Grits (Upper Llandoveryan): *Geol. Soc. London Quart. Jour.*, v. 114, pt. 2, p. 163-195, [1959].



165. EXPERIMENTS ON INTRAFORMATIONAL RECUMBENT FOLDS IN CROSSBEDDED SAND¹

By EDWIN D. MCKEE, MAX A. REYNOLDS,² and CLAUD H. BAKER, JR., Denver, Colo., Canberra, Australia, and Denver, Colo.

Equipment and materials.—Experiments on the origin of intraformational recumbent folds were conducted in a steel delta tank, 15 feet long, 2½ feet wide, and 2 feet deep, in the sedimentation laboratory of the U.S. Geological Survey, Denver, Colo. (Art. 164). The tank at its inlet end contains a feeding platform with a front sloping at 30° to the floor. A stream, after flowing across this platform, built a delta into the standing body of water in front. Three valves at the outlet end controlled the level of the water. A cross section of the delta as it built forward could be observed through a clear plastic side of the tank.

Relatively clean and well-sorted sand of two varieties was used for this set of experiments. One variety of sand, from dunes east of Denver, was brown, angular, low in sphericity, and showed the following size grades (Wentworth scale) on analysis:

	Analysis 1 (percent)	Analysis 2 (percent)
Coarse grains.....	11	6
Medium grains.....	53	56
Fine grains.....	31	34
Very fine grains.....	4	3
Silt.....	1	1

The second variety was mechanically screened ("flint shot," Ottawa Silica Co., Ottawa, Ill.) and averaged somewhat coarser than the dune sand: coarse grains 78 percent, medium grains 22 percent. It was white, well rounded, and had fairly high sphericity. The two varieties gave similar results and, as the

white was better for photographing, it was used in most final tests.

Magnetite grains were used to mark stratification surfaces and were sprinkled periodically on planes of deposition. They made structure patterns conspicuous and were sufficiently heavy to be relatively stable once deposited.

Preparation of sand deposits.—In ancient sandstones and in modern deposits of sand, intraformational recumbent folds commonly are formed within sets of cross strata, either tabular planar or trough (McKee and Weir, 1953, p. 385). This is shown not only by association of the folded structures with cross strata of such types, but also by successions of recumbent folds that form lateral transitions into sets of normal foreset beds. In order to test fold development in this environment, each experiment was begun with a set of planar cross beds, having foresets dipping between 15° and 25° and surfaces 10 to 30 inches long, formed in the delta tank. The degree of dip was controlled by the rate of depositing current; the length of foreset by the depth of water.

Experimental procedure.—Pressure great enough to produce deformation was applied to sets of planar cross strata by each of several principal methods. These were: (1) loading from above with weights, (2) undercutting foresets by ground-water seepage and by water currents near base, (3) oversteepening foreset tops to initiate gravity slumping, (4) pushing of near-surface part with a lateral force, and (5) dragging surface with an overriding force. Each of these processes was applied independently to saturated sand, wet sand with water withdrawn, and dry sand.

¹ The experimental work described in this article was done by M. A. Reynolds and Claud Baker, Jr. under the direction of Edwin D. McKee. Mr. Y. Nir of the Geological Survey of Israel assisted during the early stages.

² Geologist, Australian Bureau of Mineral Resources.

Theories of origin proposed by other researchers.—The cause of intraformational recumbent folds in unconsolidated sand has been discussed by many geologists, and numerous theories, some very ingenious, have been suggested to explain them. Among these theories are (1) drag from the overriding force of sand-laden waters (Robson, 1956, p. 251), (2) the buildup of water pressure within a sand body covered by a mantle of silt, causing mass movement when a rapid lowering of water level outside took place (Harms, MacKenzie, and McCubbin, 1962), (3) the result of stresses set up between zones of freezing in water-impregnated sand, thawed out during summer, and the permafrost below (Moskvitin, 1959, p. 727), (4) continued movement of loosely packed sand (quicksand) after the lower part of a mass has settled (Stewart, 1961), (5) slumping due to an oversteepening of the profile (Kiersch, 1950, p. 923).

Slumping from undercutting.—Gravity slump in pure sand caused by undercutting of foreset beds undoubtedly is responsible for some contorted stratification. The undercutting may result from internal weakening through ground-water seepage, from external attack through rising water level, or from erosion by currents. All of these methods were tried experimentally.

With ground-water seepage through sets of cross strata, water followed a well-defined gently sloping plane and caused a zone of weakness where it emerged at the delta front. The resulting scarp retreated so gradually, however, that all trace of structure was destroyed as its front periodically collapsed. Similar results came from gradual undercutting by rising water level.

Other experiments in undercutting were done by suddenly removing a sizeable mass of sand at the base of a deposit, simulating the effects of strong wave or current cutting. This was done by withdrawing a shingle from beneath the foreset front, causing collapse and drop of several inches. With both dry and saturated sand, planes of stratification were contorted but maintained definition (fig. 165.1A and B). Strata showed a marked tendency to curve forward and downward and to become wavy. Structures retained some degree of regularity but did not resemble recumbent folds.

Gravity slumping from oversteepening.—Gravity-slumping structures were formed in two ways. In one, a maximum angle of repose was developed by feeding sand very slowly with merely a trickle of water, after which the delicate balance was disturbed by thumping the tank. A small avalanche of sand resulted and a more stable angle of repose was devel-

oped, but the slumping sand failed to preserve any clear-cut recumbent fold structures (fig. 165.1C). The second experiment, involving a very rapid flow and a sudden cascading of sand masses down the delta front, likewise failed to bend over the laminae. In both experiments the slumping caused a flowing movement of sand with a tendency to eliminate, "stretch," or weakly contort the strata.

Vertical loading.—In experiments in which heavy weights were localized on the upper bounding surfaces of planar cross-strata sets, recumbent folds did not develop. Where the sand was below water level and saturated, a slight compaction resulted in warping (fig. 165.1 D and E). Where the sand was still wet, but water was drained off the mass, no effects could be detected. Where strata of dry sand close to the angle of repose were tested, a crinkling developed in the upper parts (fig. 165.1F).

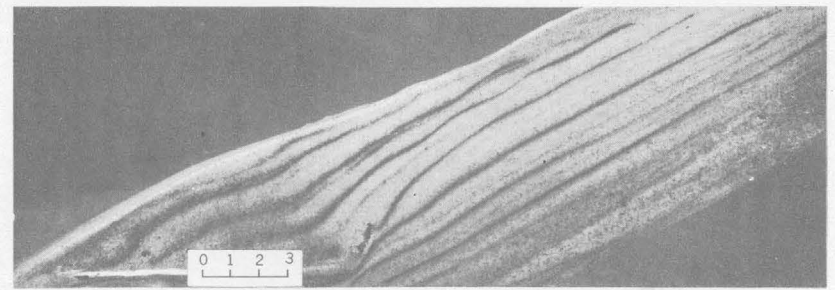
Pushing with lateral force.—A laterally applied force similar to that of an advancing glacier has been suggested (Sussmilch and David, 1919; Slater, 1927 a, b; Hansen and others, 1961, p. 1415) as a possible cause of some contorted stratification. Such force was developed in laboratory experiments by pushing a board against the dissected end of a series of foreset beds (fig. 165.2 A, B, and C). In this experiment, particles of sand were pushed forward along thrust planes parallel to the base of the board. The net result was a set of recumbent folds in which the upper limb was crinkled and particles within it displaced forward.

The same experiment conducted with wet sand, stabilized and firm following withdrawal of water, produced no deformation under moderate pressure, but with greater pressure caused the strata to buckle, break, and move forward along what seemed to be thrust planes. In dry sand a folded appearance was developed, but commonly the beds were not completely overturned as with a drag process.

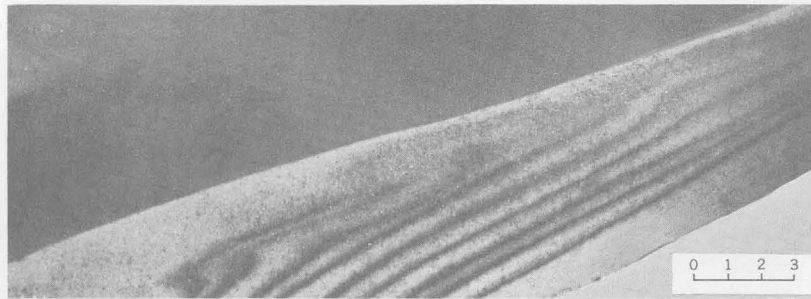
Drag from overriding force.—A sandbag was employed in order to simulate conditions of an overriding force such as a mass of sediment or a body of ice moving across a set of planar cross strata. When testing wet sand with the water drained off, dragging the sandbag with a rope caused only a beveling of the surface. When saturated sand was used, either immediately after deposition or several hours later, the cross strata were strongly distorted with a dominant forward drag. On the other hand, when sand deposited under water had the water drained off and was then resaturated, the effect of dragging the sandbag over the surface was the same as for wet sand, and only beveling occurred.



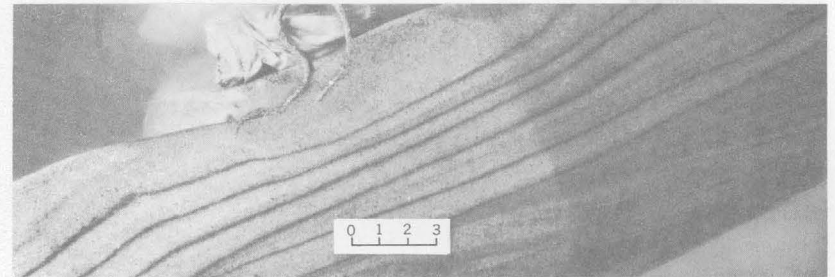
A



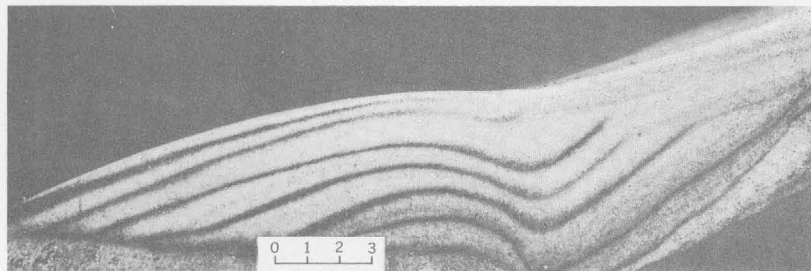
B



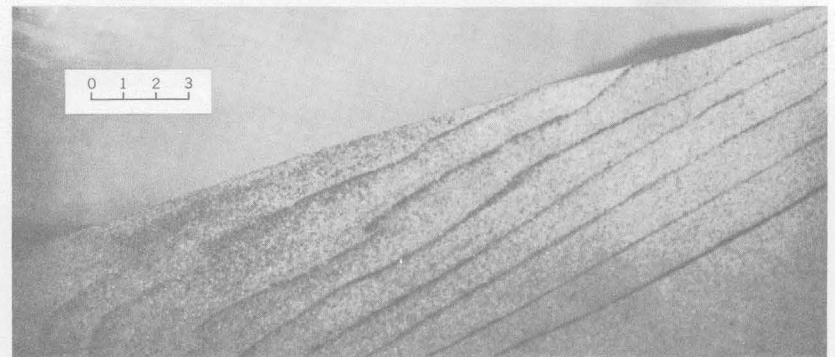
C



D



E



F

FIGURE 165.1.—Deformation of crossbedding in unconsolidated sand (scale in inches). *A*, Contorted bedding in dry sand caused by undercutting base of foresets. *B*, Contorted bedding in saturated sand caused by undercutting base of foresets. *C*, Contorted bedding in saturated sand caused by gravity slumping from oversteepening. *D*, Warping of beds in saturated sand resulting from vertical loading. *E*, Warping of beds in "quicksand" resulting from vertical loading. *F*, Crinkling of beds in dry sand resulting from vertical loading.

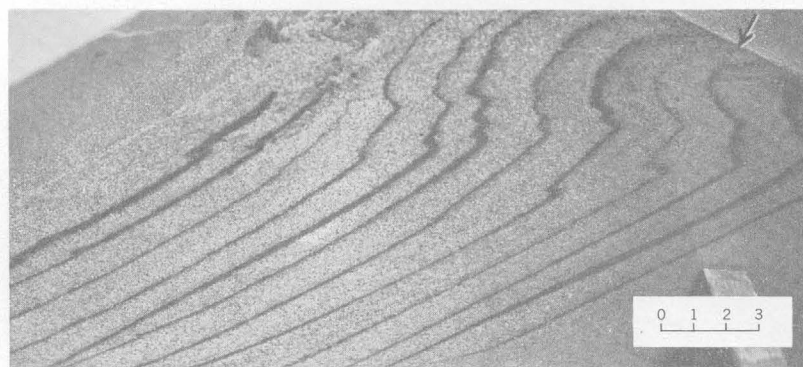
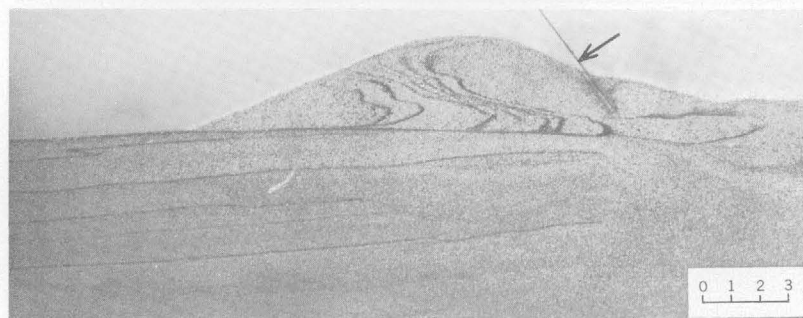
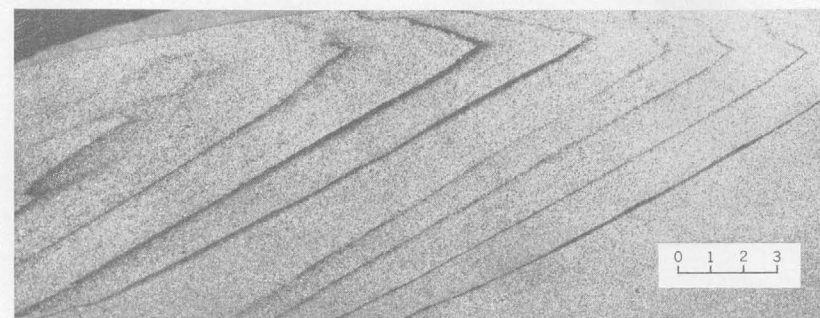
*A**B**C**D**E**F*

FIGURE 165.2.—Deformation of crossbedding in unconsolidated sand (scale in inches). *A* and *B*, Crinkling in steeply dipping beds of dry sand caused by lateral push with board, from right to left as shown by the arrows. *C*, Crinkling in dipping beds of saturated sand caused by lateral push with board, from right to left as shown by the arrow. *D*, Recumbent folds in steeply dipping dry sand formed by dragging sandbag across upper surface. *E* and *F*, Recumbent folds in foresets of saturated sand caused by drag effect as mass of sand is moved across surface by strong current.

In dry sand accumulated by avalanching, as on a dune-slip face, dragging a sandbag caused deformation resembling that formed in saturated sand (fig. 165.2D). The beds were not completely "overturned," however, and many minor crenulations developed.

Recumbent folds similar to those formed by dragging a sandbag were formed where a mass of loose but saturated sand moved as a body, pushed by the force of water behind, across the top of a set of fore-set beds (fig. 165.2E and F). The moving mass of sand and water dragged the tops of the cross strata into recumbent folds, demonstrating that the mechanics of movement within the folded beds was the same as in beds dragged over with a sandbag, and that no gravity slumping is involved. It is concluded, therefore, that either a rigid mass like moving ice or the sudden movement of a body of sediment, as by flood waters, is capable of developing these structures in sediment that is saturated.

Numerous variations in the form of intraformational folds produced in these experiments are readily explained by differences in several factors involved in the process as shown by repeated experiments:

- (1) The dip of the axial plane of the fold was directly related to the initial dip of the deformed beds; that is, the steeper the beds were initially, the greater the dip of the fold axis.
- (2) The point of folding seemed to be controlled by the water level in front of the delta; the folding occurred at or just below water level.
- (3) The form of each fold varied according to the speed and duration of the overriding movement; other factors were constant. Where the drag was rapid and its distance of movement relatively large, the folds tended to be V-shaped; with slower movements over a shorter distance, more rounded folds were formed.

In experimental work, S-shaped folds commonly developed with initial stress from drag. The upper lesser parts normally were soon removed by stream-current planation. This upper bounding surface, therefore, in folded as well as in undeformed sets of cross strata, commonly marks the surface above which a variable but unknown amount of the original deposit was removed. In some cases the entire upper half of a fold was stripped away, leaving no record of deformation.

Intraformational recumbent folds in the geologic record.—Primary structures of this type are common in sandstones of various ages and in many parts of the world (see table). Most of these structures are in fluvial deposits. Similar ones also have been recorded from modern stream deposits, including point bars of the Mississippi River (Frazier and Osanik,

Records of typical intraformational recumbent folds in crossbedded sandstone

Rock unit	Age	Locality	Reference
Nubian Sandstone.	Cretaceous.	Libya, Egypt.	McKee (1962).
Adigrat Sandstone.	Jurassic(?)	Ethiopia	Do.
Shinarump member of Chinle Formation.	Triassic	Utah	McKee, Evensen, Grundy, 1953, p. 38.
Mossback member of Chinle Formation.	do	do	Stewart, 1961.
Caseyville Group.	Pennsylvanian.	Illinois	Potter, 1957, p. 2703, fig. 7.
"lower group"	Carboniferous.	Sinai	McKee (1962).
Fell Sandstone.	do	England	Robson, 1956, p. 251.
Old Red Sandstone.	Devonian	Scotland	Westoll (in Robson, 1956, p. 251).
Aberystwyth Grits.	Silurian	Great Britain.	Wood and Smith, 1957, p. 171, fig. 5.
Caniston Grits	do	do	Prentice, 1960, p. 217, fig. 1.
Ram Sandstone.	Paleozoic	Jordan	McKee (1962).
Torridan Sandstone.	Precambrian.	Scotland	Hemmingway (in Robson, 1956, p. 251).

1961, p. 135, fig. 10), the Red River, La. (Harms, MacKenzie, and McCubbin, 1962), and flood-plain deposits of the Colorado River, Ariz. (McKee, 1938, p. 81).

REFERENCES

- Frazier, D. E. and Osanik, A., 1961, Point-bar deposits, Old River Locksite, Louisiana: Gulf Coast Assoc. Geol. Soc. Trans., v. 11, p. 121-137.
- Hansen, E., Porter, S. C., Hall, B. A. and Hills, A. 1961, De-collement structures in glacial-lake sediments: Geol. Soc. America Bull., v. 72, p. 1415-1418.
- Harms, J. C., MacKenzie, D. B., and McCubbin, D. G., 1962, Stratification in modern sands of the Red River, Louisiana: Jour. Geology.
- Kiersch, G. A., 1950, Small-scale structures and other features of Navajo Sandstone, northern part of San Rafael Swell, Utah: Am. Assoc. Petroleum Geologists Bull., v. 34, p. 923-942.
- McKee, E. D., 1938, Original structures in Colorado River flood deposits of Grand Canyon: Jour. Sed. Petrology, v. 8, no. 3, p. 77-83.
- McKee, E. D., 1962, Origin of the Nubian and similar sandstones: Geologische Rundschau. (In press)
- McKee, E. D., Evensen, C. G., and Grundy, W. D., 1953, Studies in sedimentology of the Shinarump Conglomerate of northeastern Arizona: U.S. Atomic Energy Comm., RME-3089, 48 p.
- McKee, E. D., and Weir, G. W., 1953, Terminology for stratification and cross stratification in sedimentary rocks: Geol. Soc. America Bull., v. 64, p. 381-390.

- Moskvitin, A. I., 1959, New evidence of very early glaciation of the Russian Plain: *Dok. Akad. Nauk SSSR*, v. 127, no. 1-6, p. 852-856; English translation published by American Geol. Inst. in 1960 (p. 725-729).
- Potter, P. E., 1957, Breccia and small-scale Lower Pennsylvanian overthrusting in southern Illinois: *Am. Assoc. Petroleum Geologists Bull.*, v. 41, no. 12, p. 2695-2709.
- Prentice, J. E., 1960, Flow structures in sedimentary rocks: *Jour. Geology*, v. 68, no. 2, p. 217-224.
- Robson, D. A., 1956, A sedimentary study of the Fell sandstones of the Coquet Valley, Northumberland: *Geol. Soc. London Quart. Jour.*, v. 112, p. 241-262.
- Slater, G., 1927a, The structure of the disturbed deposits of Møens Klint, Denmark: *Royal Soc. Edinburgh Trans.*, v. 55, pt. 2, no. 12, p. 289-302.
- 1927b, The disturbed glacial deposits in the neighborhood of Lønstrup, near Hjørring, North Denmark: *Royal Soc. Edinburgh Trans.*, v. 55, pt. 2, no. 13, p. 303-315.
- Stewart, J. H., 1961, Origin of cross-strata in fluvial sandstone layers in the Chinle Formation (Upper Triassic) on the Colorado Plateau: *Art. 54 in U.S. Geol. Survey Prof. Paper 424-B*, p. B127-B129.
- Sussmilch, C. A., and David T. W. E., 1919, Sequence, glaciation, and correlation of the Carboniferous rocks of the Hunter River District, New South Wales: *Royal Soc. New South Wales Jour. and Proc.*, v. 53, p. 246-338.
- Wood, Alan, and Smith, J. A., 1957, The sedimentation and sedimentary history of the Aberystwyth Grits (Upper Llandoveryan): *Geol. Soc. London Quart. Jour.*, v. 114, pt. 2, p. 163-195. [1959]



ILLUSTRATIVE AND MAPPING TECHNIQUES

166. EDGE ISOLATION IN PHOTOGRAMMETRY AND GEOLOGIC PHOTOGRAPHY

By ALVA B. CLARKE, Washington, D.C.

A process called edge isolation has been devised which transforms a normal continuously toned photograph into a photodiagrammatic representation. The areas of a photograph containing gradual tonal variations are subdued or eliminated while abrupt changes in density are rendered as gray or black lines.

In order to produce edge-isolated photographs a special contact printer is needed, the essentials of which are a phosphor screen, a source of ultraviolet light, and a source of infrared light. Such a printer can be modified from one that is manufactured commercially for making aerial photographic prints. Basic to this photographic printing system is the phenomenon of photoluminescence, which is the property of certain substances (zinc sulfide, here) to absorb radiation of one wavelength and emit radiation of another wavelength. Absorption of ultraviolet radiation causes the phosphor to luminesce. The phosphor is inversely sensitive to infrared, however, so that exposure to this radiation causes a suppression of the luminescence.

Figure 166.1 is a schematic diagram of the printer components. The lamp (*UVL*) radiates a range of ultraviolet with a peak emission of 3,650 angstrom units, exciting the phosphor screen (*P*), which luminesces. The filter (*UVF*) absorbs the ultraviolet shorter than 4,000 angstrom units and transmits vis-

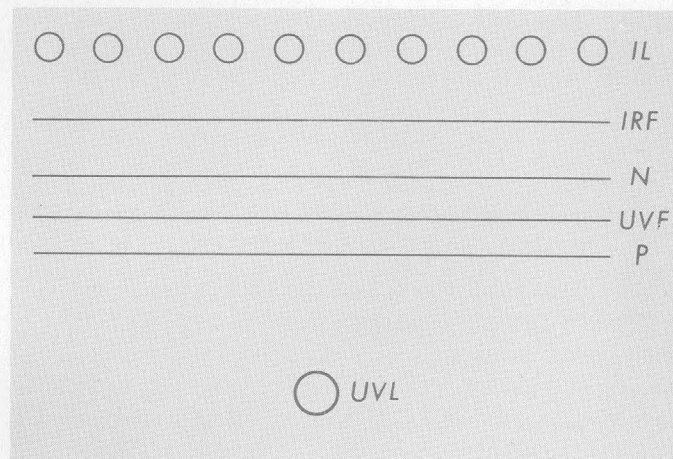


FIGURE 166.1.—Schematic diagram of the printer components.

ible light. The filter (*IRF*) transmits infrared beyond the visible range emanating from the incandescent lamps (*IL*), quenching luminescence from the phosphor screen (*P*). Thus, the quenching action through a negative (*N*) converts the phosphor screen into a point-to-point image-modulated light source.

A further aspect of the system, relative to the formation of outlines, is the manner in which abrupt changes in density are affected. Four factors determine when line formation will occur, and the ultimate

*A**B*

FIGURE 166.2.—*A*, Normal contact print of aerial photograph; *B*, edge-isolated print.

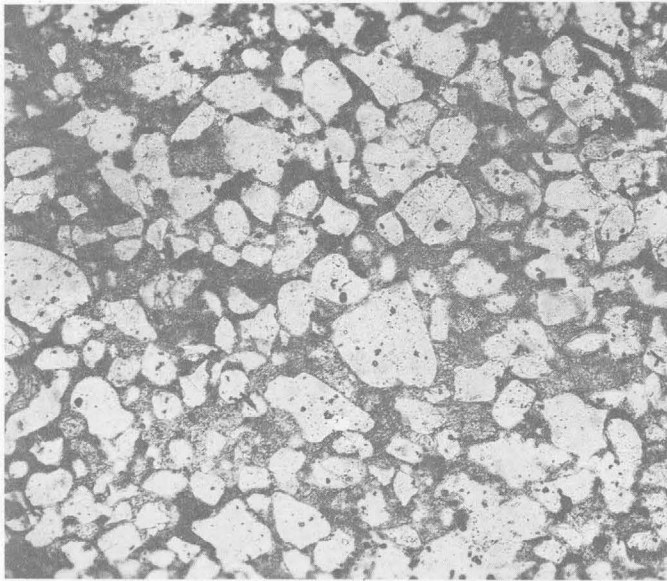
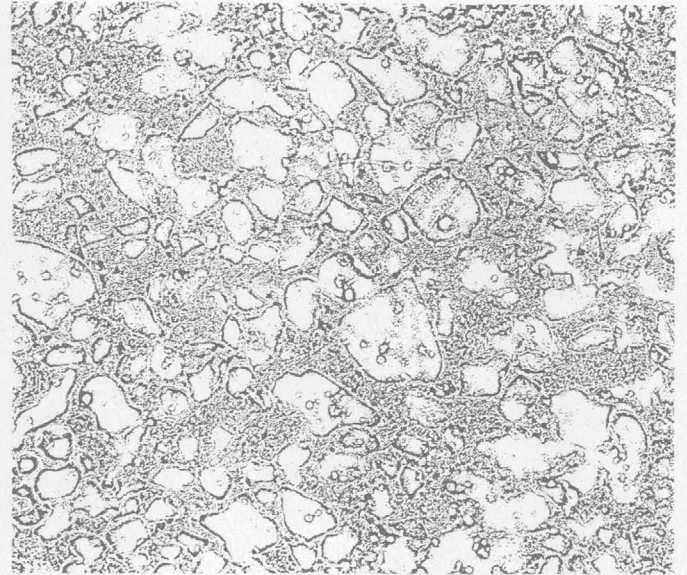
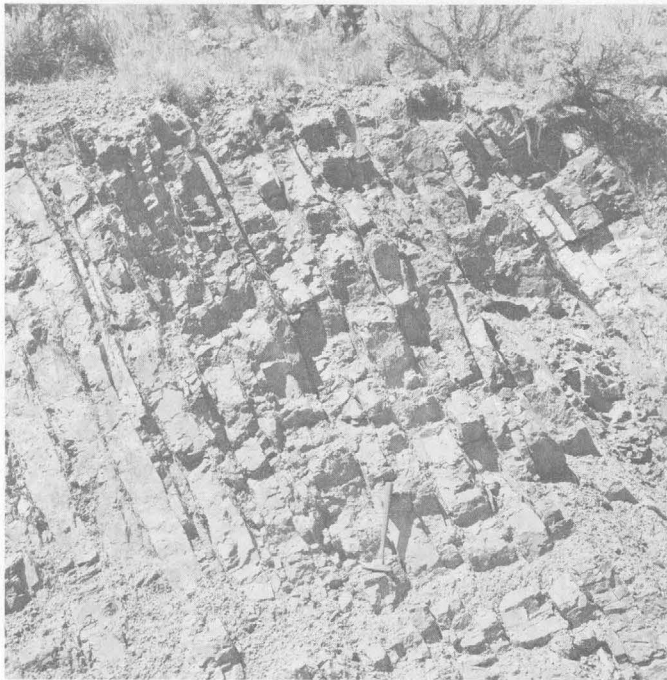
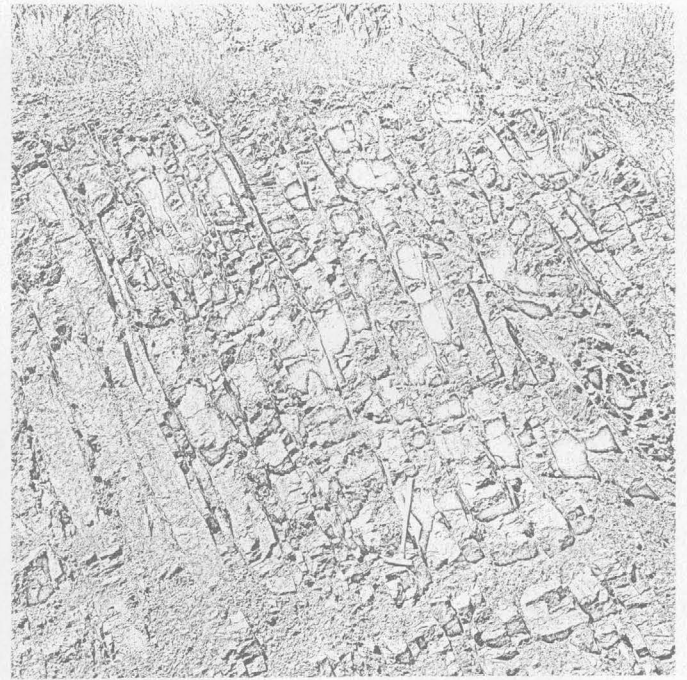
*A**B**C**D*

FIGURE 166.3.—*A*, Normal contact print of petrographic thin section; *B*, edge-isolated print. *C*, Normal contact print of rock outcrop; *D*, edge-isolated print.

width of the lines. They are (1) the distance over which the density change takes place (sharpness), (2) the amount of separation between the negative and the phosphor screen, (3) the contrast characteristics of the negative, and (4) the degree of development (gamma) given the intermediate film positive and negative. When unexposed film is placed in contact with the negative and exposed simultaneously to the luminescence from the phosphor screen and infrared from the quenching lamps, there occurs across the image edges, due to separation of the negative from the phosphor screen, an interaction of diffusion from each source of energy. After development, a line of increased density appears in juxtaposition to a line of decreased density, demarking the borders of the image. The effect produced is quite similar to the border effects of normal development, but greatly exaggerated. The effect persists over a wide range of density fluctuations on the original negative. By manipulation of the four factors outlined above it is possible to achieve any degree of edge enhancement, with or without an intermediate tone.

The procedure followed for transforming a continuous-tone negative into an edge-represented copy is much the same as that for any negative duplication process. The negative is printed on a suitable stable-base negative film, the characteristics of which are dictated by the density and contrast of the original negative and the purpose for which the result is intended. The quenching action of the infrared modulates the emission of luminescence from the phosphor screen, and upon development in a moderately contrasty developer the result is a film positive with two degrees of contrast. The continuous tone is now depicted as neutral gray bounded by narrow clear and dark lines. After processing and drying, the film

positive is placed in the printer and a negative made from it. Higher or lower contrast is obtained by varying the developer for this negative. Extremely high contrast for making pressplates or for use with other photomechanical processes is possible by developing the negative in a caustic developer, while maximum detail is retained by development in a medium-contrast developer of the type used for commercial photography.

Information in edge-isolated photographs is in a form that is in many ways more useful than in normal-perspective photographs. The geometry of the photograph is not altered, as is seen in figure 166.2. The prints can be used for stereoscopic analysis, rectification, and photomosaics, and they can be published as illustrations without using a halftone screen. Orthophotographs made with the edge-isolation technique show buildings, roads, woodlands, drainage, and other features by line images in true position. Research is being directed toward the use of this type of photoimagery in the production of standard planimetric-map substitutes. Patterns useful to geologists are often more easily identified in edge-isolated photographs than on continuous-tone photographs. The technique promises to be useful not only as an analytical tool but also as a means of preparing scientific illustrations for which an accurate line image or sketch serves better than a photograph to illustrate features of interest. It is a quick and inexpensive means, for example, of preparing faithful camera-lucida-like diagrams of petrographic thin sections (fig. 166.3A, *B*) or drawings of fossils, sketches of rock outcrops (fig. 166.3C, *D*), and perspective drawings illustrating geologic or physiographic relations from photographs or from oblique aerial photographs.



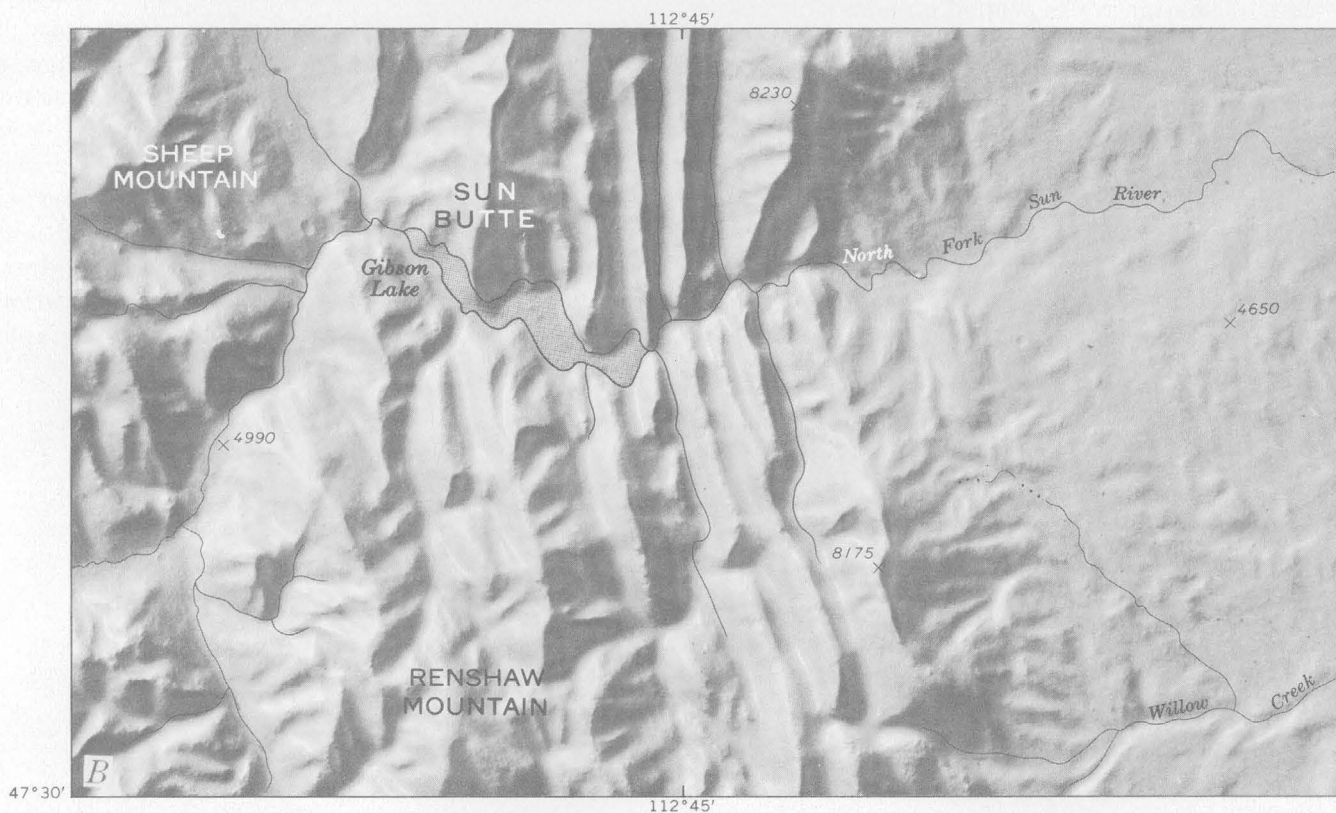


FIGURE 167.1.—A, View showing printed side of relief map. B, Identical area shown in A, but photographed from reverse side, with simplified overlay added.

167. SHORTCUT METHOD FOR THE PREPARATION OF SHADED-RELIEF ILLUSTRATIONS

By JOHN R. STACY, Denver, Colo.

Shaded-relief diagrams are a valuable adjunct to technical reports concerned with areal mapping or terrain interpretation. Such diagrams afford the reader a quick 3-dimensional impression of topographic details not otherwise readily obtained.

In the past some authors have constructed, then photographed, detailed terrain models. On occasion, the talented services of expert modelmakers have been employed. The relatively high cost for these services, however, has been a chief deterrent to their widespread use. More commonly, freehand pen and ink or airbrush drawings have been used.

A new technique now being used by the Branch of Technical Illustrations, Denver, provides excellent and inexpensive 3-dimensional illustrations for publication, for any area covered by the plastic raised-relief maps available from Army Map Service, Corps of Engineers.

A photograph of a plastic relief map as usually viewed produces an undesirable array of illegible culture intermixed with lights, shadows, wooded areas, etc., as shown in figure 167.1A. A shaded-relief

base can be prepared from the same plastic model by photographing the reverse side of the model with the light source directed from the southeast rather than the usual northwest, turning over the reverse-reading negative thus produced, and making a print. Figure 167.1B is a base map of the same area as figure 167.1A prepared by this procedure. When both sides of the model are photographed at the same scale, the photograph of the printed side (fig. 167.1A) can be used as base copy for compilation of a simplified overlay showing desired features such as coordinates, spot elevations, towns, and drainage (fig. 167.1B). Minor adjustments in drainage may be necessary to compensate for slight distortions caused by the molding process.

AMS plastic-relief maps at a scale of 1:250,000 are now available for approximately 40 percent of the United States. The maps are particularly useful at this scale for the preparation of illustrations for regional physiographic studies, index maps, and so forth. Effective lantern slides and stereopairs are also quickly obtainable with this method.



HYDROLOGIC STUDIES

GROUND WATER

168. WINTER GROUND-WATER TEMPERATURES ALONG THE MULLICA RIVER, WHARTON TRACT, NEW JERSEY

By E. C. RHODEHAMEL and S. M. LANG, Trenton, N.J.

Work done in cooperation with the New Jersey Division of Water Policy and Supply

Winter ground-water temperatures were measured at a test site along the Mullica River as part of an investigation of ground-water movement in the Wharton Tract (fig. 168.1), a State-owned water reserve. The temperature data were used in an effort to improve the understanding of the mechanism by which water is added to the zone of saturation.

Previous reports by the Geological Survey have described the well field and the geology and hydrology at the test site. Using tritium as a tracer, Carlston and others (1960) showed a distinct layering of ground water and that most of the discharge to the Mullica River was by lateral flow of ground water at the top of the zone of saturation. Lang (1961) and

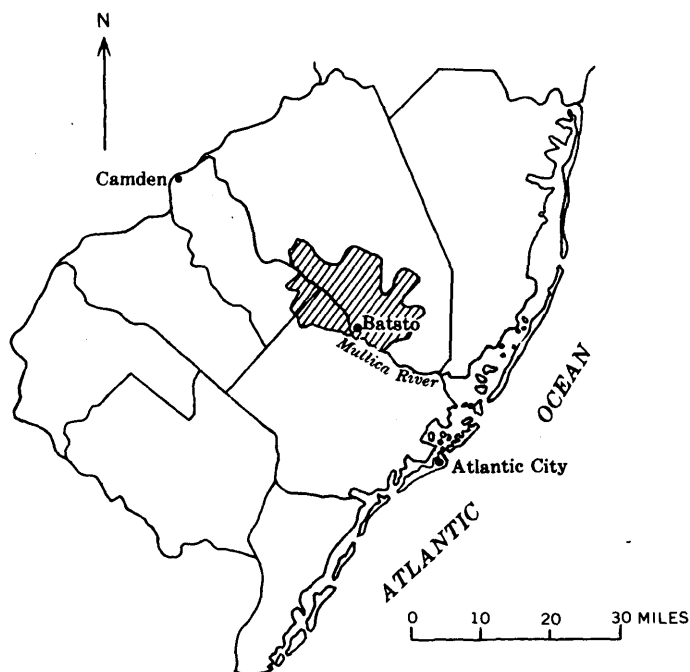


FIGURE 168.1.—Map of southern New Jersey showing location of Wharton Tract (crosshatched).

Lang and Rhodehamel (1962) confirmed this general pattern of ground-water movement by detailed studies of head distribution. The general movement is from the upland areas on either side of the river to the stream; the major ground-water discharge area is in the northern part of the site near the confluence of the river and its tributary from the west. Ground-water head—measured on February 20, 1962, prior to collection of temperature data—showed that the winter flow pattern (recharge period) was almost the same as that described by Lang (1961) for a summer flow pattern (nonrecharge period), except that the water levels were about 0.4 foot higher during the winter.

Measurements of ground-water temperature and piezometric head were made in February 1962 in 1¼-inch-diameter wells installed in groups of 3 to depths of about 25, 50, and 100 feet. Observation-well sites were at intersections of a rectangular location grid numbered from 1 to 9 from west to east, and lettered from A to N from south to north.

All the wells were pumped with a pitcher pump until the water temperature stabilized and temperatures were measured with a rapid-registering mercury thermometer calibrated to 0.1°F. Lines of equal ground-water temperature were drawn at a 0.5°F interval for the shallow, medium, and deep zones and are shown in figures 168.2, 168.3, and 168.4, respectively.

Figure 168.2 shows that the late-February pattern of temperature distribution in the shallow zone was highly complex. A U-shaped region of relatively cold water was found, the coldest water being in the vicinity of well 2E. The arms of the U extended eastward toward the Mullica River in the central and southwestern parts of the test site. East of the river the temperature distribution was relatively uniform.

Figure 168.3 indicates a less complicated pattern of temperature distribution in the medium-depth zone as compared to that in the shallow zone. The dominant temperature feature here was the irregularly circular pattern in the west-central part of the test site. The least complex pattern is shown in figure 168.4 for the deep zone, where again the dominant feature is a circular area of lower temperatures in the western part of the test site.

Cold surface water (34°F) in the swamp along the west border of the test site was observed to overflow, between wells 2C and 2B (fig. 168.2), into the channel of an ephemeral stream from which water was observed to seep into the ground. Overflow from the

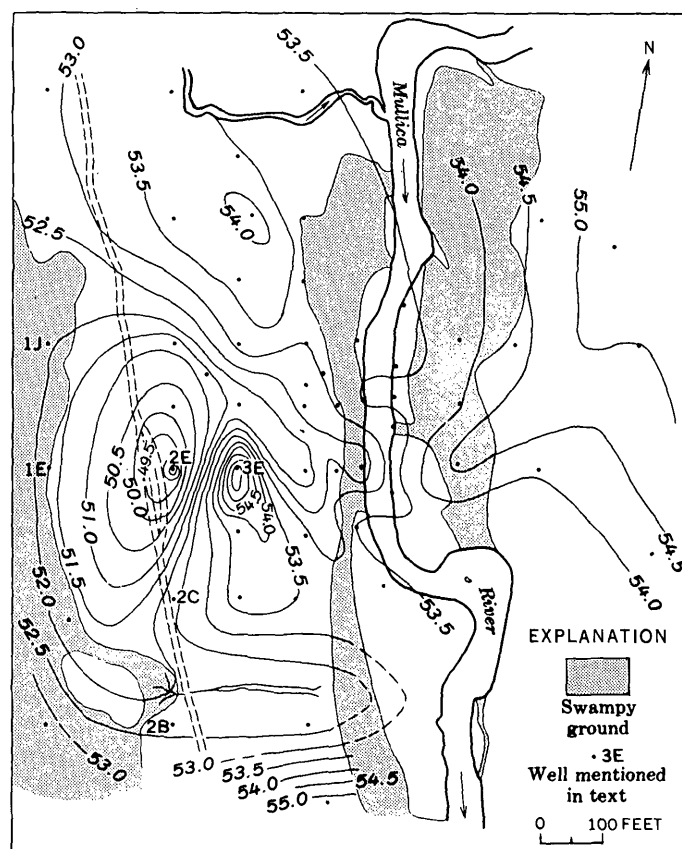


FIGURE 168.2.—Map of the Wharton Tract test site showing lines of equal ground-water temperature in the shallow water-bearing zone (25 feet) in late February 1962. Interval 0.5°F.

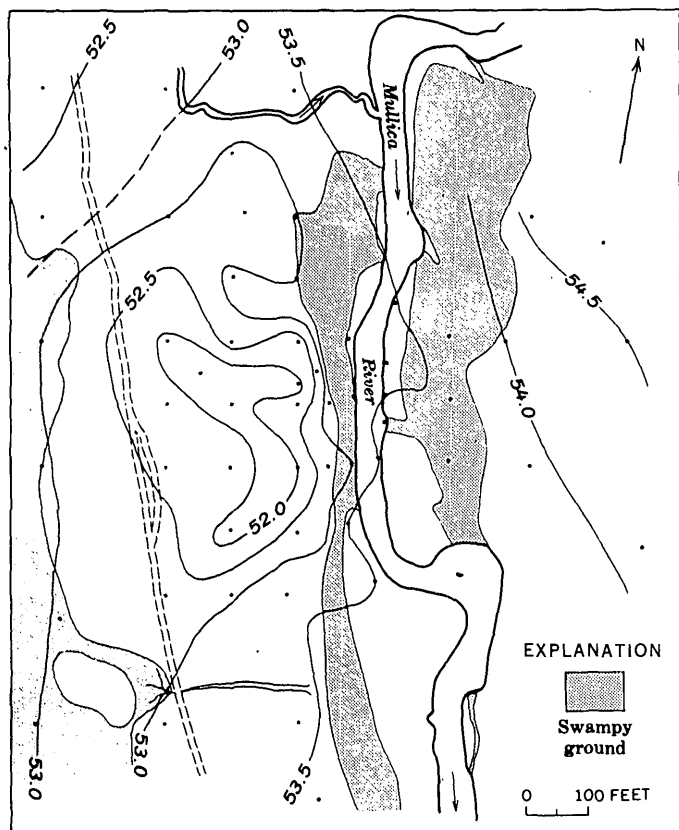


FIGURE 168.3.—Map of the Wharton Tract test site showing lines of equal ground-water temperature in the medium-depth zone (50 feet) in late February 1962. Interval 0.5°F .

swamp between wells 1J and 1E drained into a small area about 25 feet southwest of 2E, where it sank into the ground.

The temperature distribution in the shallow zone was affected directly by the concentrated recharge of cold water. However, vertical leakage between zones, which was demonstrated previously on the basis of head differentials (Lang, 1961), also was indicated by the enclosed areas of lower temperatures in the medium-depth and deep zones. The enclosed area of lower temperature in the medium zone was displaced northeastward from the area of recharge near well 2E and also displaced northeastward from the center of cold water in the shallow zone. This displacement is due to the combined effect of greater horizontal than vertical permeability and the head distribution within the zone. The cold water beneath the ephemeral stream in the southwestern part of the test site did not affect the ground-water temperatures in the medium and deep zones, for the interzonal ground-water movement near the stream was vertically upward from the deep to the medium and to the shallow zone, as indicated by the head measured in the wells prior to the temperature measurements.

The high-temperature water in the shallow zone near well 3E probably represents a body of older water not influenced by the winter cold-water recharge. Because temperatures were lower in the medium and deep zones it is suggested that a shallow layer of clayey material prevents direct downward percolation of water from the 25-foot zone.

During the period of temperature measurements there was no recharge to the aquifer east of the river. Water in the various zones in this part of the test site was of relatively uniform temperature, indicating adjustment to the geothermal gradient.

The principal conclusions from the temperature measurements are that recharge to the zone of saturation can be detected by temperature measurements, but temperature data alone cannot be relied upon to trace the movement of ground water within the test site; that details of the ground-water movement shown by the head distribution within the various depth zones, and details of leakage suggested by the differences in head between zones, are corroborated by temperature measurements in parts of the test site; and that, because the horizontal permeability is greater

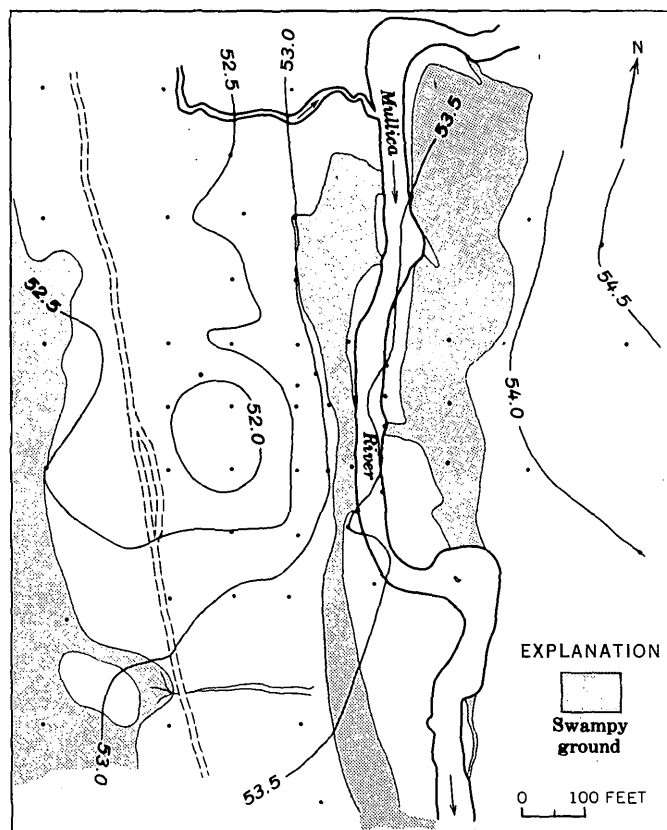


FIGURE 168.4.—Map of the Wharton Tract test site showing lines of equal ground-water temperature in the deep zone (100 feet) in late February 1962. Interval 0.5°F .

than the vertical permeability, the movement of ground water is dominantly horizontal, which appears to be the factor responsible for the layering effect previously described by Carlston and others (1960).

REFERENCES

- Carlston, C. W., Thatcher, L. L., and Rhodehamel, E. C., 1960, Tritium as a hydrologic tool—The Wharton Tract study: Internat. Assoc. Sci. Hydrologists Comm. Subterranean Waters Pub. 52, p. 503–512, 4 figs.
- Lang, S. M., 1961, Natural movement of ground water at a site on the Mullica River in the Wharton Tract, southern New Jersey: Art. 313 in U.S. Geol. Survey Prof. Paper 424-D, p. D52–D54.
- Lang, S. M., and Rhodehamel, E. C., 1962, Movement of ground water beneath the bed of the Mullica River in the Wharton Tract, southern New Jersey: Art. 36 in U.S. Geol. Survey Prof. Paper 450-B, p. B90–B91.



169. RELATION OF PERMEABILITY AND JOINTING IN CRYSTALLINE METAMORPHIC ROCKS NEAR JONESBORO, GEORGIA

By J. W. STEWART, Atlanta, Ga.

Considerable information is available on the movement of ground water in the crystalline rocks of the Piedmont physiographic province in the Southeastern States in the zone tapped by water wells. It has generally been thought that the permeability of the crystalline rocks, due mainly to jointing, decreases almost to zero within a few hundred feet of land surface. Ellis (1909, p. 68–69) stated that “* * * the greater the depth the greater must be the tendency of joints to close, owing to increased pressure * * *.” The possibility of storage of gas underground in caverns excavated in the crystalline rocks led to exploration which shows that appreciable movement of water can take place in gneiss to depths as great as 500 feet.

The feasibility of underground storage of gas at a site near Jonesboro, Ga., about 15 miles south of Atlanta, was investigated in 1961 by the Transcontinental Gas Pipe Line Corp., of Houston, Tex. Five core holes were drilled in a body of gneiss identified on the State geologic map of the Georgia Geological Survey [1939] as biotite gneiss and schist of the Carolina Series of probable Precambrian age.

The holes were spaced at distances of 0.2 to 0.4 mile and were cored to depths ranging from 490 to 509 feet. Three of the cored holes were 1 $\frac{1}{16}$ inches in diameter and two were 2 $\frac{1}{8}$ inches in diameter. The altitude of land surface at the test site ranged from about 840 to 940 feet above sea level. All the holes penetrated gneiss, ranging in composition from quartz-feldspar gneiss to hornblende-biotite gneiss (fig. 169.1). Schistose-biotite gneiss was penetrated in two

holes and jointed zones were noted at several depths in all five holes. The chief rock type was a quartz-biotite-feldspar gneiss. The crystalline rocks are overlain by a thick blanket of saprolite derived from their deep weathering. The dip of schistosity in the area is about 25° S. 30° E.

Cores were taken at selected intervals, shown on figure 169.1, for permeability and porosity tests. Upon completion of coring, formation pressure tests were made by packing off 12-foot intervals in the holes and injecting water into the packed-off intervals for a period of 15 minutes under a pressure of 100 psi (pounds per square inch).

The formation pressure tests were made with double pneumatic packers sealed with dry nitrogen at pressures ranging from 400 to 600 psi, although in 1 test hole the minimum packer pressure was 290 psi. Dry nitrogen was used to apply a constant pressure on each test section by means of a $\frac{3}{4}$ -inch connector pipe leading to the formation interval being tested. The hydrostatic pressure maintained in each test interval was in addition to the static pressure in the hole. The bottom-hole pressure was maintained at 216 to 326 psi, or about a minimum of 1 $\frac{1}{2}$ times the working pressure of the proposed cavern. The quantity of water injected into the formation for each section tested was determined by means of a water-feed measuring device on the tank. Results in terms of water loss per minute during the tests are shown graphically on figure 169.1. The field and laboratory tests were made under the supervision of Fenix Scisson, Inc., Tulsa, Okla.

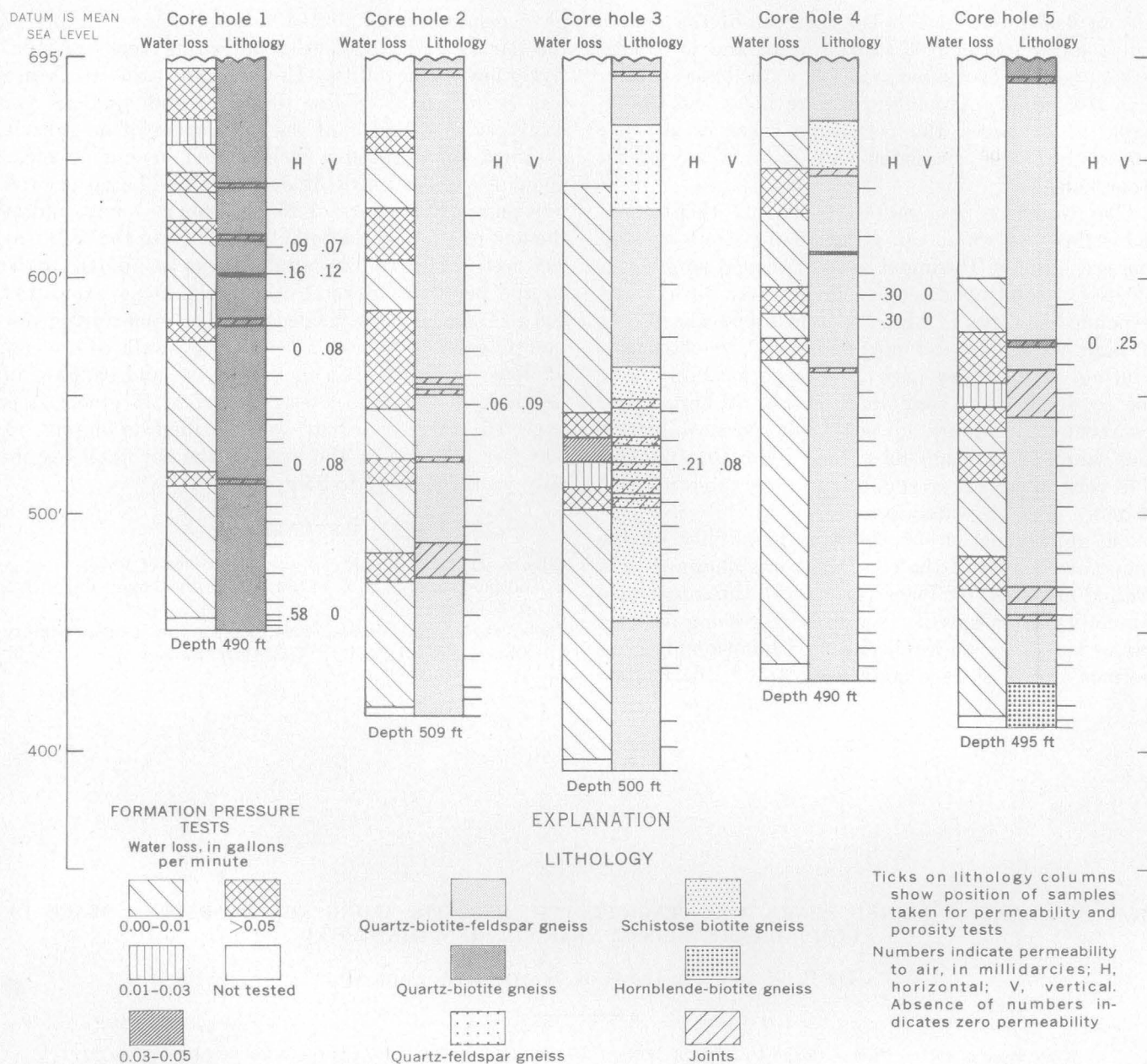


FIGURE 169.1.—Lithologic logs and results of formation pressure tests, and laboratory tests of crystalline metamorphic rocks, Jonesboro, Ga.

Permeability-to-air tests were made in the laboratory by placing core sections in rubber sleeves and maintaining a pressure differential of 50 psi for 1 minute across the sample. Determinations were made of both horizontal and vertical permeability. A permeability of 0 was assigned those cores through which no air flowed during the 1-minute period. The porosity was calculated by a comparison of the dry weight, saturated weight, and bulk volume of the samples.

The laboratory tests indicated 0 permeability for most samples. All tests indicating greater than 0

permeability are shown on figure 1. Porosity values for most samples (not shown in figure 169.1) were less than 1 percent; only 2 samples, from 458 feet and 613 feet in core hole 1, were significantly higher, 1.28 and 1.26 percent, respectively.

The total footage tested in each core hole during the formation pressure tests ranged from 185 to 244 feet. In 5 holes about 60 to 85 percent of the total sections tested showed water losses ranging from 0 to 0.01 gpm (gallons per minute); in 3 holes 4 to 10 percent of the sections had water losses ranging from

0.01 to 0.03 gpm; in 1 hole 4 percent of the section had a water loss of 0.03 to 0.05 gpm; and in 5 holes 8 to 40 percent of the sections had water losses greater than 0.05 gpm. Although all core holes had appreciable water losses, the permeable zones in any one hole could not be correlated with those of any of the other holes.

The formation pressure tests indicate that appreciable flows of water can occur in the dense crystalline rocks of the Piedmont even at depths as great as 500 feet. Jointing noted in cores nearly always corresponded to zones of high water loss, but many zones of high water loss did not correspond to observable jointing. Laboratory tests of core permeability were not as definitive. Tests in intervals of high water loss commonly indicated negligible permeability in core samples, although most tests indicating measurable permeability corresponded to observable jointing or zones of high water loss.

An approximation of the transmissibility of the gneiss at the site of the core holes was obtained by a method described by Theis (1954) of estimating transmissibility from specific capacity. By using a water loss of 0.05 gpm, a pressure head of 100 psi on the test sections, and a storage coefficient of 10^{-4} , the method

gave results which plotted below the lower limits of the curves given by Theis, indicating rocks of relatively low permeability. However, the transmissibility was estimated to be less than 100 gpd (gallons per day) per foot, and is of the same order of magnitude obtained for a 400-foot well drilled in similar rocks about 9½ miles north of Jonesboro. The latter well was pumped at a rate of 25 gpm for 24 hours, and at the end of the test the total drawdown in the well was 295 feet. The transmissibility was computed to be 45 gpd per foot. Several other wells in the same area 300 to 750 feet deep yielded 24 to 48 gpm during test pumping for 24 hours. In addition, 5 wells of the city of Jonesboro drilled in biotite gneiss, and ranging in depth from 200 to 370 feet, yield 7 to 18 gpm. It is expected, therefore, that wells drilled to depths of 500 feet or more in the area of the core holes probably would yield 10 to 25 gpm.

REFERENCES

- Ellis, E. E., 1909, A study of the occurrence of water in crystalline rocks: U.S. Geol. Survey Water-Supply Paper 232, p. 54-101.
Theis, C. V. and others, 1954, Estimating transmissibility from specific capacity: U.S. Geol. Survey open-file rept., 11 p.



170. AQUIFERS IN BURIED SHORE AND GLACIOFLUVIAL DEPOSITS ALONG THE GLADSTONE BEACH OF GLACIAL LAKE AGASSIZ NEAR STEPHEN, MINNESOTA

By R. W. MACLAY and G. R. SCHINER, St. Paul, Minn.

Work done in cooperation with the Division of Waters, Minnesota Department of Conservation and the Village of Stephen, Minnesota

Beach and glaciofluvial deposits are the principal sources of ground water in the basin of glacial Lake Agassiz; the clayey lacustrine deposits yield little water, and the underlying bedrock aquifers generally yield highly mineralized water. In the Halma-Lake Bronson area, beach and lake sand mantle productive aquifers in the underlying outwash deposits. Similar shore deposits in the Stephen area are covered by silty lacustrine clay, but will yield moderate quantities of water. The trend of these buried deposits is reflected locally by low linear mounds that parallel the Gladstone beach line of Upham (1896, p. 463). Recogni-

tion of these subdued topographic expressions of buried beach deposits was of great assistance in locating test holes, in which substantial supplies of ground water for municipal use in the Stephen area were discovered.

The floor of glacial Lake Agassiz may be divided on the basis of physiography and geology into two subareas along a line extending through Argyle and Stephen (fig. 170.1). In the western subarea the surface slopes westward about 5 feet per mile and is underlain by lacustrine silty clay and dense clay. In the eastern subarea the surface slopes about 20 feet per

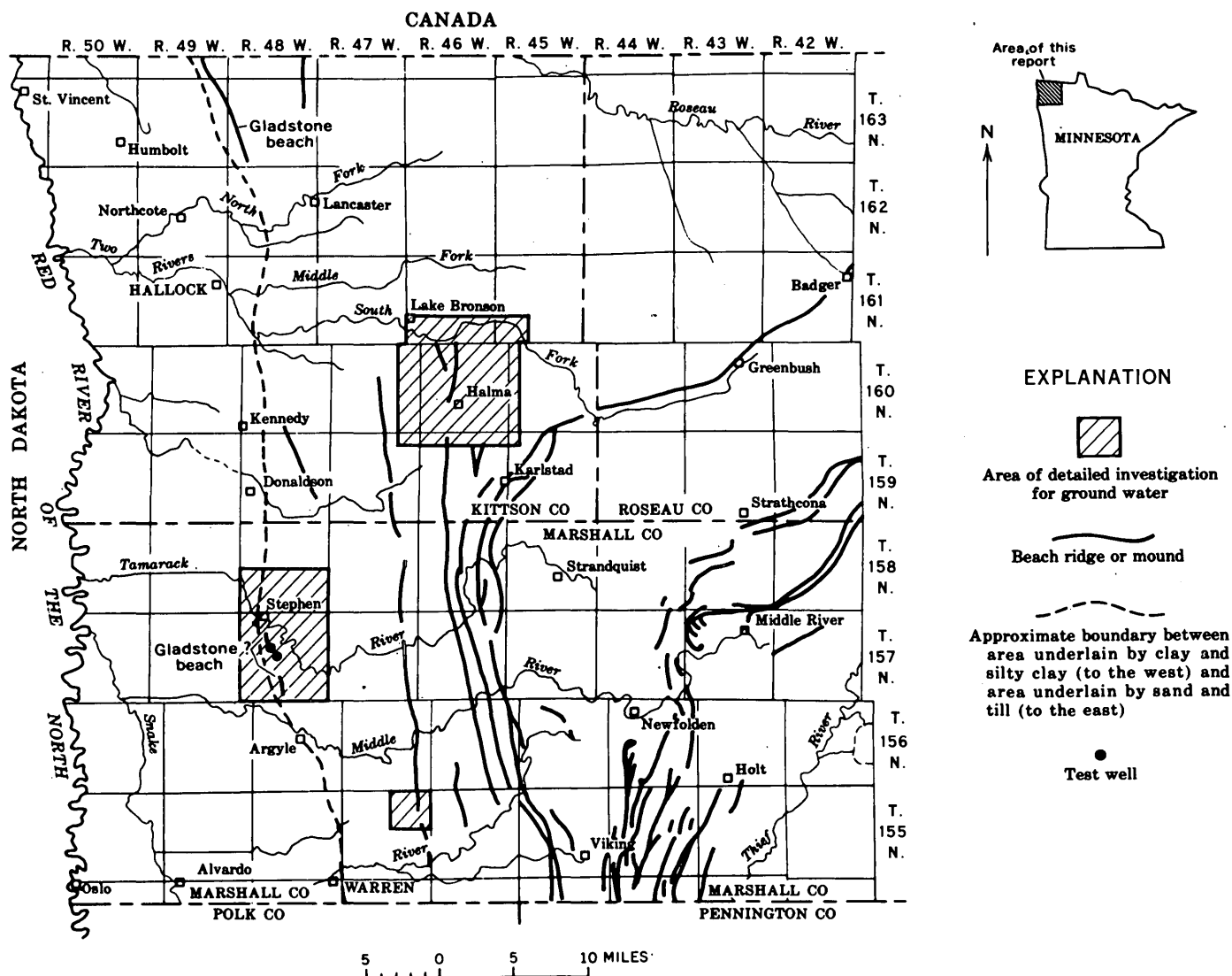


FIGURE 170.1.—Map of northwestern Minnesota showing areas of ground-water investigations and trends of several beaches of glacial Lake Agassiz.

mile westward and is underlain by lacustrine silty clay, lake-washed till, and shore and glaciofluvial deposits. The surface of the eastern subarea is characterized by a series of gentle north-trending beach ridges. The boundary between the eastern and western subareas is transitional, but in most places it is marked by a belt of discontinuous mounds or by a slight steepening toward the east.

Most of the Stephen area is mantled by clayey lacustrine deposits. Several test holes were drilled in search of beach and glaciofluvial deposits, and sandy glaciofluvial deposits about 20 feet thick were penetrated below 5 to 10 feet of lake clay near Argyle. These deposits had no topographic expression; however, they lie approximately in line with the trend of the Gladstone beach and could be traced northward

along the trend of the Gladstone beach between Argyle and Stephen. Samples from some auger holes indicate an upper sand unit of well-sorted fine- to coarse-grained quartzose sand over less well sorted glaciofluvial deposits, which consist largely of sand but also contain silt, gravel, and clay lenses (fig. 170.2). In some places the glaciofluvial deposits are missing and the upper sand unit rests on sandy clay till.

The upper sand unit presumably is a beach deposit that was reworked from the glaciofluvial deposits. Auger logs indicate that in the Stephen area as much as 70 feet of permeable glaciofluvial deposits underlie the beach deposits. All these beach and glaciofluvial deposits are covered by lacustrine clay, which probably was deposited during a lake transgression after the Gladstone beach was formed.

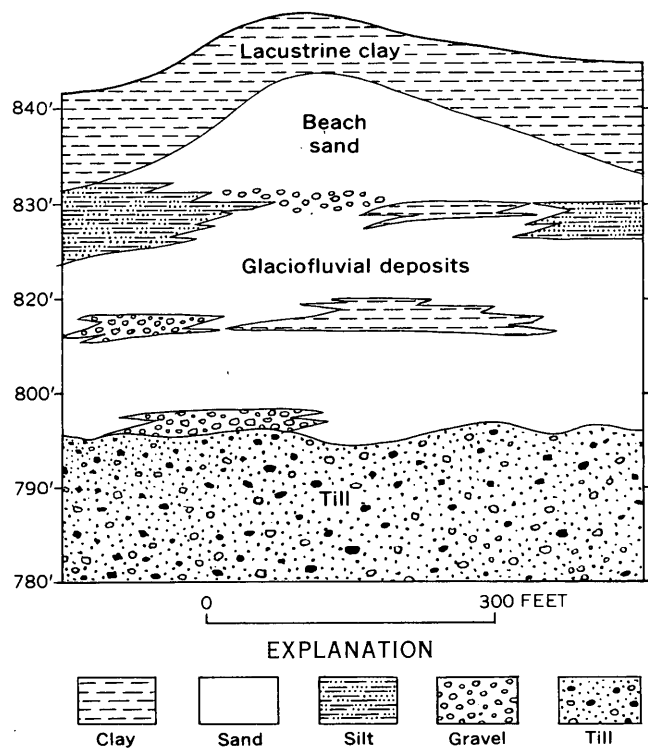


FIGURE 170.2.—Generalized section across buried beach ridge near Stephen, Minn.

Ground water in the buried beach and glaciofluvial deposits in the Stephen area is confined by the lacustrine clay. Water levels in most auger holes rose quickly in the overlying clay to within 5 to 15 feet of the land surface. Most of the recharge to the confined deposits probably occurs on the mounds where the overlying clay is silty.

Two auger holes were cased with 2-inch pipe and pumped with a centrifugal pump to test the water-bearing capacity of the beach and glaciofluvial deposits. One well, equipped with a 2-foot screen extending to 27 feet, yielded 25 gpm (gallons per minute) for 2 hours from a clean fine- to coarse-grained sand. The second well tapped a similar sand but was not equipped with a screen. The pipe was suspended from the ground surface and hung free in an open hole; the well was pumped at 80 gpm for 4 hours with no noticeable decline in production.

Most of the deeper aquifers in the Stephen area contain highly mineralized chloride water. In general, water from the shallow outwash and beach deposits is less mineralized and has a lower chloride content than water from deeper aquifers, although there is much variation in the quality of water. Field analyses suggest that the chloride content of water from the glaciofluvial deposits is lowest in areas where the clay cover is thin and recharge occurs by infiltration through the clay. Water from the well where the clay cover was only about 10 feet thick contained about 30 ppm (parts per million) of chloride, and water from the other well, where the clay cover was about 16 feet thick, contained about 280 ppm of chloride.

SELECTED BIBLIOGRAPHY

- Schiner, G. R., 1962, Ground-water exploration and test pumping in the Halma-Lake Bronson area, Kittson County, Minnesota: U.S. Geol. Survey open-file rept.
- Upham, Warren, 1896, The glacial Lake Agassiz: U.S. Geol. Survey Mon. 25.



171. POTENTIAL YIELD OF DEEP WATER WELLS IN THE SOUTHERN PART OF THE JICARILLA APACHE INDIAN RESERVATION AND VICINITY, SAN JUAN BASIN, NEW MEXICO

By ELMER H. BALTZ, S. W. WEST, and S. R. ASH, Albuquerque, N. Mex.

Work done in cooperation with the Jicarilla Apache Tribe

Subsurface geologic information from oil and gas tests suggests that large supplies of ground water for irrigation could be obtained from wells tapping consolidated Upper Cretaceous and Tertiary rocks in the southern part of the Jicarilla Apache Indian Reservation and vicinity, southeastern San Juan Basin, N. Mex. In favorable locations yields of as much as 3,500 gpm (gallons per minute) appear possible; at present few wells in northwestern New Mexico yield more than 300 gpm.

The southern part of the Jicarilla Apache Indian Reservation and the adjacent region to the south and east (fig. 171.1) include an area of about 1,300 square miles in the east-central part of the San Juan Basin. The Upper Cretaceous and Tertiary rocks of this region consist of complexly related sandstone and shale facies, which were studied by detailed surface mapping and by subsurface correlation based on electric logs of wells drilled for oil and gas. The distribution and thickness of potential sandstone aquifers were deter-

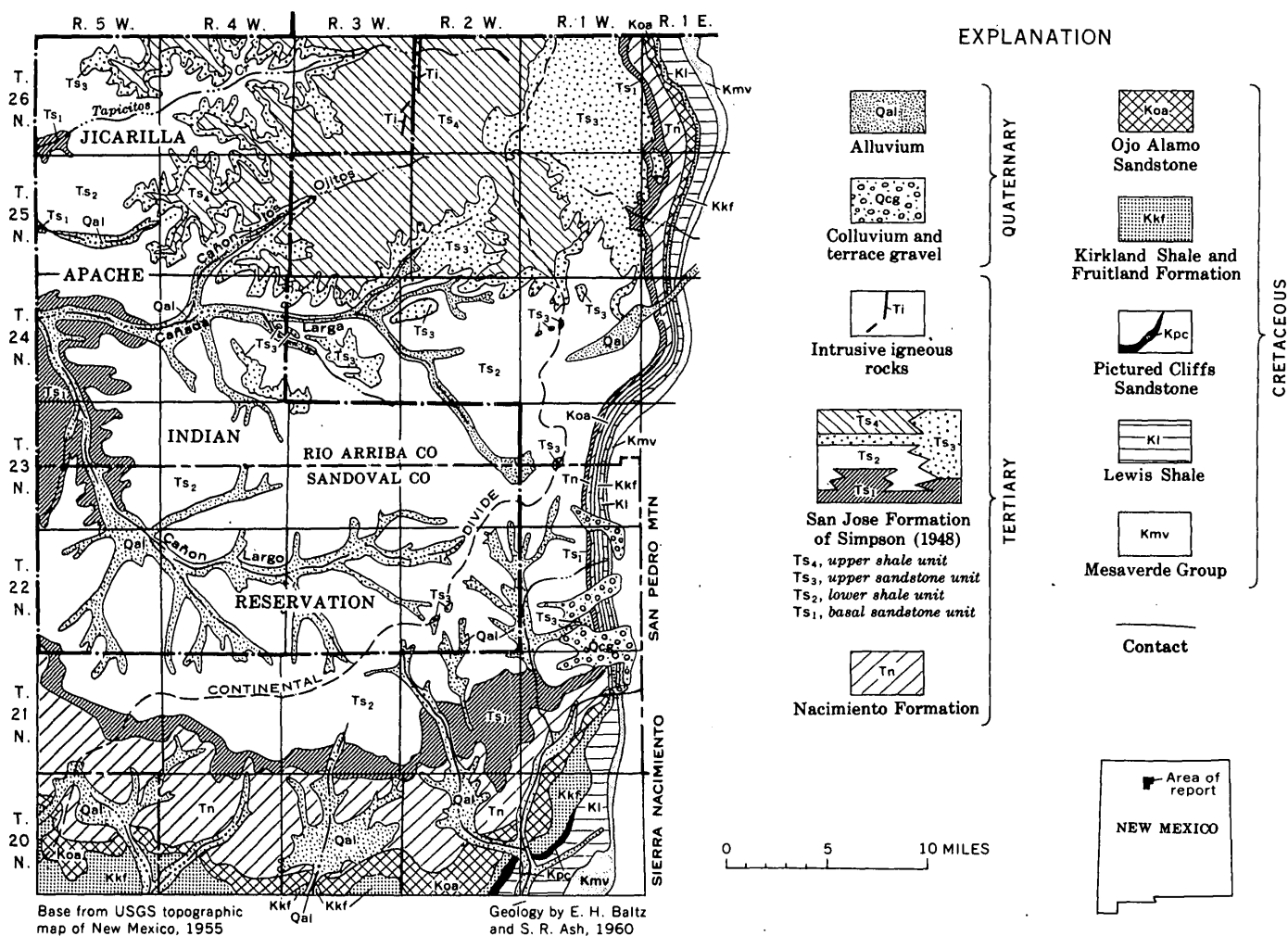


FIGURE 171.1.—Generalized geologic map of the southern part of the Jicarilla Apache Indian Reservation and vicinity, San Juan Basin, N. Mex.

mined, and the potential yield of deep water wells in the reservation was estimated.

The oldest rocks mapped are those of the Mesaverde Group of Late Cretaceous age (fig. 171.1). Other Upper Cretaceous rocks mapped include, in ascending order: the Lewis Shale, the Pictured Cliffs Sandstone, the undivided Fruitland Formation and Kirtland Shale, and the Ojo Alamo Sandstone. The Ojo Alamo Sandstone, which ranges in thickness from 70 to 200 feet, is the deepest aquifer from which large amounts of potable water may be expected in most of the area.

Rocks of Tertiary age include, in ascending order, the Nacimiento Formation, the San Jose Formation of Simpson (1948), and several igneous dikes. The Nacimiento Formation of Paleocene age ranges in thickness from 540 feet in the east-central part of the area to 1,750 feet in the north-central part. In the southern half of the area, the Nacimiento consists mostly of shale with a few intercalated beds of sandstone, and it does not yield water to wells. In the northern half of the area, the Nacimiento consists of shale and thick beds of sandstone which yield potable water to wells at a few places. These sandstone beds locally constitute more than half of the Nacimiento Formation and may be feasible sources of large supplies of water from deep wells.

The San Jose Formation of Eocene age ranges in thickness from 200 to 750 feet in the southern part of the area to 1,800 feet in the northern part. Four lithologic units of the San Jose were mapped: a basal sandstone unit, mostly conglomeratic arkosic sandstone ranging in thickness from 40 to 780 feet; a lower shale unit containing interbedded thick to thin sandstone and ranging in thickness from 400 to 800 feet in the southern part of the area to 1,640 feet in the east-central part; an upper sandstone unit, consisting mainly of conglomeratic arkosic sandstone as much as 1,300 feet thick; and an upper shale unit, consisting of red shale and interbedded thin to thick sandstone. Sandstone beds in all the units of the San Jose yield water to wells, and the thick sandstones of the basal sandstone unit and the upper sandstone unit may be practical sources of large amounts of water from deep wells in parts of the area.

Unconsolidated colluvium and gravel of Tertiary (?) and Quaternary age cap several terraces and occur in stream channels and valleys. These deposits yield small supplies of potable water to wells and springs. Alluvial deposits of Quaternary age in the major valleys contain small amounts of water at many places.

The principal sources of recharge are precipitation and streamflow on outcrops of the aquifers in the

eastern and southern parts of the area, at altitudes of 7,000 to 8,000 feet. Ground water discharges from outcrops at lower altitudes, mainly in the western part of the area, but this water is dissipated largely by evapotranspiration. Investigations of the flow of the San Juan River northwest of the area indicate that the increment of ground-water discharge to that river is too small to detect.

Water in the Ojo Alamo Sandstone and the San Jose Formation varies widely in chemical quality. Some of the water is undesirable for irrigation owing to high concentrations of sodium relative to calcium and magnesium, and some of the water is undesirable for drinking because of a high sulfate content.

Small supplies of ground water, most of which is potable, can be obtained at depths of a few feet to a few hundred feet at most places throughout the area. Deep water wells have not been drilled, but the potential yield of deep wells will depend largely on the cumulative thickness of sandstone penetrated.

The specific capacity of 59 wells that tap sandstone aquifers in the San Juan Basin, including 8 in the area investigated, ranged from 0.0002 to 0.015 gpm per foot of drawdown per foot of sandstone penetrated. The average was 0.008 for the 8 wells, which penetrated only a few feet of saturated sandstone in different aquifers in the Ojo Alamo, Nacimiento, and San Jose Formations. The total cumulative thickness of sandstone below 200 feet—the assumed average depth to the water table—and above the base of the Ojo Alamo Sandstone ranges from 80 to 1,840 feet, and sandstone makes up 10 to 50 percent of the saturated section in 29 wells drilled for oil and gas. The total thickness of sandstone in the saturated zone above the base of the San Jose Formation ranges from a few to 840 feet, and sandstone makes up 20 to 60 percent of the saturated section. The most favorable place for developing large-capacity deep wells is in T. 25 N., R. 5 W., where the section consists of 50 to 60 percent sandstone.

Using the average specific capacity per foot of sandstone penetrated (0.008) of the 8 wells in the area, the calculated potential yield of a well in sec. 25, T. 25 N., R. 5 W., that tapped all the sandstone (600 feet total thickness) to the base of the San Jose Formation might be expected to be as much as 1,400 gpm at a drawdown of 300 feet, and a well that tapped all the sandstone (1,470 feet, total thickness) to the base of the Ojo Alamo Sandstone might yield as much as 3,500 gpm at the same drawdown. These calculated potential yields of deep wells warrant test drilling for irrigation supplies.

The composite water that would be produced from the Ojo Alamo, Nacimiento, and San Jose Formations probably would be suitable for irrigation with proper soil-management precautions, and would be suitable also for many types of industrial uses.

REFERENCE

- Simpson, G. G., 1948, The Eocene of the San Juan Basin, New Mexico: *Am. Jour. Sci.*, v. 246, pt. 1, p. 257-282; pt. 2, p. 363-385.



172. COMPACTION OF THE AQUIFER SYSTEM AND LAND SUBSIDENCE IN THE SANTA CLARA VALLEY, CALIFORNIA

By J. H. GREEN, Sacramento, Calif.

Land in the central part of the Santa Clara Valley, Calif., has been subsiding for many years as a result of pressure decline in the intensively pumped artesian aquifer system (Poland and Green, 1962). About 230 square miles of urban and agricultural land extending from Palo Alto and Niles to San Jose subsided at rates up to 0.3 foot per year between 1954 and 1960. Periodic releveing of bench marks throughout the area indicates two "bowls" of maximum subsidence since 1912; Sunnyvale, with a subsidence of 11 feet and San Jose, 7.4 to 9 feet. The subsidence is due to compaction of the aquifer system, which takes place as overburden load is transferred from the water to the sediments of the aquifer system as the artesian pressure is depleted.

Two 1,000-foot core holes were drilled in 1960, one at each center of maximum subsidence. Compaction recorders, of the type described by Lofgren (1961), were installed in these and other wells of shallower depth to measure the compaction within the deposits. The field installations show that the measured compaction is comparable to the observed subsidence.

Results of laboratory tests on cores, and records of changes in artesian pressure since 1915, were used to compute the compaction in the water-bearing deposits. The purpose of this article is to outline the procedure for computing the compaction, to present the results of the computation, and to compare computed compaction with subsidence observed from precise leveling.

METHOD OF COMPUTATION

The procedure for computing the compaction of aquifer systems as a result of water-level decline has been described more fully by Miller (1961), and is based on Terzaghi's theory of consolidation (1943).

The total thickness of unconsolidated deposits affected by the pressure decline is subdivided, on the basis of interpretation of electric logs, into a reasonable number of zones of relatively uniform lithology. For each zone a one-dimensional consolidation test is made of a representative core sample. Using values of specific gravity and dry density determined in the Denver Hydrologic Laboratory of the Geological Survey, the effective overburden stress (grain-to-grain load) on each zone is computed for several periods of artesian-pressure change. The compaction of each lithologic zone is then computed, using these values of effective stress, and using laboratory consolidation-test data for the same range of loads determined by the Earth Laboratory, U.S. Bureau of Reclamation, Denver, Colo.

The compaction that occurs in each zone is computed from the relationship

$$\Delta m = \frac{e_0 - e_1}{1 + e_0} m,$$

in which Δm = compaction, in feet, m = thickness of zone, in feet, and e_0 and e_1 are initial and final void ratios. The total aquifer compaction is equal to the sum of compaction of all zones subject to increase in effective stress.

In fine-grained deposits, compaction (and subsidence) does not take place immediately as the effective stress increases. In relatively impermeable clayey zones, many years may be required before escape of water permits the internal fluid pressure to reach equilibrium with that in contiguous beds of more permeable sand and gravel, which adjust quickly in response to pressure changes. Furthermore, a thick clayey zone containing thin sand stringers will compact more quickly than an equally thick clayey bed without interbedded

sand stringers, because the more permeable interbeds permit quicker escape of water from the clayey segments. The percentage of ultimate compaction for a specific number of years may be estimated by utilizing the consolidation coefficient (determined as part of the consolidation test) and Terzaghi's (1943) equation and graphs for computing compaction time.

Residual compaction, which results in lag of subsidence, is the ultimate computed compaction less the percentage of computed compaction for that number of years. The reliability of the computation of residual compaction depends largely on how representative the tested consolidation sample is of the entire lithologic zone. The total compaction computed for any load change should equal the land-surface subsidence for that same period of time. Thus the reliability of the computed compaction can be checked in areas where precise leveling data are available.

COMPACTION AT CORE HOLE 6S/2W-24C7

The table below shows the effective loading and computed compaction at core hole 6S/2W-24C7, at Sunnyvale.

The artesian system was divided into nine zones, each of relatively uniform lithology. The clay bed confining the artesian system lies between the depths of 150 and 185 feet, thus all compaction was assumed to occur in the 7 zones below 185 feet. It is only below the confining bed that the effective load varies owing to changes of artesian pressure.

The artesian-pressure decline used for the computations in the table was that recorded at well 6S/2W-25C1, 500-foot deep and about a mile south of the core hole. Cumulative effective loading on the individual zones was computed from this pressure decline for the years shown in the table, and for the ultimate effective load, assuming an artesian-pressure decline to atmospheric (depth to water, 185 feet) at some future date.

Effective loading and computed compaction at core hole 6S/2W-24C7

Zone depth (feet)	Effective load (psi)					Compaction (ft)				
	1915	1934	1954	1960	Ultimate ¹	1915-34	1934-54	1954-60	Lag as of 1960	1960-ultimate ¹
0-150										
150-185	129	129	129	129	129					
185-215	79	123	125	130	159	0.70	0.04	0.08	0.01	0.36
215-415	93	137	139	144	173	3.40	1.11	.37	1.01	2.6
415-550	184	228	230	235	264	1.06	.45	.17	.49	1.1
550-680	248	292	294	299	328	.40	.22	.06	1.17	.92
680-800	309	353	355	361	389	1.04	.29	.12	.18	.91
800-905	362	406	408	413	442	.84	.20	.08	.12	.60
905-1,000	411	455	457	462	491	.20	.11	.01	.57	.48
Total						7.64	2.42	.89	3.55	6.97

¹ Computed for artesian-pressure reduction to atmospheric pressure at base of confining layer (185 feet).

Because the deposits at core hole 6S/2W-24C7 are chiefly fine grained and relatively impermeable, compaction lag was evaluated for each zone. Three zones containing sandy interbeds were divided into several segments (not shown in table) for computation of compaction lag.

Compaction of each zone was computed for the periods shown; the lag in subsidence was computed as the residual compaction as of January 1960. If the artesian pressure remained at the January 1960 level, the computation indicates that the area eventually would subside an additional 3.5 feet. If, in the future, the artesian pressure should decline to atmospheric, the computed additional subsidence would amount to about 7 feet. Therefore, subsidence after 1960 may eventually total as much as 10 or 11 feet.

Figure 172.1 compares the total computed subsidence and the computed subsidence, less lag, at core hole 6S/2W-24C7, for the periods 1915-34, 1934-54, and 1954-60; the actual subsidence of a nearby bench mark; and the hydrograph for well 6S/2W-25C1.

Releveling of bench marks by the U.S. Coast and Geodetic Survey furnished the evidence on land subsidence. Bench mark J111 Reset is only a few hundred feet from the core hole. Subsidence of this bench mark since 1934 is plotted on figure 172.1. The subsidence shown from 1912 to 1934 at J111 Reset was estimated from a proportional plot of subsidence at bench mark M7,¹ about 3 miles southeast.

The hydrograph of figure 172.1 is generalized and shows only the high-water level for each year of record. This simplified form is adequate to illustrate major changes in artesian pressure and to aid in the analysis of bench-mark subsidence. High-water levels for the years 1915, 1934, 1954, and 1960 were used to compute subsidence.

The rate of subsidence and water-level decline prior to the early 1930's probably was not uniform, as shown in figure 172.1, but data were not available for intermediate control. However, the downward trend of water levels in the Santa Clara Valley started about 1917.

A comparison of the total calculated subsidence and the calculated subsidence, less lag, in figure 172.1 shows the estimated amount of lag in subsidence remaining in the aquifer system as of 1934, 1954, and 1960. The estimated time required for the ultimate subsidence to occur after 1960, if artesian pressure stayed at the 1960 level, would be about 350 years.

¹ Bench mark M7 was established in 1912, whereas J111 Reset was not established until 1934. The leveling record for these bench marks overlapped for 2 years between 1934 and 1936. During this time, J111 Reset subsided at a rate 2.5 times that of M7. This proportion was applied to M7 for the period 1912-34 and assumed to be the approximate subsidence of J111 Reset.

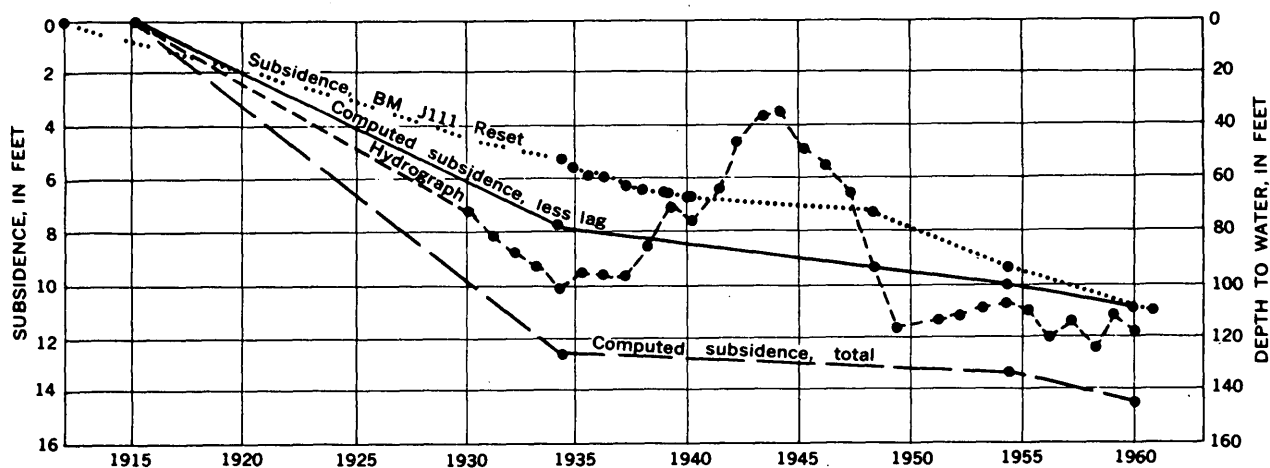


FIGURE 172.1.—Computed and actual subsidence at core hole 6S/2W-24C7 and hydrograph of nearby water well.

Calculations indicate that more than half this amount would occur in the first 75 years.

A comparison of actual subsidence at bench mark J111 Reset with the hydrograph of well 6S/2W-25C1 shows the rate of subsidence to be greater in periods of steep water-level decline than in periods of water-level rise. The recovery of artesian pressure between 1935 and 1943 acted to decrease the rate of subsidence to less than half that of the 1912-34 period. However, some subsidence continued, indicating that internal fluid pressure in the thickest beds of low permeability still exceeded the recovered artesian pressure in the more permeable beds during at least part of the 1935-43 period. As shown in figure 172.1, subsidence resumed at about the pre-1934 rate in 1948 when the artesian pressure was drawn down below its prior low (1934 level).

Figure 172.1 shows that computed subsidence, less lag, compares favorably with actual subsidence at bench mark J111 Reset. Computed subsidence, less

lag, for the period 1915-60 is 10.95 feet, whereas actual subsidence was 10.98 feet.

COMPACTION AT CORE HOLE 7S/1E-16C6

Similar computations were made for core hole 7S/1E-16C6, in the city of San Jose. The stratigraphic section was divided into 16 zones; artesian confinement was assumed in the zones below 245 feet. The water-level record for a well 800 feet deep and only a few feet from the core hole was used for the artesian-pressure change.

Figure 172.2 shows computed subsidence at core hole 7S/1E-16C6 for the periods 1915-34, 1934-54, and 1954-60; also subsidence of a nearby bench mark, and the hydrograph for well 7S/1E-16C1. Interpretations and computations were made on the same basis as for core hole 6S/2W-24C7, except that compaction lag was considered to be negligible on the basis of consolidation tests. Computed subsidence for the period

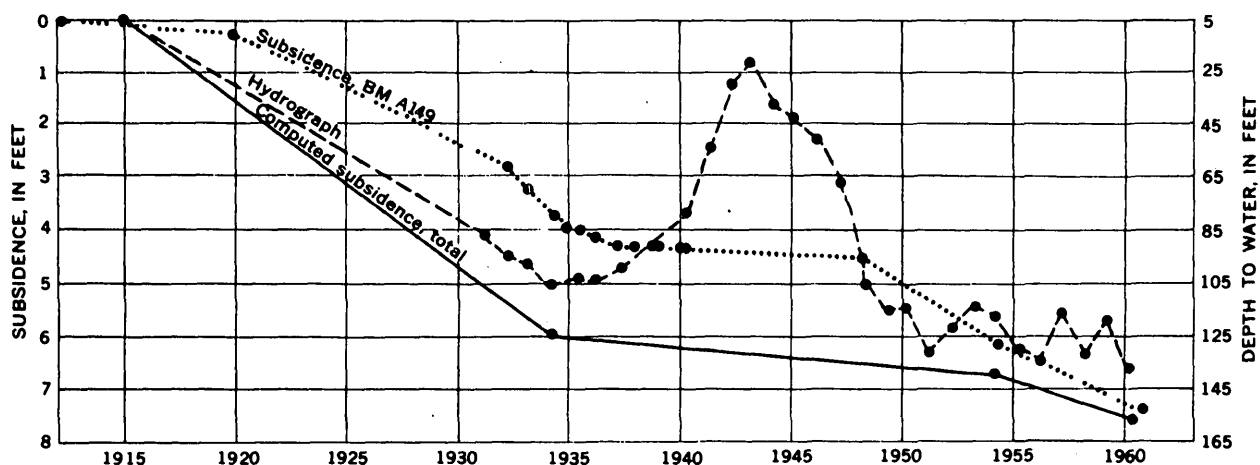


FIGURE 172.2.—Computed and actual subsidence at core hole 7S/1E-16C6, and hydrograph of nearby water well.

1915-60 was 7.6 feet, whereas subsidence of bench mark A149, nearby, determined from leveling by the U.S. Coast and Geodetic Survey was 7.4 feet.

REFERENCES

Lofgren, B. E., 1961, Measurement of compaction of aquifer systems in areas of land subsidence: Art. 24 in *U.S. Geol. Survey Prof. Paper 424-B*, p. B49-B52.

Miller, R. E., 1961, Compaction of an aquifer system computed from consolidation tests and decline in artesian head: Art. 26 in *U.S. Geol. Survey Prof. Paper 424-B*, p. B54-B58.

Poland, J. F., and Green, J. H., 1962, Subsidence in the Santa Clara Valley, California—a progress report: *U.S. Geol. Survey Water-Supply Paper 1619-C*, 16 p., 12 figs.

Terzaghi, Karl, 1943, *Theoretical soil mechanics*: New York, John Wiley & Sons, 510 p.



SURFACE WATER

173. USE OF SHORT RECORDS OF RUNOFF TO ESTIMATE A 25-YEAR AVERAGE RUNOFF IN THE POTOMAC RIVER BASIN

By WILLIAM S. EISENLOHR, JR., Denver, Colo.

The accompanying table can be used to estimate average annual runoff in the Potomac River basin for the period 1931-55 from short streamflow records of that period. It was computed as part of the preparation of a runoff map of the Potomac River and smaller basins interjacent to Delaware Bay. To use the table,

Cumulative annual runoff, in percent of the total runoff for the period 1931-55, for regions A, B, and C

Water year	Region			Water year	Region			Water year	Region		
	A	B	C		A	B	C		A	B	C
1931.....	2.4	1.2	1.8	1940.....	39.2	39.0	37.8	1948.....	68.2	68.2	69.4
1932.....	5.5	3.3	4.0	1941.....	42.0	42.0	41.1	1949.....	74.3	74.5	73.8
1933.....	10.5	9.0	10.1	1942.....	45.3	44.5	45.3	1950.....	78.3	78.2	77.4
1934.....	12.6	12.4	13.1	1943.....	51.0	49.4	50.4	1951.....	83.7	83.2	83.1
1935.....	17.5	17.2	17.1	1944.....	54.1	52.4	53.9	1952.....	88.2	88.8	88.9
1936.....	23.0	22.2	22.1	1945.....	58.1	56.7	57.8	1953.....	92.4	94.5	94.3
1937.....	27.8	27.7	27.0	1946.....	61.9	61.2	62.4	1954.....	94.7	96.7	96.5
1938.....	31.5	31.9	30.4	1947.....	64.3	63.8	65.5	1955.....	100.0	100.0	100.0
1939.....	35.3	35.6	33.9								

one needs only to determine by subtraction, for the proper region (fig. 173.1), the tabular value of cumulative annual runoff, in percent, for the period of record available and divide 0.25 times that value into the amount of runoff, in inches, observed during complete water years of record to obtain the estimated average annual runoff for 1931-55.

For example, the total runoff of Cacapon River at Yellow Spring, W. Va., in region A, was 136.68 inches for the 12 water years 1940-51. From the table, runoff in region A during these 12 years was 48.4 percent (83.7-35.3) of the 25-year total runoff. The

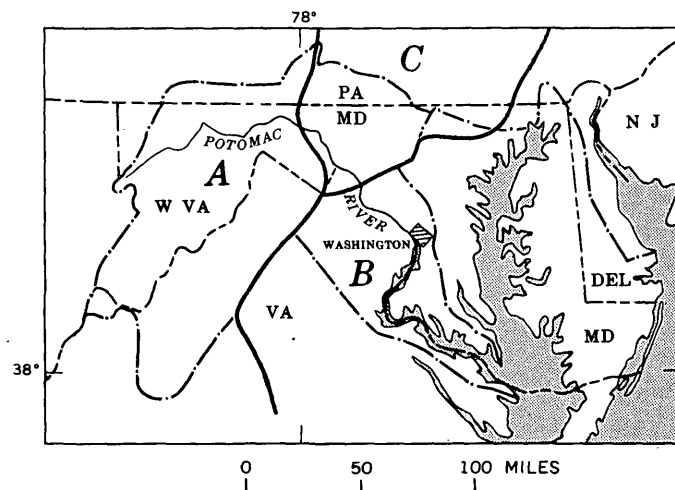


FIGURE 173.1.—Map of Potomac River basin and smaller basins interjacent to Delaware Bay, showing regions A, B, and C (heavy lines) described in text. (Dashed-and-dotted lines are boundaries of drainage basins.)

25-year average runoff is then estimated as $136.68 / (0.25 \times 48.4)$, which equals 11.3 inches per year. This record was chosen as the best one to illustrate the method; most records require a much larger adjustment.

The table was computed in the following manner. In and near the Potomac River basin and smaller basins interjacent to Delaware Bay there are 27 stream-gaging stations for which (a) the records of stream-flow are complete for the water years 1931-55, (b) the

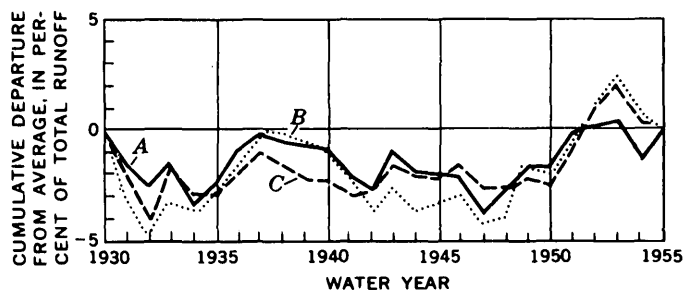


FIGURE 173.2.—Annual runoff in regions A, B, and C shown as cumulative departure from average, in percent of total runoff, for the period 1931–55.

drainage areas are more than 5 square miles but less than 1,000 square miles, and (c) effects of manmade regulation and diversion can be eliminated. A plot of the cumulative departures of annual runoff from the average annual runoff for the 25-year period, expressed in percent of total runoff, showed remarkably little variation among the records. There was enough variation, however, that it was considered best to divide the area into three regions. The plotted departures for each gaging-station record were compared separately with sketched plots of tentative regional averages (such as shown in fig. 173.2) to determine the regional classification of the station. Re-

gional averages were then computed on the basis of this classification. A single repetition of this process was sufficient to assure that each record was classified properly, and then the outlines of the regions were drawn as shown in figure 173.1.

The cumulative departures of annual runoff from average runoff for each region are plotted in figure 173.2. Approximately horizontal lines indicate average runoff whereas steeply sloping lines indicate runoff either much greater or much less than average. The departures from average runoff are almost wholly the result of differences in weather from year to year. The effects of such basin characteristics as topography, geology, and vegetation appear in the 25-year runoff and are thus almost eliminated insofar as they affect runoff, although the effect of vegetation varies slightly with precipitation.

The standard errors of estimate of the points used to define the regional curves in figure 173.2 (with loss of 25 degrees of freedom—one for each year's average) were found to be: Region A, 0.6 percent; region B, 0.6 percent; and region C, 0.5 percent. This means that about two-thirds of the points lie closer to the curve they define than the stated values of percent of total runoff for the period 1931–55.



174. USE OF REGIONALIZED FLOOD-FREQUENCY CURVES IN ADJUSTING FLOW-DURATION CURVES

By G. A. KIRKPATRICK and J. A. McCABE, Louisville, Ky.

As part of an intensive study of water resources in the Eastern Coal Field of Kentucky, duration curves of daily flow have been prepared from records of streamflow at gaging stations in the region. Because flow-duration curves based on short periods of record are unreliable for predicting the future pattern of flow, all curves in the Eastern Coal Field are being adjusted to represent a long-term base period. These adjusted curves can be defined at the upper end by use of regional flood-frequency curves.

The Eastern Coal Field covers about 10,400 square miles of the eastern part of Kentucky. Within this region are parts of the Kanawha, Cumberland Plateau, and Cumberland Mountain sections of the Appalachian Plateaus physiographic province. Principal stream basins are those of the Big Sandy River, Little Sandy

River, Tygarts Creek, upper Licking River, upper Kentucky River, and upper Cumberland River. The upper Cumberland River, Rockcastle River (a tributary of Cumberland River), and the South Fork of Cumberland River are particularly referred to in this article.

A flow-duration curve is a cumulative-frequency curve that shows the percentage of time during which specified discharges are equaled or exceeded (Searcy, 1959, p. 1). Duration curves of daily flow referred to herein are computed from figures of daily mean flow for all complete water years of streamflow record.

The method used to adjust curves prepared from short-term records to represent curves from long-term records is sometimes called the index-station method (Searcy, 1959, p. 12). A relation is estab-

lished between the index station and a short-term station for the short period of concurrent record by plotting a graph of the discharges for given durations at one station against the corresponding discharges at the other station. This graph is assumed to represent the relation between stations for a long period as well as for the short period from which it is drawn. The discharges for various percentage-duration values at the long-term index station are applied to the graph to determine the adjusted discharges for the corresponding percentage-duration values at the short-term site.

For this method to be valid, both the index station and the short-term station must be influenced by similar weather conditions. That similar conditions generally exist in the Eastern Coal Field is substantiated

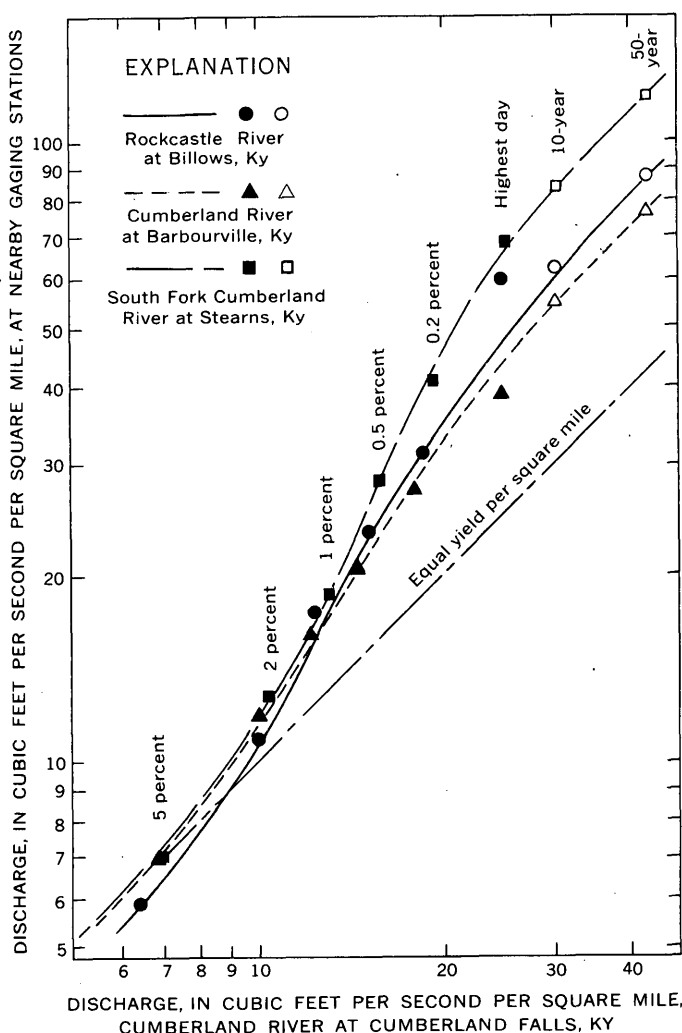


FIGURE 174.1.—Curves of relation between streamflow at gaging station Cumberland River at Cumberland Falls, and flow at three nearby stations. Solid symbols show discharge at equal-percentage duration; open symbols show peak discharge at recurrence intervals of 10 and 50 years.

by the satisfactory correlations of streamflow at one gaging station with that at other stations. The coefficient of correlation of monthly mean discharges between the Cumberland River at Cumberland Falls and 13 other gaging stations in the upper Cumberland River basin ranges from 0.72 to 0.98. Only two of these coefficients are less than 0.84.

Above its low-flow end, the relation curve between discharges at pairs of gaging stations is generally near to or converges toward the equal-yield line, because storm runoff predominates at high flow, and base runoff, which is affected by geologic conditions, is a negligible part of the total flow. The equal-yield line defines the relation curve when flow at the two sites is proportional to the respective drainage areas above the sites. If the shape and slope of the basin upstream from one gaging station are such that the effect of storm precipitation is distributed over an extended time period, and if storm runoff from the other basin is concentrated in a much shorter time period, the line of discharge relation deviates from the equal-yield line toward the coordinate scale for the station with less retention (see fig. 174.1). For high daily discharges the ratio of maximum daily discharge to peak discharge tends to become constant for each gaging station as implied by the unit hydrograph theory. Thus, at high discharges the relation line between daily discharge tends to become parallel to the equal-yield line in approximately the same position as the relation line between peak discharges.

Curves relating the flow of the gaging station Cumberland River at Cumberland Falls, Ky., to the flow at three other gaging stations in the upper Cumberland River basin are shown in figure 174.1. These gaging stations with their respective drainage areas, flood regions and hydrologic areas of Kentucky in which they are located and the number of years of record used with the concurrent record for Cumberland River at Cumberland Falls are given below.

Station name	Drainage area (square mile)	Region and area ¹	Number of concurrent years
Cumberland River at Cumberland Falls	1,977	B	-----
South Fork Cumberland River at Stearns	954	B1	14
Rockcastle River at Billows	604	B2	20
Cumberland River at Barbourville	960	B2	13

¹ See text below for explanation.

The flood region indicated by the letter B in the preceding table, and the hydrologic area within the region indicated by the numeral following the letter, are defined by a regional flood-frequency analysis for Kentucky streams being conducted by the junior author using methods described by Dalrymple (1960,

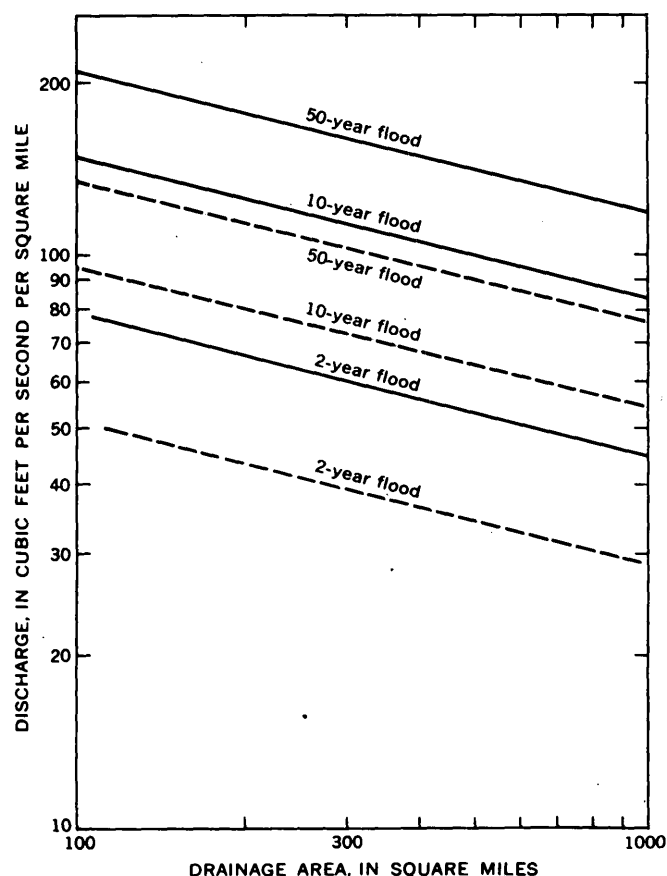


FIGURE 174.2.—Variation of 2-, 10-, and 50-year floods in flood region B, Kentucky. Solid lines are for hydrologic area 1 and dotted lines for hydrologic area 2, as defined by a flood-frequency analysis.

p. 25-46). The position of the upper ends of the relation curves shown in figure 174.1 have been defined by using the results of this regional flood-frequency analysis. The analysis gives graphs whereby an annual flood for a selected recurrence interval may be determined for a given site if the drainage area of the site is known. Regionalized flood-frequency data, rather than single station data, are used to define adjusted flow-duration curves, because evidence indicates that a flood-frequency graph that is based on the combined records of a group of stations has firmer support than one drawn to fit the data of a single station (Dalrymple, 1960, p. 65).

An example of the information available in the junior author's analysis is shown in figure 174.2. The curves therein show the variation of annual floods of selected recurrence intervals with drainage area. A 50-year flood is a flood that is equaled or exceeded once

in a period of time that averages 50 years, or one that has a 2-percent chance of being exceeded in any year. Likewise, a 10-year flood is a flood that is equaled or exceeded once in a period of time that averages 10 years, or one that has a 10-percent chance of being exceeded in any year. The plotting positions of the 10- and 50-year floods shown in figure 174.1 for the gaging stations South Fork Cumberland River at Stearns, Rockcastle River at Billows, and Cumberland River at Barbourville are picked from the curves shown in figure 174.2. The plotting positions for the gaging station Cumberland River at Cumberland Falls, a main-stem station, are from a flood-frequency curve of the flood peaks observed at the station.

Twenty-four relation curves similar to those shown in figure 174.1 have been prepared using 7 additional gaging stations in the upper Cumberland River basin, 6 gaging stations in the Big Sandy River basin, and 7 gaging stations in the upper Kentucky River basin. These relations strongly indicate that the peak discharges having an average recurrence interval of 10 years define a point that lies very close to a point on the flow-duration relation curve above which the curve tends to become parallel with the equal-yield line. Relation curves drawn through this point, as illustrated in figure 174.1, are usually better than curves defined only by the higher equal-percentage duration points.

Reference to figure 174.1 shows that the relation curve for South Fork Cumberland River at Stearns could have been drawn nearly as well without the flood-frequency data. The upper end of the curve for Rockcastle River at Billows would have been drawn above its proper position, and that for Cumberland River at Barbourville would have been drawn too low. The use of flood-frequency data in this manner helps in defining the relation between those stations having only a few years of concurrent record, because points of equal-percentage duration plot more erratically as the length of concurrent record becomes less. Such data also help if a longer period of concurrent record has no high flow, because the relation curve would then need to be extrapolated before it could be used in adjusting the short record to the long-term base period.

REFERENCES

- Dalrymple, Tate, 1960, Flood-frequency analyses: U.S. Geol. Survey Water-Supply Paper 1543-A, 80 p.
- Searcy, J. A., 1959, Flow-duration curves: U.S. Geol. Survey Water-Supply Paper 1542-A, 33 p.

175. A CONTROL STRUCTURE FOR MEASURING WATER DISCHARGE AND SEDIMENT LOAD

By E. V. RICHARDSON and D. D. HARRIS, Fort Collins, Colo., and Denver, Colo.

A control structure was designed for the Rio Grande conveyance channel near Bernardo, N. Mex., to stabilize the stage-discharge relation and to facilitate the measurement of the total sediment load. With modification for various site conditions the control should be suitable for installation on other sand-channel streams to improve their water and sediment-discharge records. The stage-discharge relation for the conveyance channel is very unstable, as it is for many other sand-bed streams (Colby, 1960; Dawdy, 1961). The stage may change 1 to 3 feet without a change in discharge or, conversely, the discharge may change without a change in stage. The proposed control provides for the determination of the total sediment discharge, whereas with no control only the suspended sediment would be measured. The design of the control was based on a model study and observed channel conditions.

Two factors contribute to the unstable stage-discharge relation in a sand-channel stream: changes in the mean elevation of the channel bed, and changes in the configuration of the bed. Either one or both of these changes can occur with or without a change in the water discharge. In the conveyance channel the mean bed elevation varies about 4 feet. An increase in discharge is usually accompanied by an increase in bed elevation, and a decrease in discharge by a decrease in bed elevation.

The effect of changes in bed configuration on the depth-discharge relation is illustrated in figure 175.1. The variation in the depth-discharge relation is caused by the bed configuration changing from dunes, which occur at low flows and which have a large resistance to flow, to a plane bed, which occurs at high flows and has a much lower resistance to flow. The stage-discharge relation for a sand-channel stream is subject to this variation of the depth-discharge relation as well as to the variation due to changes in mean bed elevation.

The conveyance channel is about 80 feet wide, and its bed and banks are composed of fine sand (median diameter 0.24 mm). Maximum flow is about 2,000 cfs (cubic feet per second), median flow is 280 cfs, and the flow exceeds 1,000 cfs 16 percent of the time. Flow in excess of 2,000 cfs is carried by the natural river channel. The bed form is characterized by dunes for discharges up to 500 cfs, changing to a plane bed at discharges between 500 and 1,200 cfs, although dunes have been observed for flows as large as 2,000 cfs and

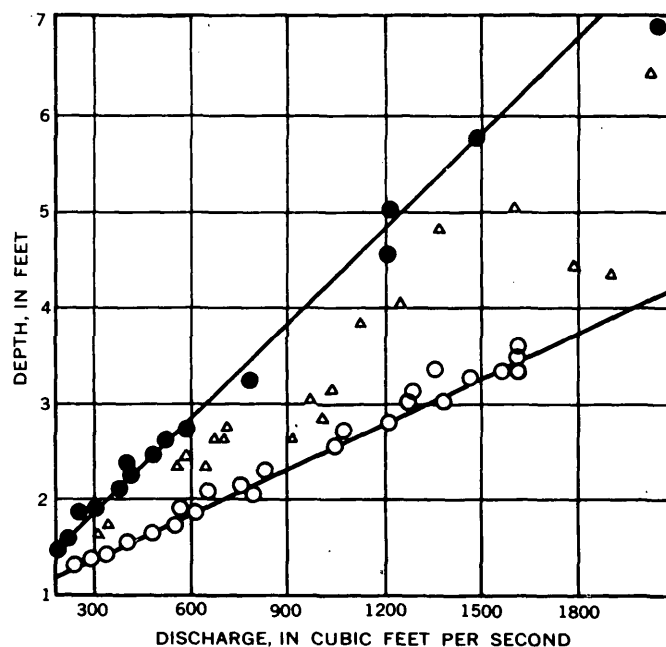


FIGURE 175.1.—Depth-discharge relation for the conveyance channel. Plotted points are from discharge measurements made when bed configuration was characterized by dunes (solid circles), by a plane surface (open circles), or in transition (triangles).

a plane bed for flows as small as 200 cfs. A combination of a high bed elevation and a dune bed configuration has caused the channel to flow bankfull (gage height 9.5 feet) at a discharge of 2,100 cfs.

A model study was conducted at Colorado State University to devise a control structure that would improve the water and sediment-discharge records for the channel. The objectives of the model study were to (1) determine the shape of a control that would stabilize and increase the sensitivity of the stage-discharge relation, (2) determine the maximum elevation at which the control could be placed in the channel without restricting the bankfull flow to less than 2,000 cfs, (3) determine the best method of controlling any scour that the control might create, and (4) provide a suitable place for measurement of water and sediment discharge.

Several shapes were studied as two-dimensional models (1:8 scale ratio) in a sand-bed flume 2 feet wide and 60 feet long. The most promising shape was then modeled (1:10 scale ratio) and modified in a sand-bed flume 8 feet wide and 150 feet long. In this study the discharges were modeled using the Froude criterion ($Q_r = L_r^{5/2}$ where Q_r is the dis-

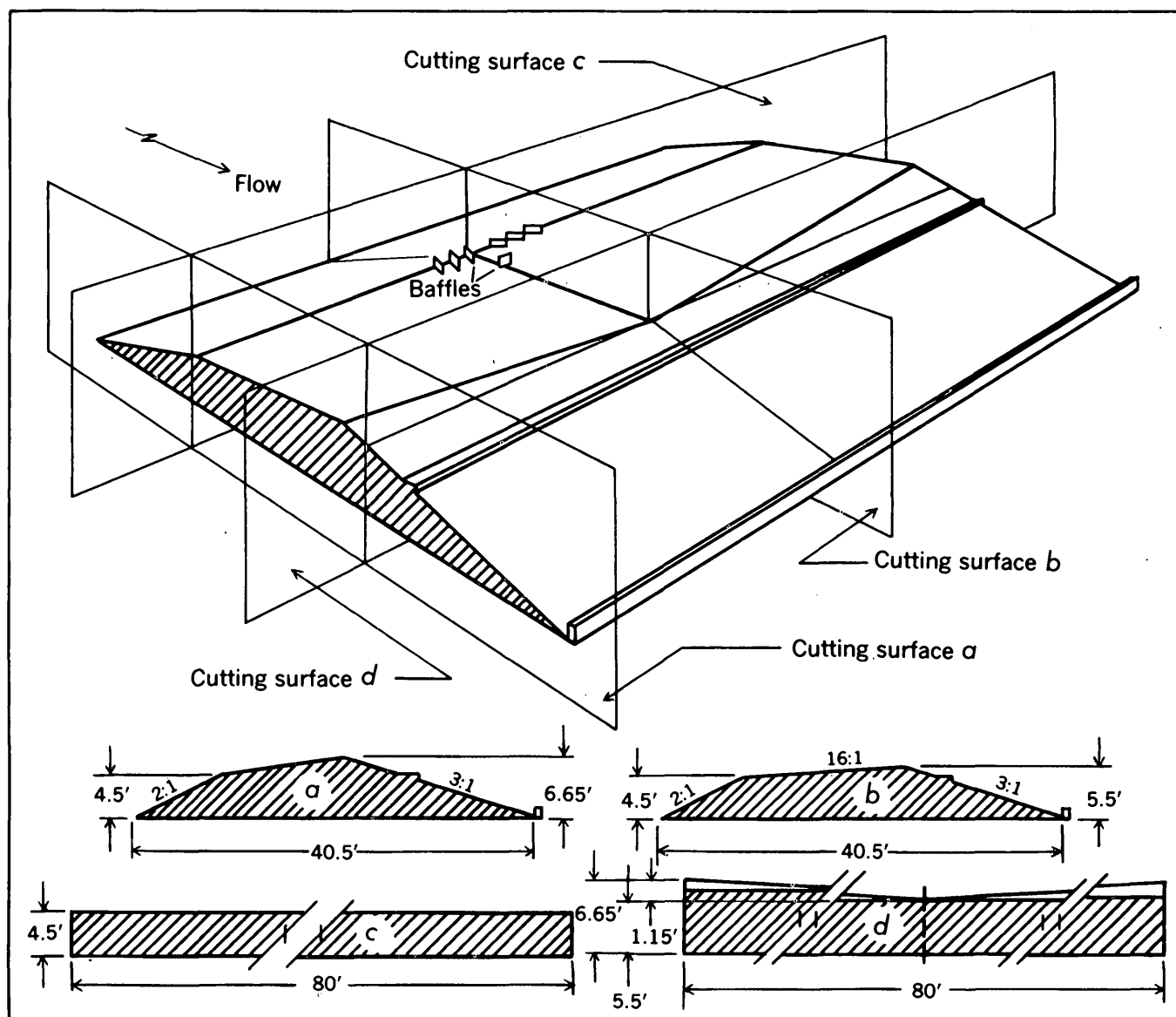


FIGURE 175.2—Details of the proposed control structure.

charge ratio and L_r is the length ratio), and flume slopes were varied so that the bed material moved and either a dune or plane bed configuration developed.

The design for the control structure for the conveyance channel was based on the model study and is illustrated in figure 175.2. The baffles indicated on the figure were installed to prevent the deposition of sediment on the control by increasing the turbulence of the flow. As illustrated in figure 175.3, the stage-discharge relation for the model control was affected only slightly by the sediment load or by the changes in the bed configuration. The desired sensitivity of the stage-discharge relation for the control was a 1.5-percent change in discharge for a 0.01-foot change in

stage. In the study of the model, however, which had a transverse crest slope of 40:1, the change in discharge was less than 1.5 percent for each 0.01-foot change in stage, for discharges greater than 400 cfs. Below 400 cfs the sensitivity decreased so that at 30 cfs the change in discharge for a 0.01-foot change in stage was 7 percent. For the proposed structure (fig. 175.2), a transverse crest slope of 35:1 was used to improve the sensitivity of the stage-discharge relation. Slopes steeper than 35:1 are not recommended because in the model study they caused large waves over the control and excessive erosion downstream.

The model control has a stable stage-discharge relation at all discharges, but the prototype control will not. The low bankfull stage limited the design eleva-

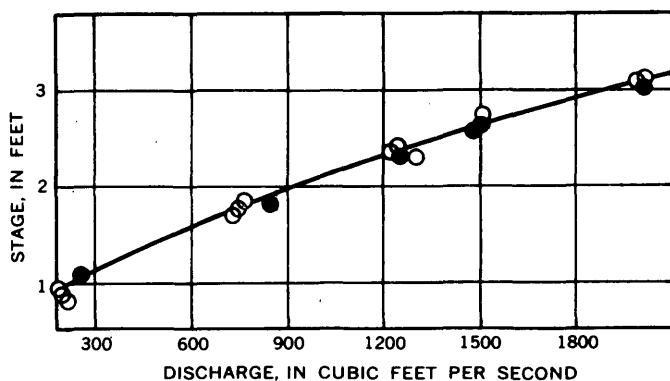


FIGURE 175.3.—Stage-discharge relation for the model control. Solid circles indicate that bed configuration was characterized by dunes; open circles, by a plane surface. Stage is measured at the low point on the control 4 feet upstream from the crest.

tion of the prototype control to 4.5 feet below bank-full stage or 0.5 feet above maximum bed elevation. As a result, downstream variation in the tailwater elevation will cause variable submergence. Tailwater elevations estimated from the prototype stage-discharge relation indicate that free fall (less than 70-percent submergence) should exist for all discharges up to 1,100 cfs under average conditions. With maximum observed tailwater elevations, free fall would exist only for flows up to 300 cfs. For discharges of 2,000 cfs the control will be completely submerged, regardless of the tailwater conditions, and will not restrict the maximum capacity of the channel. An

auxiliary gage could be used downstream in the conveyance channel to determine the degree of submergence and thus improve the discharge records. On streams where the elevation of the control crest is not limited, the crest elevation could be made high enough to eliminate the effect of variable submergence on the stability of the stage-discharge relation.

The model study indicated that for transverse slopes no steeper than 35:1, excessive downstream scour in the prototype can be prevented if a sill 1.5 feet high is placed at the downstream toe of the control with its crest at, or slightly below, low-bed elevation. In a field installation, however, some riprapping of the banks and bed near the sill may be necessary.

The proposed control structure provides for the measurement of both the water discharge and the total sediment concentration. Velocity profiles obtained in the model study indicate that accurate measurements of water discharge can be made at a section 9 feet upstream from the crest. The total sediment concentration can be measured along the fillet, which is located on the downstream apron (fig. 175.2), by traversing a conventional sampler through the entire depth of flow.

REFERENCES

- Colby, B. R., 1960, Discontinuous rating curves for Pigeon Roost and Cuffawa Creeks in Northern Mississippi: U.S. Dept. Agriculture, ARS 41-36.
- Dawdy, D. R., 1961, Depth-discharge relations of alluvial streams—discontinuous rating curves: U.S. Geol. Survey Water-Supply Paper 1498-C, 16 p.

176. USE OF A RADIOISOTOPE TO MEASURE WATER DISCHARGE

By B. J. FREDERICK; C. W. RECK, and R. W. CARTER: Oak Ridge, Tenn.; Washington, D.C.

Work done in cooperation with the U.S. Atomic Energy Commission

Laboratory tests were conducted to evaluate the use of radioisotopes in the dilution method of flow measurement. The rate of flow in a 2-inch pipe 120 feet long was measured volumetrically and compared with the rate of flow computed by measuring the radioactivity of a concentrated solution of radioactive gold (Au^{198}).

In the dilution method of flow measurement a solution with a high concentration of radioactivity is injected into the flow at a constant rate, and samples are withdrawn at some point downstream where the concentrated solution has completely mixed with the flow. According to the principle of continuity, the following relationship exists:

$$QC_0 + qC_1 = (Q + q)C_2 \quad (1)$$

in which

Q = discharge through the pipe, in cubic feet per second;
 q = discharge from injection system, in cubic feet per second;

C_0 = concentration of radioactivity in the discharge pipe upstream from injection, in microcuries per cubic foot;

C_1 = concentration of radioactivity in injection system, in microcuries per cubic foot; and

C_2 = concentration of radioactivity in discharge pipe at sampling point, in microcuries per cubic foot.

As q is very small compared to Q , the qC_2 term can be neglected, and as C_0 is very small compared to C_2 , the QC_0 term can be neglected. Consequently equation 1 can be reduced to

$$Q = q \left(\frac{C_1}{C_2} \right) \quad (2)$$

In these tests the constant injection rate was obtained from the gravity-feed system shown in figure 176.1. The flow rate q was controlled by the valve and was measured by the volume displaced per unit of time.

Samples were taken from the pipe at a location 120 feet downstream from the point of injection and transferred to a special container for the detection of radioactive concentration. The sample size was 37 liters (9.8 gallons). The count rate was determined with a counter as shown in figure 176.2.

Samples taken from the injection system were diluted before being tested, because the concentration of

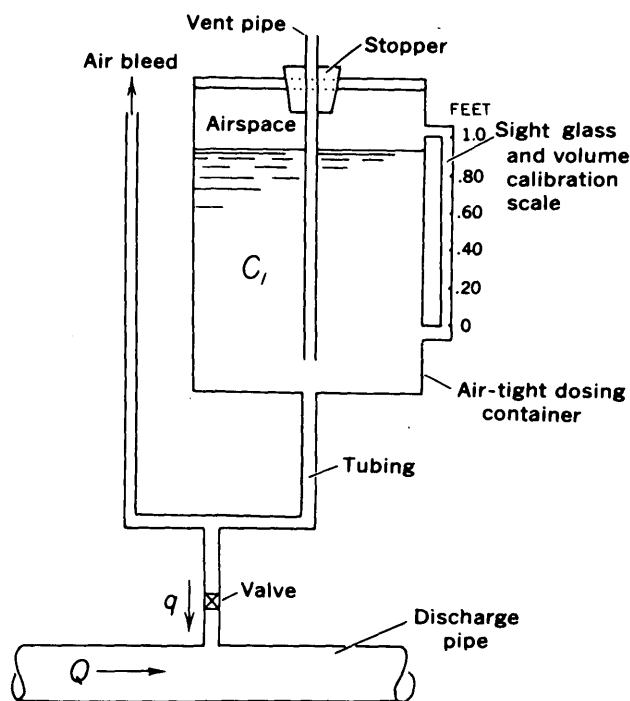


FIGURE 176.1.—System for injection of concentrated solution.

activity in the undiluted sample was so great that the count rate would have been considerably above the capacity of the detection system. A 150-ml (0.32 pint) sample from the injection was added to 37,000 ml (9.8 gallons) of background water, and the radioactivity of the diluted sample was counted in the counting container. The relationship between the count rate in this diluted sample (C_3) and the count rate in the injection system (C_1) is:

$$C_1 = \frac{37,150}{150} C_3 = 247.7 C_3.$$

The counting period was sufficiently long (10,000 counts) to make the statistical standard error less than 1 percent. Because all samples were counted in the same geometry, and because the count rate was well within the reliable range of the detection system, the count-rate figures could be used rather than an absolute value of concentration of activity in solving equation 2.

Flows computed from equation 2 are compared in the following table with flows measured volumetrically.

Comparison of measured and computed flow

Run	Measured Q (cfs)	Dosing (mlg per sec)	Concentration (counts per min)		Computed Q (cfs)	Error (per- cent)
			C ₂	C ₃		
1-----	0.0928	12.64	726	608	0.0928	0.0
2-----	.0902	12.95	11,292	9,038	.0907	+ .1
3-----	.0895	13.59	17,598	12,914	.0873	-2.5
4-----	.0890	13.42	5,756	4,424	.0906	+1.8
5-----	.0891	13.26	9,051	7,020	.0900	+1.0
Total--	.4496	-----	-----	-----	.4514	+ .1

The comparisons suggest that the accuracy of the dilution method is within about 1-percent. With some refinements in the equipment, this order of accuracy could probably be achieved in measuring the discharge of open channels at field sites provided there was no loss of radioactive material between the injection and sampling points. The adsorption problem will be considered in other experiments.

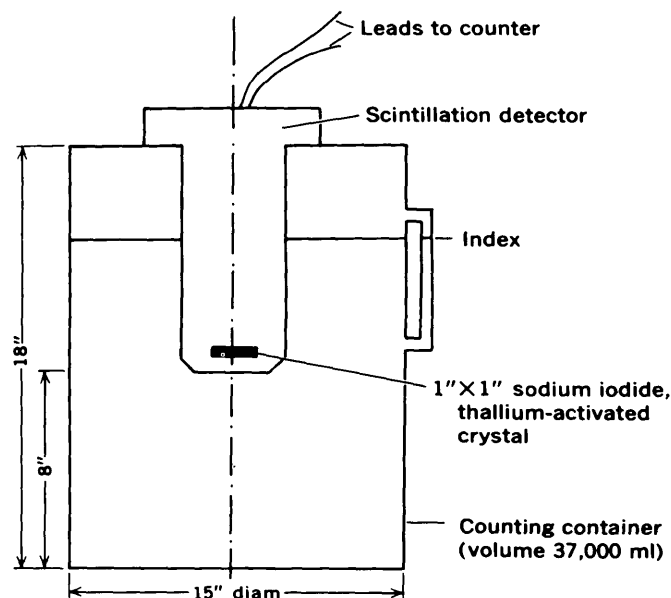


FIGURE 176.2.—System for counting radioactivity.

QUALITY OF WATER

177. SOLUTE DEGRADATION IN THE POTOMAC RIVER BASIN

By H. R. FELTZ and J. W. WARK, Washington, D.C., and Rockville, Md.

Work done in cooperation with the U.S. Army Engineer District, Baltimore, Md.

One of the processes by which rock material is eroded and transported is the solvent action of water. Previous studies show that solute degradation rates are related closely to rock type, precipitation, and runoff characteristics. This article describes some effects of both lithologic and climatic controls on chemical degradation in the Potomac River basin.

The dissolved-solids content of several streams in the Potomac basin was related to the concurrent water discharge. These relationships (fig. 177.1) and flow-duration tables (unpublished records of the Geological Survey) were used to compute the average annual solute discharges of 11 tributaries in the basin.

Corrections were made for the dissolved solids contributed to the basin by precipitation. The average solute content of 6 rainfall events in 1961 was 8 parts per million. Reported values compare favorably with data given by Junge and Werby (1958). Average

precipitation over individual drainage basins was estimated from U.S. Weather Bureau data, and for ease of correction a curve was prepared relating the dissolved solids in tons per square mile to annual precipitation. Dissolved solids carried to earth by precipitation were subtracted from the computed load of dissolved solids in stream flow. Corrections ranged from 24 tons per sq mi per yr (square miles per year) for the upper reaches of the basin to 20 tons per sq mi per yr for parts of the Shenandoah Valley.

Net solute degradation rates range from 11 to 354 tons per sq mi per yr (see table). The high solute load of the North Branch Potomac River reflects pollution from strip mining of coal. Streams such as the North Fork Shenandoah River at Cootes Store, Va., which drain sandstone and shale of Devonian age, have low solute loads. Excluding the North Branch Potomac River, streams such as Antietam Creek,

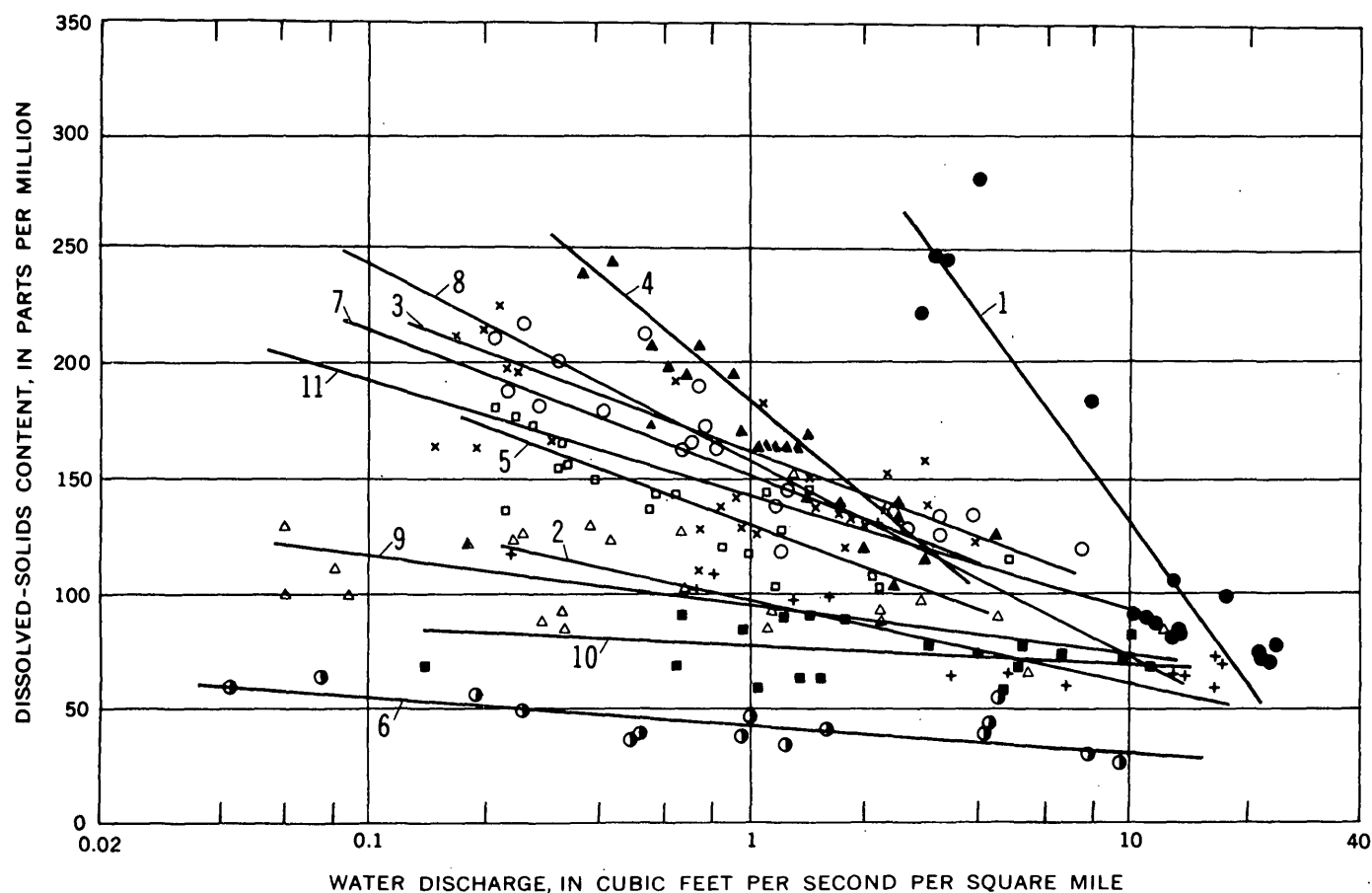


FIGURE 177.1.—Relation of dissolved-solids content to water discharge for streams in the Potomac River basin. (See table for stream name and location.)

Conococheague Creek, and the South Fork Shenandoah River, which drain areas underlain by limestone, dolomite, and shale, have the highest solute loads.

Annual runoff and average dissolved-solids content of streams in the upper reaches of the basin are about twice those in the lower reaches. Of the streams plotted in figure 177.1, Goose Creek, which drains primarily greenstone and granite, exhibits the least change in dissolved-solids content for concurrent

changes in discharge. Solute concentrations of all streams is nearly uniform when water discharge exceeds 10 cubic feet per second per square mile.

REFERENCE

Junge, C. E., and Werby, R. T., 1958, The concentration of chloride, sodium, potassium, calcium, and sulfate in rain water over the United States: Jour. Meteorology, v. 15, no. 5, p. 417-425.

Computed average annual solute degradation rates in the Potomac River basin

Reference no. (fig. 177.1)	Station	Drainage area (sq mi)	Gross solute discharge (tons per sq mi)	Precipitation (inches)	Dissolved solids in precipitation (tons per sq mi)	Net solute degradation (tons per sq mi)
1	North Branch Potomac River at Pinto, Md.	596	378	41	24	354
2	South Branch Potomac River near Springfield, W. Va.	1,471	73	35	20	53
3	Conococheague Creek at Fairview, Md.	494	162	39	22	140
4	Antietam Creek near Waynesboro, Pa.	93.5	198	40	23	175
5	South Fork Shenandoah River at Front Royal, Va.	1,638	112	38	22	90
6	North Fork Shenandoah River at Cootes Store, Va.	215	33	38	22	11
7	North Fork Shenandoah River near Strasburg, Va.	772	104	34	20	84
8	Potomac River at Point of Rocks, Md.	9,651	132	36	21	111
9	Monocacy River at Bridgeport, Md.	173	97	43	25	72
10	Goose Creek near Leesburg, Va.	338	66	40	23	43
11	Potomac River near Washington, D.C.	11,560	120	37	21	99

178. FOAMING CHARACTERISTICS OF SYNTHETIC-DETERGENT SOLUTIONS

By C. H. WAYMAN, J. B. ROBERTSON, and H. G. PAGE, Denver, Colo.

Work done in cooperation with the Federal Housing Administration

Synthetic detergents are of three general types: (1) Anionic, which contains a surfactant (surface-tension lowering agent) in which the oil-soluble portion of the molecule is negatively charged; (2) cationic, which contains a surfactant in which the oil-soluble portion of the molecule is positively charged; and (3) nonionic, which is not ionized but which acquires hydrophilic character from an oxygenated side chain such as polyoxyethylene. Anionic alkylbenzenesulfonate (ABS) is the chief surfactant in commercial detergents.

Because anionic surfactants in commercial-detergent formulations resist breakdown either after sewage treatment or in septic tanks, these compounds are contributing to the pollution of both ground water and surface water. One of the effects produced from detergent pollution is foaming. Most persistent foams are attributed to soaps, synthetic detergents, and soluble proteins (Moillet and others, 1961, p. 203). In the bulk of a solution the concentration of surfactants commonly is about 10 ppm (parts per million), but in foams such concentrations may exceed 1,000 ppm. Because of the Geological Survey's interest in ground-water pollution, a study was made to determine the influence of such factors as detergent concentrations, temperature, counter ions, pH, anionic builders, and bacteria on foaming characteristics of synthetic-detergent solutions.

Much of the profuse literature on detergent foams suggests that foaming is caused by as little as 0.5 ppm of ABS, but our study showed that sodium salts of ABS and of nonionic types of detergents will not foam stably at concentrations of less than 2 to 3 ppm. Foaming at lesser concentrations probably can be attributed to other surfactants, such as organic proteins. Cationic detergents, such as Hyamine 1622, require concentrations of 8 to 10 ppm for foaming.

Foam stability of numerous commercial anionic, nonionic, and cationic detergents is shown in figure 178.1. Anionic and nonionic types are more stable than the one cationic surfactant tested. Foam stability of nonionic surfactants increases as the ratio of the hydrophobic to hydrophilic groups of the molecule increases. Hyonic PE 70 represents a surfactant containing 70 percent hydrophobic and 30 percent hydrophilic groups.

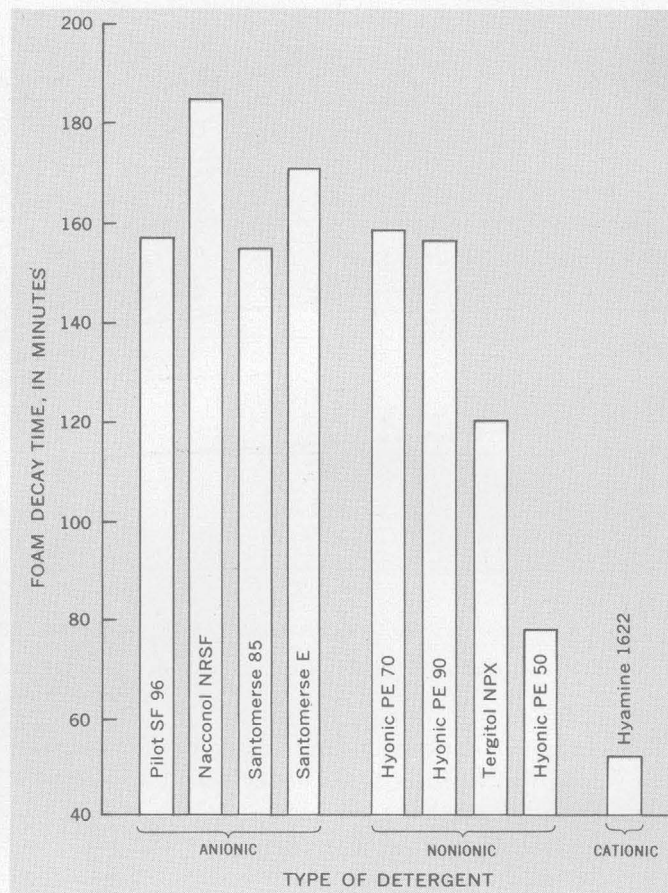


FIGURE 178.1.—Time required for a column of foam 56 cm high to decay to 0.3 cm for various anionic, nonionic, and cationic detergents.

Tests indicate that the relation between detergent concentration and foam stability is nonlinear. For pure detergent solutions containing 10, 100, and 1,000 ppm of ABS at 10°C, the time for a column of foam 56 cm high to decay to 0.3 cm is 1, 40, and 280 minutes, respectively.

Foam stability seems to increase as the temperature decreases. At temperatures of 10°C, 20°C, and 30°C, the foam height of solutions containing 100 ppm of ABS decayed from 56 to 0.3 cm in 50, 40, and 20 minutes, respectively.

Counter ions in solution generally impede the formation of a given attainable foam height. This phenomenon is illustrated in figure 178.2 where the foam-

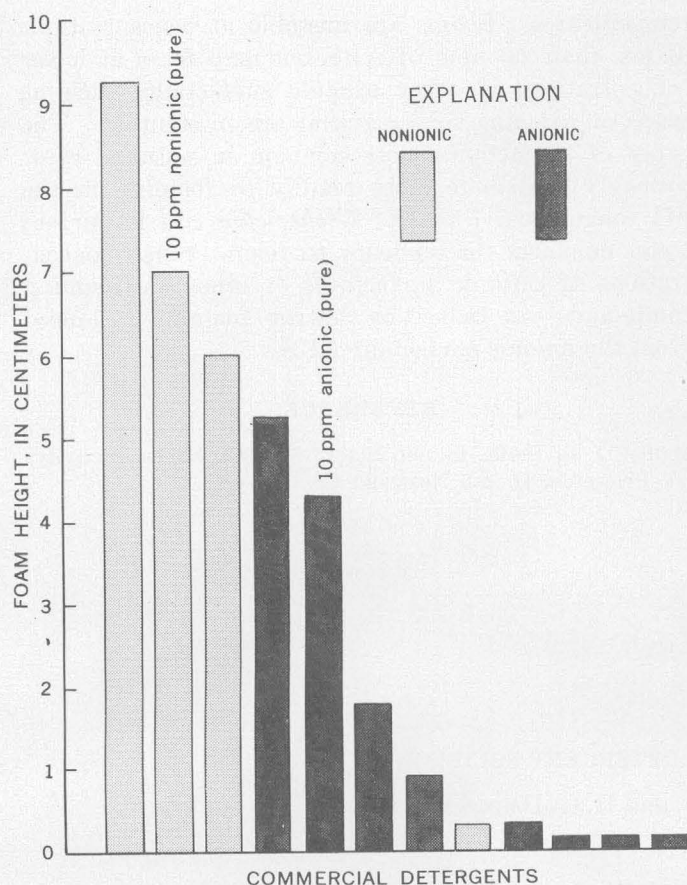


FIGURE 178.2.—Foam height of various commercial household detergents in solution containing 20 mg per l at 20°C.

ing characteristics of several commercially available detergents that contain counter ions are compared to pure anionic and nonionic surfactants.

Foaming is influenced markedly by changes in pH. As shown in figure 178.3, cationic surfactants are extremely unstable at a pH of more than 7. Anionic and nonionic types are stable throughout a large range of pH, the anionic type being more stable at higher pH and the nonionic being virtually unaffected.

Anionic builders (detergent components in addition to the surfactant) such as phosphate, silicate, and carboxymethylcellulose (CMC) ions enhance the tendency of anionic detergent solutions to foam; this effect becomes more intense when the solution contains bacteria such as *Escherichia coli*. A mixture of a cationic detergent (Hyamine) and anionic builders produces virtually no foam (fig. 178.3).

Foaming tests on a sample of sewage effluent containing 1,000 ppm of dissolved solids, 6.0 ppm of ABS, and 1×10^6 bacteria per ml indicated a poor tendency to foam. Because this sample contained the requisite amounts of ABS and bacteria to produce foaming and because foaming did not occur, the tests indicate that some sewage effluents contain natural antifoaming agents. As little as 10 to 100 ppm of antifoaming agents can prevent foaming of anionic surfactant solutions containing as much as 100 ppm of ABS. Experiments on solutions containing 100 ppm of Dow Corning Antifoam "B" and 100 ppm of ABS gave

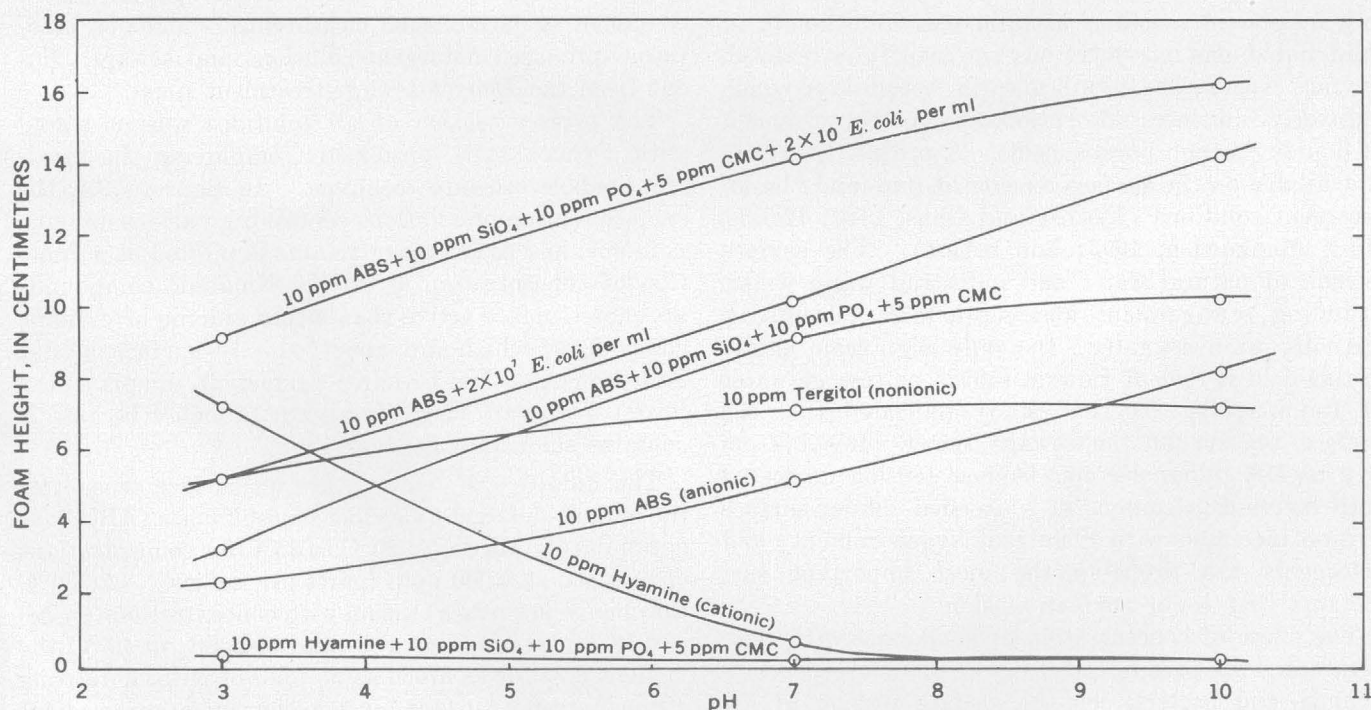


FIGURE 178.3.—The influence of pH, bacteria (*Escherichia coli*), and builders on foam height for various surfactants.

no measurable amount of foam. Similar tests on solutions containing 40 ppm of ABS and 10 ppm of the cationic Hyamine 1622 failed to create any measurable amount of foam. Therefore, small concentrations of natural antifoams, such as cationic surfactants, can destroy potential foaming in sewage effluents. Cationic surfactants like Hyamine 1622, which is a germicide, might function to destroy bacteria and foams simultaneously.

This study indicates that water supplies tapping ground water aquifers should not foam vigorously at ABS concentrations of less than 2.0 ppm, if ABS is the only surfactant present.

The stability of foams in natural water is influenced by several variables. Foams are more stable at lower

temperatures. Foams are unstable at concentrations of less than 2.0 ppm of ABS but may foam at lower concentrations if other organic surfactants such as soaps or proteinaceous material are in solution. The types of surfactants most common in natural water probably contribute more readily to foaming in the pH range from 7 to 10. *Escherichia coli* in surface water enhances the tendency to foam. Small concentrations of cationic surfactants or other antifoaming compounds can reduce or destroy foaming produced from the anionic surfactant ABS.

REFERENCE

Mollet, J. L., Collie, B., and Black, W., 1961, Surface activity: Princeton, D. van Nostrand Co., 518 p.



179. SURFACE TENSION OF DETERGENT SOLUTIONS

By C. H. WAYMAN, J. B. ROBERTSON, and H. G. PAGE, Denver, Colo.

Work done in cooperation with the Federal Housing Administration

The importance of the physicochemical property surface tension in reactions at solid-gas, solid-liquid, or solid-liquid-gas interfaces has not been fully realized. Surface tension has significance in wettability, which indirectly influences adsorption, and in the movement of liquids through porous media. A profuse literature is available on the surface tension of pure and "built" detergent solutions (Fischer and Gans, 1946; Harris, 1946; Mankowich, 1953; and others). The surface tension of natural water and industrial waste water, including sewage-plant and septic-tank effluents, is virtually uninvestigated; the only significant study in this field is that of Bowers (1952) on sewage water of Indianapolis. Bowers' study indicated that the surface tension of the sewage water ranged from 38.9 to 71.6 dynes per cm; surface tension decreased with increase in content of suspended solids; surface tension increased with dissolved-oxygen content; and detergents are probably the most important surfactants that lower surface tension.

The effect of concentration of surfactant, pH, temperature, ions present in commercial detergent compounds, and bacteria, on the surface tension of de-

tergent solutions is discussed in this paper. Data consist of surface-tension measurements made on laboratory-prepared detergent solutions and sewage effluent from the Denver sewage-treatment plant.

The surface tension of all solutions was measured with a Cassel-type tensiometer, employing the maximum-bubble-pressure technique. In figure 179.1, the surface tension of solutions containing various anionic, nonionic, and cationic surfactants is plotted as a function of concentration at 20°C. Nonionic compounds are more surface active than either anionic or cationic compounds, which are about equally surface active. Santomerse, a low-foaming surfactant, displays the lowest degree of surface activity, probably because it contains surfactant depressants.

The influence of temperature on surface tension of the anionic detergent alkylbenzenesulfonate (ABS) was determined in the range 20°C to 35°C for concentrations of as much as 3,000 ppm (parts per million). At 20°C the change in surface tension with concentration ($\partial\gamma/\partial c$) is 0.18 for as much as 110 ppm of ABS; at 35°C the value is 0.36 for as much as 55 ppm of ABS, indicating a much steeper surface tension-concentration gradient

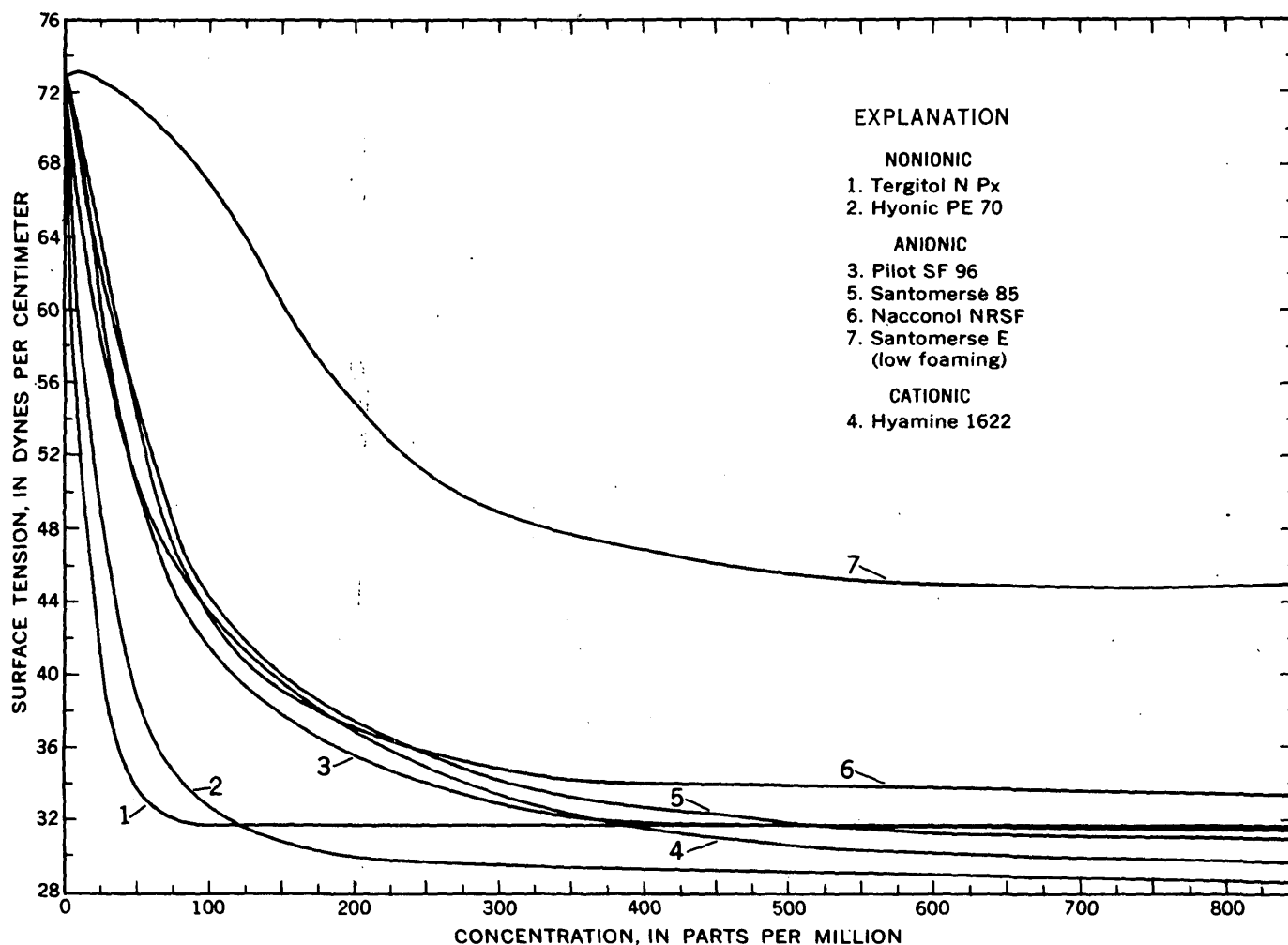


FIGURE 179.1.—Variation of surface tension with concentration for various surfactants at 20 °C.

at higher temperatures. The Gibbs adsorption equation for surface excess (Γ , in moles per cm^2) is:

$$\Gamma = \frac{c}{RT} \frac{\partial \gamma}{\partial c} \quad (1)$$

where

c = concentration in moles per liter

R = gas constant

T = absolute temperature

and $\partial \gamma / \partial c$ = slope of surface tension-concentration curve.

Calculations based on equation 1 indicate that $\partial \gamma / \partial c$ changes only slightly for as much as 140 ppm of ABS in the temperature range 20°C to 35°C. Hence, temperature has a greater influence on surface tension than concentration for the range of conditions indicated.

Because most commercial detergents contain other compounds as well as ABS, the surface tension was determined for solutions of 17 different commercial

detergent products. Enough of each product was used to give 100 ppm of ABS in solution. At this concentration of ABS and at 20°C, the surface tension of the 17 detergent solutions ranged from 50 to 63 dynes per cm. These data indicate that, in detergents, compounds other than ABS increase surface tension. Solutions of commercial products containing 10 ppm of ABS plus 100 million bacteria per ml at 20°C gave surface tensions ranging from 70.5 to 72.0 dynes per cm as compared to about 68 without bacteria; apparently, bacteria reduce the surface activity of surfactants in solution.

The influence of pH on surface tension is shown in figure 179.2. In dilute solutions of anionic surfactants, surface tension increases with increase in pH, whereas in solutions of cationic and nonionic surfactants, surface tension decreases with increase in pH. Phosphate, silicate, and carboxymethylcellulose, along with ABS, tend to inhibit the influence of

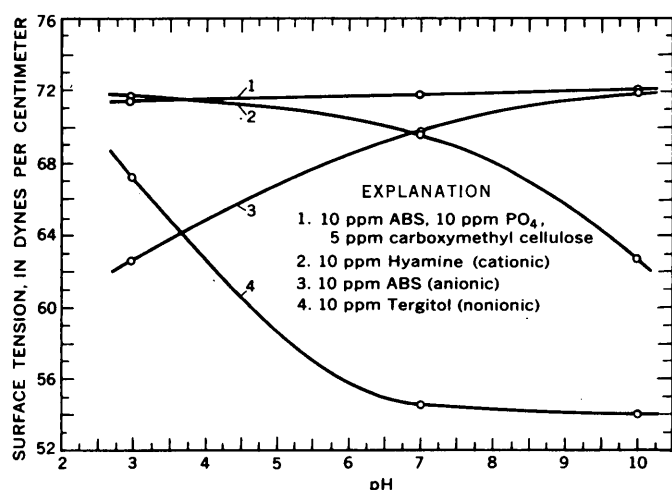


FIGURE 179.2.—Variation of surface tension of surfactant solutions with pH, at 20°C.

pH on the surface tension of a surfactant solution. Mankowich (1953) has indicated that pH and other ions have little influence on surface tension in highly concentrated surfactant solutions (1,000 to 4,000 ppm); evidently, the pH effect is masked at higher concentrations by surfactant saturation at the air-solution interface.

Surface-tension measurements of the sewage effluent from the Denver sewage-treatment plant were made for a 2-month period. The surface tension of the effluent ranged from 63 to 71.5 dynes per cm at 20°C; the surface tension of pure water at 20°C is 72.75 dynes per cm. Weekly determinations of certain constituents in this water had the following ranges: detergent (ABS), 5.5 to 6.5 ppm; dissolved solids, 750 to 1,120 ppm; bacteria (*Escherichia coli*), 150,000 to 250,000 per ml; and dissolved oxygen, 0.0 to 3.5 ppm. For a sewage effluent at Indianapolis, Bowers found that the surface tension ranged from 45 to 60 dynes per cm at 25°C. Although a minor amount of the difference between the surface tension of sewage effluents at Denver and Indianapolis can be attributed to a difference in temperature of measurement (20°C

at Denver and 25°C at Indianapolis), most of the difference probably is due to variation in composition of the sewage effluent at the two cities. The composition of a sewage effluent is influenced by waste disposal from industry, agriculture, and other sources. Because no two cities are likely to have sewage effluents of identical compositions, differences in surface tensions of their sewage effluents are to be expected.

In areas of sewage spreading or storage of natural water containing surfactants, knowledge of the surface tension of these liquids is important because the rate at which water wets and infiltrates soils depends in part on the surface tension of the liquid phase. As of March 1962, the detergent (ABS) concentration of most surface-water supplies is less than 10 ppm; at this concentration, the surface tension of water containing ABS surfactant is only slightly less than that of pure water.

This study shows that the concentration of ABS found in natural water cannot lower surface tension appreciably below that of pure water. At temperatures of more than 20°C, the surface tension-concentration gradient increases considerably for dilute surfactant solutions. In solutions containing less than 10 ppm of ABS, ions other than surfactants tend to increase surface tension above that of the pure surfactant alone; bacteria make the effect more pronounced. The results of this study will be applied to investigations of the influence of surface tension on wettability of soils and aquifer materials. The evaluation of surface tension in flow theory has received no significant consideration to date.

REFERENCES

- Bowers, D. R., 1952, Measurement of surface tension of sewage II. Indianapolis studies: Sewage and Indus. Wastes, v. 24, p. 1447-1455.
- Fischer, E. K., and Gans, D. M., 1946, Surface-active agents at interfaces: New York Acad. Sci., v. 46, p. 371-406.
- Harris, J. C., 1946, Builders with synthetic detergents: Oil and Soap, v. 23, p. 101-110.
- Mankowich, A. M., 1953, Physiochemical properties of surfactants: Indus. and Eng. Chem., v. 45, p. 2759-2766.



SUBJECT INDEX

[For major topic headings such as "Economic Geology," "Stratigraphy," "Ground Water," see under State names or refer to table of contents]

A	Article
ABS, effect on foaming of water	178
Agassiz, glacial Lake, stratigraphy	170
Alaska, stratigraphy, McCarthy C-5 quad-range	133
Alteration, hydrothermal, hot springs	153
relation to occurrence of uranium	122
Alunite, in hot-spring alteration	153
Wyoming, Aspen Mountain	123
Ansonia Gneiss, Connecticut, definition	128
Aquifers, compaction	172
glacial drift	157
glaciocluvial and shore deposits	170
sandstone	171
Arizona, economic geology, southeastern	120
geophysics, Meteor Crater	149
paleontology, northeastern	161
sedimentation, Colorado Plateau	163
structural geology, Navajo County	143
Arkansas, stratigraphy, Washington County	130, 131
Atoka Formation, Arkansas, type section	130
Avalanches, erosional features	155

B	
Blloyd Formation, Brentwood Limestone Member, Arkansas, type section.	130
Dye Shale Member, Arkansas, type section.....	131
Kessler Limestone Member, Arkansas, type section.....	130
Trace Creek Shale Member, Arkansas, type section.....	131
Woolsey Member, Arkansas, type section.	130
Bonanza King Formation, Nevada, definition.	127
Buttress Diabase, Connecticut, definition.....	128

	C
California, geomorphology, Kings River area	155
geophysics, San Bernadino County.....	150
ground water, Santa Clara Valley.....	172
igneous petrology, Inyo Mountains.....	145
structural geology, Inyo Mountains.....	145
Owens Valley.....	145
San Joaquin Valley.....	146
Sierra Nevada.....	145
Cambrian, Nevada, paleontology and stratigraphy.....	127
Nevada, stratigraphy.....	126
Campito Formation, Montenegro Member, Nevada, stratigraphic relations...	126
Canyon Creek fault, Arizona, description...	143
Carbon-14 age determinations, Pleistocene strata.....	160
Carboniferous. See Mississippian, Pennsylvanian.	
Carrara Formation, Nevada, definition.....	127
Cedar Ridge Till, Wyoming, definition.....	159
Chile, structural geology, San Pedro de Atacama.....	147
Clausthalite, thermal expansion.....	152
Clay minerals, in hot springs.....	153
Clays, relation to uranium deposits.....	124
Coesite, thermal expansion.....	152

	Article
Colorado, economic geology, Teller County.....	121
igneous petrology, central Front Range.....	154
mineralogy, Teller County.....	121
paleontology and stratigraphy, Glenwood Canyon.....	129
sedimentation, Colorado Plateau.....	163
Colorado, stratigraphy, Minturn quadrangle.....	132
Connecticut, stratigraphy, south-central.....	128
Convolute bedding, definition.....	164
Copper porphyries, K-Ar and Rb-Sr age determinations.....	120
Cretaceous, western interior, paleontology.....	161
Wyoming, strand lines.....	134
Crustal deformation, Idaho, Snake River Plain.....	141
Cryptovolcanoes, Serpent Mound, Ohio.....	148
<i>Cytherelloidea</i> , possible indicator of paleotemperatures.....	162

D	
Deep Spring Formation, Nevada, stratigraphic relations.....	126
Degradation, solute, rates	177
Delaware, surface water, Potomac River basin.....	173
Derby Hill Schist, Connecticut, definition....	128
<i>Desmoscapites</i> , Range Zone.....	161
Detergents, foaming characteristics.....	178
surface tension of solutions.....	179
Devonian, Connecticut, regional metamorphism.....	128
Dinwoody Lake Till, Wyoming, definition....	159
Discharge, stream, measurement with radio-isotopes.....	176
Dunderberg Shale, Nevada, definition.....	127

E	
Eagle Valley Evaporite, Colorado, correlation.....	132
Edge isolation, description of technique.....	166
Electrical resistivity, magnetite deposits.....	150
Emigrant Formation, Nevada, stratigraphic relations.....	126
Eocene, Florida, stratigraphy.....	136

F	
Faults and faulting, Arrowhead fault, Nevada	144
Faults and faulting, geohydrologic evidence	142
Inyo Mountains, Calif.	145
Owens Valley, Calif.	145
Jackson, Wyo.	160
Navajo County, Ariz.	143
Sierra Nevada, Calif.	145
Tooele Valley, Utah	142
Feldspars, in hot-spring alteration	153
Flood-frequency curves, in adjusting flow-duration curves	174
Florida, stratigraphy and structure, Escambia County	136
stratigraphy and structure, Santa Rosa County	136

	Article
Flow-duration curves, defining relations between.....	174
Foam stability, factors affecting.....	178
Folds and folding, laboratory studies.....	164, 165
Forsterite, thermal expansion.....	152

G	
Galena, thermal expansion.....	152
Georgia, ground water, Jonesboro.....	169
Glacial drift, aquifers.....	157
Glaciofluvial deposits, as aquifers.....	170
Gradiometer, declination, use in field deter- mination of polarity.....	151
Granitic rocks, correlation.....	145
Gravity studies, Idaho, Snake River Plain.....	141
Basin and Range province.....	140

H	
Hale Formation, Cane Hill Member, Arkansas, type section.....	130
Prairie Grove Member, Arkansas, type section.....	130
Harkless Formation, Nevada, stratigraphic relations.....	128
Hot springs, hydrothermal alteration.....	153
Hydraulics, model of control structure.....	175

I	
Idaho, geophysics, Gem Valley.....	140
geophysics, Snake River Plain.....	141
structural geology, Gem Valley.....	140
Snake River Plain.....	141
Impact craters, Serpent Mound, Ohio.....	148
Indiana, glacial geology, Lake County.....	157
Indonesia, engineering geology, West Java....	125
Interior drainage, structural control.....	146
Intraformational recumbent folds, laboratory studies.....	164, 165
Intraformational thrust structures, definition..	164
Irregularly contorted beds, definition.....	164

Joints and jointing, relation to permeability..	169
Juana Díaz Formation, Puerto Rico, ground water.....	137
Jurassic, Alaska, McCarthy C-5 quadrangle, Colorado Plateau, wind direction.....	133 163

K	
Kentucky, surface water, Eastern Coal Field..	174
Klondike Mountain Formation, Washington, definition.....	135

L	
Lake Agassiz, Vermilion end moraine.....	158
Land subsidence, relation to compaction of aquifers.....	172
Tulare Lake bed, California.....	146
Leadville Limestone, Colorado, age.....	129

Note.—Numbers refer to articles.

D193

M	Article	Article	Article		
Magnetic surveys, basalt flows.....	140	Pennsylvania, surface water, Potomac River basin.....	173	Surfactants, effect on foaming of detergents....	178
Magnetic susceptibility, magnetite deposits..	150	Pennsylvanian, Arkansas, stratigraphy.....	130, 131	Surface tension, detergent solutions.....	179
Magnetite deposits, electric and magnetic properties.....	150	Pennsylvanian, Colorado, stratigraphy.....	132		
Maps, edge isolation.....	166	Colorado Plateau, wind direction.....	163	T	
shaded relief, method of preparation.....	167	Permeability, relation to jointing in rocks.....	169	Temperature, ground water.....	168
Maroon Formation, Colorado, correlation.....	132	Permian, Colorado, stratigraphy.....	132	Tertiary, Chile, salt domes.....	147
Maroon Formation, Jacque Mountain Limestone Member, Colorado.....	132	Permian, Colorado Plateau, wind direction....	163	Washington, stratigraphy.....	135
Maryland, quality of water, Potomac River....	177	Pine Mountain overthrust, Virginia.....	139	Wyoming, stratigraphy.....	123
surface water, Potomac River basin.....	173	Pitkin Limestone, Arkansas, type section....	130	See also Eocene, Oligocene, Miocene, Pliocene.	
Massachusetts, geophysics, Merrimack River valley.....	156	Pleistocene, Florida, marine terraces.....	136	Thalenite, occurrence in Colorado.....	121
glacial geology, Merrimack River valley....	156	Indiana, glacial drift.....	157	Thermal expansion, minerals.....	152
ground water, Merrimack River valley....	156	Wyoming, glacial tills.....	159	Thermoluminescence of rocks, as an indicator of shock.....	149
Mesaverde Formation, Wyoming, correlation and facies.....	134	stratigraphy.....	160	Triassic, Colorado Plateau, wind direction...	163
Metamorphic rocks, relation of jointing to permeability.....	169	Pliocene, Florida, stratigraphy.....	136		
Minnesota, glacial geology, Nett Lake Indian Reservation.....	158	Poleta Formation, Nevada, stratigraphic relations.....	126	U	
glacial geology, Stephen.....	170	Potassium-argon age determinations, copper porphyries.....	120	Uranium, alteration related to.....	122
ground water, Stephen.....	170	Precambrian, Colorado, igneous petrology....	154	relation of deposits to clays.....	124
Minturn Formation, Colorado, correlation....	132	Precambrian, Nevada, stratigraphy.....	126	Utah, ground water, Tooele Valley.....	142
Miocene, Florida, stratigraphy.....	136	Prospect Gneiss, Connecticut, definition....	128	paleontology, eastern.....	161
Mississippian, Arkansas, stratigraphy.....	130	Prospecting, uranium.....	122	sedimentation, Colorado Plateau.....	163
Colorado, paleontology and stratigraphy....	129	Puerto Rico, ground water, Yanco area.....	137	structural geology, Tooele Valley.....	142
Montana, paleontology, western.....	161	stratigraphy, Yanco area.....	137		
Morrison Formation, New Mexico, clay content.....	124			V	
Morrow Series. See Bloyd Formation, Hale Formation.		Q		Virginia, quality of water, Potomac River....	177
Mule Spring Limestone, Nevada, stratigraphic relations.....	126	Quaternary. See Pleistocene, Recent.		structural geology, Powell River valley....	139
				surface water, Potomac River basin.....	173
N		R		Volcanic ash, carbon-14 ages.....	138
Nacimiento Formation, New Mexico, aquifers..	171	Radiolotopes, in measuring stream discharge..	176	Volcanism, Idaho, Snake River Plain.....	141
Nevada, geochemistry, Steamboat Springs....	153	Recent, Washington, pyroclastic deposits....	138		
stratigraphy, Esmeralda County.....	126	Reed Dolomite, Nevada, stratigraphic relations.....	126	W	
Nevada Test Site.....	127	Remanent magnetism, field measurement....	151	Washington, stratigraphy, Ferry County.....	135
structural geology, Muddy Mountains.....	144	Rubidium-strontium age determinations, copper porphyries.....	120	stratigraphy, Mount Rainier.....	138
New Jersey, ground water, Wharton Tract....	168	Runoff, estimation from short records.....	173	Mount St. Helens.....	138
New Mexico, economic geology, Ambrosia Lake area.....	124			Washington, D.C., quality of water, Potomac River.....	177
ground water, San Juan Basin.....	171	S		Wepawong Schist, Connecticut, definition....	128
mineralogy, Ambrosia Lake area.....	124	Sacagawea Ridge Till, Wyoming, definition..	159	West Rock Diabase, Connecticut, definition..	128
paleontology, western.....	161	Salt domes, formation of.....	147	West Virginia, quality of water, Potomac River.....	177
sedimentation, Colorado Plateau.....	163	San Jose Formation, New Mexico, aquifers....	171	surface water, Potomac River basin.....	173
surface water, Rio Grande.....	175	Sandstone, eolian, Colorado Plateau.....	163	Wisconsin age, Minnesota, glacial geology....	158
		ground water in.....	171	Woodbridge Granite, Connecticut, definition..	128
O		Sanpoil Volcanics, Washington, definition....	135	Woodtick Gneiss, Connecticut, definition....	128
O'Brien Creek Formation, Washington, definition.....	135	Scatter Creek Rhyodacite, Washington, definition.....	135	Wurtzite, thermal expansion.....	152
Ohio, economic geology, southern.....	148	Sedimentation, structure for measuring rate..	175	Wyman Formation, Nevada, stratigraphic relations.....	126
structural geology, southern.....	148	Sediments, studies of folds and folding.....	164, 165	Wyoming, economic geology, Aspen Mountain.....	123
Ojo Alamo Sandstone, New Mexico, aquifers..	171	Seismic investigations, depth of fill in river valleys.....	156	economic geology, Shirley Basin.....	122
Oligocene, Florida, stratigraphy.....	136	Shore deposits, as aquifers.....	170	glacial geology, Jackson.....	160
Puerto Rico, stratigraphy.....	137	Southington Mountain Schist, Connecticut, definition.....	128	Wind River Mountains.....	159
Ostracodes, Cretaceous.....	162	Snow chutes, formation.....	155	paleontology western.....	161
		Sphalerite, thermal expansion.....	152	paleontology and stratigraphy, southern..	134
		See also Zinc.			
P		Stilleite, thermal expansion.....	152	Y	
Paleomagnetism, field determination.....	151	Straits Schists, Connecticut, definition.....	128	Yttrium silicate, thalenite.....	121
Paleotemperatures, indicators.....	162	Streamflow, estimation from short records....	173		
		measurement with radiolotopes.....	176	Z	
		structure for measuring.....	175	Zinc, in explosion structures.....	14
		Strontianite, thermal expansion.....	152		
		Surfactant solutions, surface tension.....	179		

Note.—Numbers refer to articles.

AUTHOR INDEX

	Article
Adams, J. W.....	121
Albers, J. P.....	126
Armstrong, F. C.....	140
Ash, S. R.....	171
Baker, C. H., Jr.....	164, 165
Baltz, E. H.....	171
Barnes, Harley.....	127
Blackmon, P. D.....	123
Brock, M. R.....	148
Byers, F. M., Jr.....	127
Carter, R. W.....	176
Christiansen, R. L.....	127
Clarke, A. B.....	166
Cobban, W. A.....	134, 161
Cox, Allan.....	151
Crandell, D. R.....	138
Creasey, S. C.....	120
Davis, G. H.....	146, 155
Dingman, R. J.....	147
Doell, R. R.....	151
Eisenlohr, W. S., Jr.....	173
Feltz, H. R.....	177
Finnell, T. L.....	143
Frederick, B. J.....	176
Fritts, C. E.....	128
Gates, J. S.....	142
Granger, H. C.....	124
Green, J. H.....	146, 172
Grossman, I. G.....	137

	Article
Hallgarth, W. E.....	129
Harris, D. D.....	175
Harshman, E. N.....	122
Havens, R. G.....	121
Henbest, L. G.....	130, 131
Heyl, A. O.....	148
Hildebrand, F. A.....	121
Johnson, G. R.....	149
Kirkpatrick, G. A.....	174
Kistler, R. W.....	120
LaFehr, T. R.....	141
Lang, S. M.....	168
Longwell, C. R.....	144
Love, J. D.....	123, 160
Lovering, T. S.....	132
Mabey, D. R.....	140
McCabe, J. A.....	174
McGrath, J. G.....	149
McKee, D. M.....	164, 165
MacKevett, E. M., Jr.....	133
MacLay, R. W.....	170
Mallory, W. W.....	132
Marsh, O. T.....	136
Miller, R. D.....	138
Miller, R. L.....	139
Muessig, Siegfried.....	135
Mullineaux, D. R.....	138
Norvitch, R. F.....	158
Page, H. G.....	178, 179

	Article
Pakiser, L. C.....	141
Poole, F. G.....	163
Reck, C. W.....	176
Reynolds, M. A.....	164, 165
Richardson, E. V.....	175
Richmond, G. M.....	159
Rhodehamel, E. C.....	168
Roach, C. H.....	149
Robertson, J. B.....	178, 179
Rosenshein, J. S.....	157
Ross, D. C.....	145
Rubin, Meyer.....	138
Sammel, E. A.....	156
Schlner, G. R.....	170
Sigvaldason, G. E.....	153
Sims, P. K.....	154
Skinner, B. J.....	152
Skipp, B. A. L.....	129
Sohn, I. G.....	162
Stacy, J. R.....	167
Sterrett, T. S.....	149
Stewart, J. H.....	126
Stewart, J. W.....	169
Taylor, D. W.....	160
Taylor, R. B.....	154
Waldron, H. A.....	125
Wark, J. W.....	177
Wayman, C. H.....	178, 179
West, S. W.....	171
White, D. E.....	153
Zablocki, C. J.....	150
Zapp, A. D.....	134

Note.—Numbers refer to articles.

D195